frontiers | Research Topics

New insights into the molecular basis of long-term plasticity underlying addiction and addictive behaviours

Edited by
Elisabeth Piccart, Vidhya Kumaresan and Juan Marín-Lahoz

Published in
Frontiers in Molecular Neuroscience

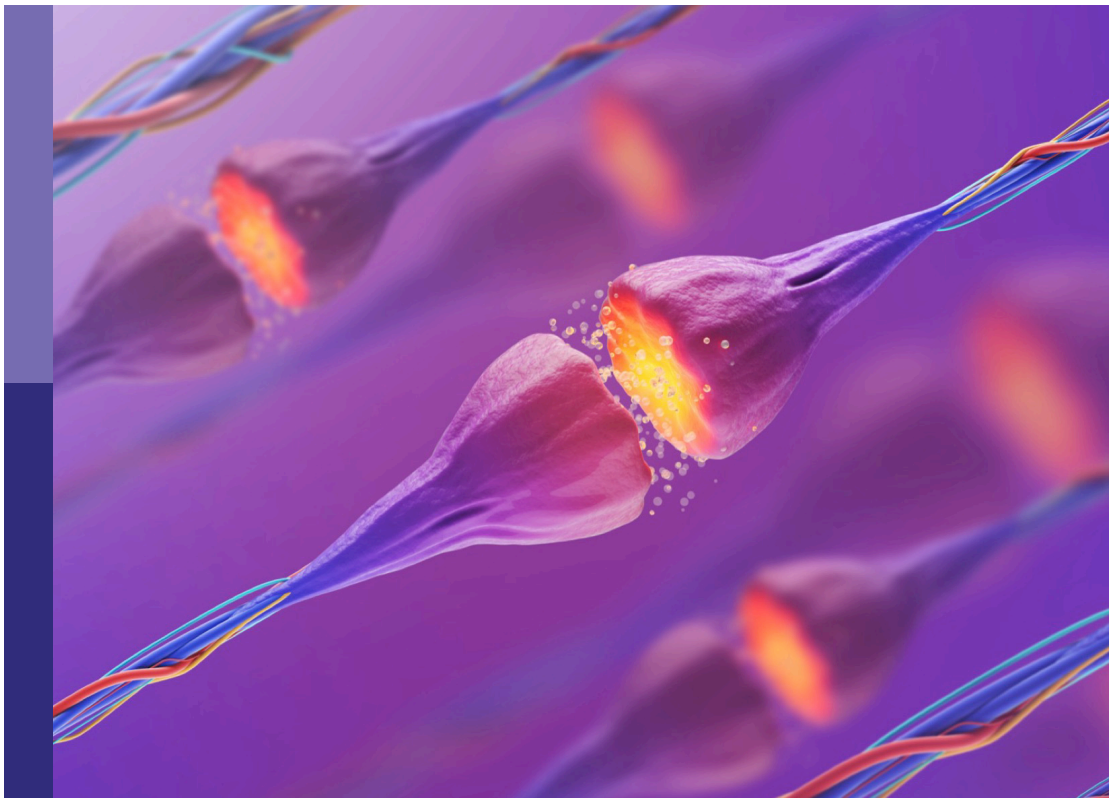

ISSN 1664-8714
ISBN 978-2-8325-2810-5
DOI 10.3389/978-2-8325-2810-5

About Frontiers

Frontiers is more than just an open access publisher of scholarly articles: it is a pioneering approach to the world of academia, radically improving the way scholarly research is managed. The grand vision of Frontiers is a world where all people have an equal opportunity to seek, share and generate knowledge. Frontiers provides immediate and permanent online open access to all its publications, but this alone is not enough to realize our grand goals.

Frontiers journal series

The Frontiers journal series is a multi-tier and interdisciplinary set of open-access, online journals, promising a paradigm shift from the current review, selection and dissemination processes in academic publishing. All Frontiers journals are driven by researchers for researchers; therefore, they constitute a service to the scholarly community. At the same time, the *Frontiers journal series* operates on a revolutionary invention, the tiered publishing system, initially addressing specific communities of scholars, and gradually climbing up to broader public understanding, thus serving the interests of the lay society, too.

Dedication to quality

Each Frontiers article is a landmark of the highest quality, thanks to genuinely collaborative interactions between authors and review editors, who include some of the world's best academicians. Research must be certified by peers before entering a stream of knowledge that may eventually reach the public - and shape society; therefore, Frontiers only applies the most rigorous and unbiased reviews. Frontiers revolutionizes research publishing by freely delivering the most outstanding research, evaluated with no bias from both the academic and social point of view. By applying the most advanced information technologies, Frontiers is catapulting scholarly publishing into a new generation.

What are Frontiers Research Topics?

Frontiers Research Topics are very popular trademarks of the *Frontiers journals series*: they are collections of at least ten articles, all centered on a particular subject. With their unique mix of varied contributions from Original Research to Review Articles, Frontiers Research Topics unify the most influential researchers, the latest key findings and historical advances in a hot research area.

Find out more on how to host your own Frontiers Research Topic or contribute to one as an author by contacting the Frontiers editorial office: frontiersin.org/about/contact

New insights into the molecular basis of long-term plasticity underlying addiction and addictive behaviours

Topic editors

Elisabeth Piccart — University of Hasselt, Belgium

Vidhya Kumaresan — Boston University, United States

Juan Marín-Lahoz — Hospital Universitario Miguel Servet, Spain

Citation

Piccart, E., Kumaresan, V., Marín-Lahoz, J., eds. (2023). *New insights into the molecular basis of long-term plasticity underlying addiction and addictive behaviours*. Lausanne: Frontiers Media SA. doi: 10.3389/978-2-8325-2810-5

Table of contents

frontiers | Frontiers in Molecular Neuroscience

TYPE Editorial
PUBLISHED 12 June 2023
DOI 10.3389/fnmol.2023.1226345

OPEN ACCESS

EDITED AND REVIEWED BY
Clive R. Bramham,
University of Bergen, Norway

*CORRESPONDENCE
Juan Marín-Lahoz
✉ juanmarinlahoz@gmail.com

RECEIVED 21 May 2023
ACCEPTED 29 May 2023
PUBLISHED 12 June 2023

CITATION
Marín-Lahoz J (2023) Editorial: New insights into the molecular basis of long-term plasticity underlying addiction and addictive behaviors. *Front. Mol. Neurosci.* 16:1226345. doi: 10.3389/fnmol.2023.1226345

Editorial: New insights into the molecular basis of long-term plasticity underlying addiction and addictive behaviors

Juan Marín-Lahoz[1,2,3]*

[1]Neurology Department, Hospital Universitario Miguel Servet, Zaragoza, Spain, [2]Grupo de Investigación en Neurociencias, IIS Aragón, Zaragoza, Spain, [3]Center for Biomedical Research on Neurodegenerative Diseases (CIBERNED), Madrid, Spain

KEYWORDS

addiction, synaptic plasticity, behavioral addictions, animal models, molecular pathways

Editorial on the Research Topic
New insights into the molecular basis of long-term plasticity underlying addiction and addictive behaviors

As editor of this Research Topic on neurobiology of addictions I am glad to present the interesting manuscripts that are finally included. I feel really grateful for the reviewers who have done a thoughtful job and for Frontiers that facilitates the process of producing a Research Topic enormously. But the ones that more strongly deserve my gratitude are the authors who not only shared their work with us but also trusted us to take care of it, review it and suggest changes.

This Research Topic contains 10 manuscripts. There is no reason to believe that this sample is completely representative of the current scientific production on addiction neurobiology. Nevertheless, it is tempting to check how the focus of the manuscripts is distributed, and also serves to introduce them.

From the point of view of the **mechanisms**, the sample is varied. As expected, much of the research evaluates synaptic plasticity and neurotransmitter pathways. Nevertheless the studied pathways are really diverse and barely overlap. Dopamine is obviously there, but only one manuscript really focuses on **dopaminergic pathways** (Bimpisidis et al.). Other neurotransmitter pathways that are explored in this topic are **glutamate** (Giangrasso et al.), and **cannabinoid** for drugs other than cannabinoids (Lucente et al.), while another evaluates the interaction of two pathways: **sigma and adenosine** (Borroto-Escuela et al.).

Nevertheless some manuscripts do not focus on neurotransmitters. Other manuscripts focus on intracellular pathways: **rho GTPases** (Ru et al.) and **Glycogen synthase kinase-3β** (Yan et al.). Some focus on the relationship between neurons from a point of view other than neurotransmitters, this is the case of the works focusing on **neuronal excitability** (Gimenez-Gomez et al.; Domi et al.) and mRNA expression of **cell adhesion molecules** (Munoz et al.). Last but not the least, one manuscript is not focused on the mechanisms but is mainly **behavioral,** focusing on the preferences to different drug concentrations (Schneider et al.).

Regarding the **species**, the two reviews include several species, one uses **zebrafish larvae** (Schneider et al.), two use **mice** (Bimpisidis et al.; Yan et al.) and all the rest use **rats**. This distribution of preclinical models seems to match the global trend but it also shows how when focusing on the internal mechanisms most of what we know

about **humans** is extrapolated from animal models. There are obvious reasons why it is easier (and more efficient) to research neurotransmitter pathways, RNA expression or synapse structure in these animal models than in humans. But for the most part, the real target is to understand human addiction and the tools to investigate these mechanisms in human subjects are increasingly available: nuclear imaging, MRI connectivity, microRNA expression, and exosomes might be considered among the options.

Addiction is about **drugs**. Or is it not? Regarding the object of addiction, all of the manuscripts focus on substances. More concretely, each of them focus on a substance except for one which reviews a target for **multiple substances** (Ru et al.). Interestingly all of the manuscript but one focus on substances usually classified as drugs: **ethanol** (Gimenez-Gomez et al.), **nicotine** (Lucente et al.; Domi et al.; Schneider et al.), **methamphetamine** (Munoz et al.; Yan et al.), and **cocaine** (Borroto-Escuela et al.). The one not focused on a drug, focuses on **sucrose** (Bimpisidis et al.). Sucrose is a common sugar in modern diets and is usually referred to as a nutrient and not a drug. Nevertheless, most of the population in the history of humankind had little or no access to sucrose in a purified form and most natural foods contain no sucrose or little sucrose. Sucrose has no direct effect on reward circuits, contrary to substances considered drugs. Accordingly, the work of Bimpisidis et al. fosters the understanding of reward processing in the absence of drugs, a paramount topic to understand **behavioral addictions**, notwithstanding its usefulness to understand the addictions in which sweets are involved. As a researcher myself, I have focused my previous work in addictions not directed toward drugs but toward behaviors. Some of their mechanisms may be shared with substance overuse disorder but the knowledge on the mechanisms of behavioral addictions lags behind that of the mechanisms of drug addiction. The burden of this kind of behavior is also high and possibly growing. But the knowledge of the knowledge of its intimate mechanisms lags behind that of drug addiction.

Yet, this Research Topic shows a great predominance of drug studies over studies targeting other objects of addiction. This predominance has occurred despite an inclusive Research Topic title: New Insights Into the Molecular Basis of Long-Term Plasticity Underlying Addiction and *Addictive Behaviors*. It has also occurred despite my efforts to engage researchers focused on behavioral addictions (due to my aforementioned interest). As I stated above, this Research Topic, does not have to be a representative sample. And maybe the current research in the neurobiology of behavioral addictions is blooming somewhere else. But maybe the researchers focused on behavioral addictions are not the ones focused on neurobiology and vice versa.

I hope this trend changes in the near future with more efforts to understand the neurobiology of behavioral addictions, and no decrease in the efforts to understand drug effects. In the meantime, I hope you find this Research Topic useful and enjoy the reading.

Author contributions

The author confirms being the sole contributor of this work and has approved it for publication.

Funding

This research was supported by the Ministerio de Ciencia e Innovación of the Spanish Government (Grant number: JR20700007).

Conflict of interest

The author declares that the research was conducted in the absence of any commercial or financial relationships that could be construed as a potential conflict of interest.

Publisher's note

frontiers | Frontiers in Molecular Neuroscience

TYPE Original Research
PUBLISHED 12 January 2023
DOI 10.3389/fnmol.2022.1104648

OPEN ACCESS

EDITED BY
Juan Marín-Lahoz,
Hospital Universitario Miguel Servet, Spain

REVIEWED BY
Yonatan M. Kupchik,
Hebrew University of Jerusalem, Israel
Steven M. Graves,
University of Minnesota Twin Cities, United States

*CORRESPONDENCE
Louise Adermark
✉ Louise.adermark@gu.se

SPECIALTY SECTION
This article was submitted to Neuroplasticity and Development, a section of the journal Frontiers in Molecular Neuroscience

RECEIVED 21 November 2022
ACCEPTED 21 December 2022
PUBLISHED 12 January 2023

CITATION
Lucente E, Söderpalm B, Ericson M and Adermark L (2023) Acute and chronic effects by nicotine on striatal neurotransmission and synaptic plasticity in the female rat brain.
Front. Mol. Neurosci. 15:1104648.
doi: 10.3389/fnmol.2022.1104648

Acute and chronic effects by nicotine on striatal neurotransmission and synaptic plasticity in the female rat brain

Erika Lucente[1], Bo Söderpalm[2], Mia Ericson[2] and Louise Adermark[1]*

[1]Integrative Neuroscience Unit, Department of Pharmacology, Institute of Neuroscience and Physiology, The Sahlgrenska Academy, University of Gothenburg, Gothenburg, Sweden, [2]Addiction Biology Unit, Department of Psychiatry and Neurochemistry, Institute of Neuroscience and Physiology, The Sahlgrenska Academy, University of Gothenburg, Gothenburg, Sweden

Introduction: Tobacco use is in part a gendered activity, yet neurobiological studies outlining the effect by nicotine on the female brain are scarce. The aim of this study was to outline acute and sub-chronic effects by nicotine on the female rat brain, with special emphasis on neurotransmission and synaptic plasticity in the dorsolateral striatum (DLS), a key brain region with respect to the formation of habits.

Methods: *In vivo* microdialysis and *ex vivo* electrophysiology were performed in nicotine naïve female Wistar rats, and following sub-chronic nicotine exposure (0.36 mg/kg free base, 15 injections). Locomotor behavior was assessed at the first and last drug-exposure.

Results: Acute exposure to nicotine *ex vivo* depresses excitatory neurotransmission by reducing the probability of transmitter release. Bath applied nicotine furthermore facilitated long-term synaptic depression induced by high frequency stimulation (HFS-LTD). The cannabinoid 1 receptor (CB1R) agonist WIN55,212-2 produced a robust synaptic depression of evoked potentials, and HFS-LTD was blocked by the CB1R antagonist AM251, suggesting that HFS-LTD in the female rat DLS is endocannabinoid mediated. Sub-chronic exposure to nicotine *in vivo* produced behavioral sensitization and electrophysiological recordings performed after 2-8 days abstinence revealed a sustained depression of evoked population spike amplitudes in the DLS, with no concomitant change in paired pulse ratio. Rats receiving sub-chronic nicotine exposure further demonstrated an increased neurophysiological responsiveness to nicotine with respect to both dopaminergic- and glutamatergic signaling. However, a tolerance towards the plasticity facilitating property of bath applied nicotine was developed during sub-chronic nicotine exposure *in vivo*. In addition, the dopamine D2 receptor agonist quinpirole selectively facilitate HFS-LTD in slices from nicotine naïve rats, suggesting that the tolerance may be associated with changes in dopaminergic signaling.

Conclusion: Nicotine produces acute and sustained effects on striatal neurotransmission and synaptic plasticity in the female rat brain, which may contribute to the establishment of persistent nicotine taking habits.

KEYWORDS
dopamine, electrophysiology, endocannabinoid, female, LTD, nicotine, striatum

Introduction

Nicotine addiction is a major preventable risk factor for morbidity and mortality, yet few manage to maintain abstinent when exchanging cigarettes for nicotine replacement therapy (Livingstone-Banks et al., 2019). Defining underlying mechanism associated with nicotine addiction is thus pivotal to outline new strategies for successful nicotine cessation. Experimental studies have shown that drugs of abuse elicit glutamatergic synaptic plasticity that contributes to the reorganization of neural circuits, and putatively, the establishment of addictive behaviors (van Huijstee and Mansvelder, 2014; Christian et al., 2021; Pascoli et al., 2022). Dopamine, which is released in response to nicotine exposure, is a prerequisite for drug-induced plasticity (Belin et al., 2009; Lee et al., 2020; Rivera et al., 2021), and a key regulator of structural and synaptic plasticity (Urakubo et al., 2020; Speranza et al., 2021). In addition, nicotine activates nicotinic acetylcholine receptors (nAChRs), which also has been demonstrated to be important for synaptic plasticity at both inhibitory and excitatory synapses (Dani et al., 2001; Partridge et al., 2002; Adermark, 2011). By activating nAChRs and increasing dopamine levels, nicotine may thus facilitate the induction of synaptic plasticity mechanisms and elicit long-term neuroadaptations, which will outlast the presence of the drug.

Studies performed in male rodents have shown that nicotine especially facilitate synaptic plasticity in the form of endocannabinoid-mediated long-term depression (eCB-LTD; Adermark et al., 2019), and both nicotine self-administration as well as yoked nicotine exposure increase VTA dialysate levels of the cannabinoid 1 receptor (CB1R) agonist 2-arachidonoyl glycerol (2-AG; Buczynski et al., 2013). Antagonists targeting the CB1R furthermore blocks the motivational and dopamine-releasing effects of nicotine (Cohen et al., 2002; Cheer et al., 2007), and mice with a genetic deletion of the CB1R does not show conditioned place preference toward nicotine (Castane et al., 2002). The addictive properties of nicotine may in this extent be connected to facilitation of eCB signaling, which apart from its rewarding properties drive neuronal adaptations that may contribute to the formation of persistent drug-related habits and addictive behaviors (Hilario et al., 2007; Merritt et al., 2008; Hernandez et al., 2014; Bystrowska et al., 2019; Iyer et al., 2022). Repeated exposure to nicotine, however, has been shown to lead to decreased eCB levels in the striatum, without affecting CB1R expression (Gonzalez et al., 2002).

Importantly, smoking cigarettes is in part a gendered activity with sex-specific uptake trends and cessation patterns (Benowitz and Hatsukami, 1998). Smoking is more anxiolytic in women, and women are more likely to smoke in situations associated with stress or in response to negative affect (Perkins et al., 2012; Antin et al., 2017). Interestingly, human studies indicate that there is disparity with regards to nicotine-induced dopamine-release in women and men, where the reward system and ventral striatum is activated by nicotine in men, while dorsal striatal regions are recruited in women (Cosgrove et al., 2014). The dorsal striatum may thus be a key brain region of interest when assessing nicotine-induced neuroplasticity in females. Furthermore, animal studies indicate that female rats display higher tonic 2-AG signaling (Melis et al., 2013), which may affect the responsiveness to the putative nicotine-induced eCB release. Since previous studies outlining nicotine-induced facilitation of eCB signaling has been performed in male rats, the aim of this study was to study acute and sub-chronic effects by nicotine on neurotransmission and synaptic plasticity in the female rat brain. To this end, female Wistar rats were studied using *ex vivo* electrophysiology and *in vivo* microdialysis, and nicotine was administered through experimenter-controlled injections. Neurotransmission was monitored in the dorsolateral striatum, a brain region associated with the development of drug-related habits but also linked to neurophysiological responses to nicotine in women (Gerdeman et al., 2003; Belin et al., 2009; Cosgrove et al., 2014).

Materials and methods

Research outline

In the first set of experiments, acute effects displayed by nicotine on neurotransmission and long-term synaptic depression induced by high frequency stimulation (HFS-LTD) were assessed using *ex vivo* electrophysiology ($n = 26$ rats). In the next set of experiments, sustained neuroadaptations elicited by repeated nicotine exposure were outlined. Female rats received 15 experimenter-controlled nicotine injections (0.36 mg/kg, free base) distributed over 3 weeks and locomotor activity was measured at the first and last exposure ($n = 30$). Baseline dopamine levels and dopamine release evoked by nicotine were recorded in the DLS using *in vivo* microdialysis, while synaptic activity and HFS-LTD were monitored by *ex vivo* electrophysiology.

Animals

Female Wistar rats (Envigo, Netherlands) were group housed (3/cage) and kept on a 12/12-h light/dark cycle at 22°C with 50% humidity with free access to food and water. All experiments were approved by the Gothenburg Animal Research Ethics Committee and conducted during the light time cycle. Estrous cycle was

estimated by visual assessment of vaginal smear at the time point for neurophysiological assessments.

Electrophysiological recordings

Brain slice preparation

Electrophysiological recordings were conducted in brain slices from naïve rats (10–14 weeks old, Figure 1) and animals receiving sub-chronic treatment (15 injections over 3 weeks) of either nicotine or saline (approximately 4 months old). In brief, animals were anesthetized with isoflurane and the brain was quickly removed and submerged in ice-cold modified aCSF containing (in mM): 220 sucrose, 2 KCl, 6 $MgCl_2$, 26 $NaHCO_3$, 1.3 NaH_2PO_4, 0.2 $CaCl_2$, and 10 D-glucose, continuously bubbled with a gas mixture of 95% O_2/5% CO_2. Brains were sectioned coronally at 250 µm using a VT 1200S Vibratome (Leica Microsystems, Bromma, Sweden). The slices were transferred to a custom-made incubation chamber with conventional aCSF containing (in mM): 124 NaCl, 4.5 KCl, 2 $CaCl_2$, 1 $MgCl_2$, 26 $NaHCO_3$, 1.2 NaH_2PO_4, and 10 D-glucose, with osmolarity adjusted to 315–320 mOsm with sucrose, and continuously bubbled with 95% O_2/5% CO_2. Slices were incubated in aCSF for 30 min at 30°C and at room temperature for the remainder of the day.

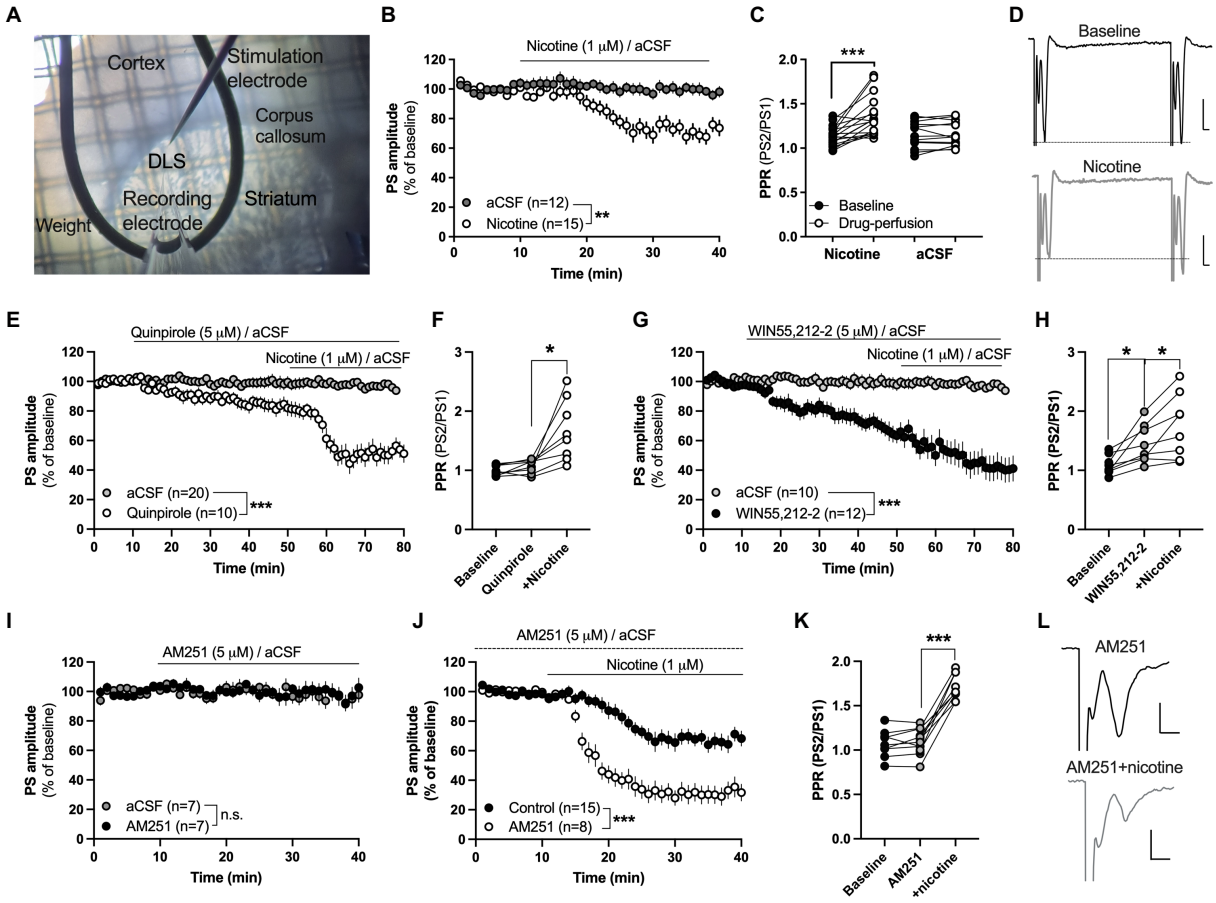

FIGURE 1
Acute nicotine exposure depresses evoked potentials and promotes HFS-LTD in the female rat striatum. **(A)** Micrograph showing the position of recording and stimulation electrode in the DLS. Recording and stimulating electrodes were positioned close to the corpus callosum in the lateral part of the dorsal striatum. Note the visual texture of the striatum and the dark shade of the corpus callosum which clearly marks the transition to the cortex. **(B)** Evoked field potentials were significantly depressed by bath perfusion of nicotine (1µM). **(C)** Nicotine perfusion significantly increased PPR. **(D)** Example traces showing field potentials evoked with a paired pulse stimulation protocol delivered with a 50ms interpulse interval at baseline (upper trace) and after 25min nicotine perfusion (lower trace). Note that the first pulse decreases to a greater extent in response to nicotine perfusion, thereby resulting in increased PPR. Calibration: 0.2mV, 2ms. **(E,F)** The dopamine D2 receptor agonist quinpirole (5µM) slightly depressed PS amplitude but did not occlude nicotine-induced synaptic depression or the increase in PPR. **(G,H)** Bath perfusion of the CB1R agonist WIN55,212-2 (3µM) significantly depressed PS amplitude and increased PPR, and nicotine co-perfusion further potentiated synaptic depression. **(I)** The CB1R antagonist AM251 (3µM) did not modulate PS amplitude by itself. **(J)** Synaptic depression induced by acute nicotine perfusion was significantly enhanced in AM251-pretreated slices. **(K)** PPR was not modulated by AM251, but robustly enhanced when nicotine was co-administered. **(L)** Example traces showing evoked PS amplitude at AM251-treated baseline (upper trace) and following nicotine co-perfusion (lower trace). Not that the pre pulse is not affected during nicotine co-perfusion demonstrating that nicotine affects synaptic transmission. Data are mean values±SEM. *n*=number of slices, taken from at least three animals. *p<0.05, ***p<0.001.

Field potential recordings

Field potential recordings were performed as previously described (Adermark et al., 2011a). In brief, one hemisphere of the slice was perfused with prewarmed aCSF (30°C) and field population spikes (PSs) were evoked with a stimulation electrode positioned dorsal in close vicinity (0.2–0.3 mm) to the recording electrode (World Precision Instruments, FL, United States; Figure 2A). Striatal field potential recordings primarily reflect AMPA-receptor activation (Lagstrom et al., 2019), and the experiments were performed in order to outline the effects displayed by acute and repeated nicotine exposure on striatal neurotransmission and stimulation-induced plasticity. Changes in release probability was measured by employing a paired pulse stimulation protocol with a 50 ms interpulse interval. Paired pulse stimulation was evoked at 0.1 Hz, and paired pulse ratio (PPR) was calculated by dividing the second PS amplitude with the first evoked response.

In the first set of experiments the acute effect displayed by nicotine on striatal neurotransmission was determined. Response amplitudes were set to approximately 60% of the maximal response, and a stable baseline was recorded for at least 10 min before drugs were administered through bath perfusion. Nicotine was perfused at a concentration of 1 μM, which has previously been shown to depress the frequency of glutamatergic inputs onto striatal MSNs in brain slices from male rats (Licheri et al., 2018). To determine putative signaling pathways activated by nicotine, slices were pre-treated with the dopamine D2 receptor agonist quinpirole (dissolved in H_2O to 50 mM and used at 5 μM), the CB1R agonist WIN55,212-2 (dissolved in DMSO to 20 mM and used at 3 μM) or the CB1R antagonist AM251 (dissolved in DMSO to 20 mM and used at 3 μM).

In the next set of recordings, the ability for nicotine to facilitate synaptic plasticity in the form of long-term depression (LTD) was assessed by administering four trains of 100 pulses delivered at 100 Hz (HFS). This protocol has previously been shown to elicit robust eCB-mediated LTD in brain slices from male rats (HFS-LTD; Adermark and Lovinger, 2009). To further determine if CB1R signaling may underly HFS-LTD also in brain slices from female rats, slices were pre-treated with the CB1R antagonist AM251 (3 μM) prior to HFS.

In the last set of experiments, sustained effects elicited by repeated nicotine exposure on neurotransmission and stimulation-induced plasticity were determined. To this end, stimulation/response curves were evoked with increasing stimulation intensity (12–48 μA) in slices from rats receiving either sub-chronic nicotine exposure or vehicle injections. Changes in the responsiveness to acute nicotine perfusion and HFS-LTD were also assessed. eCB-LTD in male rats requires dopamine D2 signaling (Kreitzer and Malenka, 2005), and nicotine has been suggested to facilitate eCB-LTD by stimulating dopamine D2 receptor activation (Adermark et al., 2019). In a subset of recordings brain slices were thus perfused with the dopamine D2 receptor agonist quinpirole (5 μM) prior to HFS-stimulation. Signals were amplified with a custom-made amplifier, filtered at 3 kHz, and digitized at 8 kHz.

Nicotine-treatment and behavioral sensitization

Rats (10–12 weeks old) were randomly assigned to receive either nicotine (0.36 mg/kg, free base, pH normalized with $NaHCO_3$) or saline (0.9% NaCl) over a period of 3 weeks. Subcutaneous injections of nicotine or saline were given in a discontinuous manner over 3 weeks (15 injections in total). This treatment protocol has previously been shown to induce a long-lasting behavioral sensitization to nicotine that sustains for at least 7 months in male rats (Morud et al., 2016).

A behavioral sensitization toward the locomotor stimulatory properties of psychostimulants with repeated drug-exposure is well established in animal models and is believed to be associated with aberrant dopamine signaling (Jackson and Moghaddam, 2001; Phillips et al., 2003; Rouillon et al., 2008; Jones et al., 2010). As a proxy to establish that repeated nicotine exposure had elicit behavioral and neurophysiological transformations locomotor behavior was monitored in a subset of rats (nine vehicle, 10 nicotine) during the first and last (15th) injection to either vehicle or nicotine. Vertical and horizontal movements were registered in an open-field arena (Med Assoc., Fairfax, VT, United States) placed in a sound attenuated, ventilated, and dim lit box (Adermark et al., 2015). The open-field arena was equipped with a two-layer grid, consisting of rows of photocell beams, and consecutive beam breaks were tracked by a computer-based system (Activity Monitor 7, Med Assoc., St. Albans, VT, United States). Rats were allowed to habituate to the box for 30 min and were then injected with nicotine (0.36 mg/kg, s.c.) or vehicle (0.9% NaCl), after which locomotor behavior was registered for another 30 min. Data was registered to determine if the locomotor stimulatory property of nicotine would increase with repeated nicotine administration, and if repeated nicotine exposure would lead to changes in locomotion also during the drug-free habituation period.

Microdialysis

Surgery for *in vivo* microdialysis was performed 3 days after the last nicotine injection and the experiments were performed after a total of 5 days abstinence. Microdialysis probe placement was performed as previously described (Adermark et al., 2022). In brief, a custom-made I-shaped dialysis probe was lowered into the DLS [A/P: +1.2, M/L: −3.5 relative to bregma, D/V: −5.5 relative to dura mater (Paxinos and Watson, 2007)] and fixed to the scull, together with the anchoring screws, using Harvard cement (DAB Dental AB, Gothenburg, Sweden). Rats were allowed to recover for 48 h before initiation of the *in vivo* microdialysis experiment.

Microdialysis experiments were performed in awake and freely moving animals [$n = 19$, weight 230–250 g (approximately 4 months old)]. In brief, the dialysis probe was perfused with Ringer's solution at a rate of 2 μl/min and dialysate samples were collected every 20 min. When four stable dopamine baseline

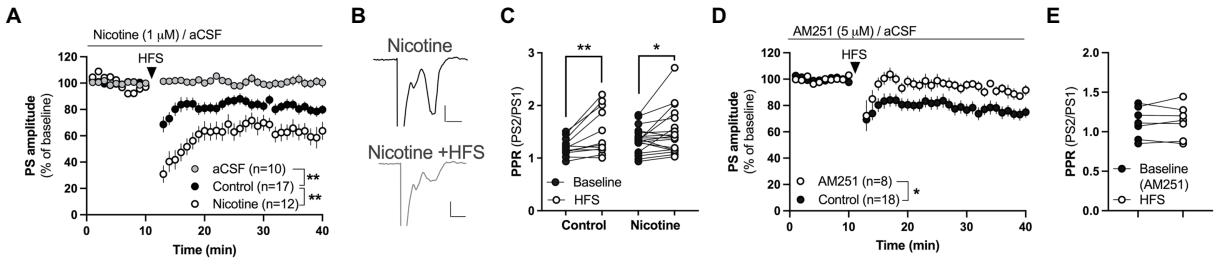

FIGURE 2
Nicotine facilitates endocannabinoid-mediated LTD in the DLS. **(A)** HFS produced LTD in both aCSF-treated control slices and in nicotine pre-treated slices, but synaptic depression was significantly enhanced by nicotine. **(B)** Example traces showing evoked potentials at nicotine-treated baseline (upper trace) and 25min after HFS (lower trace). Calibration: 0.2mV, 2ms. **(C)** HFS increased PPR in both aCSF-treated control slices and slices treated with nicotine, indicating that HFS decreases the probability of transmitter release. **(D,E)** HFS did not induce LTD in brain slices-pre-treated with AM251. Data are mean values±SEM. *n*=number of slices, taken from at least three animals. *p<0.05, **p<0.01.

samples (less than ±10% fluctuation) had been retrieved, nicotine (0.36 mg/kg) was administered subcutaneously. The dialysate samples were analyzed online using high performance liquid chromatography (HPLC) with electrochemical detection as described previously (Ulenius et al., 2020). After the experiment, brains were removed, fixed in formaline-free fixative (Accustain, Sigma-Aldrich, Stockholm, Sweden) and stored (+4°C) for 4–7 days until verification of probe placement. One rat was excluded for incorrect probe placement.

Statistical analysis

Electrophysiological data were extracted using Clampfit 10.2 and Microsoft excel. All data were assembled and analyzed using GraphPad Prism 9 (GraphPad Software, San Diego, CA, United States). Two-way analysis of variance (ANOVA) was used for comparisons over time, and input/output function, while paired or unpaired t tests were used when applicable. All parameters are given as mean ± standard error of the mean (SEM), and the level of significance was set to $p < 0.05$.

Results

Acute nicotine perfusion depresses evoked field potentials in the female rat striatum

In the first set of experiments, the effect displayed by acute nicotine exposure on striatal neurotransmission was assessed by electrophysiological field potential recordings in brain slices from nicotine-naïve rats. Bath perfusion of nicotine (1 μM) depressed evoked field potentials and increased PPR indicating that nicotine reduces the probability of transmitter release (PS amplitude: Repeated measures ANOVA: main effect treatment$_{(\text{nicotine acute})}$: $F_{(1,25)} = 13.68$, $p = 0.0011$; time: $F_{(27,625)} = 15.88$, $p < 0.001$; time × treatment: $F_{(27,625)} = 7.716$, $p < 0.001$; PPR$_{(\text{nicotine acute})}$: Student's t test: $t_{(16)} = 4.408$, $p < 0.001$; Figures 1B,C). aCSF perfusion alone did not affect PPR ($t_{(12)} = 0.7358$, $p = 0.4760$; Figure 1C).

Nicotine increases dopaminergic neurotransmission and the dopamine D2 receptor agonist quinpirole has been shown to occlude nicotine-induced synaptic depression in brain slices from male rats (Licheri et al., 2018). Quinpirole (5 μM) depressed PS amplitude compared to aCSF-treated control (main effect treatment$_{(\text{quinpirole acute})}$: $F_{(1,28)} = 8.537$, $p = 0.0068$; time: $F_{(35,980)} = 3.060$, $p < 0.001$; time × treatment: $F_{(35,980)} = 1.938$, $p = 0.0010$; Figure 1E), with a trend toward increased PPR following 40 min quinpirole perfusion ($t_{(7)} = 2.147$, $p = 0.0689$; Figure 1F). Pre-treatment with quinpirole, however, did not prevent nicotine-induced depression (main effect treatment$_{(\text{nicotine acute})}$: $F_{(1,16)} = 27.18$, $p < 0.001$; time: $F_{(25,400)} = 6.619$ $p < 0.001$; time × treatment: $F_{(25,400)} = 5.796$, $p < 0.001$) or the nicotine-induced increase in PPR (stats; PPR: $t_{(7)} = 3.473$, $p = 0.0104$; Figures 1E,F).

Nicotine has also been postulated to stimulate eCB signaling and might thus depress PS amplitude *via* activation of presynaptic CB1Rs. Perfusion of the CB1R agonist WIN55,212-2 (3 μM) depressed PS amplitude (main effect treatment$_{(\text{WIN55,212-2 acute})}$: $F_{(1,20)} = 16.37$, $p < 0.001$; time: $F_{(35,700)} = 7.295$, $p < 0.001$; time × treatment: $F_{(35,700)} = 4.992$, $p < 0.0001$) and increased PPR by itself (PPR: $t_{(7)} = 3.473$, $p = 0.0104$; Figures 1G,H). Co-perfusion with nicotine resulted in a continuous depression of PS amplitude (main effect treatment$_{(\text{nicotine acute})}$: $F_{(1,14)} = 24.37$, $p < 0.001$; time: $F_{(25,350)} = 5.513$, $p < 0.001$; time × treatment: $F_{(25,\ 350)} = 4.510$, $p < 0.0001$) and a further increase in PPR ($t_{(7)} = 3.019$, $p = 0.0194$; Figures 1G,H). Since the baseline was steadily decreasing by WIN55,212-2-perfusion alone, another experiment was performed where slices were pre-treated with the CB1R antagonist AM251 (3 μM) prior to nicotine. AM251 did not affect PS amplitude or PPR by itself (AM251 vs. aCSF: treatment: $F_{(1,12)} = 0.1056$, $p = 0.7508$; time: $F_{(25,300)} = 0.7813$, $p = 0.7655$; time × drug: $F_{(25,300)} = 0.6216$, $p = 0.9228$; PPR: $t_{(8)} = 1.083$, $p = 0.3105$; Figures 1I,K). Co-administration with nicotine, however, demonstrated an enhanced synaptic depression by nicotine when compared to control slices (main effect treatment$_{(\text{nicotine acute})}$: $F_{(1,18)} = 28.70$, $p < 0.001$; time: $F_{(25,450)} = 34.88$,

$p < 0.001$; time × drug: $F_{(25,450)} = 2.336$, $p < 0.001$), and a robust increase in PPR ($t_{(8)} = 11.12$, $p < 0.001$; Figures 1J,K).

Nicotine promotes synaptic plasticity in the form of endocannabinoid-mediated LTD

In the next set of experiments the ability for nicotine to promote HFS-LTD was assessed. HFS produced a robust synaptic depression of PS amplitude in control slices that was concomitant with an increase in PPR indicative of a reduced probability of transmitter release [$F_{(1,30)} = 11.16$, $p = 0.0022$; time: $F_{(25,750)} = 8.134$, $p < 0.001$; time × drug: $F_{(25,750)} = 1.067$, $p = 0.3752$; PPR ($t_{(11)} = 3.324$, $p = 0.0068$; Figures 2A,C)]. While HFS-LTD in DLS has been suggested to be mediated by eCB-signaling in male rats (Gerdeman and Lovinger, 2001), CB1R expression has been shown to be lower in the female mouse striatum compared to males (Liu et al., 2020). To determine if HFS-LTD was associated with eCB signaling also in the female rat striatum, slices were bath perfused with the CB1R antagonist AM251 (3 μM). AM251 blocked synaptic depression mediated by HFS (main effect treatment$_{(\text{AM251 vs. control})}$: $F_{(1,24)} = 6.630$, $p = 0.0166$; time: $F_{(25,600)} = 2.482$, $p < 0.001$; time × drug: $F_{(25,600)} = 0.4267$, $p = 0.9940$; Figure 2D), and the increase in PPR ($t_{(6)} = 0.3975$, $p = 0.7048$; Figure 2E). Importantly, pre-treatment for 30 min with bath applied nicotine (1 μM) significantly enhanced HFS-LTD (aCSF vs. nicotine acute: treatment: $F_{(1,31)} = 2.60$, $p = 0.0013$; time: $F_{(27,837)} = 8.134$, $p < 0.001$; time × drug: $F_{(27,837)} = 2.794$, $p < 0.001$; PPR$_{(\text{nicotine acute + HFS})}$: $t_{(18)} = 2.267$, $p = 0.03609$), suggesting that acute nicotine exposure facilitates HFS-LTD also in the DLS of female rats (Figures 2A–C).

Repeated nicotine exposure produces robust behavioral sensitization in female rats

Acute administration depressed evoked potentials in the DLS and facilitated LTD. In a way to outline if repeated nicotine exposure would lead to sustained neuroadaptations, female rats underwent sub-chronic nicotine exposure through experimenter-controlled nicotine injections (0.36 mg/kg, s.c., total of 15 injections) delivered over a period of 3 weeks. As a proxy for behavioral and neurophysiological transformations, nicotine-induced behavioral sensitization was monitored in locomotion boxes. Repeated nicotine exposure produced robust behavioral sensitization demonstrated as increased locomotor activity in response to a nicotine challenge following sub-chronic nicotine treatment (paired *t*-test, 1st vs. 15th injection: horizontal beam breaks: vehicle: $t_{(8)} = 0.9802$, $p = 0.3557$; nicotine: $t_{(9)} = 5.325$, $p < 0.001$; vertical beam breaks: vehicle: $t_{(8)} = 1.177$, $p = 0.2729$; nicotine: $t_{(9)} = 4.223$, $p = 0.0022$; Figures 3B–F). In addition, following drug-administration, an increase in the time spent in center zone was seen selectively in rats receiving repeated nicotine exposures (paired *t*-test, 1st vs. 15th injection vehicle: $t_{(8)} = 1.884$, $p = 0.0962$; nicotine: $t_{(9)} = 3.752$, $p = 0.0045$; Figures 3G,H). Neither time spent in center zone (vehicle 15th vs. nicotine 15th: $t_{(13)} = 0.4298$, $p = 0.6744$) nor baseline locomotion (vehicle 15th vs. nicotine 15th: $t_{(13)} = 0.1657$, $p = 0.8709$) were affected by sub-chronic nicotine administration when monitored during the habituation to the locomotor box (first 30 min, prior to drug-administration), suggesting that locomotor behavior during drug-free conditions were not significantly altered.

Neurophysiological transformations following sub-chronic nicotine exposure

In the next step, neurophysiological assessments were conducted *in vivo* and *ex vivo* in animals previously receiving sub-chronic administration of either saline or nicotine. Estimation of estrus phase did not reveal any significant deviations between treatment groups (Chi square test: $p = 0.7652$; Figure 4A). There was also no effect by repeated nicotine exposure on weight ($t_{(16)} = 0.7734$, $p = 0.4506$; Figure 4B).

In vivo microdialysis performed in the DLS 5 days after the last drug-treatment demonstrated no change in baseline extracellular dopamine levels in the DLS following sub-chronic nicotine exposure ($t_{(28)} = 1.439$, $p = 0.1614$; Figure 4D). The relative responsiveness to acute nicotine administration (0.36 mg/kg), however, was significantly enhanced in animals previously receiving sub-chronic nicotine exposure (sub-chronic nicotine vs. vehicle: treatment: $F_{(1,16)} = 6.431$, $p = 0.0220$; time: $F_{(2,32)} = 36.93$, $p < 0.001$; time × treatment: $F_{(2,32)} = 0.8087$, $p = 0.4543$; Figure 4E), indicative of a sensitized response to nicotine with regards to the relative dopamine release.

Electrophysiological recordings performed on nicotine abstinent rats 2–7 days after the last nicotine exposure demonstrated a sustained synaptic depression of evoked potentials in brain slices from rats receiving sub-chronic nicotine treatment (treatment: $F_{(1,56)} = 4.179$, $p = 0.00456$; time: $F_{(6,336)} = 52.47$, $p < 0.001$; time × drug: $F_{(6,336)} = 0.8307$, $p = 0.5468$; Figures 4F,G), with no concomitant change in PPR ($t_{(49)} = 0.28$, $p = 0.7806$; Figure 4H), indicating that repeated nicotine exposure may lead to sustained postsynaptic transformations that outlasts the presence of the drug. In addition, bath perfused nicotine (1 μM) further depressed PS amplitude to a significantly greater extent in brain slices from animals previously receiving nicotine (sub-chronic nicotine vs. vehicle: treatment: $F_{(1,45)} = 8.898$, $p = 0.0046$; time: $F_{(15,675)} = 0.878$, $p < 0.001$; time × treatment: $F_{(15,675)} = 0.818$, $p = 0.659$; Figure 4I), indicating a sensitized response to nicotine also with respect to glutamatergic neurotransmission. Bath perfused nicotine increased PPR also in slices from rats receiving sub-chronic nicotine exposure (stats $t_{(14)} = 2.501$, $p = 0.0254$; Figure 4J).

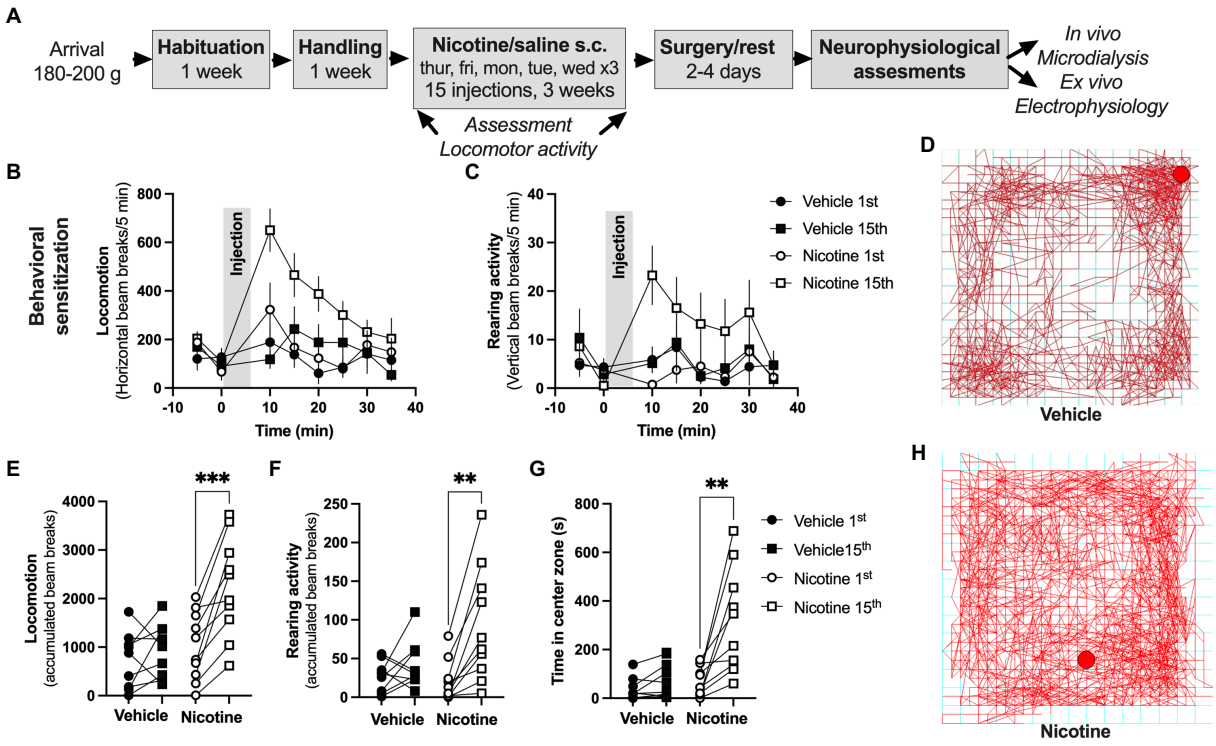

FIGURE 3
Repeated nicotine exposure produces behavioral sensitization in female rats. **(A)** Timeline for the described experiments. **(B,C)** Time-course graphs showing locomotor activity and rearing activity in response to nicotine injection. **(D)** Example picture showing ambulatory movement in a rat receiving vehicle injection. **(E,F)** Accumulated beam breaks elicited by either saline or nicotine exposure during the first and last injection demonstrated a selective increase in locomotion in rats receiving repeated nicotine injections. **(G)** Time spent in center zone was increased in response to repeated nicotine injections. **(H)** Example picture showing ambulatory movement in a rat receiving nicotine injection. Data are mean values±SEM and based on 9–10 rats/treatment-group. *p<0.05, **p<0.01.

Regulation of synaptic plasticity in the form of HFS-LTD is modulated by repeated nicotine exposure in the female rat brain

In the last sets of experiments, the influence displayed by sub-chronic nicotine exposure *in vivo* on the induction and expression of striatal long-term synaptic plasticity was outlined. While eCB levels have been reported to be depressed following repeated nicotine exposure in male rats (Gonzalez et al., 2002), HFS-LTD was not impaired in brain slices from rats receiving sub-chronic nicotine exposure (sub-chronic nicotine vs. vehicle: treatment: $F_{(1,31)} = 0.7419$, $p = 0.3957$; time: $F_{(27,837)} = 19.68$, $p < 0.001$; time × treatment: $F_{(27,837)} = 1.396$, $p = 0.0878$; Figure 5A). However, bath perfused nicotine (1 μM) facilitated HFS-LTD in brain slices from vehicle treated rats (treatment$_{(\text{nicotine acute})}$: $F_{(1,25)} = 4.678$, $p = 0.0403$; time: $F_{(27,675)} = 18.89$, $p < 0.001$; time × treatment: $F_{(27,675)} = 1.480$, $p = 0.0566$; Figure 5B), but not in brain slices from rats receiving sub-chronic nicotine treatment (treatment$_{(\text{nicotine acute})}$: $F_{(1,30)} = 0.1912$, $p = 0.6651$; time: $F_{(27,810)} = 13.74$, $p < 0.001$; time × treatment: $F_{(27,\ 810)} = 2.306$, $p = 0.0002$; Figure 5C).

eCB-LTD in male rats requires dopamine D2 signaling (Kreitzer and Malenka, 2005), and nicotine has been suggested to facilitate eCB-LTD by stimulating dopamine D2 receptor activation (Adermark et al., 2019). Previous studies performed on brain slices from male rats has suggested that nicotine produces changes in dopamine D2 receptor signaling which leads to distorted synaptic plasticity mechanisms (Adermark et al., 2019). In the last set of experiments responsiveness to dopamine D2 receptor activation and effects on HFS-LTD were assessed in brain slices from female rats receiving either sub-chronic treatment with nicotine or vehicle. Administration of the dopamine D2 receptor agonist quinpirole slightly depressed PS amplitude to a similar extent in both treatment groups (vehicle vs. sub-chronic nicotine: treatment: $F_{(1,20)} = 0.7264$, $p = 0.4042$; time: $F_{(15,300)} = 7.064$, $p < 0.001$; time × treatment: $F_{(15,300)} = 2.348$, $p = 0.0034$; data not shown). Pre-treatment with quinpirole selectively enhanced HFS-LTD in brain slices from vehicle-treated rats (vehicle aCSF vs. vehicle quinpirole: treatment: $F_{(1,21)} = 4.343$, $p = 0.04961$; time: $F_{(27,567)} = 8.182$, $p < 0.001$; time × treatment: $F_{(27,567)} = 4.297$, $p < 0.001$), and HFS-LTD in quinpirole-treated brain slices was significantly reduced in slices from rats receiving sub-chronic nicotine-treatment compared to slices from vehicle-treated

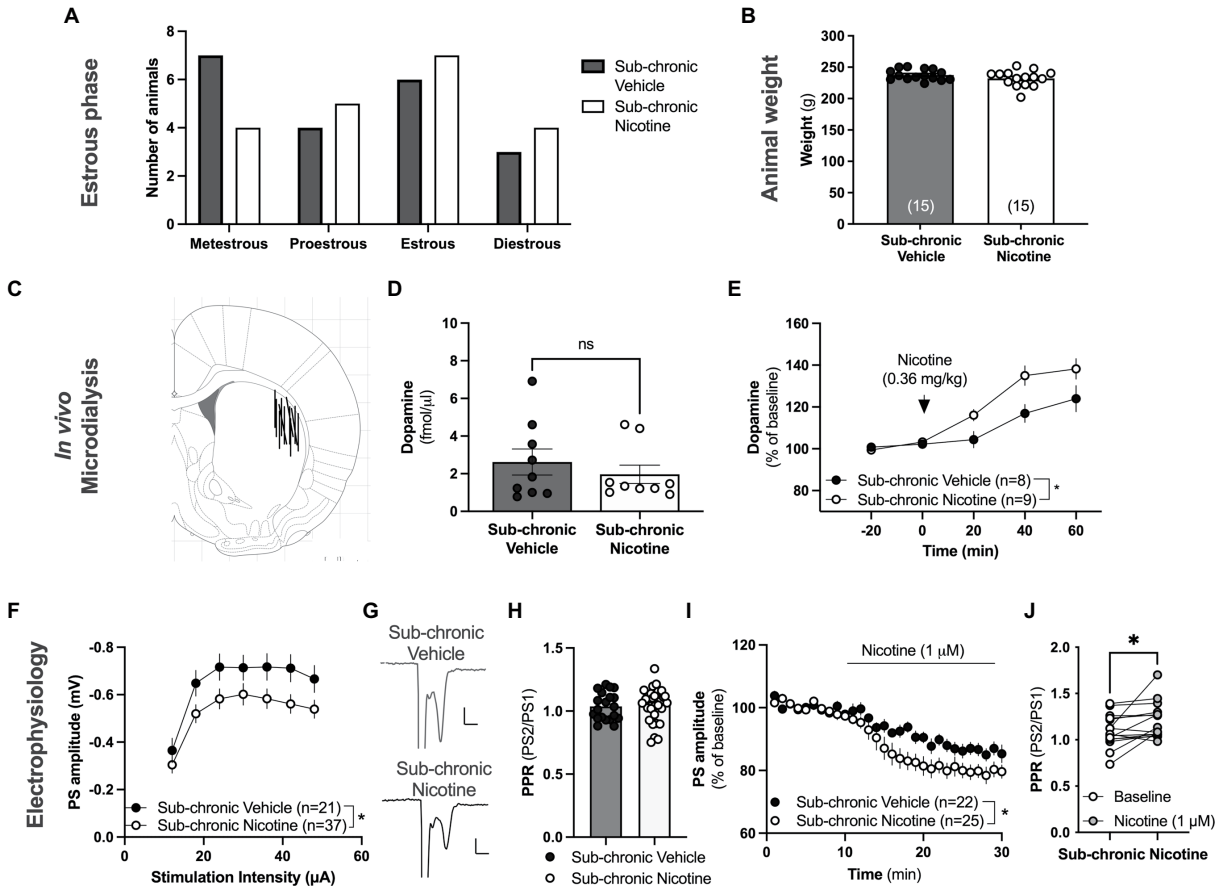

FIGURE 4
Neurophysiological transformations following sub-chronic nicotine exposure. **(A)** Estimated estrus phase based on vaginal smears for animals used during neurophysiological assessments. **(B)** Animal weight did not differ between treatment groups at the time point for neurophysiological assessments. **(C)** Schematic drawing showing the position of the active space of the microdialysis probe. **(D)** The microdialysate level of dopamine was not significantly altered by sub-chronic nicotine exposure. **(E)** Acute administration of nicotine, as indicated by the arrow, increased striatal dopamine to a significantly greater extent in animals receiving sub-chronic nicotine exposure. **(F)** *Ex vivo* electrophysiological recordings demonstrated that the amplitude of evoked potentials was significantly depressed in the DLS of animals previously receiving nicotine. **(G)** Example traces showing evoked PSs in a brain slice from a vehicle-treated rat (upper trace) and a rat receiving sub-chronic nicotine exposure (lower trace). **(H)** PPR was not significantly modulated by sub-chronic nicotine exposure. **(I)** Bath perfused nicotine depressed evoked potentials to a significantly greater extent in brain slices from rats receiving sub-chronic nicotine exposure. **(J)** Synaptic depression induced by acute nicotine exposure was accompanied by an increase in PPR, indicating that nicotine reduces the probability of transmitter release. Data are mean values±SEM. *n*=number of animals in **(B,E)**, and number of slices in **(F,I)**. Slices were taken from at least five animals/treatment. *$p<0.05$, **$p<0.01$.

control (vehicle vs. sub-chronic nicotine: treatment: $F_{(1,17)}=11.87$, $p=0.0031$; time: $F_{(27,459)}=7.035$, $p<0.001$; time × treatment: $F_{(27,459)}=1.758$, $p=0.0116$; Figure 5D).

Discussion

The data presented here shows that nicotine acutely depresses neurotransmission in a manner that is not driven by CB1R activation or dopamine D2 receptor activation, indicating that dopamine may regulate these acute effects in a partially sex-dependent manner (Licheri et al., 2018). In addition, HFS produced eCB mediated long-standing synaptic plasticity in the DLS of female rats, and nicotine pre-exposure significantly enhanced this form of LTD. This finding is in agreement with previous data retrieved from male rats (Adermark et al., 2019). We also show that repeated exposure to nicotine produces a sustained depression of evoked potentials in the DLS and give rise to a sensitized response to nicotine with regards to both locomotor behavior, as well as dopaminergic and glutamatergic signaling in the DLS. At the same time, our data show that the plasticity facilitating property of nicotine vanishes following repeated nicotine exposure. We also demonstrate that dopamine D2 receptor activation is insufficient to facilitate HFS-LTD in slices from rats previously receiving nicotine. These findings suggest that repeated nicotine exposure produces neuroplastic transformations in the DLS and impaired regulation of

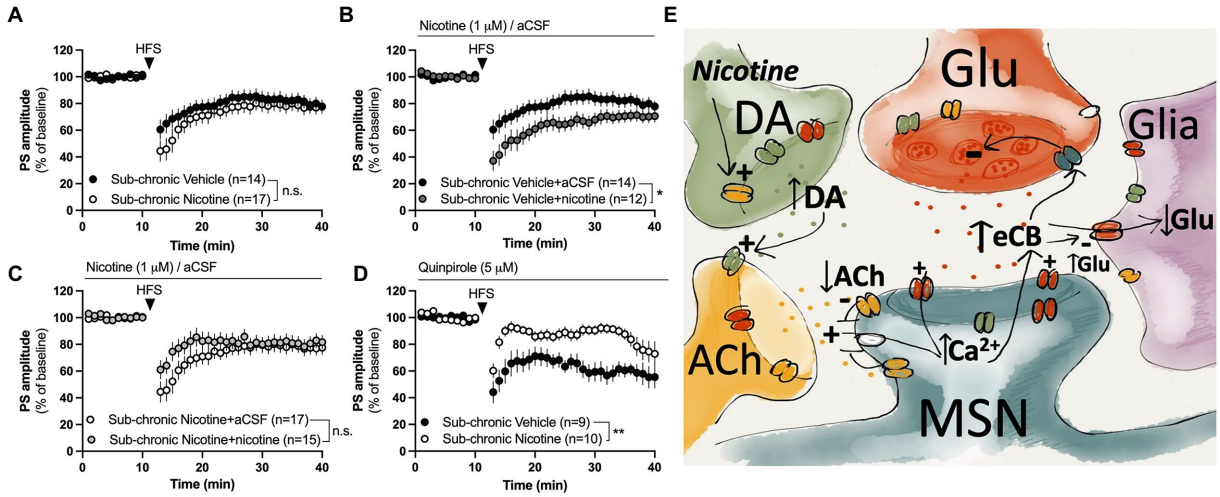

FIGURE 5
Nicotine or dopamine D2 receptor activation does not facilitate LTD in slices from female rats receiving sub-chronic nicotine treatment. **(A)** HFS-LTD was not significantly modulated during acute withdrawal (2–7days) after the last nicotine exposure. **(B,C)** Bath perfusion of nicotine facilitated HFS-LTD in slices from vehicle-treated rats but not from nicotine-treated rats. **(D)** The dopamine D2 receptor agonist quinpirole selectively facilitated HFS-LTD in slices from vehicle-treated rats. **(E)** Simplified schematic drawing depicting putative signaling pathways that nicotine may recruit to modulate neurotransmission and HFS-LTD in the DLS. Acute administration of nicotine may weakly stimulate eCB production and release by activating nAChRs located on dopaminergic terminals, thereby increasing the inhibitory tone by dopamine on cholinergic neurons. Reduced cholinergic tone relieves the inhibition of L-type calcium channels (Wang et al., 2006), thereby facilitating calcium influx and eCB production in MSNs. When nicotine is combined with HFS, eCB signaling is potentiated compared to HFS alone, thereby leading to a more robust depression of PS amplitude. Following sub-chronic nicotine exposure, however, the regulatory role of dopamine D2 receptors appears to be altered. Endocannabinoids may also reduce glutamate uptake (Brown et al., 2003), thereby increasing extrasynaptic glutamate levels and further promoting eCB signaling and synaptic depression. Data are mean values±SEM. *n*=number of slices, taken from at least three animals. **p*<0.05, ***p*<0.01.

stimulation-induced long-term depression, which in the extension may reduce behavioral flexibility and contribute to the development of persistent habits.

Acute administration of nicotine depressed PS amplitude in a manner that was concomitant with a decrease in the probability of transmitter release. This finding is in agreement with previous studies performed on male rats, showing that nicotine acutely depresses the frequency but not amplitude of spontaneous excitatory post synaptic currents in medium spiny neurons in the DLS (Licheri et al., 2018). The exact mechanisms underlying nicotine-induced neuroplasticity in the striatum is not fully understood, but dopamine D2 receptor signaling appears to mediate the down-stream effects of nAChR activation (Licheri et al., 2018; Grieder et al., 2022). Dopamine D2 receptors are also critical for induction of nicotine-induced conditioned place preference (CPP) in mice (Wilar et al., 2019), and the improving effect of nicotine on stress-induced memory impairment (Keshavarzian et al., 2018). Increased levels of dopamine D2 receptor mRNA and receptor binding has also been reported following repeated nicotine administration in experimental studies (Metaxas et al., 2010; Adermark et al., 2016), while a decrease in DAT availability is associated with tobacco addiction in humans (Leroy et al., 2012). Changes in dopaminergic neurotransmission may thus be involved in mediating both acute and protracted neuroplasticity elicited by nicotine. However, while data from male rats has shown that nicotine-induced synaptic depression is occluded by dopamine D2 receptor activation and blocked by dopamine D2 receptor antagonist (Licheri et al., 2018), this was not supported by the data presented here. While the net effect by nicotine on striatal neurotransmission appears to be the same, the mechanisms underlying synaptic depression may thus be partially sex-dependent. Interestingly, while HFS-LTD was enhanced by nicotine, synaptic depression elicited by nicotine alone was potentiated by CB1R antagonist. Since low levels of eCBs has been proposed to act primarily on GABAergic terminals (Uchigashima et al., 2007; Adermark and Lovinger, 2009), it is possible that nicotine stimulates eCB release but that the amount released is insufficient to affect glutamatergic synapses. When combined with HFS, however, eCB-levels are high enough to act on both excitatory and inhibitory terminals (Adermark and Lovinger, 2009). Importantly, the data presented here shows that nicotine-induced synaptic depression engage several signaling pathways and more research is required to fully understand the mechanisms involved.

HFS induced a long-term depression of PS amplitude with a concomitant increase in PPR indicating that synaptic depression is expressed presynaptically. While eCB-signaling has been shown to be important for HFS-LTD in the DLS of male rats (Gerdeman and Lovinger, 2001; Kreitzer and Malenka, 2005; Adermark and Lovinger, 2009), CB1R expression has been shown to be lower in the female mouse striatum compared to males (Liu et al., 2020), and other signaling pathways may thus be recruited. However, HFS-LTD was blocked in slices pre-treated with the CB1R antagonist

AM251, showing that eCB-signaling is important for LTD also in the DLS of female rats. Endocannabinoids are produced on demand and the indiction of eCB signaling involves a complex interplay of dopaminergic, glutamatergic and cholinergic receptors (Kreitzer and Malenka, 2005; Wang et al., 2006; Adermark, 2011; Liput et al., 2022). Direct activation of L-type calcium channels produces eCB signaling that is independent on dopamine D2 receptors or mGluR group 1 receptors, suggesting that these signaling pathways are required for facilitating a postsynaptic calcium increase to enable eCB production and release (Adermark and Lovinger, 2007; outlined in schematic drawing, Figure 5E). Quinpirole has previously been shown to robustly increase striatal release of the eCB anandamide in a dopamine D2 dependent manner (Giuffrida et al., 1999). Nicotine could thus facilitate eCB signaling by increasing dopamine D2 receptor signaling, thereby inhibiting cholinergic neurons, and reliving the muscarinic break on post synaptic calcium channels to promote eCB signaling (Wang et al., 2006; Adermark and Lovinger, 2007; Figure 5E). Furthermore, eCB may further suppress activity at striatal synapses by decreasing glutamate transporter activity, resulting in elevated extrasynaptic glutamate concentrations and an indirect suppression of presynaptic glutamate release (Brown et al., 2003; Adermark et al., 2022). While it remains to be determined, the data presented here suggest that nicotine increases eCB signaling, but that HFS is warranted to reach the threshold required for synaptic depression at excitatory terminals (Uchigashima et al., 2007; Adermark and Lovinger, 2009).

Importantly, while drugs of abuse produce synaptic plasticity mechanisms in the acute phase, repeated exposure has been shown to impair eCB signaling (Blanco et al., 2016; Wang et al., 2020). This holds true not only for nicotine (Baca et al., 2013; Xia et al., 2017; Adermark et al., 2019), but also for alcohol and cocaine (Adermark et al., 2011b; Wang et al., 2020). Especially, repeated nicotine exposure appears to impair dopamine D2R-dependent induction of LTD, rather than CB1R signaling *per se* (Baca et al., 2013; Adermark et al., 2019). In fact, HFS-LTD in male rats have been shown to be restored by quinpirole alone (Adermark et al., 2019), or by quinpirole in combination with the NMDA receptor antagonist APV (Xia et al., 2017). While the data presented here shows that pre-treatment with quinpirole enhance HFS-LTD in slices from vehicle-treated rats, it did not facilitate HFS-LTD in slices from rats receiving sub-chronic nicotine exposure. Interestingly, elevated levels of acetylcholine, which has been reported during nicotine abstinence (Rada et al., 2001), may transform dopamine D2 receptor signaling (Scarduzio et al., 2017). If this is a factor underlying the shifted response to quinpirole remains to be determined.

Repeated exposure to nicotine produced a robust behavioral sensitization, which is in agreement with previous studies (Benwell and Balfour, 1992; Ericson et al., 2010; Hamilton et al., 2014; Morud et al., 2016; Honeycutt et al., 2020). Behavioral sensitization to repeated psychostimulant administration has been proposed to reflect many of the neurochemical changes that are characteristic for drug addiction (Robinson and Berridge, 1993; Steketee and Kalivas, 2011), and is in this regard a well-established model to outline behavioral transformations elicited by drugs of abuse. Behavioral sensitization elicited by psychostimulants has been proposed to be driven by an interplay between dopaminergic and glutamatergic neuroadaptations (Robinson and Becker, 1982; Vezina, 1996; Kim and Vezina, 2002; Bamford et al., 2008; Yoon et al., 2008; Jing et al., 2018; Kim et al., 2022), and neuroplasticity in the dorsal striatum appears to be especially important for establishing these behavioral transformations (Durieux et al., 2012; Kim et al., 2022; Lotfi et al., 2022). The neurophysiological data presented here demonstrated a sensitized response to nicotine with respect to both dopaminergic-and glutamatergic signaling, thereby supporting a role for striatal neuroplasticity in behavioral sensitization. Part of these findings may be linked to increased number of nAChRs, which has been observed in the brains of experimental animals during nicotine treatment and in the brains of human smokers at autopsy (Benwell et al., 1988; Collins et al., 1994; Breese et al., 1997; Alasmari et al., 2021). However, the establishment of behavioral sensitization may also be linked to other forms of striatal neuroplasticity. In fact, inhibition of CB1R has been shown to enhance the motor stimulatory property of the dopamine D2 agonist quinpirole (Giuffrida et al., 1999). This finding suggests that the eCB system may act as an inhibitory feedback mechanism counteracting dopamine-induced facilitation of locomotion. This is especially interesting considering the finding that synaptic depression induced by acute nicotine exposure was potentiated in slices pre-treated with CB1R antagonist. In addition, the data presented here showed reduced HFS-LTD in response to dopamine D2 receptor activation in slices from rats receiving sub-chronic nicotine exposure. It is thus possible that impaired eCB signaling contributes the potentiation of behavioral and neurophysiological response to acute nicotine in rats receiving sub-chronic nicotine exposure.

While nicotine preferentially increases dopamine in the ventral as compared to dorsal striatum in animal studies (Imperato et al., 1986; Shim et al., 2001; Danielsson et al., 2021b), raclopride binding in dorsal striatum of humans have been shown to correlate with subjective measures of the rewarding properties of nicotine (Montgomery et al., 2007). Furthermore, when characterizing the effects of smoking on the mesolimbic dopamine system in humans, dopamine elevations in ventral striatum were consistent with studies performed in men, whereas dopamine responses in women were associated with subregions of dorsal striatum (Cosgrove et al., 2014). Nicotine may thus display sex-specific effects on striatal dopamine transmission. The data presented here show that nicotine elevates the microdialysate concentration of dopamine in the DLS, and that repeated exposure

produces a sensitized response to the dopamine-elevating property of nicotine. The sensitized dopamine response may contribute to behavioral transformations and enhanced neuroplasticity in response to nicotine. While sensitized responses to nicotine-induced dopamine elevations have primarily been studied in the nucleus accumbens (Balfour et al., 1998; Vezina et al., 2007), our finding is in agreement with a previous study showing an increased dopamine elevation in dorsal striatum following local administration of nicotine (5 mM) in nicotine exposed rats (Shim et al., 2001). However, more research outlining dopaminergic neurotransmission in dorsal striatal subregions in females is warranted to outline putative sex-specific effects.

Abstinence to nicotine is associated with reduced dopamine levels (Rada et al., 2001; Rahman et al., 2004; Domino and Tsukada, 2009; Rademacher et al., 2016), and withdrawal-induced by the nAChR antagonist mecamylamine has been shown to produce a more pronounced decrease in dopamine levels in the nucleus accumbens of female compared to male rats (Carcoba et al., 2018). However, *in vivo* microdialysis performed in the DLS revealed no significant decrease in baseline dopamine levels at the time-point assessed here (5 days after the last nicotine injection). This finding may be associated with the fact that drug-induced changes in baseline dopamine levels are more pronounced in the nucleus accumbens compared to the dorsal striatum (Balfour et al., 1998; Danielsson et al., 2021a). In addition, findings may also be highly dependent on the time-point when dopamine levels were assessed (Hirth et al., 2016).

Repeated administration of nicotine resulted in a sustained suppression of evoked potentials in the DLS of female rats. This is partially in agreement with studies performed in male rats, although the neuroadaptations described here arise at an earlier time-point (Adermark et al., 2016). While increased eCB signaling in response to nicotine exposure might contribute to the sustained synaptic depression, decreased PS amplitude in nicotine abstinent rats was not associated with a change in PPR indicating that postsynaptic transformations may underly the sustained synaptic depression. While it remains to be determined what changes that underly the decrease in PS amplitude, impaired glutamate uptake may be one contributing factor. Both nicotine and eCB signaling impair glutamate uptake (Brown et al., 2003; Lim and Kim, 2003a,b; Alasmari et al., 2021), and elevated glutamate levels are reported following repeated nicotine exposure (Carcoba et al., 2018). Reduced glutamate clearance may thus contribute to both acute and sustained neuroplasticity elicited by nicotine (Adermark et al., 2022), possibly through remodeling of synaptic networks and post-translational modifications of glutamate receptors and their interacting proteins (Zheng et al., 2008; outlined in schematic drawing, Figure 5E).

Sex hormones may have the potential to modulate neurohormonal responses to nicotine and influence the psychoactive and reinforcing properties of the drug (Bertrand et al., 1991). Estradiol treatment decreased striatal dopamine D2 receptor binding, and variations in dopamine levels and binding are seen in different phases of the estrous cycle in rats (Bazzett and Becker, 1994; Al Sweidi et al., 2013). Still, there appears to be no estrous cycle dependent changes or sex differences when monitoring nicotine self-administration and reinstatement of nicotine-seeking (Feltenstein et al., 2012; Leyrer-Jackson et al., 2021). *In vivo* spontaneous activity of dopamine neurons, as well as *ex vivo* intrinsic and synaptic properties, have also been reported to be similar in male and female rats (Melis et al., 2013), even though there appears to be a sex difference with regards to tonic 2-AG signaling on to dopaminergic neurons (Melis et al., 2013).

There are several limitations with this study. Especially, electrophysiological recordings are conducted *ex vivo* and the reciprocal connection with other brain regions is thus lost. Field potential recordings also represent the collective activity of hundreds of neurons evoked by electrical stimulation, and differences in direct–indirect pathway neurons can thus not be assessed. Still, eCB-induced LTD is reported in glutamatergic synapses targeting both dopamine D1 and D2 expressing MSNs (Adermark and Lovinger, 2007). Another limitation is that plasticity in the DLS may be especially important during contingent administration and operant behaviors, but nicotine was administered in a non-volitional manner. While the data presented here demonstrates that nicotine produces acute and long-lasting effects on neurotransmission even without the involvement of instrumental learning, it is thus important to further evaluate nicotine-induced neuroplasticity following operant self-administration.

In conclusion, the data presented here demonstrates that nicotine facilitates eCB-mediated LTD and produces striatal synaptic depression by reducing the probability of transmitter release. These findings are similar to what has previously been reported in male rats suggesting that the acute effects mediated by nicotine on excitatory neurotransmission are independent on sex (Licheri et al., 2018; Adermark et al., 2019). However, a sustained depression of evoked PS amplitudes was observed at an earlier time-point in female rats, suggesting that they might be more susceptible to nicotine-induced neuroplasticity (Adermark et al., 2016). In addition, the acute effect of nicotine on PS amplitude was not occluded by dopamine D2 receptor activation, and D2 stimulation did also not facilitate HFS-LTD following sub-chronic nicotine exposure, which also disagrees with findings from male rats (Adermark et al., 2019). Considering the plastic interplay between dopamine and acetylcholine in eCB signaling and glutamate-induced synaptic depression (Calabresi et al., 1999; Wang et al., 2006; Adermark, 2011), these findings might be explained by the proposed sex specificity observed with regards to dopaminergic neurotransmission and dopaminergic regulation of reward-related behavior (Melis et al., 2013; Hynes et al., 2020, 2021). But more studies are required to fully establish sex-specific neuroplasticity associated with repeated nicotine exposure.

Data availability statement

The raw data supporting the conclusions of this article will be made available by the authors, without undue reservation.

Ethics statement

The animal study was reviewed and approved by Göteborgs djurförsöksetiska nämnd, Gothenburg Sweden.

Author contributions

LA designed the study, conducted electrophysiological recordings, assembled figures, and drafted the manuscript. EL handled the animals, conducted behavioral experiments, and assisted during electrophysiological recordings. BS and ME assisted in data interpretation. All authors contributed to the article and approved the submitted version.

Funding

This work was supported by the Swedish research council (vetenskapsrådet: Dnr: 2018-02814, 2020-00559, 2020-01346, 2020-02105), and governmental support under the ALF agreement (ALFGBG-966287).

Acknowledgments

We greatly appreciate the assistance provided by Davide Cadeddu, Rosita Stomberg, Jonas Smith, Marcus Burman, Tobias Eriksson, and Edvin Vestin.

Conflict of interest

The authors declare that the research was conducted in the absence of any commercial or financial relationships that could be construed as a potential conflict of interest.

Publisher's note

All claims expressed in this article are solely those of the authors and do not necessarily represent those of their affiliated organizations, or those of the publisher, the editors and the reviewers. Any product that may be evaluated in this article, or claim that may be made by its manufacturer, is not guaranteed or endorsed by the publisher.

References

Adermark, L. (2011). Modulation of endocannabinoid-mediated long-lasting disinhibition of striatal output by cholinergic interneurons. *Neuropharmacology* 61, 1314–1320. doi: 10.1016/j.neuropharm.2011.07.039

Adermark, L., Clarke, R. B., Soderpalm, B., and Ericson, M. (2011a). Ethanol-induced modulation of synaptic output from the dorsolateral striatum in rat is regulated by cholinergic interneurons. *Neurochem. Int.* 58, 693–699. doi: 10.1016/j.neuint.2011.02.009

Adermark, L., Jonsson, S., Ericson, M., and Soderpalm, B. (2011b). Intermittent ethanol consumption depresses endocannabinoid-signaling in the dorsolateral striatum of rat. *Neuropharmacology* 61, 1160–1165. doi: 10.1016/j.neuropharm.2011.01.014

Adermark, L., Lagstrom, O., Loften, A., Licheri, V., Havenang, A., Loi, E. A., et al. (2022). Astrocytes modulate extracellular neurotransmitter levels and excitatory neurotransmission in dorsolateral striatum via dopamine D2 receptor signaling. *Neuropsychopharmacology* 47, 1493–1502. doi: 10.1038/s41386-021-01232-x

Adermark, L., and Lovinger, D. M. (2007). Combined activation of L-type Ca2+ channels and synaptic transmission is sufficient to induce striatal long-term depression. *J. Neurosci.* 27, 6781–6787. doi: 10.1523/JNEUROSCI.0280-07.2007

Adermark, L., and Lovinger, D. M. (2009). Frequency-dependent inversion of net striatal output by endocannabinoid-dependent plasticity at different synaptic inputs. *J. Neurosci.* 29, 1375–1380. doi: 10.1523/JNEUROSCI.3842-08.2009

Adermark, L., Morud, J., Lotfi, A., Danielsson, K., Ulenius, L., Soderpalm, B., et al. (2016). Temporal rewiring of striatal circuits initiated by nicotine. *Neuropsychopharmacology* 41, 3051–3059. doi: 10.1038/npp.2016.118

Adermark, L., Morud, J., Lotfi, A., Ericson, M., and Soderpalm, B. (2019). Acute and chronic modulation of striatal endocannabinoid-mediated plasticity by nicotine. *Addict. Biol.* 24, 355–363. doi: 10.1111/adb.12598

Adermark, L., Morud, J., Lotfi, A., Jonsson, S., Soderpalm, B., and Ericson, M. (2015). Age-contingent influence over accumbal neurotransmission and the locomotor stimulatory response to acute and repeated administration of nicotine in Wistar rats. *Neuropharmacology* 97, 104–112. doi: 10.1016/j.neuropharm.2015.06.001

Al Sweidi, S., Morissette, M., Rouillard, C., and Di Paolo, T. (2013). Estrogen receptors and lesion-induced response of striatal dopamine receptors. *Neuroscience* 236, 99–109. doi: 10.1016/j.neuroscience.2012.12.058

Alasmari, F., Crotty Alexander, L. E., Hammad, A. M., Horton, A., Alhaddad, H., Schiefer, I. T., et al. (2021). E-cigarette aerosols containing nicotine modulate nicotinic acetylcholine receptors and astroglial glutamate transporters in mesocorticolimbic brain regions of chronically exposed mice. *Chem. Biol. Interact.* 333:109308. doi: 10.1016/j.cbi.2020.109308

Antin, T. M. J., Annechino, R., Hunt, G., Lipperman-Kreda, S., and Young, M. (2017). The gendered experience of smoking stigma: implications for tobacco control. *Crit. Public Health* 27, 443–454. doi: 10.1080/09581596.2016.1249825

Baca, M., Allan, A. M., Partridge, L. D., and Wilson, M. C. (2013). Gene-environment interactions affect long-term depression (LTD) through changes in dopamine receptor affinity in Snap25 deficient mice. *Brain Res.* 1532, 85–98. doi: 10.1016/j.brainres.2013.08.012

Balfour, D. J., Benwell, M. E., Birrell, C. E., Kelly, R. J., and Al-Aloul, M. (1998). Sensitization of the mesoaccumbens dopamine response to nicotine. *Pharmacol. Biochem. Behav.* 59, 1021–1030. doi: 10.1016/s0091-3057(97)00537-6

Bamford, N. S., Zhang, H., Joyce, J. A., Scarlis, C. A., Hanan, W., Wu, N. P., et al. (2008). Repeated exposure to methamphetamine causes long-lasting presynaptic corticostriatal depression that is renormalized with drug readministration. *Neuron* 58, 89–103. doi: 10.1016/j.neuron.2008.01.033

Bazzett, T. J., and Becker, J. B. (1994). Sex differences in the rapid and acute effects of estrogen on striatal D2 dopamine receptor binding. *Brain Res.* 637, 163–172. doi: 10.1016/0006-8993(94)91229-7

Belin, D., Jonkman, S., Dickinson, A., Robbins, T. W., and Everitt, B. J. (2009). Parallel and interactive learning processes within the basal ganglia: relevance for the understanding of addiction. *Behav. Brain Res.* 199, 89–102. doi: 10.1016/j.bbr.2008.09.027

Benowitz, N. L., and Hatsukami, D. (1998). Gender differences in the pharmacology of nicotine addiction. *Addict. Biol.* 3, 383–404. doi: 10.1080/13556219871930

Benwell, M. E., and Balfour, D. J. (1992). The effects of acute and repeated nicotine treatment on nucleus accumbens dopamine and locomotor activity. *Br. J. Pharmacol.* 105, 849–856. doi: 10.1111/j.1476-5381.1992.tb09067.x

Benwell, M. E., Balfour, D. J., and Anderson, J. M. (1988). Evidence that tobacco smoking increases the density of (−)-[3H]nicotine binding sites in human brain. *J. Neurochem.* 50, 1243–1247. doi: 10.1111/j.1471-4159.1988.tb10600.x

Bertrand, D., Valera, S., Bertrand, S., Ballivet, M., and Rungger, D. (1991). Steroids inhibit nicotinic acetylcholine receptors. *Neuroreport* 2, 277–280. doi: 10.1097/00001756-199105000-00016

Blanco, E., Galeano, P., Palomino, A., Pavon, F. J., Rivera, P., Serrano, A., et al. (2016). Cocaine-induced behavioral sensitization decreases the expression of endocannabinoid signaling-related proteins in the mouse hippocampus. *Eur. Neuropsychopharmacol.* 26, 477–492. doi: 10.1016/j.euroneuro.2015.12.040

Breese, C. R., Marks, M. J., Logel, J., Adams, C. E., Sullivan, B., Collins, A. C., et al. (1997). Effect of smoking history on [3H]nicotine binding in human postmortem brain. *J. Pharmacol. Exp. Ther.* 282, 7–13. PMID: 9223534

Brown, T. M., Brotchie, J. M., and Fitzjohn, S. M. (2003). Cannabinoids decrease corticostriatal synaptic transmission via an effect on glutamate uptake. *J. Neurosci.* 23, 11073–11077. doi: 10.1523/JNEUROSCI.23-35-11073.2003

Buczynski, M. W., Polis, I. Y., and Parsons, L. H. (2013). The volitional nature of nicotine exposure alters anandamide and oleoylethanolamide levels in the ventral tegmental area. *Neuropsychopharmacology* 38, 574–584. doi: 10.1038/npp.2012.210

Bystrowska, B., Frankowska, M., Smaga, I., Niedzielska-Andres, E., Pomierny-Chamiolo, L., and Filip, M. (2019). Cocaine-induced reinstatement of cocaine seeking provokes changes in the endocannabinoid and N-Acylethanolamine levels in rat brain structures. *Molecules* 24:1125. doi: 10.3390/molecules24061125

Calabresi, P., Centonze, D., Gubellini, P., Marfia, G. A., and Bernardi, G. (1999). Glutamate-triggered events inducing corticostriatal long-term depression. *J. Neurosci.* 19, 6102–6110. doi: 10.1523/JNEUROSCI.19-14-06102.1999

Carcoba, L. M., Flores, R. J., Natividad, L. A., and O'Dell, L. E. (2018). Amino acid modulation of dopamine in the nucleus accumbens mediates sex differences in nicotine withdrawal. *Addict. Biol.* 23, 1046–1054. doi: 10.1111/adb.12556

Castane, A., Valjent, E., Ledent, C., Parmentier, M., Maldonado, R., and Valverde, O. (2002). Lack of CB1 cannabinoid receptors modifies nicotine behavioural responses, but not nicotine abstinence. *Neuropharmacology* 43, 857–867. doi: 10.1016/s0028-3908(02)00118-1

Cheer, J. F., Wassum, K. M., Sombers, L. A., Heien, M. L., Ariansen, J. L., Aragona, B. J., et al. (2007). Phasic dopamine release evoked by abused substances requires cannabinoid receptor activation. *J. Neurosci.* 27, 791–795. doi: 10.1523/JNEUROSCI.4152-06.2007

Christian, D. T., Stefanik, M. T., Bean, L. A., Loweth, J. A., Wunsch, A. M., Funke, J. R., et al. (2021). GluN3-containing NMDA receptors in the rat nucleus accumbens core contribute to incubation of cocaine craving. *J. Neurosci.* 41, 8262–8277. doi: 10.1523/JNEUROSCI.0406-21.2021

Cohen, C., Perrault, G., Voltz, C., Steinberg, R., and Soubrie, P. (2002). SR141716, a central cannabinoid (CB(1)) receptor antagonist, blocks the motivational and dopamine-releasing effects of nicotine in rats. *Behav. Pharmacol.* 13, 451–463. doi: 10.1097/00008877-200209000-00018

Collins, A. C., Luo, Y., Selvaag, S., and Marks, M. J. (1994). Sensitivity to nicotine and brain nicotinic receptors are altered by chronic nicotine and mecamylamine infusion. *J. Pharmacol. Exp. Ther.* 271, 125–133. PMID: 7965705

Cosgrove, K. P., Wang, S., Kim, S. J., McGovern, E., Nabulsi, N., Gao, H., et al. (2014). Sex differences in the brain's dopamine signature of cigarette smoking. *J. Neurosci.* 34, 16851–16855. doi: 10.1523/JNEUROSCI.3661-14.2014

Dani, J. A., Ji, D., and Zhou, F. M. (2001). Synaptic plasticity and nicotine addiction. *Neuron* 31, 349–352. doi: 10.1016/s0896-6273(01)00379-8

Danielsson, K., Lagstrom, O., Ericson, M., Soderpalm, B., and Adermark, L. (2021a). Subregion-specific effects on striatal neurotransmission and dopamine-signaling by acute and repeated amphetamine exposure. *Neuropharmacology* 194:108638. doi: 10.1016/j.neuropharm.2021.108638

Danielsson, K., Stomberg, R., Adermark, L., Ericson, M., and Soderpalm, B. (2021b). Differential dopamine release by psychosis-generating and non-psychosis-generating addictive substances in the nucleus accumbens and dorsomedial striatum. *Transl. Psychiatry* 11:472. doi: 10.1038/s41398-021-01589-z

Domino, E. F., and Tsukada, H. (2009). Nicotine sensitization of monkey striatal dopamine release. *Eur. J. Pharmacol.* 607, 91–95. doi: 10.1016/j.ejphar.2009.02.011

Durieux, P. F., Schiffmann, S. N., and de Kerchove d'Exaerde, A. (2012). Differential regulation of motor control and response to dopaminergic drugs by D1R and D2R neurons in distinct dorsal striatum subregions. *EMBO J.* 31, 640–653. doi: 10.1038/emboj.2011.400

Ericson, M., Norrsjo, G., and Svensson, A. I. (2010). Behavioral sensitization to nicotine in female and male rats. *J. Neural Transm.* 117, 1033–1039. doi: 10.1007/s00702-010-0449-9

Feltenstein, M. W., Ghee, S. M., and See, R. E. (2012). Nicotine self-administration and reinstatement of nicotine-seeking in male and female rats. *Drug Alcohol Depend.* 121, 240–246. doi: 10.1016/j.drugalcdep.2011.09.001

Gerdeman, G., and Lovinger, D. M. (2001). CB1 cannabinoid receptor inhibits synaptic release of glutamate in rat dorsolateral striatum. *J. Neurophysiol.* 85, 468–471. doi: 10.1152/jn.2001.85.1.468

Gerdeman, G. L., Partridge, J. G., Lupica, C. R., and Lovinger, D. M. (2003). It could be habit forming: drugs of abuse and striatal synaptic plasticity. *Trends Neurosci.* 26, 184–192. doi: 10.1016/S0166-2236(03)00065-1

Giuffrida, A., Parsons, L. H., Kerr, T. M., Rodriguez de Fonseca, F., Navarro, M., and Piomelli, D. (1999). Dopamine activation of endogenous cannabinoid signaling in dorsal striatum. *Nat. Neurosci.* 2, 358–363. doi: 10.1038/7268

Gonzalez, S., Cascio, M. G., Fernandez-Ruiz, J., Fezza, F., Di Marzo, V., and Ramos, J. A. (2002). Changes in endocannabinoid contents in the brain of rats chronically exposed to nicotine, ethanol or cocaine. *Brain Res.* 954, 73–81. doi: 10.1016/s0006-8993(02)03344-9

Grieder, T. E., Yee, M., Vargas-Perez, H., Maal-Bared, G., George, S., Ting, A. K. R., et al. (2022). Administration of BDNF in the ventral tegmental area produces a switch from a nicotine-non-dependent D1R-mediated motivational state to a nicotine-dependent-like D2R-mediated motivational state. *Eur. J. Neurosci.* 55, 714–724. doi: 10.1111/ejn.15579

Hamilton, K. R., Elliott, B. M., Berger, S. S., and Grunberg, N. E. (2014). Environmental enrichment attenuates nicotine behavioral sensitization in male and female rats. *Exp. Clin. Psychopharmacol.* 22, 356–363. doi: 10.1037/a0037205

Hernandez, G., Oleson, E. B., Gentry, R. N., Abbas, Z., Bernstein, D. L., Arvanitogiannis, A., et al. (2014). Endocannabinoids promote cocaine-induced impulsivity and its rapid dopaminergic correlates. *Biol. Psychiatry* 75, 487–498. doi: 10.1016/j.biopsych.2013.09.005

Hilario, M. R., Clouse, E., Yin, H. H., and Costa, R. M. (2007). Endocannabinoid signaling is critical for habit formation. *Front. Integr. Neurosci.* 1:2007. doi: 10.3389/neuro.07.006.2007

Hirth, N., Meinhardt, M. W., Noori, H. R., Salgado, H., Torres-Ramirez, O., Uhrig, S., et al. (2016). Convergent evidence from alcohol-dependent humans and rats for a hyperdopaminergic state in protracted abstinence. *Proc. Natl. Acad. Sci. U. S. A.* 113, 3024–3029. doi: 10.1073/pnas.1506012113

Honeycutt, S. C., Garrett, P. I., Barraza, A. G., Maloy, A. N., and Hillhouse, T. M. (2020). Repeated nicotine vapor inhalation induces behavioral sensitization in male and female C57BL/6 mice. *Behav. Pharmacol.* 31, 583–590. doi: 10.1097/FBP.0000000000000562

Hynes, T. J., Ferland, J. M., Feng, T. L., Adams, W. K., Silveira, M. M., Tremblay, M., et al. (2020). Chemogenetic inhibition of dopaminergic projections to the nucleus accumbens has sexually dimorphic effects in the rat gambling task. *Behav. Neurosci.* 134, 309–322. doi: 10.1037/bne0000372

Hynes, T. J., Hrelja, K. M., Hathaway, B. A., Hounjet, C. D., Chernoff, C. S., Ebsary, S. A., et al. (2021). Dopamine neurons gate the intersection of cocaine use, decision making, and impulsivity. *Addict. Biol.* 26:e13022. doi: 10.1111/adb.13022

Imperato, A., Mulas, A., and Di Chiara, G. (1986). Nicotine preferentially stimulates dopamine release in the limbic system of freely moving rats. *Eur. J. Pharmacol.* 132, 337–338. doi: 10.1016/0014-2999(86)90629-1

Iyer, V., Rangel-Barajas, C., Woodward, T. J., Kulkarni, A., Cantwell, L., Crystal, J. D., et al. (2022). Negative allosteric modulation of CB1 cannabinoid receptor signaling suppresses opioid-mediated reward. *Pharmacol. Res.* 185:106474. doi: 10.1016/j.phrs.2022.106474

Jackson, M. E., and Moghaddam, B. (2001). Amygdala regulation of nucleus accumbens dopamine output is governed by the prefrontal cortex. *J. Neurosci.* 21, 676–681. doi: 10.1523/JNEUROSCI.21-02-00676.2001

Jing, L., Liu, B., Zhang, M., and Liang, J. H. (2018). Involvement of dopamine D2 receptor in a single methamphetamine-induced behavioral sensitization in C57BL/6J mice. *Neurosci. Lett.* 681, 87–92. doi: 10.1016/j.neulet.2018.02.067

Jones, J. L., Day, J. J., Aragona, B. J., Wheeler, R. A., Wightman, R. M., and Carelli, R. M. (2010). Basolateral amygdala modulates terminal dopamine release in the nucleus accumbens and conditioned responding. *Biol. Psychiatry* 67, 737–744. doi: 10.1016/j.biopsych.2009.11.006

Keshavarzian, E., Ghasemzadeh, Z., and Rezayof, A. (2018). The basolateral amygdala dopaminergic system contributes to the improving effect of nicotine on stress-induced memory impairment in rats. *Prog. Neuro-Psychopharmacol. Biol. Psychiatry* 86, 30–35. doi: 10.1016/j.pnpbp.2018.05.008

Kim, S., Sohn, S., and Choe, E. S. (2022). Phosphorylation of Glu A1-Ser831 by CaMKII activation in the caudate and putamen is required for behavioral sensitization after challenge nicotine in rats. *Int. J. Neuropsychopharmacol.* 25, 678–687. doi: 10.1093/ijnp/pyac034

Kim, J. H., and Vezina, P. (2002). The mGlu2/3 receptor agonist LY379268 blocks the expression of locomotor sensitization by amphetamine. *Pharmacol. Biochem. Behav.* 73, 333–337. doi: 10.1016/s0091-3057(02)00827-4

Kreitzer, A. C., and Malenka, R. C. (2005). Dopamine modulation of state-dependent endocannabinoid release and long-term depression in the striatum. *J. Neurosci.* 25, 10537–10545. doi: 10.1523/JNEUROSCI.2959-05.2005

Lagstrom, O., Danielsson, K., Soderpalm, B., Ericson, M., and Adermark, L. (2019). Voluntary ethanol intake produces subregion-specific neuroadaptations in striatal and cortical areas of Wistar rats. *Alcohol. Clin. Exp. Res.* 43, 803–811. doi: 10.1111/acer.14014

Lee, J. H., Ribeiro, E. A., Kim, J., Ko, B., Kronman, H., Jeong, Y. H., et al. (2020). Dopaminergic regulation of nucleus accumbens cholinergic interneurons demarcates susceptibility to cocaine addiction. *Biol. Psychiatry* 88, 746–757. doi: 10.1016/j.biopsych.2020.05.003

Leroy, C., Karila, L., Martinot, J. L., Lukasiewicz, M., Duchesnay, E., Comtat, C., et al. (2012). Striatal and extrastriatal dopamine transporter in cannabis and tobacco addiction: a high-resolution PET study. *Addict. Biol.* 17, 981–990. doi: 10.1111/j.1369-1600.2011.00356.x

Leyrer-Jackson, J. M., Holter, M., Overby, P. F., Newbern, J. M., Scofield, M. D., Olive, M. F., et al. (2021). Accumbens cholinergic interneurons mediate Cue-induced nicotine seeking and associated glutamatergic plasticity. *eNeuro* 8:ENEURO.0276-20.2020. doi: 10.1523/ENEURO.0276-20.2020

Licheri, V., Lagstrom, O., Lotfi, A., Patton, M. H., Wigstrom, H., Mathur, B., et al. (2018). Complex control of striatal neurotransmission by nicotinic acetylcholine receptors via excitatory inputs onto medium spiny neurons. *J. Neurosci.* 38, 6597–6607. doi: 10.1523/JNEUROSCI.0071-18.2018

Lim, D. K., and Kim, H. S. (2003a). Chronic exposure of nicotine modulates the expressions of the cerebellar glial glutamate transporters in rats. *Arch. Pharm. Res.* 26, 321–329. doi: 10.1007/BF02976963

Lim, D. K., and Kim, H. S. (2003b). Opposite modulation of glutamate uptake by nicotine in cultured astrocytes with/without cAMP treatment. *Eur. J. Pharmacol.* 476, 179–184. doi: 10.1016/s0014-2999(03)02186-1

Liput, D. J., Puhl, H. L., Dong, A., He, K., Li, Y., and Lovinger, D. M. (2022). 2-Arachidonoylglycerol mobilization following brief synaptic stimulation in the dorsal lateral striatum requires glutamatergic and cholinergic neurotransmission. *Neuropharmacology* 205:108916. doi: 10.1016/j.neuropharm.2021.108916

Liu, X., Li, X., Zhao, G., Wang, F., and Wang, L. (2020). Sexual dimorphic distribution of cannabinoid 1 receptor mRNA in adult C57BL/6J mice. *J. Comp. Neurol.* 528, 1986–1999. doi: 10.1002/cne.24868

Livingstone-Banks, J., Norris, E., Hartmann-Boyce, J., West, R., Jarvis, M., Chubb, E., et al. (2019). Relapse prevention interventions for smoking cessation. *Cochrane Database Syst. Rev.* 2019:CD003999. doi: 10.1002/14651858.CD003999.pub6

Lotfi, A., Licheri, V., Andersson, J., Soderpalm, B., Ericson, M., and Adermark, L. (2022). Sustained inhibitory transmission but dysfunctional dopamine D2 receptor signaling in dorsal striatal subregions following protracted abstinence from amphetamine. *Pharmacol. Biochem. Behav.* 218:173421. doi: 10.1016/j.pbb.2022.173421

Melis, M., De Felice, M., Lecca, S., Fattore, L., and Pistis, M. (2013). Sex-specific tonic 2-arachidonoylglycerol signaling at inhibitory inputs onto dopamine neurons of Lister hooded rats. *Front. Integr. Neurosci.* 7:93. doi: 10.3389/fnint.2013.00093

Merritt, L. L., Martin, B. R., Walters, C., Lichtman, A. H., and Damaj, M. I. (2008). The endogenous cannabinoid system modulates nicotine reward and dependence. *J. Pharmacol. Exp. Ther.* 326, 483–492. doi: 10.1124/jpet.108.138321

Metaxas, A., Bailey, A., Barbano, M. F., Galeote, L., Maldonado, R., and Kitchen, I. (2010). Differential region-specific regulation of alpha4beta2* nAChRs by self-administered and non-contingent nicotine in C57BL/6J mice. *Addict. Biol.* 15, 464–479. doi: 10.1111/j.1369-1600.2010.00246.x

Montgomery, A. J., Lingford-Hughes, A. R., Egerton, A., Nutt, D. J., and Grasby, P. M. (2007). The effect of nicotine on striatal dopamine release in man: a [11C]raclopride PET study. *Synapse* 61, 637–645. doi: 10.1002/syn.20419

Morud, J., Adermark, L., Perez-Alcazar, M., Ericson, M., and Soderpalm, B. (2016). Nicotine produces chronic behavioral sensitization with changes in accumbal neurotransmission and increased sensitivity to re-exposure. *Addict. Biol.* 21, 397–406. doi: 10.1111/adb.12219

Partridge, J. G., Apparsundaram, S., Gerhardt, G. A., Ronesi, J., and Lovinger, D. M. (2002). Nicotinic acetylcholine receptors interact with dopamine in induction of striatal long-term depression. *J. Neurosci.* 22, 2541–2549. doi: 10.1523/JNEUROSCI.22-07-02541.2002

Pascoli, V., Hiver, A., Li, Y., Harada, M., Esmaeili, V., and Luscher, C. (2022). Cell-type specific synaptic plasticity in dorsal striatum is associated with punishment-resistance compulsive-like cocaine self-administration in mice. *Neuropsychopharmacology*. doi: 10.1038/s41386-022-01429-8 [Epub ahead of print]

Paxinos, G., and Watson, C. (2007). *The Rat Brain in Stereotaxic Coordinates*. Amsterdam: Elsevier, Academic Press.

Perkins, K. A., Giedgowd, G. E., Karelitz, J. L., Conklin, C. A., and Lerman, C. (2012). Smoking in response to negative mood in men versus women as a function of distress tolerance. *Nicotine Tob. Res.* 14, 1418–1425. doi: 10.1093/ntr/nts075

Phillips, A. G., Ahn, S., and Howland, J. G. (2003). Amygdalar control of the mesocorticolimbic dopamine system: parallel pathways to motivated behavior. *Neurosci. Biobehav. Rev.* 27, 543–554. doi: 10.1016/j.neubiorev.2003.09.002

Rada, P., Jensen, K., and Hoebel, B. G. (2001). Effects of nicotine and mecamylamine-induced withdrawal on extracellular dopamine and acetylcholine in the rat nucleus accumbens. *Psychopharmacology* 157, 105–110. doi: 10.1007/s002130100781

Rademacher, L., Prinz, S., Winz, O., Henkel, K., Dietrich, C. A., Schmaljohann, J., et al. (2016). Effects of smoking cessation on presynaptic dopamine function of addicted male smokers. *Biol. Psychiatry* 80, 198–206. doi: 10.1016/j.biopsych.2015.11.009

Rahman, S., Zhang, J., Engleman, E. A., and Corrigall, W. A. (2004). Neuroadaptive changes in the mesoaccumbens dopamine system after chronic nicotine self-administration: a microdialysis study. *Neuroscience* 129, 415–424. doi: 10.1016/j.neuroscience.2004.08.010

Rivera, A., Suarez-Boomgaard, D., Miguelez, C., Valderrama-Carvajal, A., Baufreton, J., Shumilov, K., et al. (2021). Dopamine D4 receptor is a regulator of morphine-induced plasticity in the rat dorsal striatum. *Cells* 11:31. doi: 10.3390/cells11010031

Robinson, T. E., and Becker, J. B. (1982). Behavioral sensitization is accompanied by an enhancement in amphetamine-stimulated dopamine release from striatal tissue in vitro. *Eur. J. Pharmacol.* 85, 253–254. doi: 10.1016/0014-2999(82)90478-2

Robinson, T. E., and Berridge, K. C. (1993). The neural basis of drug craving: an incentive-sensitization theory of addiction. *Brain Res. Brain Res. Rev.* 18, 247–291. doi: 10.1016/0165-0173(93)90013-p

Rouillon, C., Abraini, J. H., and David, H. N. (2008). Prefrontal cortex and basolateral amygdala modulation of dopamine-mediated locomotion in the nucleus accumbens core. *Exp. Neurol.* 212, 213–217. doi: 10.1016/j.expneurol.2008.04.002

Scarduzio, M., Zimmerman, C. N., Jaunarajs, K. L., Wang, Q., Standaert, D. G., and McMahon, L. L. (2017). Strength of cholinergic tone dictates the polarity of dopamine D2 receptor modulation of striatal cholinergic interneuron excitability in DYT1 dystonia. *Exp. Neurol.* 295, 162–175. doi: 10.1016/j.expneurol.2017.06.005

Shim, I., Javaid, J. I., Wirtshafter, D., Jang, S. Y., Shin, K. H., Lee, H. J., et al. (2001). Nicotine-induced behavioral sensitization is associated with extracellular dopamine release and expression of c-Fos in the striatum and nucleus accumbens of the rat. *Behav. Brain Res.* 121, 137–147. doi: 10.1016/s0166-4328(01)00161-9

Speranza, L., di Porzio, U., Viggiano, D., de Donato, A., and Volpicelli, F. (2021). Dopamine: the neuromodulator of long-term synaptic plasticity, reward and movement control. *Cells* 10:735. doi: 10.3390/cells10040735

Steketee, J. D., and Kalivas, P. W. (2011). Drug wanting: behavioral sensitization and relapse to drug-seeking behavior. *Pharmacol. Rev.* 63, 348–365. doi: 10.1124/pr.109.001933

Uchigashima, M., Narushima, M., Fukaya, M., Katona, I., Kano, M., and Watanabe, M. (2007). Subcellular arrangement of molecules for 2-arachidonoyl-glycerol-mediated retrograde signaling and its physiological contribution to synaptic modulation in the striatum. *J. Neurosci.* 27, 3663–3676. doi: 10.1523/JNEUROSCI.0448-07.2007

Ulenius, L., Andren, A., Adermark, L., Soderpalm, B., and Ericson, M. (2020). Sub-chronic taurine administration induces behavioral sensitization but does not influence ethanol-induced dopamine release in the nucleus accumbens. *Pharmacol. Biochem. Behav.* 188:172831. doi: 10.1016/j.pbb.2019.172831

Urakubo, H., Yagishita, S., Kasai, H., and Ishii, S. (2020). Signaling models for dopamine-dependent temporal contiguity in striatal synaptic plasticity. *PLoS Comput. Biol.* 16:e1008078. doi: 10.1371/journal.pcbi.1008078

van Huijstee, A. N., and Mansvelder, H. D. (2014). Glutamatergic synaptic plasticity in the mesocorticolimbic system in addiction. *Front. Cell. Neurosci.* 8:466. doi: 10.3389/fncel.2014.00466

Vezina, P. (1996). D1 dopamine receptor activation is necessary for the induction of sensitization by amphetamine in the ventral tegmental area. *J. Neurosci.* 16, 2411–2420. doi: 10.1523/JNEUROSCI.16-07-02411.1996

Vezina, P., McGehee, D. S., and Green, W. N. (2007). Exposure to nicotine and sensitization of nicotine-induced behaviors. *Prog. Neuro-Psychopharmacol. Biol. Psychiatry* 31, 1625–1638. doi: 10.1016/j.pnpbp.2007.08.038

Wang, R., Hausknecht, K. A., Gancarz-Kausch, A. M., Oubraim, S., Shen, R. Y., and Haj-Dahmane, S. (2020). Cocaine self-administration abolishes endocannabinoid-mediated long-term depression of glutamatergic synapses in the ventral tegmental area. *Eur. J. Neurosci.* 52, 4517–4524. doi: 10.1111/ejn.14980

Wang, Z., Kai, L., Day, M., Ronesi, J., Yin, H. H., Ding, J., et al. (2006). Dopaminergic control of corticostriatal long-term synaptic depression in medium spiny neurons is mediated by cholinergic interneurons. *Neuron* 50, 443–452. doi: 10.1016/j.neuron.2006.04.010

Wilar, G., Shinoda, Y., Sasaoka, T., and Fukunaga, K. (2019). Crucial role of dopamine D2 receptor signaling in nicotine-induced conditioned place preference. *Mol. Neurobiol.* 56, 7911–7928. doi: 10.1007/s12035-019-1635-x

Xia, J., Meyers, A. M., and Beeler, J. A. (2017). Chronic nicotine alters corticostriatal plasticity in the striatopallidal pathway mediated by NR2B-containing silent synapses. *Neuropsychopharmacology* 42, 2314–2324. doi: 10.1038/npp.2017.87

Yoon, H. S., Jang, J. K., and Kim, J. H. (2008). Blockade of group II metabotropic glutamate receptors produces hyper-locomotion in cocaine pre-exposed rats by interactions with dopamine receptors. *Neuropharmacology* 55, 555–559. doi: 10.1016/j.neuropharm.2008.07.012

Zheng, K., Scimemi, A., and Rusakov, D. A. (2008). Receptor actions of synaptically released glutamate: the role of transporters on the scale from nanometers to microns. *Biophys. J.* 95, 4584–4596. doi: 10.1529/biophysj.108.129874

frontiers | Frontiers in Molecular Neuroscience

TYPE Original Research
PUBLISHED 13 January 2023
DOI 10.3389/fnmol.2022.1104657

OPEN ACCESS

EDITED BY
Vidhya Kumaresan,
Boston University,
United States

REVIEWED BY
Chitra D. Mandyam,
VA San Diego Healthcare System,
United States
Habibeh Khoshbouei,
University of Florida,
United States

*CORRESPONDENCE
Jean Lud Cadet
✉ jcadet@inta.nida.nih.gov

SPECIALTY SECTION
This article was submitted to Neuroplasticity and Development, a section of the journal Frontiers in Molecular Neuroscience

RECEIVED 21 November 2022
ACCEPTED 19 December 2022
PUBLISHED 13 January 2023

CITATION
Munoz C, Jayanthi S, Ladenheim B and Cadet JL (2023) Compulsive methamphetamine self-administration in the presence of adverse consequences is associated with increased hippocampal mRNA expression of cellular adhesion molecules.
Front. Mol. Neurosci. 15:1104657.
doi: 10.3389/fnmol.2022.1104657

Compulsive methamphetamine self-administration in the presence of adverse consequences is associated with increased hippocampal mRNA expression of cellular adhesion molecules

Ceiveon Munoz, Subramaniam Jayanthi, Bruce Ladenheim and Jean Lud Cadet*

Molecular Neuropsychiatry Research Branch, DHHS/NIH/NIDA, Intramural Research Program, Baltimore, MD, United States

Methamphetamine (METH) is a popular but harmful psychostimulant. METH use disorder (MUD) is characterized by compulsive and continued use despite adverse life consequences. METH users experience impairments in learning and memory functions that are thought to be secondary to METH-induced abnormalities in the hippocampus. Recent studies have reported that about 50% of METH users develop MUD, suggesting that there may be differential molecular effects of METH between the brains of individuals who met criteria for addiction and those who did not after being exposed to the drug. The present study aimed at identifying potential transcriptional differences between compulsive and non-compulsive METH self-administering male rats by measuring global gene expression changes in the hippocampus using RNA sequencing. Herein, we used a model of METH self-administration (SA) accompanied by contingent foot-shock punishment. This approach led to the separation of animals into shock-resistant rats (compulsive) that continued to take METH and shock-sensitive rats (non-compulsive) that suppressed their METH intake in the presence of punished METH taking. Rats were euthanized 2h after the last METH SA plus foot-shock session. Their hippocampi were immediately removed, frozen, and used later for RNA sequencing and qRT-PCR analyses. RNA sequencing analyses revealed differential expression of mRNAs encoding cell adhesion molecules (CAMs) between the two rat phenotypes. qRT-PCR analyses showed significant higher levels of *Cdh1*, *Glycam1*, *and Mpzl2* mRNAs in the compulsive rats in comparison to non-compulsive rats. The present results implicate altered CAM expression in the hippocampus in the behavioral manifestations of continuous compulsive METH taking in the presence of adverse consequences. Our results raise the novel possibility that altered CAM expression might play a role in compulsive METH taking and the cognitive impairments observed in MUD patients.

KEYWORDS

methamphetamine, hippocampus, gene expression, electric foot-shocks, cell adhesion

Introduction

Methamphetamine (METH) is an amphetamine-type psychostimulant drug which is among the most misused substances in the world (UNODC (United Nations Office on Drug and Crime), 2022). METH can be taken orally, *via* snorting, smoking, and intravenously, with the intravenous route being mostly involved in METH-related overdose deaths (Han et al., 2021; Jones et al., 2022). Humans who use the drug experience a multitude of physiological, neurological, and behavioral sequelae including neuroinflammatory responses and cognitive impairments (Moszczynska and Callan, 2017; Paulus and Stewart, 2020). METH exerts its effects *via* the release of monoamines such as dopamine and noradrenaline from synaptic vesicles and causing changes in their metabolism (Moszczynska and Callan, 2017; Jayanthi et al., 2021; Daiwile et al., 2022b).

About 50% of METH users develop METH use disorder (MUD) which is characterized by repeated drug misuse, loss of control over drug use, compulsive use despite negative consequences, and multiple relapse episodes, according to the Diagnostic Statistical Manual (DSM5) of the American Psychiatric Association (APA) DSM5 (2022). Patients also show changes in learning and memory functions (Shukla and Vincent, 2021) that are subserved by the hippocampus (Golsorkhdan et al., 2020). The substrates for METH-associated cognitive disturbances might include epigenetic modifications, altered gene expression, changes in synaptic plasticity, and dysfunctional neurotransmission (Chojnacki et al., 2020; Golsorkhdan et al., 2020; Shukla and Vincent, 2021). This line of reasoning suggests that METH might influence the expression of genes including cell adhesion molecules (CAMs) that participate in regulating hippocampal synaptic plasticity (Cotman et al., 1998; Gnanapavan and Giovannoni, 2013) and other drug-induced neuroadaptions during addictive processes (Muskiewicz et al., 2018).

As a step toward identifying genes that might be differentially regulated during compulsive METH taking in the presence of adverse consequences, we used the discovery approach of RNA sequencing using the model of foot-shock-induced compulsive and non-compulsive rat METH SA (Cadet et al., 2016, 2019; Subu et al., 2020; Jayanthi et al., 2022). We also used quantitative PCR to validate changes in some CAMs that were identified by RNA Sequencing as showing differential expression between compulsive and non-compulsive METH takers in the presence of foot-shocks. Herein, we discuss the potential role of hippocampal CAMs in mediating METH-induced compulsive METH taking.

Materials and methods

Animals and drug treatment

Male Sprague–Dawley rats each weighing 350-400 g were used (Charles River Labs, Raleigh, NC, United States). Animals were housed in a humidity and temperature controlled (22.2 ± 0.2°C) room with free access to food and water. All animals were handled as outlined in the Guide for the Care and Use of Laboratory Animals (ISBN: 0–309–05377-3) and animal protocol was approved by the National Institute of Drug Abuse Animal Care and Use Committee (NIDA, ACUC).

Intravenous surgery

Rats were anesthetized using ketamine (100 mg/kg i.p.) and xylazine (5 mg/kg i.p.) and silastic catheters were put into the jugular vein. After surgery, animal health was monitored daily, and catheters were flushed with sterile saline containing gentamicin (Butler Schein; 5 mg/ml) and allowed to recover for 5–10 days before start of METH self-administration training. Upon wake from anesthesia, rats received meloxicam (1 mg/kg s.c.), as an analgesic, and a second dose the following day.

Training and punishment phases

As mentioned, our METH self-administration training procedure was performed according to the previously designed protocol for our lab (Cadet et al., 2016; Subu et al., 2020; Jayanthi et al., 2022). Rats were housed in self-administration chambers with free access to food and water, made available in water bottles and feeders hanging from each chamber wall. We trained rats to self-administer dl-methamphetamine HCl (NIDA), by pressing an active infusion pump lever, for three 3-h sessions per day, for 21 days. To achieve this, rat catheters were connected to a modified cannula (Plastics One, Minneapolis, MN) attached to a liquid swivel (Instech Laboratories, Inc., Plymouth Meeting, PA, United States) *via* polyethylene-50 tubing protected by a metal spring. To prevent overdose, each 3-h self-administration training session was separated by a 30-min timeout during which the animals had no access to the active lever. Rats self-administered METH at a dose of 0.1 mg/kg/infusion over 3.5 s, and the number of infusions was limited to 35 per each 3-h training session, and each pressed lever infusion was given a 20-s recess timeout. To

reinforce, active lever presses were accompanied by a compound tone-light cue, and presses on inactive lever induced no reinforcement cues. Rats were trained 5 days a week, with 2 days off to minimize weight loss for a total of 21 days of METH self-administration training. During the 2 days off, rats remained housed in chambers but were disconnected from the intravenous self-administration connection and cannulas were covered with dust prevention caps. We started self-administration sessions at the onset of the dark cycle and sessions began with insertion of the active lever and the illumination of a red light that remained on during the entire 3 h session. At the end of each session, and during 30-min timeouts, the red light was turned off, and the active lever was removed. Control rats self-administered saline, under the same conditions.

During the 8-day foot-shock punishment phase, rats continued METH self-administration for 8 days straight under the same 3-h session schedule used during the training phase. However, a 0.5-s foot-shock was delivered through the grid floor on 50% of all active METH lever presses. This electrical current was set at 0.18 mA on day 1, which was increased as the 8-day foot-shock phase proceeded. Shock intensity was set to 0.24 mA on day 2, 0.30 mA on days 3–5, and 0.36 mA on days 6–8. As an important addition, some control rats that self-administered saline were "yoked" connected to a METH taking rat and received a contingent shock whenever the rat it was paired to pressed for METH. As a control for the effects of shock on biochemical and molecular markers within the brain, the METH taking rat and the yoke-saline rat that it was paired to, received the same number of foot-shocks. Totally, after the 8-day foot-shock phase was complete, rats were separated into 5 groups CT (Saline, no foot-shock), SR (Methamphetamine, Shock Resistant), SS (Methamphetamine, Shock Sensitive), YSR (Saline, SR contingent foot-shock), and YSS (Saline, SS contingent foot-shock).

RNA extraction and sequencing

Immediately after the last 3 h foot-shock session, rats were euthanized by decapitation, and the brains were removed and dissected by region. We dissected out the entire hippocampus using the coordinates A/P -5 to -7 mm bregma, mediolateral ±6 mm, D/V -2 to -8 mm, corresponding to *The Rat Brain in Stereotaxic Coordinates* (Paxinos and Watson, 2013).Total RNA was extracted from samples of the total hippocampal region using Qiagen RNeasy Mini kit (Qiagen, Valencia, CA, United States). RNA integrity was assessed using an Agilent 2,100 Bioanalyzer (Agilent, Palo Alto, CA, United States), and RNA samples showed no signs of degradation. RNA sequencing was performed by GeneWiz (GeneWiz, South Plainfield, NJ, United States) using Illumina HiSeq instrument according to manufacturer's instructions and was converted into fastq files and de-multiplexed using the Illumina bcl2fastq 2.17 software. The samples were sequenced using a 2×150bp Paired End (PE) configuration (GeneWiz, South Plainfield, NJ, United States). Sequence reads were filtered to remove any poor-quality reads using Trimmomatic v.0.36 and this data has been submitted to Gene Expression Omnibus[1] under accession number GSE203268.

Ingenuity pathway analysis

We used Ingenuity Pathway Analysis (IPA) software (Qiagen, Valencia, CA, United States) to analyze genes that showed differential expression in RNA sequencing data and identify molecular functions, biochemical networks, and validated canonical gene pathways.

Quantitative RT-PCR analysis of mRNA

To analyze mRNA levels, for each sample in each group (CT, SR, SS, YSR, YSS), we reversed-transcribed individual total RNA into cDNA using Advantage RT-for-PCR kit (Clontech, Mountain View, CA, United States). Using this kit, 500 nanograms(ng) of RNA was reversed-transcribed with oligo dT primers to create cDNA. We generated PCR primers using NIH accredited NCBI primer-BLAST website and ordered gene-specific primers from the Synthesis and Sequencing Facility of Johns Hopkins University (Baltimore, MD, United States). RT-qPCR was performed with the Roche LightCycler 480 II using iQ SYBR Green Supermix (Bio-Rad Laboratories, Hercules CA, United States). Relative amounts of mRNA in each sample were normalized to a combined mean of OAZ1 and Clathrin mRNA, used as housekeeping reference genes.

Statistical analysis

Behavioral data, RNA sequencing data, and qRT-PCR data were analyzed using the statistical program GraphPad Prism version 9 (Dotmatics, San Diego, CA, United States). Behavioral data was analyzed using repeated measures two-way ANOVA. For the behavioral experiments, the dependent variable used was the number of METH or saline infusions during the 21-day training and 8-day foot-shock phases, for each group. RNA sequencing and qRT-PCR data was analyzed using one-way ANOVA followed by Tukey's multiple comparison *post hoc* test. Statistical significance level for all tests was set to 0.05, and the null hypothesis was rejected at value of $p<0.05$.

1 http://www.ncbi.nlm.nih.gov/geo/

Results

Foot-shocks separate methamphetamine self-administering rats into compulsive (shock-resistant) and non-compulsive (shock-sensitive) behavioral phenotypes

Figure 1A shows the experimental timeline of the behavioral experiment. It includes METH SA training and contingent foot-shock phases. Figure 1B depicts the number of infusions of either METH or saline during the 21-day SA training period. All METH-trained rats ($n = 15$) significantly increased their drug intake whereas control rats ($n = 9$) did not change their saline intake during the training phase (Figure 1B). The repeated measure analysis using 2-way ANOVA for the SA training phase included the between-subject factor of groups: control (CT $n = 9$), yoked saline (YS $n = 19$), shock-resistant (SR $n = 8$), and shock-sensitive (SS $n = 7$), and the within-subject factor of training days (experimental days 1–21). There were significant differences in the number of infusions between groups [$F_{(3,35)} = 139.9$, $p < 0.0001$] over training days [$F_{(20,700)} = 34.29$, $p < 0.0001$], with there being significant interaction of day × group [$F_{(60,700)} = 21.31$, $p < 0.0001$].

On day 22, foot-shocks were introduced and increased in intensity from 0.18–0.36 mA over 8 days (experimental days 22–29). Foot-shocks helped to separate the rats into 2 different behavioral phenotypes. The group of rats that continued to compulsively press the active lever for METH infusions despite foot-shocks were labeled shock-resistant (SR) or compulsive METH takers ($n = 8$) whereas the rats that decreased their active lever pressing under punishment were termed shock-sensitive (SS) or non-compulsives ($n = 7$; Figure 1B). The repeated measures analysis for the foot-shock phase included the SR and SS groups, and the within-subject factor of days (experimental days 22–29). We found significant differences in the number of METH infusions between groups [$F_{(1,13)} = 46.53$, $p < 0.0001$] and over shock days [$F_{(7,91)} = 6.654$, $p < 0.0001$]. The interaction of day × group [$F_{(7,91)} = 9.348$, $p < 0.0001$] was also significant.

The total METH intake (mg/kg) of the SR and SS rats during the training and foot-shock phases are shown in Figure 1C. During SA training, all METH SA rats took comparable amounts of the drug. During the foot-shock/punishment phase, both groups decreased their drug intake, with the SS rats decreasing their active lever pressing significantly more than the SR rats. Overall, SS rats took significantly less METH [$F_{(1,6)} = 66.86$; $p = 0.0002$; Figure 1C] and received significantly less foot-shocks [$F_{(1,13)} = 64.69$; $p < 0.0001$; Figure 1D] than SR rats. The 2-way

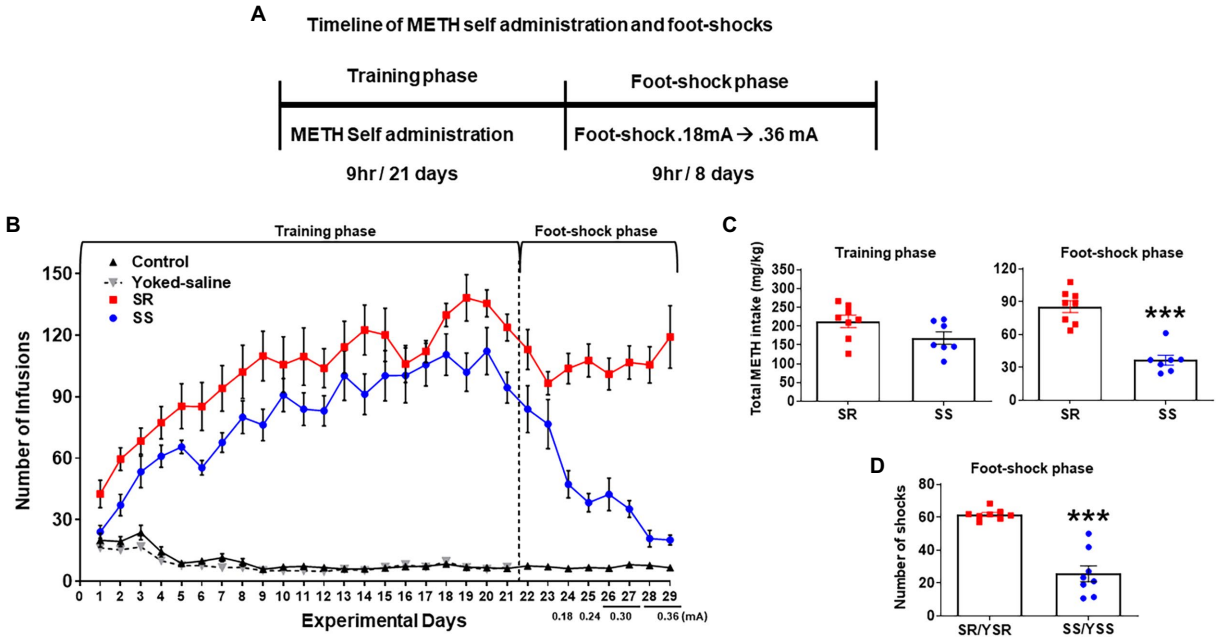

FIGURE 1
Contingent foot-shocks during METH self-administration (SA) are associated with continued compulsive drug taking behaviors. **(A)** Experimental timeline for METH SA training and punishment phases. **(B)** Average number of infusions (METH or saline) over the training phase (21days) showed increases in METH infusions during SA training. The introduction of contingent shocks for 8days suppressed lever pressing in non-compulsive, shock-sensitive (SS, *n*=7) rats but not in shock-resistant rats (SR, *n*=8). **(C)** Average total METH intake of SR rats (212.6±15.35mg/kg) and SS rats (168.1±14.99mg/kg) during the training phase (*first panel*) showed no significant differences. Foot-shocks (*second panel*) had significant differences in METH intake between SR rats (85.4±5.38mg/kg) and SS rats (36.5±4.21mg/kg). **(D)** Total numbers of shocks administered to the SR rats and their yoked-shock controls (YSR) were significantly higher than those received by SS rats and their yoked-shock control group (YSS). *Key to statistics:* ***$p<0.001$ significant SR vs. SS.

ANOVA for number of foot-shocks was also significant for groups [$F_{(1,13)} = 64.69$, $p < 0.0001$], days [$F_{(7,91)} = 6.920$, $p < 0.0001$], and interaction of day × group [$F_{(7,91)} = 9.892$, $p < 0.0001$; Figure 1D].

As mentioned in the Methods, some rats that self-administered saline were individually connected to METH taking rats. These yoked rats received foot-shocks whenever the METH SA rat to which they were paired received a shock, such that individual yoked-saline rats and paired METH-taking rats received the same number of shocks by the end of the behavioral experiment. These paired rats were labeled yoked shock-resistant (YSR) or yoked shock-sensitive (YSS).

Genome-wide transcriptional analyses revealed significant differences in gene expression between hippocampus of compulsive vs. non-compulsive methamphetamine taking rats

To identify potential transcriptional changes in the resistant and sensitive rats, we used RNA sequencing using RNA obtained from whole hippocampal tissues (CT, $n = 7$; SR, $n = 7$; SS, $n = 6$; YSR, $n = 5$; YSS, $n = 5$). We then calculated RNA expression fold changes to find differentially expressed genes (DEGs) between 8 pairings (SR vs. CT, SS vs. CT, YSR vs. CT, YSS vs. CT, SR vs. SS, SR vs. YSR, SS vs. YSS, YSR vs. YSS).

Using GraphPad Prism (Version 9), we created volcano plots to visualize the entire sets of DEGs obtained from the sequencing data (Figures 2A,H). The volcano plots, showing up- and downregulated genes, were plotted using fold-changes scaled on the x-axis, and value of p shown on the y-axis. Note that SR group comparisons (SR vs. CT and SR vs. YSR; Figures 2A,F) showed more total DEGs than the SS group comparisons (SS vs. CT and SS vs. YSS; Figures 2B,G). The YSR vs. CT (Figure 2C) and YSS vs. CT (Figure 2D) comparisons showed clearly that shock-induced stress had significant effects on hippocampal gene expression.

To identify potential overlaps of DEGs between the various comparisons, we created Venn diagrams[2] (Figures 2I,J). For these comparisons, we used fold-changes of greater or less that 1.7-fold

2 http://www.interactivenn.net/

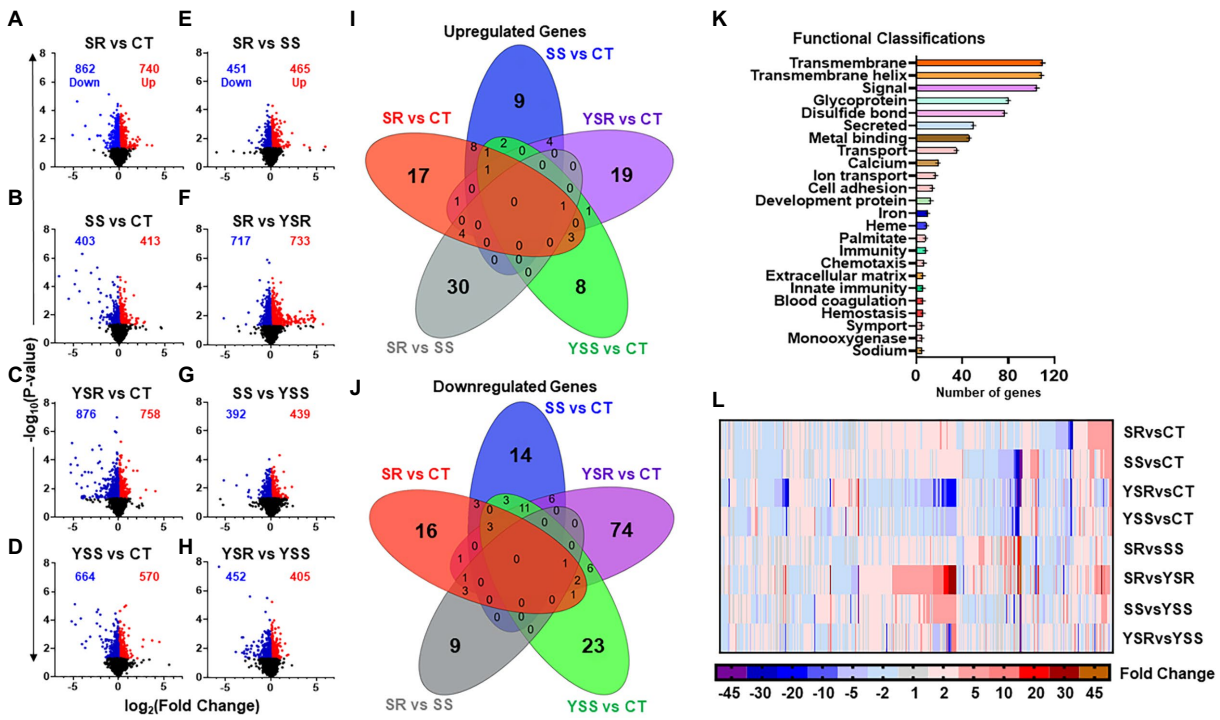

FIGURE 2
(A–H) Volcano plots illustrating the number of significant genes ($p<0.05$) between each pair-wise comparison. Volcano plots were created using GraphPad Prism version 9 (Dotmatics, San Diego, CA) with scaled fold changes [$\log_2$ (foldchange)] on the *X*-axis, and value of ps [$-\log_{10}$ (value of *p*)] scaled on *Y*-axis. **(I)** The Venn diagram shows significant upregulated genes ($p<0.05$, fold change 1.7F) in control comparisons, with unique genes specific to that comparison in outer rings. This Venn analysis identified 30 upregulated genes that were found exclusively in the SR vs. SS comparison. **(J)** Overlap of downregulated genes showed fewer total genes in the SR vs. SS comparison. There was also a higher number of 354 downregulated genes in the SS vs. CT comparison. **(K)** Functional annotation analysis of differentially expressed genes (DEGs), using DAVID bioinformatics database, revealed their functional classifications. Prominent among these annotations were transmembrane function, cell signaling, ion transport, and cell adhesion molecules. **(L)** Heatmap illustrating fold changes between pair-wise comparisons of DEGs that met the criterion of 1.7-fold-change and $p<0.05$, with blue to purple indicating downregulated gene expression, and red to orange indicating increased gene expression.

and *p*-values of 0.05. We found that 30 upregulated genes (Figure 2I) and 9 downregulated genes (Figure 2J) were unique to the SR vs. SS comparison. Figures 2I,J showed very little overlaps between the pairwise comparisons.

We used DAVID gene functional annotation tool (DAVID Bioinformatics) to examine functional classifications for the significant DEGs among the eight comparisons (Figure 2K). The DEGs fall within functional classes that included cell signaling, metal-binding, transport of ions, calcium signaling, and cell adhesion (Figure 2K). Figure 2L shows a heatmap (GraphPad Prism) that illustrates relative changes in mRNA expression in the 8 pair-wise comparisons.

Kyoto encyclopedia of genes and genomes pathway and Sankey analyses of differentially expressed genes in the hippocampus of compulsive and non-compulsive rats

Kyoto encyclopedia of genes and genomes pathway analysis was also used to further identify relevant pathways that were differentially impacted in the compulsive and non-compulsive rats. Many DEGs participated in pathways related to neuronal ligand-receptor interactions, neuroinflammation, metabolism and absorption, and CAMs (Figure 3A).

We used Sankey diagrams to further show the interactions of up- (Figure 3B) and downregulated (Figure 3C) genes located in various KEGG pathways. The diagrams show that single genes that participate in multiple functions in the hippocampus are impacted by compulsive METH taking behaviors.

Compulsive methamphetamine self-administration increased hippocampal expression of cell adhesion molecules

We also used Ingenuity Pathway Analysis (IPA) to identify biological networks affected by METH SA and foot-shocks (Figures 4A,B). Figure 4A showed upregulation of glycosylation dependent cell adhesion molecule (*Glycam1)* and myelin protein zero-like 2 (*Mpzl2*) in the comparison between the shock-resistant vs. -sensitive rats. Figure 4B showed that there was increased expression of L-dopachrome Tautomerase (*Dct*) in the resistant group in comparison to the sensitive rats.

To further validate the RNA sequencing results, we ran qRT-PCR using primers for some CAMs of interest. The PCR

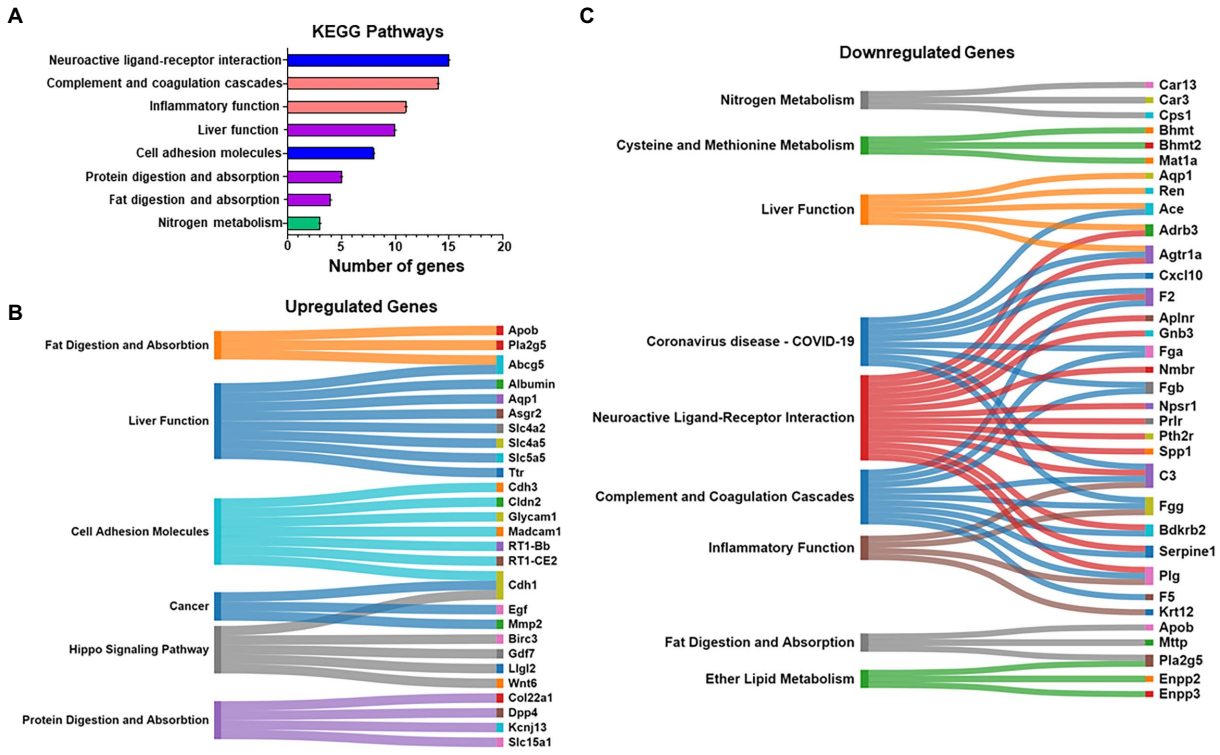

FIGURE 3
(A) Kyoto Encyclopedia of Genes and Genomes (KEGG) pathway analysis was also performed on the DEGs of all the eight pair-wise comparisons similar to the *Heatmap* in Figure 2L. A pathway prominently highlighted was cell adhesion molecules (CAMs). **(B,C)** The list of mapped genes included in the above KEGG pathways is represented as Sankey diagrams (Sankomatic.com) that display overlap of up- **(B)** and downregulated **(C)** genes involved in shared and unique KEGG pathways.

results showing fold-changes in mRNA levels are shown in Figures 4C–H. *Cdh1* (cadherin 1), a member of the cadherin family of CAMs was significantly decreased [$F_{(4,26)} = 3.445$; $p = 0.0219$] in the SS group compared to SR (Figure 4C). *Mpzl2* [$F_{(4,25)} = 9.393$; $p < 0.0001$], *Glycam1* [$F_{(4,23)} = 18.62$; $p < 0.0001$], and *Dct* [$F_{(4,27)} = 6.290$; $p < 0.0010$], all showed significant increases in the compulsive group in comparison to the other groups (Figures 4E–G).

Discussion

The main findings of these experiments are: (*i*) all METH taking rats increased their active lever pressing for the drug during METH SA training. The application of contingent foot-shocks caused clear separation of rats into compulsive/SR and non-compulsive/SS rats; (*ii*) RNA sequencing identified 354 DEGs that met the criterion of ±1.7-fold changes at $p < 0.05$. We found further that (*iii*) the DEGs were involved in cell signaling, and binding and transport of ions, or were CAMs; (*iv*) IPA helped to highlight networks that included *Glycam1*, *Mpzl2*, and *Dct*. Below, we discuss the potential roles of hippocampal CAMs in mediating compulsive METH taking by rats in the presence of adverse consequences.

The observed differences in *Cdh1* mRNA expression between the compulsive and non-compulsive rats are reminiscent, in part, of the results of our previous microarray experiments that identified increased expression of cadherin 4 (*Cdh4*) mRNA in the dorsal striatum of compulsive rats (Krasnova et al., 2017). Together, these results suggest that members of that family of genes might be involved in promoting drug taking behaviors in the presence of foot-shock punishment. Cadherins are a family of transmembrane protein characterized by 5 CDH repeats that participate in calcium-regulated interactions (Troyanovsky, 2022). These proteins also play important roles in synaptic changes involved in learning and memory *via* their interactions with beta-catenin (Bozdagi et al., 2000; Huber et al., 2001). In addition, cadherins interact directly and indirectly with AMPA receptors (Saglietti et al., 2007; Silverman et al., 2007). Therefore, the significant decreases in Cdh1 mRNA expression in the non-compulsive rats suggest the possibility that continued compulsive behaviors observed even during

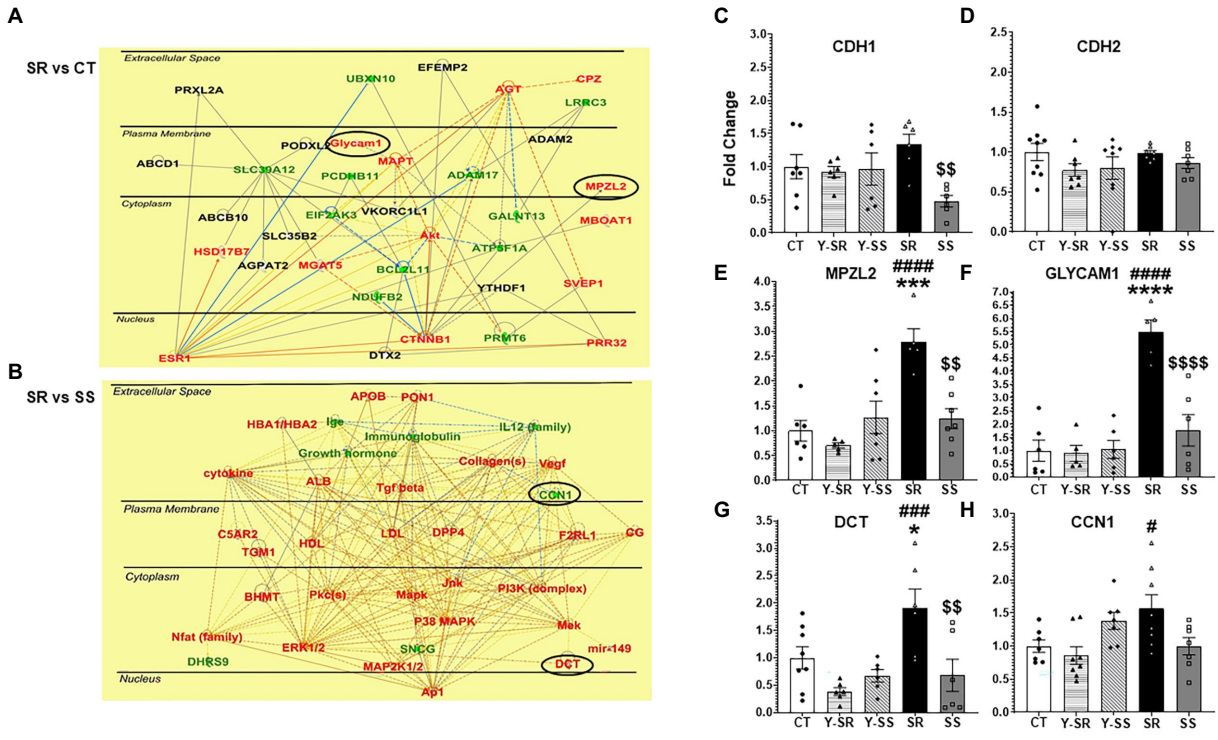

FIGURE 4
(A) Ingenuity Pathway Analysis (IPA, www.qiagen.com/ingenuity) shows the pathways that included CAMs like *Glycam1* and *Mpzl2* that exhibited higher mRNA expression in compulsive SR rats compared to CT rats. **(B)** IPA also illustrates other genes that *Dct* and *Ccn1* interact with. The red color represents upregulated transcripts whereas the green color represents downregulated transcripts. **(C–H)** We used qRT-PCR to validate the changes in some CAM-related transcripts identified by the sequencing experiments. The data in the bar graphs are shown as fold-changes in comparison to control. *Key to statistics:* *significant to CT, #significant to paired YSR/YSS, $significant between SR and SS; *p-values*: *$p<0.05$, **$p<0.01$, ***$p<0.001$, ****$p<0.0001$.

punishment might be dependent, in part, to normal functioning of the cadherin-beta catenin adhesion complex.

We found, in addition, that *Mpzl2/Eva1* mRNA expression is increased in the compulsive rats in comparison to the other groups including the non-compulsive rats (see Figure 4E). *Mpzl2/Eva1* is highly expressed in the epithelial cells of choroid plexus and helps to regulate the permeability of the blood/cerebrospinal fluid barrier (Chatterjee et al., 2008). Although *Mpzl2/Eva1* expression has not been studied extensively in the peripheral or central nervous system, except for studies on its role in hearing loss (Bademci et al., 2018; Wesdorp et al., 2018), upregulation of *Mpzl2* expression has been reported in the substantia nigra (SN) in a MPTP mouse model of Parkinson's disease (PD) using microarray analyses (Yeo et al., 2015). *Cdh1* expression was also increased by MPTP. When taken together with our present results in the compulsive rats, these results suggest that *Cdh1* and *Mpzl2/Eva1* might be co-regulated by substances that impact dopaminergic systems in the brain. It remains to be determined to what extent these two proteins might work in concert in the hippocampus to cause neuroadaptive changes that might affect compulsive drug taking.

The mRNA of another well-known CAM, *Glycam1*, was also upregulated in the hippocampus of compulsive rats, with this mRNA showing the highest fold change (5.5-fold; compare Figures 4E–G). Glycam1 is a sialomucin-like ligand for L-selectin (Imai et al., 1991; Lasky et al., 1992). It is involved in the regulation of inflammatory responses *via* its interaction with L-selectin (Ivetic et al., 2019). These observations support the notion that METH use disorder might involve the activation of neuroinflammatory cascades in the brain (Sekine et al., 2008; Agarwal et al., 2022), with METH-induced neuroinflammation being responsible, in part, for the learning and memory deficits reported in patients with MUD (Moszczynska and Callan, 2017; Paulus and Stewart, 2020). Neuroinflammation-induced changes in the basic processes that regulate synaptic plasticity (Cornell et al., 2022; Mancini et al., 2022) might also promote the perpetuation of substance use disorders.

The paper has some limitations. One of the limitations has to do with our use of only male rats in the present study. The accumulated evidence indicates that there exist sex-dependent differences in the behavioral and molecular consequences of METH self-administration (Daiwile et al., 2021, 2022a,b). Although many studies use male rodents to investigate molecular and biochemical mechanisms of substance use disorders (SUDs), the evidence is clear that there exist sex differences in the clinical courses and responses to therapies in those populations (McHugh et al., 2018, 2021). Sex differences in animal models of SUDs have also been reviewed (Quigley et al., 2021). Cadet (2021) has suggested that these differences might be dependent on both neurobiological and psychosocial/environmental determinants of SUDs. Sexual dimorphism was proposed to probably be secondary to potential interactions of licit and illicit substances with endogenous systems that might show baseline sex-based differences (Cadet, 2021). These ideas were supported by the work of Daiwile et al. (2022b) that had documented baseline differences in stress-related genes (2021) and in markers of dopaminergic systems in some brain regions. Daiwile et al. (2022a) have reviewed these issues in great length in the case of METH, and previous studies from our laboratory have investigated sex differences in some genes (Daiwile et al., 2021). Future studies have already been planned for us to measure regional and more global transcriptional responses in rats of both sexes.

Another limitation in the present study is that we measured gene expression in whole tissue collected from the hippocampus. This approach did not allow us to specify whether the changes were occurring in cells of specific neuronal or glial phenotypes or in specific hippocampal sub-regions. Given the importance of cellular diversity in various brain sub-regions of brain structures, we have been engaged in discussions to conduct these types of investigations in our future studies.

In conclusion, overexpression of cell adhesion genes in compulsive METH SA may influence hippocampus-based molecular changes affecting learning and memory processes in repeated METH users. These changes could include differences in synaptic plasticity and neurotransmission in the hippocampus and cause cognitive impairments (Huntley et al., 2002; Golsorkhdan et al., 2020). These cognitive changes might influence responses to treatment as well as relapses to drug seeking and taking behaviors. Future studies will focus on elucidating the manner by which CAMs might impact compulsive METH taking by measuring and manipulating their expression in specific cellular phenotypes of both sexes.

Data availability statement

The datasets presented in this study can be found in online repositories. The names of the repository/repositories and accession number(s) can be found at: https://www.ncbi.nlm.nih.gov/geo/, GSE203268.

Ethics statement

The animal study was reviewed and approved by National Institutes of Health (NIH) Guide for the Care and Use of Laboratory Animals (ISBN: 978-0-309-15401-7) and the study was approved by the National Institute of Drug Abuse Animal Care and Use Committee.

Author contributions

JC and SJ conceived the study and designed the methodology. SJ and CM analyzed the differential expressed genes of the RNA sequencing data obtained from GeneWiz. CM performed the RT-PCR experiments and wrote the first draft of the article with

contributions from SJ. SJ and BL performed the behavioral experiment. JC reviewed the final manuscript. All authors contributed to the article and approved the submitted version.

Funding

This research was supported by funds of the Intramural Research Program of the DHHS/NIH/NIDA.

Acknowledgments

We thank Michael Mccoy for submitting the RNA sequencing data onto the NCBI GEO website.

Conflict of interest

The authors declare that the research was conducted without any commercial or financial relationships that could be construed as a potential conflict of interest.

Publisher's note

References

Agarwal, K., Manza, P., Chapman, M., Nawal, N., Biesecker, E., McPherson, K., et al. (2022). Inflammatory markers in substance use and mood disorders: a neuroimaging perspective. *Front. Psych.* 13:863734. doi: 10.3389/fpsyt.2022.863734

American Psychiatric Association. (2022). *Dsm-5-text revision 5th Ed. (diagnostic and statistical manual of mental disorders)* 5th Edition, eds. D. J. Kupfer and D. A. Regier. Washington DC: American Psychiatric Association Generic.

Bademci, G., Abad, C., Incesulu, A., Rad, A., Alper, O., Kolb, S. M., et al. (2018). MPZL2 is a novel gene associated with autosomal recessive non-syndromic moderate hearing loss. *Hum. Genet.* 137, 479–486. doi: 10.1007/s00439-018-1901-4

Bozdagi, O., Shan, W., Tanaka, H., Benson, D. L., and Huntley, G. W. (2000). Increasing numbers of synaptic puncta during late-phase LTP. *Neuron* 28, 245–259. doi: 10.1016/s0896-6273(00)00100-8

Cadet, J. L. (2021). Sex in the nucleus accumbens: ΔFosB, addiction, and affective states. *Biol. Psychiatry* 90, 508–510. doi: 10.1016/j.biopsych.2021.08.002

Cadet, J. L., Krasnova, I. N., Walther, D., Brannock, C., Ladenheim, B., McCoy, M. T., et al. (2016). Increased expression of proenkephalin and prodynorphin mRNAs in the nucleus accumbens of compulsive methamphetamine taking rats. *Sci. Rep.* 6:37002. doi: 10.1038/srep37002

Cadet, J. L., Patel, R., and Jayanthi, S. (2019). Compulsive methamphetamine taking and abstinence in the presence of adverse consequences: epigenetic and transcriptional consequences in the rat brain. *Pharmacol. Biochem. Behav.* 179, 98–108. doi: 10.1016/j.pbb.2019.02.009

Chatterjee, G., Carrithers, L. M., and Carrithers, M. D. (2008). Epithelial V-like antigen regulates permeability of the blood–CSF barrier. *Biochem. Biophys. Res. Commun.* 372, 412–417. doi: 10.1016/j.bbrc.2008.05.053

Chojnacki, M. R., Jayanthi, S., and Cadet, J. L. (2020). Methamphetamine pre-exposure induces steeper escalation of methamphetamine self-administration with consequent alterations in hippocampal glutamate AMPA receptor mRNAs. *Eur. J. Pharmacol.* 889:173732. doi: 10.1016/j.ejphar.2020.173732

Cornell, J., Salinas, S., Huang, H. Y., and Zhou, M. (2022). Microglia regulation of synaptic plasticity and learning and memory. *Neural Regen. Res.* 17, 705–716. doi: 10.4103/1673-5374.322423

Cotman, C. W., Hailer, N. P., Pfister, K., Soltesz, I., and Schachner, M. (1998). Cell adhesion molecules in neural plasticity and pathology: similar mechanisms, distinct organizations? *Prog. Neurobiol.* 55, 659–669. doi: 10.1016/s0301-0082(98)00025-2

Daiwile, A. P., Jayanthi, S., and Cadet, J. L. (2021). Sex- and brain region-specific changes in gene expression in male and female rats as consequences of methamphetamine self-administration and abstinence. *Neuroscience* 452, 265–279. doi: 10.1016/j.neuroscience.2020.11.025

Daiwile, A. P., Jayanthi, S., and Cadet, J. L. (2022a). Sex differences in methamphetamine use disorder perused from pre-clinical and clinical studies: potential therapeutic impacts. *Neurosci. Biobehav. Rev.* 137:104674. doi: 10.1016/j.neubiorev.2022.104674

Daiwile, A. P., Sullivan, P., Jayanthi, S., Goldstein, D. S., and Cadet, J. L. (2022b). Sex-specific alterations in dopamine metabolism in the brain after methamphetamine self-administration. *Int. J. Mol. Sci.* 23:4353. doi: 10.3390/ijms23084353

Gnanapavan, S., and Giovannoni, G. (2013). Neural cell adhesion molecules in brain plasticity and disease. *Mult. Scler. Relat. Disord.* 2, 13–20. doi: 10.1016/j.msard.2012.08.002

Golsorkhdan, S. A., Boroujeni, M. E., Aliaghaei, A., Abdollahifar, M. A., Ramezanpour, A., Nejatbakhsh, R., et al. (2020). Methamphetamine administration impairs behavior, memory and underlying signaling pathways in the hippocampus. *Behav. Brain Res.* 379:112300. doi: 10.1016/j.bbr.2019.112300

Han, B., Compton, W. M., Jones, C. M., Einstein, E. B., and Volkow, N. D. (2021). Methamphetamine use, methamphetamine use disorder, and associated overdose deaths among United States adults. *JAMA Psychiat.* 78, 1329–1342. doi: 10.1001/jamapsychiatry.2021.2588

Huber, A. H., Stewart, D. B., Laurents, D. V., Nelson, W., and Weis, W. I. (2001). The cadherin cytoplasmic domain is unstructured in the absence of β-catenin. *J. Biol. Chem.* 276, 12301–12309. doi: 10.1074/jbc.m010377200

Huntley, G. W., Gil, O., and Bozdagi, O. (2002). The cadherin family of cell adhesion molecules: multiple roles in synaptic plasticity. *Neuroscientist* 8, 221–233. doi: 10.1177/1073858402008003008

Imai, Y., Singer, M. S., Fennie, C., Lasky, L. A., and Rosen, S. D. (1991). Identification of a carbohydrate-based endothelial ligand for a lymphocyte homing receptor. *J. Cell Biol.* 113, 1213–1221. doi: 10.1083/jcb.113.5.1213

Ivetic, A., Hoskins Green, H. L., and Hart, S. J. (2019). L-selectin: a major regulator of leukocyte adhesion, migration and signaling. *Front. Immunol.* 10:1068. doi: 10.3389/fimmu.2019.01068

Jayanthi, S., Daiwile, A. P., and Cadet, J. L. (2021). Neurotoxicity of methamphetamine: Main effects and mechanisms. *Exp. Neurol.* 344:113795. doi: 10.1016/j.expneurol.2021.113795

Jayanthi, S., Ladenheim, B., Sullivan, P., McCoy, M. T., Krasnova, I. N., Goldstein, D. S., et al. (2022). Biochemical neuroadaptations in the rat striatal dopaminergic system after prolonged exposure to methamphetamine self-administration. *Int. J. Mol. Sci.* 23:10092. doi: 10.3390/ijms231710092

Jones, C. M., Han, B., Seth, P., Baldwin, G., and Compton, W. M. (2022). Increases in methamphetamine injection among treatment admissions in the U.S. *Addict. Behav.* 136:107492. doi: 10.1016/j.addbeh.2022.107492

Krasnova, I. N., Gerra, M. C., Walther, D., Jayanthi, S., Ladenheim, B., McCoy, M. T., et al. (2017). Compulsive methamphetamine taking in the presence of punishment is associated with increased oxytocin expression in the nucleus accumbens of rats. *Sci. Rep.* 7:8331. doi: 10.1038/s41598-017-08898-8

Lasky, L. A., Singer, M. S., Dowbenko, D., Imai, Y., Henzel, W. J., Grimley, C., et al. (1992). An endothelial ligand for L-selectin is a novel mucin-like molecule. *Cells* 69, 927–938. doi: 10.1016/0092-8674(92)90612-g

Mancini, A., de Iure, A., and Picconi, B. (2022). "Basic mechanisms of plasticity and learning" in *Handbook of clinical neurology*, eds. M. J. Aminoff, F. Boller and D. F. Swaab (Elsevier) vol. *184* doi: 10.1016/b978-0-12-819410-2.00002-3

McHugh, R. K., Nguyen, M. D., Chartoff, E. H., Sugarman, D. E., and Greenfield, S. F. (2021). Gender differences in the prevalence of heroin and opioid analgesic misuse in the United States, 2015–2019. *Drug Alcohol Depend.* 227:108978. doi: 10.1016/j.drugalcdep.2021.108978

McHugh, R. K., Votaw, V. R., Sugarman, D. E., and Greenfield, S. F. (2018). Sex and gender differences in substance use disorders. *Clin. Psychol. Rev.* 66, 12–23. doi: 10.1016/j.cpr.2017.10.012

Moszczynska, A., and Callan, S. P. (2017). Molecular, behavioral, and physiological consequences of methamphetamine neurotoxicity: implications for treatment. *J. Pharmacol. Exp. Ther.* 362, 474–488. doi: 10.1124/jpet.116.238501

Muskiewicz, D. E., Uhl, G. R., and Hall, F. S. (2018). The role of cell adhesion molecule genes regulating neuroplasticity in addiction. *Neural Plast.* 2018, 1–17. doi: 10.1155/2018/9803764

Paulus, M. P., and Stewart, J. L. (2020). Neurobiology, clinical presentation, and treatment of methamphetamine use disorder. *JAMA Psychiat.* 77, 959–966. doi: 10.1001/jamapsychiatry.2020.0246

Paxinos, G., and Watson, C. (2013). *The rat brain in stereotaxic coordinates* Amsterdam: Elsevier Academic Press.

Quigley, J. A., Logsdon, M. K., Turner, C. A., Gonzalez, I. L., Leonardo, N., and Becker, J. B. (2021). Sex differences in vulnerability to addiction. *Neuropharmacology* 187:108491. doi: 10.1016/j.neuropharm.2021.108491

Saglietti, L., Dequidt, C., Kamieniarz, K., Rousset, M. C., Valnegri, P., Thoumine, O., et al. (2007). Extracellular interactions between Glu R2 and N-cadherin in spine regulation. *Neuron* 54, 461–477. doi: 10.1016/j.neuron.2007.04.012

Sekine, Y., Ouchi, Y., Sugihara, G., Takei, N., Yoshikawa, E., Nakamura, K., et al. (2008). Methamphetamine causes microglial activation in the brains of human abusers. *J. Neurosci.* 28, 5756–5761. doi: 10.1523/jneurosci.1179-08.2008

Shukla, M., and Vincent, B. (2021). Methamphetamine abuse disturbs the dopaminergic system to impair hippocampal-based learning and memory: An overview of animal and human investigations. *Neurosci. Biobehav. Rev.* 131, 541–559. doi: 10.1016/j.neubiorev.2021.09.016

Silverman, J. B., Restituito, S., Lu, W., Lee-Edwards, L., Khatri, L., and Ziff, E. B. (2007). Synaptic Anchorage of AMPA receptors by Cadherins through neural Plakophilin-related arm protein AMPA receptor-binding protein complexes. *J. Neurosci.* 27, 8505–8516. doi: 10.1523/jneurosci.1395-07.2007

Subu, R., Jayanthi, S., and Cadet, J. L. (2020). Compulsive methamphetamine taking induces autophagic and apoptotic markers in the rat dorsal striatum. *Arch. Toxicol.* 94, 3515–3526. doi: 10.1007/s00204-020-02844-w

Troyanovsky, S. M. (2022). Adherens junction: the ensemble of specialized cadherin clusters. *Trends Cell Biol.* doi: 10.1016/j.tcb.2022.08.007

UNODC (United Nations Office on Drug and Crime) (2022). *World drug report 2022*. Available at: https://www.unodc.org/unodc/en/data-and-analysis/wdr2022_annex.html

Wesdorp, M., Murillo-Cuesta, S., Peters, T., Celaya, A. M., Oonk, A., Schraders, M., et al. (2018). MPZL2, encoding the epithelial junctional protein myelin protein zero-like 2, is essential for hearing in man and mouse. *Am. J. Hum. Genet.* 103, 74–88. doi: 10.1016/j.ajhg.2018.05.011

Yeo, S., An, K. S., Hong, Y. M., Choi, Y. G., Rosen, B., Kim, S. H., et al. (2015). Neuroprotective changes in degeneration-related gene expression in the substantia nigra following acupuncture in an MPTP mouse model of parkinsonism: microarray analysis. *Genet. Mol. Biol.* 38, 115–127. doi: 10.1590/s1415-475738120140137

frontiers | Frontiers in Molecular Neuroscience

TYPE Original Research
PUBLISHED 25 January 2023
DOI 10.3389/fnmol.2023.1105388

OPEN ACCESS

EDITED BY
Vidhya Kumaresan,
Boston University,
United States

REVIEWED BY
Jean Lud Cadet,
National Institute on Drug Abuse (NIH),
United States
Jérémie Naudé,
Centre National de la Recherche Scientifique,
France

*CORRESPONDENCE
Ana Domi
✉ ana.domi@gu.se

SPECIALTY SECTION
This article was submitted to Neuroplasticity and Development, a section of the journal Frontiers in Molecular Neuroscience

RECEIVED 22 November 2022
ACCEPTED 09 January 2023
PUBLISHED 25 January 2023

CITATION
Domi A, Lucente E, Cadeddu D and Adermark L (2023) Nicotine but not saline self-administering or yoked control conditions produces sustained neuroadaptations in the accumbens shell.
Front. Mol. Neurosci. 16:1105388.
doi: 10.3389/fnmol.2023.1105388

Nicotine but not saline self-administering or yoked control conditions produces sustained neuroadaptations in the accumbens shell

Ana Domi[1,2]*, Erika Lucente[1], Davide Cadeddu[1] and Louise Adermark[1,2]

[1]Department of Pharmacology, Institute of Neuroscience and Physiology, The Sahlgrenska Academy, University of Gothenburg, Gothenburg, Sweden, [2]Addiction Biology Unit, Department of Psychiatry and Neurochemistry, Institute of Neuroscience and Physiology, The Sahlgrenska Academy, University of Gothenburg, Gothenburg, Sweden

Introduction: Using yoked animals as the control when monitoring operant drug-self-administration is considered the golden standard. However, instrumental learning *per se* recruits several neurocircuits that may produce distinct or overlapping neuroadaptations with drugs of abuse. The aim of this project was to assess if contingent responding for nicotine or saline in the presence of a light stimulus as a conditioned reinforcer is associated with sustained neurophysiological adaptations in the nucleus accumbens shell (nAcS), a brain region repeatedly associated with reward related behaviors.

Methods: To this end, nicotine-or saline-administrating rats and yoked-saline stimulus-unpaired training conditions were assessed in operant boxes over four consecutive weeks. After four additional weeks of home cage forced abstinence and subsequent cue reinforced responding under extinction conditions, *ex vivo* electrophysiology was performed in the nAcS medium spiny neurons (MSNs).

Results: Whole cell recordings conducted in voltage and current-clamp mode showed that excitatory synapses in the nAcS were altered after prolonged forced abstinence from nicotine self-administration. We observed an increase in sEPSC amplitude in animals with a history of contingent nicotine SA potentially indicating higher excitability of accumbal MSNs, which was further supported by current clamp recordings. Interestingly no sustained neuroadaptations were elicited in saline exposed rats from nicotine associated visual cues compared to the yoked controls.

Conclusion: The data presented here indicate that nicotine self-administration produces sustained neuroadaptations in the nAcS while operant responding driven by nicotine visual stimuli has no long-term effects on MSNs in nAcS.

KEYWORDS

nicotine, electrophysiology, whole-cell recording, operant self-administration, abstinence, conditioned stimuli (cues), smoking

Introduction

Self-administration (SA) of drugs of abuse has been widely used as a preclinical investigative tool to study behavioral, neurobiological, and genetic factors associated with drug addiction (Spealman and Goldberg, 1978; Panlilio and Goldberg, 2007). Besides the drug consummatory

response, operant self-administration paradigms evaluate, appetitive and motivational components of drug seeking, taking and relapse (for review see Belin-Rauscent et al., 2016). Nicotine, the main component of tobacco smoke, is highly addictive in humans and intravenous nicotine self-administration (IVSA) is considered the gold standard for studying the rewarding and motivational aspects of the drug in rodents (Donny et al., 1995; Palmatier et al., 2006; Henningfield et al., 2016).

A widely-used procedure for demonstrating specificity of effect during drug self-administration sessions is to include a yoked control condition that passively receives either the psychoactive drug or saline (Lecca et al., 2007; Mathieson et al., 2022). Generally, a yoked-saline design is used as a control when assessing for the pharmacological effects of nicotine and possible neuroadaptations elicited by the drug (Palmatier et al., 2007; Gipson et al., 2013b; Pittenger et al., 2018; Jin et al., 2020). However, more than in any other drug of abuse, the reinforcing properties of nicotine are strongly driven by paired sensory stimuli that through associative learning processes maintain smoking behavior (Caggiula et al., 2001; Bevins and Palmatier, 2004; Markou and Paterson, 2009). In the yoked-saline control there is not Pavlovian conditioning and instrumental performance such as nose-poking or pressing a lever has no consequences. Conversely, a saline self-administering group can be used to control for neurophysiological transformations that may be shielded by neuroadaptations produced when conditioned visual cues are associated with operant responding. As a matter of fact, saline self-administering rats that respond for nicotine associated visual cues, present a stimulus-driven operant learning and are able to discriminate between active (rewarded) and inactive (non-rewarded) responses (Donny et al., 2003; Garcia-Rivas et al., 2019).

When learning to lever press for nicotine in the presence of contingent visual stimuli, several brain regions involved in instrumental learning or stimulus–response associations are recruited (for review see Schmidt et al., 2019). In particular the nucleus accumbens (nAc) appears to play a central role in the way reward-related cues influence instrumental performance (Corbit et al., 2001; Di Ciano et al., 2008). Lesions and pharmacological manipulations of the nAc impair the ability of conditioned stimuli (CS) to promote operant responding for psychostimulants (Ito et al., 2004; Di Ciano et al., 2008; Floresco et al., 2008). For instance, response-contingent nicotine SA paired with a visual stimulus preferentially increases the dopamine output in the nAc shell (nAcS) as compared to that in the core subdivision, at different training periods but not following extinction (Lecca et al., 2006).

Changes in dopaminergic activity in the nAcS seem to involve mGluR 2/3 receptors signaling (Karasawa et al., 2006; Liechti et al., 2007; Karasawa et al., 2010) and during nicotine intake and withdrawal there is an interplay between compensatory mechanisms involving mGluR 2/3 and AMPA/kainite receptor within the mesolimbic dopamine pathway (Kenny et al., 2003; Liechti et al., 2007). In fact, mGluR2/3 in nAcS has been proposed to be involved in mediating the rewarding effects of nicotine and potentially also in cue-induced nicotine-seeking behavior (Liechti et al., 2007). Furthermore, accumbal AMPA receptor signaling has been shown to play a role both cue-induced nicotine seeking behavior (Gipson et al., 2013b), as well as cocaine seeking behavior (Gipson et al., 2013a), and changes in calcium-permeable AMPARs are associated with incubation of cocaine and methamphetamine craving (Conrad et al., 2008; Scheyer et al., 2016; Murray et al., 2019). Studies outlining nicotine-induced glutamatergic neuroplasticity in the accumbens may thus be important for defining neurobiological mechanisms underlying reinstatement to nicotine-cues.

In the present study we assessed long-lasting changes in nAcS neurotransmission elicited by nicotine operant self-administration in the presence of environmental stimuli. We controlled both for the pharmacological effects of nicotine using yoked-saline rats and for the effects of the nicotine associated visual cues using a group that self-administered saline in an identical environment. *Ex vivo* whole-cell patch-clamp and field potential electrophysiological recordings were conducted in the nAcS 1 month after discontinuing nicotine self-administration.

Materials and methods

Animals

Male Wistar rats (Charles River, Germany), 150–170 g at arrival, were paired-housed in a temperature and humidity-controlled environment under a reversed 12:12-h light/dark cycle (lights off at 8:00 a.m.) with food and water *ad libitum*. Rats were habituated to the facility and handled prior to experiments. Experiments were conducted during the dark phase of the cycle and all efforts were made to minimize rats' suffering and distress. Procedures were conducted in accordance with the National Committee for Animal Research in Sweden and approved by the Local Ethics Committee for Animal Care and Use at Gothenburg University.

Drugs

The (−)-Nicotine hydrogen tartrate salt (Sigma-Aldrich, St. Louis, MO) was dissolved in sterile physiological saline and administered intravenously at a concentration of 30.0 μg/kg/0.1 mL infusion. The pH of the solution was adjusted to 7.4 with NaOH 5 M. The GABAA receptor antagonist bicuculline-methiodide (bicuculline) was diluted in Milli-Q to 20 mM and further diluted in aCSF (20 μM). The NMDA receptor antagonist D-(−)-2-Amino-5-phosphonopentanoic acid (APV; 50 μM) and the AMPA receptor antagonist CNQX (10 μM) were dissolved in aCSF shortly before use. All drugs were purchased from Sigma Aldrich (Stockholm, Sweden).

Catheter implantation

Chronic jugular intravenous catheter implantation was conducted as previously described (Domi et al., 2022). Briefly, animals were anesthetized with isoflurane anesthesia: 5% induction and 2% maintenance. For intravenous surgery, incisions were made to expose the right jugular vein and a catheter made from micro-renathane tubing (ID = 0.020″, OD = 0.037″; Braintree Scientific) was positioned subcutaneously between the vein and the back. Rats were treated subcutaneously with 10 mg/kg of enrofloxacin (50 mg/mL, Baytril, Germany) for 3 days post-surgery and allowed 3 week of recovering before self-administration training. Catheters were daily flushed with 0.1–0.2 mL of sterile saline mixed with heparin (20 U/mL, Italfarmaco S.p.A, Milan, Italy) for the entire duration of the experiments. Patency of the catheters was confirmed by intravenous injection of 150 μL/rat of Sodium Pentothal (25 mg/mL, Intervet, Italy) at the end of experimental procedures.

Operant training

SA apparatus

The self-administration stations consisted of operant conditioning chambers (29.5 cm × 32.5 cm × 23.5 cm; Med Associates, St. Albans, VT) enclosed in sound-attenuating, ventilated environmental cubicles. Each chamber was equipped with two retractable levers located in the front panel with two stimulus light placed above each lever, a house light at the top of the opposite panel and a tone generator. Infusions were delivered through a system composed by an infusion pump, swivel, counterbalanced arm assembly, tether and a plastic tube that was connected to the catheter before the beginning of the session. Activation of the pump by responses in the "active lever" resulted in a delivery of 0.1 mL of fluid while responses on the "inactive" lever were recorded but did not result in any programmed consequences. An IBM compatible computer controlled the delivery of fluids and the recording of the behavioral data with MED-PC® IV windows-compatible software.

Operant self-administration

A week after surgery rats (≈70 days old) were randomly assigned to self-administer either nicotine (30 μg/kg/0.1 mL infusion) or saline (0.9% NaCl) and a third yoked-saline group was yoked to the rats that self-administered nicotine. Rats in the nicotine-SA and saline-SA group were trained for 2 h/daily (5 days/week) under Fixed Ratio 1 (FR1) contingency in which every lever response resulted in the delivery of a single dose of nicotine or saline. After 7 days in FR1 the response requirement for each infusion was then incremented to FR3 to ensure stable nicotine self-administration rates for the remainder of the training. Each infusion was followed by the activation of a cue-light above the active lever for 5-s and a total of 20-s time out period (TO) where responses at the active lever were not reinforced. The stimulus light presented to the nicotine group (nicotine associated visual stimuli) was the same for the saline-SA and yoked-saline rats. The yoked-saline rats received the identical infusion and stimulus light onsets/offsets as the animals that learned to self-inject nicotine.

The entire duration of the 120-min session was signaled by the intermittent cue-tone (1 s ON/1 s OFF; 7 kHz, 70 dB) as previously described (Cippitelli et al., 2015).

Forced abstinence and cue-reinforced responding under extinction conditions

Following training rats entered the abstinence phase in which they were left undisturbed in their home cages for 28 days. In this forced abstinence period rats were handled daily and received standard care. After this period rats were subjected to a single session of cue-reinforced responding under extinction conditions for the duration of 2 h. Pressing on the active lever resulted in illumination of the cue light above the lever under an FR3 schedule but nicotine or saline were no longer delivered. Cue responding was measured as the number of responses on the active lever throughout the test session, including during the timeout periods. Inactive lever presses were also recorded as a measure of non-specific responding.

Brain slice preparation

To obtain brain slices, rats were deeply anesthetized with isoflurane and decapitated. Brains were rapidly removed and transferred into a constantly oxygenated (95% O2, 5% CO2) modified artificial cerebrospinal fluid solution (aCSF) containing (in mM): 220 sucrose, 2 KCl, 0.2 CaCl2, 6 MgCl2, 26 NaHCO3, 1.3 NaH2PO4 and 10 D-glucose. Coronal brain slices (250 μm) containing the nAcS were obtained using a Leica VT 1200S Vibratome (Leica Microsystems AB, Bromma, Sweden), and submerged in a continuously oxygenated standard aCSF containing (in mM): 124 NaCl, 4.5 KCl, 2 CaCl2, 1 MgCl2, 26 NaHCO3, 1.2 NaH2PO4 and 10 D-glucose. After an incubation for 30 min in 33°C, slices were allowed to rest for additionally 30 min before electrophysiological recordings were performed. Slices were maintained at room temperature for the rest of the day.

Field potential recordings

Glutamatergic plasticity has been linked to behavioral transformations elicited by prolonged withdrawal from psychostimulants (Conrad et al., 2008; Ping et al., 2008; Mameli et al., 2009; McCutcheon et al., 2011), and to outline if sustained neurophysiological transformations also would be present in the nAcS after a history of nicotine SA, electrophysiological field potential recordings were performed as previously described (Adermark et al., 2011; Licheri et al., 2019). In brief, population spikes (PS) were evoked with a stimulation frequency of 0.05 Hz in the nAc shell. Stimulation electrodes (type TM33B, World Precision Instruments, Sarasota, FL) were positioned locally, 0.2–0.3 mm from the recording electrode (borosilicate glass, 2.5 to 4.5 MΩ, World Precision Instruments), and the amplitude of PSs were measured. To assess long-lasting effects by treatment on synaptic output, stimulus response curves were conducted by stepwise increasing the afferent stimulation strength creating a stimulus/response curve. To estimate changes in the probability of transmitter release, responses were evoked with a paired pulse stimulation protocol (50 ms interpulse interval), and the paired pulse ratio (PPR) was calculated by dividing the second pulse (PS2) with the first pulse (PS1).

To monitor changes in inhibitory tone, slices were treated with bicuculline (20 μM). For these measurements, the stimulus intensity was set to yield a PS amplitude of approximately half the size of the maximal amplitude of the evoked response, and a stable baseline was monitored for 10 min before drug-perfusion. Following 20 min of bath perfusion, stimulus/response curves were recorded to assess changes in synaptic output.

Whole-cell recordings

A Nikon Eclipse FN-1 microscope equipped with a 10x/0.30 objective identified the nAcS, and a 40×/0.80 water-immersion objective was used to identify medium spiny neurons (MSNs) for whole-cell recordings. Recording pipettes were prepared from borosilicate glass using a micropipette puller (Sutter Instruments, Novato, CA) with a resistance ranging from 2.5 to 5.5 MΩ. Pipettes were filled with an internal solution containing (in mM): 135 K-Glu, 20 KCl, 2 $MgCl_2$, 0.1 EGTA, 10 Hepes, 2 Mg-ATP and 0.3 Na-GTP, pH adjusted to 7.3 with KOH, and osmolarity to 295 mOsm with sucrose. Whole-cell recordings were conducted under constant flow (2 mL/min) of standard aCSF at the temperature of 33°C–34°C. To record spontaneous excitatory postsynaptic currents (sEPSCs) in voltage clamp mode, neurons were clamped at-65 mV using a MultiClamp 700B amplifier (Molecular Devices, Axon CNS, San Jose, CA), digitized at 10 kHz and filtered at 2 kHz using Clampex (Molecular devices).

In a subpopulation of these neurons, after the voltage clamp recording, a current clamp protocol was applied. Current was injected with a duration of 1,000 ms and an increasing intensity (in intervals of 20 pA) from −80 to 160 pA in order to hyperpolarize and depolarize the neuronal membrane.

Statistics and data analysis

We examined for significant violations for assumptions of homogeneity of variance by using Levene's test. Behavioral and electrophysiological data were analyzed by analysis of variance (ANOVA) with factors for the respective analysis indicated in conjunction with its results. When appropriate, *post hoc* comparisons were performed using Newman–Keuls test. Paired or unpaired Student's *t*-tests were used for statistical analysis when appropriate. Data were analyzed using STATISTICA, stat soft 13.0 (RRID:SCR_014213), Clampfit 10.2 (Molecular devices, Axon CNS, CA, United States), Minianalysis 6.0 (Synaptosoft), Microsoft Excel and GraphPad Prism 9 (GraphPad Software, San Diego, CA). All parameters are given as mean +/− SEM, and differences between groups were considered statistically significant at $p < 0.05$.

Results

Cue-maintained responding during training and reinstatement in nicotine and saline self-administering rats

Nicotine ($n = 9$) and saline ($n = 8$) rats were trained to operant responding for 7 days under FR1 schedule of reinforcement followed by 13 days on FR3 (Figure 1). A third yoked-saline group ($n = 8$) underwent passive saline administration at the same time as the animals that learned to self-inject nicotine. Analysis of active lever responses over training showed a significant effect of group [Repeated measures ANOVA: main effect group $F_{(2,22)} = 72.64$, $p < 0.0001$, session $F_{(19,418)} = 11.47$, $p < 0.0001$ and

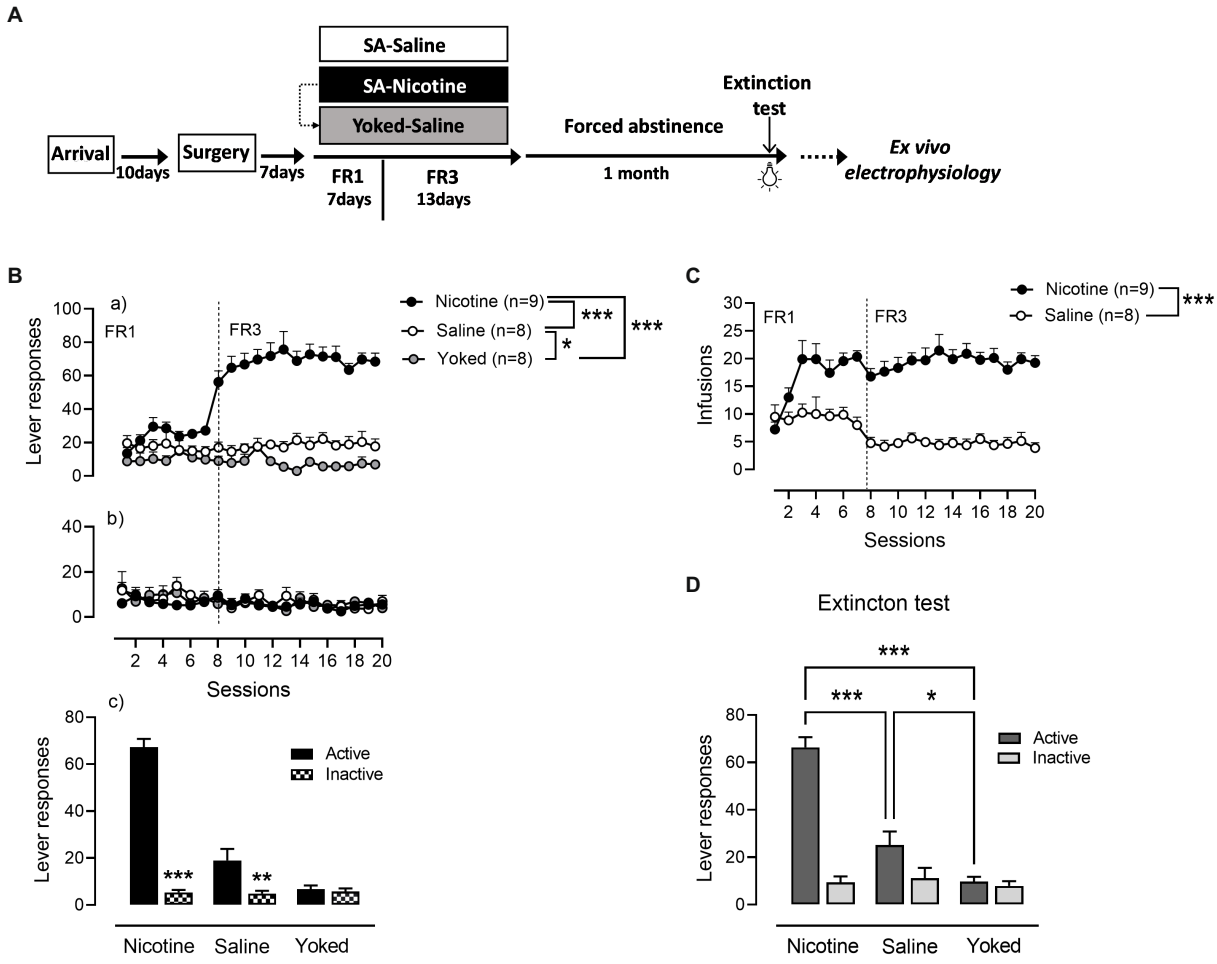

FIGURE 1
Cue-maintained responding during training and reinstatement in nicotine and saline self-administering rats. **(A)** Timeline of the experimental procedures that includes behavioral and neurophysiological assessments. **(B) (a)** During operant training nicotine-SA rats showed higher number of active lever presses over time compared to the control groups. Active responding for saline-SA rats was as well significantly higher than in yoked-saline control group. **(b)** Inactive lever pressing was very low with no differences between groups. **(c)** Both nicotine-SA and saline-SA rats discriminated between active and inactive lever presses while the yoked-saline group presented the same responding on both levers. **(C)** In accordance with the reported active lever presses, the number of infusions achieved over time was significantly higher in the rat self-administering nicotine compared to the saline-SA group. **(D)** Cue reinforced responding under extinction conditions 1 month after the last training session produced a significant higher operant responding in rats with a history of contingent nicotine-SA compared to saline-SA rats and yoked-saline control with the saline-SA group presenting higher active lever pressing than the yoked control, ***p<0.001, **p<0.01, *p<0.01.

group × session interaction $F_{(19,418)} = 13.05$, $p < 0.0001$]. As expected and demonstrated in Figures 1Ba, rats self-administering nicotine produced a higher number of active lever presses compared with the saline-SA and yoked-saline group (Newman–Keuls *post-hoc* test: N vs. S, $p = 0.0014$; N vs. Y, $p = 0.0013$). In addition, operant responding for saline produced significant increases in lever presses compared to the yoked-saline control group where lever presses were recorded but led to no consequences (S vs. Y, $p = 0.0305$). Inactive lever responses were very low and without differences between the three groups (main effect group: $F_{(2,22)} = 0.3586$, $p = 0.7026$; Figures 1Bb). However, while nicotine and saline rats were able to discriminate between levers [N_A (67.26 ± 3.51) vs. N_I (5.41 ± 1.02), $p < 0.0001$; S_A (19 ± 4.8) vs. S_I (4.83 ± 1.2), $p = 0.0042$] in yoked-saline rats the difference in pressing the active vs. the inactive lever was not significant [Y_A (6.75 ± 1.62) vs. Y_I (5.7 ± 1.34), $p = 0.7860$; Figures 1Bc]. This suggest that cue-contingency in saline-SA rats, present some intrinsic reinforcing properties in driving self-administration behavior. In accordance with the active lever responding data and the known pharmacological effects of nicotine, the number of self-infusions was significantly higher in the nicotine-SA than in the saline-SA rats [main effect group: $F_{(1,15)} = 61.99$, $p < 0.0001$; Figure 1C].

After a month of forced abstinence in their homecage rats were tested for cue-reinforced responding under extinction conditions (Figure 1D). An overall two-way ANOVA analysis yielded significant main effect of group: [$F_{(2,22)} = 24.3$, $p < 0.0001$], lever [$F_{(1,22)} = 92.74$, $p < 0.0001$] and a significant group × lever interaction [$F_{(2,22)} = 45.57$, $p < 0.0001$]. Rats with a history of nicotine SA exhibited a significant higher cue-reinforced responding as compared with rats trained with saline and yoked-saline group [N_A (66.33 ± 4.28) vs. S_A (25.13 ± 5.7), $p = 0.0001$; N_A (66.33 ± 4.28) vs. Y_A (9.75 ± 1.98), $p = 0.0001$]. In addition, cue-presentation alone during reinstatement produced a higher number of active lever presses in the saline-SA rats compared to yoked-saline rats that during training received yoked presentations of the same cue as the nicotine-SA group [S_A (25.13 ± 5.7) vs. Y_A (9.75 ± 1.98), $p = 0.0495$]. These results suggest that the conditioned-cue becomes motivationally salient not only if previously paired with a drug of abuse such as nicotine but as well with a neutral substance such as saline.

Nicotine associated visual cue does not produce sustained neuroadaptations in the nAcS when paired with saline-SA rats

During training and reinstatement rats responding for saline showed at a certain extent active lever pressing driven by nicotine visual stimuli as they distinguished between active and inactive lever. Thus, we first examined if operant responding maintained by environmental cues produces long-lasting neurophysiological transformations in the nAcS of saline-SA compared to the yoked-saline controls. To this end, electrophysiological recordings were conducted *ex vivo* in nAcS in brain slices from yoked-saline rats and saline-SA controls (Figure 2A) at least 2 days after the reinstatement test to avoid putative effects on transmission produced by the reinstatement session *per se*. Stimulus/response curves assessing evoked field potentials showed no differences between groups [main effect treatment: $F_{(1, 35)} = 0.01195$, $p = 0.9136$; time $F_{(6, 210)} = 179.7$, $p < 0.001$; time × drug: $F_{(6,210)} = 1.258$, $p = 0.2783$]. Even though there was a trend toward increased PPR in brain slices from yoked animals, the effect was not significant [Student's *t*-test: $t_{(36)} = 1.95$, $p = 0.060$; Figures 2B, C]. CNQX blocked evoked potentials showing that recorded PS amplitudes are mediated through AMPA receptor activation (Figures 2Ha).

To further outline changes in accumbal neurotransmission induced by saline self-administration, whole cell recordings were conducted in medium spiny neurons. Recordings performed in voltage clamp mode demonstrated no effect by treatment on spontaneous activity. Neither the frequency [$t_{(33)} = 0.3360$, $p = 0.7390$], nor the amplitude [amplitude $t_{(33)} = 1.342$, $p = 0.1888$; decay time: $t_{(33)} = 1.117$, $p = 0.2719$; rise-time: $t_{(33)} = 1.449$, $p = 0.1594$] of spontaneous events were significantly affected (Figures 2D–G). CNQX and APV blocked all spontaneous events suggesting that all events are excitatory (Figures 2Hb).

Nicotine self-administration followed by forced abstinence produces sustained neuroadaptations in nAc shell

Since there were no significant differences between yoked-saline and saline-SA control when assessing spontaneous activity in voltage-clamp mode, these groups were pooled to increase the number of animals assessed in each comparison. To examine if nicotine SA would produce more sustained neuroadaptations in the nAcS, we compared the control with nicotine-SA rats after 1 month of forced abstinence.

Field potential recording revealed a trend toward an increase in PS amplitude in the nAc shell of rats self-administering nicotine [main effect treatment: $F_{(1, 54)} = 3.199$, $p = 0.0793$; time $F_{(6, 324)} = 231.6$, $p < 0.001$; time × drug $F_{(6,324)} = 1.212$, $p = 0.2997$; Figures 3A, E]. PPR was not modulated by treatment [yoked/saline: 0.9871 ± 0.02117, nicotine: 0.9469 ± 0.02118; $t_{(59)} = 1.263$, $p = 0.2116$; Figure 3B]. In a way to assess inhibitory tone over evoked potentials the $GABA_A$ receptor antagonist bicuculline (20 μM) was bath perfused. Bicuculline disinhibited PS amplitude to a similar extent in both treatment groups [yoked/saline: 138.9 ± 9.001%, nicotine: 145.8 ± 12.20%; main effect treatment: $F_{(1, 43)} = 0.2253$, $p = 0.6374$; time $F_{(15, 645)} = 1.948$, $p = 0.0168$; time × drug $F_{(15, 645)} = 0.6246$, $p = 0.8559$; Figure 3C]. However, when monitoring stimulus–response curves in bicuculline-treated slices, synaptic output was significantly enhanced in rats previously receiving nicotine [main effect treatment: $F_{(1, 42)} = 5.747$, $p = 0.0210$; time $F_{(6, 252)} = 207.5$, $p < 0.001$; time × drug $F_{(6,252)} = 0.3426$, $p = 0.9138$; Figure 3D]. PPR did not differ between the treatment groups in bicuculline-treated slices [yoked/saline: 1.083 ± 0.02135, nicotine: 1.042 ± 0.01620; $t_{(44)} = 1.357$, $p = 0.1818$; data not shown].

Whole cell recordings demonstrated no significant effect on passive membrane properties. Neither membrane resistance [yoked/saline: 161.0 ± 16.96 MΩ, nicotine: 154.9 ± 18.51 MΩ; $t_{(61)} = 0.2402$, $p = 0.8110$] nor capacitance [yoked/saline: 55.97 ± 3.011 pF, nicotine: 51.31 ± 3.638 pF; $t_{(61)} = 0.3279$, $p = 0.7441$] were significantly affected by nicotine SA followed by 1 month abstinence (Figures 3F, G). Recordings of spontaneous activity demonstrated no change in the frequency of excitatory inputs [sEPSC frequency: yoked/saline: 1.336 ± 0.1510 Hz, nicotine: 1.653 ± 0.2199 Hz; $t_{(57)} = 1.231$, $p = 0.2233$; Figure 3H]. However, sEPSCs amplitude was significantly enhanced in MSNs from nicotine-exposed rats [yoked/saline: −7.552 ± 0.2276 pA, nicotine: −8.503 ± 0.3483 pA; $t_{(57)} = 2.403$, $p = 0.0195$; Figure 3I, L], with no concomitant change in rise-or decay-time [rise-time: yoked/saline: 1.394 ± 0.0762 pA, nicotine: 1.296 ± 0.0630 pA; $t_{(57)} = 0.7588$, $p = 0.4511$; decay-time: yoked/saline: 6.200 ± 0.2275 pA, nicotine: 6.043 ± 0.3616 pA; $t_{(57)} = 0.9447$, $p = 0.3488$; Figures 3H, J, K].

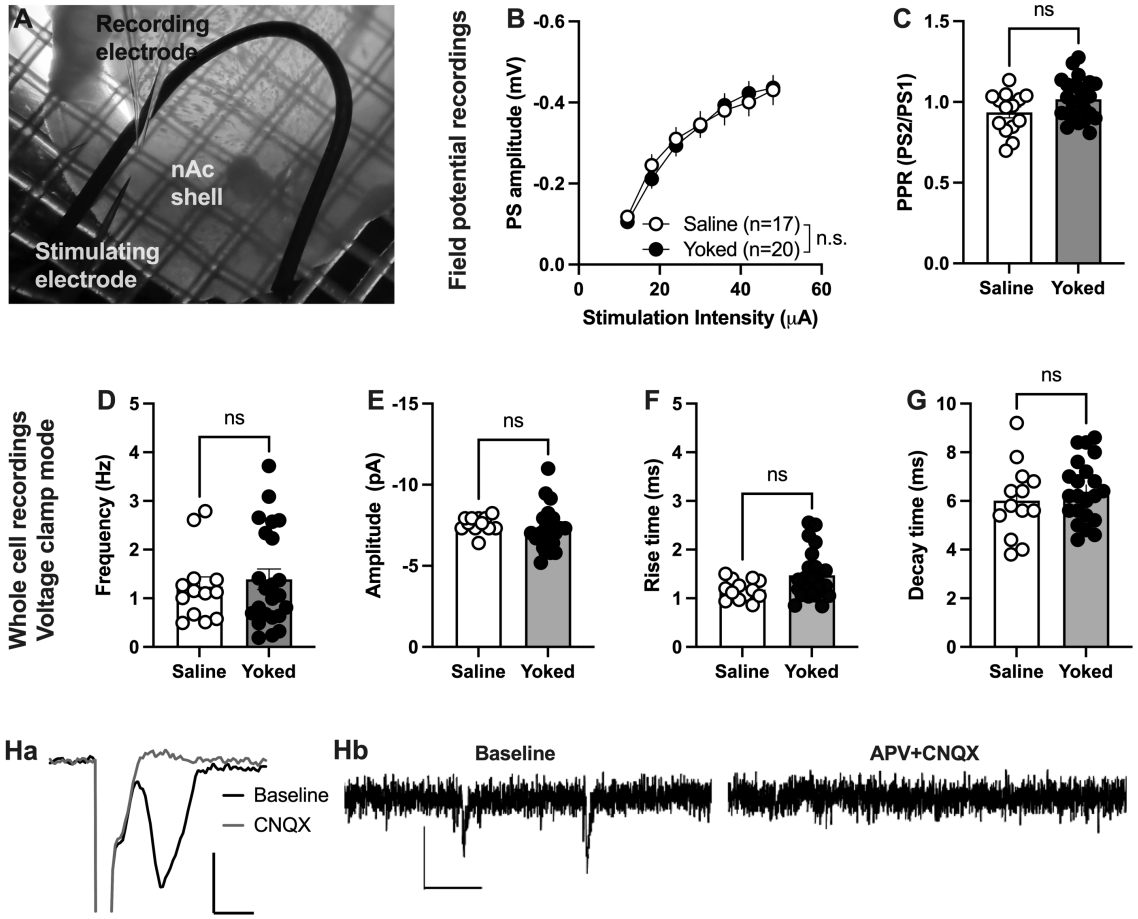

FIGURE 2
Neuronal transmission is not significantly altered in the nAcS of animals self-administering saline. **(A)** Micrograph showing the region of recording. **(B,C)** Evoked PS amplitudes were not significantly modulated by saline-self-administration, even though there was a trend toward increased PPR in brain slices from yoked-saline rats. **(D–G)** Whole cell recordings conducted in voltage clamp mode showed no effect by saline self-administration on neither frequency nor amplitude of spontaneous events. **(H)** Both evoked field potentials and sEPSCs were rapidly blocked by bath perfusion of CNQX and APV indicating that recorded activity is excitatory. Calibration: Ha: 2ms, 0.2mV. Hb: 50ms, 10 pA. Values are presented as mean (±SEM), *n*=number of slices, taken from at least four animals.

A history of nicotine self-administration produces sustained changes in accumbal MSNs excitability

The increase in sEPSC amplitude and evoked potentials indicates that a history of nicotine self-administration may act to increase excitability of accumbal MSNs that persist during prolonged abstinence. In the last set of experiments, current clamp recordings were thus performed to assess changes in excitability. Recordings from yoked animals were not significantly different compared to rats self-administrating saline [delta voltage: $F_{(1,\ 21)} = 1.395$, $p = 0.2508$; rheobase: $t_{(21)} = 0.6529$, $p = 0.5209$; threshold: $t_{(21)} = 0.9214$, $p = 0.3673$; AP latency: $F_{(1,\ 21)} = 0.1149$, $p = 0.7380$; AP frequency: $F_{(1,\ 21)} = 0.006849$, $p = 0.9348$] and the groups were thus pooled.

Membrane voltage was not significantly affected when comparing current clamp recordings performed in MSNs from yoked/saline controls with nicotine-self-administering rats [yoked/saline: −73.36 ± 1.443 mV, nicotine: −71.57 ± 0.9277 mV, student's *t*-test: $t_{(39)} = 0.9456$, $p = 0.3502$; Figure 4A]. However, the relative change in membrane voltage (delta voltage) elicited by current injection was more pronounced in MSNs from rats self-administrating nicotine [repeated measures ANOVA, main effect treatment: $F_{(1,\ 39)} = 6.097$, $p = 0.0180$; time $F_{(12,\ 468)} = 458.7$, $p < 0.0001$; time × drug $F_{(12,\ 468)} = 6.587$, $p < 0.001$; Figures 4B, C]. A trend toward decreased rheobase was found in brain slices from nicotine-exposed rats [yoked/saline: 100.9 ± 10.25 pA, nicotine: 74.44 ± 8.371 pA: $t_{(39)} = 1.920$, $p = 0.0622$] but not for threshold for action potential firing [yoked/saline: −42.03 ± 2.084 mV, nicotine: −40.48 ± 1.586 mV, $t_{(39)} = 0.5658$, $p = 0.5748$; Figures 4D,E]. Action potential firing elicited by current injection showed a trend toward increased excitability [repeated measures ANOVA, main effect treatment: $F_{(1,\ 39)} = 3.672$, $p = 0.0627$; time $F_{(7,273)} = 62.99$, $p < 0.0001$; time × drug $F_{(7,273)} = 1.237$, $p = 0.2825$; Figure 4F], and reduced latency for AP firing [repeated measures ANOVA, main effect treatment: $F_{(1,\ 39)} = 3.435$, $p = 0.0714$; time $F_{(7,\ 273)} = 70.88$, $p < 0.001$; time × drug $F_{(7,\ 273)} = 0.9778$, $p = 0.4476$; Figure 4G].

Discussion

Despite being a brain region involved in drug reinforcement, studies in the nAcS that outline neuroplasticity elicited by nicotine self-administration are scarce. In fact, this study is to our knowledge the

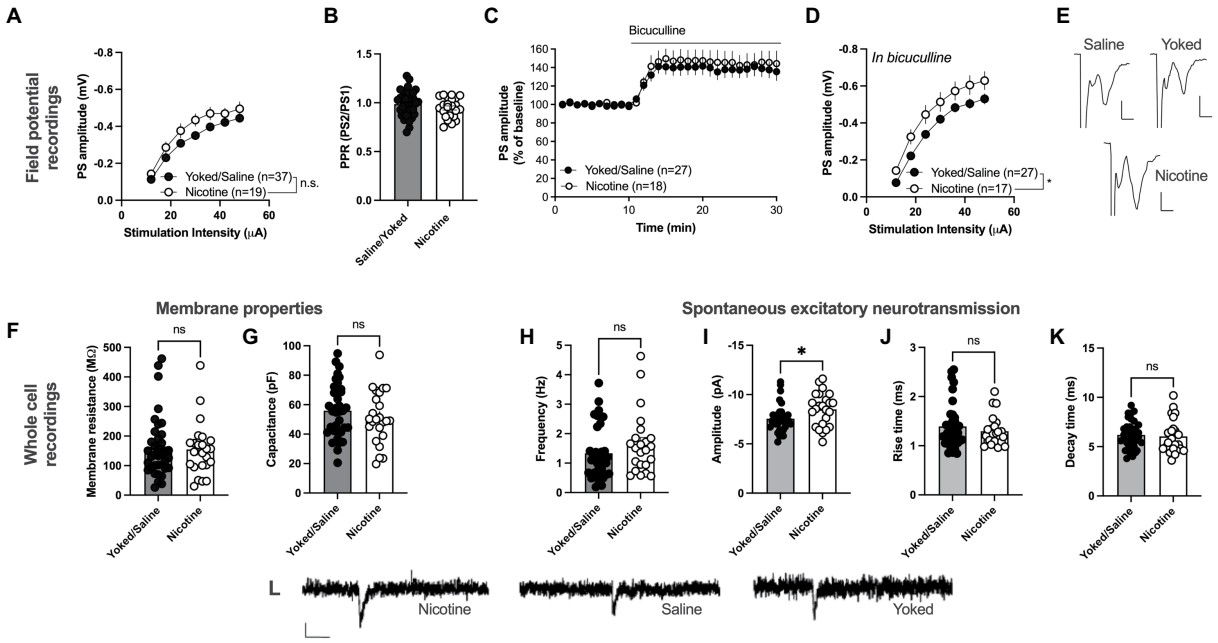

FIGURE 3
Nicotine SA increases excitatory neurotransmission in nAcS MSNs. **(A)** Field potential recordings demonstrated a trend toward potentiated stimulus–response curves in brain slices from nicotine-SA rats. **(B)** PPR was not modulated by nicotine-SA. **(C)** The GABAA receptor antagonist bicuculline disinhibited evoked potentials to a similar extent in both treatment groups. **(D)** Isolation of excitatory currents revealed a significantly enhanced stimulus–response curve in brain slices from nicotine-SA. **(E)** Example traces based on a mean of 5 traces at baseline for each treatment group. Calibration: 2ms, 0.2mV. **(F,G)** Membrane properties were not significantly modulated by treatment. **(H–K)** Recordings of spontaneous activity demonstrated a significant increase in sEPSC amplitude, indicating that nicotine-SA increases MSN responsiveness to excitatory inputs. **(L)** Example traces showing recorded sEPSCs in brain slices from all treatment groups. Calibration: 10 pA, 50ms. Values are presented as mean (±SEM), *n*=number of slices, taken from at least four animals. *$p<0.05$.

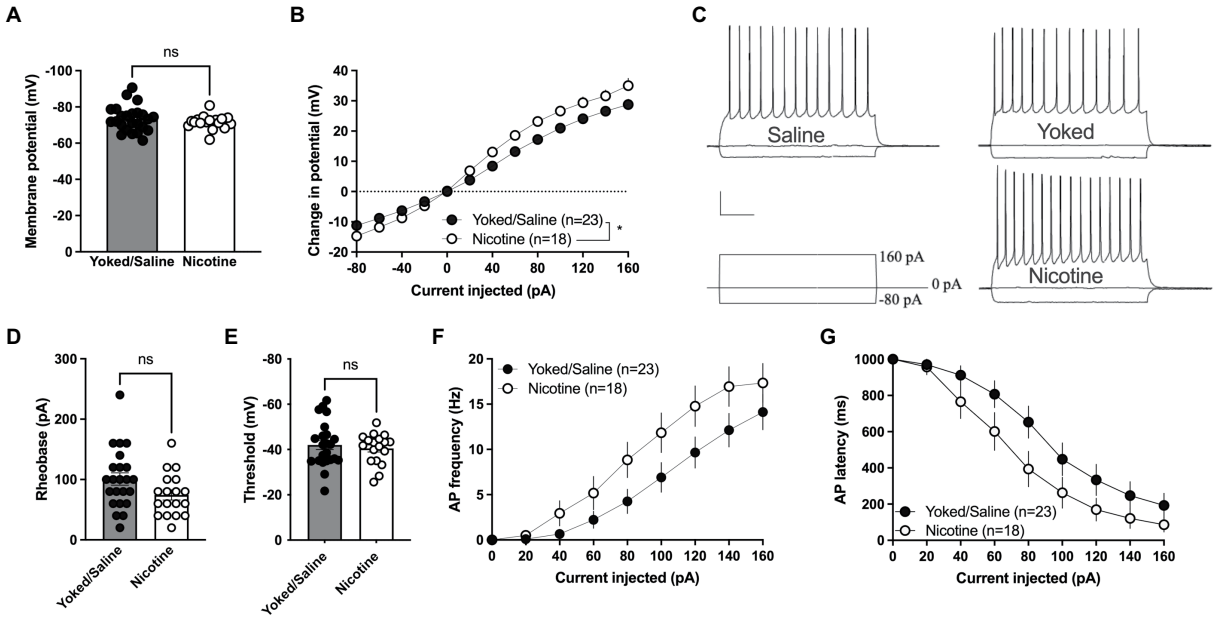

FIGURE 4
Increased excitability in nAcS MSNs after nicotine SA. **(A)** Membrane voltage was not affected by nicotine SA. **(B)** Relative change in membrane potential evoked by current injection was significantly bigger in MSNs from nicotine SA rats. **(C)** Representative traces of current clamp recordings from all treatment groups. Calibration: 0.2s, 20mV. **(D,E)** A trend toward reduced rheobase was observed in MSNs from nicotine SA rats, while threshold was not modulated. **(F,G)** MSNs from nicotine SA rats further demonstrated a trend toward increased AP frequency and decreased AP latency, but the effects were not significant. Values are presented as mean (±SEM), *n*=number of slices, taken from at least four animals. *$p<0.05$.

first to monitor sustained neuroadaptations in the nAc after a period of nicotine-self-administration followed by 1 month of forced abstinence. We show that after prolonged forced abstinence from nicotine self-administration excitatory synapses in the nAcS are altered. We observed an increase in evoked field potentials and sEPSC amplitude in animals with a history of contingent nicotine SA potentially indicating higher excitability of accumbal MSNs compared to control. This finding was further supported by current clamp recordings, showing a strong trend toward reduced rheobase and AP latency, with a concomitant increase in AP frequency of MSNs.

Interestingly, saline self-administering rats presented an operant responding behavior maintained by nicotine paired visual stimuli. When the reinforcement effort was incremented from FR1 to FR3 saline-SA rats decreased the number of active responses to a stable level. However their active lever pressing was maintained significantly higher than the inactive lever responding and reinstated to baseline during cue-reinforced responding under extinction conditions. Other previous studies have confirmed the contribution of environmental cues in driving self-administration behavior, that when paired with contingent saline-SA produced even stronger responding than nicotine-SA in the absence of these stimuli (Donny et al., 2003; Garcia-Rivas et al., 2019). However, this mild reinforcing effect of visual cues in driving operant behavior did not produce any sustained neuroadaptations in the saline-SA group when compared to yoked-treated control within the accumbens shell. This finding indicates that sustained effects on accumbens shell neurotransmission is produced by the drug itself or the drug in combination with instrumental conditioning rather than the cue-conditioned reinforcer alone.

The lack of sustained neurophysiological transformations in the shell of saline self-injecting rats makes it a reliable control group when studying the involvement of this brain region in incubation of drug craving and relapse to environmental stimuli. On the other hand, short self-administration of saline paired with cue presentation has been shown to produce changes in neuronal activity by c-fos expression in the nAcS and other brain structures (Zahm et al., 2010). It is also possible that selective neuronal ensembles are recruited, and that we do not capture these transitions when monitoring subsets of cells in whole cell recordings or collective activity of hundreds cells through field potential recordings. In addition, it should be noted that other subregions within the striatum or the amygdala may be more robustly recruited during operant behavior invigorated by conditioned stimuli. In particular, dorsal striatal circuits encode consolidating new instrumental actions (Smith et al., 2021), and the nucleus accumbens core has been shown to be relevant in pavlovian drug seeking behavior elicited by psychostimulants (Corbit et al., 2001; Ito et al., 2004; Corbit and Balleine, 2011). Studies performed in other brain regions may thus be more sensitive to the choice of control group.

Both accumbens core and shell have been shown to be involved in abstinence-induced incubation of cocaine and methaphetamine craving (Conrad et al., 2008; Lee et al., 2013; Xi et al., 2013; Cruz et al., 2014; Scheyer et al., 2016) while evidences on nicotine are scarce. Previous studies have shown that 2 weeks of nicotine withdrawal presented c-fos activation in both core and shell while potentiation of excitatory synapses in the nAc core was observed at the same abstinence period (Gipson et al., 2013a; Funk et al., 2016). In our study, measures from whole cell voltage clamp and evoked field potential recordings showed that also excitatory synapses in the nAcS were altered after prolonged forced abstinence from nicotine self-administration. sEPSC amplitude was significantly enhanced in accumbal MSNs from rats self-administering nicotine. Since neither decay nor rise time were significantly affected it is possible that the change in amplitude is linked to an increase in the number of excitatory receptors on accumbal MSNs. While a cocktail of CNQX and APV blocked recorded sEPSCs, neurons are voltage clamped at-65 mv and the amplitude is thus most likely associated with activation of postsynaptic AMPA receptors. In addition, voltage clamp recordings were supported by field potential recordings that presented a potentiation of stimulus–response curves in slices from nicotine-SA rats. Evoked potentials in the nAcS were robustly blocked by CNQX, indicating that these recordings primarily reflect activation of AMPA receptors.

AMPA/kainate receptors has been suggested to be selectively involved in the relapse of nicotine seeking after a period of abstinence (Gipson et al., 2013b; Ruda-Kucerova et al., 2021). Interestingly, studies on cocaine seeking have shown that both accumbens shell and core undergo similar AMPAR plasticity after prolonged withdrawal and these neuroadaptations contribute to the expression of incubation of cocaine craving (Conrad et al., 2008; Ping et al., 2008; Mameli et al., 2009; McCutcheon et al., 2011). For instance, both increased AMPA receptors expression and changes in subunit composition is observed in the accumbens following withdrawal from cocaine or methamphetamine (Conrad et al., 2008; Wolf and Tseng, 2012; Scheyer et al., 2016; Murray et al., 2019). Electrophysiological studies support synaptic potentiation of nAc excitatory synapses where prolonged abstinence following cocaine, enhances AMPAR-dependent synaptic strength with both increases in mEPSC amplitude and AMPA/NMDA ratio (Kourrich et al., 2007; Ortinski et al., 2012). Our findings suggest a possibly common AMPAR nAcS metaplasticity during forced abstinence for both nicotine and cocaine beyond the other evidences of shared molecular effects within the accumbens of these two drugs of abuse (Di Chiara and Imperato, 1988; Pich et al., 1997; McClung et al., 2004; Ciccocioppo et al., 2021). Importantly negative affective states, generally experienced during late nicotine withdrawal, are characterized by increased AMPA receptor expression in nAcS selectively in dopamine D1 MSNs (Pignatelli et al., 2021) In addition, cocaine abstinence has been shown to selectively increase the rectification of AMPA receptor-mediated currents in nAcS dopamine D1 receptor expressing MSNs (Inbar et al., 2022). The data presented in this study did not distinguish between dopamine D1 and D2 receptor expressing MSNs. If withdrawal induced stress responses contribute to the transformations retrieved here, it is thus possible that more pronounced effects would have been observed if separating recordings associated with the direct or indirect pathway.

While we observed changes in sEPSC amplitude, voltage clamp recordings revealed no significant increase in the frequency of synaptic inputs onto MSNs. However, nAc shell is innervated by glutamatergic projections arising from several distinct areas including the infralimbic cortex, basal amygdaloid complex, hippocampus and ventral prelimbic cortex (Voorn et al., 2004). It is thus possible that changes in specific inputs exist, but that these transformations are shielded by inputs arising from other regions.

Changes in neuronal excitability of nAc MSNs are critical for the manifestation of behavioral alterations related to drugs of abuse (Hu et al., 2004; Dong et al., 2006; Mu et al., 2010; Liu et al., 2012; Ma et al., 2013), and the data presented here indicated an increased excitability of MSNs in nicotine-SA male rats. Injected current produced a significantly greater change in membrane voltage, and there was a strong trend toward increased AP frequency and reduced rheobase and AP latency. This is partially supported by a previous study showing that nicotine addicted mice presented hyperexcitability of nAcS MSNs due to a decrease in potassium conductance mediated by large-conductance Ca^{2+}-activated K+ channels (Ma et al., 2013). Our observation of increased excitability of nAcS during nicotine forced abstinence in male rats might further be a factor that could drive

relapse to nicotine seeking. One limitation of the study is that only male rats were used. Considering that women experience more severe withdrawal symptoms including greater negative affect compared to men (Piasecki et al., 2003; Pang and Leventhal, 2013; O'Dell and Torres, 2014), nicotine abstinence-induced neuroadaptations may be more pronounced in female rats. Future research in both sexes will be essential to prove a functional role of the presented shell MSNs alterations and nicotine seeking behavior.

In conclusion, our findings suggest that a history of nicotine self-administration produces sustained neuroadaptations in the nAcS while operant responding driven by nicotine visual stimuli has no long-term effects on MSNs in the nAcS. The observed neuronal alterations in excitatory activity of nAcS MSNs during nicotine forced abstinence suggest that normalization of these synapses activity has implications for the treatment of nicotine seeking and relapse prevention.

Data availability statement

The raw data supporting the conclusions of this article will be made available by the authors, without undue reservation.

Ethics statement

Procedures were conducted in accordance with the National Committee for Animal Research in Sweden and approved by the Local Ethics Committee for Animal Care and Use at Gothenburg University: ID 2510, decision 25/09/2019.

Author contributions

AD and LA were responsible for the study concept and design. AD designed and performed the behavioral and field potential electrophysiological experiments, collected and analyzed the data, and wrote and revised the manuscript. LA contributed in analyzing, interpreting, and assembling the data and revising the manuscript. EL and DC performed and analyzed whole-cell electrophysiological recordings. All authors contributed to the article and approved the submitted version.

Funding

This work was supported by the Swedish Research Council (vetenskapsrådet: 2018-02814 and 2020-00559), Governmental support under the ALF agreement (ALFGBG-966287), and Fredrik and Ingrid Thurings Stiftelse (2020-00593).

Acknowledgments

We thank Elisabet Jerlhag, Alfredo Fiorelli, Mia Ericson, and Rosita Stomberg for technical assistance.

Conflict of interest

The authors declare that the research was conducted in the absence of any commercial or financial relationships that could be construed as a potential conflict of interest.

Publisher's note

References

Adermark, L., Clarke, R. B., Söderpalm, B., and Ericson, M. (2011). Ethanol-induced modulation of synaptic output from the dorsolateral striatum in rat is regulated by cholinergic interneurons. *Neurochem. Int.* 58, 693–699. doi: 10.1016/j.neuint.2011.02.009

Belin-Rauscent, A., Fouyssac, M., Bonci, A., and Belin, D. (2016). How preclinical models evolved to resemble the diagnostic criteria of drug addiction. *Biol. Psychiatry* 79, 39–46. doi: 10.1016/j.biopsych.2015.01.004

Bevins, R. A., and Palmatier, M. I. (2004). Extending the role of associative learning processes in nicotine addiction. *Behav. Cogn. Neurosci. Rev.* 3, 143–158. doi: 10.1177/1534582304272005

Caggiula, A. R., Donny, E. C., White, A. R., Chaudhri, N., Booth, S., Gharib, M. A., et al. (2001). Cue dependency of nicotine self-administration and smoking. *Pharmacol. Biochem. Behav.* 70, 515–530. doi: 10.1016/S0091-3057(01)00676-1

Ciccocioppo, R., Guglielmo, G., Li, H., Melis, M., Caffino, L., Shen, Q., et al. (2021). Selective inhibition of phosphodiesterase 7 enzymes reduces motivation for nicotine use through modulation of mesolimbic dopaminergic transmission. *J. Neurosci.* 41, 6128–6143. doi: 10.1523/JNEUROSCI.3180-20.2021

Cippitelli, A., Wu, J., Gaiolini, K. A., Mercatelli, D., Schoch, J., Gorman, M., et al. (2015). At-1001: a high-affinity A3β4 Nachr ligand with novel nicotine-suppressive pharmacology. *Br. J. Pharmacol.* 172, 1834–1845. doi: 10.1111/bph.13034

Conrad, K. L., Tseng, K. Y., Uejima, J. L., Reimers, J. M., Heng, L. J., Shaham, Y., et al. (2008). Formation of Accumbens Glur2-lacking Ampa receptors mediates incubation of cocaine craving. *Nature* 454, 118–121. doi: 10.1038/nature06995

Corbit, L. H., and Balleine, B. W. (2011). The general and outcome-specific forms of Pavlovian-instrumental transfer are differentially mediated by the nucleus Accumbens Core and Shell. *J. Neurosci.* 31, 11786–11794. doi: 10.1523/JNEUROSCI.2711-11.2011

Corbit, L. H., Muir, J. L., and Balleine, B. W. (2001). The role of the nucleus Accumbens in instrumental conditioning: evidence of a functional dissociation between Accumbens Core and Shell. *J. Neurosci.* 21, 3251–3260. doi: 10.1523/JNEUROSCI.21-09-03251.2001

Cruz, F. C., Babin, K. R., Leao, R. M., Goldart, E. M., Bossert, J. M., Shaham, Y., et al. (2014). Role of nucleus Accumbens Shell neuronal ensembles in context-induced reinstatement of cocaine-seeking. *J. Neurosci.* 34, 7437–7446. doi: 10.1523/JNEUROSCI.0238-14.2014

Di Chiara, G., and Imperato, A. (1988). Drugs abused by humans preferentially increase synaptic dopamine concentrations in the mesolimbic system of freely moving rats. *Proc. Natl. Acad. Sci. U. S. A.* 85, 5274–5278. doi: 10.1073/pnas.85.14.5274

Di Ciano, P., Robbins, T. W., and Everitt, B. J. (2008). Differential effects of nucleus Accumbens Core, Shell, or dorsal striatal Inactivations on the persistence, reacquisition, or reinstatement of responding for a drug-paired conditioned Reinforcer. *Neuropsychopharmacology* 33, 1413–1425. doi: 10.1038/sj.npp.1301522

Domi, A., Lunerti, V., Petrella, M., Domi, E., Borruto, A. M., Ubaldi, M., et al. (2022). Genetic deletion or pharmacological blockade of Nociceptin/Orphanin Fq receptors in the ventral tegmental area attenuates nicotine-motivated behaviour. *Br. J. Pharmacol.* 179, 2647–2658. doi: 10.1111/bph.15762

Dong, Y., Green, T., Saal, D., Marie, H., Neve, R., Nestler, E. J., et al. (2006). Creb modulates excitability of nucleus Accumbens neurons. *Nat. Neurosci.* 9, 475–477. doi: 10.1038/nn1661

Donny, E. C., Caggiula, A. R., Knopf, S., and Brown, C. (1995). Nicotine self-administration in rats. *Psychopharmacology (Berl)* 122, 390–394. doi: 10.1007/BF02246272

Donny, E. C., Chaudhri, N., Caggiula, A. R., Evans-Martin, F. F., Booth, S., Gharib, M. A., et al. (2003). Operant responding for a visual Reinforcer in rats is enhanced by noncontingent nicotine: implications for nicotine self-administration and reinforcement. *Psychopharmacology (Berl)* 169, 68–76. doi: 10.1007/s00213-003-1473-3

Floresco, S. B., Mclaughlin, R. J., and Haluk, D. M. (2008). Opposing roles for the nucleus Accumbens Core and Shell in Cue-induced reinstatement of food-seeking behavior. *Neuroscience* 154, 877–884. doi: 10.1016/j.neuroscience.2008.04.004

Funk, D., Coen, K., Tamadon, S., Hope, B. T., Shaham, Y., and Lê, A. D. (2016). Role of central amygdala neuronal ensembles in incubation of nicotine craving. *J. Neurosci.* 36, 8612–8623. doi: 10.1523/JNEUROSCI.1505-16.2016

Garcia-Rivas, V., Fiancette, J. F., Cannella, N., Carbo-Gas, M., Renault, P., Tostain, J., et al. (2019). Varenicline targets the reinforcing-enhancing effect of nicotine on its associated salient Cue during nicotine self-administration in the rat. *Front. Behav. Neurosci.* 13:159. doi: 10.3389/fnbeh.2019.00159

Gipson, C. D., Kupchik, Y. M., Shen, H., Reissner, K. J., Thomas, C. A., and Kalivas, P. W. (2013a). Relapse induced by cues predicting cocaine depends on rapid, transient synaptic potentiation. *Neuron* 77, 867–872. doi: 10.1016/j.neuron.2013.01.005

Gipson, C. D., Reissner, K. J., Kupchik, Y. M., Smith, A. C., Stankeviciute, N., Hensley-Simon, M. E., et al. (2013b). Reinstatement of nicotine seeking is mediated by glutamatergic plasticity. *Proc. Natl. Acad. Sci. U. S. A.* 110, 9124–9129. doi: 10.1073/pnas.1220591110

Henningfield, J. E., Smith, T. T., Kleykamp, B. A., Fant, R. V., and Donny, E. C. (2016). Nicotine self-administration research: the legacy of Steven R. Goldberg and implications for regulation, health policy, and research. *Psychopharmacologia* 233, 3829–3848. doi: 10.1007/s00213-016-4441-4

Hu, X. T., Basu, S., and White, F. J. (2004). Repeated cocaine administration suppresses Hva-Ca2+ potentials and enhances activity of K+ channels in rat nucleus Accumbens neurons. *J. Neurophysiol.* 92, 1597–1607. doi: 10.1152/jn.00217.2004

Inbar, K., Levi, L. A., and Kupchik, Y. M. (2022). Cocaine induces input and cell-type-specific synaptic plasticity in ventral pallidum-projecting nucleus Accumbens medium spiny neurons. *Neuropsychopharmacology* 47, 1461–1472. doi: 10.1038/s41386-022-01285-6

Ito, R., Robbins, T. W., and Everitt, B. J. (2004). Differential control over cocaine-seeking behavior by nucleus Accumbens Core and Shell. *Nat. Neurosci.* 7, 389–397. doi: 10.1038/nn1217

Jin, X. T., Tucker, B. R., and Drenan, R. M. (2020). Nicotine self-administration induces plastic changes to nicotinic receptors in medial Habenula. *Eneuro* 7, ENEURO.0197–ENEU20.2020. doi: 10.1523/ENEURO.0197-20.2020

Karasawa, J., Kotani, M., Kambe, D., and Chaki, S. (2010). Ampa receptor mediates Mglu 2/3 receptor antagonist-induced dopamine release in the rat nucleus Accumbens Shell. *Neurochem. Int.* 57, 615–619. doi: 10.1016/j.neuint.2010.07.011

Karasawa, J., Yoshimizu, T., and Chaki, S. (2006). A metabotropic glutamate 2/3 receptor antagonist, Mgs0039, increases extracellular dopamine levels in the nucleus Accumbens Shell. *Neurosci. Lett.* 393, 127–130. doi: 10.1016/j.neulet.2005.09.058

Kenny, P. J., Gasparini, F., and Markou, A. (2003). Group ii metabotropic and alpha-Amino-3-Hydroxy-5-Methyl-4-Isoxazole propionate (Ampa)/Kainate glutamate receptors regulate the deficit in brain reward function associated with nicotine withdrawal in rats. *J. Pharmacol. Exp. Ther.* 306, 1068–1076. doi: 10.1124/jpet.103.052027

Kourrich, S., Rothwell, P. E., Klug, J. R., and Thomas, M. J. (2007). Cocaine experience controls bidirectional synaptic plasticity in the nucleus Accumbens. *J. Neurosci.* 27, 7921–7928. doi: 10.1523/JNEUROSCI.1859-07.2007

Lecca, D., Cacciapaglia, F., Valentini, V., Acquas, E., and Di Chiara, G. (2007). Differential neurochemical and behavioral adaptation to cocaine after response contingent and noncontingent exposure in the rat. *Psychopharmacology (Berl)* 191, 653–667. doi: 10.1007/s00213-006-0496-y

Lecca, D., Cacciapaglia, F., Valentini, V., Gronli, J., Spiga, S., and Di Chiara, G. (2006). Preferential increase of extracellular dopamine in the rat nucleus Accumbens Shell as compared to that in the Core during acquisition and maintenance of intravenous nicotine self-administration. *Psychopharmacology (Berl)* 184, 435–446. doi: 10.1007/s00213-005-0280-4

Lee, B. R., Ma, Y. Y., Huang, Y. H., Wang, X., Otaka, M., Ishikawa, M., et al. (2013). Maturation of silent synapses in amygdala-Accumbens projection contributes to incubation of cocaine craving. *Nat. Neurosci.* 16, 1644–1651. doi: 10.1038/nn.3533

Licheri, V., Eckernas, D., Bergquist, F., Ericson, M., and Adermark, L. (2019). Nicotine-induced neuroplasticity in striatum is subregion-specific and reversed by motor training on the Rotarod. *Addict. Biol.* 24. doi: 10.1111/adb.12757

Liechti, M. E., Lhuillier, L., Kaupmann, K., and Markou, A. (2007). Metabotropic glutamate 2/3 receptors in the ventral tegmental area and the nucleus Accumbens Shell are involved in behaviors relating to nicotine dependence. *J. Neurosci.* 27, 9077–9085. doi: 10.1523/JNEUROSCI.1766-07.2007

Liu, Z., Zhang, J. J., Liu, X. D., and Yu, L. C. (2012). Inhibition of Camkii activity in the nucleus Accumbens Shell blocks the reinstatement of morphine-seeking behavior in rats. *Neurosci. Lett.* 518, 167–171. doi: 10.1016/j.neulet.2012.05.003

Ma, L., Wu, Y. M., Guo, Y. Y., Yang, Q., Feng, B., Song, Q., et al. (2013). Nicotine addiction reduces the large-conductance ca(2+)-activated potassium channels expression in the nucleus Accumbens. *Neuromolecular Med.* 15, 227–237. doi: 10.1007/s12017-012-8213-y

Mameli, M., Halbout, B., Creton, C., Engblom, D., Parkitna, J. R., Spanagel, R., et al. (2009). Cocaine-evoked synaptic plasticity: persistence in the Vta triggers adaptations in the Nac. *Nat. Neurosci.* 12, 1036–1041. doi: 10.1038/nn.2367

Markou, A., and Paterson, N. E. (2009). Multiple motivational forces contribute to nicotine dependence. *Nebr. Symp. Motiv.* 55, 65–89. doi: 10.1007/978-0-387-78748-0_5

Mathieson, E., Irving, C., Koberna, S., Nicholson, M., Otto, M. W., and Kantak, K. M. (2022). Role of preexisting inhibitory control deficits vs. drug use history in mediating insensitivity to aversive consequences in a rat model of polysubstance use. *Psychopharmacology (Berl)* 239, 2377–2394. doi: 10.1007/s00213-022-06134-4

Mcclung, C. A., Ulery, P. G., Perrotti, L. I., Zachariou, V., Berton, O., and Nestler, E. J. (2004). Deltafosb: a molecular switch for long-term adaptation in the brain. *Brain Res. Mol. Brain Res.* 132, 146–154. doi: 10.1016/j.molbrainres.2004.05.014

Mccutcheon, J. E., Loweth, J. A., Ford, K. A., Marinelli, M., Wolf, M. E., and Tseng, K. Y. (2011). Group I Mglur activation reverses cocaine-induced accumulation of calcium-permeable Ampa receptors in nucleus Accumbens synapses via a protein kinase C-dependent mechanism. *J. Neurosci.* 31, 14536–14541. doi: 10.1523/JNEUROSCI.3625-11.2011

Mu, P., Moyer, J. T., Ishikawa, M., Zhang, Y., Panksepp, J., Sorg, B. A., et al. (2010). Exposure to cocaine dynamically regulates the intrinsic membrane excitability of nucleus Accumbens neurons. *J. Neurosci.* 30, 3689–3699. doi: 10.1523/JNEUROSCI.4063-09.2010

Murray, C. H., Loweth, J. A., Milovanovic, M., Stefanik, M. T., Caccamise, A. J., Dolubizno, H., et al. (2019). Ampa receptor and metabotropic glutamate receptor 1 adaptations in the nucleus Accumbens Core during incubation of methamphetamine craving. *Neuropsychopharmacology* 44, 1534–1541. doi: 10.1038/s41386-019-0425-5

O'dell, L. E., and Torres, O. V. (2014). A mechanistic hypothesis of the factors that enhance vulnerability to nicotine use in females. *Neuropharmacology* 76 Pt B, 566–580. doi: 10.1016/j.neuropharm.2013.04.055

Ortinski, P. I., Vassoler, F. M., Carlson, G. C., and Pierce, R. C. (2012). Temporally dependent changes in cocaine-induced synaptic plasticity in the nucleus Accumbens Shell are reversed by D1-like dopamine receptor stimulation. *Neuropsychopharmacology* 37, 1671–1682. doi: 10.1038/npp.2012.12

Palmatier, M. I., Evans-Martin, F. F., Hoffman, A., Caggiula, A. R., Chaudhri, N., Donny, E. C., et al. (2006). Dissociating the primary reinforcing and reinforcement-enhancing effects of nicotine using a rat self-administration paradigm with concurrently available drug and environmental Reinforcers. *Psychopharmacology (Berl)* 184, 391–400. doi: 10.1007/s00213-005-0183-4

Palmatier, M. I., Liu, X., Matteson, G. L., Donny, E. C., Caggiula, A. R., and Sved, A. F. (2007). Conditioned reinforcement in rats established with self-administered nicotine and enhanced by noncontingent nicotine. *Psychopharmacology (Berl)* 195, 235–243. doi: 10.1007/s00213-007-0897-6

Pang, R. D., and Leventhal, A. M. (2013). Sex differences in negative affect and lapse behavior during acute tobacco abstinence: a laboratory study. *Exp. Clin. Psychopharmacol.* 21, 269–276. doi: 10.1037/a0033429

Panlilio, L. V., and Goldberg, S. R. (2007). Self-administration of drugs in animals and humans as a model and an investigative tool. *Addiction* 102, 1863–1870. doi: 10.1111/j.1360-0443.2007.02011.x

Piasecki, T. M., Jorenby, D. E., Smith, S. S., Fiore, M. C., and Baker, T. B. (2003). Smoking withdrawal dynamics: iii. Correlates of withdrawal heterogeneity. *Exp. Clin. Psychopharmacol.* 11, 276–285. doi: 10.1037/1064-1297.11.4.276

Pich, E. M., Pagliusi, S. R., Tessari, M., Talabot-Ayer, D., Hooft Van Huijsduijnen, R., and Chiamulera, C. (1997). Common neural substrates for the addictive properties of nicotine and cocaine. *Science* 275, 83–86. doi: 10.1126/science.275.5296.83

Pignatelli, M., Tejeda, H. A., Barker, D. J., Bontempi, L., Wu, J., Lopez, A., et al. (2021). Cooperative synaptic and intrinsic plasticity in a Disynaptic limbic circuit drive stress-induced anhedonia and passive coping in mice. *Mol. Psychiatry* 26, 1860–1879. doi: 10.1038/s41380-020-0686-8

Ping, A., Xi, J., Prasad, B. M., Wang, M. H., and Kruzich, P. J. (2008). Contributions of nucleus Accumbens Core and Shell Glur1 containing Ampa receptors in Ampa-and cocaine-primed reinstatement of cocaine-seeking behavior. *Brain Res.* 1215, 173–182. doi: 10.1016/j.brainres.2008.03.088

Pittenger, S. T., Schaal, V. L., Moore, D., Guda, R. S., Koul, S., Yelamanchili, S. V., et al. (2018). Microrna cluster Mir199a/214 are differentially expressed in female and male rats following nicotine self-administration. *Sci. Rep.* 8:17464. doi: 10.1038/s41598-018-35747-z

Ruda-Kucerova, J., Amchova, P., Siska, F., and Tizabi, Y. (2021). Nbqx attenuates relapse of nicotine seeking but not nicotine and methamphetamine self-administration in rats. *World J. Biol. Psychiatry* 22, 733–743. doi: 10.1080/15622975.2021.1907714

Scheyer, A. F., Loweth, J. A., Christian, D. T., Uejima, J., Rabei, R., Le, T., et al. (2016). Ampa receptor plasticity in Accumbens Core contributes to incubation of methamphetamine craving. *Biol. Psychiatry* 80, 661–670. doi: 10.1016/j.biopsych.2016.04.003

Schmidt, H. D., Rupprecht, L. E., and Addy, N. A. (2019). Neurobiological and neurophysiological mechanisms underlying nicotine seeking and smoking relapse. *Mol. Neuropsychiatry* 4, 169–189. doi: 10.1159/000494799

Smith, A. C. W., Jonkman, S., Difeliceantonio, A. G., O'connor, R. M., Ghoshal, S., Romano, M. F., et al. (2021). Opposing roles for Striatonigral and Striatopallidal neurons in dorsolateral striatum in consolidating new instrumental actions. *Nat. Commun.* 12:5121. doi: 10.1038/s41467-021-25460-3

Spealman, R. D., and Goldberg, S. R. (1978). Drug self-administration by laboratory animals: control by schedules of reinforcement. *Annu. Rev. Pharmacol. Toxicol.* 18, 313–339. doi: 10.1146/annurev.pa.18.040178.001525

Voorn, P., Vanderschuren, L. J., Groenewegen, H. J., Robbins, T. W., and Pennartz, C. M. (2004). Putting a spin on the dorsal-ventral divide of the striatum. *Trends Neurosci.* 27, 468–474. doi: 10.1016/j.tins.2004.06.006

Wolf, M. E., and Tseng, K. Y. (2012). Calcium-permeable Ampa receptors in the Vta and nucleus Accumbens after cocaine exposure: when, how, and why? *Front. Mol. Neurosci.* 5:72.

Xi, Z. X., Li, X., Li, J., Peng, X. Q., Song, R., Gaál, J., et al. (2013). Blockade of dopamine D3 receptors in the nucleus Accumbens and central amygdala inhibits incubation of cocaine craving in rats. *Addict. Biol.* 18, 665–677. doi: 10.1111/j.1369-1600.2012.00486.x

Zahm, D. S., Becker, M. L., Freiman, A. J., Strauch, S., Degarmo, B., Geisler, S., et al. (2010). Fos after single and repeated self-administration of cocaine and saline in the rat: emphasis on the basal forebrain and recalibration of expression. *Neuropsychopharmacology* 35, 445–463. doi: 10.1038/npp.2009.149

frontiers | Frontiers in Molecular Neuroscience

TYPE Original Research
PUBLISHED 07 February 2023
DOI 10.3389/fnmol.2023.1069834

OPEN ACCESS

EDITED BY
Vidhya Kumaresan,
Boston University,
United States

REVIEWED BY
Sho Yagishita,
The University of Tokyo,
Japan
Fuyong Jiao,
Xi'an Jiaotong University,
China

*CORRESPONDENCE
Zisis Bimpisidis
✉ Zisis.Bimpisidis@iit.it;
✉ Zisis.Bimpisidis@gmail.com

†PRESENT ADDRESS
Zisis Bimpisidis,
Istituto Italiano di Tecnologia,
Genova, Italy

SPECIALTY SECTION
This article was submitted to Neuroplasticity and Development, a section of the journal Frontiers in Molecular Neuroscience

RECEIVED 14 October 2022
ACCEPTED 11 January 2023
PUBLISHED 07 February 2023

CITATION
Bimpisidis Z, Serra GP, König N and Wallén-Mackenzie Å (2023) Increased sucrose consumption in mice gene-targeted for *Vmat2* selectively in NeuroD6-positive neurons of the ventral tegmental area.
Front. Mol. Neurosci. 16:1069834.
doi: 10.3389/fnmol.2023.1069834

Increased sucrose consumption in mice gene-targeted for *Vmat2* selectively in NeuroD6-positive neurons of the ventral tegmental area

Zisis Bimpisidis*†, Gian Pietro Serra, Niclas König and Åsa Wallén-Mackenzie

Unit of Comparative Physiology, Department of Organismal Biology, Uppsala University, Uppsala, Sweden

Ventral tegmental area (VTA) dopamine (DA) neurons are implicated in reward processing, motivation, reward prediction error, and in substance use disorder. Recent studies have identified distinct neuronal subpopulations within the VTA that can be clustered based on their molecular identity, neurotransmitter profile, physiology, projections and behavioral role. One such subpopulation is characterized by expression of the *NeuroD6* gene, and projects primarily to the nucleus accumbens medial shell. We recently showed that optogenetic stimulation of these neurons induces real-time place preference while their targeted deletion of the *Vmat2* gene caused altered response to rewarding substances, including ethanol and psychostimulants. Based on these recent findings, we wanted to further investigate the involvement of the NeuroD6-positive VTA subpopulation in reward processing. Using the same *NeuroD6*$^{Cre+/wt}$;*Vmat2*$^{flox/flox}$ mice as in our prior study, we now addressed the ability of the mice to process sucrose reward. In order to assess appetitive behavior and motivation to obtain sucrose reward, we tested conditional knockout (cKO) and control littermate mice in an operant sucrose self-administration paradigm. We observed that cKO mice demonstrate higher response rates to the operant task and consume more sucrose rewards than control mice. However, their motivation to obtain sucrose is identical to that of control mice. Our results highlight previous observations that appetitive behavior and motivation to obtain rewards can be served by distinct neuronal circuits, and demonstrate that the NeuroD6 VTA subpopulation is involved in mediating the former, but not the latter. Together with previous studies on the NeuroD6 subpopulation, our findings pinpoint the importance of unraveling the molecular and functional role of VTA subpopulations in order to better understand normal behavior and psychiatric disease.

KEYWORDS

dopamine, NeuroD6, VTA, sucrose, VMAT2, motivation, self-administration

Introduction

The midbrain dopamine (DA) system has been implicated in reinforcement learning, reward prediction error (Schultz et al., 1997), motivation (Berke, 2018), incentive salience (Berridge and Robinson, 1998) and in diseases where these functions are compromised, such as substance use disorder (Lüscher, 2016). Expanding on the classical classification of DA circuits into nigrostriatal and mesolimbic systems (Björklund and Dunnett, 2007), recent studies have focused on the

heterogeneity of DA neurons within the midbrain, in terms of gene expression, projection patterns and behavioral role (Chung et al., 2005; Greene et al., 2005; Lammel et al., 2008, 2011, 2012; Poulin et al., 2014, 2018; Viereckel et al., 2016; Bimpisidis et al., 2019; Heymann et al., 2020; König et al., 2020; Serra et al., 2021). Characterizing differences between previously considered homogeneous DA populations will lead in deciphering the functional role of distinct subpopulations, make it possible to selectively target them for treatment of disease and eventually avoiding unwanted side effects that might occur by targeting the DA system as a whole.

It is increasingly understood that DAergic systems can mediate distinct aspects of behavior depending on the target projection area. Substantia nigra pars compacta (SNc) and ventral tegmental area (VTA) DA neurons have different topographical projections that in turn mediate diverse aspects of reward-related behavior. For example, incentive value attribution is mediated by nucleus accumbens (NAc) core projecting DA neurons and not by those projecting to the NAc shell (NAcSh; Saunders et al., 2018). Within the SNc, separate DA neuron groups project to the dorsolateral (DLS) and to the dorsomedial striatum (DMS), have distinct electrophysiological properties, and respond differently to reward delivery and aversive stimuli. Those neurons projecting to DMS reduce, while those projecting in DLS increase their activity in response to foot shock (Lerner et al., 2015).

Regarding the behavioral role of the VTA, recent fiber photometry studies have demonstrated that the activity of DA neurons in the medial and lateral parts is correlated with reward prediction error and salience, respectively, and the overall aftermath is dependent on the temporal scale of activation of these subareas (Cai et al., 2020). Sophisticated analysis of complex behavioral data and Ca^{2+} transients of VTA DA neurons showed that these neurons form clusters that respond more strongly to specific aspects of a reward task (sensory, motor, cognitive), a function related to anatomical location of the cluster. However, neurons in each cluster do not seem to be "specialized" in only one behavioral variable but to respond to more than one (Engelhard et al., 2019).

The specific input–output circuitry characteristics of subgroups of VTA DA neurons defines their profile in terms of behavioral role (Lammel et al., 2011, 2012; de Jong et al., 2019). Separate subpopulations within the VTA receive different inputs and mediate opposite types of behavior, rewarding or aversive. A rewarding stimulus such as cocaine, affects mostly medial VTA DA neurons projecting to the medial NAcSh (mNAcSh) while aversive stimuli like foot shocks are processed by those DA neurons projecting to the medial prefrontal cortex (mPFC). VTA DA neurons connected to the NAc lateral shell respond to both types of stimuli in a similar way (Lammel et al., 2011).

Exploiting the unique gene expression patterns of different neuronal subtypes has been recently employed to unravel the projection patterns and role in behavior of distinct neuronal subpopulations within the VTA (Bimpisidis et al., 2019; Heymann et al., 2020; König et al., 2020; Kramer et al., 2021; Serra et al., 2021). For example, Heymann and colleagues (Heymann et al., 2020) used genetic and viral approaches to target VTA neurons characterized by specific expression of peptides. They showed that VTA neurons expressing *Crhr1* project selectively to the NAc core and those expressing *Cck* to the mNAcSh. Behaviorally, activation of VTA-NAc core neurons is sufficient to promote acquisition of an instrumental behavior while VTA-NAc shell activation is responsible for maintaining an instrumental response. However, the two different subpopulations act in synergy to optimize behavior (Heymann et al., 2020). More recently, Serra and colleagues, using conditioned knock-out (cKO) approaches, showed that the medially located VTA DA population characterized by the expression of *TrpV1* is involved in modulating amphetamine-induced locomotion (Serra et al., 2021).

A recently described VTA subpopulation is characterized by the expression of the *NeuroD6* gene (also known as *NEX1M*). The gene is selectively expressed within subsets of VTA DA neurons but not in those of the neighboring substantia nigra compacta (SNc; Viereckel et al., 2016; Khan et al., 2017; Kramer et al., 2018). We recently showed that NeuroD6- (or NEX-Cre)-expressing neurons constitute 12% of all VTA tyrosine hydroxylase (TH) positive neurons, are mostly located in the medial nuclei of the VTA and project preferentially to the medial part of the nucleus accumbens shell (mNAcSh). A small percentage of them (12%) co-releases glutamate and optogenetic stimulation of these neurons induces real-time place preference. To address the role of DA released by this VTA subpopulation, we generated a conditional knock-out (cKO) mouse line, created by crossing $NEX^{Cre+/wt}$ mice and mice having the gene coding for the vesicular monoamine transporter – 2 (*Vmat2*) flanked by LoxP sites ($Vmat2^{flox/flox}$; Narboux-Nême et al., 2011). We observed that disruption of NEX-Cre neurons' ability to release DA renders mice hypersensitive to the locomotor effects of repeated injections of amphetamine and results in altered responses toward ethanol consumption (Bimpisidis et al., 2019).

The mesolimbic DAergic system is involved in processing both drug and natural rewards (Di Chiara and Bassareo, 2007; Ikemoto, 2007). It remains to be answered whether the NeuroD6 DA subpopulation is involved in reinforcement learning and motivation for food reward. To answer this question, we used the cKO mouse line generated and characterized previously (Bimpisidis et al., 2019) to ablate DA release selectively from NeuroD6-expressing neurons. We tested cKO and littermate control mice in an operant sucrose self-administration task consisting of different phases modeling separate behavioral aspects of appetitive behavior. We assessed the consumption of sucrose rewards under fixed ratio schedules of reinforcement, and the motivation to obtain reward using the well-established progressive ratio schedule. We observed that cKO mice nose-poke for, receive and consume/ingest more sucrose rewards than control littermates in fixed ratio schedules. Interestingly, when tested in the progressive ratio schedule, their motivation or will to work for sucrose remained unaltered. Finally, during a cue-induced reinstatement phase of the protocol, cKO mice had higher number of magazine entries, suggesting that the ability of that mice to process cues paired to reward was impaired. Our results add up to the increasing knowledge on the involvement of distinct DA subpopulations in behavior and suggest that separate subcircuits within the VTA might serve the appetitive and motivational aspects of reward-related behaviors. This is of interest in better understanding DA-related diseases such as drug or food addiction and relevant in developing novel therapeutic approaches aiming to target well-defined neuronal subpopulations.

Materials and methods

Animals

$NEX^{Cre-/wt}$;$Vmat2^{flox/flox}$ (Control) and $NEX^{Cre+/wt}$;$Vmat2^{flox/flox}$ (cKO) were generated as described previously (Bimpisidis et al., 2019) and as depicted in Figure 1C. Briefly, $NeuroD6/NEX^{Cre+/wt}$ transgenic mice (Goebbels et al., 2006) were bred with $Vmat2^{flox/flox}$ mice, in which exon 2 of the Vmat2 gene is flanked by LoxP sites (Narboux-Nême et al., 2011) to generate cKO mice in which Vmat2 exon 2 is ablated on NEX-Cre-mediated recombination of LoxP sites. VMAT2 is responsible for concentrating monoamines in synaptic vesicles and thus for their

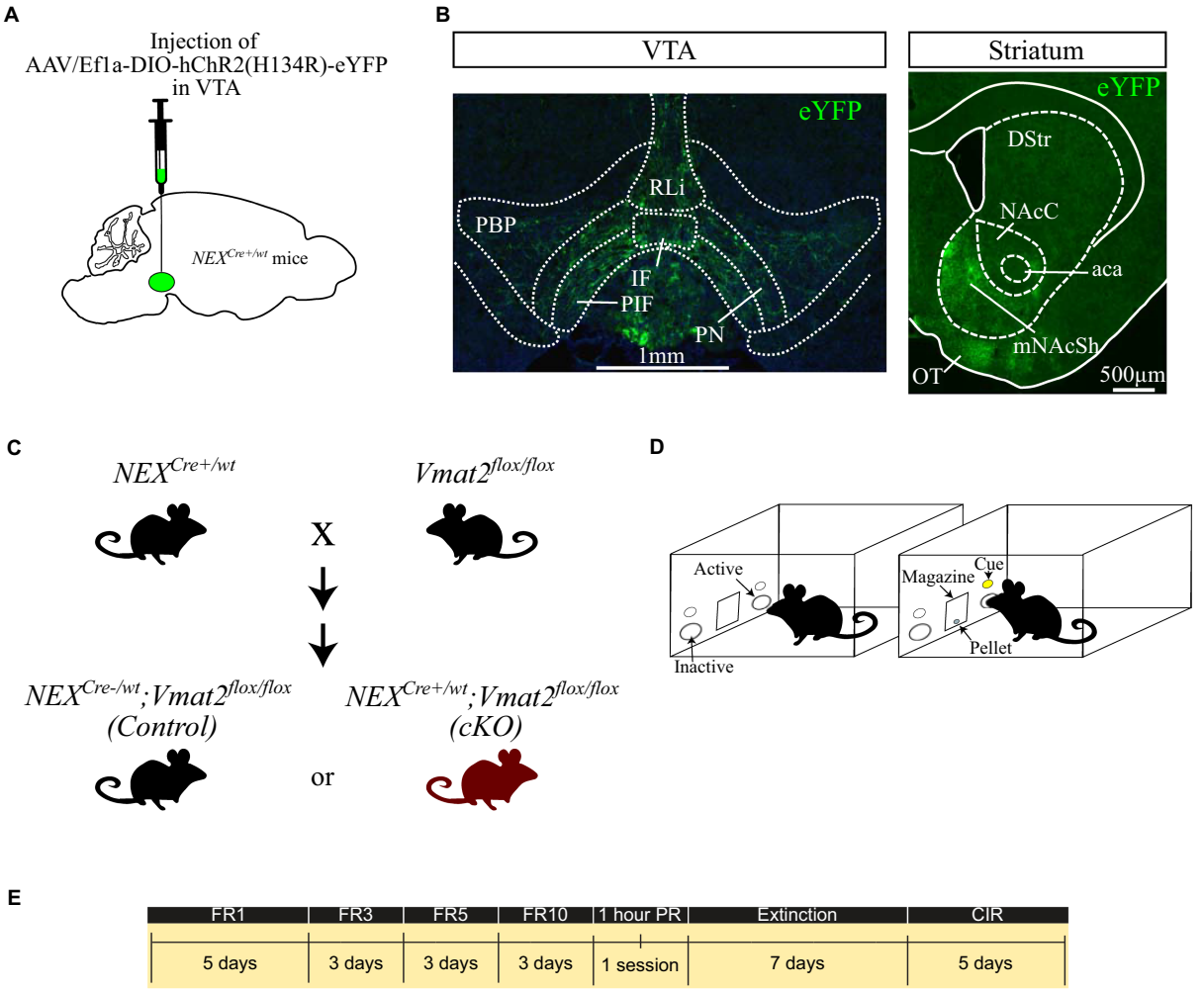

FIGURE 1
Schematic representation of the virus injection in *NEX*$^{Cre+/wt}$ mice **(A)**. Fluorescent images showing the distribution of NEX-Cre neurons in the VTA (**B**, left panel) and their main projections to the mNAcSh (**B**, right). Breeding strategy to obtain *NEX*$^{Cre-/wt}$;Vmat2$^{flox/flox}$ (Control) and *NEX*$^{Cre+/wt}$;*Vmat2*$^{floxf/lox}$ (cKO) mice **(C)**. Schematic of the apparatus **(D)** and the schedule of the behavioral experiments **(E)**. aca: anterior commissure, anterior part, DStr: dorsal striatum, NAcC: nucleus accumbens core, mNAcSh: nucleus accumbens medial shell, IF: interfascicular nucleus, OT: olfactory tubercule, PBP: parabranchial pigmented nucleus, PIR: parainterfascicular nucleus, PN: paranigral nucleus, RLi: rostral linear nucleus. CIR: Cue-induced reinstatement.

release in the synaptic cleft; abnormal expression of the transporter leads to impaired neurotransmission (Narboux-Nême et al., 2011). Littermates negative for NEX-Cre served as controls (Control). Mice were genotyped by PCR as described previously (Bimpisidis et al., 2019) with the following primers: Cre: 5'-ACG AGT GAT GAG GTT CGC AAG A-3′; 5'-ACC GAC GAT GAA GCA TGT TTA G-3′; Vmat2Lox: 5'-GAC TCA GGG CAG CAC AAA TCT CC-3′; 5′-GAA ACA TGA AGG ACA ACT GGG ACC C-3′. All animals were housed on a standard 12 h sleep/wake cycle (7:00 A.M. lights on, 7:00 P.M. lights off) and housed according to Swedish (Animal Welfare Act SFS 1998:56) and European Union legislation (Convention ETS 123 and Directive 2010/63/EU). Mice were food restricted (85% of initial body weight) throughout the experiments. All experiments were conducted with permission from Uppsala University Ethical Committee for Use of Animals.

Stereotaxic injections

AAV5-EF1a-DIO-ChR2 (H134)-eYFP virus was purchased from University of North Carolina, Vector Core Facilities, and delivered to the VTA by stereotaxic surgery as previously described (Bimpisidis et al., 2019, 2020; Figure 1A) in order to visualize VTA NEX-Cre positive neurons and their projections. Briefly, *NEX*$^{Cre+/wt}$ mice (>8 weeks old; >20 g) were deeply anesthetized with isoflurane and received 300 nl of virus in the right VTA (AP: −3.45 mm, L: −0.2 mm, V:-4.4 mm according to Franklin and Paxinos, 2008) at 100 nl min^{-1} flow rate. Four weeks after injection the mice were transcardially perfused, their brains were collected and cut in a vibratome at 30um-thick sections. The sections were mounted, coverslipped and imaged using a Leica epifluorescent microscope.

Operant apparatus

Instrumental testing was performed in operant chambers (Med Associates Inc., Fairfax, United States) equipped with nosepoke devices on each side of a food magazine. Nose-poking to the active nosepoke (right) activated a cue light above the nose poke and a pellet dispenser which delivered a 20 mg sucrose pellet (5TUT, TestDiet, St. Louis, United States; Figure 1D) according to the different phases of the task.

Sucrose self-administration paradigm

Operant sucrose Self-Administration (SA) was performed as described previously (Alsiö et al., 2011). We used operant conditioning to assess incentive-guided behaviors similarly to what has been used to study addiction-related behaviors. Thus, we included Fixed Ratio (FR) schedules of reinforcement to measure sucrose "taking" or consumption, a Progressive Ratio (PR) schedule of reinforcement to express quantitively the motivation to obtain sucrose, an extinction phase and a final cue-induced reinstatement (CIR) phase to model sucrose seeking and/or the efficacy of sucrose-related cues to elicit instrumental responses (Roberts et al., 1989; Epstein et al., 2006; Grimm and Sauter, 2020; Tsibulsky and Norman, 2021).

The timeline of the experiments is depicted in Figure 1E. At the first phase of the task, food restricted mice were placed in the chambers under a FR1 schedule in which each active nose poke resulted in the delivery of 1 sucrose pellet. The learning criterion was met if the mouse obtained ≥10 rewards and then having stable responses in terms of active nose pokes (<15% difference between sessions) for 3 consecutive days. For FR1, 2 days before the aforementioned criterion was met were included in the graph and analysis. The mice were then moved to FR3, where 3 active nose pokes resulted the delivery of 1 reward. When mice demonstrated stable responses in the active nose poke (<15% difference between sessions) for 3 days were moved to increased ratios, firstly to FR5 and finally to FR10. The FR sessions were followed by a single, one-hour PR session where the increase in number of responses required to obtain each pellet during the sessions was increased and calculated according to the formula $5e^{(\text{reinforcer number x } 0.2)}$-5, rounded to the nearest integer (Richardson and Roberts, 1996). As breaking point was considered the last number of poke requirement before the session end. After the PR session the mice underwent 7 days of extinction where nose-poking did not result in any sucrose delivery or cue-presentation. The experiment was finalized with 5-days of CIR sessions. During this phase each nose poke resulted in cue-presentation but not sucrose pellet delivery. All sessions except PR lasted for 30 min.

Statistical analysis

All data are expressed as mean ± SEM and were analyzed with GraphPad 8.0 (RRID:SCR_002798). Statistical significance was set at $p < 0.05$ and details on tests can be found in the "Results" sections and/or in figure legends.

Results

NEX-Cre neurons are confined within the VTA and project mainly to the nucleus accumbens medial shell

Brain tissue analysis of *NEX*$^{Cre+/wt}$ mice injected with optogenetic viruses confirmed that NEX-Cre neurons are located within the medial aspects of the VTA. The majority were located in the paranigral, parainterfascicular and parabranchial pigmented nuclei, while smaller numbers were scattered in the interfascicular and rostral linear nuclei (Figure 1B, left panel). The strongest projections of eYFP labeled neurons was observed in the mNAcSh (Figure 1B, right panel), in accordance with previous studies (Bimpisidis et al., 2019; Kramer et al., 2021).

NEX$^{Cre+/wt}$;*Vmat2*$^{flox/flox}$ mice demonstrate more consummatory behavior than their wild-type littermates

The first phase of the operant sucrose SA experiment consisted of increasing FR schedules of reinforcement and when met, a single reward was delivered in the food magazine. cKO mice poked the active nose-poke more than controls throughout this phase of the task, with greater differences revealed with increasing ratio demands [session x genotype x nose poke effect, $F_{(13,1,338)} = 2.195$, $p = 0.0081$, mixed effects model; Figure 2A]. Two-way ANOVA analysis on the average active nose pokes for each schedule of reinforcement (Figure 2B) revealed significant effects of schedule [$F_{(3,204)} = 4{,}450$, $p < 0.0001$], genotype [$F_{(1,204)} = 146.3$, $p < 0.0001$] and schedule x genotype interaction [$F_{(3,204)} = 24.99$, $p < 0.0001$]. Sidak's multiple comparisons test showed that cKO mice displayed a trend toward increased average numbers of active nose pokes for FR1 and FR3 schedules compared to controls ($p = 0.0751$ and $p = 0.0669$, respectively), that reached statistical significance during FR5 ($p < 0.0001$) and FR10 ($p < 0.0001$; Average active nose pokes for each schedule of reinforcement: cKO FR1: 30.92 ± 0.67, N = 34; Control FR1: 23.29 ± 0.77, N = 34; cKO FR3: 85.18 ± 1.18, N = 26; Control FR3: 76.76 ± 1.45, N = 29; cKO FR5: 172 ± 1.295, N = 21; Control FR5: 146.5 ± 2.54, N = 25; cKO FR10: 347 ± 5.93, N = 20; Control FR10: 297.9 ± 6.15, N = 20; Figure 2B).

The increased number of responses on the active nose pokes by the cKO mice was accompanied by a larger number of consumed rewards throughout the 14 sessions of the experiment [effect of session $F_{(13,669)} = 41.4$, $p < 0.001$; effect of genotype $F_{(1,66)} = 9.56$, $p = 0.003$ but not of session x genotype $F_{(13,669)} = 0.478$, $p = 0.937$, mixed effects model; Figure 2C]. Thus, the average number of rewards obtained by cKO mice was consistently higher than control mice for every FR schedule of reinforcement [Two-way ANOVA, effect of schedule: $F_{(3,204)} = 351.3$, $p < 0.0001$; genotype $F_{(1,204)} = 252.7$, $p < 0.0001$; schedule x genotype $F_{(3,204)} = 1.607$, $p = 01888$. Sidak's multiple comparisons test on averages: FR1: cKO 21.93 ± 0.48, Control 17.36 ± 0.19, $p < 0.0001$; FR3: cKO 24.31 ± 0.28, Control 21.11 ± 0.18, $p < 0.0001$; FR5: cKO 29.62 ± 0.2, Control 25.61 ± 0.32, $p < 0.0001$; FR10: cKO 32.05 ± 0.52, Control 27.82 ± 0.47, $p = 0.0001$; Figure 2D].

These results indicate that cKO mice, that lack the capacity to release DA from the NEX-Cre positive VTA subpopulation, work more to obtain sucrose and thus demonstrate increased consummatory behavior compared to their wild-type littermates.

Motivation to obtain sucrose is not altered in *NEX*$^{Cre+/wt}$;*Vmat2*$^{flox/flox}$ mice

When tested in a progressive ratio schedule of reinforcement, where the subsequent reward delivery demanded higher-effort poking behavior, cKO mice did not differ on their level of motivation to obtain sucrose from control mice. Thus, cKO and their wild-type littermates had similar number of active nose pokes (cKO: 664.2 ± 51.73, N = 20; Control 622 ± 65.32, N = 20; $p = 0.615$; Figure 3A), inactive nose pokes (cKO: 24.95 ± 3.22; Control 21.1 ± 2.51; $p = 0.352$; Figure 3B), magazine entries (cKO: 464.4 ± 43.29; Control: 543.4 ± 62.95; $p = 0.308$; Figure 3C)

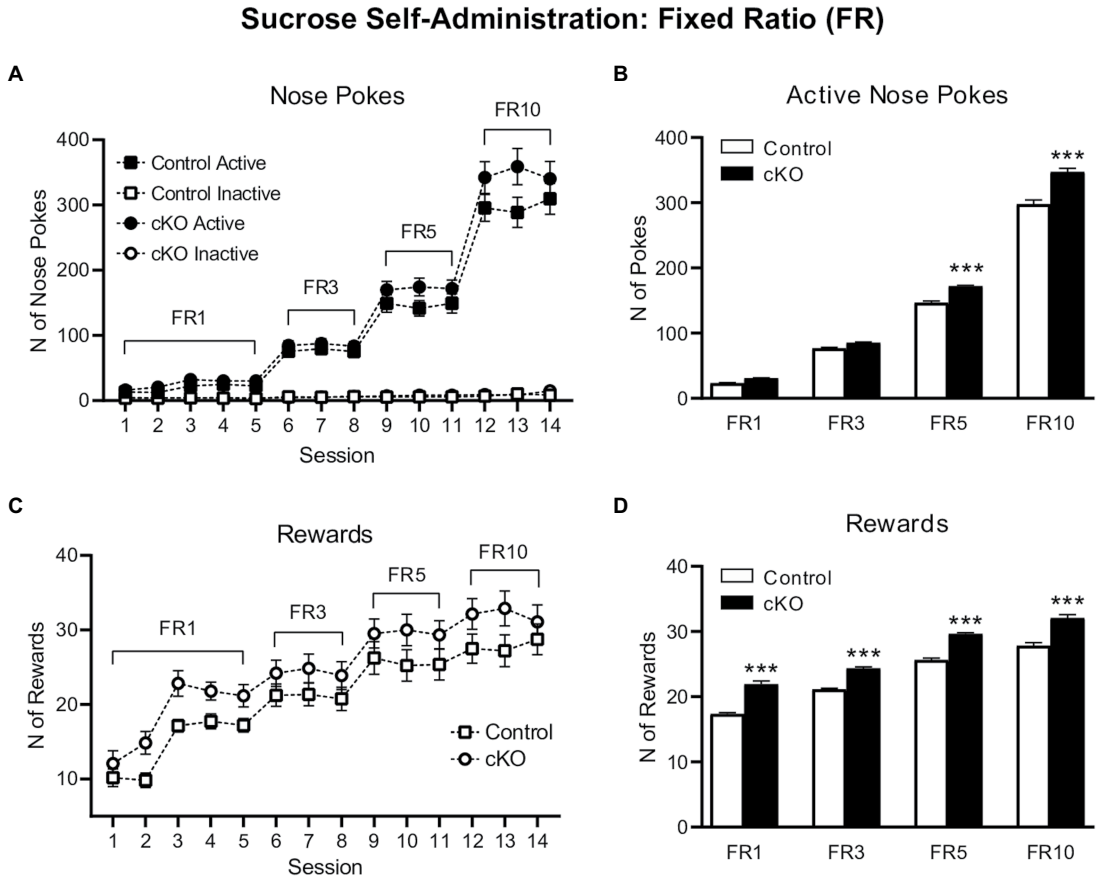

FIGURE 2
Active (filled symbols) and inactive (clear symbols) nose pokes of control (squares) and cKO (circles) mice throughout the Fixed Ratio (FR) sessions **(A)**. Average of active nose pokes of control (white bars) and cKO (black bars) mice in FR1, FR3, FR5 and FR10 sessions **(B)**. Rewards obtained by control (squares) and cKO (circles) throughout the Fixed Ratio (FR) sessions **(C)**. Average of rewards gained by control (white bars) and cKO (black bars) mice in FR1, FR3, FR5 and FR10 sessions **(D)**. Data are expressed as mean±SEM. ***p <0.001 Sidak's multiple comparisons test vs. control mice.

and breaking point (cKO 145.6 ± 10.44, Control 140.2 ± 14.17, $p = 0.758$; Figure 3D), a quantitative measurement of motivation to obtain a reward. Unlike consummatory behavior, the motivational processes to obtain a highly salient food reward do not seem to depend on DA released by the NEX-Cre positive VTA subpopulation.

NEX$^{Cre+/wt}$;*Vmat2*$^{flox/flox}$ and control mice do not differ in extinction and cue-induced reinstatement of operant behavior in the sucrose SA paradigm

After the progressive ratio session, cKO and control mice underwent a seven-day extinction phase, followed by 5 days of CIR. Responding in nose pokes did not differ between genotypes throughout the testing period [effect of session x genotype x nose poke, $F_{(11,432)} = 1.299$, $p = 0.3192$, 3-way ANOVA; Figure 4A]. Similarly, the average of pokes during extinction [active cKO: 80.05 ± 32.06 N = 19, Control:71.99 ± 26.23 N = 19, $p = 0.849$; inactive cKO: 9.79 ± 1.630, Control 7.5 ± 1.612, $p = 0.339$, unpaired t-test; Figures 4B,C] and CIR [active cKO: 26.28 ± 1.42, Control:24.83 ± 1.47, $p = 0.498$; inactive cKO: 5.16 ± 0.71, Control 4.47 ± 0.38, $p = 0.421$, unpaired t-test; Figures 4D,E] did not differ between genotypes. Furthermore, magazine entries did not differ when analyzed for each session [effect of session x genotype $F_{(11,396)} = 0.656$, $p = 0.780$, 2-way ANOVA; Figure 4F]. The average of magazine entries during extinction was not different between genotypes (cKO: 175 ± 17.78; Control:146.4 ± 21.63, $p = 0.328$, unpaired t-test) but was higher in cKO compared to control mice in CIR sessions (cKO: 151.3 ± 3.27; Control:110.5 ± 5.63, $p < 0.001$, unpaired t-test; Figures 4G,H). While both genotypes extinguish their operant responses in a similar manner, cKO mice visit the magazine more frequently during CIR, a behavior possibly reflecting abnormal sensitivity to cues.

Discussion

The gene encoding the transcription factor NeuroD6 is expressed in a relatively small number of DA neurons of the VTA primarily located in paranigral, parainterfascicular and parabranchial pigmented subnuclei of the VTA (Viereckel et al., 2016; Khan et al., 2017; Kramer et al., 2018, 2021; Bimpisidis et al., 2019). Using our previously published cKO approach to target the NeuroD6 DA subpopulation, we here tested cKO mice in an operant sucrose SA task, and compared their performance with that of age-and sex-matched control mice. The operant SA task differs from the sucrose preference test we used before (Bimpisidis et al., 2019) and can reveal different behaviors affected by the given genetic manipulation. Thus, while the later can give information for anhedonia-like symptoms (Liu et al., 2018), the

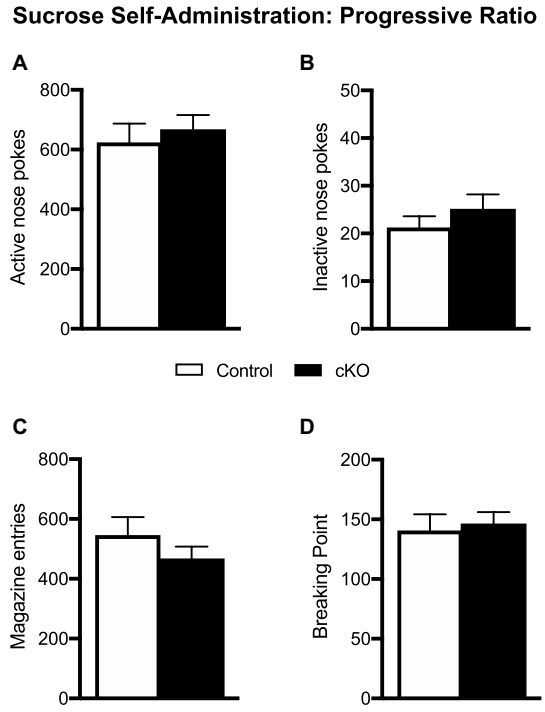

FIGURE 3
Active **(A)** and inactive pokes **(B)**, magazine entries **(C)** and breaking point **(D)** of control (white bars) and cKO (black bars) mice during the one-hour progressive ratio session. Data are expressed as mean±SEM.

complexity of the former can answer questions on whether consumption, motivation or cue-induced behavior is altered in cKO mice with respect to wt littermate controls. It is possible that knocking-out genes within the DA system can induce alterations in homeostatic feeding behavior. Nevertheless, the fact that cKO mice and littermate controls show no differences in weight (Bimpisidis et al., 2019; current study, data not shown) led us to exclude this possibility. The operant SA task made evident that cKO mice demonstrated more responses and obtained more rewards under several FR schedules compared to controls. This shows that NeuroD6 neurons are involved in regulating consummatory behavior through DA release. On the other hand, motivation to receive sucrose rewards did not differ between cKO and control mice, as measured by a PR schedule, suggesting that the NeuroD6 VTA subpopulation is not involved in motivational aspects related to food reward. Finally, no differences in active and inactive nose pokes were observed during extinction and CIR schedules but cKO mice visited the food magazine more times than their control littermates during this latter phase of the experiment, possibly indicating that cKO mice show abnormal sensitivity to reward-related cues.

In a previous study (Bimpisidis et al., 2019), we described that NEX-Cre neurons project mainly to the mNAcSh and that ablation of Vmat2 from these neurons results in elevated locomotor responses to amphetamine. In the current study we demonstrate that these same cKO mice make more operant responses to obtain sucrose rewards. These results might seem counterintuitive, given the well characterized role of DA in both motor and consummatory behaviors provided by studies targeting the DAergic systems unselectively. A possible explanation of our results could be given by the fact that only a small percentage of VTA DA neurons express *NeuroD6* (about 12%; Bimpisidis et al., 2019) and their inability to release DA might lead to different behavioral outcomes from those expected when larger ablations or disturbances of the DA system take place.

NeuroD6 is already expressed at E14.5 in cells positive for other dopaminergic markers, indicating that the processes to form a unique DA subpopulation within the VTA begin early in development (Dumas and Wallén-Mackenzie, 2019). Studies on NeuroD6 knock-out mice, have highlighted the importance of the gene in the normal development of the DA system; KO mice show reduced number of midbrain DA neurons (Khan et al., 2017). It is possible that the cKO approach we followed in the current study also affected the maturation of the developing DA system by disrupting DA transmission from NeuroD6+ cells. Furthermore, reduced DA tone from this subpopulation might have induced post-synaptic adaptive changes in other systems, that could explain our findings. For instance, the higher number of operant responding during fixed ratios of reinforcement might reflect increased positive experiences that are mainly non-DA related; indeed, they seem to be mediated by GABAergic and opioidergic systems (Berridge and Robinson, 1998). Possibly, cKO mice work for and consume more sucrose because they experience greater pleasurable effects due to occurrence of developmental changes following the absence of DA release from NeuroD6+ neurons throughout the lifespan, but this is a hypothesis that has to be tested experimentally. A way to verify this hypothesis would be to use inducible Cre lines or viral strategies to target this specific neuronal subpopulation in combination with behavioral tests that assess hedonic reactions (Berridge and Robinson, 1998).

Additional plastic changes, such as the overactivity of the rest, non NeuroD6+, neurons of the DA system cannot be excluded. Different DA subcircuits work in synergy to mediate behavior and transform incentive to actions. In this direction, disruption of DA release toward mNAcShell (and as mentioned throughout development) might render DA target areas more sensitive to DA deriving from intact DA populations and in consequence to enhance response-outcome associations relevant to food reward delivery, or more sensitive to cues related to it. The increases in magazine entries during the CIR phase of the experiment may support this notion, but it requires further investigation.

Manipulations of the DA system affect higher effort schedules of reinforcement rather than actions of lower cost (Salamone et al., 1991; Cheeta et al., 1995; Ikemoto and Panksepp, 1996; Aberman and Salamone, 1999; Reilly, 1999; Barbano and Cador, 2006; Veeneman et al., 2012). In the current study, no changes in performance during higher effort/increasing demand-related schedules of reinforcement were observed when cKO and control mice were tested in the progressive ratio test. Our results suggest that consummatory and motivational aspects of reward-related behavior are served by distinct DA circuits and that the NeuroD6-positive DA neurons are involved in the former and not the latter. A possible limitation of our study design is the relatively short period of the PR sessions. It remains unknown if testing for longer time periods would be sufficient to reveal differences between cKO and control mice. However, given the fact that we already observed significant differences between genotypes during the 30-minute-long FR sessions, it is likely that one-hour sessions of PR testing were appropriate for the scope of our study, and in accordance to the literature.

Newer molecular methods permit the separation and characterization of DA neurons within the midbrain based on their molecular profile, both between SNc and VTA, but also within each region (Poulin et al., 2014, 2018; La Manno et al., 2016; Viereckel et al., 2016; Nagaeva et al., 2020). The identification of unique neuronal subtypes based on molecular markers gives the opportunity to selectively target neurons intermingled

10.3389/fnmol.2023.1069834

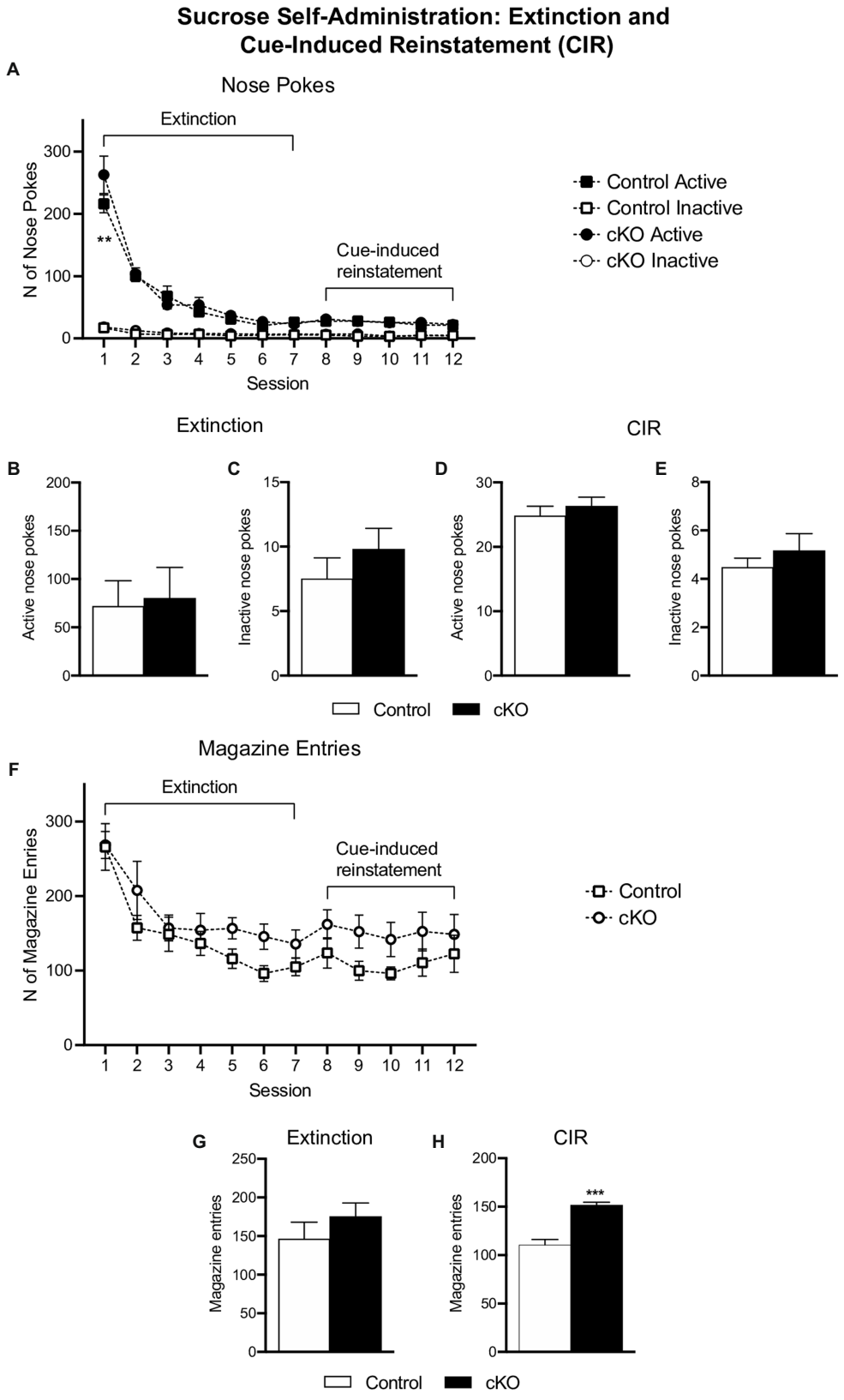

FIGURE 4
Active (filled symbols) and inactive (clear symbols) nose pokes of control (squares) and cKO (circles) mice throughout the extinction and cue-induced reinstatement (CIR) phases **(A)**. Average of active **(B,D)** and inactive **(C,E)** nose pokes of control (white bars) and cKO (black bars) mice in extinction and CIR phases. Magazine entries throughout the extinction and CIR phases **(F)** and average of responses separate for each phase **(G,H)**. Data are expressed as mean±SEM. $^{**}p=0.0011$, Tukey's *post-hoc* comparison test vs. control mice; $^{***}p<0.001$ vs. control mice unpaired *t*-test.

within others in a given area, and describe their behavioral character. We here used gene targeting based on molecular profile and provide evidence that a distinct group of VTA DA neurons characterized by the expression of *NeuroD6* is involved in consummatory and not motivated behavior toward sucrose reward, adding information on the current knowledge of the function of the VTA DA system. Altogether, studies using advanced targeting of isolated DA subpopulations are crucial for understanding the underlying physiology of normal reward-related behavior and for providing a theoretical framework to explain conditions where these processes are compromised, such as drug use disorder, food disorders and depression. By aiming to manipulate only specific neurons implicated in disease, more efficient therapeutic approaches can be developed and unwanted side-effects by targeting the whole DA system can be avoided. Our results provide insights on the role of one of those VTA DA subpopulations in behavior, toward this direction.

Data availability statement

The raw data supporting the conclusions of this article will be made available by the authors, without undue reservation.

Ethics statement

The animal study was reviewed and approved by Uppsala University Ethical Committee for Use of Animals in accordance to Swedish and EU legislation.

Author contributions

ZB conceived planned and performed experiments, analyzed data, and wrote the manuscript (original draft, editing, and revision). GPS and NK performed experiments. ÅW-M: project design, organization and funding, and manuscript editing. All authors reviewed the manuscript, contributed to the article, and approved the submitted version.

Funding

This work was supported by Uppsala University and by grants to ÅW-M from the Swedish Research Council (Vetenskapsrådet 2017–02039), the Swedish Brain Foundation (Hjärnfonden), Parkinsonfonden, Bertil Hållsten Research Foundation, Zoologiska stiftelsen and Åhlénstiftelsen.

Acknowledgments

The authors thank Bruno Giros (McGill University, Montreal, Canada) for generously providing the *Vmat2*$^{flox/flox}$ mice and Professor Klaus-Armin Nave and Sandra Goebbels (Max Plank Institute of Experimental Medicine, Goettingen, Germany) for the NEX-Cre mice.

Conflict of interest

The authors declare that the research was conducted in the absence of any commercial or financial relationships that could be construed as a potential conflict of interest.

Publisher's note

All claims expressed in this article are solely those of the authors and do not necessarily represent those of their affiliated organizations, or those of the publisher, the editors and the reviewers. Any product that may be evaluated in this article, or claim that may be made by its manufacturer, is not guaranteed or endorsed by the publisher.

References

Aberman, J. E., and Salamone, J. D. (1999). Nucleus accumbens dopamine depletions make rats more sensitive to high ratio requirements but do not impair primary food reinforcement. *Neuroscience* 92, 545–552. doi: 10.1016/S0306-4522(99)00004-4

Alsiö, J., Nordenankar, K., Arvidsson, E., Birgner, C., Mahmoudi, S., Halbout, B., et al. (2011). Enhanced sucrose and cocaine self-administration and Cue-induced drug seeking after loss of VGLUT2 in midbrain dopamine neurons in mice. *J. Neurosci.* 31, 12593–12603. doi: 10.1523/jneurosci.2397-11.2011

Barbano, M. F., and Cador, M. (2006). Differential regulation of the consummatory, motivational and anticipatory aspects of feeding behavior by dopaminergic and opioidergic drugs. *Neuropsychopharmacology* 31, 1371–1381. doi: 10.1038/sj.npp.1300908

Berke, J. D. (2018). What does dopamine mean? *Nat. Neurosci.* 21, 787–793. doi: 10.1038/s41593-018-0152-y

Berridge, K. C., and Robinson, T. E. (1998). What is the role of dopamine in reward: hedonic impact, reward learning, or incentive salience? *Brain Res. Rev.* 28, 309–369. doi: 10.1016/S0165-0173(98)00019-8

Bimpisidis, Z., König, N., Stagkourakis, S., Zell, V., Vlcek, B., Dumas, S., et al. (2019). The NeuroD6 subtype of VTA neurons contributes to psychostimulant sensitization and behavioral reinforcement. *eNeuro* 6, ENEURO.0066–ENEU19.2019. doi: 10.1523/ENEURO.0066-19.2019

Bimpisidis, Z., König, N., and Wallén-Mackenzie, Å. (2020). Two different real-time place preference paradigms using Optogenetics within the ventral tegmental area of the mouse. *JoVE Journal Vis. Exp* 2020:e60867. doi: 10.3791/60867

Björklund, A., and Dunnett, S. B. (2007). Dopamine neuron systems in the brain: an update. *Trends Neurosci.* 30, 194–202. doi: 10.1016/j.tins.2007.03.006

Cai, L. X., Pizano, K., Gundersen, G. W., Hayes, C. L., Fleming, W. T., Holt, S., et al. (2020). Distinct signals in medial and lateral VTA dopamine neurons modulate fear extinction at different times. *elife* 9, 1–23. doi: 10.7554/ELIFE.54936

Cheeta, S., Brooks, S., and Willner, P. (1995). Effects of reinforcer sweetness and the D2/D3 antagonist raclopride on progressive ratio operant performance. *Behav. Pharmacol.* 6:127. doi: 10.1097/00008877-199503000-00004

Chung, C. Y., Seo, H., Sonntag, K. C., Brooks, A., Lin, L., and Isacson, O. (2005). Cell type-specific gene expression of midbrain dopaminergic neurons reveals molecules involved in their vulnerability and protection. *Hum. Mol. Genet.* 14, 1709–1725. doi: 10.1093/hmg/ddi178

de Jong, J. W., Afjei, S. A., Pollak Dorocic, I., Peck, J. R., Liu, C., Kim, C. K., et al. (2019). A neural circuit mechanism for encoding aversive stimuli in the mesolimbic dopamine system. *Neuron* 101, 133–151.e7. doi: 10.1016/j.neuron.2018.11.005

Di Chiara, G., and Bassareo, V. (2007). Reward system and addiction: what dopamine does and doesn't do. *Curr. Opin. Pharmacol.* 7, 69–76. doi: 10.1016/j.coph.2006.11.003

Dumas, S., and Wallén-Mackenzie, Å. (2019). Developmental co-expression of Vglut2 and Nurr1 in a Mes-Di-encephalic continuum Preceeds dopamine and glutamate neuron specification. *Front. Cell Dev. Biol.* 7:307. doi: 10.3389/fcell.2019.00307

Engelhard, B., Finkelstein, J., Cox, J., Fleming, W., Jang, H. J., Ornelas, S., et al. (2019). Specialized coding of sensory, motor and cognitive variables in VTA dopamine neurons. *Nature* 570, 509–513. doi: 10.1038/s41586-019-1261-9

Epstein, D. H., Preston, K. L., Stewart, J., and Shaham, Y. (2006). Toward a model of drug relapse: an assessment of the validity of the reinstatement procedure. *Psychopharmacology* 189, 1–16. doi: 10.1007/s00213-006-0529-6

Franklin, K. B. J., and Paxinos, G. (2008). *The mouse brain in stereotaxic coordinates*. Boston: Academic Press.

Goebbels, S., Bormuth, I., Bode, U., Hermanson, O., Schwab, M. H., and Nave, K.-A. (2006). Genetic targeting of principal neurons in neocortex and hippocampus of NEX-Cre mice. *Genesis* 44, 611–621. doi: 10.1002/dvg.20256

Greene, J. G., Dingledine, R., and Greenamyre, J. T. (2005). Gene expression profiling of rat midbrain dopamine neurons: implications for selective vulnerability in parkinsonism. *Neurobiol. Dis.* 18, 19–31. doi: 10.1016/j.nbd.2004.10.003

Grimm, J. W., and Sauter, F. (2020). Environmental enrichment reduces food seeking and taking in rats: a review. *Pharmacol. Biochem. Behav.* 190:172874. doi: 10.1016/J.PBB.2020.172874

Heymann, G., Jo, Y. S., Reichard, K. L., McFarland, N., Chavkin, C., Palmiter, R. D., et al. (2020). Synergy of distinct dopamine projection populations in behavioral reinforcement. *Neuron* 105, 909–920.e5. doi: 10.1016/j.neuron.2019.11.024

Ikemoto, S. (2007). Dopamine reward circuitry: two projection systems from the ventral midbrain to the nucleus accumbens-olfactory tubercle complex. *Brain Res. Rev.* 56, 27–78. doi: 10.1016/j.brainresrev.2007.05.004

Ikemoto, S., and Panksepp, J. (1996). Dissociations between appetitive and consummatory responses by pharmacological manipulations of reward-relevant brain regions. *Behav. Neurosci.* 110, 331–345. doi: 10.1037//0735-7044.110.2.331

Khan, S., Stott, S. R. W., Chabrat, A., Truckenbrodt, A. M., Spencer-Dene, B., Nave, K. A., et al. (2017). Survival of a novel subset of midbrain dopaminergic neurons projecting to the lateral septum is dependent on neurod proteins. *J. Neurosci.* 37, 2305–2316. doi: 10.1523/JNEUROSCI.2414-16.2016

König, N., Bimpisidis, Z., Dumas, S., and Wallén-Mackenzie, Å. (2020). Selective knockout of the vesicular monoamine transporter 2 (Vmat2) gene in Calbindin2/Calretinin-positive neurons results in profound changes in behavior and response to drugs of abuse. *Front. Behav. Neurosci.* 14:443. doi: 10.3389/fnbeh.2020.578443

Kramer, D. J., Aisenberg, E. E., Kosillo, P., Friedmann, D., Stafford, D. A., Lee, A. Y. F., et al. (2021). Generation of a DAT-P2A-Flpo mouse line for intersectional genetic targeting of dopamine neuron subpopulations. *Cell Rep.* 35:109123. doi: 10.1016/j.celrep.2021.109123

Kramer, D. J., Risso, D., Kosillo, P., Ngai, J., and Bateup, H. S. (2018). Combinatorial expression of Grp and NeuroD6 defines dopamine neuron populations with distinct projection patterns and disease vulnerability. *eNeuro.* 5. doi: 10.1523/ENEURO.0152-18.2018

La Manno, G., Gyllborg, D., Codeluppi, S., Nishimura, K., Salto, C., Zeisel, A., et al. (2016). Molecular diversity of midbrain development in mouse, human, and stem cells. *Cells* 167, 566–580.e19. doi: 10.1016/j.cell.2016.09.027

Lammel, S., Hetzel, A., Häckel, O., Jones, I., Liss, B., and Roeper, J. (2008). Unique properties of Mesoprefrontal neurons within a dual Mesocorticolimbic dopamine system. *Neuron* 57, 760–773. doi: 10.1016/j.neuron.2008.01.022

Lammel, S., Ion, D. I., Roeper, J., and Malenka, R. C. (2011). Projection-specific modulation of dopamine neuron synapses by aversive and rewarding stimuli. *Neuron* 70, 855–862. doi: 10.1016/j.neuron.2011.03.025

Lammel, S., Lim, B. K., Ran, C., Huang, K. W., Betley, M. J., Tye, K. M., et al. (2012). Input-specific control of reward and aversion in the ventral tegmental area. *Nature* 491, 212–217. doi: 10.1038/nature11527

Lerner, T. N., Shilyansky, C., Davidson, T. J., Evans, K. E., Beier, K. T., Zalocusky, K. A., et al. (2015). Intact-brain analyses reveal distinct information carried by SNc dopamine subcircuits. *Cells* 162, 635–647. doi: 10.1016/j.cell.2015.07.014

Liu, M. Y., Yin, C. Y., Zhu, L. J., Zhu, X. H., Xu, C., Luo, C. X., et al. (2018). Sucrose preference test for measurement of stress-induced anhedonia in mice. *Nat. Protoc 2018* 137, 1686–1698. doi: 10.1038/s41596-018-0011-z

Lüscher, C. (2016). The emergence of a circuit model for addiction. *Annu. Rev. Neurosci.* 39, 257–276. doi: 10.1146/annurev-neuro-070815-013920

Nagaeva, E., Zubarev, I., Gonzales, C. B., Forss, M., Nikouei, K., de Miguel, E., et al. (2020). Heterogeneous somatostatin-expressing neuron population in mouse ventral tegmental area. *elife* 9:328. doi: 10.7554/ELIFE.59328

Narboux-Nême, N., Sagné, C., Doly, S., Diaz, S. L., Martin, C. B. P., Angenard, G., et al. (2011). Severe serotonin depletion after conditional deletion of the vesicular monoamine transporter 2 gene in serotonin neurons: neural and behavioral consequences. *Neuropsychopharmacology* 36, 2538–2550. doi: 10.1038/npp.2011.142

Poulin, J.-F., Caronia, G., Hofer, C., Cui, Q., Helm, B., Ramakrishnan, C., et al. (2018). Mapping projections of molecularly defined dopamine neuron subtypes using intersectional genetic approaches. *Nat. Neurosci.* 21, 1260–1271. doi: 10.1038/s41593-018-0203-4

Poulin, J. F., Zou, J., Drouin-Ouellet, J., Kim, K. Y. A., Cicchetti, F., and Awatramani, R. (2014). Defining midbrain dopaminergic neuron diversity by single-cell gene expression profiling. *Cell Rep.* 9, 930–943. doi: 10.1016/j.celrep.2014.10.008

Reilly, S. (1999). Reinforcement value of gustatory stimuli determined by progressive ratio performance. *Pharmacol. Biochem. Behav.* 63, 301–311. doi: 10.1016/S0091-3057(99)00009-X

Richardson, N. R., and Roberts, D. C. S. (1996). Progressive ratio schedules in drug self-administration studies in rats: a method to evaluate reinforcing efficacy. *J. Neurosci. Methods* 66, 1–11. doi: 10.1016/0165-0270(95)00153-0

Roberts, D. C. S., Loh, E. A., and Vickers, G. (1989). Self-administration of cocaine on a progressive ratio schedule in rats: dose-response relationship and effect of haloperidol pretreatment. *Psychopharmacology* 97, 535–538. doi: 10.1007/BF00439560

Salamone, J. D., Steinpreis, R. E., McCullough, L. D., Smith, P., Grebel, D., and Mahan, K. (1991). Haloperidol and nucleus accumbens dopamine depletion suppress lever pressing for food but increase free food consumption in a novel food choice procedure. *Psychopharmacology* 104, 515–521. doi: 10.1007/BF02245659

Saunders, B. T., Richard, J. M., Margolis, E. B., and Janak, P. H. (2018). Dopamine neurons create Pavlovian conditioned stimuli with circuit-defined motivational properties. *Nat. Neurosci.* 21, 1072–1083. doi: 10.1038/s41593-018-0191-4

Schultz, W., Dayan, P., and Montague, P. R. (1997). A neural substrate of prediction and reward. *Science* 275, 1593–1599. doi: 10.1126/science.275.5306.1593

Serra, G. P., Guillaumin, A., Dumas, S., Vlcek, B., and Wallén-Mackenzie, Å. (2021). Midbrain dopamine neurons defined by TrpV1 modulate psychomotor behavior. *Front. Neural Circuits* 15:119. doi: 10.3389/FNCIR.2021.726893

Tsibulsky, V. L., and Norman, A. B. (2021). Methodological and analytical issues of progressive ratio schedules: definition and scaling of breakpoint. *J. Neurosci. Methods* 356:109146. doi: 10.1016/j.jneumeth.2021.109146

Veeneman, M. M. J., Van Ast, M., Broekhoven, M. H., Limpens, J. H. W., and Vanderschuren, L. J. M. J. (2012). Seeking-taking chain schedules of cocaine and sucrose self-administration: effects of reward size, reward omission, and α-flupenthixol. *Psychopharmacology* 220, 771–785. doi: 10.1007/s00213-011-2525-8

Viereckel, T., Dumas, S., Smith-Anttila, C. J. A., Vlcek, B., Bimpisidis, Z., Lagerström, M. C., et al. (2016). Midbrain gene screening identifies a new Mesoaccumbal glutamatergic pathway and a marker for dopamine cells Neuroprotected in Parkinson's disease. *Sci. Rep.* 6, 1–16. doi: 10.1038/srep35203

frontiers | Frontiers in Molecular Neuroscience

TYPE Review
PUBLISHED 14 February 2023
DOI 10.3389/fnmol.2023.1098211

OPEN ACCESS

EDITED BY
Juan Marín-Lahoz,
Hospital Universitario Miguel Servet,
Spain

REVIEWED BY
Lawrence Judson Chandler,
Medical University of South Carolina,
United States
Paul Slesinger,
Icahn School of Medicine at Mount Sinai,
United States
Marsida Kallupi,
University of California,
San Diego,
United States

*CORRESPONDENCE
Pablo Gimenez-Gomez
✉ pablo.gimenezgomez@umassmed.edu
Gilles E. Martin
✉ gilles.martin@umassmed.edu

SPECIALTY SECTION
This article was submitted to Neuroplasticity and Development, a section of the journal Frontiers in Molecular Neuroscience

RECEIVED 14 November 2022
ACCEPTED 19 January 2023
PUBLISHED 14 February 2023

CITATION
Gimenez-Gomez P, Le T and Martin GE (2023) Modulation of neuronal excitability by binge alcohol drinking.
Front. Mol. Neurosci. 16:1098211.
doi: 10.3389/fnmol.2023.1098211

Modulation of neuronal excitability by binge alcohol drinking

Pablo Gimenez-Gomez[1,2]*, Timmy Le[1,2,3] and Gilles E. Martin[1,2]*

[1]Department of Neurobiology, University of Massachusetts Chan Medical School, Worcester, MA, United States, [2]The Brudnick Neuropsychiatric Research Institute, Worcester, MA, United States, [3]Graduate Program in Neuroscience, Morningside Graduate School of Biomedical Sciences, UMass Chan Medical School, Worcester, MA, United States

Drug use poses a serious threat to health systems throughout the world. The number of consumers rises every year being alcohol the drug of abuse most consumed causing 3 million deaths (5.3% of all deaths) worldwide and 132.6 million disability-adjusted life years. In this review, we present an up-to-date summary about what is known regarding the global impact of binge alcohol drinking on brains and how it affects the development of cognitive functions, as well as the various preclinical models used to probe its effects on the neurobiology of the brain. This will be followed by a detailed report on the state of our current knowledge of the molecular and cellular mechanisms underlying the effects of binge drinking on neuronal excitability and synaptic plasticity, with an emphasis on brain regions of the meso-cortico limbic neurocircuitry.

KEYWORDS

alcohol, binge alcohol drinking, neuroadaptation, neuronal excitability, ion channel

1. Introduction

Traces of alcohol, an organic compound that results from the fermentation of grain, fruit juice and honey, have been identified in early 7,000 BC settlements in China (McGovern et al., 2004) and in jars from the Middle East and Egyptian settlements dating back to 3,000 BC (Cavalieri et al., 2003; Gately, 2008). These archeological findings arguably place alcohol as one of the first, if not the first, drug used by humans. Today, it is the most widely used and abused legal drug, becoming a major global health problem as the United Nations Office on Drugs and Crime admits. Worldwide, 57% of the global population aged 15 years and over consumed alcohol in the previous 12 months producing 3 million deaths (5.3% of all deaths) worldwide and 132.6 million disability-adjusted life years. In the U.S. alone, excessive alcohol consumption is responsible for 13% and 20% of total deaths among adults 20 to 64 and 20 to 49 years old, respectively (Esser et al., 2022). Alcohol is consumed in a variety of methods, from light social drinking to more abusive forms. Early enquiries focused primarily on the development of tolerance and dependence resulting from prolonged and repeated heavy drinking. Over the past decade, binge alcohol drinking has received increased attention in part due to the recognition that it is the preferred mode of consumption of adolescents and young adults. As school surveys show alcohol use starts before the age of 15 and the prevalence of alcohol use can be in the range of 50%–70% with no remarkable differences between sexes (Substance Abuse and Mental Health Services Administration, 2019). Moreover, the prevalence of heavy episodic drinking using binge alcohol drinking is 18.2% with a peak in young adults, an age group particularly susceptible to the drug effects owing to the biological vulnerability of their still developing brains (Kwan et al., 2020). In the present review we tried to discuss all the relevant bibliography for the topic discussed. In order to do so we used Pubmed as a main resource for publications using keywords such as "alcohol," "EtOH," "Ethanol," "Drinking in the dark" or the name of other relevant models along with keywords related to each topic discussed (Neuronal excitability, potassium channels, sodium, channels, ion channels, neuronal firing, synaptic transmission, plasticity,

glutamate, GABA, glutamate receptors, gaba receptors, AMPA, NMDA or synaptic gating).

1.1. Consequences of binge alcohol drinking on behavior

As originally described by Tomsovic (1974), binge alcohol drinking is defined as repeated periods of heavy drinking, followed by periods of abstinence. Although the number of drinks consumed during a 2-h period was initially considered as the main marker, a recent attempt to standardize studies led to an updated definition stipulating that binge drinking must elevate blood alcohol levels to 80 mg/dl or above. This typically corresponds to consuming five or more drinks (male), or four or more drinks (female), in approximately 2 h (NIAAA, 2004). Such drinking pattern has been primarily studied in young adults (e.g., college students) as they represent by far the largest group affected by this behavior (Naimi et al., 2003), although this drinking pattern is also increasingly common in adolescents as young as 12 (Sun et al., 2008; SAMHSA, 2014). Furthermore, this pattern of drinking may be exacerbated in adolescents and young adults during the 2020 COVID-19 lockdown as a means to cope with social isolation (Skrzynski and Creswell, 2020).

Regarding the brain areas affected by binge alcohol drinking, there is strong cumulative evidence that the frontal lobes, which mature later compared to the rest of the brain (Giedd et al., 1999) and play a major role in controlling inhibitory responses, are particularly susceptible to this pattern of consumption. Accordingly, just one episode of binge drinking during 3 months produces thinner and lower volumes of the prefrontal cortex (PFC) and cerebellar regions, and attenuated white matter development (Cservenka and Brumback, 2017). These changes translate into alterations in a number of cognitive tasks such as self-control, working memory, decision making and social and emotional processing. Thus, Scaife and Duka (2009) showed specific impairments in the dorsolateral PFC of females, and the temporal lobes of males and females in binge drinkers compared to non-drinkers. Not only does heavy binge alcohol drinking potentially lead to destructive behaviors such as suicide, drunk driving (Wechsler et al., 1994), and cognitive deficits (Duka et al., 2004), but it is also recognized as being the precursor to long-term alcohol-related problems like sleep disorders, stroke, and social anxiety (Townshend and Duka, 2002; Weissenborn and Duka, 2003; Hartley et al., 2004). Importantly, binge drinkers, contrary to light drinkers, typically display a stronger response to early euphoric effects but are less sensitive to the sedative effects of alcohol, indicative of a predisposition for the development of alcohol addiction (Schuckit, 1994; Schuckit et al., 2008). While the PFC appears particularly vulnerable (Moorman, 2018), probing the effects of binge drinking showed ethanol widespread reach to other brain regions, as we will describe below, including those associated with the neurocircuitry of drug addiction.

Over the past two decades, spurred by the need to work with animals whose blood alcohol levels could be rapidly raised to 80 mg/dL or higher, a level that is generally considered to be intoxicating and representative of excessive drinking (Bell et al., 2006), a number of models were developed, ranging from alcohol consumption without access to water, to gavage, two-bottle choice, and alcohol liquid diet (Crabbe et al., 2011). Two additional protocols seemed to have gathered a general agreement regarding their usefulness. Indeed, most of the data discussed here have mostly been obtained with these two models, the Drinking-in-the-dark (DID) and the chronic intermittent alcohol vapor exposure (CIE) paradigms. DID protocol, originally described by Rhodes et al. (2005), consists in substituting the free access to water to free access to EtOH during 2 h the first 3 days and 4 h during the last day. Ethanol is offered at a concentration of 20% in tap water and the mice drink voluntarily (Thiele and Navarro, 2014). CIE is an EtOH dependence and relapse drinking model described by Becker and Lopez which *via* repeated cycles of chronic intermittent exposure to EtOH vapors in inhalation chambers and periods of withdrawal generate an escalation in voluntary EtOH consumption simulating the transition to EtOH dependence in mice (Becker and Lopez, 2004) and rats (Gilpin et al., 2008). The chief advantages of the DID model are its simplicity, its short duration, as well as its ability to quickly drive blood alcohol concentrations to levels associated with robust intoxication (Ryabinin et al., 2003; Rhodes et al., 2005; Sharpe et al., 2005). Although more complex and costly in its implementation, CIE also promotes a rapid escalation and large EtOH intake (O'Dell et al., 2004). The chief advantage of the DID strategy is that mice can reach intoxication levels at a faster rate relative to that of the CIE model (the mice only need 4 days of consumption using DID protocol; Thiele and Navarro, 2014). Furthermore, the DID is a cost-effective strategy do not require the delivery of vapors or any type of injections (e.g., CIE protocols usually requires the use of Pyrazole and EtOH i.p). On the other hand, the CIE model, unlike DID, produces symptoms in mice compatible with dependence (Becker and Lopez, 2004).

2. Regulation of neuronal excitability by binge drinking

In contrast to its deleterious effects on the liver, heart, blood, and pancreas that typically appear following prolonged and repeated heavy consumption (Rehm et al., 2009; Mostofsky et al., 2016), alcohol affects brain functions as early as the first experience and at lower concentrations (Mukherjee, 2013). With the principal consequences of binge drinking being behavioral alterations, it is imperative to identify the origins of these effects. Considering that the primary function of neurons is to transport information from one part of the brain to another, early research sought to identify the cellular mechanisms underlying alcohol effects on neuronal excitability. The ability of nerve cells to fire action potentials, the electrical signals that support cell-to-cell communication, results from a subtle balance between neuronal intrinsic and extrinsic (i.e., synaptic) homeostatic states (Franklin et al., 1992; Turrigiano et al., 1994). While intrinsic excitability is controlled by a variety of sodium, potassium and calcium channels, synaptic transmission results from the interplay between the release of neurotransmitters, the availability of their endogenous receptors and their biophysical and pharmacological properties defined by their subunit composition (Citri and Malenka, 2008). Additionally, these features are tightly controlled by a number of neuromodulators such as Neuropeptide Y (van den Pol, 2012) Corticotropin Releasing Factor (Joshi et al., 2020) or dopamine (Tritsch and Sabatini, 2012). We will review the state of our current knowledge about the various mechanisms that binge drinking employs to alter behaviors through its effects on neuronal excitability. Although, for clarity, we have classically divided the molecular targets of binge drinking in broad categories, it should not be construed that they are strictly independent and compartmentalized. Instead, their activation is carefully orchestrated as exemplified with voltage-gated sodium and calcium channels that amplify synaptic

potentials in dendrites of hippocampal CA1 pyramidal neurons (Magee and Johnston, 1995) while hyperpolarization-activated cyclic nucleotide-gated cation channels (HCN) inhibit EPSPs the same neurons (George et al., 2009).

3. Binge drinking regulation of ion channel properties and neuronal excitability

3.1. Potassium channels

In addition to shaping neuronal excitability, voltage-gated K^+ channels regulate synaptic transmission and plasticity as they are recruited during depolarization induced by synaptic events (Frick et al., 2004; Truchet et al., 2012).

Therefore, changes in their expression and biophysical properties in the presence of alcohol may directly affect the excitability of neurons and their ability to integrate and process synaptic events. As pharmacological tools and electrophysiological techniques improved, so did the isolation of many ion channels that had previously been inaccessible. However, given the staggering diversity of these channels, compounded by the existence of a number of splice variants for some of these genes, and the sheer difficulty for some to be fully isolated from other ionic currents, only a few have been thoroughly characterized.

It is worth noting that the sensitivity of K^+ channels to physiologically relevant concentrations of acute EtOH (i.e., ≤50 mM) is generally weak. While, in Xenopus oocytes, Kv4 (mShall) and Kv1 (Shaker) channels are insensitive to ethanol, Kv3 (Shaw2) potassium currents are inhibited at only very high concentrations (i.e., ≥100 mM; Covarrubias and Rubin, 1993), confirming an earlier study where none of the 10 different voltage-gated K+ channels expressed in oocytes were sensitive to EtOH (Anantharam et al., 1992). Similarly, in invertebrates, A-currents (I_A) are marginally inhibited by very high EtOH concentrations (Alekseev et al., 1997), and the activity of the G-protein-activated inwardly rectifying potassium channels (GIRKs), in both homomeric and heteromeric forms, is significantly enhanced only at highly intoxicating concentrations of alcohol, an effect believed to depend on the interactions of EtOH with a short sequence of 43 amino acids in the carboxyl terminus (Kobayashi et al., 1999; Lewohl et al., 1999). However, exceptions to this seeming rule exist. One is the calcium- and voltage-sensitive potassium channel (KCNM, mSlo) or BK channel. This channel, that strongly repolarizes membrane potential when activated due to its uniquely large conductance (i.e., ~200 pS and higher), is found in all brain regions of the addiction circuitry. It is potentiated by acute EtOH concentrations as low as 10 mM (Dopico et al., 1996, 1999; Martin et al., 2004). The other is the KCNQ channel which drives the sustained M-current to prevent excessive depolarization by mediating persistent outward K^+ currents at depolarized potentials. Like the BK channels, KCNQ channels are highly expressed in the cortex, hippocampus and nucleus accumbens (NAc), and are inhibited by low (~10 mM) acute EtOH concentrations in drosophila (Cavaliere et al., 2012).

The molecular site of action of ethanol has been a long-standing question in the field of alcohol research (see Abrahao et al., 2017 for a thorough review). Ethanol was initially thought to solely alter channel properties by interacting with the protein lipid environment, a mechanism that is experimentally supported (Crowley et al., 2003; Yuan et al., 2004; Crowley et al., 2005) albeit at high concentrations of EtOH (Ingólfsson and Andersen, 2011). More recently, an elegant study by Bukiya et al. (2014) identified a distinct pocket as the EtOH-recognition site that is placed between the calcium-sensors and gate of the channel α subunit, supporting a direct interaction between EtOH and the BK channel. Although it is unclear whether a similar interaction exists for other ion channels, this is likely because no dedicated EtOH receptors have so far been identified. This observation followed that of Aryal et al. (2009) who identified the cytoplasmic hydrophobic alcohol-binding pocket in GIRK channels. Recent observations also indicate that ligand-gated ion channels are similarly equipped with an EtOH-binding site (see for review Trudell et al., 2014). These EtOH-protein and EtOH–lipid interactions, which probably coexist, provide alcohol with a wealth of options to modulate channel function. Although a low sensitivity to acute EtOH may seemingly disqualify most K^+ channels as contributing to the effects of binge drinking, it may not be so. Other factors like channel subunit expression may be equally, if not more important. Indeed, subunit composition is instrumental in regulating the properties of ion channels (Torres et al., 2007), and by extension their influence on neuronal excitability (Brenner et al., 2005). A recent in-depth analysis of the genes encoding various K^+ channels in the NAc and PFC revealed a significant correlation between K^+ channel transcripts and voluntary drinking in the naïve BXD strain of mouse (Rinker et al., 2017). This study also reported that the expression of genes encoding a K^+ delayed rectifier, the A-current, and G protein-gated inwardly rectifying K+ channels (GIRKs) was significantly altered following intermittent alcohol exposure in both the PFC and NAc. Using a two-bottle choice drinking model, McGuier et al. (2016) recently reported that genes that encode Kv7 channels (i.e., KCNQ2/3) are related to alcohol consumption and preference in rodent NAc, confirming previous findings showing differential expression of KCNQ2 in the NAc of mice selectively bred for high alcohol consumption (Metten et al., 2014). Similarly, You et al. (2019) showed that ethanol increases VTA neurons excitability in part by inhibiting KCNK13, a two-pore potassium channel that also contribute to excessive alcohol consumption in binge drinking mice, further underscoring the potential role of voltage-gated potassium channels in mediating alcohol effects on neuronal excitability. These results demonstrate that the lack of sensitivity of some K^+ channels to acute EtOH is not a reliable criterion to define their contribution to neuronal adaptation in binge drinking animals. Interestingly, ethanol metabolites, such as acetaldehyde and acetic acid, may also contribute to modulating potassium channels function as shown in GH3 cells where acetic acid activates BK channels, leading to membrane hyperpolarization, cessation of Ca2+ oscillations and decrease of growth hormone release (Ghatta et al., 2007; Shaidullov et al., 2021).

3.2. Sodium channels

Their importance cannot be overstated given their role not only in helping propagate information to downstream neurons, but also in informing the dendritic arborization on the level of excitability reached by the soma. This retrograde propagation into the dendritic compartment controls the induction of synaptic plasticity by interacting in a precise time-dependent fashion with excitatory postsynaptic potentials in a number of neuronal populations such as pyramidal neurons in the cortex and hippocampus (Caporale and Dan, 2008; Sjostrom et al., 2008) as well as in medium spiny neurons (MSNs) of the

dorsal (Fino and Venance, 2010) and ventral striatum (Ji and Martin, 2012; Bosch-Bouju et al., 2016). These channels are formed by the association of a large pore-forming α subunit with accessory proteins or β subunits (Catterall, 2000). Although a single α subunit forms the core of the channel and is functional on its own (Barchi, 1988), each of the various β subunits (β1 to β4) modulates α subunit gating properties in unique ways (Brackenbury and Isom, 2011).

Of particular interest is the β4 subunit, encoded by the Scn4b gene, as it prevents normal inactivation, thus conferring channels the ability to evoke a resurgent current upon repolarization (Grieco et al., 2005; Aman et al., 2009; Bant and Raman, 2010). While all brain regions express one or more variants of the gene encoding the Na^+ channel α subunit (Goldin et al., 2000; Goldin, 2001), those expressing Scn4b are restricted to discreet brain regions particularly the dorsal striatum and the NAc (Oyama et al., 2006; Miyazaki et al., 2014), where this subunit selectively controls long-term depression (Ji et al., 2017a). Although this channel is insensitive to acute EtOH (Wu and Kendig, 1998), chronic EtOH exposure markedly altered expression of mRNA encoding the Scn4b subunit in alcohol-preferring mice and rats (Mulligan et al., 2006; Tabakoff et al., 2008), and more recently in populations of alcoholics (Farris et al., 2014). While Scn4b subunit may not be directly implicated in regulating alcohol consumption in mice, some evidence suggest that nucleus accumbens sodium leak currents may be responsible for EtOH's acute hypnotic effects (Blednov et al., 2019) and for alterating alcohol-mediated locomotor sensitization (Wu et al., 2021).

3.3. Effects of binge drinking on neuronal firing

In light of these findings, it is reasonable to expect that changes in neuronal intrinsic excitability reflect the high sensitivity of these ion channels to binge alcohol drinking.

No significant difference in the baseline firing rate of VTA DA neurons in slices from alcohol drinking mice compared to EtOH-naïve control mice was reported (Avegno et al., 2016). Doyon et al. (2021) showed that a gradual infusion of ethanol significantly altered VTA DA neurons firing rate in a concentration-dependent manner providing. However, those findings may mask the effects of lower alcohol concentrations. Thus, in the same brain region, Juarez et al. (2017) recently reported higher bursting and firing activity in dopamine neurons, a phenomenon absent in mice consuming higher level of alcohol. In contrast, in the NAc core region, prolonged withdrawal from CIE treatment induces a sharp increase of the inward rectification caused by larger K_{ir} currents (Marty and Spigelman, 2012), these channels are the major determinants of the input resistance and the hyperpolarized resting membrane potential of MSNs during the down-state (Nisenbaum and Wilson, 1995). This effect was associated with a lower input resistance, faster action potentials (APs), and larger fast afterhyperpolarizations (fAHPs) compared to MSNs from control animals. Interestingly, EtOH drinking modulates the expression of mRNAs encoding the K_{ir} channel subunits in the NAc of alcohol-preferring rats (Mulholland et al., 2011). The same study also reported that CIE enhanced I_A current amplitudes. Surprisingly, they found no change in the firing rate of MSNs. Using a different consumption protocol, Hopf et al. (2010) showed that a protracted withdrawal following a fixed ratio EtOH self-administration protocol increases the firing of core NAc MSNs, an effect they attributed to the inhibition of SK channels. In the orbitofrontal cortex, chronic intermittent ethanol exposure increased firing in large regular-spiking cells, an effect attributed to a decrease of functional activity of SK channels (Nimitvilai et al., 2016). In the inferior colliculus dorsal cortex, intragastric ethanol also increased intrinsic excitability by lowering the action potential threshold while leaving the resting membrane potential unaffected (Evans et al., 2000). In the central nucleus of the amygdala (CeA), and the ventral bed nucleus of the stria terminalis, binge drinking followed by a 3-day withdrawal period induced a net inhibition and hyperexcitability, respectively (Pleil et al., 2015).

Taken together, these studies underscore the complex interactions of EtOH with neurons of the cortico-limbic circuitry, and highlight the notion that binge drinking impacts neuronal excitability in ways that likely reflect the idiosyncratic expression of a variety of ion channels unique to each brain region and neuronal population. This is well illustrated by the BK channels that controls neuronal repolarization following action potential firing. BK channels present a complex of subunits that include the pore forming α subunit and four regulatory β1-4 subunits, products of four distinct genes. Whereas the BK α subunit is ubiquitously expressed in the brain (Chang et al., 1997), among the β(1–4) subunits, only the β1 and β4 have been reported in the central nervous system (Behrens et al., 2000; Brenner et al., 2000). In rat NAc MSNs, the expression of the β1 and β4 subunits is compartment-specific, with the former expressed in the dendritic arborization while the latter is found mostly in the soma (Martin et al., 2004). To further muddle the picture, their expression patterns is likely reversed in mouse MSNs, illustrating the perils of drawing broad conclusions based on data from one species. Moreover, the sensitivity of BK channels to EtOH is markedly different depending upon the subunit composition of the channels, with the αβ1 subtype being totally insensitive, while the αβ4 subtype is enhanced by the drug (Martin et al., 2004). Although it is unknown whether a comparable differential expression pattern between soma and dendrites apply to other ion channels, these data nevertheless underscore the necessity to break down ion channel expression at the subcompartment level to obtain a comprehensive view of their influence on neuronal excitability and how binge drinking might affect dendritic and somatic excitability independently. Finally, it is important to underscore the idea that an ion channel insensitivity to acute EtOH does not necessarily disqualify it as a potentially important alcohol target. Indeed, as noted above, acute EtOH fails to alter I_A (Kv4) potassium channel properties. Yet, prolonged exposure to the drug reduces expression of I_A channels (Mulholland et al., 2015), an effect associated with increased backpropagating action potential-evoked Ca^{2+} transients in the distal apical dendrites of CA1 pyramidal neurons that may profoundly alter synaptic integration.

4. Binge drinking modulation of synaptic transmission and plasticity

In addition to modulating intrinsic neuronal excitability, binge drinking alters the strength of synaptic transmission mediated by a number of neurotransmitters. Glutamate- and GABA-mediated synaptic transmission have been the major focus of past research owing to their central role in the nervous system as the primary excitatory and inhibitory neurotransmitters, respectively, as well as to their sensitivity to acute EtOH being an area beneficiated by the impulse in transgenic and gene "knockout" development (Hoffman et al., 2001). Unlike most voltage-gated K+ channels, both glutamate

and GABA receptors are highly sensitive to low acute EtOH concentrations. While physiologically relevant concentrations of acute EtOH (i.e., 5–50 mM) inhibited NMDA receptor-mediated transmission in the hippocampus (Lovinger et al., 1990), the PFC (Weitlauf and Woodward, 2008), the amygdala (Roberto et al., 2004), and the NAc (Nie et al., 1994), they consistently enhanced $GABA_A$ receptor in expression systems (Harris et al., 1995; Dildy-Mayfield et al., 1996), neuronal cell culture, and in fresh slices of tissue from the cortex and the amygdala (Celentano et al., 1988; Deitrich et al., 1989; Aguayo and Pancetti, 1994; Mehta and Ticku, 1994) as well as the NAc (Nie et al., 2000). As with BK channels, interactions between EtOH and NMDA/$GABA_A$ receptors (Blednov et al., 2011; den Hartog et al., 2013) likely result from the effect of EtOH on the channel itself since it is limited by the size of its carboxyl chain (Lobo and Harris, 2008).

4.1. Binge drinking and glutamate-mediated synaptic transmission

Receptors for the amino acid L-glutamate that contribute to excitatory synaptic transmission are expressed throughout the brain and spinal cord. Beginning in the late 1970s, glutamate receptors in the vertebrate central nervous system (CNS) were classified into three families on the basis of pharmacological tools such as the agonists α-amino-3-hydroxy-methylisoxazolepropionic acid (AMPA), kainic acid, and N-methyl-D-aspartic acid (NMDA), and the antagonists such as 2- amino-5-phosphonopentanoic acid (AP5), also referred to as APV, and 6-cyano-7-nitroquinoxaline-2,3-dione (CNQX; Watkins and Evans, 1981). Subsequently, it was shown that while the majority of the first-recognized glutamate receptors were ligand-gated ion channels, a large number of G protein-coupled (i.e., metabotropic) glutamate receptors are also expressed throughout the CNS (Nakanishi, 1992). For the purpose of this review, we will limit the discussion to AMPA and NMDA receptors because of their central role in both synaptic transmission and plasticity. Further description of the glutamate transmission in the CNS can be found in Zhou and Danbolt (2014).

NAc can be divided into two anatomically and functionally distinct subregions: The sell and the core. While the core is involved in motor functions related to reward among other behaviors, the shell is involved in the cognitive processing of reward (Malenka et al., 2009). In the core, but not the shell, two subdivisions of the nucleus accumbens that present different functional and anatomical properties (Salgado and Kaplitt, 2015), binge drinking increases the expression of the gene encoding the NMDA receptors NR2B subunit but not the NR2A subunit, two NMDA receptor auxiliary subunits that are components of the heteromultimeric NMDA receptors. In primary cultured cortical neurons, the surface expression of both NR1 and NR2B subunits increased after CIE treatment (Qiang et al., 2007), a finding that mirrors a similar increase of NR2A and NR2B membrane expression in CA1 hippocampal neurons following 7 days of withdrawal from CIE treatment, a phenomenon that was accompanied by a significant enhancement of NMDA receptor-mediated synaptic response (Nelson et al., 2005). However, in the orbitofrontal cortex, CIE led to an increase of the AMPA/NMDA ratio in part through a decrease of NMDA NR2B subunit expression (Nimitvilai et al., 2016). Interestingly, changes of NMDA receptor subunit expression do not appear to occur in all addiction-related brain regions. Thus, in the CeA, a liquid diet treatment showed no effects on NMDA NR1 and NR2B subunit expression (Lack et al., 2005). Although the mechanisms leading to changes in genes expression remain poorly understood, there is growing evidence that histone demethylation at H3K9 and H3K36 in PFC and hippocampus may be implicated (Qiang et al., 2014; Finegersh et al., 2015; Simon-O'Brien et al., 2015; Sakharkar et al., 2016; Ponomarev et al., 2017; Wolstenholme et al., 2017). Functionally, a similar treatment in adolescent rats leads to an increase of electrically-evoked NMDA currents in CA1 hippocampal pyramidal neurons (Swartzwelder et al., 2017). The opposite finding was reported in the medial PFC area where CIE reduced the amplitude of electrically evoked NMDA currents, possibly through the downregulation of the NMDA NR1 subunit expression (Holmes et al., 2012). As with EtOH's effects on neuronal firing, these findings underscore again the complex, and sometime seemingly contradictory interactions between alcohol and NMDA receptors, likely reflecting brain regions, alcohol treatments, and neuronal subtypes heterogeneity.

Regarding AMPA receptors, intermittent access to alcohol in young rats induces an increase in basal glutamate in the NAc core that is accompanied by a decrease in the frequency of spontaneous AMPA events (Pati et al., 2016), confirming data from an earlier study in the same region (Griffin et al., 2014). Surprisingly, using western blotting, the authors also detected a marked increase in surface expression of the AMPA GluA1 subunit, a result that seems inconsistent with a lack of change in the amplitude of spontaneous EPSCs events A possible explanation for this apparent discrepancy between electrophysiological and western blotting data is that newly formed AMPA receptors were extrasynaptic. This could provide MSNs with a pool of readily available AMPA receptors for further rapid insertion of AMPA receptors at synapses. Combining new biosensors with high resolution microscopy may help resolve this issue (Choquet et al., 2021). At thalamic inputs to CeA neurons, CIE enhanced glutamate release probability, as shown by a reduction of paired-pulse facilitation (Christian et al., 2013). The relationship between AMPA and NMDA receptor subunits and binge drinking has been tested using a number of knock out mouse models. Surprisingly, in a 2-bottle choice drinking model, Cowen et al. (2003) found no significant differences between the wild-type and AMPA GluR1 KO mice in the acquisition of voluntary ethanol consumption (Cowen et al., 2003). A similar lack of EtOH consumption was reported in AMPA GluR3 KO mice compared to wild-type littermates (Sanchis-Segura et al., 2006). Regarding NMDA receptors, the absence of the NR2A subunit has no effect on EtOH consumption (Boyce-Rustay and Holmes, 2006). Taken together these data show that knocking down particular genes associated with AMPA and NMDA synaptic transmission has overall little impact on alcohol consumption, a somewhat surprising result considering the large body of research supporting a link between NMDA receptor pharmacology and alcohol dependence in humans (Krystal et al., 2003).

Although it might be tempting to dismiss the role of these ion channels in mediating alcohol effects on behavior, some explanation can be proposed to account for such apparent negative results (i) although some early studies showed no apparent compensatory mechanisms in the hippocampus in AMPA GluR1 using KO mice (Sakimura et al., 1995; Jia et al., 1996), it remains that this question has been examined in too few brain regions to draw broad conclusions as to the existence (or lack thereof) of such mechanisms in other regions associated with alcohol addiction, (ii) A more focused approach using conditional knockout techniques (e.g., the Cre-lox recombination system) might prove useful by enabling the removal of specific genes in specific neuronal populations.

4.2. Binge drinking and glutamate-mediated synaptic plasticity

There is agreement that at the heart of alcohol's persistent effects on behavior lays its ability to modulate "Long-term potentiation" (LTP), and long-term depression or LTD (Lovinger et al., 2003; Zorumski et al., 2014). Although the tetanic stimulation originally described by Bliss and Lømo (1973) remains the stimulation paradigm of choice in the majority of brain regions studied, another induction protocol called spike-timing dependent plasticity (STDP) is now being used in the NAc (Ji and Martin, 2012) where classic tetanic stimulations fail to reliably induce LTP (Kombian and Malenka, 1994; Robbe et al., 2002; Schramm et al., 2002), and in the cortex (Kroener et al., 2012). STDP is based on the timing (typically within a critical time window of 10–20 ms) and the pairing order between pre-and postsynaptic action potentials at low frequency (i.e., ~ 1 Hz; Sjostrom et al., 2008). There are little doubts that the AMPA and NMDA receptors, which control the initial rise of intracellular calcium that triggers phosphorylation of calcium kinases, are essential for the induction of LTP. Regarding LTD, the situation is somewhat more complex. While NMDA receptors do play an important role in some brain regions and under some experimental conditions, they are not necessary in others. Our understanding of synaptic plasticity is further complicated in the NAc where several forms of LTD have been recorded. Those include the NMDA-, mGluR- (see for review Winder et al., 2002) and action potential-dependent LTDs (Ji and Martin, 2012), a situation that contrasts with that of the dorsal striatum where both LTD and LTP are NMDAR-dependent (Partridge et al., 2000).

Several groups have explored the changes in LTP and LTD in models of binge alcohol drinking (Roberto et al., 2002, 2003; Stephens et al., 2005; Bernier et al., 2011; Kroener et al., 2012; Agoglia et al., 2015; Risher et al., 2015; Gruol et al., 2021). Field potential recordings in CA1 hippocampus display a larger LTP at the lowest stimulus intensity tested in CIE Sprague–Dawley rats, a difference that was abolished when stronger intensities were tested (Risher et al., 2015). This result contrasts with earlier studies in the same brain region where the post-tetanic field potentials were totally inhibited by CIE treatment (Roberto et al., 2002), an effect the authors later attributed in part to inhibition of the MAP kinase pathway (Roberto et al., 2003), a family of intracellular signaling molecules that regulate synaptic plasticity and learning (Thomas and Huganir, 2004), and whose inhibition decreases binge drinking (Agoglia et al., 2015). These data were subsequently replicated, also in the CA1 hippocampus, in a different rat strain (Stephens et al., 2005). Interestingly, regarding LTD, only two consecutive binges of EtOH (9 h apart) were sufficient to fully inhibit it in the same region, an effect that was reversed 8 days following the last EtOH exposure (Silvestre de Ferron et al., 2015). In both the VTA and PFC, the amplitude of tetanic stimulation- and STDP-mediated LTPs is enhanced (Bernier et al., 2011; Kroener et al., 2012). Although how EtOH alters LTP is not fully understood, a key role for IL-6 has been proposed (Gruol et al., 2021). In the NAc, the situation is somewhat more complex owing to different stimulation protocols (i.e., tetanic vs. STDP) and to the existence of MSNs expressing either dopamine D1 or D2 receptors. While D1-MSNs project to the VTA and to some extend to the ventral pallidum, D2-MSNs project exclusively to the ventral pallidum (Gerfen, 1984; Kupchik et al., 2015). Importantly, D1-MSN activation is related to positive rewarding events, inducing persistent reinforcement, whereas D2-MSN signaling is thought to mediate aversion (Hikida et al., 2010; Lobo et al., 2010; Kravitz et al., 2012), although this dichotomy might be more complex than initially thought (Soares-Cunha et al., 2020). Yet, despite many limitations, some commonalities have emerged among all these studies. In the NAc shell, LTD was inhibited by CIE exposure in MSNs, an effect that dissipated 72 h following the last treatment (Jeanes et al., 2011). Following up on their initial observations, the same group demonstrated a remarkable complexity in basic synaptic plasticity properties in MSNs expressing D1 and D2 receptors, but also a remarkable divergence in their respective responses to binge drinking. Thus, in transgenic Drd1-eGFP naïve mice, they could evoke LTD in D1R- but not in putative D2R-expressing MSNs. Interestingly, four consecutive days of CIE treatment totally blocked LTD in the former, while they observed LTD in the latter MSNs population, an effect that took 2 weeks to reverse (Jeanes et al., 2014). Comparison between the shell and core subregions revealed that CIE-mediated inhibition of LTD in D1R-MSNs was circumscribed to the shell while the core region seemed unaffected by the treatment (Renteria et al., 2018). These data provide critical evidence that binge drinking differentially modulates synaptic plasticity in D1R- and D2R-expressing MSNs. The same group shows that CIE-induced escalation of EtOH consumption produces NMDAr-dependent LTD in D1R (Renteria et al., 2018). In the NAc core, the same STDP stimulation paradigm evoked both tLTP and tLTD. While LTP was conventionally NMDAR-dependent, tLTD was controlled entirely by backpropagating action potentials (Ji and Martin, 2012). In another study, our group showed that tLTD and tLTP were primarily found in D1R- and D2R-expressing MSNs, respectively (Ji et al., 2017b). Two weeks of binge drinking led plasticity to switch from tLTD to tLTP in D1R-expressing MSNs, mirroring the findings by the Morrisett group, while tLTP in D2R-expressing MSNs was only mildly and not significantly attenuated. Interestingly, alterations of plasticity by binge drinking were not accompanied by changes in AMPA or NMDA current properties at PFC, hippocampal or amygdala synapses; only significant changes of the AMPA/NMDA ratio, a widely accepted index of plasticity, were reported (Ji et al., 2017b).

As noted above, because spike-timing-dependent LTD is controlled by backpropagating action potentials, it is possible that the tLTD-to-tLTP switch reflects a weakening of these electrical events as they invade the dendritic tree retrogradely, a phenomenon that does not exclude insertion of AMPA receptors vs. changes in their subunit composition as seen in other brain regions. The strengthening of glutamate synaptic transmission in D1R-expressing MSNs seems to be supported by findings in the dorsal striatum of mice trained to consume alcohol using an intermittent-access two-bottle-choice drinking paradigm. In this study, Cheng et al. (2017) demonstrated a similar increase in the AMPA/NMDA ratio, increase found in D1R- but not in D2R-expressing MSNs. Using a chemogenetic approach, the study also reported that the excitation of D1R-expressing MSNs promoted alcohol drinking, establishing a strong correlation between the enhance excitation in these neurons and drinking. Much remains to be understood about the molecular underpinnings responsible for the differential effects of binge drinking on the glutamatergic synaptic transmission of striatal D1R- and D2R-expressing MSNs, and the increase of the AMPA/NMDA ratio. In light of NMDA receptor subunit expression sensitivity to alcohol, as seen in the previous section, binge drinking may trigger the expression of different NMDA receptor subunits with higher unitary conductance. Our group measured the deactivation rates of optogenetically-driven NMDA currents, a feature controlled by the receptor subunit composition (Monyer et al., 1992). Surprisingly, we showed that NMDA

current decay kinetics remained unchanged after binge EtOH, seemingly ruling out this possibility (Ji et al., 2017b). Irrespective of the specifics of the alterations of the glutamate synaptic transmission in MSNs, binge drinking effects on NAc direct pathway (D1R) point to a remarkable degree of specificity that mirrors what has been reported with cocaine in the same brain region (Bock et al., 2013; Heinsbroek et al., 2017) and engages with the stablished dichotomy that shows that D1 is involved in reinforcement and reward and D2 has been associated with punishment and aversion (Soares-Cunha et al., 2016). It is likely that this specificity is functionally relevant as striatal D1R- and D2R-expressing MSNs project to different brain regions (Gerfen and Surmeier, 2011), even though new data are now challenging the strict anatomical segregation of these projections in mice NAc (Kupchik et al., 2015).

Importantly, alterations of the AMPA/NMDA synaptic transmission in the striatum may merely reflect alcohol-glutamate receptors interactions occurring simultaneously at multiple levels in the local circuitry. Indeed, glutamate synaptic transmission and plasticity in striatal MSNs are under the control of dopamine (Shen et al., 2008; Ji et al., 2017b), whose release is regulated in part by cholinergic interneurons (ACh INs). The putative role of these interneurons is particularly intriguing. Despite their rarity as they represent between 1 and 2% of the total neuronal population of the rat striatum (Lim et al., 2014), ACh INs are critical players in regulating the output of this region due to their direct connection to MSNs (Hsu et al., 1996; Galarraga et al., 1999; Shen et al., 2005), as well as through the control of dopamine (Threlfell et al., 2010; Cachope et al., 2012), GABA (Witten et al., 2010), and glutamate (Bonsi et al., 2011; de Kloet et al., 2015; Silberberg and Bolam, 2015) release from terminals that synapse on MSNs. Alterations of the properties of ACh INs have been associated with neurological disorders such as depression and emotional control (Warner-Schmidt et al., 2012; Atallah et al., 2014). They have also been implicated in a number of neurological disorders in task attention, memory, and aversive behavior (Aosaki et al., 1994; Ravel et al., 1999; Anagnostaras et al., 2003; Furey et al., 2008). With respect to drugs of reward and addiction, their spontaneous firing is influenced by event context and by cocaine reward-related cues *in vivo* preparations (Apicella et al., 1997; Williams and Adinoff, 2008; Witten et al., 2010; Schmidt et al., 2011; Tuesta et al., 2011; Atallah et al., 2014). There is also evidence that acetylcholine mediates EtOH's effects by modulating the release of dopamine from terminals originating in the VTA (Adamantidis et al., 2011; Abrahao et al., 2012; Bahi and Dreyer, 2012; Engel and Jerlhag, 2014). Binge alcohol drinking in adolescents profoundly reduces both the expression of 11 of the 14 genes encoding nicotinic acetylcholine receptors (Colbert et al., 1997), and the density of ACh INs in the NAc of human alcoholics (Vetreno et al., 2014) as well as in an adolescent intermittent alcohol drinking model in rats (Hauser et al., 2019). Similarly, chronic alcohol consumption reduces the number of striatal cholinergic varicosities (Pereira et al., 2014). There is also evidence that ACh INs spontaneous firing is inhibited by EtOH (Blomeley et al., 2011). In a recent study, Kolpakova et al. (2022) detailed the complex cellular mechanisms underlying ACh INs-mediated inhibition of glutamate release in D1 and D2 MSNs. Thus, NAc ChIs decreased MSN synaptic excitability through different mechanisms in D1- vs. D2-MSNs. While decrease of ChI-mediated sEPSCs frequency in D1-MSNs was mediated by dopamine, the same effect in D2-MSNs resulted from a direct control of glutamate release by ChIs. Interestingly, after 2 weeks of binge alcohol drinking, optogenetic stimulation of ChIs enhanced glutamate release in D1-MSNs, while its effect on D2-MSNs remained unchanged (Kolpakova et al., 2022). Taken together, these studies suggest that binge drinking may initiate a carefully orchestrated cascade of events, starting with ACh INs through their control of dopamine release, that ultimately favors synaptic transmission and plasticity of MSNs belonging to the direct pathway. Also, restoring the balance between the NAc direct and indirect pathways in favor of the latter, possibly through manipulations of ACh INs excitability, may help protect individuals against the long-term consequences of alcohol consumption.

4.3. Synaptic gating as a model of synaptic adaptation to binge alcohol drinking

The nucleus accumbens receives glutamatergic afferents primarily from the prefrontal cortex, hippocampus, basolateral amygdala (BLA), and hippocampus (Ikemoto, 2007; Humphries and Prescott, 2010; Li et al., 2018), allowing integration of emotional, contextual, and cognitive information. There is evidence that these inputs do not behave independently of each other. Thus, early *in vivo* recordings by O'Donnell and Grace (1995) revealed that hippocampal inputs facilitate the transmission of information originating in the prefrontal cortex in NAc MSNs, a mechanism called synaptic gating (O'Donnell and Grace, 1995; Katz, 2003). In 2005, based in part on earlier observations in human subjects (Bechara et al., 1995), Bechara proposed that the loss of control over alcohol consumption in adolescents was be caused by an imbalance between the reflective and impulsive systems that are, respectively, associated with the prefrontal cortex (PFC) and the basolateral amygdala (BLA), respectively (Bechara, 2005). While the PFC is responsible for planning, evaluating long-term consequences and is instrumental in retrieving drug-associated memories (Dalley et al., 2004; Zhang et al., 2019), the BLA encodes emotions that shape impulsive behavior and the response to associative learning (Gallagher and Chiba, 1996; Cardinal et al., 2002; Lalumiere, 2014). More specifically, Bechara hypothesized that the impulsive system could override the reflective system upon repeated drugs of abuse consumption. To identify the molecular basis of a putative disruption of synaptic integration between cortical and amygdala inputs, Kolpakova et al. (2021) used a double optogenetics approach (i.e., Channelrhodopsin and ChrimsonR) to independently stimulate the PFC and BLA afferents, respectively, to elucidate how executive and emotional information is processed by MSNs in alcohol-naïve and binge alcohol drinking mice (Kolpakova et al., 2021). This approach revealed that PFC and BLA inputs synapse onto the same MSNs where they reciprocally inhibit each other presynaptically in a strict time-dependent manner. In alcohol-naïve mice, this temporal gating of BLA-inputs by PFC afferents is stronger than the reverse, revealing that MSNs prioritize high-order executive processes information from the PFC. Importantly, binge alcohol drinking alters this reciprocal inhibition by unilaterally strengthening BLA inhibition of PFC inputs. In line with this observation, we demonstrate that *in vivo* optogenetic stimulation of the BLA, but not PFC, blocks binge alcohol drinking escalation in mice (Kolpakova et al., 2021). Overall, this study identified a new mechanism through which NAc MSNs integrate executive and emotional information and showed that this integration is dysregulated during binge alcohol drinking. It also highlights the idea to fully understand the effects of alcohol on synaptic transmission and neuronal excitability in the NAc and elsewhere it is important to consider the network in its globality and diversity, and the dynamic interplay between various inputs (Kolpakova et al., 2021).

4.4. CIE and GABA- and glycine-mediated synaptic transmission

$GABA_A$ receptors are formed by the association of 5 subunits (α1-6, β1-3, γ1-3, δ1, ε, Θ, and π) asymmetrically arranged around the central chloride anion conduction pore. Although their stoichiometry and composition vary with cell types and brain regions, most neurons express a combination of αβγ subunits (Sigel and Steinmann, 2012). Of all these subunits, the α subunits seems to be particularly sensitive to binge drinking.

Thus, the examination of subunit expression in the hippocampus revealed a decrease of mRNA encoding the α1 and an increase in α4 subunit mRNA expression in CIE rats (Cagetti et al., 2003). In the dentate gyrus, protein levels for the α4-$GABA_A$ receptor subunits were significantly reduced, but mRNA levels were increased, 26 days after the last intermittent alcohol exposure in mice (Centanni et al., 2014). Interestingly, in the same publication, Cagetti et al. (2003) found no effect on expression of any of these subunits following CIE exposure during adulthood, underscoring the idea of adolescence as a time window particularly sensitive to the effect of EtOH. While a two-day withdrawal following CIE treatment leads to a significant increase in the α4 subunit mRNA levels in the dentate gyrus, the CA3, and the CA1 regions, no significant change in the α5 subunit expression was observed in the same regions. There is also evidence of a reorganization of the α4 synaptic and extrasynaptic $GABA_A$ receptor subunit in CA1 pyramidal neurons (Liang et al., 2006). A similar reorganization of $GABA_A$ receptor subunit composition in the hippocampus of CIE animals appears to be supported by mIPSCs with markedly different activation/deactivation kinetics, an effect that was associated with upregulation of the α2, and not the α4, subunit, an effect the authors associated with the anxiolytic response to EtOH exposure (Lindemeyer et al., 2017). Interestingly, a point mutation that renders the α2 subunit insensitive to benzodiazepine blunted alcohol intake in mice with an intermittent access to EtOH, suggesting that neurosteroid action on α2-containing receptors may be necessary for escalation of chronic EtOH intake (Newman et al., 2016). The role of the α2 subunit appears to be supported by data showing that a point mutation from histidine at 270 to alanine decreased alcohol consumed and reduced preference for ethanol (Blednov et al., 2011). Also in the hippocampal CA1 pyramidal neurons, intermittent ethanol exposure modulated $GABA_AR$ δ but not α4 subunit expression (Follesa et al., 2015). Regarding the δ-$GABA_A$ receptors, a significant reduction in its protein levels was observed in the dentate gyrus, in the absence of any changes in mRNA levels, at 48 h and 26 days after the last ethanol CIE exposure (Centanni et al., 2014). Possibly related to changes in subunit expression, in hippocampal dentate granule cells, alcohol exposure during adolescence decreased the tonic noise driven by extrasynaptic $GABA_A$ receptors, in CIE animals compared to untreated animals, suggesting a weaker baseline inhibition (Fleming et al., 2012). In CIE rats, $GABA_A$ receptor-mediated synaptic transmission was depressed in CA1 hippocampus as suggested by a decrease in agonist-evoked $^{36}Cl^-$ efflux, of the paired-pulse inhibition in the CA1 area, and alterations of $GABA_A$ receptor subunit expression. Taken together, these studies seem to point to the hippocampal α2 and α4 subunits as being particularly sensitive to binge drinking.

In other brain regions, similar adaptations of GABA receptor subunit expression were observed, with again the α subunits playing a central role. Thus, in rat cerebellum, an increase of $GABA_A$ α6 subunit expression was detected following CIE treatment (Petrie et al., 2001). In the PFC, CIE decreased the levels of α1 and α2 subunits, and increased the level of α4 (Sheela Rani and Ticku, 2006), while it reduced the amplitude of tonic GABA currents in layer V pyramidal neurons, perhaps reflecting an attenuation of currents mediated by δ-subunit containing receptors (Centanni et al., 2017). Finally, a recent study shows that in these regions, withdrawal impairs α1subunit affecting synaptic neurotransmission (Hughes et al., 2019). In the NAc, CIE decreased the frequency of fast-rising miniature IPSCs (Liang et al., 2014a), mirroring reports in dorsal striatum MSNs (Wilcox et al., 2014), an effect that the authors interpreted as consistent with a possible decrease in somatic GABAergic synapses in MSNs from CIE rats. In a separate study, the same group reported that dopamine, at concentrations consistent with those measured *in vivo* (0.01–1 μM), modulated extrasynaptic $GABA_A$ receptors of NAc MSNs, without affecting the postsynaptic kinetics of miniature inhibitory postsynaptic currents (mIPSCs), highlighting the differential sensitivity of synaptic and extrasynaptic GABA receptors to CIE treatment (Liang et al., 2014b). Interestingly, RNA sequencing demonstrated that the expression of most (6 of 8) $GABA_A$ receptor subunit genes decreased in the periacqueductal gray (McClintick et al., 2016) and increased in the dorsal raphe (McClintick et al., 2015) following CIE treatment. Because these brain regions are not believed to play a direct role in addiction but rather are central in processing pain and anxiety, it seems somewhat surprising to see $GABA_A$ receptor subunit expression change in response to intermittent EtOH exposure. However, this effect may be related to finding by Fu et al. (2015) who showed that CIE induces hyperalgesia in rats and to the well-known anxiogenic effects of repeated EtOH consumption associated with withdrawal (Hamilton et al., 2013). Finally, in the CeA region, CIE effects on tonic GABA-mediated synaptic transmission is complex due in part to the presence of different neuronal populations (i.e., low-threshold bursting [LTB], regular spiking and late spiking neurons), a mosaic further complicated by the expression (or not) of the corticotropin releasing factor receptors (CRF1). While the frequency of spontaneous events (i.e., phasic GABA response) was markedly reduced in CeA neurons expressing the CRF1 receptor, it was enhanced in CRF1-negative late spiking cells (Herman et al., 2016). Additionally, the study reported a loss of the tonic GABA current in CRF1 but not in CRF1-negative neurons, an effect that persisted into withdrawal.

These data highlight two key facts. First, the expression of GABAR α subunits seems to be particularly sensitive to repeated alcohol exposure. Second, they underscore the idea that GABA-EtOH interactions are complex and cannot be strictly described in terms of inhibitory or excitatory effects. These seemingly disparate outcomes may reflect the unique expression pattern of the GABA receptor subunits in different neuronal populations and their response to binge drinking. Equally important is that the overall effects of CIE on neuronal excitability through $GABA_A$ synaptic transmission depend on the specific electrical characteristics of the neurons studied and particularly on their resting membrane potentials (RMPs). Thus, considering that the reversal potential for chloride (E_{Cl}^-) typically ranges between −70 and −75 mV in nerve cells (Deisz and Prince, 1989), neurons presenting more depolarized RMPs will display increased excitability upon a decrease of inhibitory activity, due to weakening of the ability of $GABA_A$ receptors to prevent the cells from further depolarizing. In contrast, in neurons whose RMP is much more hyperpolarized (i.e., ~ − 85 mV) such as NAc MSNs, $GABA_A$ receptors likely mediate depolarization at rest. As such, a weakening of the GABA transmission will further dampen MSNs neuronal

excitability. Regarding CIE effects on GABA tonic currents, in neurons with resting potentials close to E_{Cl}^-, this tonic current is likely to shunt the membrane, which would primarily negatively impact neuronal cable properties and the propagation of synaptic events from their point of inception in spines to the soma by attenuating the amplitude of these events and slowing their kinetics. Therefore, associating changes of GABA synaptic transmission with an overall inhibitory or excitatory effect should be carefully weighted in light of the basic electrical properties of the neurons considered.

Less is known about interactions between alcohol and the $GABA_B$ receptor, a metabotropic receptor that inhibits neuronal excitability through its action on g-protein-coupled inward rectifying potassium (GIRK) channels (Padgett and Slesinger, 2010). In BLA neurons, $GABA_B$ receptors appear to be responsible for tolerance to acute ethanol-mediated increase in the frequency of spontaneous GABAergic synaptic currents (Zhu and Lovinger, 2006). Interestingly, in the hippocampus, inhibition of $GABA_B$ receptor function enhances ethanol-mediated potentiation of distal $GABA_A$ IPSCs (Proctor et al., 2006), bolstering the idea that they may counter the effects of EtOH on $GABA_A$ receptors. In a two-bottle choice alcohol drinking model, Herman et al. (2015) showed that constitutive deletion of $GIRK_3$, one of the three GIRK subunits, selectively increased ethanol binge-like drinking. Additionally, they reported that $GIRK_3$ is responsible for EtOH-mediated increase of VTA DA neurons firing and EtOH-mediated DA release in the NAc.

Glycine, alongside GABA, is the other fast inhibitory neurotransmitter in the central nervous system. Like GABA receptors, activation of glycine receptors opens an anionic conductance that hyperpolarizes the membrane potential. Although it was initially believed that glycine receptors were almost exclusively found in the spinal cord and brainstem of adult rats (Rajendra et al., 1997), their expression was subsequently reported in forebrain structures associated with the addiction neurocircuitry (Yoon et al., 1998; McCool and Botting, 2000; McCool and Farroni, 2001; Martin and Siggins, 2002; Mori et al., 2002). As with GABA receptors, acute EtOH generally enhances glycine currents in a number of preparations (Celentano et al., 1988; Aguayo and Pancetti, 1994; Mascia et al., 1996; Ye et al., 2001) even though inhibition of glycine currents was also reported in the ventral tegmental area (Tao and Ye, 2002). Interestingly, in the lateral orbital frontal cortex, acute EtOH enhances glycine currents without affecting GABA currents (Badanich et al., 2013). Unfortunately, there is currently little information as to how these receptors adapt to binge drinking. On the model of GABA receptors and other ionotropic receptors, the GlyR is a pentameric receptor constituted as either α-homomers or α-β heteromers. In the amygdala and NAc, GlyR α2 and α3 subunits show equal or greater expression compared with α1 (Jonsson et al., 2009; Delaney et al., 2010). In light of the sensitivity of the expression of the various subunits forming GABA and AMPA/NMDARs, it is tempting to speculate that GlyRs may similarly respond to binge drinking by altering their subunit composition, an adaptation that would not only influence their intrinsic channel properties (Grudzinska et al., 2005) but also their location (Laube et al., 2002). A study by McClintick et al. (2016) showed a reduced expression of 4 glycine receptor-related genes in the periacqueductal gray of DID rats. Recently the field has been expanded to acknowledge the role that other glycine receptor agonists, such as Taurine, can play in alcohol dependence, in this sense has been demonstrated that alcohol dependence disrupts the taurine-mediated inhibition of the GABAergic tone in the amygdala (Kirson et al., 2020).

Behaviorally, microinjections of glycine into the VTA decreased EtOH intake, but not sucrose or water, in rats chronically exposed to ethanol under the intermittent-access protocol (Li et al., 2012). Regarding GABA receptors, their role has been examined using both the two-bottle choice and the DID models in knockout mouse. While all GABAR subunits do not have the same influence on binge drinking, those that do alter the behavior consistently decrease drinking. Thus, alcohol consumption of α1, α5 and δ knockout mice was lower than that of wild-type littermates (Mihalek et al., 2001; Blednov et al., 2003; Boehm et al., 2004; June et al., 2007). In contrast, α2 and β2 knockout mice had no effects on alcohol consumption (Blednov et al., 2003; Boehm et al., 2004). Although limited in scope, these studies appear to indicate that alterations of GABA and Glycine-mediated inhibitory synaptic transmission attenuate alcohol drinking.

5. What is the role of ion channels on neuronal excitability in binge alcohol drinking animals?

Data presented here offer a strong rationale for some voltage- and ligand-gated ion channels as potential direct candidates that mediate the effects of binge alcohol drinking on neuronal excitability and communication. Indeed, for good reasons, glutamate has long held a central role in various models of addiction (Berke and Hyman, 2000; Kauer and Malenka, 2007; Kalivas, 2009; Kalivas et al., 2009). However, to fully appreciate the role of glutamate in binge alcohol drinking and how precisely it exerts its effects, it is critical to understand not only how individually it affects neuronal excitability and how AMPA/NMDA receptors properties are influenced by alcohol, but also how they work in the broader context of the constantly changing and dynamic neuronal excitability. As already alluded to in this review, voltage- and ligand-gated channels do not work separately and independently. For example, there is a wealth of evidence that membrane depolarization following the release of glutamate recruits a number of voltage-gated calcium and potassium channels that contribute to modulating the kinetics of synaptic potentials (Cai et al., 2004; Kim et al., 2007; Lin et al., 2008) and by extension how synaptic events temporally and spatially aggregate to trigger action potentials and how they may in some situations modulate neurotransmitter release (Debanne et al., 2013). This is probably a phenomenon more exacerbated in dendritic spines than in synapses on the dendritic shaft and cell body since spines are a fairly well isolated electrical compartment. Thus, when considering the modulation of LTP by binge drinking, one may want to go beyond the generally accepted and critical role of AMPA and NMDA receptors to include a direct participation of voltage-gated ion channels. For example, Ia, SK and BK channels are widely expressed in both dendritic spines where they control glutamate-mediated depolarization and calcium influx (Isaacson and Murphy, 2001; Faber et al., 2005; Wang et al., 2014). By altering their subunit composition or by undergoing endocytosis in response to binge drinking, they may contribute to changing the long-lasting strength of synaptic transmission independently of the effects of alcohol on AMPA/NMDA receptors. Thus, in the NAc, binge drinking promotes LTP in D1R-MSNs, an effect that is not accompanied by a corresponding increase of AMPA/NMDA ratio, a classic measure of AMPA receptor insertion, at hippocampal glutamatergic synaptic inputs compared to cortical and amygdala synapses (Ji et al., 2017b). This suggests that the mechanisms underlying synaptic plasticity may differ in the same

neuronal population based on the origin of the afferents. While interacting with ligand-gated channels in dendrites, the same ion channels will concomitantly shape action potentials generated at their point of inception in the initial segment near the soma. By the same token, when expressed in the membrane of the dendritic shaft, they will not only modulate the strength of back-propagating action potentials but also the degree of filtering to which synaptic events reaching the soma are subjected based on the cable theory proposed by W. Rall more than 50 years ago (RALL, 1959). This shows that to fully capture the complexity of the contribution of ion channels to neuronal excitability necessitates integration of various dimensions of all ion channels in a unifying model, a goal that we have not reached yet, in part due to the challenges of probing hard-to-reach neuronal compartments such as dendritic spines.

6. Future perspectives

The present survey of the literature is a testimony to the progress accomplished over the recent decades toward understanding how neurons of the central nervous system adapt to repeated alcohol consumption. To some measure, the origin of each advance can be traced back to specific technological breakthroughs. Thus, following the widespread adoption of the voltage-clamp technique that enabled whole-cell and single-channel recordings of specific ion channels in the 80s, the 90s capitalized on the advancement of cloning techniques to identify the many subunits of a host of ligand- and voltage-gated ion channels, to determine their influence on biological and pharmacological properties of these channels, and to establish their influence on interactions with alcohol. The turn of the century witnessed dramatic progress in genome wide sequencing analysis that led to a better appreciation of the expression patterns of these targets as well as many others, in binge drinking animals, and the regulation of their expression by non-coding RNA and epigenetic mechanisms. More recently, opto- and chemogenetic approaches have been instrumental in helping to disentangle the complex neuronal circuitry by enabling the targeting of specific pathways or neuronal populations, a goal that was for the most part unattainable with more conventional pharmacological and electrical approaches. Yet, despite this wealth of information, it remains difficult to ascribe EtOH a simple excitatory or inhibitory value. As highlighted here, EtOH's influence on ion channel physiology and more broadly on neuronal excitability depends on a number of variables such as the ion channel subunit composition, their sensitivity to the drug and their site of expression (e.g., soma vs. dendrites). Also, when studying the effects of binge drinking on a particular ion channel, we tend to draw conclusions through the prism of this channel while ignoring all other interactions. All these factors combined often lead to a truncated interpretation of the influence of binge drinking on brain function. Interestingly, during the last years a vast body of evidence regarding the role that the epigenetic changes plays in alcohol consumption is growing and shows clearly that the adaptations produced by the epigenetic landscape and their interlinked pathways plays a key role in the development of AUD (see for review Egervari et al., 2021). Finally, a emboldened body of evidence shows that the immune system and stress can also modulate the effect of alcohol in the brain in different stages of consumption (i. e. binge drinking, tolerance, dependence) being a promising area of study (de Guglielmo et al., 2019; Blednov et al., 2021).

The contribution of these bottom-up approaches do not mask the fact that a broad narrative of the effects of binge drinking on brain function remains elusive, and poses the question of the best way forward in decades to come. It could be argued that a renewed focus on top-down approaches, typically represented by *in vivo* simultaneous recordings of multiple neurons, may prove beneficial for the field assuming that recent technological progress are harnessed. As successful as such an approach has proved in the past in providing a general sense of the overall neuronal excitability in any given brain region, it has been limited in its ability to concomitantly pinpoint specific neurons or their inputs. Fortunately, such limitations are fading as new techniques become available. One exciting recent development is the miniaturized fluorescence microscopy system that simultaneously monitor calcium transients (a proxy for neuronal excitability) in a large number of visually identified individual neurons in freely moving mice and rats (Kitamura et al., 2017). Through this approach, it is now possible to study the concept of the engram (i.e., a collection of neurons simultaneously activated) and to identify the location and physical basis of "memory traces" left in the brain by repeated binge drinking. Although miniaturized fluorescence microscopy remains the purview of few laboratories due to its cost and complexity, its dissemination in years to come will undoubtedly be instrumental in advancing the field of alcohol research.

Interestingly, a number of laboratories are now leveraging the power of sophisticated transgenic mice models (e.g., fos/arc-TRAP2, TetTag, and fos-^{TVA} mice) initially developed to identify and characterize neurons encoding fear retrieval memories (Liu et al., 2012; Sakurai et al., 2016; DeNardo et al., 2019), with various approaches like viral delivery technique, opto- and chemogenetics to establish a causal relationship between engram excitability and alcohol consumption and to elucidate what makes these neurons unique at the molecular (i.e., transcript profile) and functional (electrophysiological properties) levels. This approach may offer a unique opportunity to develop therapeutics that would selectively target neurons recruited by alcohol, such as the neuronal ensemble described in the amygdala that plays a key role in alcohol dependence (de Guglielmo et al., 2016) potentially resulting in higher efficacy and fewer side effects unlike what is reported with currently available drugs (Litten et al., 2016).

Author contributions

GM wrote the manuscript with inputs from PG-G and TL. All authors contributed to the article and approved the submitted version.

Funding

This work was supported by the National Institute on Alcohol Abuse and Alcoholism, grant nos. AA027807 and AA020501.

Conflict of interest

The authors declare that the research was conducted in the absence of any commercial or financial relationships that could be construed as a potential conflict of interest.

Publisher's note

References

Abrahao, K. P., Quadros, I. M., Andrade, A. L., and Souza-Formigoni, M. L. (2012). Accumbal dopamine D2 receptor function is associated with individual variability in ethanol behavioral sensitization. *Neuropharmacology* 62, 882–889. doi: 10.1016/j.neuropharm.2011.09.017

Abrahao, K. P., Salinas, A. G., and Lovinger, D. M. (2017). Alcohol and the brain: neuronal molecular targets, synapses, and circuits. *Neuron* 96, 1223–1238. doi: 10.1016/j.neuron.2017.10.032

Adamantidis, A. R., Tsai, H. C., Boutrel, B., Zhang, F., Stuber, G. D., Budygin, E. A., et al. (2011). Optogenetic interrogation of dopaminergic modulation of the multiple phases of reward-seeking behavior. *J. Neurosci.* 31, 10829–10835. doi: 10.1523/JNEUROSCI.2246-11.2011

Agoglia, A. E., Sharko, A. C., Psilos, K. E., Holstein, S. E., Reid, G. T., and Hodge, C. W. (2015). Alcohol alters the activation of ERK1/2, a functional regulator of binge alcohol drinking in adult C57BL/6J mice. *Alcohol. Clin. Exp. Res.* 39, 463–475. doi: 10.1111/acer.12645

Aguayo, L. G., and Pancetti, F. C. (1994). Ethanol modulation of the gamma-aminobutyric acidA- and glycine-activated cl-current in cultured mouse neurons. *J. Pharmacol. Exp. Ther.* 270, 61–69. PMID: 8035343

Alekseev, S. I., Alekseev, A. S., and Ziskin, M. C. (1997). Effects of alcohols on A-type K+ currents in Lymnaea neurons. *J. Pharmacol. Exp. Ther.* 281, 84–92. PMID: 9103483

Aman, T. K., Grieco-Calub, T. M., Chen, C., Rusconi, R., Slat, E. A., Isom, L. L., et al. (2009). Regulation of persistent Na current by interactions between beta subunits of voltage-gated Na channels. *J. Neurosci.* 29, 2027–2042. doi: 10.1523/JNEUROSCI.4531-08.2009

Anagnostaras, S. G., Murphy, G. G., Hamilton, S. E., Mitchell, S. L., Rahnama, N. P., Nathanson, N. M., et al. (2003). Selective cognitive dysfunction in acetylcholine M1 muscarinic receptor mutant mice. *Nat. Neurosci.* 6, 51–58. doi: 10.1038/nn992

Anantharam, V., Bayley, H., Wilson, A., and Treistman, S. N. (1992). Differential effects of ethanol on electrical properties of various potassium channels expressed in oocytes. *Mol. Pharmacol.* 42, 499–505. PMID: 1406600

Aosaki, T., Tsubokawa, H., Ishida, A., Watanabe, K., Graybiel, A. M., and Kimura, M. (1994). Responses of tonically active neurons in the primate's striatum undergo systematic changes during behavioral sensorimotor conditioning. *J. Neurosci.* 14, 3969–3984. doi: 10.1523/JNEUROSCI.14-06-03969.1994

Apicella, P., Legallet, E., and Trouche, E. (1997). Responses of tonically discharging neurons in the monkey striatum to primary rewards delivered during different behavioral states. *Exp. Brain Res.* 116, 456–466. doi: 10.1007/PL00005773

Aryal, P., Dvir, H., Choe, S., and Slesinger, P. A. (2009). A discrete alcohol pocket involved in GIRK channel activation. *Nat. Neurosci.* 12, 988–995. doi: 10.1038/nn.2358

Atallah, H. E., McCool, A. D., Howe, M. W., and Graybiel, A. M. (2014). Neurons in the ventral striatum exhibit cell-type-specific representations of outcome during learning. *Neuron* 82, 1145–1156. doi: 10.1016/j.neuron.2014.04.021

Avegno, E. M., Salling, M. C., Borgkvist, A., Mrejeru, A., Whitebirch, A. C., Margolis, E. B., et al. (2016). Voluntary adolescent drinking enhances excitation by low levels of alcohol in a subset of dopaminergic neurons in the ventral tegmental area. *Neuropharmacology* 110, 386–395. doi: 10.1016/j.neuropharm.2016.07.031

Badanich, K. A., Mulholland, P. J., Beckley, J. T., Trantham-Davidson, H., and Woodward, J. J. (2013). Ethanol reduces neuronal excitability of lateral orbitofrontal cortex neurons via a glycine receptor dependent mechanism. *Neuropsychopharmacology* 38, 1176–1188. doi: 10.1038/npp.2013.12

Bahi, A., and Dreyer, J. L. (2012). Involvement of nucleus accumbens dopamine D1 receptors in ethanol drinking, ethanol-induced conditioned place preference, and ethanol-induced psychomotor sensitization in mice. *Psychopharmacology (Berl)* 222, 141–153. doi: 10.1007/s00213-011-2630-8

Bant, J. S., and Raman, I. M. (2010). Control of transient, resurgent, and persistent current by open-channel block by Na channel beta4 in cultured cerebellar granule neurons. *Proc. Natl. Acad. Sci. U. S. A.* 107, 12357–12362. doi: 10.1073/pnas.1005633107

Barchi, R. L. (1988). Probing the molecular structure of the voltage-dependent sodium channel. *Annu. Rev. Neurosci.* 11, 455–495. doi: 10.1146/annurev.ne.11.030188.002323

Bechara, A. (2005). Decision making, impulse control and loss of willpower to resist drugs: a neurocognitive perspective. *Nat. Neurosci.* 8, 1458–1463. doi: 10.1038/nn1584

Bechara, A., Tranel, D., Damasio, H., Adolphs, R., Rockland, C., and Damasio, A. R. (1995). Double dissociation of conditioning and declarative knowledge relative to the amygdala and hippocampus in humans. *Science* 269, 1115–1118. doi: 10.1126/science.7652558

Becker, H. C., and Lopez, M. F. (2004). Increased ethanol drinking after repeated chronic ethanol exposure and withdrawal experience in C57BL/6 mice. *Alcohol. Clin. Exp. Res.* 28, 1829–1838. doi: 10.1097/01.ALC.0000149977.95306.3A

Behrens, R., Nolting, A., Reimann, F., Schwarz, M., Waldschutz, R., and Pongs, O. (2000). hKCNMB3 and hKCNMB4, cloning and characterization of two members of the large-conductance calcium-activated potassium channel beta subunit family. *FEBS Lett.* 474, 99–106. doi: 10.1016/S0014-5793(00)01584-2

Bell, R. L., Rodd, Z. A., Lumeng, L., Murphy, J. M., and McBride, W. J. (2006). The alcohol-preferring P rat and animal models of excessive alcohol drinking. *Addict. Biol.* 11, 270–288. doi: 10.1111/j.1369-1600.2005.00029.x

Berke, J. D., and Hyman, S. E. (2000). Addiction, dopamine, and the molecular mechanisms of memory. *Neuron* 25, 515–532. doi: 10.1016/S0896-6273(00)81056-9

Bernier, B. E., Whitaker, L. R., and Morikawa, H. (2011). Previous ethanol experience enhances synaptic plasticity of NMDA receptors in the ventral tegmental area. *J. Neurosci.* 31, 5205–5212. doi: 10.1523/JNEUROSCI.5282-10.2011

Blednov, Y. A., Bajo, M., Roberts, A. J., Da Costa, A. J., Black, M., Edmunds, S., et al. (2019). Scn4b regulates the hypnotic effects of ethanol and other sedative drugs. *Genes Brain Behav.* 18:e12562. doi: 10.1111/gbb.12562

Blednov, Y. A., Borghese, C. M., McCracken, M. L., Benavidez, J. M., Geil, C. R., Osterndorff-Kahanek, E., et al. (2011). Loss of ethanol conditioned taste aversion and motor stimulation in knockin mice with ethanol-insensitive α2-containing GABA(a) receptors. *J. Pharmacol. Exp. Ther.* 336, 145–154. doi: 10.1124/jpet.110.171645

Blednov, Y. A., Da Costa, A., Mayfield, J., Harris, R. A., and Messing, R. O. (2021). Deletion of Tlr3 reduces acute tolerance to alcohol and alcohol consumption in the intermittent access procedure in male mice. *Addict. Biol.* 26:e12932. doi: 10.1111/adb.12932

Blednov, Y. A., Walker, D., Alva, H., Creech, K., Findlay, G., and Harris, R. A. (2003). GABAA receptor alpha 1 and beta 2 subunit null mutant mice: behavioral responses to ethanol. *J. Pharmacol. Exp. Ther.* 305, 854–863. doi: 10.1124/jpet.103.049478

Bliss, T. V., and Lomo, T. (1973). Long-lasting potentiation of synaptic transmission in the dentate area of the anaesthetized rabbit following stimulation of the perforant path. *J Physiol* 232, 331–356. doi: 10.1113/jphysiol.1973.sp010273

Blomeley, C. P., Cains, S., Smith, R., and Bracci, E. (2011). Ethanol affects striatal interneurons directly and projection neurons through a reduction in cholinergic tone. *Neuropsychopharmacology* 36, 1033–1046. doi: 10.1038/npp.2010.241

Bock, R., Shin, J. H., Kaplan, A. R., Dobi, A., Markey, E., Kramer, P. F., et al. (2013). Strengthening the accumbal indirect pathway promotes resilience to compulsive cocaine use. *Nat. Neurosci.* 16, 632–638. doi: 10.1038/nn.3369

Boehm, S. L., Ponomarev, I., Jennings, A. W., Whiting, P. J., Rosahl, T. W., Garrett, E. M., et al. (2004). Gamma-aminobutyric acid a receptor subunit mutant mice: new perspectives on alcohol actions. *Biochem. Pharmacol.* 68, 1581–1602. doi: 10.1016/j.bcp.2004.07.023

Bonsi, P., Cuomo, D., Martella, G., Madeo, G., Schirinzi, T., Puglisi, F., et al. (2011). Centrality of striatal cholinergic transmission in basal ganglia function. *Front. Neuroanat.* 5:6. doi: 10.3389/fnana.2011.00006

Bosch-Bouju, C., Larrieu, T., Linders, L., Manzoni, O. J., and Layé, S. (2016). Endocannabinoid-mediated plasticity in nucleus Accumbens controls vulnerability to anxiety after social defeat stress. *Cell Rep.* 16, 1237–1242. doi: 10.1016/j.celrep.2016.06.082

Boyce-Rustay, J. M., and Holmes, A. (2006). Ethanol-related behaviors in mice lacking the NMDA receptor NR2A subunit. *Psychopharmacology (Berl)* 187, 455–466. doi: 10.1007/s00213-006-0448-6

Brackenbury, W. J., and Isom, L. L. (2011). Na Channel beta subunits: overachievers of the Ion Channel family. *Front. Pharmacol.* 2:53. doi: 10.3389/fphar.2011.00053

Brenner, R., Chen, Q. H., Vilaythong, A., Toney, G. M., Noebels, J. L., and Aldrich, R. W. (2005). BK channel beta4 subunit reduces dentate gyrus excitability and protects against temporal lobe seizures. *Nat. Neurosci.* 8, 1752–1759. doi: 10.1038/nn1573

Brenner, R., Jegla, T. J., Wickenden, A., Liu, Y., and Aldrich, R. W. (2000). Cloning and functional characterization of novel large conductance calcium-activated potassium channel beta subunits, hKCNMB3 and hKCNMB4. *J. Biol. Chem.* 275, 6453–6461. doi: 10.1074/jbc.275.9.6453

Bukiya, A. N., Kuntamallappanavar, G., Edwards, J., Singh, A. K., Shivakumar, B., and Dopico, A. M. (2014). An alcohol-sensing site in the calcium- and voltage-gated, large conductance potassium (BK) channel. *Proc Natl Acad Sci U S A.* 24, 9313–9318. doi: 10.1073/pnas.1317363111

Cachope, R., Mateo, Y., Mathur, B. N., Irving, J., Wang, H. L., Morales, M., et al. (2012). Selective activation of cholinergic interneurons enhances accumbal phasic dopamine release: setting the tone for reward processing. *Cell Rep.* 2, 33–41. doi: 10.1016/j.celrep.2012.05.011

Cagetti, E., Liang, J., Spigelman, I., and Olsen, R. W. (2003). Withdrawal from chronic intermittent ethanol treatment changes subunit composition, reduces synaptic function,

and decreases behavioral responses to positive allosteric modulators of GABAA receptors. *Mol. Pharmacol.* 63, 53–64. doi: 10.1124/mol.63.1.53

Cai, X., Liang, C. W., Muralidharan, S., Kao, J. P., Tang, C. M., and Thompson, S. M. (2004). Unique roles of SK and Kv4.2 potassium channels in dendritic integration. *Neuron* 44, 351–364. doi: 10.1016/j.neuron.2004.09.026

Caporale, N., and Dan, Y. (2008). Spike timing-dependent plasticity: a hebbian learning rule. *Annu. Rev. Neurosci.* 31, 25–46. doi: 10.1146/annurev.neuro.31.060407.125639

Cardinal, R. N., Parkinson, J. A., Hall, J., and Everitt, B. J. (2002). Emotion and motivation: the role of the amygdala, ventral striatum, and prefrontal cortex. *Neurosci. Biobehav. Rev.* 26, 321–352. doi: 10.1016/S0149-7634(02)00007-6

Catterall, W. A. (2000). From ionic currents to molecular mechanisms: the structure and function of voltage-gated sodium channels. *Neuron* 26, 13–25. doi: 10.1016/S0896-6273(00)81133-2

Cavaliere, S., Gillespie, J. M., and Hodge, J. J. (2012). KCNQ channels show conserved ethanol block and function in ethanol behaviour. *PLoS One* 7:e50279. doi: 10.1371/journal.pone.0050279

Cavalieri, D., McGovern, P. E., Hartl, D. L., Mortimer, R., and Polsinelli, M. (2003). Evidence for S. cerevisiae fermentation in ancient wine. *J. Mol. Evol.* 57 Suppl 1, S226–S232. doi: 10.1007/s00239-003-0031-2

Celentano, J. J., Gibbs, T. T., and Farb, D. H. (1988). Ethanol potentiates GABA- and glycine-induced chloride currents in chick spinal cord neurons. *Brain Res.* 455, 377–380. doi: 10.1016/0006-8993(88)90098-4

Centanni, S. W., Burnett, E. J., Trantham-Davidson, H., and Chandler, L. J. (2017). Loss of δ-GABAA receptor-mediated tonic currents in the adult prelimbic cortex following adolescent alcohol exposure. *Addict. Biol.* 22, 616–628. doi: 10.1111/adb.12353

Centanni, S. W., Teppen, T., Risher, M. L., Fleming, R. L., Moss, J. L., Acheson, S. K., et al. (2014). Adolescent alcohol exposure alters GABAA receptor subunit expression in adult hippocampus. *Alcohol. Clin. Exp. Res.* 38, 2800–2808. doi: 10.1111/acer.12562

Chang, C. P., Dworetzky, S. I., Wang, J., and Goldstein, M. E. (1997). Differential expression of the alpha and beta subunits of the large-conductance calcium-activated potassium channel: implication for channel diversity. *Brain Res. Mol. Brain Res.* 45, 33–40. doi: 10.1016/S0169-328X(96)00230-6

Cheng, Y., Huang, C. C. Y., Ma, T., Wei, X., Wang, X., Lu, J., et al. (2017). Distinct Synaptic Strengthening of the Striatal Direct and Indirect Pathways Drives Alcohol Consumption. *Biol Psychiatry* 81, 918–929. doi: 10.1016/j.biopsych.2016.05.016

Choquet, D., Sainlos, M., and Sibarita, J. B. (2021). Advanced imaging and labelling methods to decipher brain cell organization and function. *Nat. Rev. Neurosci.* 22, 237–255. doi: 10.1038/s41583-021-00441-z

Christian, D. T., Alexander, N. J., Diaz, M. R., and McCool, B. A. (2013). Thalamic glutamatergic afferents into the rat basolateral amygdala exhibit increased presynaptic glutamate function following withdrawal from chronic intermittent ethanol. *Neuropharmacology* 65, 134–142. doi: 10.1016/j.neuropharm.2012.09.004

Citri, A., and Malenka, R. C. (2008). Synaptic plasticity: multiple forms, functions, and mechanisms. *Neuropsychopharmacology* 33, 18–41. doi: 10.1038/sj.npp.1301559

Colbert, C. M., Magee, J. C., Hoffman, D. A., and Johnston, D. (1997). Slow recovery from inactivation of Na+ channels underlies the activity-dependent attenuation of dendritic action potentials in hippocampal CA1 pyramidal neurons. *J. Neurosci.* 17, 6512–6521. doi: 10.1523/JNEUROSCI.17-17-06512.1997

Covarrubias, M., and Rubin, E. (1993). Ethanol selectively blocks a noninactivating K+ current expressed in Xenopus oocytes. *Proc. Natl. Acad. Sci. U. S. A.* 90, 6957–6960. doi: 10.1073/pnas.90.15.6957

Cowen, M. S., Schroff, K. C., Gass, P., Sprengel, R., and Spanagel, R. (2003). Neurobehavioral effects of alcohol in AMPA receptor subunit (GluR1) deficient mice. *Neuropharmacology* 45, 325–333. doi: 10.1016/S0028-3908(03)00174-6

Crabbe, J. C., Harris, R. A., and Koob, G. F. (2011). Preclinical studies of alcohol binge drinking. *Ann. N. Y. Acad. Sci.* 1216, 24–40. doi: 10.1111/j.1749-6632.2010.05895.x

Crowley, J. J., Treistman, S. N., and Dopico, A. M. (2003). Cholesterol antagonizes ethanol potentiation of human brain BKCa channels reconstituted into phospholipid bilayers. *Mol. Pharmacol.* 64, 365–372. doi: 10.1124/mol.64.2.365

Crowley, J. J., Treistman, S. N., and Dopico, A. M. (2005). Distinct structural features of phospholipids differentially determine ethanol sensitivity and basal function of BK channels. *Mol. Pharmacol.* 68, 4–10. doi: 10.1124/mol.105.012971

Cservenka, A., and Brumback, T. (2017). The burden of binge and heavy drinking on the brain: effects on adolescent and young adult neural structure and function. *Front. Psychol.* 8:1111. doi: 10.3389/fpsyg.2017.01111

Dalley, J. W., Cardinal, R. N., and Robbins, T. W. (2004). Prefrontal executive and cognitive functions in rodents: neural and neurochemical substrates. *Neurosci. Biobehav. Rev.* 28, 771–784. doi: 10.1016/j.neubiorev.2004.09.006

de Guglielmo, G., Crawford, E., Kim, S., Vendruscolo, L. F., Hope, B. T., Brennan, M., et al. (2016). Recruitment of a neuronal Ensemble in the Central Nucleus of the amygdala is required for alcohol dependence. *J. Neurosci.* 36, 9446–9453. doi: 10.1523/JNEUROSCI.1395-16.2016

de Guglielmo, G., Kallupi, M., Pomrenze, M. B., Crawford, E., Simpson, S., Schweitzer, P., et al. (2019). Inactivation of a CRF-dependent amygdalofugal pathway reverses addiction-like behaviors in alcohol-dependent rats. *Nat. Commun.* 18:1238. doi: 10.1523/JNEUROSCI.1395-16.2016

de Kloet, S. F., Mansvelder, H. D., and De Vries, T. J. (2015). Cholinergic modulation of dopamine pathways through nicotinic acetylcholine receptors. *Biochem. Pharmacol.* 97, 425–438. doi: 10.1016/j.bcp.2015.07.014

Debanne, D., Bialowas, A., and Rama, S. (2013). What are the mechanisms for analogue and digital signaling in the brain? *Nat. Rev. Neurosci.* 14, 63–69. doi: 10.1038/nrn3361

Deisz, R. A., and Prince, D. A. (1989). Frequency-dependent depression of inhibition in Guinea-pig neocortex in vitro by GABAB receptor feed-back on GABA release. *J. Physiol.* 412, 513–541. doi: 10.1113/jphysiol.1989.sp017629

Deitrich, R. A., Dunwiddie, T. V., Harris, R. A., and Erwin, V. G. (1989). Mechanism of action of ethanol: initial central nervous system actions. *Pharmacol. Rev.* 41, 489–537. PMID: 2700603

Delaney, A. J., Esmaeili, A., Sedlak, P. L., Lynch, J. W., and Sah, P. (2010). Differential expression of glycine receptor subunits in the rat basolateral and central amygdala. *Neurosci. Lett.* 469, 237–242. doi: 10.1016/j.neulet.2009.12.003

den Hartog, C. R., Beckley, J. T., Smothers, T. C., Lench, D. H., Holseberg, Z. L., Fedarovich, H., et al. (2013). Alterations in ethanol-induced behaviors and consumption in knock-in mice expressing ethanol-resistant NMDA receptors. *PLoS One* 8:e80541. doi: 10.1371/journal.pone.0080541

DeNardo, L. A., Liu, C. D., Allen, W. E., Adams, E. L., Friedmann, D., Fu, L., et al. (2019). Temporal evolution of cortical ensembles promoting remote memory retrieval. *Nat. Neurosci.* 22, 460–469. doi: 10.1038/s41593-018-0318-7

Dildy-Mayfield, J. E., Mihic, S. J., Liu, Y., Deitrich, R. A., and Harris, R. A. (1996). Actions of long chain alcohols on GABAA and glutamate receptors: relation to in vivo effects. *Br. J. Pharmacol.* 118, 378–384. doi: 10.1111/j.1476-5381.1996.tb15413.x

Dopico, A. M., Chu, B., Lemos, J. R., and Treistman, S. N. (1999). Alcohol modulation of calcium-activated potassium channels. *Neurochem. Int.* 35, 103–106. doi: 10.1016/S0197-0186(99)00051-0

Dopico, A. M., Lemos, J. R., and Treistman, S. N. (1996). Ethanol increases the activity of large conductance, ca(2+)-activated K+ channels in isolated neurohypophysial terminals. *Mol. Pharmacol.* 49, 40–48. PMID: 8569710

Duka, T., Gentry, J., Malcolm, R., Ripley, T. L., Borlikova, G., Stephens, D. N., et al. (2004). Consequences of multiple withdrawals from alcohol. *Alcohol. Clin. Exp. Res.* 28, 233–246. doi: 10.1097/01.ALC.0000113780.41701.81

Doyon, W. M., Ostroumov, A., Ontiveros, T., Gonzales, R. A., and Dani, J. A. (2021). Ethanol produces multiple electrophysiological effects on ventral tegmental area neurons in freely moving rats. *Addict Biol.* 26:e12899. doi: 10.1111/adb.12899

Egervari, G., Siciliano, C. A., Whiteley, E. L., and Ron, D. (2021). Alcohol and the brain: from genes to circuits. *Trends Neurosci.* 44, 1004–1015. doi: 10.1016/j.tins.2021.09.006

Engel, J. A., and Jerlhag, E. (2014). Alcohol: mechanisms along the mesolimbic dopamine system. *Prog. Brain Res.* 211, 201–233. doi: 10.1016/B978-0-444-63425-2.00009-X

Esser, M. B., Leung, G., Sherk, A., Bohm, M. K., Liu, Y., Lu, H., et al. (2022). Estimated deaths attributable to excessive alcohol use among US adults aged 20 to 64 years, 2015 to 2019. *JAMA Netw. Open* 5:e2239485. doi: 10.1001/jamanetworkopen.2022.39485

Evans, M. S., Li, Y., and Faingold, C. (2000). Inferior colliculus intracellular response abnormalities in vitro associated with susceptibility to ethanol withdrawal seizures. *Alcohol. Clin. Exp. Res.* 24, 1180–1186. doi: 10.1111/j.1530-0277.2000.tb02081.x

Faber, E. S., Delaney, A. J., and Sah, P. (2005). SK channels regulate excitatory synaptic transmission and plasticity in the lateral amygdala. *Nat. Neurosci.* 8, 635–641. doi: 10.1038/nn1450

Farris, S. P., Arasappan, D., Hunicke-Smith, S., Harris, R. A., and Mayfield, R. D. (2014). Transcriptome organization for chronic alcohol abuse in human brain. *Mol. Psychiatry* 20, 1438–1447. doi: 10.1038/mp.2014.159

Finegersh, A., Ferguson, C., Maxwell, S., Mazariegos, D., Farrell, D., and Homanics, G. E. (2015). Repeated vapor ethanol exposure induces transient histone modifications in the brain that are modified by genotype and brain region. *Front. Mol. Neurosci.* 8:39. doi: 10.3389/fnmol.2015.00039

Fino, E., and Venance, L. (2010). Spike-timing dependent plasticity in the striatum. *Front. Synaptic Neurosci.* 2:6. doi: 10.3389/fnsyn.2010.00006

Fleming, R. L., Acheson, S. K., Moore, S. D., Wilson, W. A., and Swartzwelder, H. S. (2012). In the rat, chronic intermittent ethanol exposure during adolescence alters the ethanol sensitivity of tonic inhibition in adulthood. *Alcohol. Clin. Exp. Res.* 36, 279–285. doi: 10.1111/j.1530-0277.2011.01615.x

Follesa, P., Floris, G., Asuni, G. P., Ibba, A., Tocco, M. G., Zicca, L., et al. (2015). Chronic intermittent ethanol regulates hippocampal GABA(a) Receptor Delta subunit gene expression. *Front. Cell. Neurosci.* 9:445. doi: 10.3389/fncel.2015.00445

Franklin, J. L., Fickbohm, D. J., and Willard, A. L. (1992). Long-term regulation of neuronal calcium currents by prolonged changes of membrane potential. *J. Neurosci.* 12, 1726–1735. doi: 10.1523/JNEUROSCI.12-05-01726.1992

Frick, A., Magee, J., and Johnston, D. (2004). LTP is accompanied by an enhanced local excitability of pyramidal neuron dendrites. *Nat. Neurosci.* 7, 126–135. doi: 10.1038/nn1178

Fu, R., Gregor, D., Peng, Z., Li, J., Bekker, A., and Ye, J. (2015). Chronic intermittent voluntary alcohol drinking induces hyperalgesia in Sprague-Dawley rats. *Int J Physiol Pathophysiol Pharmacol.* 13, 136–144.

Furey, M. L., Pietrini, P., Haxby, J. V., and Drevets, W. C. (2008). Selective effects of cholinergic modulation on task performance during selective attention. *Neuropsychopharmacology* 33, 913–923. doi: 10.1038/sj.npp.1301461

Galarraga, E., Hernández-López, S., Reyes, A., Miranda, I., Bermudez-Rattoni, F., Vilchis, C., et al. (1999). Cholinergic modulation of neostriatal output: a functional antagonism between different types of muscarinic receptors. *J. Neurosci.* 19, 3629–3638. doi: 10.1523/JNEUROSCI.19-09-03629.1999

Gallagher, M., and Chiba, A. A. (1996). The amygdala and emotion. *Curr. Opin. Neurobiol.* 6, 221–227. doi: 10.1016/S0959-4388(96)80076-6

Gately, I. (2008). *Drink: a cultural history of alcohol*, penguin, Publishing Group, New York, US, 546.

George, M. S., Abbott, L. F., and Siegelbaum, S. A. (2009). HCN hyperpolarization-activated cation channels inhibit EPSPs by interactions with M-type K(+) channels. *Nat. Neurosci.* 12, 577–584. doi: 10.1038/nn.2307

Gerfen, C. R. (1984). The neostriatal mosaic: compartmentalization of corticostriatal input and striatonigral output systems. *Nature* 311, 461–464. doi: 10.1038/311461a0

Gerfen, C. R., and Surmeier, D. J. (2011). Modulation of striatal projection systems by dopamine. *Annu. Rev. Neurosci.* 34, 441–466. doi: 10.1146/annurev-neuro-061010-113641

Giedd, J. N., Blumenthal, J., Jeffries, N. O., Castellanos, F. X., Liu, H., Zijdenbos, A., et al. (1999). Brain development during childhood and adolescence: a longitudinal MRI study. *Nat. Neurosci.* 2, 861–863. doi: 10.1038/13158

Gilpin, N. W., Richardson, H. N., and Koob, G. F. (2008). Effects of CRF1-receptor and opioid-receptor antagonists on dependence-induced increases in alcohol drinking by alcohol-preferring (P) rats. *Alcohol. Clin. Exp. Res.* 32, 1535–1542. doi: 10.1111/j.1530-0277.2008.00745.x

Ghatta, S., Lozinskaya, I., Lin, Z., Gordon, E., Willette, R. N., Brooks, D. P., et al. (2007). Acetic acid opens large-conductance Ca2+-activated K+ channels in guinea pig detrusor smooth muscle cells. *Eur J Pharmacol.* 563, 203–208. doi: 10.1016/j.ejphar.2007.02.037

Goldin, A. L. (2001). Resurgence of sodium channel research. *Annu. Rev. Physiol.* 63, 871–894. doi: 10.1146/annurev.physiol.63.1.871

Goldin, A. L., Barchi, R. L., Caldwell, J. H., Hofmann, F., Howe, J. R., Hunter, J. C., et al. (2000). Nomenclature of voltage-gated sodium channels. *Neuron* 28, 365–368. doi: 10.1016/S0896-6273(00)00116-1

Grieco, T. M., Malhotra, J. D., Chen, C., Isom, L. L., and Raman, I. M. (2005). Open-channel block by the cytoplasmic tail of sodium channel beta4 as a mechanism for resurgent sodium current. *Neuron* 45, 233–244. doi: 10.1016/j.neuron.2004.12.035

Griffin, W. C., Haun, H. L., Hazelbaker, C. L., Ramachandra, V. S., and Becker, H. C. (2014). Increased extracellular glutamate in the nucleus accumbens promotes excessive ethanol drinking in ethanol dependent mice. *Neuropsychopharmacology* 39, 707–717. doi: 10.1038/npp.2013.256

Grudzinska, J., Schemm, R., Haeger, S., Nicke, A., Schmalzing, G., Betz, H., et al. (2005). The beta subunit determines the ligand binding properties of synaptic glycine receptors. *Neuron* 45, 727–739. doi: 10.1016/j.neuron.2005.01.028

Gruol, D. L., Hernandez, R. V., and Roberts, A. (2021). Alcohol enhances responses to high frequency stimulation in hippocampus from transgenic mice with increased astrocyte expression of IL-6. *Cell. Mol. Neurobiol.* 41, 1299–1310. doi: 10.1007/s10571-020-00902-6

Hamilton, K. R., Ansell, E. B., Reynolds, B., Potenza, M. N., and Sinha, R. (2013). Self-reported impulsivity, but not behavioral choice or response impulsivity, partially mediates the effect of stress on drinking behavior. *Stress* 16, 3–15. doi: 10.3109/10253890.2012.671397

Harris, R. A., Proctor, W. R., McQuilkin, S. J., Klein, R. L., Mascia, M. P., Whatley, V., et al. (1995). Ethanol increases GABAA responses in cells stably transfected with receptor subunits. *Alcohol. Clin. Exp. Res.* 19, 226–232. doi: 10.1111/j.1530-0277.1995.tb01496.x

Hartley, D. E., Elsabagh, S., and File, S. E. (2004). Binge drinking and sex: effects on mood and cognitive function in healthy young volunteers. *Pharmacol. Biochem. Behav.* 78, 611–619. doi: 10.1016/j.pbb.2004.04.027

Hauser, S. R., Knight, C. P., Truitt, W. A., Waeiss, R. A., Holt, I. S., Carvajal, G. B., et al. (2019). Adolescent intermittent ethanol increases the sensitivity to the reinforcing properties of ethanol and the expression of select cholinergic and dopaminergic genes within the posterior ventral tegmental area. *Alcohol. Clin. Exp. Res.* 43, 1937–1948. doi: 10.1111/acer.14150

Heinsbroek, J. A., Neuhofer, D. N., Griffin, W. C., Siegel, G. S., Bobadilla, A. C., Kupchik, Y. M., et al. (2017). Loss of plasticity in the D2-Accumbens Pallidal pathway promotes cocaine seeking. *J. Neurosci.* 37, 757–767. doi: 10.1523/JNEUROSCI.2659-16.2016

Herman, M. A., Contet, C., and Roberto, M. (2016). A functional switch in tonic GABA currents alters the output of central amygdala Corticotropin releasing factor Receptor-1 neurons following chronic ethanol exposure. *J. Neurosci.* 36, 10729–10741. doi: 10.1523/JNEUROSCI.1267-16.2016

Herman, M. A., Sidhu, H., Stouffer, D. G., Kreifeldt, M., Le, D., Cates-Gatto, C., et al. (2015). GIRK3 gates activation of the mesolimbic dopaminergic pathway by ethanol. *Proc. Natl. Acad. Sci. U. S. A.* 112, 7091–7096. doi: 10.1073/pnas.1416146112

Hikida, T., Kimura, K., Wada, N., Funabiki, K., and Nakanishi, S. (2010). Distinct roles of synaptic transmission in direct and indirect striatal pathways to reward and aversive behavior. *Neuron* 66, 896–907. doi: 10.1016/j.neuron.2010.05.011

Hopf, F. W., Bowers, M. S., Chang, S. J., Chen, B. T., Martin, M., Seif, T., et al. (2010). Reduced nucleus accumbens SK channel activity enhances alcohol seeking during abstinence. *Neuron.* 65, 682–694. doi: 10.1016/j.neuron.2010.02.015

Hoffman, P. L., Yagi, T., Tabakoff, B., Phillips, T. J., Kono, H., Messing, R. O., et al. (2001). Transgenic and gene "knockout" models in alcohol research. *Alcohol. Clin. Exp. Res.* 25, 60S–66S. doi: 10.1097/00000374-200105051-00011

Holmes, A., Fitzgerald, P. J., MacPherson, K. P., DeBrouse, L., Colacicco, G., Flynn, S. M., et al. (2012). Chronic alcohol remodels prefrontal neurons and disrupts NMDAR-mediated fear extinction encoding. *Nat. Neurosci.* 15, 1359–1361. doi: 10.1038/nn.3204

Hsu, K. S., Yang, C. H., Huang, C. C., and Gean, P. W. (1996). Carbachol induces inward current in neostriatal neurons through M1-like muscarinic receptors. *Neuroscience* 73, 751–760. doi: 10.1016/0306-4522(96)00066-8

Hughes, B. A., Bohnsack, J. P., O'Buckley, T. K., Herman, M. A., and Morrow, A. L. (2019). Chronic ethanol exposure and withdrawal impair synaptic $GABA_A$ receptor-mediated neurotransmission in deep-layer prefrontal cortex. *Alcohol. Clin. Exp. Res.* 43, 822–832. doi: 10.1111/acer.14015

Humphries, M. D., and Prescott, T. J. (2010). The ventral basal ganglia, a selection mechanism at the crossroads of space, strategy, and reward. *Prog. Neurobiol.* 90, 385–417. doi: 10.1016/j.pneurobio.2009.11.003

Ikemoto, S. (2007). Dopamine reward circuitry: two projection systems from the ventral midbrain to the nucleus accumbens-olfactory tubercle complex. *Brain Res. Rev.* 56, 27–78. doi: 10.1016/j.brainresrev.2007.05.004

Ingólfsson, H. I., and Andersen, O. S. (2011). Alcohol's effects on lipid bilayer properties. *Biophys. J.* 101, 847–855. doi: 10.1016/j.bpj.2011.07.013

Isaacson, J. S., and Murphy, G. J. (2001). Glutamate-mediated extrasynaptic inhibition: direct coupling of NMDA receptors to ca(2+)-activated K+ channels. *Neuron* 31, 1027–1034. doi: 10.1016/S0896-6273(01)00428-7

Jeanes, Z. M., Buske, T. R., and Morrisett, R. A. (2011). In vivo chronic intermittent ethanol exposure reverses the polarity of synaptic plasticity in the nucleus accumbens shell. *J. Pharmacol. Exp. Ther.* 336, 155–164. doi: 10.1124/jpet.110.171009

Jeanes, Z. M., Buske, T. R., and Morrisett, R. A. (2014). Cell type-specific synaptic encoding of ethanol exposure in the nucleus accumbens shell. *Neuroscience* 277, 184–195. doi: 10.1016/j.neuroscience.2014.06.063

Ji, X., and Martin, G. E. (2012). New rules governing synaptic plasticity in core nucleus accumbens medium spiny neurons. *Eur. J. Neurosci.* 36, 3615–3627. doi: 10.1111/ejn.12002

Ji, X., Saha, S., Gao, G., Lasek, A. W., Homanics, G. E., Guildford, M., et al. (2017a). The Sodium Channel β4 auxiliary subunit selectively controls long-term depression in Core nucleus Accumbens medium spiny neurons. *Front. Cell. Neurosci.* 11:17. doi: 10.3389/fncel.2017.00017

Ji, X., Saha, S., Kolpakova, J., Guildford, M., Tapper, A. R., and Martin, G. E. (2017b). Dopamine receptors differentially control binge alcohol drinking-mediated synaptic plasticity of the Core nucleus Accumbens direct and indirect pathways. *J. Neurosci.* 37, 5463–5474. doi: 10.1523/JNEUROSCI.3845-16.2017

Jia, Z., Agopyan, N., Miu, P., Xiong, Z., Henderson, J., Gerlai, R., et al. (1996). Enhanced LTP in mice deficient in the AMPA receptor GluR2. *Neuron* 17, 945–956. doi: 10.1016/S0896-6273(00)80225-1

Jonsson, S., Kerekes, N., Hyytia, P., Ericson, M., and Soderpalm, B. (2009). Glycine receptor expression in the forebrain of male AA/ANA rats. *Brain Res.* 1305, S27–S36. doi: 10.1016/j.brainres.2009.09.053

Joshi, N., McAree, M., and Chandler, D. (2020). Corticotropin releasing factor modulates excitatory synaptic transmission. *Vitam. Horm.* 114, 53–69. doi: 10.1016/bs.vh.2020.04.003

Juarez, B., Morel, C., Ku, S. M., Liu, Y., Zhang, H., Montgomery, S., et al. (2017). Midbrain circuit regulation of individual alcohol drinking behaviors in mice. *Nat. Commun.* 8, 1–15. doi: 10.1038/s41467-017-02365-8

June, H. L., Foster, K. L., Eiler, W. J., Goergen, J., Cook, J. B., Johnson, N., et al. (2007). Dopamine and benzodiazepine-dependent mechanisms regulate the EtOH-enhanced locomotor stimulation in the GABAA alpha1 subunit null mutant mice. *Neuropsychopharmacology* 32, 137–152. doi: 10.1038/sj.npp.1301097

Kalivas, P. W. (2009). The glutamate homeostasis hypothesis of addiction. *Nat. Rev. Neurosci.* 10, 561–572. doi: 10.1038/nrn2515

Kalivas, P. W., Lalumiere, R. T., Knackstedt, L., and Shen, H. (2009). Glutamate transmission in addiction. *Neuropharmacology* 56, 169–173. doi: 10.1038/nrn2515

Katz, P. S. (2003). Synaptic gating: the potential to open closed doors. *Curr. Biol.* 13, R554–R556. doi: 10.1016/S0960-9822(03)00471-8

Kauer, J. A., and Malenka, R. C. (2007). Synaptic plasticity and addiction. *Nat. Rev. Neurosci.* 8, 844–858. doi: 10.1038/nrn2234

Kim, J., Jung, S. C., Clemens, A. M., Petralia, R. S., and Hoffman, D. A. (2007). Regulation of dendritic excitability by activity-dependent trafficking of the A-type K+ channel subunit Kv4.2 in hippocampal neurons. *Neuron* 54, 933–947. doi: 10.1016/j.neuron.2007.05.026

Kirson, D., Oleata, C. S., and Roberto, M. (2020). Taurine suppression of central amygdala GABAergic inhibitory signaling via glycine receptors is disrupted in alcohol dependence. *Alcohol. Clin. Exp. Res.* 44, 445–454. doi: 10.1111/acer.14252

Kitamura, T., Ogawa, S. K., Roy, D. S., Okuyama, T., Morrissey, M. D., Smith, L. M., et al. (2017). Engrams and circuits crucial for systems consolidation of a memory. *Science* 356, 73–78. doi: 10.1126/science.aam6808

Kobayashi, T., Ikeda, K., Kojima, H., Niki, H., Yano, R., Yoshioka, T., et al. (1999). Ethanol opens G-protein-activated inwardly rectifying K+ channels. *Nat. Neurosci.* 2, 1091–1097. doi: 10.1038/16019

Kolpakova, J., van der Vinne, V., Gimenez-Gomez, P., Le, T., and Martin, G. E. (2022). Binge alcohol drinking alters the differential control of cholinergic interneurons over nucleus accumbens D1 and D2 medium spiny neurons. *Front. Cell. Neurosci.* 16:1010121. doi: 10.3389/fncel.2022.1010121

Kolpakova, J., van der Vinne, V., Giménez-Gómez, P., Le, T., You, I. J., Zhao-Shea, R., et al. (2021). Binge alcohol drinking alters synaptic processing of executive and emotional information in Core nucleus Accumbens medium spiny neurons. *Front. Cell. Neurosci.* 15:742207. doi: 10.3389/fncel.2021.742207

Kombian, S. B., and Malenka, R. C. (1994). Simultaneous LTP of non-NMDA- and LTD of NMDA-receptor-mediated responses in the nucleus accumbens. *Nature* 368, 242–246. doi: 10.1038/368242a0

Kravitz, A. V., Tye, L. D., and Kreitzer, A. C. (2012). Distinct roles for direct and indirect pathway striatal neurons in reinforcement. *Nat. Neurosci.* 15, 816–818. doi: 10.1038/nn.3100

Kroener, S., Mulholland, P. J., New, N. N., Gass, J. T., Becker, H. C., and Chandler, L. J. (2012). Chronic alcohol exposure alters behavioral and synaptic plasticity of the rodent prefrontal cortex. *PLoS One* 7:e37541. doi: 10.1371/journal.pone.0037541

Krystal, J. H., Petrakis, I. L., Krupitsky, E., Schutz, C., Trevisan, L., and D'Souza, D. C. (2003). NMDA receptor antagonism and the ethanol intoxication signal: from alcoholism risk to pharmacotherapy. *Ann. N. Y. Acad. Sci.* 1003, 176–184. doi: 10.1196/annals.1300.010

Kupchik, Y. M., Brown, R. M., Heinsbroek, J. A., Lobo, M. K., Schwartz, D. J., and Kalivas, P. W. (2015). Coding the direct/indirect pathways by D1 and D2 receptors is not valid for accumbens projections. *Nat. Neurosci.* 18, 1230–1232. doi: 10.1038/nn.4068

Kwan, L. Y., Eaton, D. L., Andersen, S. L., Dow-Edwards, D., Levin, E. D., Talpos, J., et al. (2020). This is your teen brain on drugs: in search of biological factors unique to dependence toxicity in adolescence. *Neurotoxicol. Teratol.* 81:106916. doi: 10.1016/j.ntt.2020.106916

Lack, A. K., Floyd, D. W., and McCool, B. A. (2005). Chronic ethanol ingestion modulates proanxiety factors expressed in rat central amygdala. *Alcohol* 36, 83–90. doi: 10.1016/j.alcohol.2005.07.004

Lalumiere, R. T. (2014). Optogenetic dissection of amygdala functioning. *Front. Behav. Neurosci.* 8:107. doi: 10.3389/fnbeh.2014.00107

Laube, B., Maksay, G., Schemm, R., and Betz, H. (2002). Modulation of glycine receptor function: a novel approach for therapeutic intervention at inhibitory synapses. *Trends Pharmacol. Sci.* 23, 519–527. doi: 10.1016/S0165-6147(02)02138-7

Lewohl, J. M., Wilson, W. R., Mayfield, R. D., Brozowski, S. J., Morrisett, R. A., and Harris, R. A. (1999). G-protein-coupled inwardly rectifying potassium channels are targets of alcohol action. *Nat. Neurosci.* 2, 1084–1090. doi: 10.1038/16012

Li, Z., Chen, Z., Fan, G., Li, A., Yuan, J., and Xu, T. (2018). Cell-type-specific afferent innervation of the nucleus Accumbens Core and Shell. *Front. Neuroanat.* 12:84. doi: 10.3389/fnana.2018.00084

Li, J., Nie, H., Bian, W., Dave, V., Janak, P. H., and Ye, J. H. (2012). Microinjection of glycine into the ventral tegmental area selectively decreases ethanol consumption. *J. Pharmacol. Exp. Ther.* 341, 196–204. doi: 10.1124/jpet.111.190058

Liang, J., Lindemeyer, A. K., Suryanarayanan, A., Meyer, E. M., Marty, V. N., Ahmad, S. O., et al. (2014a). Plasticity of GABA(a) receptor-mediated neurotransmission in the nucleus accumbens of alcohol-dependent rats. *J. Neurophysiol.* 112, 39–50. doi: 10.1152/jn.00565.2013

Liang, J., Marty, V. N., Mulpuri, Y., Olsen, R. W., and Spigelman, I. (2014b). Selective modulation of GABAergic tonic current by dopamine in the nucleus accumbens of alcohol-dependent rats. *J. Neurophysiol.* 112, 51–60. doi: 10.1152/jn.00564.2013

Liang, J., Zhang, N., Cagetti, E., Houser, C. R., Olsen, R. W., and Spigelman, I. (2006). Chronic intermittent ethanol-induced switch of ethanol actions from extrasynaptic to synaptic hippocampal GABAA receptors. *J. Neurosci.* 26, 1749–1758. doi: 10.1523/JNEUROSCI.4702-05.2006

Lim, S. A., Kang, U. J., and McGehee, D. S. (2014). Striatal cholinergic interneuron regulation and circuit effects. *Front. Synaptic Neurosci.* 6:22. doi: 10.3389/fnsyn.2014.00022

Lin, M. T., Luján, R., Watanabe, M., Adelman, J. P., and Maylie, J. (2008). SK2 channel plasticity contributes to LTP at Schaffer collateral-CA1 synapses. *Nat. Neurosci.* 11, 170–177. doi: 10.1038/nn2041

Lindemeyer, A. K., Shen, Y., Yazdani, F., Shao, X. M., Spigelman, I., Davies, D. L., et al. (2017). α2 subunit-containing GABAA receptor subtypes are upregulated and contribute to alcohol-induced functional plasticity in the rat hippocampus. *Mol. Pharmacol.* 92, 101–112. doi: 10.1124/mol.116.107797

Litten, R. Z., Wilford, B. B., Falk, D. E., Ryan, M. L., and Fertig, J. B. (2016). Potential medications for the treatment of alcohol use disorder: an evaluation of clinical efficacy and safety. *Subst. Abus.* 37, 286–298. doi: 10.1080/08897077.2015.1133472

Liu, X., Ramirez, S., Pang, P. T., Puryear, C. B., Govindarajan, A., Deisseroth, K., et al. (2012). Optogenetic stimulation of a hippocampal engram activates fear memory recall. *Nature* 484, 381–385. doi: 10.1038/nature11028

Lobo, M. K., Covington, H. E., Chaudhury, D., Friedman, A. K., Sun, H., Damez-Werno, D., et al. (2010). Cell type-specific loss of BDNF signaling mimics optogenetic control of cocaine reward. *Science* 330, 385–390. doi: 10.1126/science.1188472

Lobo, I. A., and Harris, R. A. (2008). GABA(a) receptors and alcohol. *Pharmacol. Biochem. Behav.* 90, 90–94. doi: 10.1016/j.pbb.2008.03.006

Lovinger, D. M., Partridge, J. G., and Tang, K. C. (2003). Plastic control of striatal glutamatergic transmission by ensemble actions of several neurotransmitters and targets for drugs of abuse. *Ann. N. Y. Acad. Sci.* 1003, 226–240. doi: 10.1196/annals.1300.014

Lovinger, D. M., White, G., and Weight, F. F. (1990). NMDA receptor-mediated synaptic excitation selectively inhibited by ethanol in hippocampal slice from adult rat. *J. Neurosci.* 10, 1372–1379. doi: 10.1523/JNEUROSCI.10-04-01372.1990

Magee, J. C., and Johnston, D. (1995). Synaptic activation of voltage-gated channels in the dendrites of hippocampal pyramidal neurons. *Science* 268, 301–304. doi: 10.1126/science.7716525

Malenka, R. C., Nestler, E. J., and Hyman, S. E. (2009) in Excitatory and Inhibitory Amino Acids, *Molecular neuropharmacology: A Foundation for Clinical Neuroscience*. eds. A. Sydor and R. Y. Brown. *2nd* ed (New York, US: McGraw-Hill Medical), 147–148.

Martin, G., Puig, S., Pietrzykowski, A., Zadek, P., Emery, P., and Treistman, S. (2004). Somatic localization of a specific large-conductance calcium-activated potassium channel subtype controls compartmentalized ethanol sensitivity in the nucleus accumbens. *J. Neurosci.* 24, 6563–6572. doi: 10.1523/JNEUROSCI.0684-04.2004

Martin, G., and Siggins, G. R. (2002). Electrophysiological evidence for expression of glycine receptors in freshly isolated neurons from nucleus accumbens. *J. Pharmacol. Exp. Ther.* 302, 1135–1145. doi: 10.1124/jpet.102.033399

Marty, V. N., and Spigelman, I. (2012). Long-lasting alterations in membrane properties, k(+) currents, and glutamatergic synaptic currents of nucleus accumbens medium spiny neurons in a rat model of alcohol dependence. *Front. Neurosci.* 6:86. doi: 10.3389/fnins.2012.00086

Mascia, M. P., Machu, T. K., and Harris, R. A. (1996). Enhancement of homomeric glycine receptor function by long-chain alcohols and anaesthetics. *Br. J. Pharmacol.* 119, 1331–1336. doi: 10.1111/j.1476-5381.1996.tb16042.x

McClintick, J. N., McBride, W. J., Bell, R. L., Ding, Z. M., Liu, Y., Xuei, X., et al. (2015). Gene expression changes in serotonin, GABA-A receptors, neuropeptides and ion channels in the dorsal raphe nucleus of adolescent alcohol-preferring (P) rats following binge-like alcohol drinking. *Pharmacol. Biochem. Behav.* 129, 87–96. doi: 10.1016/j.pbb.2014.12.007

McClintick, J. N., McBride, W. J., Bell, R. L., Ding, Z. M., Liu, Y., Xuei, X., et al. (2016). Gene expression changes in glutamate and GABA-A receptors, neuropeptides, ion channels, and cholesterol synthesis in the periaqueductal gray following binge-like alcohol drinking by adolescent alcohol-preferring (P) rats. *Alcohol. Clin. Exp. Res.* 40, 955–968. doi: 10.1111/acer.13056

McCool, B. A., and Botting, S. K. (2000). Characterization of strychnine-sensitive glycine receptors in acutely isolated adult rat basolateral amygdala neurons. *Brain Res.* 859, 341–351. doi: 10.1016/S0006-8993(00)02026-6

McCool, B. A., and Farroni, J. S. (2001). Subunit composition of strychnine-sensitive glycine receptors expressed by adult rat basolateral amygdala neurons. *Eur. J. Neurosci.* 14, 1082–1090. doi: 10.1046/j.0953-816x.2001.01730.x

McGuier, N. S., and Griffin, W. C. 3rd., Gass, J. T., Padula, A. E., Chesler, E. J., and Mulholland, P. J. (2016) Kv7 channels in the nucleus accumbens are altered by chronic drinking and are targets for reducing alcohol consumption. *Addict Biol.* 21, 1097-1112. doi:10.1111/adb.12279.

McGovern, P. E., Zhang, J., Tang, J., Zhang, Z., Hall, G. R., Moreau, R. A., et al. (2004). Fermented beverages of pre- and proto-historic China. *Proc. Natl. Acad. Sci. U. S. A.* 101, 17593–17598. doi: 10.1073/pnas.0407921102

Mehta, A. K., and Ticku, M. K. (1994). Ethanol enhancement of GABA-induced 36Cl-influx does not involve changes in Ca2+. *Pharmacol. Biochem. Behav.* 47, 355–357. doi: 10.1016/0091-3057(94)90022-1

Metten, P., Iancu, O. D., Spence, S. E., Walter, N. A., Oberbeck, D., Harrington, C. A., et al. (2014). Dual-trait selection for ethanol consumption and withdrawal: genetic and transcriptional network effects. *Alcohol. Clin. Exp. Res.* 38, 2915–2924. doi: 10.1111/acer.12574

Mihalek, R. M., Bowers, B. J., Wehner, J. M., Kralic, J. E., VanDoren, M. J., Morrow, A. L., et al. (2001). GABA(a)-receptor delta subunit knockout mice have multiple defects in behavioral responses to ethanol. *Alcohol. Clin. Exp. Res.* 25, 1708–1718. PMID: 11781502

Miyazaki, H., Oyama, F., Inoue, R., Aosaki, T., Abe, T., Kiyonari, H., et al. (2014). Singular localization of sodium channel beta4 subunit in unmyelinated fibres and its role in the striatum. *Nat. Commun.* 5:5525. doi: 10.1038/ncomms6525

Monyer, H., Sprengel, R., Schoepfer, R., Herb, A., Higuchi, M., Lomeli, H., et al. (1992). Heteromeric NDMA receptors: molecular and functional distinction of subtypres. *Science* 256, 1217–1221. doi: 10.1126/science.256.5060.1217

Mori, M., Gähwiler, B. H., and Gerber, U. (2002). Beta-alanine and taurine as endogenous agonists at glycine receptors in rat hippocampus in vitro. *J. Physiol.* 539, 191–200. doi: 10.1113/jphysiol.2001.013147

Moorman, D. E. (2018). The role of the orbitofrontal cortex in alcohol use, abuse, and dependence. *Prog Neuropsychopharmacol Biol Psychiatry.* 87, 85–107. doi: 10.1016/j.pnpbp.2018.01.010

Mostofsky, E., Chahal, H. S., Mukamal, K. J., Rimm, E. B., and Mittleman, M. A. (2016). Alcohol and immediate risk of cardiovascular events: a systematic review and dose-response meta-analysis. *Circulation* 133, 979–987. doi: 10.1161/CIRCULATIONAHA.115.019743

Mukherjee, S. (2013). Alcoholism and its effects on the central nervous system. *Curr. Neurovasc. Res.* 10, 256–262. doi: 10.2174/15672026113109990004

Mulholland, P. J., Becker, H. C., Woodward, J. J., and Chandler, L. J. (2011). Small conductance calcium-activated potassium type 2 channels regulate alcohol-associated plasticity of glutamatergic synapses. *Biol. Psychiatry* 69, 625–632. doi: 10.1016/j.biopsych.2010.09.025

Mulholland, P. J., Spencer, K. B., Hu, W., Kroener, S., and Chandler, L. J. (2015). Neuroplasticity of A-type potassium channel complexes induced by chronic alcohol exposure enhances dendritic calcium transients in hippocampus. *Psychopharmacology (Berl)* 232, 1995–2006. doi: 10.1007/s00213-014-3835-4

Mulligan, M. K., Ponomarev, I., Hitzemann, R. J., Belknap, J. K., Tabakoff, B., Harris, R. A., et al. (2006). Toward understanding the genetics of alcohol drinking through transcriptome meta-analysis. *Proc. Natl. Acad. Sci. U. S. A.* 103, 6368–6373. doi: 10.1073/pnas.0510188103

Naimi, T. S., Brewer, R. D., Mokdad, A., Denny, C., Serdula, M. K., and Marks, J. S. (2003). Binge drinking among US adults. *JAMA* 289, 70–75. doi: 10.1001/jama.289.1.70

Nakanishi, S. (1992). Molecular diversity of glutamate receptors and implications for brain function. *Science* 258, 597–603. doi: 10.1126/science.1329206

Nelson, T. E., Ur, C. L., and Gruol, D. L. (2005). Chronic intermittent ethanol exposure enhances NMDA-receptor-mediated synaptic responses and NMDA receptor expression in hippocampal CA1 region. *Brain Res.* 1048, 69–79. doi: 10.1016/j.brainres.2005.04.041

Newman, E. L., Gunner, G., Huynh, P., Gachette, D., Moss, S. J., Smart, T. G., et al. (2016). Effects of Gabra2 point mutations on alcohol intake: increased binge-like and blunted chronic drinking by mice. *Alcohol. Clin. Exp. Res.* 40, 2445–2455. doi: 10.1111/acer.13215

NIAAA, (2004). NIH Publication No. 04–5346. Web address: http://www.niaaa.nih.gov; Email: NIAAAnewsletter@nih.gov. Editor: Gregory Roa. NIAAA Office of Research Translation and Communications 5635 Fishers Lane, MSC 9304 Bethesda, MD 20892–9304.

Nie, Z., Madamba, S., and Siggins, G. R. (1994). Ethanol inhibits glutamatergic neurotransmission in nucleus accumbens neurons by multiple mechanisms. *J. Pharmacol. Exp. Ther.* 271, 1566–1573. PMID: 7527857

Nie, Z., Madamba, S. G., and Siggins, G. R. (2000). Ethanol enhances gamma-aminobutyric acid responses in a subpopulation of nucleus accumbens neurons: role of metabotropic glutamate receptors. *J. Pharmacol. Exp. Ther.* 293, 654–661. PMID: 10773041

Nimitvilai, S., Lopez, M. F., Mulholland, P. J., and Woodward, J. J. (2016). Chronic intermittent ethanol exposure enhances the excitability and synaptic plasticity of lateral orbitofrontal cortex neurons and induces a tolerance to the acute inhibitory actions of ethanol. *Neuropsychopharmacology* 41, 1112–1127. doi: 10.1038/npp.2015.250

Nisenbaum, E. S., and Wilson, C. J. (1995). Potassium currents responsible for inward and outward rectification in rat neostriatal spiny projection neurons. *J. Neurosci.* 15, 4449–4463. doi: 10.1523/JNEUROSCI.15-06-04449.1995

O'Dell, L. E., Roberts, A. J., Smith, R. T., and Koob, G. F. (2004). Enhanced alcohol self-administration after intermittent versus continuous alcohol vapor exposure. *Alcohol. Clin. Exp. Res.* 28, 1676–1682. doi: 10.1097/01.ALC.0000145781.11923.4E

O'Donnell, P., and Grace, A. A. (1995). Synaptic interactions among excitatory afferents to nucleus accumbens neurons: hippocampal gating of prefrontal cortical input. *J. Neurosci.* 15, 3622–3639. doi: 10.1523/JNEUROSCI.15-05-03622.1995

Oyama, F., Miyazaki, H., Sakamoto, N., Becquet, C., Machida, Y., Kaneko, K., et al. (2006). Sodium channel beta4 subunit: down-regulation and possible involvement in neuritic degeneration in Huntington's disease transgenic mice. *J. Neurochem.* 98, 518–529. doi: 10.1111/j.1471-4159.2006.03893.x

Padgett, C. L., and Slesinger, P. A. (2010). GABAB receptor coupling to G-proteins and ion channels. *Adv. Pharmacol.* 58, 123–147. doi: 10.1016/S1054-3589(10)58006-2

Partridge, J. G., Tang, K. C., and Lovinger, D. M. (2000). Regional and postnatal heterogeneity of activity-dependent long-term changes in synaptic efficacy in the dorsal striatum. *J. Neurophysiol.* 84, 1422–1429. doi: 10.1152/jn.2000.84.3.1422

Pati, D., Kelly, K., Stennett, B., Frazier, C. J., and Knackstedt, L. A. (2016). Alcohol consumption increases basal extracellular glutamate in the nucleus accumbens core of Sprague-Dawley rats without increasing spontaneous glutamate release. *Eur. J. Neurosci.* 44, 1896–1905. doi: 10.1111/ejn.13284

Pereira, P. A., Neves, J., Vilela, M., Sousa, S., Cruz, C., and Madeira, M. D. (2014). Chronic alcohol consumption leads to neurochemical changes in the nucleus accumbens that are not fully reversed by withdrawal. *Neurotoxicol. Teratol.* 44, 53–61. doi: 10.1016/j.ntt.2014.05.007

Petrie, J., Sapp, D. W., Tyndale, R. F., Park, M. K., Fanselow, M., and Olsen, R. W. (2001). Altered Gabaa receptor subunit and splice variant expression in rats treated with chronic intermittent ethanol. *Alcohol. Clin. Exp. Res.* 25, 819–828. doi: 10.1111/j.1530-0277.2001.tb02285.x

Pleil, K. E., Lowery-Gionta, E. G., Crowley, N. A., Li, C., Marcinkiewcz, C. A., Rose, J. H., et al. (2015). Effects of chronic ethanol exposure on neuronal function in the prefrontal cortex and extended amygdala. *Neuropharmacology* 99, 735–749. doi: 10.1016/j.neuropharm.2015.06.017

Ponomarev, I., Stelly, C. E., Morikawa, H., Blednov, Y. A., Mayfield, R. D., and Harris, R. A. (2017). Mechanistic insights into epigenetic modulation of ethanol consumption. *Alcohol* 60, 95–101. doi: 10.1016/j.alcohol.2017.01.016

Proctor, W. R., Diao, L., Freund, R. K., Browning, M. D., and Wu, P. H. (2006). Synaptic GABAergic and glutamatergic mechanisms underlying alcohol sensitivity in mouse hippocampal neurons. *J. Physiol.* 575, 145–159. doi: 10.1113/jphysiol.2006.112730

Qiang, M., Denny, A. D., and Ticku, M. K. (2007). Chronic intermittent ethanol treatment selectively alters N-methyl-D-aspartate receptor subunit surface expression in cultured cortical neurons. *Mol. Pharmacol.* 72, 95–102. doi: 10.1124/mol.106.033043

Qiang, M., Li, J. G., Denny, A. D., Yao, J. M., Lieu, M., Zhang, K., et al. (2014). Epigenetic mechanisms are involved in the regulation of ethanol consumption in mice. *Int. J. Neuropsychopharmacol.* 18, 1–11. doi: 10.1093/ijnp/pyu072

Rajendra, S., Lynch, J. W., and Schofield, P. R. (1997). The glycine receptor. *Pharmacol. Ther.* 73, 121–146. doi: 10.1016/S0163-7258(96)00163-5

RALL, W. (1959). Branching dendritic trees and motoneuron membrane resistivity. *Exp. Neurol.* 1, 491–527. doi: 10.1016/0014-4886(59)90046-9

Ravel, S., Legallet, E., and Apicella, P. (1999). Tonically active neurons in the monkey striatum do not preferentially respond to appetitive stimuli. *Exp. Brain Res.* 128, 531–534. doi: 10.1007/s002210050876

Rehm, J., Mathers, C., Popova, S., Thavorncharoensap, M., Teerawattananon, Y., and Patra, J. (2009). Global burden of disease and injury and economic cost attributable to alcohol use and alcohol-use disorders. *Lancet* 373, 2223–2233. doi: 10.1016/S0140-6736(09)60746-7

Renteria, R., Buske, T. R., and Morrisett, R. A. (2018). Long-term subregion-specific encoding of enhanced ethanol intake by D1DR medium spiny neurons of the nucleus accumbens. *Addict. Biol.* 23, 689–698. doi: 10.1111/adb.12526

Rhodes, J. S., Best, K., Belknap, J. K., Finn, D. A., and Crabbe, J. C. (2005). Evaluation of a simple model of ethanol drinking to intoxication in C57BL/6J mice. *Physiol. Behav.* 84, 53–63. doi: 10.1016/j.physbeh.2004.10.007

Rinker, J. A., Fulmer, D. B., Trantham-Davidson, H., Smith, M. L., Williams, R. W., Lopez, M. F., et al. (2017). Differential potassium channel gene regulation in BXD mice reveals novel targets for pharmacogenetic therapies to reduce heavy alcohol drinking. *Alcohol* 58, 33–45. doi: 10.1016/j.alcohol.2016.05.007

Risher, M. L., Fleming, R. L., Risher, W. C., Miller, K. M., Klein, R. C., Wills, T., et al. (2015). Adolescent intermittent alcohol exposure: persistence of structural and functional hippocampal abnormalities into adulthood. *Alcohol. Clin. Exp. Res.* 39, 989–997. doi: 10.1111/acer.12725

Robbe, D., Kopf, M., Remaury, A., Bockaert, J., and Manzoni, O. J. (2002). Endogenous cannabinoids mediate long-term synaptic depression in the nucleus accumbens. *Proc. Natl. Acad. Sci. U. S. A.* 99, 8384–8388. doi: 10.1073/pnas.122149199

Roberto, M., Nelson, T. E., Ur, C. L., Brunelli, M., Sanna, P. P., and Gruol, D. L. (2003). The transient depression of hippocampal CA1 LTP induced by chronic intermittent ethanol exposure is associated with an inhibition of the MAP kinase pathway. *Eur. J. Neurosci.* 17, 1646–1654. doi: 10.1046/j.1460-9568.2003.02614.x

Roberto, M., Nelson, T. E., Ur, C. L., and Gruol, D. L. (2002). Long-term potentiation in the rat hippocampus is reversibly depressed by chronic intermittent ethanol exposure. *J. Neurophysiol.* 87, 2385–2397. doi: 10.1152/jn.2002.87.5.2385

Roberto, M., Schweitzer, P., Madamba, S. G., Stouffer, D. G., Parsons, L. H., and Siggins, G. R. (2004). Acute and chronic ethanol alter glutamatergic transmission in rat central amygdala: an in vitro and in vivo analysis. *J. Neurosci.* 24, 1594–1603. doi: 10.1523/JNEUROSCI.5077-03.2004

Ryabinin, A. E., Galvan-Rosas, A., Bachtell, R. K., and Risinger, F. O. (2003). High alcohol/sucrose consumption during dark circadian phase in C57BL/6J mice: involvement of hippocampus, lateral septum and urocortin-positive cells of the Edinger-Westphal nucleus. *Psychopharmacology (Berl)* 165, 296–305. doi: 10.1007/s00213-002-1284-y

Sakharkar, A. J., Vetreno, R. P., Zhang, H., Kokare, D. M., Crews, F. T., and Pandey, S. C. (2016). A role for histone acetylation mechanisms in adolescent alcohol exposure-induced deficits in hippocampal brain-derived neurotrophic factor expression and neurogenesis markers in adulthood. *Brain Struct. Funct.* 221, 4691–4703. doi: 10.1007/s00429-016-1196-y

Sakimura, K., Kutsuwada, T., Ito, I., Manabe, T., Takayama, C., Kushiya, E., et al. (1995). Reduced hippocampal LTP and spatial learning in mice lacking NMDA receptor epsilon 1 subunit. *Nature* 373, 151–155. doi: 10.1038/373151a0

Sakurai, K., Zhao, S., Takatoh, J., Rodriguez, E., Lu, J., Leavitt, A. D., et al. (2016). Capturing and manipulating activated neuronal ensembles with CANE delineates a hypothalamic social-fear circuit. *Neuron* 92, 739–753. doi: 10.1016/j.neuron.2016.10.015

Salgado, S., and Kaplitt, M. G. (2015). The nucleus Accumbens: a comprehensive review. *Stereotact. Funct. Neurosurg.* 93, 75–93. doi: 10.1159/000368279

SAMHSA, (2014). Results from the 2013 National Survey on Drug Use and Health: Summary of National Findings, NSDUH Series H-48, HHS Publication No. (SMA) 14-4863. Rockville, MD: Substance Abuse and Mental Health Services Administration

Scaife, J. C., and Duka, T. (2009). Behavioural measures of frontal lobe function in a population of young social drinkers with binge drinking pattern. *Pharmacol Biochem Behav.* 93, 354–362. doi: 10.1016/j.pbb.2009.05.015

Shaidullov, I., Ermakova, E., Gaifullina, A., Mosshammer, A., Yakovlev, A., Weiger, T. M., et al. (2021). Alcohol metabolite acetic acid activates BK channels in a pH-dependent manner and decreases calcium oscillations and exocytosis of secretory granules in rat pituitary GH3 cells. *Pflugers Arch.* 473, 67–77. doi: 10.1007/s00424-020-02484-0

Substance Abuse and Mental Health Services Administration (2019). "Key substance use and mental health indicators in the United States: Results from the 2019 National Survey on Drug Use and Health (HHS Publication No. PEP20-07-01-001, NSDUH Series H-55)" in *Rockville, MD: Center for Behavioral Health Statistics and Quality, Substance Abuse and Mental Health Services Administration*

Sanchis-Segura, C., Borchardt, T., Vengeliene, V., Zghoul, T., Bachteler, D., Gass, P., et al. (2006). Involvement of the AMPA receptor GluR-C subunit in alcohol-seeking behavior and relapse. *J. Neurosci.* 26, 1231–1238. doi: 10.1523/JNEUROSCI.4237-05.2006

Schmidt, L. S., Thomsen, M., Weikop, P., Dencker, D., Wess, J., Woldbye, D. P., et al. (2011). Increased cocaine self-administration in M4 muscarinic acetylcholine receptor knockout mice. *Psychopharmacology (Berl)* 216, 367–378. doi: 10.1007/s00213-011-2225-4

Schramm, N. L., Egli, R. E., and Winder, D. G. (2002). LTP in the mouse nucleus accumbens is developmentally regulated. *Synapse* 45, 213–219. doi: 10.1002/syn.10104

Schuckit, M. A. (1994). Low level of response to alcohol as a predictor of future alcoholism. *Am. J. Psychiatry* 151, 184–189. doi: 10.1176/ajp.151.2.184

Schuckit, M. A., Smith, T. L., Hesselbrock, V., Bucholz, K. K., Bierut, L., Edenberg, H., et al. (2008). Clinical implications of tolerance to alcohol in nondependent young drinkers. *Am. J. Drug Alcohol Abuse* 34, 133–149. doi: 10.1080/00952990701877003

Sharpe, A. L., Tsivkovskaia, N. O., and Ryabinin, A. E. (2005). Ataxia and c-Fos expression in mice drinking ethanol in a limited access session. *Alcohol. Clin. Exp. Res.* 29, 1419–1426. doi: 10.1097/01.alc.0000174746.64499.83

Sheela Rani, C. S., and Ticku, M. K. (2006). Comparison of chronic ethanol and chronic intermittent ethanol treatments on the expression of GABA(a) and NMDA receptor subunits. *Alcohol* 38, 89–97. doi: 10.1016/j.alcohol.2006.05.002

Shen, W., Flajolet, M., Greengard, P., and Surmeier, D. J. (2008). Dichotomous dopaminergic control of striatal synaptic plasticity. *Science* 321, 848–851. doi: 10.1126/science.1160575

Shen, W., Hamilton, S. E., Nathanson, N. M., and Surmeier, D. J. (2005). Cholinergic suppression of KCNQ channel currents enhances excitability of striatal medium spiny neurons. *J. Neurosci.* 25, 7449–7458. doi: 10.1523/JNEUROSCI.1381-05.2005

Sigel, E., and Steinmann, M. E. (2012). Structure, function, and modulation of GABA(a) receptors. *J. Biol. Chem.* 287, 40224–40231. doi: 10.1074/jbc.R112.386664

Silberberg, G., and Bolam, J. P. (2015). Local and afferent synaptic pathways in the striatal microcircuitry. *Curr. Opin. Neurobiol.* 33, 182–187. doi: 10.1016/j.conb.2015.05.002

Silvestre de Ferron, B., Bennouar, K. E., Kervern, M., Alaux-Cantin, S., Robert, A., Rabiant, K., et al. (2015). Two binges of ethanol a day keeps the memory away in adolescent rats: key role for Glun2B subunit. *Int. J. Neuropsychopharmacol.* 19:pyv087. doi: 10.1093/ijnp/pyv087

Simon-O'Brien, E., Alaux-Cantin, S., Warnault, V., Buttolo, R., Naassila, M., and Vilpoux, C. (2015). The histone deacetylase inhibitor sodium butyrate decreases excessive ethanol intake in dependent animals. *Addict. Biol.* 20, 676–689. doi: 10.1111/adb.12161

Sjostrom, P. J., Rancz, E. A., Roth, A., and Hausser, M. (2008). Dendritic excitability and synaptic plasticity. *Physiol. Rev.* 88, 769–840. doi: 10.1152/physrev.00016.2007

Skrzynski, C. J., and Creswell, K. G. (2020). Associations between solitary drinking and increased alcohol consumption, alcohol problems, and drinking to cope motives in adolescents and young adults: a systematic review and meta-analysis. *Addiction* 115, 1989–2007. doi: 10.1111/add.15055

Soares-Cunha, C., Coimbra, B., David-Pereira, A., Borges, S., Pinto, L., Costa, P., et al. (2016). Activation of D2 dopamine receptor-expressing neurons in the nucleus accumbens increases motivation. *Nat. Commun.* 7:11829. doi: 10.1038/ncomms11829

Soares-Cunha, C., de Vasconcelos, N. A. P., Coimbra, B., Domingues, A. V., Silva, J. M., Loureiro-Campos, E., et al. (2020). Nucleus accumbens medium spiny neurons subtypes signal both reward and aversion. *Mol. Psychiatry* 25, 3241–3255. doi: 10.1038/s41380-019-0484-3

Stephens, D. N., Ripley, T. L., Borlikova, G., Schubert, M., Albrecht, D., Hogarth, L., et al. (2005). Repeated ethanol exposure and withdrawal impairs human fear conditioning and depresses long-term potentiation in rat amygdala and hippocampus. *Biol. Psychiatry* 58, 392–400. doi: 10.1016/j.biopsych.2005.04.025

Sun, X., Yao, H., Zhou, D., Gu, X., and Haddad, G. G. (2008). Modulation of hSlo BK current inactivation by fatty acid esters of CoA. *J. Neurochem.* 104, 1394–1403. doi: 10.1111/j.1471-4159.2007.05083.x

Swartzwelder, H. S., Park, M. H., and Acheson, S. (2017). Adolescent ethanol exposure enhances NMDA receptor-mediated currents in hippocampal neurons: reversal by gabapentin. *Sci. Rep.* 7:13133. doi: 10.1038/s41598-017-12956-6

Tabakoff, B., Saba, L., Kechris, K., Hu, W., Bhave, S. V., Finn, D. A., et al. (2008). The genomic determinants of alcohol preference in mice. *Mamm. Genome* 19, 352–365. doi: 10.1007/s00335-008-9115-z

Tao, L., and Ye, J. H. (2002). Protein kinase C modulation of ethanol inhibition of glycine-activated current in dissociated neurons of rat ventral tegmental area. *J. Pharmacol. Exp. Ther.* 300, 967–975. doi: 10.1124/jpet.300.3.967

Thiele, T. E., and Navarro, M. (2014). Drinking in the dark (DID) procedures: a model of binge-like ethanol drinking in non-dependent mice. *Alcohol* 48, 235–241. doi: 10.1016/j.alcohol.2013.08.005

Thomas, G. M., and Huganir, R. L. (2004). MAPK cascade signalling and synaptic plasticity. *Nat. Rev. Neurosci.* 5, 173–183. doi: 10.1038/nrn1346

Threlfell, S., Clements, M. A., Khodai, T., Pienaar, I. S., Exley, R., Wess, J., et al. (2010). Striatal muscarinic receptors promote activity dependence of dopamine transmission via distinct receptor subtypes on cholinergic interneurons in ventral versus dorsal striatum. *J. Neurosci.* 30, 3398–3408. doi: 10.1523/JNEUROSCI.5620-09.2010

Torres, Y. P., Morera, F. J., Carvacho, I., and Latorre, R. (2007). A marriage of convenience: beta-subunits and voltage-dependent K+ channels. *J. Biol. Chem.* 282, 24485–24489. doi: 10.1074/jbc.R700022200

Townshend, J. M., and Duka, T. (2002). Patterns of alcohol drinking in a population of young social drinkers: a comparison of questionnaire and diary measures. *Alcohol Alcohol.* 37, 187–192. doi: 10.1093/alcalc/37.2.187

Tritsch, N. X., and Sabatini, B. L. (2012). Dopaminergic modulation of synaptic transmission in cortex and striatum. *Neuron* 76, 33–50. doi: 10.1016/j.neuron.2012.09.023

Truchet, B., Manrique, C., Sreng, L., Chaillan, F. A., Roman, F. S., and Mourre, C. (2012). Kv4 potassium channels modulate hippocampal EPSP-spike potentiation and spatial memory in rats. *Learn. Mem.* 19, 282–293. doi: 10.1101/lm.025411.111

Trudell, J. R., Messing, R. O., Mayfield, J., and Harris, R. A. (2014). Alcohol dependence: molecular and behavioral evidence. *Trends Pharmacol. Sci.* 35, 317–323. doi: 10.1016/j.tips.2014.04.009

Tuesta, L. M., Fowler, C. D., and Kenny, P. J. (2011). Recent advances in understanding nicotinic receptor signaling mechanisms that regulate drug self-administration behavior. *Biochem. Pharmacol.* 82, 984–995. doi: 10.1016/j.bcp.2011.06.026

Turrigiano, G., Abbott, L. F., and Marder, E. (1994). Activity-dependent changes in the intrinsic properties of cultured neurons. *Science* 264, 974–977. doi: 10.1126/science.8178157

Tomsovic, M. (1974). "Binge" and continuous drinkers. Characteristics and treatment follow-up. *Q J Stud Alcohol.* 35, 558–564.

van den Pol, A. N. (2012). Neuropeptide transmission in brain circuits. *Neuron* 76, 98–115. doi: 10.1016/j.neuron.2012.09.014

Vetreno, R. P., Broadwater, M., Liu, W., Spear, L. P., and Crews, F. T. (2014). Adolescent, but not adult, binge ethanol exposure leads to persistent global reductions of choline acetyltransferase expressing neurons in brain. *PLoS One* 9:e113421. doi: 10.1371/journal.pone.0113421

Wang, K., Lin, M. T., Adelman, J. P., and Maylie, J. (2014). Distinct Ca2+ sources in dendritic spines of hippocampal CA1 neurons couple to SK and Kv4 channels. *Neuron* 81, 379–387. doi: 10.1016/j.neuron.2013.11.004

Warner-Schmidt, J. L., Schmidt, E. F., Marshall, J. J., Rubin, A. J., Arango-Lievano, M., Kaplitt, M. G., et al. (2012). Cholinergic interneurons in the nucleus accumbens regulate depression-like behavior. *Proc. Natl. Acad. Sci. U. S. A.* 109, 11360–11365. doi: 10.1073/pnas.1209293109

Watkins, J. C., and Evans, R. H. (1981). Excitatory amino acid transmitters. *Annu. Rev. Pharmacol. Toxicol.* 21, 165–204. doi: 10.1146/annurev.pa.21.040181.001121

Wechsler, H., Davenport, A., Dowdall, G., Moeykens, B., and Castillo, S. (1994). Health and behavioral consequences of binge drinking in college. A national survey of students at 140 campuses. *JAMA* 272, 1672–1677. doi: 10.1001/jama.1994.03520210056032

Weissenborn, R., and Duka, T. (2003). Acute alcohol effects on cognitive function in social drinkers: their relationship to drinking habits. *Psychopharmacology (Berl)* 165, 306–312. doi: 10.1007/s00213-002-1281-1

Weitlauf, C., and Woodward, J. J. (2008). Ethanol selectively attenuates NMDAR-mediated synaptic transmission in the prefrontal cortex. *Alcohol. Clin. Exp. Res.* 32, 690–698. doi: 10.1111/j.1530-0277.2008.00625.x

Wilcox, M. V., Cuzon Carlson, V. C., Sherazee, N., Sprow, G. M., Bock, R., Thiele, T. E., et al. (2014). Repeated binge-like ethanol drinking alters ethanol drinking patterns and depresses striatal GABAergic transmission. *Neuropsychopharmacology* 39, 579–594. doi: 10.1038/npp.2013.230

Williams, M. J., and Adinoff, B. (2008). The role of acetylcholine in cocaine addiction. *Neuropsychopharmacology* 33, 1779–1797. doi: 10.1038/sj.npp.1301585

Winder, D. G., Egli, R. E., Schramm, N. L., and Matthews, R. T. (2002). Synaptic plasticity in drug reward circuitry. *Curr. Mol. Med.* 2, 667–676. doi: 10.2174/1566524023361961

Witten, I. B., Lin, S. C., Brodsky, M., Prakash, R., Diester, I., Anikeeva, P., et al. (2010). Cholinergic interneurons control local circuit activity and cocaine conditioning. *Science* 330, 1677–1681. doi: 10.1126/science.1193771

Wolstenholme, J. T., Mahmood, T., Harris, G. M., Abbas, S., and Miles, M. F. (2017). Intermittent ethanol during adolescence leads to lasting behavioral changes in adulthood and alters gene expression and histone methylation in the PFC. *Front. Mol. Neurosci.* 10:307. doi: 10.3389/fnmol.2017.00307

Wu, J. V., and Kendig, J. J. (1998). Differential sensitivities of TTX-resistant and TTX-sensitive sodium channels to anesthetic concentrations of ethanol in rat sensory neurons. *J. Neurosci. Res.* 54, 433–443. doi: 10.1002/(SICI)1097-4547(19981115)54:4<433::AID-JNR1>3.0.CO;2-A

Wu, Y., Zhang, D., Liu, J., Yang, Y., Ou, M., Liu, B., et al. (2021). Sodium Leak Channel in the nucleus Accumbens modulates ethanol-induced acute stimulant responses and locomotor sensitization in mice: a brief research report. *Front. Neurosci.* 15:687470. doi: 10.3389/fnins.2021.687470

Ye, J. H., Tao, L., Ren, J., Schaefer, R., Krnjevic, K., Liu, P. L., et al. (2001). Ethanol potentiation of glycine-induced responses in dissociated neurons of rat ventral tegmental area. *J. Pharmacol. Exp. Ther.* 296, 77–83. PMID: 11123365

Yoon, K. W., Wotring, V. E., and Fuse, T. (1998). Multiple picrotoxinin effect on glycine channels in rat hippocampal neurons. *Neuroscience* 87, 807–815. doi: 10.1016/S0306-4522(98)00158-4

You, C., Savarese, A., Vandegrift, B. J., He, D., Pandey, S. C., Lasek, A. W., et al. (2019). Ethanol acts on KCNK13 potassium channels in the ventral tegmental area to increase firing rate and modulate binge-like drinking. *Neuropharmacology* 144, 29–36. doi: 10.1016/j.neuropharm.2018.10.008

Yuan, C., O'Connell, R. J., Feinberg-Zadek, P. L., Johnston, L. J., and Treistman, S. N. (2004). Bilayer thickness modulates the conductance of the BK channel in model membranes. *Biophys. J.* 86, 3620–3633. doi: 10.1529/biophysj.103.029678

Zhang, W. H., Cao, K. X., Ding, Z. B., Yang, J. L., Pan, B. X., and Xue, Y. X. (2019). Role of prefrontal cortex in the extinction of drug memories. *Psychopharmacology (Berl)* 236, 463–477. doi: 10.1007/s00213-018-5069-3

Zhou, Y., and Danbolt, N. C. (2014). Glutamate as a neurotransmitter in the healthy brain. *J. Neural Transm.* 121, 799–817. doi: 10.1007/s00702-014-1180-8

Zhu, P. J., and Lovinger, D. M. (2006). Ethanol potentiates GABAergic synaptic transmission in a postsynaptic neuron/synaptic Bouton preparation from basolateral amygdala. *J. Neurophysiol.* 96, 433–441. doi: 10.1152/jn.01380.2005

Zorumski, C. F., Mennerick, S., and Izumi, Y. (2014). Acute and chronic effects of ethanol on learning-related synaptic plasticity. *Alcohol* 48, 1–17. doi: 10.1016/j.alcohol.2013.09.045

frontiers | Frontiers in Molecular Neuroscience

TYPE Original Research
PUBLISHED 06 March 2023
DOI 10.3389/fnmol.2023.1129553

OPEN ACCESS

EDITED BY
Elisabeth Piccart,
Hasselt University,
Belgium

REVIEWED BY
Lorenz S. Neuwirth,
State University of New York at Old Westbury,
United States
David F. Werner,
Binghamton University,
United States

*CORRESPONDENCE
Shuguang Wei
✉ weisg@mail.xjtu.edu.cn
Jianghua Lai
✉ laijh1011@mail.xjtu.edu.cn

SPECIALTY SECTION
This article was submitted to Neuroplasticity and Development, a section of the journal Frontiers in Molecular Neuroscience

RECEIVED 22 December 2022
ACCEPTED 13 February 2023
PUBLISHED 06 March 2023

CITATION
Yan P, Liu J, Ma H, Feng Y, Cui J, Bai Y, Huang X, Zhu Y, Wei S and Lai J (2023) Effects of glycogen synthase kinase-3β activity inhibition on cognitive, behavioral, and hippocampal ultrastructural deficits in adulthood associated with adolescent methamphetamine exposure. *Front. Mol. Neurosci.* 16:1129553. doi: 10.3389/fnmol.2023.1129553

Effects of glycogen synthase kinase-3β activity inhibition on cognitive, behavioral, and hippocampal ultrastructural deficits in adulthood associated with adolescent methamphetamine exposure

Peng Yan[1], Jincen Liu[1], Haotian Ma[1], Yue Feng[1], Jingjing Cui[2], Yuying Bai[1], Xin Huang[1], Yongsheng Zhu[1], Shuguang Wei[1]*and Jianghua Lai[1]*

[1]NHC Key Laboratory of Forensic Science, School of Forensic Sciences, Xi'an Jiaotong University, Xi'an, China, [2]Forensic Identification Institute, The Fourth People's Hospital of Yancheng, Yancheng, China

Objective: Glycogen synthase kinase-3β (GSK3β) has been implicated in the maintenance of synaptic plasticity, memory process, and psychostimulant-induced behavioral effects. Hyperactive GSK3β in the Cornu Ammonis 1 (CA1) subregion of the dorsal hippocampus (DHP) was associated with adolescent methamphetamine (METH) exposure-induced behavioral and cognitive deficits in adulthood. This study aimed to evaluate the possible therapeutic effects of GSK3β inhibition in adulthood on adolescent METH exposure-induced long-term neurobiological deficits.

Methods: Adolescent male mice were treated with METH from postnatal day (PND) 45–51. In adulthood, three intervention protocols (acute lithium chloride systemic administration, chronic lithium chloride systemic administration, and chronic SB216763 administration within CA1) were used for GSK3β activity inhibition. The effect of GSK3β intervention on cognition, behavior, and GSK3β activity and synaptic ultrastructure in the DHP CA1 subregion were detected in adulthood.

Results: In adulthood, all three interventions reduced adolescent METH exposure-induced hyperactivity (PND97), while only chronic systemic and chronic within CA1 administration ameliorated the induced impairments in spatial (PND99), social (PND101) and object (PND103) recognition memory. In addition, although three interventions reversed the aberrant GSK3β activity in the DHP CA1 subregion (PND104), only chronic systemic and chronic within CA1 administration rescued adolescent METH exposure-induced synaptic ultrastructure changes in the DHP CA1 subregion (PND104) in adulthood.

Conclusion: Rescuing synaptic ultrastructural abnormalities in the dHIP CA1 subregion by chronic administration of a GSK3β inhibitor may be a suitable therapeutic strategy for the treatment of behavioral and cognitive deficits in adulthood associated with adolescent METH abuse.

KEYWORDS

methamphetamine, adolescence, glycogen synthase kinase-3β (GSK3β), CA1 – Cornu ammonis region 1, recognition memory, hyperactivity

Introduction

Methamphetamine (METH) is a highly addictive psychoactive substance, and its abuse has become an important global public health concern (UNODC, 2019). Adolescence is a special period of susceptibility to drug abuse, and METH use is often initiated during this period (Ye et al., 2014). Although a large number of METH users are adults, the number of adolescent METH users has increased rapidly over the past decade (Nazari et al., 2020; Basedow et al., 2021). Adolescence is also a substantial period of brain development, making this an especially vulnerable period for neurotoxic damage (Luikinga et al., 2018). METH exposure in adolescence can cause long-lasting effects on the developing brain, resulting in a series of abnormalities in behavior, cognition, and brain structures in adulthood, even after prolonged periods of drug abstinence (Spear, 2016). Thus, studying how to improve adolescent METH exposure-induced long-term neurobiological deficits in adulthood is necessary.

One key reason why adolescent METH exposure induces long-lasting impairments is that METH may disorganize the normal pattern of growth and maturation of the brain (Westbrook et al., 2020). The hippocampus is one of the important regions of the limbic system, undergoing significant restructuring and maturation in adolescence (Fuhrmann et al., 2015; Lee and Kim, 2019). The hippocampus not only plays a crucial role in learning, memory, and locomotion but is also a target for psychostimulants (Tanimizu et al., 2017; Shukla and Vincent, 2021). Adolescent METH exposure induces profound impairments in reference memory and spatial memory, decreases hippocampal plasticity, and leads to hippocampal cell damage in adulthood (Vorhees et al., 2005; North et al., 2013; García-Cabrerizo et al., 2018). In addition, a previous study showed that adult mice with a history of METH administration in adolescence exhibited significant alterations in locomotor activity, novel spatial exploration, and social recognition memory, as well as abnormalities in excitatory synapse density and postsynaptic density (PSD) thickness in the Cornu Ammonis 1 (CA1) subregion of the dorsal hippocampus (DHP; Yan et al., 2019). These results highlight that the hippocampus is sensitive to adolescent METH exposure-induced long-term nerve damage in adulthood, indicating that recovery of hippocampal function may be a treatment strategy for behavioral and cognitive deficits in adulthood associated with adolescent METH abuse.

Glycogen synthase kinase-3β (GSK3β) is a multifunctional Ser/Thr kinase that is highly expressed in the hippocampus, prefrontal cortex, and other brain regions (Demuro et al., 2021). As a regulator of several cellular processes, GSK3β has a central position in the control of emotion, locomotion, and memory (Chen et al., 2021; Jung et al., 2021). An increasing number of studies have indicated an important role of GSK3β in the effects of psychostimulants (Barr and Unterwald, 2020). METH exposure prominently modulates GSK3β activity, whereas inhibition of GSK3β activity can ameliorate METH exposure-induced hyperactivity, locomotor sensitization, and neurotoxicity (Xu et al., 2011; Wu et al., 2015; Xing et al., 2015). Moreover, adolescent METH exposure significantly enhanced GSK3β activity in both the medial prefrontal cortex (mPFC) and DHP by regulating the phosphorylation pattern of GSK3β, but after prolonged METH abstinence, in adulthood, the increased GSK3β activity remained only in the DHP instead of the mPFC (Yan et al., 2019). Thus, METH exposure during adolescence induced long-term dysregulation of GSK3β activity in DHP, which may be a key factor in that induced deficit in cognition and behavior in adulthood. Dysfunction of GSK3β is involved in the pathogenesis of several psychoneuroses; therefore, GSK3β has been considered a therapeutic target for Alzheimer's disease and bipolar disorder (Bhat et al., 2018; Ochoa, 2022). However, it is unclear whether recovering GSK3β activity in the DHP in adulthood is beneficial to adolescent METH exposure-induced long-term deficits.

The activity of GSK3β depends on site-specific phosphorylation, phosphorylation of Tyr216 (Y216) on GSK3β activates GSK3β, while phosphorylation of Ser9 (S9) on GSK3β inhibits its activity. The role of Ser9 phosphorylation may be much bigger than the role of Tyr216 phosphorylation in GSK3β activity regulation (Takahashi-Yanaga et al., 2004), and Ser9 phosphorylation is the most frequently suggested mechanism regulating GSK3β activity (Beurel et al., 2015). Lithium (Li) is the first GSK3β inhibitor to be identified and widely used in prescription medicine for bipolar disorder treatment (King et al., 2014), and SB216763 has been widely used in GSK3β-related studies and has been found to improve memory impairment, stimulants-induced hyperactivity, behavioral sensitization, and synaptic transmission dysfunction (Xu et al., 2011; Zhao et al., 2016; Lin et al., 2018). Both agents can inhibit GSK3β activity by increasing Ser9 phosphorylation (Xu et al., 2011; Demuro et al., 2021). In the present study, we performed three GSK3β intervention protocols by using Li chloride (LiCl) and SB216763, and aimed to investigate the possible therapeutic effects of GSK3β activity inhibition in adulthood on adolescent METH exposure-induced long-term alterations in behavior, cognition, and hippocampal synaptic plasticity.

Materials and methods

Study design

To assess the therapeutic effects of GSK3β inhibition on cognition, behavior, and hippocampal ultrastructural deficits in adulthood associated with adolescent METH exposure, three intervention protocols were used, as schematically shown in Figure 1. In each protocol, mice received the same daily (o.d.) i.p. injection of METH (1 mg/kg) or saline (similar volume to METH) in late adolescence for 7 days from PND 45 to 51 and participated in the same behavioral tests (Brust et al., 2015; Spear, 2015). In our previous study, we found adult mice with a history of METH administration in adolescence exhibited impairments in locomotor activity, novel spatial exploration behavior and social recognition memory, instead of working memory and anxiety-and depressive-like behaviors (Yan et al., 2019). According to this, in the present study, the behavioral tests were selected and performed in the following sequence: an open field test (OFT) for detecting locomotor activity (PND 97), a modified two-trial Y-maze test for detecting novel spatial exploration behavior (PND 99), a three-chamber social behavior test for detecting sociability and social recognition memory (PND 101), and a novel object recognition (NOR) test for further detection of recognition memory (PND 103). Moreover, a standard two-trial Y-maze test was performed in a separate cohort to explain the results of the modified two-trial Y-maze test and to detect spatial recognition memory (PND 99). An overview of the timing of the behavioral tests is provided in Figure 1.

In the acute systemic intervention protocol (Li–acute) (Figure 1A), the mice were randomly divided into the following groups:

10.3389/fnmol.2023.1129553

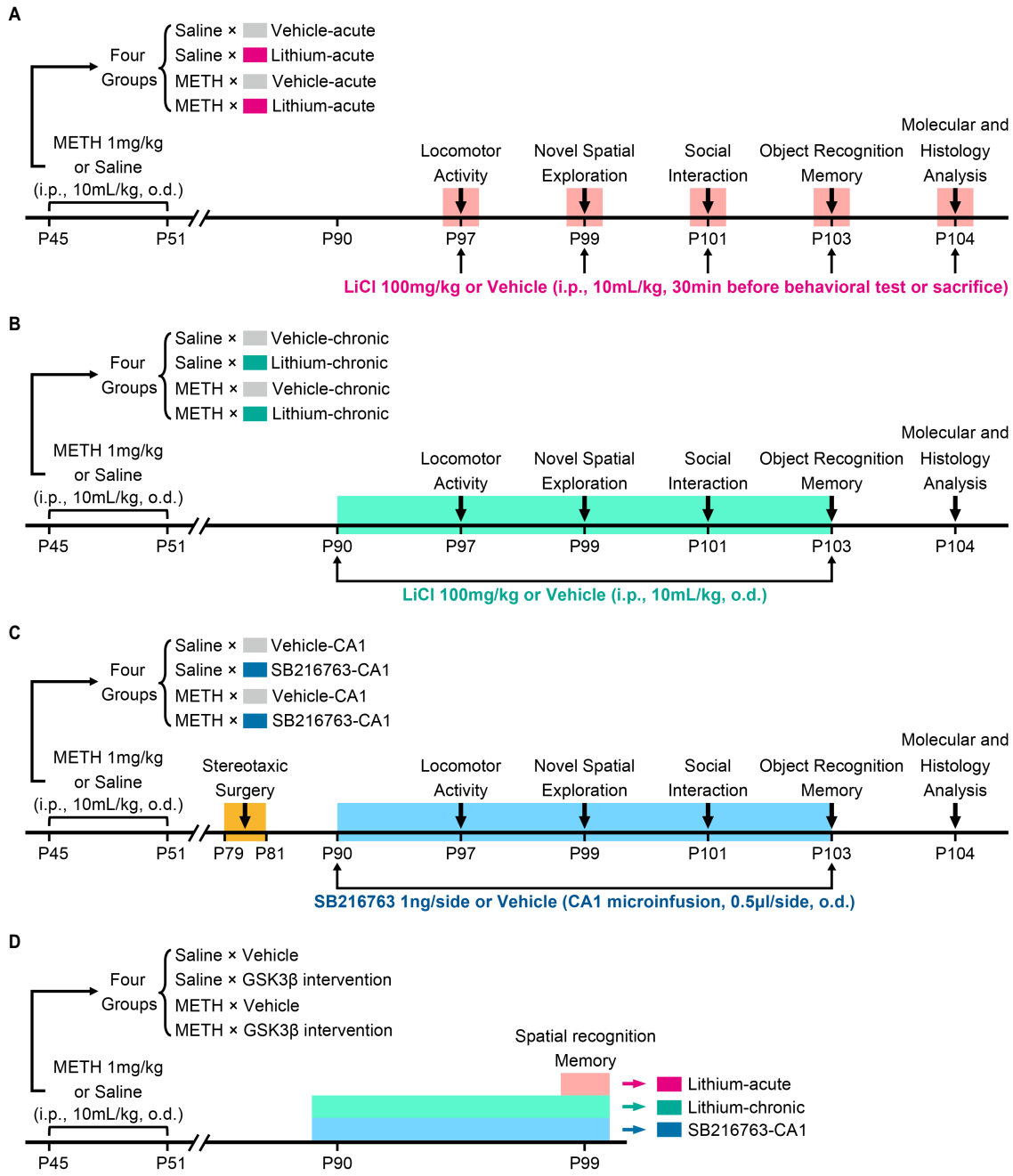

FIGURE 1
Schematic diagram of GSK3β intervention protocols and experimental time courses. Acute systemic intervention **(A)**, chronic systemic intervention **(B)**, and chronic intervention within CA1 **(C)** were performed to detect the therapeutic effects of GSK3β inhibition on adolescent METH exposure-induced cognitive, behavioral, and hippocampal ultrastructural deficits in adulthood. To further explain the results of novel spatial exploration, spatial recognition memory was detected in a separate cohort of mice **(D)**.

saline × vehicle–acute, saline × Li–acute, METH × vehicle–acute, and METH × Li–acute. In each group, LiCl (100 mg/kg, i.p.) or saline (similar volume to LiCl, i.p.) was injected 30 min before the behavioral tests and sacrifice.

In the chronic systemic intervention protocol (Li–chronic) (Figure 1B), mice were randomly divided into the following groups: saline × vehicle–chronic, saline × Li–chronic, METH × vehicle–chronic, and METH × Li–chronic. LiCl (100 mg/kg, i.p., o.d.) or saline (similar volume to LiCl, i.p., o.d.) injection was carried out at 18:00 on each day from PND 90 to PND 103.

The therapeutic potential of GSK3β is highly dependent on the brain region. Thus, in the chronic CA1 intervention protocol (SB–CA1) (Figure 1C), we investigated the effect of GSK3β inhibition within the CA1 subregion of the DHP. Mice were randomly divided into the following groups: saline × vehicle–CA1, saline × SB216763–CA1, METH × vehicle–CA1, and METH × SB216763–CA1. SB216763 (1 ng/side, CA1 infusion, o.d.) or vehicle (similar volume to SB216763, CA1 infusion, o.d.) injection was carried out at 18:00 on each day from PND 90 to PND 103.

Animals

All adolescent male C57BL/6J mice were obtained at PND 35 and were housed in pathogen-free rooms in groups of four under controlled conditions (12-h light/dark cycle, 50 ± 5% humidity, and 22 ± 3°C temperature control) with food and water *ad libitum*. All mice were acclimated to the environment for 7 days and handled daily for 4 days before the experiment. All animal procedures were approved by the Institutional Animal Care and Use Committee of Xi'an Jiaotong University.

Drug preparation and administration

Methamphetamine hydrochloride (The Third Research Institute of The Ministry of Public Security, Shanghai, China) and LiCl (Sigma, St. Louis, MO, United States) were dissolved in 0.9% saline to final concentrations of 0.1 and 10 mg/mL, respectively. SB216763 (Sigma, St. Louis, MO, United States) was dissolved in 3% (vol/vol) DMSO, 3% (vol/vol) Tween 80, and distilled water (3:3:94) to a final concentration of 2 ng/μL. All drugs were freshly prepared before use and i.p. injected at a volume of 10 ml/kg or microinfused into CA1 at a volume of 0.5 μL/side.

For CA1 microinfusions, stereotaxic surgery was performed on PND 79–81 to prevent the effects of surgery on brain development. The mice were anesthetized with sodium pentobarbital (65 mg/kg, i.p.) and fixed in a stereotaxic frame. Stainless steel guide cannulae (27G, RWD Life Science, Shenzhen, China) were bilaterally implanted into the CA1 subregion of the DHP at the following stereotaxic coordinates: AP −2.00 mm, ML ± 1.50 mm, and DV −1.00 mm (Gyu et al., 2012). The guide cannulae were secured to the skull using dental cement, and dummy cannulae were inserted. The mice were allowed to recover for 1 week after surgery. For intracranial injection, the mice were restrained carefully, and the dummy cannulae were replaced by internal cannulae (0.5 mm longer than the guide cannulae). SB216763 or the vehicle was bilaterally infused into CA1 at a rate of 0.1 μL/min, and the internal cannula remained in the guide cannula for 5 min after the infusion to ensure the proper delivery of the reagents.

The drug doses used in the present study were chosen based on previous reports and can produce significant biological effects (Kamei et al., 2006; Xu et al., 2011; Gyu et al., 2012; Yan et al., 2019).

Behavioral tests

All behavioral tests were performed from 8:00 to 16:00 on each test day. Tests were recorded and analyzed using the Any-maze 5.2 software (Stoelting Co., Wood Dale, IL, United States). An entry was defined as all four paws in one area. The apparatus was cleaned using 50% ethanol for different trials and phases. The distal cues consisted of different geometric shapes (including rectangle, circle, triangle, pentagon, and irregular polygon), and were changed between different types of behavioral tests. In all behavioral tests, a white LED light with diffuser plate was suspended 2.5 meters above the center of the apparatus, and the illumination of the apparatus floor was approximately 50 Lux. Previous study reported this illumination may have neither anxiogenic stimulus nor anxiolytic stimulus (Neuwirth et al., 2022).

Open field test (locomotor activity)

Mice were individually placed in a plastic box (45 × 45 × 30 cm) and allowed to freely explore the arena for 60 min. The center area (30 × 30 cm) and four corner areas (7.5 × 7.5 cm) were marked using Any-maze 5.2 software. The distance moved, movement duration, and movement in the center and at the four corners were measured.

Modified two-trial Y-maze test (novel spatial exploration)

This test was performed as described in previous study (Yan et al., 2019). We used a Y-maze in which the wall of one of the three arms was marked with a black-and-white stripe and defined as the novel arm. Each arm of the Y-maze was 30 cm in length, 6 cm in width, and 15 cm in height. The apparatus was rotated by +60° between tests. First, the novel arm was blocked, and the mice were allowed to habituate to the Y-maze for 5 min. After 30 min of rest, the novel arm was opened, and the mice were allowed to freely explore all three arms for 5 min. The time spent in the novel arm (%) was defined as the time spent in the novel arm divided by the time spent in all three arms. Entries into the novel arm (%) were defined as the number of entries into the novel arm divided by the total number of entries into all three arms. The latency to the first entry and the longest single visit to the novel arm were also recorded.

Three-chamber social behavior test (sociability and social recognition memory)

The test apparatus was a three-chambered box with two lateral chambers (lateral, 35 × 20 × 30 cm; middle, 35 × 15 × 30 cm). Mice were first allowed to habituate to the apparatus for 5 min, followed by two successive phases (T1 and T2) to investigate their sociability and social recognition memory. In the T1 phase (sociability test), an unfamiliar C57BL/6J male mouse (stranger), which had no prior contact with the subject mouse, was placed into one of the two lateral chambers and enclosed in a circular acrylic cage that only allowed nose contact between the cage bars. Another empty cage of the same design was placed in the other lateral chamber. The subject mice were placed in the central chamber and allowed to freely explore the test apparatus for 10 min. The location of the stranger mouse in the left or right chamber was interchanged between the trials. In the T2 phase (social recognition memory test, a second 10 min period), 30 min after the T1 phase, a second unfamiliar mouse (novel) was placed in the lateral chamber that had been empty in the T1 phase and enclosed in the circular acrylic cage. The subject mouse had a choice between the first, already investigated unfamiliar mouse (stranger (T1), familiar (T2)), and the novel unfamiliar mouse. The interaction was defined as the sniffing or direct contact when the subject animal oriented its nose or initiated physical contact within 2 cm of the stranger/novel mouse contained in the wired cage (Leung et al., 2018). Sociability was expressed using sociability scores that were defined as the difference between the interaction time with the stranger and empty chambers. Time in contact with the stranger (%) was defined as the interaction time with the stranger divided by the total interaction time; entries into the stranger chamber (%) were also recorded. Social recognition memory was expressed using social recognition scores that were defined as the difference between the interaction time with the novel and familiar mice. Time in contact with the novel (%) was defined as the interaction time with the novel animal divided by the

total interaction time; entries in the novel chamber (%) were also recorded.

Novel object recognition test (object recognition memory)

The test apparatus was a rectangular box (35 × 20 × 30 cm). This test consisted of three phases: habituation, training, and testing (Leger et al., 2013). On day 1 (habituation phase, PND 102), the mice were habituated to the apparatus twice for 10 min each. On day 2 (PND 103), in the training phase, two identical objects were symmetrically fixed to the floor of the apparatus, 10 cm from the walls, and the mice were allowed to freely explore the apparatus for 10 min. In the testing phase, 30 min after the training phase, one of the objects used during the training phase was replaced with a novel object, and the mice were placed back in the apparatus for free exploration for 5 min. The objects used in this test were similar in size but different in color, shape, and texture and had a similar preference for mice. Object exploration was defined as sniffing or touching an object while looking at it at a distance of <2 cm. The object preference in training (%) was defined as the exploration time of one of the two identical objects divided by the total exploration time of all objects, and the novel preference in testing (%) was defined as the exploration time of the novel object divided by the total exploration time of both objects. The total exploration time in the training and testing phases was also recorded.

Standard two-trial Y-maze test (spatial recognition memory)

The standard two-trial Y-maze test was used to assess spatial recognition memory (Dellu et al., 2000). This test was also conducted using a Y-maze, which had three identical arms, and one of the three arms was defined as the novel arm. The protocol and data recorded in this test were the same as those of the modified two-trial Y-maze test.

Molecular and histological analysis

Western blot

Mouse brains were rapidly mounted onto a cryostat, and coronal sections of the DHP CA1 subregion were obtained according to Paxino and Franklin's Stereotaxic Atlas, 2nd edition (Franklin and Paxinos, 2001); they were then stored at −80°C until processing. Western blotting was conducted as previously described (Wang et al., 2017). The dilutions of primary antibodies were as follows: phosphorylated pGSK3β-S9 (1:1000, Cell Signaling Technology, Beverly, MA, United States), total-GSK3β (t-GSK3β) (1:2000, Cell Signaling Technology), GAPDH (internal control, 1:2000, Pioneer Biotechnology, Xi'an, China). All species-appropriate horseradish peroxidase-conjugated secondary antibodies (Pioneer Biotechnology) were used at a dilution of 1:10,000.

Immunohistochemistry

Mice were anesthetized with sodium pentobarbital and intracardially perfused with 4% paraformaldehyde in 0.1 M phosphate buffer (PB; pH 7.4). Brains were immediately removed and post-fixed in 4% paraformaldehyde. After being saturated in 30% (w/v) sucrose in 0.1 M PB buffer (pH 7.4), the brains were serially cut into 20-μm thick transverse sections with a freezing microtome (CM1950, Leica). Immunohistochemical staining was performed according to the manufacturer's protocol using a Biotin-Streptavidin HRP Detection System (SP-9001, ZSGB-BIO, Beijing, China) (Yan et al., 2019). The dilution of the primary antibody pGSK3β-S9 (Cell Signaling Technology) was 1:100. Images of the processed sections were captured using a Leica MZFL III microscope. The integrated optical density (IOD) in the CA1 subregion of the DHP was evaluated using Image-Pro Plus 6.0 software (IPP, Media Cybernetics, Wokingham, United Kingdom).

Transmission electron microscopic analysis

Mice were anesthetized with sodium pentobarbital and intracardially perfused with saline and then with 0.1 M PB buffer (pH 7.4) containing 4% paraformaldehyde and 0.25% glutaraldehyde. Brains were removed immediately and stored in 0.1 M PB buffer (pH 7.4) with 4% paraformaldehyde and 2.5% glutaraldehyde at 4°C. The CA1 subregion of the DHP was extracted and dissected into ~1 mm^3 pieces. The samples were then fixed in a fresh solution of 1% osmium tetroxide for 90 min, dehydrated in ethanol, and embedded in epon-araldite resin. Ultrathin sections were cut and placed onto grids, stained with 2% aqueous uranyl acetate, and counterstained with 0.3% lead citrate. The sections were imaged using a Hitachi 7,650 electron microscope operated at 80 kV. Synapses were identified by clear pre-and postsynaptic membranes and the presence of synaptic vesicles in the presynaptic terminals. The number of gray type-1 asymmetric synapses (excitatory synapses), the thickness of the PSD at the thickest part, the length of the active zone, and the width of the synaptic cleft in asymmetrical synapses were measured. Quantification was performed using 10 random sections (more than 60 asymmetric synapses) per mouse.

Statistical analyses

Statistical analyses were performed using GraphPad Prism 9.0 (GraphPad Software Inc., La Jolla, CA, United States) and SPSS 25 (IBM, Armonk, NY, United States). The results are presented as the mean ± SEM. The parametric test (two-way ANOVA with Bonferroni's *post-hoc* test) was applied when normality and homogeneity of variance assumptions were satisfied; otherwise, the nonparametric test (Kruskal-Wallis with Dunn's *post-hoc* test) was used. For two-way ANOVA, when there was a statistical interaction were between groups comparisons done; if not, the post-hoc test was performed on the main effect variables that were significant. The investigators were blinded to the allocation of the groups and outcome assessments for all the experiments. All statistically significant differences were defined as $p < 0.05$. Detailed statistics are provided in Supplementary Table S1.

Results

The effects of GSK3β activity inhibition on the adolescent METH exposure-induced behavioral and cognitive deficits in adulthood

Inhibition of GSK3β activity reduced adolescent METH exposure-induced hyperactivity in adulthood

For the OFT, in the acute systemic intervention (Figure 2A), the adolescent METH × vehicle–acute mice were markedly more active than

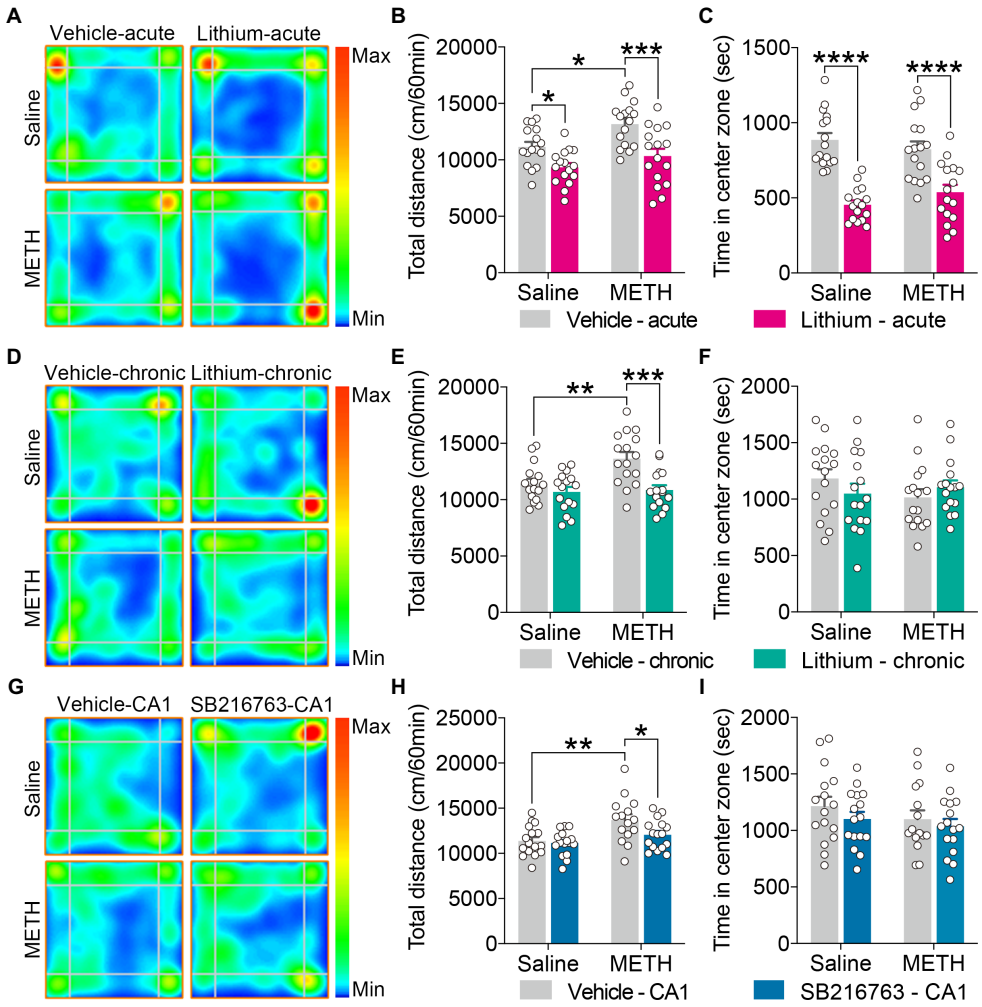

FIGURE 2
Effect of GSK3β inhibition on adolescent METH exposure-induced hyperactivity in adulthood. Acute systemic intervention **(A–C)**, chronic systemic intervention **(D–F)**, and chronic intervention within CA1 **(G–I)** reduced adolescent METH exposure-induced hyperactivity in adulthood, but Li–acute administration attenuated locomotor activity and led to anxiety-like behavior. Representative heat maps show the location of the mice during the OFT **(A,D,G)**. Histograms show the total distance moved **(B,E,H)** and time spent in the center **(C,F,I)** during the OFT. Data are presented as the mean +/− SEM, each symbol represents the independent of a single animal; two-way ANOVA followed by the Bonferroni *post hoc* test; n=16~17/group; *p<0.05, **p<0.01, ***p<0.001, and ****p<0.0001, comparison between the two indicated groups. See also Supplementary Figure S1.

the saline×vehicle–acute and the METH × Li–acute mice, and saline×Li–acute mice were less active than the saline×vehicle–acute mice (Figure 2B) (two-way ANOVA: $F_{Interaction(1,60)}=1.038$, $p=0.3124$, $F_{METH(1,60)}=9.279$, $p<0.01$, $F_{Li\text{-}acute(1,60)}=21.99$, $p<0.0001$). In addition, the saline×Li–acute mice traveled less distance in the center than the saline×vehicle–acute and METH×Li–acute mice (Supplementary Figure S1A) (two-way ANOVA: $F_{Interaction(1,60)}=2.486$, $p=0.1201$, $F_{METH(1,60)}=6.507$, $p<0.05$, $F_{Li\text{-}acute(1,60)}=20.21$, $p<0.0001$), and the METH×vehicle–acute mice traveled more distance in the corner than the saline×vehicle–acute mice (Supplementary Figure S1B) (two-way ANOVA: $F_{Interaction(1,60)}=1.192$, $p=0.2794$, $F_{METH(1,60)}=7.982$, $p<0.01$, $F_{Li\text{-}acute(1,60)}=3.446$, $p<0.0638$). Furthermore, the saline×Li–acute mice stayed shorter in the center and longer in the corner than saline×vehicle–acute mice, and the METH×Li–acute mice stayed shorter in the center and longer in the corner than METH×vehicle–acute mice (Figure 2C and Supplementary Figure S1C) (two-way ANOVA: time spent in center zone, $F_{Interaction(1,60)}=2.640$, $p=0.1095$, $F_{METH(1,60)}=0.05235$, $p=0.8198$, $F_{Li\text{-}acute(1,60)}=62.82$, $p<0.0001$; time spent in corner zone, $F_{Interaction(1,60)}=0.2303$, $p=0.6331$, $F_{METH(1,60)}=0.7871$, $p=0.3785$, $F_{Li\text{-}acute(1,60)}=16.63$, $p<0.001$).

In the chronic systemic intervention (Figure 2D), the adolescent METH×vehicle–chronic mice traveled more distance than the saline×vehicle–chronic and METH×Li–chronic mice (Figure 2E) (two-way ANOVA: $F_{Interaction(1,60)}=4.781$, $p<0.05$, $F_{METH(1,60)}=6.403$, $p<0.05$, $F_{Li\text{-}chronic(1,60)}=14.13$, $p<0.001$). In addition, the METH×vehicle–chronic mice traveled more distance in the corner than the saline×vehicle–chronic and METH×Li–chronic mice (Supplementary Figure S1E) (two-way ANOVA: $F_{Interaction(1,60)}=9.256$, $p<0.01$, $F_{METH(1,60)}=7.432$, $p<0.01$, $F_{Li\text{-}chronic(1,60)}=14.74$, $p<0.001$). There was no statistical significance of the time spent in the center between groups (Figure 2F).

In the chronic CA1 intervention (Figure 2G), the METH × vehicle–CA1 mice traveled a greater distance than the saline × vehicle–CA1 and METH × SB–CA1 mice (Figure 2H) (two-way ANOVA: $F_{Interaction(1,59)}=2.223$, $p=0.1413$,

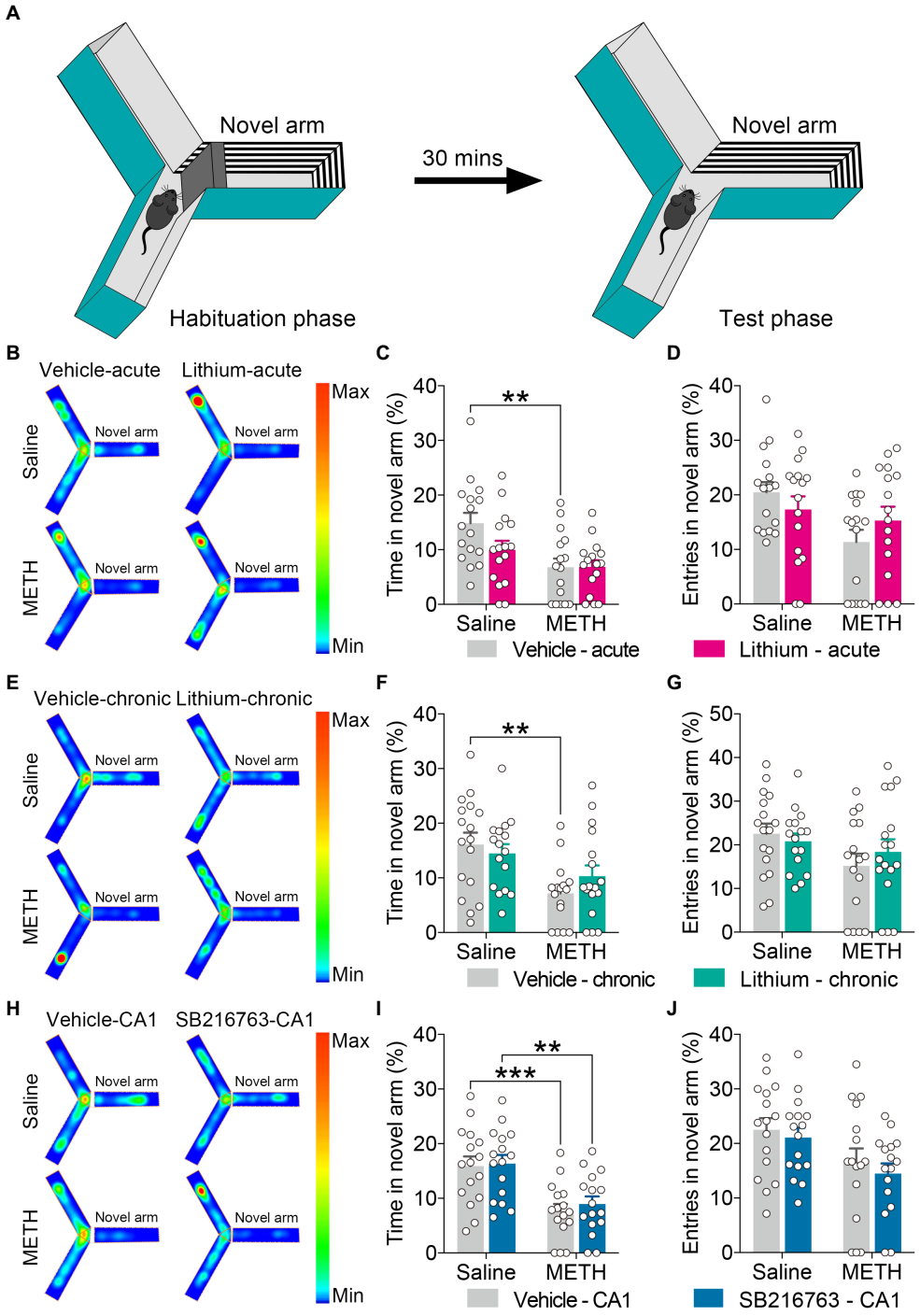

FIGURE 3
Effect of GSK3β inhibition on adolescent METH exposure-induced novel spatial exploration impairment in adulthood. Apparatus and placements of the mice for the modified two-trial Y-maze test **(A)**. There was no significant influence by the acute systemic intervention **(B–D)**, chronic systemic intervention **(E–G)**, or chronic intervention within CA1 **(H–J)** in adolescent METH exposure-induced novel spatial exploration impairment in adulthood. Representative heat maps show the location of the mice during the testing phase **(B,E,H)**. Histograms show the time spent (%) **(C,F,I)** and entries (%) **(D,G,J)** in the novel arm in this test. Data are presented as the mean +/− SEM, each symbol represents the independent of a single animal; two-way ANOVA followed by the Bonferroni *post hoc* test; n=16~17/group; **p<0.01 and ***p<0.001, comparison between the two indicated groups. See also Supplementary Figure S2.

$F_{METH(1,59)} = 12.27$, $p < 0.001$, $F_{SB\text{-}CA1(1,59)} = 4.125$, $p < 0.05$). Moreover, METH × vehicle–CA1 mice traveled more distance in the corner than saline × vehicle–CA1 and METH × SB–CA1 mice (Supplementary Figure S1H) (Kruskal-Wallis test: $H = 13.15$, $p < 0.01$). There was no statistical significance of the time spent in the center between groups (Figure 2I).

No significant effects of inhibition of GSKβ activity on adolescent METH exposure-induced novel spatial exploration impairment

For the modified two-trial Y-maze test, the apparatus and placement of the mice for this test are shown in Figure 3A. In each intervention protocol, adolescent METH-exposed mice spent less

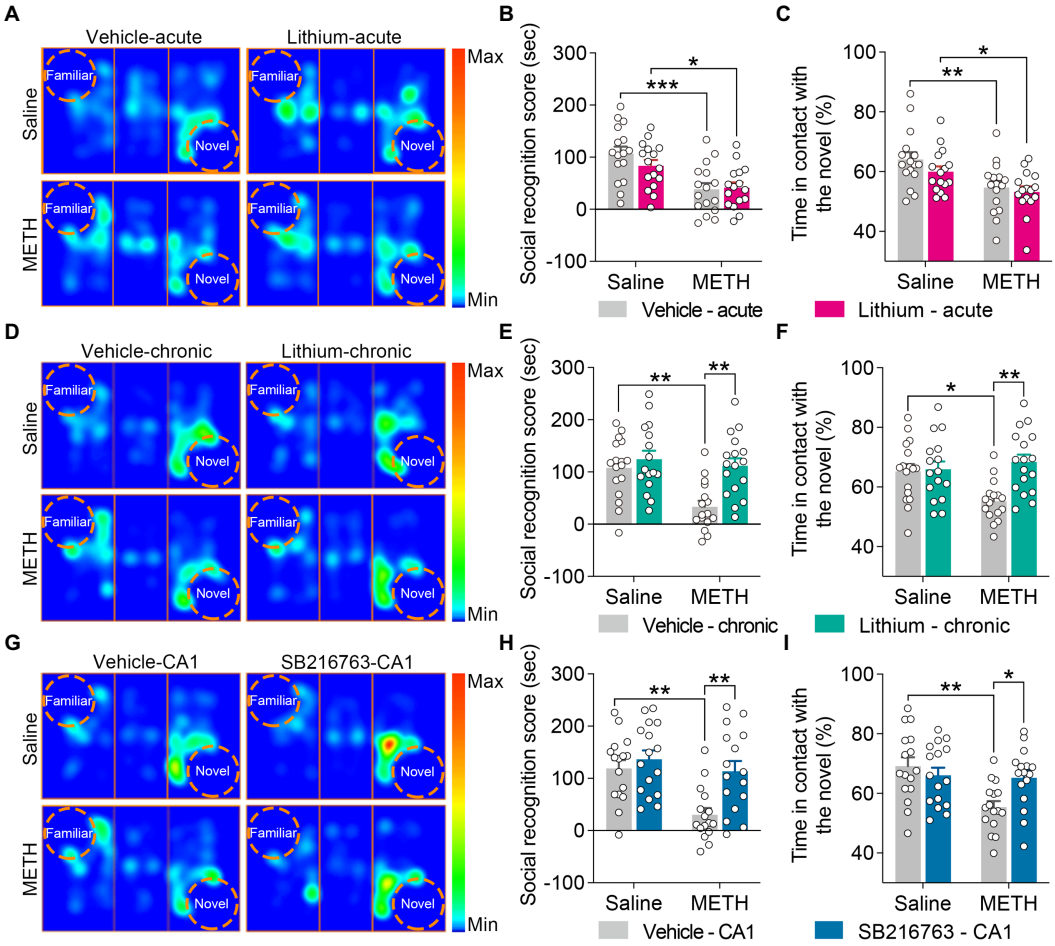

FIGURE 4
Effect of GSK3β inhibition on adolescent METH exposure-induced social recognition memory impairment in adulthood. Acute systemic intervention **(A–C)** had no significant effects on adolescent METH exposure-induced social behavioral deficit, while chronic systemic intervention **(D–F)** and chronic intervention within CA1 **(G–I)** rescued adolescent METH exposure-induced social recognition memory impairment in adulthood. Representative heat maps show the location of the mice during the social recognition memory test **(A,D,G)**. Histograms show the social recognition score **(B,E,H)** and time in contact with the novel (%) **(C,F,I)** during the social recognition memory test. Data are presented as the mean +/− SEM, each symbol represents the independent of a single animal; two-way ANOVA followed by the Bonferroni *post hoc* test; n=16~17/group; *p<0.05, **p<0.01, and ***p<0.001, comparison between the two indicated groups. See also Supplementary Figure S3.

time in the novel arm (%) than control mice (Figures 3C,F,I) (two-way ANOVA: acute systemic intervention, $F_{Interaction(1,59)} = 2.338$, $p = 0.1315$, $F_{METH(1,60)} = 11.89$, $p < 0.01$, $F_{Li\text{-}acute(1,60)} = 2.210$, $p = 0.1423$; chronic systemic intervention, $F_{Interaction(1,62)} = 1.693$, $p = 0.1981$, $F_{METH(1,62)} = 12.76$, $p < 0.001$, $F_{Li\text{-}chronic(1,62)} = 0.1917$, $p = 0.663$; chronic CA1 intervention: $F_{Interaction(1,60)} = 0.08186$, $p = 0.7758$, $F_{METH(1,60)} = 26.69$, $p < 0.0001$, $F_{SB\text{-}CA1(1,60)} = 0.3371$, $p = 0.5637$); however, METH × GSKβ inhibitor mice and METH × vehicle mice showed similar characteristics in this test (Figure 3 and Supplementary Figure S2).

Chronic treatment with the GSKβ inhibitors ameliorated adolescent METH exposure-induced social recognition memory impairment in adulthood

For the sociability test, two-way ANOVA revealed that all tested mice showed similar sociability characteristics in each intervention protocol (Supplementary Figure S3).

For social recognition memory, in the acute systemic intervention (Figure 4A), the METH × vehicle–acute and METH × Li–acute mice obtained a lower average social recognition score and decreased time in contact with the novel (%) than the saline × vehicle–acute mice (Figures 4B,C) (two-way ANOVA: social recognition score, $F_{Interaction(1,60)} = 1.326$, $p = 0.254$, $F_{METH(1,60)} = 22.73$, $p < 0.0001$, $F_{Li\text{-}acute(1,60)} = 0.7555$, $p = 0.3882$; time in contact with the novel, $F_{Interaction(1,60)} = 0.3973$, $p = 0.5309$, $F_{METH(1,60)} = 15.22$, $p < 0.001$, $F_{Li\text{-}acute(1,60)} = 1.839$, $p = 0.1802$).

In the chronic systemic intervention (Figure 4D), METH × vehicle–chronic mice obtained a lower average social recognition score than saline × vehicle–chronic and METH × Li–chronic mice (Figure 4E) (two-way ANOVA: $F_{Interaction(1,62)} = 4.850$, $p < 0.05$, $F_{METH(1,62)} = 9.470$, $p < 0.01$, $F_{Li\text{-}chronic(1,62)} = 11.34$, $p < 0.01$). In addition, METH × vehicle–chronic mice spent less time in contact with the novel (%) than the saline × vehicle–chronic mice (Figure 4F) (two-way ANOVA: $F_{Interaction(1,62)} = 6.962$, $p < 0.05$, $F_{METH(1,62)} = 2.596$, $p = 0.1122$, $F_{Li\text{-}chronic(1,62)} = 8.562$, $p < 0.01$).

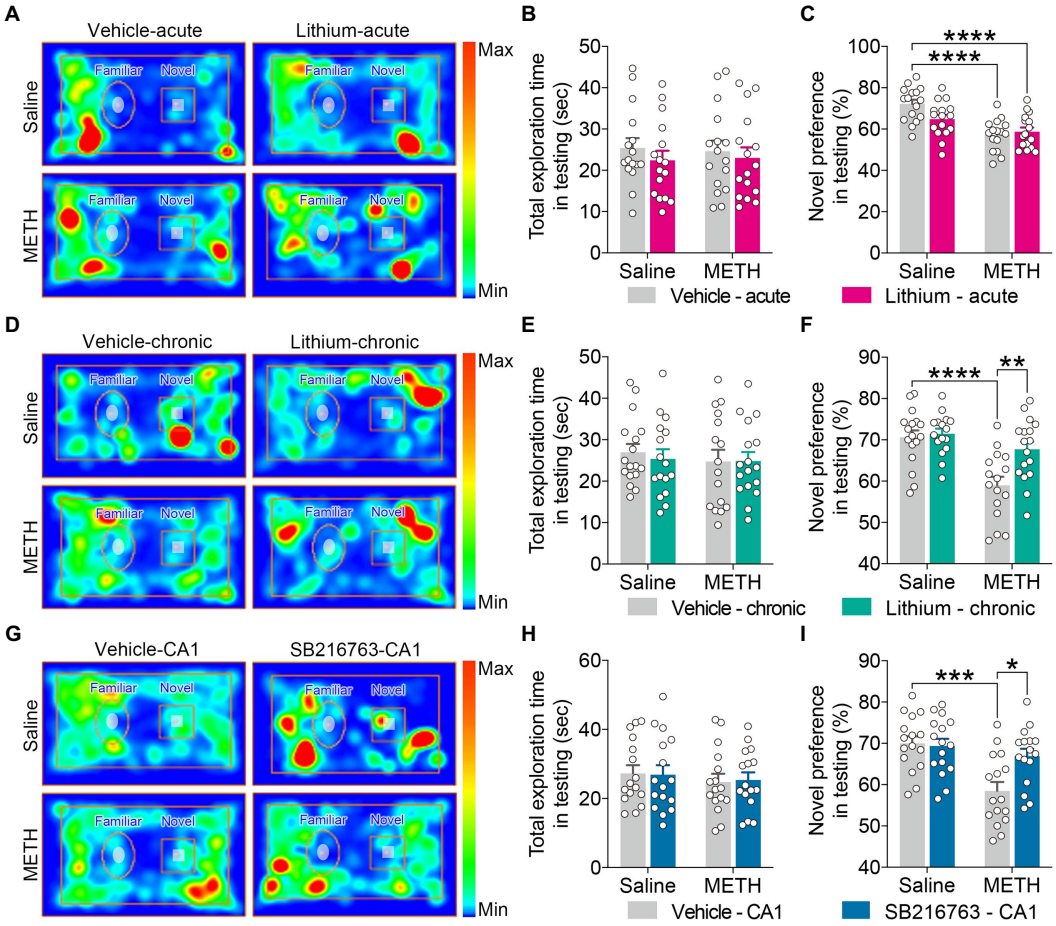

FIGURE 5
Effect of GSK3β inhibition on adolescent METH exposure-induced object recognition memory impairment in adulthood. Compared with the effect of the acute systemic intervention **(A–C)**, chronic systemic intervention **(D–F)** and chronic intervention within CA1 **(G–I)** improved adolescent METH exposure-induced object recognition memory impairment in adulthood. Representative heat maps show the location of the mice during the testing phase **(A,D,G)**. Histograms show the total exploration time **(B,E,H)** and novel preference (%) **(C,F,I)** during the testing phase. Data are presented as the mean +/− SEM, each symbol represents the independent of a single animal; two-way ANOVA followed by the Bonferroni *post hoc* test; *n*=16~17/group; **p*<0.05, ***p*<0.01, ****p*<0.001, and *****p*<0.0001, comparison between the two indicated groups. See also Supplementary Figure S4.

In the chronic CA1 intervention (Figure 4G), compared to the saline × vehicle–CA1 and METH × SB–CA1 mice, the METH × vehicle–CA1 mice had a lower average social recognition score and spent less time in contact with the novel (%) (Figures 4H,I) (two-way ANOVA: social recognition score, $F_{Interaction(1,60)} = 4.013$, $p < 0.05$, $F_{METH(1,60)} = 11.59$, $p < 0.01$, $F_{SB\text{-}CA1(1,60)} = 9.474$, $p < 0.01$; time in contact with the novel, $F_{Interaction(1,60)} = 6.518$, $p < 0.05$, $F_{METH(1,60)} = 8.344$, $p < 0.01$, $F_{SB\text{-}CA1(1,60)} = 1.761$, $p = 0.1896$).

Chronic treatment with the GSKβ inhibitors improved adolescent METH exposure-induced object recognition memory deficits in adulthood

For the NOR test, in the training phase, all test mice exhibited similar behavioral characteristics in each intervention protocol (Supplementary Figure S4).

In the testing phase, for the total exploration time, no significant differences were observed among the groups for each intervention protocol (Figures 5B,E,H).

For the exploratory preference of novel objects, in the acute systemic intervention (Figure 5A), the METH × vehicle–acute and METH × Li–acute mice exhibited significantly decreased novel preference (%) compared with the saline × vehicle–acute mice (Figure 5C) (two-way ANOVA: $F_{Interaction(1,60)} = 4.791$, $p < 0.05$, $F_{METH(1,60)} = 27.00$, $p < 0.0001$, $F_{Li\text{-}acute(1,60)} = 2.092$, $p = 0.1533$).

In the chronic systemic intervention (Figure 5D), the METH × vehicle–chronic mice showed a significantly decreased novel preference (%) compared to the saline × vehicle–chronic and METH × Li–chronic mice (Figure 5F) (two-way ANOVA: $F_{Interaction(1,62)} = 5.281$, $p < 0.05$, $F_{METH(1,62)} = 19.99$, $p < 0.0001$, $F_{Li\text{-}chronic(1,62)} = 7.543$, $p < 0.01$).

In the chronic CA1 intervention (Figure 5G), METH × vehicle–CA1 mice showed significantly decreased novel preference (%) compared to saline × vehicle–CA1 and METH × SB–CA1 mice (Figure 5I) (two-way ANOVA: $F_{Interaction(1,60)} = 6.040$, $p < 0.05$, $F_{METH(1,60)} = 14.26$, $p < 0.001$, $F_{SB\text{-}CA1(1,60)} = 4.433$, $p < 0.05$).

Chronic treatment with the GSK3β inhibitors ameliorated adolescent METH exposure-induced spatial recognition memory impairment in adulthood

For the standard two-trial Y-maze test, the apparatus and placement of the mice for this test are shown in Figure 6A. In the acute systemic.intervention (Figure 6B), reduced time spent and entries into the novel arm (%) were displayed by METH × vehicle–acute mice and METH × Li–acute mice (Figures 6C,D) (two-way ANOVA: time spent in the novel arm, $F_{Interaction(1,36)} = 0.7398$, $p = 0.3954$, $F_{METH(1,36)} = 19.83$, $p < 0.0001$, $F_{Li\text{-}acute(1,36)} = 0.01305$, $p = 9{,}097$; entries in the novel arm, $F_{Interaction(1,36)} = 0.02909$, $p = 0.8655$, $F_{METH(1,36)} = 15.52$, $p < 0.001$, $F_{Li\text{-}acute(1,36)} = 1.230$, $p = 0.2748$).

In the chronic systemic intervention (Figure 6E), the METH × vehicle–chronic mice showed significantly decreased time spent and entries into the novel arm (%) than the saline × vehicle–chronic and METH × Li–chronic mice (Figures 6F,G) (two-way ANOVA: time spent in the novel arm, $F_{Interaction(1,36)} = 7.652$, $p < 0.01$, $F_{METH(1,36)} = 12.8$, $p < 0.01$, $F_{Li\text{-}chronic(1,36)} = 2.303$, $p = 0.1379$; entries in the novel arm, $F_{Interaction(1,36)} = 9.491$, $p < 0.01$, $F_{METH(1,36)} = 5.378$, $p < 0.05$, $F_{Li\text{-}chronic(1,36)} = 3.972$, $p = 0.0539$).

In the chronic CA1 intervention (Figure 6H), the METH × vehicle–CA1 mice showed significantly decreased time spent and entries into the novel arm (%) compared to saline × vehicle–CA1 and METH × SB–CA1 mice (Figures 6I,J) (two-way ANOVA: time spent in the novel arm, $F_{Interaction(1,30)} = 4.959$, $p < 0.05$, $F_{METH(1,30)} = 8.989$, $p < 0.01$, $F_{SB\text{-}CA1(1,30)} = 6.439$, $p < 0.05$; entries in the novel arm, $F_{Interaction(1,30)} = 7.493$, $p < 0.05$, $F_{METH(1,30)} = 4.911$, $p < 0.05$, $F_{SB\text{-}CA1(1,30)} = 3.811$, $p = 0.0603$).

Taken together, these results suggest that, in adulthood, all three GSK3β interventions reduce the adolescent METH exposure-induced long-lasting hyperactivity; but only chronic systemic and chronic within CA1 interventions improve that induced social, object, and spatial recognition memory impairments; in addition, acute Li exposure reduces locomotor activity and leads to anxiety-like behavior; for novel spatial exploration impairment, all three interventions have no significant effects.

Inhibition of GSK3β activity restored adolescent METH exposure-induced increase in the GSK3β activity of the DHP CA1 subregion in adulthood

Previous study reported that in adulthood, increased GSKβ activity of the DHP CA1 subregion may be the reason for behavioral and cognitive impairments induced by adolescent METH exposure, we investigated the effects of GSKβ inhibitors on GSKβ activity in the DHP CA1 subregion (Yan et al., 2019).

Western blot analysis (Figures 7A,F,K). demonstrated no changes in the expression level of total-GSK3β in the DHP CA1 subregion among the groups in any intervention protocol (Figures 7C,H,M). However, the adolescent METH-exposed mice showed a significant decrease in the ratio of pGSK3β-Ser9/t-GSK3β compared to the control mice and the METH × GSK3β inhibitor mice in each intervention protocol (Figures 7B,G,L), and Li–acute significantly enhanced the ratio of pGSK3β-Ser9 to t-GSK3β in the DHP CA1 subregion (Figure 7B) (two-way ANOVO: acute systemic intervention: $F_{Interaction(1,16)} = 1.080$, $p = 0.3141$, $F_{METH(1,16)} = 17.93$, $p < 0.001$, $F_{Li\text{-}acute(1,16)} = 28.24$, $p < 0.0001$; chronic systemic intervention: $F_{Interaction(1,16)} = 4.998$, $p < 0.05$, $F_{METH(1,16)} = 11.42$, $p < 0.01$, $F_{Li\text{-}chronic(1,16)} = 11.80$, $p < 0.01$; chronic CA1 intervention: $F_{Interaction(1,16)} = 4.763$, $p < 0.05$, $F_{METH(1,16)} = 15.52$, $p < 0.01$, $F_{SB\text{-}CA1(1,16)} = 9.219$, $p < 0.01$).

Next, immunochemical analysis (Figures 7D,I,N). was performed to confirm the effects of GSK3β inhibitors. In agreement with the results of western blot analysis, adolescent METH-exposed mice showed a significant decrease in the IOD of pGSK3β-Ser9 compared to control mice and METH × GSKβ inhibitor mice in each intervention protocol (Figures 7E,J,O) (two-way ANOVO: acute systemic intervention: $F_{Interaction(1,11)} = 4.067$, $p = 0.0688$, $F_{METH(1,11)} = 24.47$, $p < 0.001$, $F_{Li\text{-}acute(1,11)} = 24.95$, $p < 0.001$; chronic systemic intervention: $F_{Interaction(1,12)} = 9.346$, $p < 0.01$, $F_{METH(1,12)} = 23.30$, $p < 0.001$, $F_{Li\text{-}chronic(1,12)} = 20.73$, $p < 0.001$; chronic CA1 intervention: $F_{Interaction(1,12)} = 4.928$, $p < 0.05$, $F_{METH(1,12)} = 19.54$, $p < 0.001$, $F_{SB\text{-}CA1(1,12)} = 13.76$, $p < 0.01$).

These results suggest that, in adulthood, GSK3β interventions restore adolescent METH exposure-induced long-lasting changes in GSKβ activity in the DHP CA1 subregion.

Chronic treatment with the GSK3β inhibitors rescued adolescent METH exposure-induced excitatory synaptic ultrastructure alterations of the DHP CA1 subregion in adulthood

To determine the structural basis underlying the therapeutic effects of GSK3β inhibition on adolescent METH exposure-induced behavioral and cognitive deficits in adulthood, we examined the synaptic ultrastructure in the DHP CA1 subregion using transmission electron microscopy (Figure 8 and Supplementary Figure S6).

In the acute systemic intervention, reduced excitatory synapse density and PSD thickness in the CA1 subregion were displayed by METH × vehicle–acute mice compared with saline × vehicle–acute mice, and reduced excitatory synapse density in the CA1 subregion was also displayed by METH × Li–acute mice compared with saline × Li–acute mice (Figures 8A–C) (two-way ANOVA: density of excitatory synapses, $F_{Interaction(1,12)} = 0.5632$, $p = 0.4674$, $F_{METH(1,12)} = 40.01$, $p < 0.0001$, $F_{Li\text{-}acute(1,12)} = 0.01149$, $p = 0.9164$; PSD thickness, $F_{Interaction(1,12)} = 1.599$, $p = 0.23$, $F_{METH(1,12)} = 10.02$, $p < 0.01$, $F_{Li\text{-}acute(1,12)} = 0.7341$, $p = 0.4083$).

In the chronic systemic intervention, the METH × vehicle–chronic mice showed significantly decreased excitatory synapse density and PSD thickness in the CA1 subregion compared to the saline × vehicle–chronic and METH × Li–chronic mice (Figures 8D–F) (two-way ANOVA: density of excitatory synapses, $F_{Interaction(1,12)} = 9.045$, $p < 0.05$, $F_{METH(1,12)} = 23.16$, $p < 0.001$, $F_{Li\text{-}chronic(1,12)} = 26.14$, $p < 0.001$; PSD thickness, $F_{Interaction(1,12)} = 0.3332$, $p = 0.5745$, $F_{METH(1,12)} = 11.23$, $p < 0.01$, $F_{Li\text{-}chronic(1,12)} = 10.27$, $p < 0.01$).

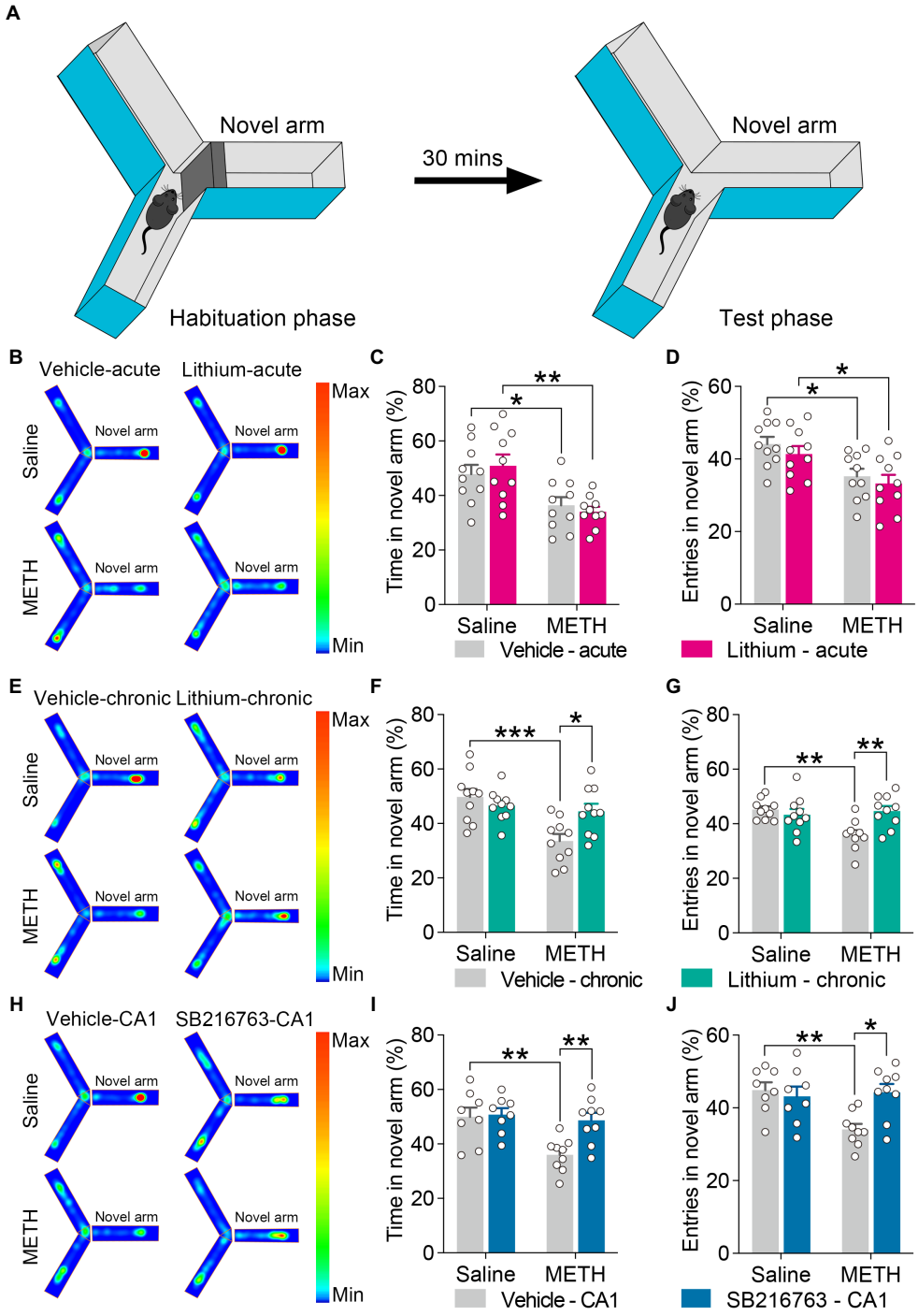

FIGURE 6
Effect of GSK3β inhibition on adolescent METH exposure-induced spatial recognition memory impairment in adulthood. Apparatus and placements of the mice for the standard two-trial Y-maze test **(A)**. Compared with the effect of the acute systemic intervention **(B–D)**, chronic systemic intervention **(E–G)** and chronic intervention within CA1 **(H–J)** ameliorated adolescent METH exposure-induced spatial recognition memory impairment in adulthood. Representative heat maps show the location of the mice during the testing phase **(B,E,H)**. Histograms show the time spent (%) **(C,F,I)** and entries (%) **(D,G,J)** in the novel arm in this test. Data are presented as the mean +/− SEM, each symbol represents the independent of a single animal; two-way ANOVA followed by the Bonferroni *post hoc* test; n=8~10/group; *p<0.05, **p<0.01, and ***p<0.001, comparison between the two indicated groups. See also Supplementary Figure S5.

In the chronic CA1 intervention, the METH × vehicle–CA1 mice showed significantly decreased excitatory synapse density and PSD thickness in the CA1 subregion compared with the saline × vehicle–CA1 and METH × SB–CA1 mice (Figures 8G–I) (two-way ANOVA: density of excitatory synapses, $F_{\text{Interaction}(1,11)} = 12.03$, $p < 0.01$, $F_{\text{METH}(1,11)} = 19.30$, $p < 0.01$, $F_{\text{SB-CA1}(1,11)} = 20.12$, $p < 0.0001$; PSD thickness, $F_{\text{Interaction}(1,11)} = 5.084$, $p < 0.05$, $F_{\text{METH}(1,11)} = 6.977$, $p < 0.05$, $F_{\text{SB-CA1}(1,11)} = 14.18$, $p < 0.01$).

These results suggest that, compared with acute treatment, chronic treatment with the GSK3β inhibitors is more effectiveness in the

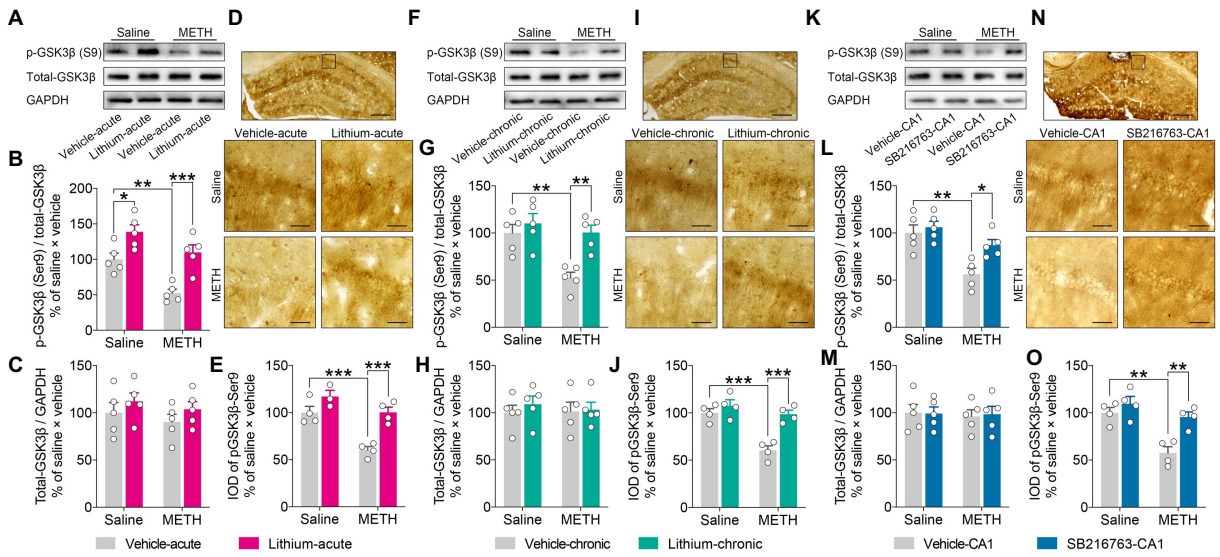

FIGURE 7
Effects of GSK3β inhibition on abnormal GSK3β activity in the adult DHP CA1 subregion induced by adolescent METH exposure. Acute systemic intervention **(A–E)**, chronic systemic intervention **(F–J)**, and chronic intervention within CA1 **(K–O)** restored the adolescent METH exposure-induced increase in the GSKβ activity of the DHP CA1 subregion in adulthood. Representative western blot of total and phosphorylated GSK3β in the DHP CA1 extract **(A,F,K)**. The relative changes in the ratio of phosphorylation of residues Ser9 (indicative of inactive protein) **(B,G,L)** and the expression of total GSK3β **(C,H,M)** were analyzed. Representative immunostaining of pGSK3β-Ser9 in the DHP CA1. The boxes indicate regions shown at higher magnification in the lower panels; scale bars represent 250μm under low magnification and 50μm under high magnification **(D,I,N)**. The relative changes in the IOD of pGSK3β-Ser9 in the DHP CA1 subregion were analyzed **(E,J,O)**. Data are presented as the mean +/− SEM, each symbol represents the independent of a single animal; two-way ANOVA followed by the Bonferroni *post hoc* test; *n*=5/group in western blot, *n*=4/group in immunohistochemistry; *p<0.05, **p<0.01, and ***p<0.001, comparison between the two indicated groups.

adolescent METH exposure-induced excitatory synaptic ultrastructural alterations of the DHP CA1 subregion in adulthood.

Discussion

Developmental METH exposure causes long-lasting neuropsychiatric consequences (Teixeira-Gomes et al., 2015). To the best of our knowledge, this is the first study to investigate how to improve adolescent METH exposure-associated behavioral and cognitive alterations in adulthood. We demonstrated that treatment with a GSK3β inhibitor in adulthood significantly ameliorated adolescent METH exposure-induced long-term deficits in locomotor activity and recognition memory by reversing the aberrant GSK3β activity and synaptic ultrastructure in the DHP CA1 subregion.

Glycogen synthase kinase-3β has extensive biological functions, and abnormal regulation of GSK3β has been observed in the onset and progression of different conditions (Beurel et al., 2015). GSK3β inhibition is not only an effective therapy for several neurological and psychiatric disorders, but is also beneficial for addictive drug-induced neurotoxicity (Takahashi-Yanaga, 2013; Barr and Unterwald, 2020). Therefore, many GSK3β-targeted pharmacological agents are being evaluated in preclinical and clinical trials (Demuro et al., 2021). In this study, we verified two GSK3β inhibitors: LiCl and SB216763, we found both agents were promising for treating adolescent METH exposure-induced behavioral and cognitive deficits in adulthood. It is well known that establishing adequate administration protocol is critical to correctly evaluate the therapeutical effects of drugs (Kim et al., 2008; Wang et al., 2021; Hiratsu et al., 2022). Herein, we performed acute (systemic) and chronic (systemic and within CA1) intervention protocols, and the results revealed that both protocols had a certain effect, but chronic intervention seemed to be better. Specifically, both protocols were effective against adolescent METH exposure-induced hyperactivity in adulthood, these results further highlight the efficacy of GSK3β-targeted therapeutic intervention in hyperactivity-associated behaviors (Mines, 2013). Compared with the ventral hippocampus, the DHP plays a more important role in locomotion (Fanselow and Dong, 2010), and local lesions of serotonin projections into DHP reduced amphetamine-induced locomotor hyperactivity (Kusljic and van den Buuse, 2004). Serotonin regulates the GSK3B activity by type 1 and type 2 serotonin receptors, in turn, GSK3β selectively interacts with 5-hydroxytryptamine-1B receptors (5-HT1BR) for modulating 5-HT1BR activity (Li and Polter, 2011). Thus, we presumed that rebalancing of the serotonin system in the DHP CA1 subregion may be one reason for improving hyperactivity by GSK3B activity inhibition. Nevertheless, for social, object, and spatial recognition memory impairments, only the chronic intervention had a positive impact.

The hippocampus is a complex brain structure that plays a vital role in memory (Borczyk et al., 2021). GSK3β has been regarded as a switch for synaptic plasticity, and hyperactivation of GSK3β is associated with memory deficiencies (Salcedo-Tello et al., 2011). Hypoxic brain damage is one of the most common manifestations of METH exposure, and among the various brain regions, the hippocampus is more vulnerable to hypoxia; thus, adolescent METH exposure may induce long-term hippocampal damage by disturbing development (Zhu et al., 2012; Weaver et al., 2014). Liang et al. (2022) recently reported that adult mice exposed to METH in adolescence had abnormal changes in the structural

10.3389/fnmol.2023.1129553

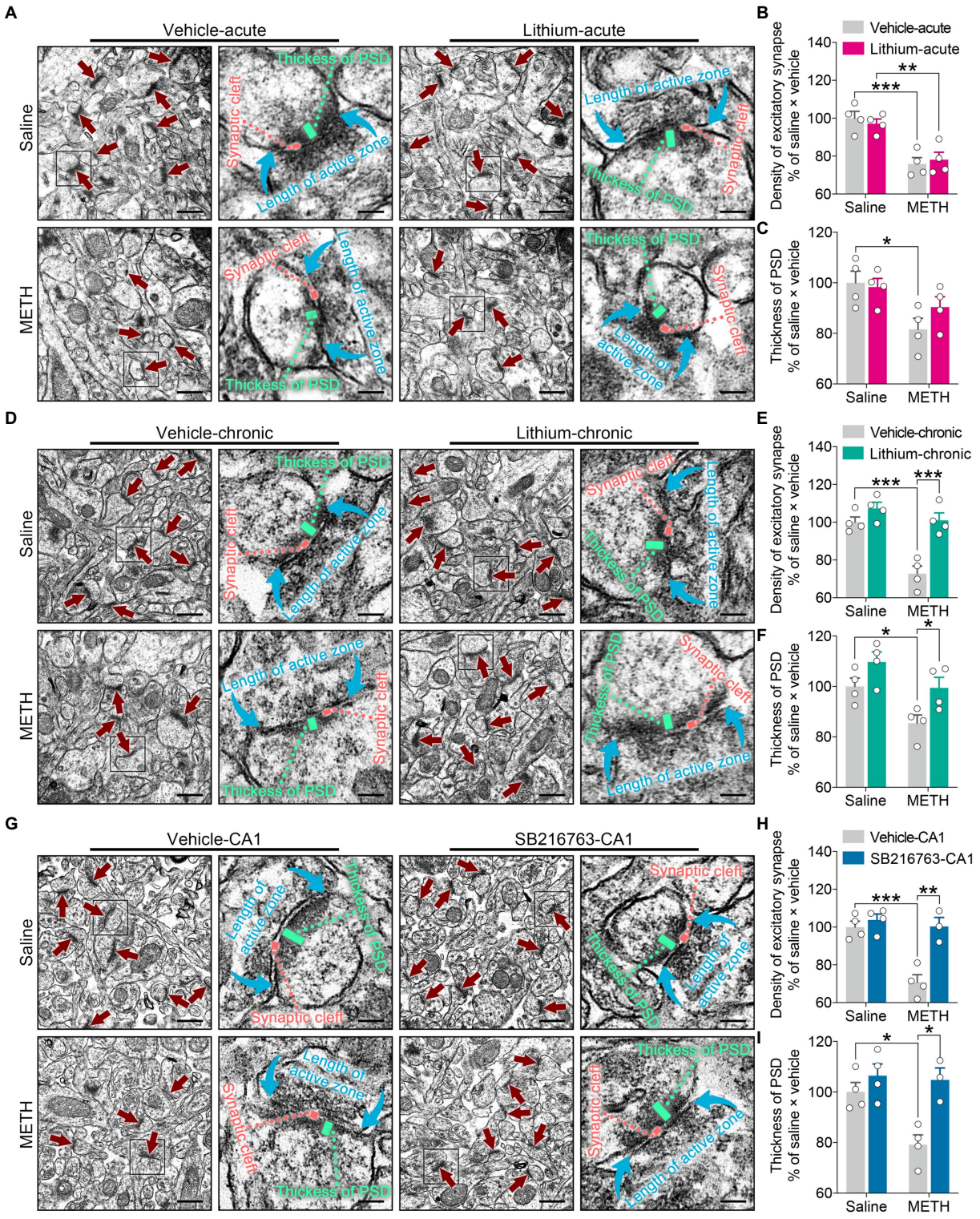

FIGURE 8
Effects of GSK3β inhibition on synaptic ultrastructural changes in the adult DHP CA1 subregion induced by adolescent METH exposure. Compared with the effect of the acute systemic intervention **(A–C)**, chronic systemic intervention **(D–F)** and chronic intervention within CA1 **(G–I)** resumed adolescent METH exposure-induced alterations in synaptic ultrastructure of the DHP CA1 subregion in adulthood. Representative electron micrographs of the DHP CA1 subregion. The straight crimson arrows indicate Gray's type-1 asymmetric synapses (excitatory synapses), the boxes indicate regions shown at higher magnification in the lower panels, and scale bars represent 500nm under low magnification and 100nm under high magnification **(A,D,G)**. Histograms show the relative changes in the total number of excitatory synapses **(B,E,H)** and the thickness of postsynaptic density (PSD) at the thickest part **(C,F,I)**. More than 60 randomly chosen excitatory synapses from each animal were analyzed. Data are presented as the mean +/− SEM, each symbol represents the independent of a single animal; two-way ANOVA followed by the Bonferroni *post hoc* test; n=4~5/group; *p<0.05, **p<0.01, and ***p<0.001, comparison between the two indicated groups. See also Supplementary Figure S6.

plasticity of the DHP. Yan et al. (2019) also found adolescent METH exposure caused decreased excitatory synapse density and PSD thickness of the DHP in adulthood, which were predominantly located in the CA1 subregion rather than in the CA3 and DG subregions. Thus, recovering synaptic ultrastructural alterations in the DHP CA1 subregion should be effective against adolescent METH exposure-induced cognitive and behavioral impairments in adulthood. However, our results indicated transient inhibition of GSK3β activity was not sufficient to resume synaptic ultrastructural alterations, which may explain why the chronic intervention is more effective than acute intervention for recognition memory impairment.

Lithium has been used for more than 70 years as one of the most effective agents for the treatment of major mood disorders (Gómez-Sintes and Lucas, 2010). However, because of the narrow therapeutic window index, several side effects of lithium maintenance treatment have been reported in clinical studies, including polyuria, polydipsia, tremor, and weight gain (Gitlin, 2016; Schoot et al., 2020). In this study, we used medium doses of GSK3β inhibitors, and previous studies reported that these dosages significantly inhibited GSK3β activity but rarely caused behavioral and cognitive deficits (Mines, 2013; Xing et al., 2016; Nguyen et al., 2017; Pan et al., 2018; Xiang et al., 2021). Accordingly, our results indicated that chronic GSK3β intervention (systemic and within CA1) did not affect locomotor activity, recognition memory, or CA1 synaptic ultrastructure during the treatment phase. However, acute systemic GSK3β intervention decreased locomotor activity and induced anxiety-like behavior in the OFT. Previously, striatal dopaminergic circuits were implicated in locomotor activity and anxiety disorders (Macpherson and Hikida, 2019; Casado-Sainz et al., 2022), while striatal physiology is affected preferentially by GSK3β inhibition compared with some other brain regions (Gómez-Sintes and Lucas, 2010); thus, the acute side effects may be due to the targeted effects of systemic administration of LiCl on the striatum. Anxiety-like behavior may also be associated with the aversive effect of LiCl, as LiCl was a classical agent for inducing condition place aversion (Cloutier et al., 2018). Therefore, the potential side effects of GSK3β inhibitors should be carefully considered when treating adult deficits associated with adolescent METH abuse, and brain region-targeting therapy may be a good strategy.

We used the modified two-trial Y-maze test to detect novel spatial exploration behavior; however, our results showed that both acute and chronic GSK3β interventions had no significant therapeutic effects on adolescent METH exposure-induced novel spatial exploration impairment in adulthood. Novel spatial exploration critically depends on the intact function of novel exploration and recognition memory (Melnikova et al., 2006; Szalardy et al., 2018). To further confirm which function was more difficult to improve by GSK3β inhibition, we performed a standard two-trial Y-maze test in a separate cohort. We verified that chronic GSK3β intervention rescued adolescent METH exposure-induced spatial recognition memory impairment in adulthood. Moreover, the mice avoided the novel arm in the modified two-trial Y-maze test because the average time spent in the novel arm (%) was less than one-third, which is typical if the mice have no preference for each arm (Dellu et al., 2000). Anxiety also gives rise to exploration behavioral deficits; however, previous study confirmed that adult mice with adolescent METH exposure did not exhibit anxiety-like behavior in a similar time window (Yan et al., 2019). In the modified two-trial Y-maze test, to increase recognition and navigation in the novel space, the wall of the novel arm was marked integrally with a black-and-white stripe that was entirely different from the other arms, and we speculated that this novel space would generate mild stress in mice, causing avoidance behavior (Aylward et al., 2019; Vogel and Schwabe, 2019; Kondev et al., 2022). The stress-related avoidance behavior in this study may be because some other brain regions are also damaged by adolescent METH exposure, which is difficult to ameliorate by GSK3β inhibition in adulthood. Further studies are required to confirm these results.

This study has three limitations that must be addressed. First, LiCl and SB216763 directly inhibit GSK3α and GSK3β. Although GSK3α is involved in fewer signaling pathways than GSK3β, and its expression level is relatively lower and decreases with age (KEGG pathway)[1] (Giese, 2009), the effect of GSK3α cannot be eliminated in the present study. Second, although LiCl and SB216763 could rescue hyperactivation of GSK3β in several disease-associated rodent models (Maixner and Weng, 2013; Barr and Unterwald, 2020), in the present study, there was still an interval of several days between behavioral tests and the molecular and ultrastructural analysis, suggesting that alterations in molecular and synaptic plasticity may not perfectly reflect behavioral alterations. Third, this study is still a preclinical work, mice cannot fully mimic human drug abuse behavior, and the side effects of GSK3β inhibitor remain elusive, investigating GSK3β inhibitor-related toxicity, behavioral and cognitive alterations is necessary in future studies.

In summary, the present results revealed that chronic GSK3β inhibition attenuates chronic METH exposure-induced hyperactivity and recognition memory impairment by rescuing synaptic ultrastructural abnormalities in the DHP CA1 subregion in adulthood. This extends the scope of potential applications of GSK3β inhibitors and suggests that chronic administration of GSK3β inhibitors maybe an option for treating behavioral and cognitive deficits associated with adolescent METH abuse in adulthood.

Data availability statement

The original contributions presented in the study are included in the article/Supplementary material, further inquiries can be directed to the corresponding authors.

Ethics statement

The animal study was reviewed and approved by the Institutional Animal Care and Use Committee of Xi'an Jiaotong University.

Author contributions

PY, SW, and JLa conceived and designed the study. PY, JLi, HM, YF, JC, and YB performed the experiments and acquired the data. XH, YZ, and SW provided technical support and analyzed the data. PY and JLa wrote the manuscript. All authors contributed to the article and approved the submitted version.

1 http://www.genome.jp/kegg/pathway.html

Funding

This work was supported by the National Natural Science Foundation of China (Grant Nos. 82001999 and 82171880), the China Postdoctoral Science Foundation (Grant No. 2020M673422), and the NHC Key Laboratory of Forensic Science (Xi'an Jiaotong University) Open Projects Fund (Grant No. 2020FYXH002).

Conflict of interest

The authors declare that the research was conducted in the absence of any commercial or financial relationships that could be construed as a potential conflict of interest.

Publisher's note

Supplementary material

The Supplementary material for this article can be found online at: https://www.frontiersin.org/articles/10.3389/fnmol.2023.1129553/full#supplementary-material

References

Aylward, J., Valton, V., Ahn, W.-Y., Bond, R. L., Dayan, P., Roiser, J. P., et al. (2019). Altered learning under uncertainty in unmedicated mood and anxiety disorders. *Nat. Hum. Behav.* 3, 1116–1123. doi: 10.1038/s41562-019-0628-0

Barr, J. L., and Unterwald, E. M. (2020). Glycogen synthase kinase-3 signaling in cellular and behavioral responses to psychostimulant drugs. *Biochim. Biophys. Acta, Mol. Cell Res.* 1867:118746. doi: 10.1016/j.bbamcr.2020.118746

Basedow, L. A., Kuitunen-Paul, S., Wiedmann, M. F., Ehrlich, S., Roessner, V., and Golub, Y. (2021). Verbal learning impairment in adolescents with methamphetamine use disorder: a cross-sectional study. *BMC Psychiatry* 21:166. doi: 10.1186/s12888-021-03169-3

Beurel, E., Grieco, S. F., and Jope, R. S. (2015). Glycogen synthase kinase-3 (GSK3): regulation, actions, and diseases. *Pharmacol. Ther.* 148, 114–131. doi: 10.1016/j.pharmthera.2014.11.016

Bhat, R. V., Andersson, U., Andersson, S., Knerr, L., Bauer, U., and Sundgren-Andersson, A. K. (2018). The conundrum of GSK3 inhibitors: is it the dawn of a new beginning? *J. Alzheimers Dis.* 64, S547–S554. doi: 10.3233/JAD-179934

Borczyk, M., Radwanska, K., and Giese, K. P. (2021). The importance of ultrastructural analysis of memory. *Brain Res. Bull.* 173, 28–36. doi: 10.1016/j.brainresbull.2021.04.019

Brust, V., Schindler, P. M., and Lewejohann, L. (2015). Lifetime development of behavioural phenotype in the house mouse (*Mus musculus*). *Front. Zool.* 12:S17. doi: 10.1186/1742-9994-12-s1-s17

Casado-Sainz, A., Gudmundsen, F., Baerentzen, S. L., Lange, D., Ringsted, A., Martinez-Tejada, I., et al. (2022). Dorsal striatal dopamine induces fronto-cortical hypoactivity and attenuates anxiety and compulsive behaviors in rats. *Neuropsychopharmacology* 47, 454–464. doi: 10.1038/s41386-021-01207-y

Chen, X., Sun, G., Tian, E., Zhang, M., Davtyan, H., Beach, T. G., et al. (2021). Modeling sporadic Alzheimer's disease in human brain organoids under serum exposure. *Adv. Sc.* 8, –e2101462. doi: 10.1002/advs.202101462

Cloutier, C. J., Kavaliers, M., and Ossenkopp, K.-P. (2018). Lipopolysaccharide (LPS) induced sickness in adolescent female rats alters the acute-phase response and lithium chloride (LiCl)- induced impairment of conditioned place avoidance/aversion learning, following a homotypic LPS challenge in adulthood. *Behav. Brain Res.* 351, 121–130. doi: 10.1016/j.bbr.2018.05.033

Dellu, F., Contarino, A., Simon, H., Koob, G. F., and Gold, L. H. (2000). Genetic differences in response to novelty and spatial memory using a two-trial recognition task in mice. *Neurobiol. Learn. Mem.* 73, 31–48. doi: 10.1006/nlme.1999.3919

Demuro, S., Di Martino, R. M. C., Ortega, J. A., and Cavalli, A. (2021). GSK-3β, FYN, and DYRK1A: master regulators in neurodegenerative pathways. *Int. J. Mol. Sci.* 22:9098. doi: 10.3390/ijms22169098

Fanselow, M. S., and Dong, H. W. (2010). Are the dorsal and ventral hippocampus functionally distinct structures? *Neuron* 65, 7–19. doi: 10.1016/j.neuron.2009.11.031

Franklin, K.B.J., and Paxinos, G. (2001). *The mouse brain in stereotaxic coordinates*. San Diego, CA: Academic Press.

Fuhrmann, D., Knoll, L. J., and Blakemore, S.-J. (2015). Adolescence as a sensitive period of brain development. *Trends Cogn. Sci.* 19, 558–566. doi: 10.1016/j.tics.2015.07.008

García-Cabrerizo, R., Bis-Humbert, C., and García-Fuster, M. J. (2018). Methamphetamine binge administration during late adolescence induced enduring hippocampal cell damage following prolonged withdrawal in rats. *Neurotoxicology* 66, 1–9. doi: 10.1016/j.neuro.2018.02.016

Giese, K. P. (2009). GSK-3: a key player in neurodegeneration and memory. *IUBMB Life*, 61:516–521. doi: 10.1002/iub.187

Gitlin, M. (2016). Lithium side effects and toxicity: prevalence and management strategies. *Int. J. Bipolar Disord.* 4:27. doi: 10.1186/s40345-016-0068-y

Gómez-Sintes, R., and Lucas, J. J. (2010). NFAT/Fas signaling mediates the neuronal apoptosis and motor side effects of GSK-3 inhibition in a mouse model of lithium therapy. *J. Clin. Invest.* 120, 2432–2445. doi: 10.1172/JCI37873

Gyu, H. J., Hyun, K. D., Hwan, L. C., Se Jin, P., Jong Min, K., Mudan, C., et al. (2012). GSK-3β activity in the hippocampus is required for memory retrieval. *Neurobiol. Learn. Mem.* 98, 122–129. doi: 10.1016/j.nlm.2012.07.003

Hiratsu, A., Tataka, Y., Namura, S., Nagayama, C., Hamada, Y., and Miyashita, M. (2022). The effects of acute and chronic oral L-arginine supplementation on exercise-induced ammonia accumulation and exercise performance in healthy young men: a randomised, double-blind, cross-over, placebo-controlled trial. *J. Exerc. Sci. Fitness* 20, 140–147. doi: 10.1016/j.jesf.2022.02.003

Jung, S., Kim, Y., Kim, M., Seo, M., Kim, S., Kim, S., et al. (2021). Exercise pills for drug addiction: forced moderate endurance exercise inhibits methamphetamine-induced hyperactivity through the striatal glutamatergic signaling pathway in male Sprague Dawley rats. *Int. J. Mol. Sci.* 22:8203. doi: 10.3390/ijms22158203

Kamei, H., Nagai, T., Nakano, H., Togan, Y., Takayanagi, M., Takahashi, K., et al. (2006). Repeated methamphetamine treatment impairs recognition memory through a failure of novelty-induced ERK1/2 activation in the prefrontal cortex of mice. *Biol. Psychiatry* 59, 75–84. doi: 10.1016/j.biopsych.2005.06.006

Kim, K.-H., Oudit, G. Y., and Backx, P. H. (2008). Erythropoietin protects against doxorubicin-induced cardiomyopathy via a phosphatidylinositol 3-kinase-dependent pathway. *J. Pharmacol. Exp. Ther.* 324, 160–169. doi: 10.1124/jpet.107.125773

King, M. K., Pardo, M., Cheng, Y., Downey, K., Jope, R. S., and Beurel, E. (2014). Glycogen synthase kinase-3 inhibitors: rescuers of cognitive impairments. *Pharmacol. Ther.* 141, 1–12. doi: 10.1016/j.pharmthera.2013.07.010

Kondev, V., Morgan, A., Najeed, M., Winters, N. D., Kingsley, P. J., Marnett, L., et al. (2022). The endocannabinoid 2-Arachidonoylglycerol Bidirectionally modulates acute and protracted effects of predator odor exposure. *Biol. Psychiatry* 92, 739–749. doi: 10.1016/j.biopsych.2022.05.012

Kusljic, S., and van den Buuse, M. (2004). Functional dissociation between serotonergic pathways in dorsal and ventral hippocampus in psychotomimetic drug-induced locomotor hyperactivity and prepulse inhibition in rats. *Eur. J. Neurosci.* 20, 3424–3432. doi: 10.1111/j.1460-9568.2004.03804.x

Lee, J. H., and Kim, D. G. (2019). Diminished food-related motivation in adult rats treated with methamphetamine during adolescence. *Neuroreport* 30, 1143–1147. doi: 10.1097/WNR.0000000000001325

Leger, M., Quiedeville, A., Bouet, V., Haelewyn, B., Boulouard, M., Schumann-Bard, P., et al. (2013). Object recognition test in mice. *Nat. Protoc.* 8, 2531–2537. doi: 10.1038/nprot.2013.155

Leung, C., Kim, J. C., and Jia, Z. (2018). Three-chamber social approach task with Optogenetic stimulation (mice). *Biol. Protoc.* 8:e3120:e3120. doi: 10.21769/BioProtoc.3120

Li, X., and Polter, A. (2011). Glycogen synthase Kinase-3 is an intermediate modulator of serotonin neurotransmission. *Front. Mol. Neurosci.* 4:31. doi: 10.3389/fnmol.2011.00031

Liang, M., Zhu, L., Wang, R., Su, H., Ma, D., Wang, H., et al. (2022). Methamphetamine exposure in adolescent impairs memory of mice in adulthood accompanied by changes in neuroplasticity in the dorsal hippocampus. *Front. Cell. Neurosci.* 16:892757. doi: 10.3389/fncel.2022.892757

Lin, L., Cao, J., Yang, S.-S., Fu, Z.-Q., Zeng, P., Chu, J., et al. (2018). Endoplasmic reticulum stress induces spatial memory deficits by activating GSK-3. *J. Cell. Mol. Med.* 22, 3489–3502. doi: 10.1111/jcmm.13626

Luikinga, S. J., Kim, J. H., and Perry, C. J. (2018). Developmental perspectives on methamphetamine abuse: exploring adolescent vulnerabilities on brain and behavior. *Prog. Neuro Psychopharmacol. Biol. Psychiatry* 87, 78–84. doi: 10.1016/j.pnpbp.2017.11.010

Macpherson, T., and Hikida, T. (2019). Role of basal ganglia neurocircuitry in the pathology of psychiatric disorders. *Psychiatry Clin. Neurosci.* 73, 289–301. doi: 10.1111/pcn.12830

Maixner, D. W., and Weng, H. R. (2013). The role of glycogen synthase kinase 3 Beta in neuroinflammation and pain. *J. Pharm. Pharmacol.* 1:001. doi: 10.13188/2327-204X.1000001

Melnikova, T., Savonenko, A., Wang, Q., Liang, X., Hand, T., Wu, L., et al. (2006). Cycloxygenase-2 activity promotes cognitive deficits but not increased amyloid burden in a model of Alzheimer's disease in a sex-dimorphic pattern. *Neuroscience* 141, 1149–1162. doi: 10.1016/j.neuroscience.2006.05.001

Mines, M. A. (2013). Hyperactivity: glycogen synthase kinase-3 as a therapeutic target. *Eur. J. Pharmacol.* 708, 56–59. doi: 10.1016/j.ejphar.2013.02.055

Nazari, A., Perez-Fernandez, C., Flores, P., Moreno, M., and Sánchez-Santed, F. (2020). Age-dependent effects of repeated methamphetamine exposure on locomotor activity and attentional function in rats. *Pharmacol. Biochem. Behav.* 191:172879. doi: 10.1016/j.pbb.2020.172879

Neuwirth, L. S., Verrengia, M. T., Harikinish-Murrary, Z. I., Orens, J. E., and Lopez, O. E. (2022). Under or absent reporting of light stimuli in testing of anxiety-like behaviors in rodents: the need for standardization. *Front. Mol. Neurosci.* 15:912146. doi: 10.3389/fnmol.2022.912146

Nguyen, T., Fan, T., George, S. R., and Perreault, M. L. (2017). Disparate effects of lithium and a GSK-3 inhibitor on neuronal oscillatory activity in prefrontal cortex and hippocampus. *Front. Aging Neurosci.* 9:434. doi: 10.3389/fnagi.2017.00434

North, A., Swant, J., Salvatore, M. F., Gamble-George, J., Prins, P., Butler, B., et al. (2013). Chronic methamphetamine exposure produces a delayed, long-lasting memory deficit. *Synapse* 67, 245–257. doi: 10.1002/syn.21635

Ochoa, E. L. M. (2022). Lithium as a neuroprotective agent for bipolar disorder: an overview. *Cell. Mol. Neurobiol.* 42, 85–97. doi: 10.1007/s10571-021-01129-9

Pan, Y., Short, J. L., Newman, S. A., Choy, K. H. C., Tiwari, D., Yap, C., et al. (2018). Cognitive benefits of lithium chloride in APP/PS1 mice are associated with enhanced brain clearance of β-amyloid. *Brain Behav. Immun.* 70, 36–47. doi: 10.1016/j.bbi.2018.03.007

Salcedo-Tello, P., Ortiz-Matamoros, A., and Arias, C. (2011). GSK3 function in the brain during development, neuronal plasticity, and neurodegeneration. *Int. J. Alzheimers Dis.* 2011:189728. doi: 10.4061/2011/189728

Schoot, T. S., Molmans, T. H. J., Grootens, K. P., and Kerckhoffs, A. P. M. (2020). Systematic review and practical guideline for the prevention and management of the renal side effects of lithium therapy. *Eur. Neuropsychopharmacol.* 31, 16–32. doi: 10.1016/j.euroneuro.2019.11.006

Shukla, M., and Vincent, B. (2021). Methamphetamine abuse disturbs the dopaminergic system to impair hippocampal-based learning and memory: an overview of animal and human investigations. *Neurosci. Biobehav. Rev.* 131, 541–559. doi: 10.1016/j.neubiorev.2021.09.016

Spear, L. P. (2015). Adolescent alcohol exposure: are there separable vulnerable periods within adolescence? *Physiol. Behav.* 148, 122–130. doi: 10.1016/j.physbeh.2015.01.027

Spear, L. P. (2016). Consequences of adolescent use of alcohol and other drugs: studies using rodent models. *Neurosci. Biobehav. Rev.* 70, 228–243. doi: 10.1016/j.neubiorev.2016.07.026

Szalardy, L., Molnar, M. F., Zadori, D., Cseh, E. K., Veres, G., Kovacs, G. G., et al. (2018). Non-motor behavioral alterations of PGC-1α-deficient mice – a peculiar phenotype with slight male preponderance and no apparent progression. *Front. Behav. Neurosci.* 12:180. doi: 10.3389/fnbeh.2018.00180

Takahashi-Yanaga, F. (2013). Activator or inhibitor? GSK-3 as a new drug target. *Biochem. Pharmacol.* 86, 191–199. doi: 10.1016/j.bcp.2013.04.022

Takahashi-Yanaga, F., Shiraishi, F., Hirata, M., Miwa, Y., Morimoto, S., and Sasaguri, T. (2004). Glycogen synthase kinase-3beta is tyrosine-phosphorylated by MEK1 in human skin fibroblasts. *Biochem. Biophys. Res. Commun.* 316, 411–415. doi: 10.1016/j.bbrc.2004.02.061

Tanimizu, T., Kenney, J. W., Okano, E., Kadoma, K., Frankland, P. W., and Kida, S. (2017). Functional connectivity of multiple brain regions required for the consolidation of social recognition memory. *J. Neurosci.* 37, 4103–4116. doi: 10.1523/jneurosci.3451-16.2017

Teixeira-Gomes, A., Costa, V. M., Feio-Azevedo, R., Bastos Mde, L., Carvalho, F., and Capela, J. P. (2015). The neurotoxicity of amphetamines during the adolescent period. *Int. J. Dev. Neurosci.* 41, 44–62. doi: 10.1016/j.ijdevneu.2014.12.001

UNODC (2019). *World drug report 2019*. New York: UNODC.

Vogel, S., and Schwabe, L. (2019). Stress, aggression, and the balance of approach and avoidance. *Psychoneuroendocrinology* 103, 137–146. doi: 10.1016/j.psyneuen.2019.01.020

Vorhees, C. V., Reed, T. M., Morford, L. L., Fukumura, M., Wood, S. L., Brown, C. A., et al. (2005). Periadolescent rats (P41–50) exhibit increased susceptibility to d-methamphetamine-induced long-term spatial and sequential learning deficits compared to juvenile (P21–30 or P31–40) or adult rats (P51–60). *Neurotoxicol. Teratol.* 27, 117–134. doi: 10.1016/j.ntt.2004.09.005

Wang, F., He, Q., Gao, Z., and Redington, A. N. (2021). Atg5 knockdown induces age-dependent cardiomyopathy which can be rescued by repeated remote ischemic conditioning. *Basic Res. Cardiol.* 116:47. doi: 10.1007/s00395-021-00888-2

Wang, Y., Yin, F., Guo, H., Zhang, J., Yan, P., and Lai, J. (2017). The role of dopamine D1 and D3 receptors in N-methyl-D-aspartate (NMDA)/GlycineB site-regulated complex cognitive behaviors following repeated morphine administration. *Int. J. Neuropsychopharmacol.* 20, 562–574. doi: 10.1093/ijnp/pyx010

Weaver, J., Yang, Y., Purvis, R., Weatherwax, T., Rosen, G. M., and Liu, K. J. (2014). In vivo evidence of methamphetamine induced attenuation of brain tissue oxygenation as measured by EPR oximetry. *Toxicol. Appl. Pharmacol.* 275, 73–78. doi: 10.1016/j.taap.2013.12.023

Westbrook, S. R., Dwyer, M. R., Cortes, L. R., and Gulley, J. M. (2020). Extended access self-administration of methamphetamine is associated with age-and sex-dependent differences in drug taking behavior and recognition memory in rats. *Behav. Brain Res.* 390:112659:112659. doi: 10.1016/j.bbr.2020.112659

Wu, J., Zhu, D., Zhang, J., Li, G., Liu, Z., and Sun, J. (2015). Lithium protects against methamphetamine-induced neurotoxicity in PC12 cells via Akt/GSK3beta/mTOR pathway. *Biochem. Biophys. Res. Commun.* 465, 368–373. doi: 10.1016/j.bbrc.2015.08.005

Xiang, J., Ran, L.-Y., Zeng, X.-X., He, W.-W., Xu, Y., Cao, K., et al. (2021). LiCl attenuates impaired learning and memory of APP/PS1 mice, which in mechanism involves α7 nAChRs and Wnt/β-catenin pathway. *J. Cell. Mol. Med.* 25, 10698–10710. doi: 10.1111/jcmm.17006

Xing, B., Li, Y. C., and Gao, W. J. (2016). GSK3beta hyperactivity during an early critical period impairs prefrontal synaptic plasticity and induces lasting deficits in spine morphology and working memory. *Neuropsychopharmacology* 41, 3003–3015. doi: 10.1038/npp.2016.110

Xing, B., Liang, X.-P., Liu, P., Zhao, Y., Chu, Z., and Dang, Y.-H. (2015). Valproate inhibits methamphetamine induced hyperactivity via glycogen synthase kinase 3β signaling in the nucleus Accumbens Core. *PLoS One* 10:e0128068. doi: 10.1371/journal.pone.0128068

Xu, C. M., Wang, J., Wu, P., Xue, Y. X., Zhu, W. L., Li, Q. Q., et al. (2011). Glycogen synthase kinase 3beta in the nucleus accumbens core is critical for methamphetamine-induced behavioral sensitization. *J. Neurochem.* 118, 126–139. doi: 10.1111/j.1471-4159.2011.07281.x

Yan, P., Xu, D., Ji, Y., Yin, F., Cui, J., Su, R., et al. (2019). LiCl pretreatment ameliorates adolescent methamphetamine exposure-induced long-term alterations in behavior and hippocampal ultrastructure in adulthood in mice. *Int. J. Neuropsychopharmacol.* 22, 303–316. doi: 10.1093/ijnp/pyz001

Ye, T., Pozos, H., Phillips, T. J., and Izquierdo, A. (2014). Long-term effects of exposure to methamphetamine in adolescent rats. *Drug Alcohol Depend.* 138, 17–23. doi: 10.1016/j.drugalcdep.2014.02.021

Zhao, R., Chen, J., Ren, Z., Shen, H., and Zhen, X. (2016). GSK-3β inhibitors reverse cocaine-induced synaptic transmission dysfunction in the nucleus accumbens. *Synapse* 70, 461–470. doi: 10.1002/syn.21922

Zhu, H., Yoshimoto, T., Imajo-Ohmi, S., Dazortsava, M., Mathivanan, A., and Yamashima, T. (2012). Why are hippocampal CA1 neurons vulnerable but motor cortex neurons resistant to transient ischemia? *J. Neurochem.* 120, 574–585. doi: 10.1111/j.1471-4159.2011.07550.x

frontiers | Frontiers in Molecular Neuroscience

TYPE Review
PUBLISHED 30 March 2023
DOI 10.3389/fnmol.2023.1125277

OPEN ACCESS

EDITED BY
Juan Marín-Lahoz,
Hospital Universitario Miguel Servet,
Spain

REVIEWED BY
Nicolas Gervasi,
Institut National de la Santé et de la Recherche Médicale (INSERM),
France
A.J. Baucum,
Indiana University Bloomington,
United States

*CORRESPONDENCE
Lin Chen
✉ hdycl@126.com
Yuxiang Wu
✉ yxwu@jhun.edu.cn

SPECIALTY SECTION
This article was submitted to Neuroplasticity and Development, a section of the journal Frontiers in Molecular Neuroscience

RECEIVED 16 December 2022
ACCEPTED 14 March 2023
PUBLISHED 30 March 2023

CITATION
Ru Q, Wang Y, Zhou E, Chen L and Wu Y (2023) The potential therapeutic roles of Rho GTPases in substance dependence.
Front. Mol. Neurosci. 16:1125277.
doi: 10.3389/fnmol.2023.1125277

The potential therapeutic roles of Rho GTPases in substance dependence

Qin Ru, Yu Wang, Enyuan Zhou, Lin Chen* and Yuxiang Wu*

Department of Health and Physical Education, Jianghan University, Wuhan, China

Rho GTPases family are considered to be molecular switches that regulate various cellular processes, including cytoskeleton remodeling, cell polarity, synaptic development and maintenance. Accumulating evidence shows that Rho GTPases are involved in neuronal development and brain diseases, including substance dependence. However, the functions of Rho GTPases in substance dependence are divergent and cerebral nuclei-dependent. Thereby, comprehensive integration of their roles and correlated mechanisms are urgently needed. In this review, the molecular functions and regulatory mechanisms of Rho GTPases and their regulators such as GTPase-activating proteins (GAPs) and guanine nucleotide exchange factors (GEFs) in substance dependence have been reviewed, and this is of great significance for understanding their spatiotemporal roles in addictions induced by different addictive substances and in different stages of substance dependence.

KEYWORDS

Rho GTPases, substance dependence, GTPase-activating proteins, guanine nucleotide exchange factors, cytoskeleton remodeling

1. Introduction

The Ras-like superfamily G proteins are monomer proteins of approximately 21 kDa that function as molecular switches to regulate a wide range of primary and versatile cellular processes (Shutes and Der, 2004; Gao et al., 2019; Casalou et al., 2020). There are nine major subgroups in the Ras-like superfamily, including Ras, Rab, and Rho families (Figure 1). Even between distantly related clades, members in the Ras-like superfamily share 65–85% amino-acid sequence similarity (Rojas et al., 2012). This extreme conservation is inconsistent with their roles in fundamental cellular functions such as F-actin dynamics and endo/exocytosis. The Ras-like proteins rely on their structural changes between guanosine triphosphate (GTP)-binding conformation and guanosine diphosphate (GDP)-binding conformation, acting as binary signaling switches biochemically, and transmitting upstream signals to downstream molecules (Bosco et al., 2009; Raimondi et al., 2011).

Among Ras-like superfamily, the Rho family (Rho GTPases) with 22 members are primary regulators of the cytoskeleton remodeling, cell adhesion, polarity, and locomotion processes (Vega and Ridley, 2007). Rho GTPases are divided into nine subfamilies (Rac, Rho, RhoD, Cdc42, RhoH, RhoF, Rnd, Miro, and RhoBTB) according to their structure and function differences (Vega and Ridley, 2007). Like other members of Ras superfamily, most Rho GTPases cycle between an active GTP-bound state in the cell membrane and an inactive GDP-bound state in the cytoplasm. Activated Rho GTPases can contact with a variety of downstream effectors that regulates numerous cellular functions, such as cytoskeleton remodeling, cell motility, cell polarity, vesicle transport, cell adhesion and other essential life processes (Jung

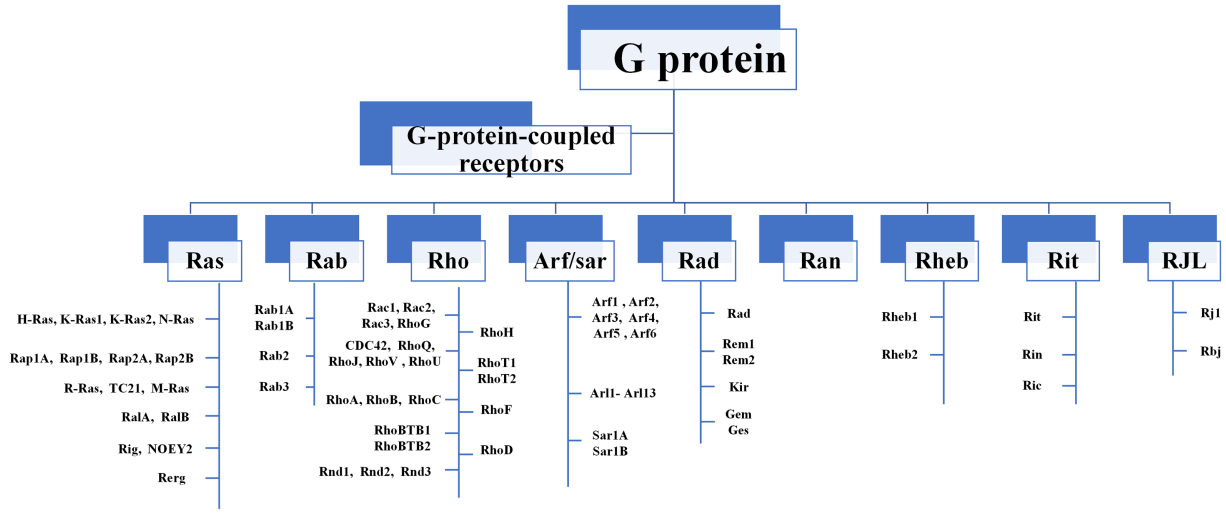

FIGURE 1
The composition of Ras-like superfamily. There are nine major subgroups in the Ras-like superfamily, including Ras, Rab, and Rho families. Rho GTPases can be divided into 9 subfamilies (Rac, Rho, RhoD, Cdc42, RhoH, RhoF, Rnd, Miro, RhoBTB) according to their structural and functional differences.

et al., 2020; Figure 2). Therefore, they are considered to be molecular switches of receptor signaling pathways on the surface of synapses, and contribute significantly in regulating the synaptic structure and neuron development, and are closely related to cognitive and emotional disorders and neurodegenerative diseases.

The high relapse rate of substance addiction mainly lies in the fact that addiction will form lasting, stubborn and environment-related memories in the human brain. The continuous morphological plasticity of dendritic spines and the functional plasticity of excitatory synaptic transmission may be the neurobiological mechanism of the abnormal behaviors induced by addictive substances. Preliminary studies showed that Rho GTPases might participate in the acquisition and extinction of addictive substances-associated contextual memory (Tu et al., 2019; Zhao et al., 2019). Therefore, in this review, we focused on several extensively investigated Rho GTPases involved in substance addiction. By detecting expression levels of these Rho GTPases and potential protein-protein interactions, we attempted to explore how these Rho GTPases and their modulators regulate specific signaling pathways spatiotemporally to affect changes in neuron structure and functional plasticity, thus participating in the pathological process of substance addiction.

2. The regulation of Rho GTPases

The activities of Rho GTPases are mainly controlled by three classes of regulators. The first-class is Rho GTPases guanine nucleotide exchange factors (Rho GEFs). Rho GEFs are classified into two subclasses, including dedicator of cytokinesis (DOCK)-related proteins (Benson and Southgate, 2021) and Dbl-like proteins, whose structure has similarity to the Dbl (diffuse B-cell lymphoma) protein (Jaiswal et al., 2013). Most Rho GEFs share a Dbl homology (DH) domain (170–190 amino acids) and Pleckstrin homology (PH) domain (approximately 100 amino acid). DH domain is responsible for the guanine nucleotide exchange activity on Rho GTPases, and the binding of DH domain to GTPases promotes the combination of Rho GTPase to GTP and catalyzes its conformational change, which can then activate a set of downstream effectors for signal transduction (Jaiswal et al., 2013). The PH domain anchors GEFs to the membrane by interacting with specific lipids on the membrane, then induces orientational and/or conformational changes on the membrane surface and activates Rho GTPase by aligning the DH domain to a particular cytoskeletal position to mediate cell transformation (Zheng et al., 1996; Baumeister et al., 2003). Rho GTPase activating proteins (Rho GAPs), which are negative regulatory factors, promote the hydrolysis of GTP into GDP within the Rho GTPase and inactivate the Rho GTPase to terminate signal transduction (Amin et al., 2016). Rho GAPs have a conserved catalytic domain named Rho GAP domain (approximately 190 amino acids), which can supply a conserved "arginine finger." Apart from conserved Rho GAP domains, Rho GAPs have several structural domains and sequence motifs, which take part in subcellular localization, lipid membrane association, and the connection to upstream signals (Jaiswal et al., 2014). Only a tiny amount of Rho GTPases are activated under normal physiological conditions, and the inactive Rho GTPases are associated with Rho GTPases guanine nucleotide dissociation inhibitors (Rho GDIs), which can isolate Rho GTPases in their GDP bound, inhibit the dissociation of GDP from Rho GTPase and stabilize the inactivation state of Rho GTPase (Matsuda et al., 2021). GDIs can be classified according to the specificity of G proteins, however, not all G proteins have GDIs (for example, the Rho and Rab families have GDIs, but the Ras family does not). Although different GDIs have some common structural and functional features, they usually have unrelated amino acid sequences, indicating that GDIs have appeared independently in the evolutionary process. To date, 3 Rho GDIs, 72 Rho GAPs, and 82 Rho GEFs have been identified in humans (Tcherkezian and Lamarche-Vane, 2007; Garcia-Mata et al., 2011; Amin et al., 2016; Fort and Blangy, 2017; Table 1). It is worth noting that post-translational modifications such as ubiquitination and phosphorylation can also regulate the activities of Rho GTPases

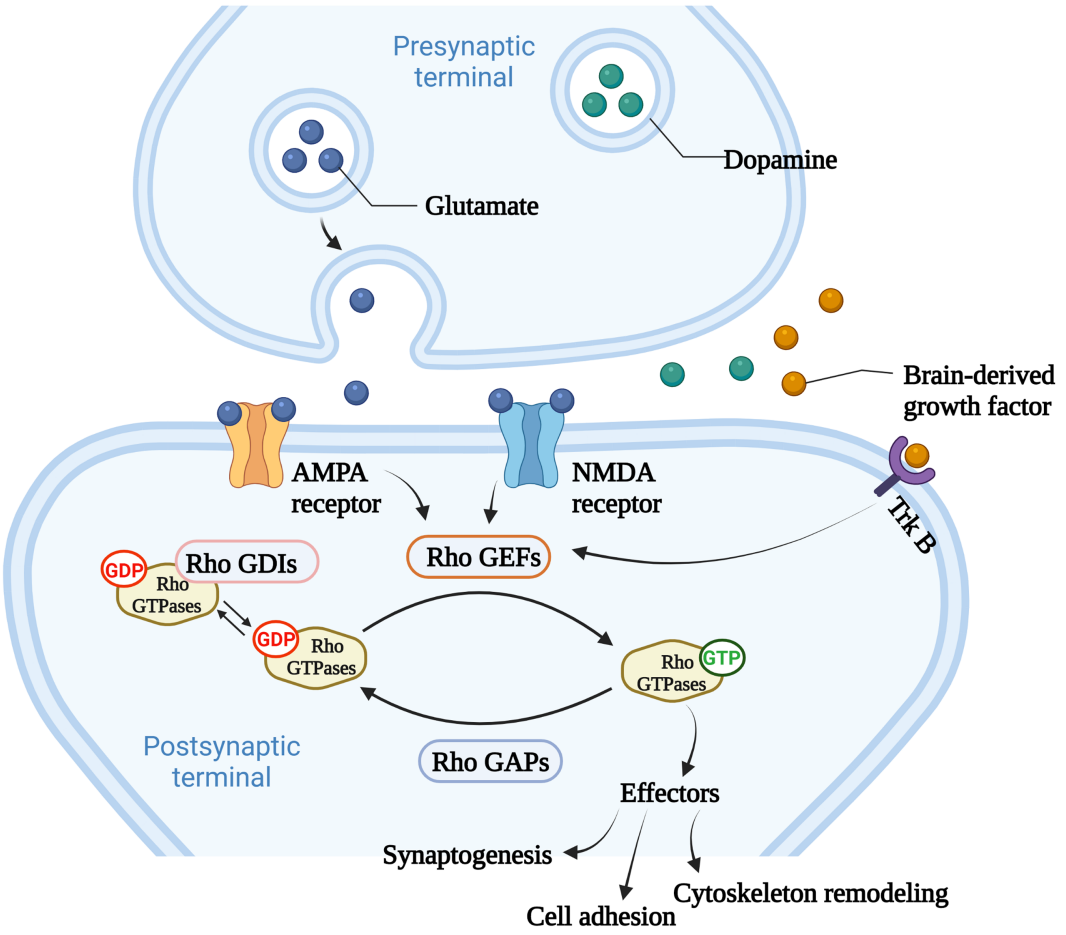

FIGURE 2
The main function of Rho GTPases. Rho GTPases cycles between an active GTP-bound state in the cell membrane and an inactive GDP-bound state in the cytoplasm, and the activity of Rho GTPases is regulated by Rho GTPases guanine nucleotide exchange factors (Rho GEFs), Rho GTPase activating proteins (Rho GAPs), and Rho GTPases guanine nucleotide dissociation inhibitors (Rho GDIs). Rho GEFs catalyze the conformational change of Rho GTPases and activate Rho GTPases. Rho GAPs facilitate the hydrolysis of GTP into GDP within Rho GTPases, and deactivate Rho GTPases. Rho GDIs inhibit the dissociation of GDP from Rho GTPases and stabilize the inactivation of Rho GTPases. Rho GTPases act as important molecular switches to transmit signals to downstream effectors that regulates numerous cellular functions, such as cytoskeleton remodeling, cell adhesion and other essential life processes.

Table 1 Addiction related Rho GTPase and their regulators.

Items	Number	Elements
Addiction related Rho GTPase	6	RHOD, RAC1, RAC2, RHOA, CDC42, RHOB
Addiction related Rho GEFs	13	FARP1, ARHGEF9, ARHGEF38, ALS2, ARHGEF12, ARHGEF2, PLEKHG2, ARHGEF3, ARHGEF1, ARHGEF6, AKAP13, SPATA13, RASGRF2
Addiction related Rho GAPs	7	ARHGAP39, OPHN1, BCR, ARHGAP28, SRGAP2, SRGAP3, ARHGAP6

(Abdrabou and Wang, 2018; Jung et al., 2020). These post-translational modifications and the regulators as mentioned above cooperatively determine the activation status, concentration, localization, and ability to bind downstream molecules of Rho GTPases.

3. The role of Rho GTPases on the regulation of synaptic plasticity

Synaptic connections between neurons are crucial to all aspects of neural activity and are therefore precisely regulated. Synaptic plasticity is the activity-dependent changes in the strength and efficacy of synaptic transmission across the synapses, and these changes are thought to underlie the neurobiology of addiction (Magee and Grienberger, 2020; Mateos-Aparicio and Rodriguez-Moreno, 2020).

The excitatory synapses of major neurons in the brain are mostly located at the tips of dendritic spines, which are dynamic structures,

and the rapid remodeling of dendritic spines is essential for synaptic formation, function, and plasticity. Inappropriate dendritic spinous morphogenesis may lead to impaired information processing in the brain. Therefore, abnormal dendritic spines are associated with many neurodevelopmental, neuropsychiatric, and neurodegenerative diseases, and dendritic spine morphology can be a proxy for synaptic strength (Tolias et al., 2011). Dendritic spines are highly enriched in filamentous actin (F-actin), and the rapid remodeling of actin cytoskeleton determines the morphologic change ability of dendritic spines. Therefore, Rho-GTPases, which are well-known for their ability to control actin cytoskeleton dynamics, are undoubtedly an important part of the regulatory mechanism of dendritic spines morphogenesis (Duman et al., 2022). Ras-related C3 botulinum toxin substrate 1 (Rac1), cell division control protein 42 homolog (Cdc42) and Ras homolog family member A (RhoA) are the most studied members of the Rho GTPase family, and Rac1 and Cdc42 promote the formation, growth and maintenance of spine, while RhoA has opposite effects (Govek et al., 2005). For instance, cofilin cuts off F-actin, creating new barbed end for polymerization or causing actin depolymerization, which is necessary to regulate the density and morphology of mature spine (Cao et al., 2017). Serine/threonine kinase PAK1 is the main downstream effect of Rac1 and Cdc42. Rac1 and Cdc42 induce phosphorylation of LIMK and cofilin through PAK1 to inhibit cofilin activity, while inhibition of cofilin phosphorylation and F-actin polymerization resulted in loss of dendritic spines (Yang et al., 2018). The Arp2/3 complex is one of the most important intracellular actins nucleators, which forms actin networks and caps the ends of actin filaments (Chou and Wang, 2016), therefore, Arp2/3 is necessary for the formation and remodeling of actin cytoskeleton to regulate spine morphology and function. The function of the Arp2/3 complex is highly regulated by nucleation promoters such as Wiskott-Aldrich Syndrome protein (WASP) or WASP-family verprolin homologous protein 2 (WAVE2) (Stradal and Scita, 2006). Cdc42 activates Arp2/3 through N-WASP, which drives actin polymerization and dendritic spine development in neurons (Hasegawa et al., 2022). Similarly, Rac1 regulates Arp2/3 mediated actin polymerization by activating WAVE2 through IRSp53, and is involved in the formation and development of synapses (Ding et al., 2022). Rho-GTPases are essential for regulating excitatory synaptic formation and plasticity of mature synapses in neurodevelopment (Figure 3). Chronic substance dependence leads to behavioral, morphological and neurochemical plasticity changes that underlie compulsive drug-seeking behavior and relapse after withdrawal. Identifying and reversing the synaptic plasticity associated with addiction is considered a potential intervention strategy for drug addiction (Smith and Kenny, 2018; Speranza et al., 2021).

4. Rho GTPases and substance dependence

Abnormal morphology and density of dendritic spines could be observed in patients and animals with addiction (Beltran-Campos et al., 2015; Yin et al., 2020), accompanied by abnormal expression and activation level of Rho GTPase and its regulatory factors (Cahill et al., 2018). Regulation of Rho GTPase activities is very crucial for treating substance dependence (Table 2).

4.1. Rho GTPases and mesolimbic dopamine (DA) system

Dopamine (DA) has long been considered as an important regulatory neurotransmitter, regulating salience encoding, memory expression, reward prediction, and addiction (Langdon and Daw, 2020; Lin et al., 2020, 2021). Both reward and aversion stimuli activate dopaminergic neurons and promote the release of DA (Lin et al., 2020; Liu et al., 2022). The mesolimbic DA system, the dopaminergic neurons in the ventral tegmental area (VTA) project to the brain regions involved in emotional, motivational, and executive functions such as the nucleus accumbens (NAc), amygdale, and prefrontal cortex (PFC) (Serafini et al., 2020). In the field of substance dependence, the mesolimbic DAsystem is the common pathway for addictive substances to induce reward effect, and it is involved in the positive reinforcement effect, pathological memory, craving caused by addictive substances, and emotional reactions such as anxiety and fear after withdrawal (Natividad et al., 2012). Addictive substances can directly or indirectly excite VTA and cause a rapid and extensive DA release, thereby producing a rewarding effect (di Volo et al., 2019; Christoffel et al., 2021). Repeated DA treatments, which could mimic the increase of DA in synaptic transmission, increased the dendritic branching spine density of primary cortex neurons (Li J. et al., 2015). The application of DA can significantly activate Rac1 whereas decrease RhoA activity (Li J. et al., 2015). At the same time, SCH23390, the inhibitor of dopamine receptor 1 (DRD1), could inhibit the morphogenesis of dendrites and spines induced by DA treatment, and SKF81297, an agonist of DRD1, could promote neuronal morphogenesis (Li J. et al., 2015). Further results have shown that the activation of Rac1 had a positive effect on DA-induced morphogenesis, while the activation of RhoA has a negative effect, and Rac1 could interact with RhoA and then inhibit RhoA activity (Li J. et al., 2015), indicating the activation of Rac1 was a necessary condition for DA to induce RhoA inactivation, and Rac1 and RhoA had different roles in the regulation of dendritic morphogenesis following DA stimulation.

4.2. Rho GTPases in morphine dependence

Growing evidence indicated that Rho GTPases were intracellular targets of addictive substances and were involved in drug-induced dendritic spines morphogenic changes and behavior changes. After morphine conditional place preference (CPP) training, the number of hippocampal thin dendritic spines was significantly reduced, and the expression of RhoA on synapses increased, and morphine-induced CPP could be prevented by microinjection of the Rho-associated protein kinase 1 (ROCK) inhibitor H1152 to block RhoA signaling (Fakira et al., 2016), showing that the RhoA/ROCK signaling pathway was involved in the formation of morphine-induced place preference, and local inhibition of this pathway in the hippocampus completely prevents morphine-associated environmental cues (Figure 4). Although acute morphine withdrawal did not alter the synaptoneurosomal expression of the RhoA pathway, the increased expression of the RhoA network in NAc has excessively engaged and facilitated the selective elimination of thin spines on medium-sized spiny neurons (MSNs) after 2 weeks of morphine withdrawal (Cahill et al., 2018), suggesting heightened RhoA signaling pathway had a

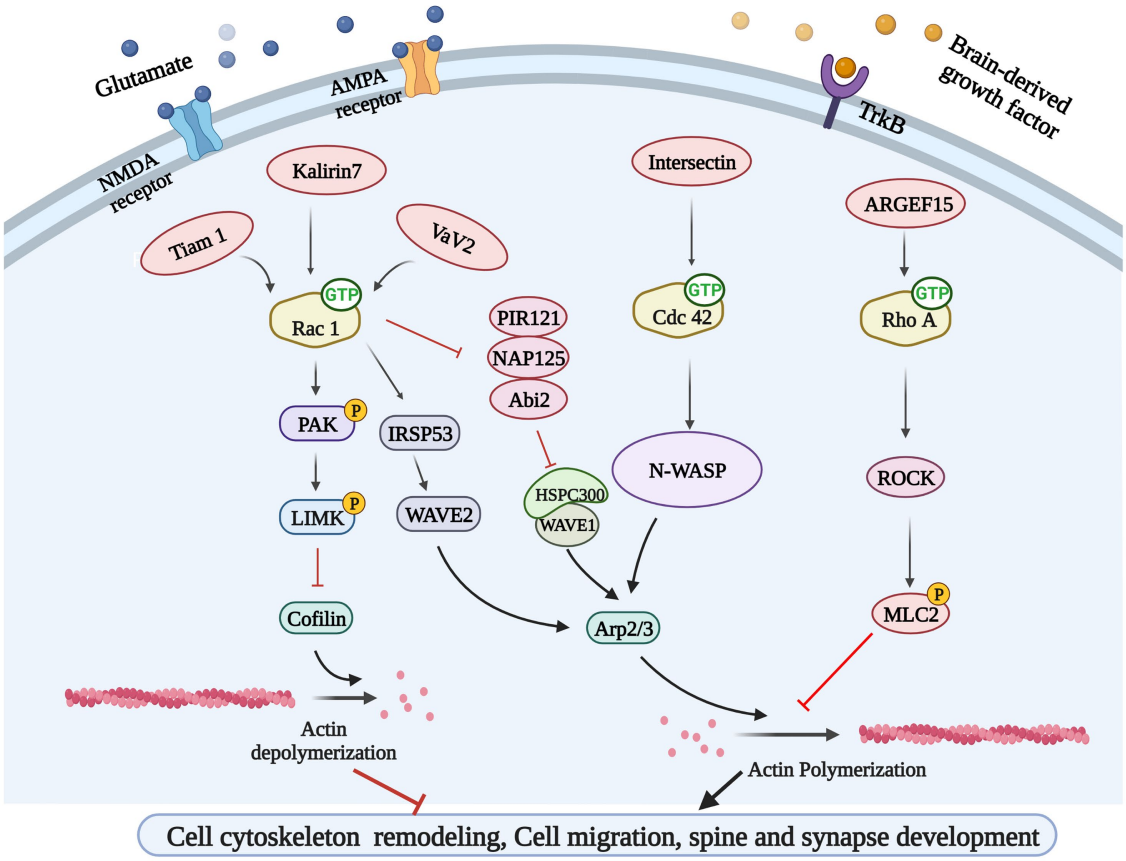

FIGURE 3
Rho GTPases-related signaling pathways. Glutamate and brain-derived neurotrophic factor (BDNF) could bind to their corresponding receptors and activate Rho GEFs, leading to Rho GTPases activation. Rho GEFs including Tiam 1, Kakirin 7, and Vav2 could activate Rac 1 and participate in cytoskeleton remodeling and synapse development through PAK/LIMK/Cofilin pathway and IRSP53/WAVE2 pathway. Rho GEF Intersection can activate N-WASP to regulate cytoskeleton remodeling by activating another GTPases Cdc42. ARGEF15 is also involved in this process by activating Rho A and its downstream ROCK.

potential contribution to the elimination of thin spines during the protracted stages of morphine withdrawal.

PFC receives dopaminergic projection from VTA and is an important brain region in the reward circuit of drug addiction. The excitability of neurons in PFC is affected by the amplitude of action potential afterhyperpolarization, suggesting that they may be regulated by small conductance calcium activated potassium (SK) channels (Shan et al., 2019), which may influence somatic excitability by promoting afterhyperpolarization and regulating synaptic plasticity. It has been shown that the excitability of the fifth layer of pyramidal neurons in infralimbic (IL) regions of the PFC was decreased at 1 week after withdrawal from morphine CPP training, and the expression of the SK3 and activated-Rac1 were enhanced compared to controls (Qu et al., 2020). Meanwhile, NSC23766, one of Rac1 inhibitors, could disrupt SK current and increase neuronal firing, while downregulation of Rac1 reduced the expression of SK channels in IL and inhibited morphine-induced CPP (Qu et al., 2020), indicating that Rac1 signaling pathway reduced neuronal excitability by regulating SK channel in PFC after morphine withdrawal, and this could help shed light on the mechanisms of opioid dependence and the development of treatment strategies.

Although the current neurobiological mechanism of opioid abuse is primarily related to synaptic plasticity of dopaminergic and glutaminergic neurons, this drug-induced plasticity may also be enhanced by glial cell activity. More and more evidence showed that glial cells, including oligodendrocytes, astrocytes and microglia, participate in cognitive impairment-and drug-induced neuronal plasticity changes, through the activity of cytokines and neurotrophins (Rahman et al., 2022). Chronic morphine therapy induces activation of astrocytes and microglia (Valentinova et al., 2019). In addition to affecting neuronal plasticity, Rac activity in glial cells is also involved in morphine addiction. Repeated morphine exposure could induce the activation of astrocytes and microglia *in vivo*, and promote the release of cytokines and glutamate from neurons. At the same time, morphine could induce morphological changes of cultured microglia from bipolar rod-like shapes or globular to lamellipodial and flat, with membrane ruffling at the edge, which was colocalized with Rac (Takayama and Ueda, 2005). These results indicated that Rac activation was involved in morphine-induced changes in neuronal synaptic plasticity and glial cell activation, which all affected morphine induced abnormal behaviors.

Table 2 Roles of Rho GTPases in substance dependence.

Substance	Behavior test	Strain	Nuclei or cell lines	Changes of Rho GTPases	References
Morphine	Conditioned place preference	C57BL/6 mice	Hippocampus	Number of dendritic spines ⇩ Rho A ⇧ ROCK⇧	Fakira et al. (2016)
	Withdrawal	C57BL/6J mice	Nucleus accumbens	Spines on medium-sized spiny neurons ⇩ Rho A ⇧	Cahill et al. (2018)
	Conditioned place preference and withdrawal	Sprague Dawley rats	Prefrontal cortex	Rac1 ⇧	Qu et al. (2020)
Heroin	Self-administration	Sprague Dawley rats	Dorsal hippocampus	RhoB⇧ ROCK⇧	Chen et al. (2017)
	Self-administration	Sprague Dawley rats	Dorsal hippocampus	Rac1 ⇧ F-actin/G-actin⇧	Chen et al. (2017)
	Behavioral sensitization	C57BL/6J mice	Nucleus accumbens	Rac1 ⇩	Zhu et al. (2016)
Cocaine	Goal-directed action	C57BL/6J mice	Prelimbic prefrontal cortex	Number of dendritic spines ⇩ ROCK⇧	Swanson et al. (2017)
	Locomotor activity	C57BL/6J mice	Prefrontal cortex	ROCK⇩	DePoy et al. (2013)
	Acute injection	CD-1 mice	Dorsal striatum, prefrontal cortex and hippocampus	Rnd3⇧	Marie-Claire et al. (2007)
	Locomotor sensitization	C57BL/6J mice × 129 mice	Nucleus accumbens	Rho-GEF Kalirin-7⇧	Kiraly et al. (2010) and Ma et al. (2012)
	Withdrawal	Sprague Dawley rats	Nucleus accumbens	Kalirin-7⇧ Rac-1⇧PAK⇧	Wang et al. (2013)
	Self-administration, locomotor activity and conditioned place preference	Mice	Nucleus accumbens	RhoGEF PDZ⇧ RhoA⇧ Rap1b⇧	Cahill et al. (2016)
	Behavioral sensitization and conditioned place preference	C57BL/10 mice	Nucleus accumbens	RhoGEF Vav2⇧	Zhu et al. (2015)
Amphetamine		Cells	SK-N-SH cells	RhoA ⇧ ROCK⇧	Wheeler et al. (2015)
		Swiss-Webster mice	Midbrain slices	RhoA ⇧ ROCK⇧	Wheeler et al. (2015)
Methamphetamine	Rearing and sniffing	Sprague–Dawley rats	Nucleus accumbens	ROCK⇧	Narita et al. (2003)
	Conditioned place preference	C57BL/6J mice	Nucleus accumbens	Rac1⇧ PAK1⇧ and Cdc42⇩	Tu et al. (2019) and Zhao et al. (2019)
	Neurotoxicity	Sprague Dawley rats	Hippocampus	RhoA⇧, ROCK⇧, cofilin⇧, p-cofilin⇧	Xue et al. (2019)
Nicotine	Neurotoxicity	Cells	PC 12 cells	RhoA⇧, ROCK⇧	Fukuda et al. (2005)
Alcohol	Alcohol preference	Wistar rats	Striatum	ROCK⇩	Kurt et al. (2015)
	Alcohol preference	Wistar rats	Hippocampus	ROCK⇧	Kurt et al. (2015)
	Self-administration	Drosophila		Rac1⇩	Butts et al. (2019)
	Sedation	Drosophila		RhoGAP18b⇧ Rac1⇩ RhoA⇩ Cdc42⇧	Rothenfluh et al. (2006)
	Self-administration	Drosophila		Arf6⇧ Rac1⇧	Peru et al. (2012)

4.3. Rho GTPases in heroin dependence

A key point with substance dependence is that abuse usually occurs in specific situations, therefore, exposure to the environment associated with addictive substance can increase craving and the odds of relapse, even after long-term withdrawal (Hitchcock and Lattal, 2018). Many brain regions play a role in environmental context-induced reinstatement of drug seeking and relapse, including dorsal

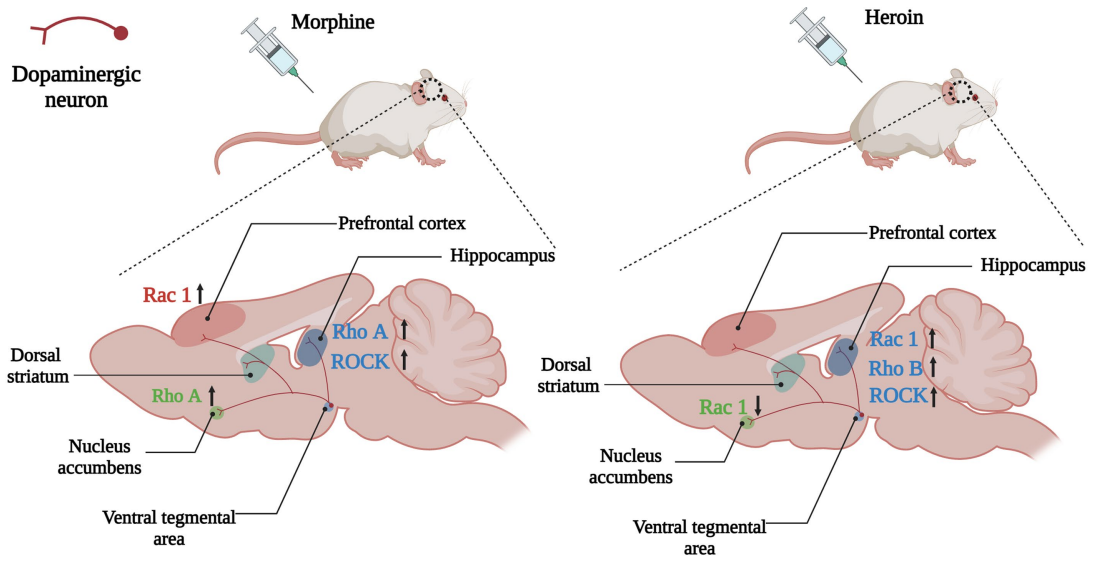

FIGURE 4
Changes of Rho GTPases expression in brain induced by opioids. In the mesolimbic dopamine system, the dopaminergic neurons in the ventral tegmental area (VTA) project to the brain regions involved in emotional, motivational, and executive functions such as the nucleus accumbens, hippocampus, dorsal striatum and prefrontal cortex. Opioids such as morphine and heroin abuse lead to changes in expressions of Rho GTPases in the mesencephalic limbic dopamine system, which in turn cause cytoskeleton remodeling and synaptic morphological and functional changes of dopamine neurons, leading to addiction and relapse. Arrows are used to represent changes in Rho GTPases and their downstream molecules in different brain regions caused by addictive substances, with upward arrows indicating increased expression and downward arrows indicating decreased expression. The color of the Rho GTPases and their downstream molecules coincides with the color of the brain regions in which they are differentially expressed. For example, the pink Rac1 in the left panel indicates changes in Rac1 expression in the prefrontal cortex (also the pink brain region) caused by morphine, and the upward arrow in the back indicates increased Rac1 expression in the prefrontal cortex caused by morphine.

and ventral PFC, dorsal striatum, basolateral amygdala and hippocampus (Marchant et al., 2015; Pelloux et al., 2018; Sun and Giocomo, 2022). Among them Hippocampus is crucial for developing and retrieving contextual and spatial memories (Sun and Giocomo, 2022). The dorsal hippocampus (DH) is the physiological basis for the learning of associations between the environmental context and unconditioned stimuli (such as drug use), and it is involved in mediating drug-taking and drug-seeking behavior and relapse (Chen et al., 2017; Hitchcock and Lattal, 2018). The expression of RhoB was increased in the DH of heroin self-administering rats, whereas blocking the RhoB/ROCK network could attenuate context-induced heroin relapse (Chen et al., 2017; Figure 4), which indicated that the RhoB pathway in the DH was necessary for the retrieval (recall) of addiction memory.

Rac1 was also particularly needed in cytoskeleton remodeling of the dendritic spine. DNA methylation is an essential mechanism for controlling gene expression, and it is essential for long-term synaptic plasticity. Calcium/calmodulin-dependent kinases (CaMKs) have become fundamental molecules that control spinal morphogenesis and dendritic development (Chang et al., 2019; Wang et al., 2019; Shibata et al., 2021). CaMKII is critical to the plasticity of activity-dependent spines (Yasuda et al., 2022). In addition to CaMKII, neurons also contain other CaMK cascades, facilitated by CaMK kinase (CaMKK) and its major downstream targets. Self-administration of heroin increased the expression of CaMKK1, which in turn activated its downstream target CaMKIα. The CaMKK1/CaMKIα pathway activated Rac1 *via* interacting with βPIX (Rac GEF) to regulate actin cytoskeleton remodeling in the DH and behavioral plasticity (Chen et al., 2021). Repeated self-administration of heroin caused the activation of Rac1 and the ratio of F-actin to G-actin in the DH increased significantly, indicating that the actin cytoskeleton was remodeled (actin polymerization). More importantly, bilateral intra-DH injection of NSC23766 significantly blocked actin polymerization and inhibited heroin self-administration (Chen et al., 2021), demonstrating that the upregulation of CaMKK1 in the DH was related to the motivation of heroin intake, and CaMKK1/CaMKIα/Rac1 pathway was required for the cytoskeleton remodeling and heroin addiction behavior of rats. However, Autism susceptibility candidate 2 (AUTS2) could inhibit the initiation and expression of heroin-induced behavioral sensitization *via* elevating Rac1 activation in NAc (Zhu et al., 2016). These results demonstrate that actin cytoskeleton remodeling is necessary for heroin addiction and hyperactive behavior, though the Rac1 signaling pathway may play different roles in different regions.

4.4. Rho GTPases in cocaine dependence

"Goal-directed" actions, the ability to choose actions based on expected consequences, are critical for the survival of individuals, which means that their performance is sensitive to the change in the connections between the action and its results. Habit-based stimulus-induced reward seeking at the expense of "goal-directed" response strategies may play an etiological role in the development and maintenance of substance dependence, especially for cocaine addiction (Everitt and Robbins, 2016). The cortex-dorsomedial striatum circuit is critical to the acquisition of "goal-directed" actions (Hart et al., 2014), and lesions of the prelimbic cortex impaired the

ability of laboratory animals to choose actions based on previously encoded action-outcome associations (Corbit and Balleine, 2003), indicating the prelimbic prefrontal cortex is essential for making "goal-oriented" decisions. Swanson et al. found that decision-making strategies could be predicted by dendrite spine density, and the intensity of action-outcome conditioning correlated with dendrite spine density in the prelimbic cortex, suggesting that the structural plasticity of prelimbic cortical neurons may play critical roles in the generation of "goal-directed" actions (Swanson et al., 2017). Systemic and local prelimbic cortical injection of the fasudil (ROCK inhibitor) could block the habitual response to food and cocaine in an actin polymerization-dependent manner, and temporarily reduce dendritic spine densities in prelimbic cortex in the process of consolidating new action-outcome associations (Swanson et al., 2017), demonstrating that blocking Rho/ROCK could impact the habit-based behaviors, including in the context of cocaine habits. HA-1077 (ROCK inhibitor) treatment during the adolescent period exaggerated cocaine-induced locomotor activity in adulthood, and administration of HA-1077 in adulthood had no psychomotor consequences in mice (DePoy et al., 2013), suggesting that early-life ROCK inhibition for destabilizing dendritic spines could confer cocaine vulnerability.

Cocaine addiction leads to persistent alterations in the brain's reward system, including increased dendrites and spine density on MSNs in the NAc and glutamatergic projection neurons in the PFC and ventral hippocampus (Li et al., 2012; Barrientos et al., 2018). Except Rho/ROCK pathway, the members of the Rnd subfamily also play essential roles in the regulation of actin cytoskeleton. Different from other small Rho GTPases, members of the Rnd subfamily (Rnd1, Rnd2, and Rnd3) do not hydrolyze GTP, therefore, Rnd proteins are not regulated by GAPs, and might be mainly regulated by transcriptional modulation (Chardin, 2003). Rnd3 is ubiquitously expressed, while Rnd1 and Rnd2 are mainly expressed in the brain. Studies have shown that Rnd1 promoted the maturation of the dendrite spine, Rnd2 stimulated dendrite branching, and Rnd3 regulated cytoskeleton remodeling and cell migration. The level of Rnd3 mRNA in the dorsal striatum, PFC and, hippocampus was significantly increased after the cocaine injection (Marie-Claire et al., 2007; Figure 5). Considering the role of the Rnd subfamily in actin cytoskeleton modulation and synaptic plasticity, cocaine regulation of Rnd3 gene expression suggests that Rnd3 is involved in the growth of neurites and modification of dendritic branches induced by cocaine abuse (Marie-Claire et al., 2007). With limited research progress in this field, it would be significant to study the direct relationship between Rnd3 and cocaine addiction and neuronal morphologic changes.

As positive regulators of Rho GTPases, Rho GEFs also become central regulators of synaptic actin dynamics. Kalirins, a well-known subfamily of Rho-GEFs promote the exchange of GDP and GTP, thereby stimulating the activity of specific Rho GTPases (Paskus et al., 2020). Kalirin-7 (Kal-7) is located on the postsynaptic side of excitatory synapses, and it is the most abundant Kalirin subtype in adult rodent brains. Kal-7 could activate Rac1, RhoA, and RhoG and is critical to the formation and stability of dendritic spines (Ma, 2010; Mazzone et al., 2012). The binding of the PH domain of Kal-7 and the NR2B (one of glutamate receptor NMDAR subunits) was necessary for synaptic plasticity (Kiraly et al., 2011). Chronic cocaine induced an increased expression of Kal-7 in the NAc of wild-type mice, and overexpression of Kal-7 in cultured MSNs increased the density of dendritic spine, while knocking out of Kal-7 inhibited the increase in spine density after cocaine treatment, indicating that Kal-7 was supposed to be indispensable for increases of dendritic spine density induced by cocaine (Kiraly et al., 2010; Ma et al., 2012). Lack of Kal-7 did not influence acute locomotor response to cocaine, but it could increase cocaine locomotor sensitization and self-administration (Kiraly et al., 2010, 2013; LaRese et al., 2017). After 2 weeks withdrawal from repeated cocaine injections, the levels Kal-7 and the activation of its downstream effectors such as Rac1 and PAK in the NAc were increased, while the surface expression of glutamate receptor AMPAR and spine density also increased (Wang et al., 2013). Kal-7 knockdown eliminated the increased expression of AMPAR and spine density, and Kal-7 knockdown rats also exhibited locomotor sensitization, however, incentive sensitization, which was assessed by the speed rats learned to self-administer a threshold dose of cocaine, was impaired severely (Wang et al., 2013). Blockade of NR2B with ifenprodil also inhibited locomotor hypersensitization of cocaine in Kal-7^{KO} mice (LaRese et al., 2017). These results indicated that Kal-7/Rac1/PAK pathway coordinated glutamate receptors to increase dendritic spine density during cocaine withdrawal, while incentive sensitization and locomotor sensitization may involve divergent mechanisms.

The synaptic structure and function of NAc MSNs in the early and late stages during cocaine withdrawal had opposing alterations. For instance, the observation of *de novo* thin spine formation at early time points indicated weakened synapses, while the increased formation of mushroom dendritic spines and related strengthened synapses were seen at later time points. After long-term exposure to cocaine, the level of PDZ-RhoGEF (one of the RhoGEFs, encoded by Arhgef11 gene) in the cytoplasm of NAc MSNs decreased, and the level of PDZ-RhoGEF in the nucleus increased (Cahill et al., 2016). This change was related to the increase in the levels of active RhoA in the nucleus, which in turn promoted the formation of F-actin. Meanwhile, the mRNA level and the synaptoneurosomal fraction level of Rap1b, which belongs to the Rap subfamily, were selectively increased after cocaine exposure, and further studies demonstrated that the elevated levels of active RhoA and Rap1b were related to the upregulation of PDZ-RhoGEF (Cahill et al., 2016). NAc infusion of Rap1b inhibitor GGTI-298 reduced locomotor activity and CPP induced by cocaine, and Rap1b could activate the PI3K-Akt-mTOR pathway, which, in turn, promoted the formation of thin spines at early time points of cocaine withdrawal. On the contrary, the activity of this pathway was reversed at late time points of cocaine withdrawal, resulting in the formation of mushroom spines (Cahill et al., 2016). These findings reveal the key role of biaxial synaptic expression of PDZ-RhoGEF/Rap1b in cocaine addiction. Although the actin dynamic changes that occur early and late time points appear to be different, synaptic remodeling during this process is a potential example of "superplasticity," with the initial formation of new fine spines early providing sites where subsequent dendritic spine maturation occurs (Wright et al., 2020).

Dopamine transporter (DAT)-mediated DA reuptake is one of the most critical mechanisms for substance dependence. Vav2 belongs to the VAV family with guanine nucleotide exchange activity. Compared with wild-type mice, the surface expression of DAT in the NAc of cocaine-treated Vav2$^{-/-}$ mice was significantly reduced, along with reduced DA levels and diminished behavioral response to cocaine (Zhu et al., 2015), demonstrating that Vav2 was a key factor of DAT trafficking and cocaine abuse.

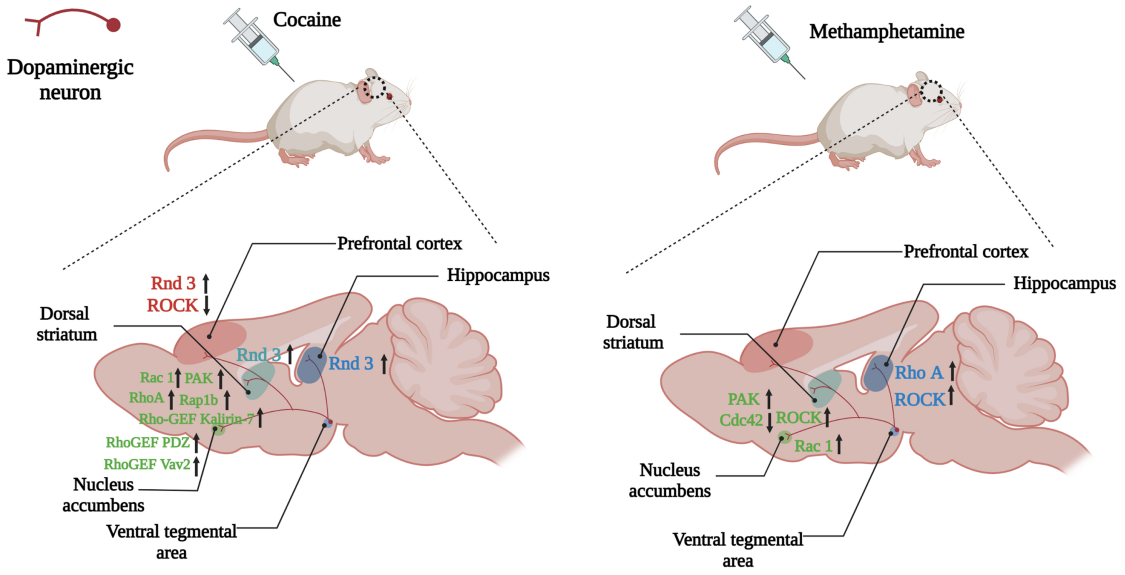

FIGURE 5
Changes of Rho GTPases expression in brain induced by psychostimulants. Dopamine plays a role in the brain's reward system, helping to reinforce certain behaviors that result in reward. Dopaminergic neuronal projections from the ventral tegmental area (VTA) to the nucleus accumbens, dorsal striatum and hippocampus, and prefrontal cortex underlie the neurobiology of this process. Psychostimulants such as cocaine and amphetamine lead to abnormal expressions of Rho GTPases (Rho A, Rac1, Rnd3) and their regulators (Kalirin-7, Vav2) in the above regions, which take part in the reinforcement, withdrawal and relapse of psychostimulants addiction. Arrows are used to represent changes in Rho GTPases and their regulators in different brain regions caused by addictive substances, with upward arrows indicating increased expression and downward arrows indicating decreased expression. The color of the Rho GTPases and their downstream molecules coincides with the color of the brain regions in which they are differentially expressed.

4.5. Rho GTPases in amphetamine dependence

Amphetamine is a psychostimulant that can increase DA content in the synaptic cleft by inhibiting DA reuptake in dopaminergic neuron terminals, and DAT is the crucial target of amphetamine actions during addiction. Different from cocaine and other psychostimulants, amphetamine can serve as a DAT substrate to stimulate the endocytosis of DAT in the plasma membrane. For instance, after injections of amphetamine (2 mg/kg), the level of DAT on the cell membrane of the midbrain slice significantly decreased (Saunders and Galli, 2015; Wheeler et al., 2015), which may be the key mechanism that leads to addiction. Wheeler et al. demonstrated that amphetamine rapidly stimulated DAT trafficking through a clathrin-independent, dynamin-dependent process in midbrain slices and cultured dopamine neurons, and this effect was mediated by activation of the RhoA (Wheeler et al., 2015). Inhibiting RhoA activity by C3 exotoxin, ROCK inhibitor Y27632, or a dominant-negative RhoA could block amphetamine-induced DAT internalization and dopamine uptake. Amphetamine also stimulated the accumulation of cAMP and PKA-dependent inactivation of RhoA, thus regulating the timing and stability of the effect of amphetamine on DAT internalization through the interaction of PKA and RhoA signaling pathways (Wheeler et al., 2015). The regulation of Rho activation/inactivation sequence provided a mechanism through which endogenous neurotransmitters and drugs could affect the response of dopaminergic neurons to amphetamine (Figure 5).

Similar to DAT, which is responsible for maintaining the DA concentration in the synaptic cleft, excitatory amino acid transporters (EAATs) are responsible for regulating the concentration of extracellular glutamate, which determines the spatial and temporal precision of glutamate neurotransmission and limits the excitotoxic effects of glutamate. EAAT3 is found predominantly in neurons and is the main subtype of glutamate transporter in dopaminergic neurons (Shin et al., 2020). Amphetamine stimulated the internalization of EAAT3, which was dependent on the activation of a RhoA, dynamin, and the expression of DAT, and decreased glutamate uptake in cultured neurons (Underhill et al., 2014). EAAT3 Trafficking from the cytomembrane after amphetamine treatment enhanced glutamate synaptic transmission by reducing glutamate clearance, proving a new mechanism for amphetamine to regulate midbrain glutamate activities.

NAc injection of ROCK inhibitor Y27632 significantly suppressed the increase of extracellular DA levels and behaviors induced by methamphetamine (METH) (Narita et al., 2003). METH regulated the Rac1 and Cdc42 signaling pathways oppositely, and inhibiting the Rac1 signaling and activating the Cdc42 signaling were crucial to CPP and structural plasticity induced by METH. DRD1 activated both the Rac1 and Cdc42 signaling, while DRD2 activated Cdc42 signaling but inhibited Rac1 signaling, thereby mediating METH-induced CPP and structural plasticity (Tu et al., 2019). These results showed both DRD1 and DRD2 in the MSNs of NAc regulated METH-induced locomotor activation, CPP, and dendritic and spine remodeling, however the possible mechanisms may differ.

The acquisition of METH-related addiction memory increased the thin dendritic spine density of DRD1-and DRD2-MSNs and it

decreased the activity of Rac1 and the expressions of its downstream p-PAK, p-Cofilin, and p-LIMK, whereas overexpression of Rac1 accelerated the extinction of METH-associated contextual memory. Additionally, although NAc microinjection of Rac1 inhibitor or activator was not sufficient to interrupt the reconsolidation of METH-associated contextual memory, the pharmacological activation of Rac1 in the NAc also promoted the elimination of thin spines and the extinction of METH-associated contextual memory. It was worth noting that Rac1 had an effect on the spine plasticity of DRD1-MSNs induced by METH, but had no effect on DRD2-MSNs. These findings indicated that Rac1 might play an opposite role in the acquisition and extinction of METH-related contextual memory, and the role of Rac1 in METH-related spine remodeling is also cell-specific, indicating that Rac1 may be a potential therapeutic target for reducing METH relapse (Zhao et al., 2019).

In addition to addiction and hyperactivity, METH is highly neurotoxic to the central nervous system. METH significantly increased blood-brain barrier (BBB) permeability, induced cytoskeleton remodeling, and reduced levels of tight junction (TJ) proteins in the hippocampus. The expressions of RhoA, ROCK, myosin light chain (MLC), p-MLC, cofilin, p-cofilin, and matrix metalloproteinase (MMP)-9 were all up-regulated, indicating that the RhoA/ROCK pathway was activated after METH treatment. After pretreatments with RhoA or ROCK inhibitors, the expressions of above-mentioned proteins significantly decreased, and the expressions of TJ proteins were increased, while the rearrangement F-actin cytoskeleton was suppressed and the permeability of rat brain microvascular endothelial cells was also reduced. These results indicated that METH could induce cytoskeleton rearrangement and TJ protein down-regulation *via* activating the RhoA/ROCK pathway, and then increase the permeability of BBB (Xue et al., 2019).

The neurotoxicity caused by METH abuse is associated with neurodegenerative damage in various brain regions such as the hippocampus and dorsal striatum. For instance, METH can cause dopaminergic neurons apoptosis, and using small interfering RNA to silence ROCK2 could increase cell viabilities and reduce apoptosis of PC12 cells (Yang et al., 2013), showing that ROCK2 may be a possible target for the treatment of METH-induced neurotoxicity. METH induced cytomorphological changes on human neuroblastoma SH-SY5Y cells including macropinocytosis through actin-dependent endocytosis (Nara et al., 2010). Further study showed that macropinosomes formed after METH exposure colocalized with activated Ras and activated Rac1, and both Rac1 inhibitor and Ras inhibitor significantly suppressed the formation of macropinosomes. Meanwhile, the levels of lysosomal-associated membrane proteins increased gradually in a time-dependent manner after METH exposure, while the proteolytic activities of cathepsin L were significantly suppressed, indicating that lysosomal function was inhibited. These results indicate that inhibition of lysosomal function through Ras-and Rac1-mediated macropinocytosis is at least partially involved in cytotoxic effects of METH (Nara et al., 2012).

4.6. Rho GTPases in alcohol dependence

Alcohol has been widely abused in many cultures for centuries, and drinking alcohol is related to the risk of chronic diseases including mental and behavioral disorders, liver cirrhosis, and cardiovascular diseases. Studies have found that the activity of ROCK in the striatum of rats was significantly reduced after being exposed to alcohol, while that in the hippocampus was significantly increased (Kurt et al., 2015), indicating that alcohol had different effects on the Rho/ROCK pathway in different brain regions. Rac1 and its target cofilin could bi-directionally change the experience-dependent alcohol preference. Dominant-negative Rac1 or activated cofilin in the mushroom bodies of Drosophila led to faster acquisition of experience-dependent alcohol preference, while activated Rac1 or dominant-negative cofilin eliminated alcohol preference, suggesting the activation state of Rac1 and cofilin were key factors to determining the rate of acquisition of alcohol preference and actin dynamics regulation played critical roles in the development of voluntary self-administration in Drosophila (Butts et al., 2019).

Low doses of alcohol (15% alcohol in the preference assays; Butts et al., 2019) caused disinhibition and hyperactivity (increased locomotion), while higher doses (alcohol vapors; Rothenfluh et al., 2006) led to dyskinesia and subsequent sedation. Small GTPase Arf6 acts downstream of Rac1 and Arfaptin and functions in the nervous system of adults. Arfaptin can directly bind to the activated Rac1 and Arf6, and Arfaptin and Arf6 mutations caused hypersensitivity to alcohol-induced sedation, demonstrating that the conservative Rac1/Arfaptin/Arf6 pathway was the main mediator of behavioral responses to alcohol in Drosophila (Peru et al., 2012).

The biological response to alcohol is highly conserved, and the reduced response to the sedative effects of alcohol indicates an increased risk of alcohol dependence in humans. RhoGAP18B is one of Rho GAPs and also affects the sensitivity to alcohol. Blockage of RhoGAP18B has strong resistance to the sedative effect of alcohol, and could enhance the GTPase activities of human Cdc42 and Rac, but has no impacts on RhoA. This resistance can be inhibited by decreasing the levels of RhoA or Rac1, indicating these GTPases were involved in the behavioral response to alcohol (Rothenfluh et al., 2006). The loss-of-function mutation in cofilin led to decreased alcohol-sensitivity and synergistic effect with RhoGAP18B, and the RhoGAP18B-PA subtype acted on Cdc42, while PC and PD activated cofilin through Rac1 and Rho, indicating that different RhoGAP18B subtypes acted on different Rho GTPases subgroups to regulate actin polymerization and depolymerization, and alcohol-induced behaviors (Ojelade et al., 2015).

The central nervous system has mechanisms to ensure the process of forming appropriate neuron polarity and regulating the growth time of the processes, and alcohol can destroy these mechanisms and alter the normal establishment of neuronal polarity. For instance, cultured pyramidal neurons of the fetal rat hippocampus developed abnormally small dendritic branches after being exposed to alcohol in the early stages of cultivation (Clamp and Lindsley, 1998), and long term alcohol treatment led to a reduction in the total length of dendrites, the number of dendrites and the number of synapses (Yanni and Lindsley, 2000). Ca^{2+} signaling pathway is a key regulator of axon growth and guidance, altered Ca^{2+} signaling in growth cone were associated with abnormal neuromorphogenesis caused by fetal alcohol exposure (Mah et al., 2011). Alcohol exposure inhibited Rac1/Cdc42 activation induced by BDNF in a dose-dependent manner, and in the early stages of hippocampus development, alcohol inhibited growth

cone signaling through regulating the activities of small Rho GTPases (Lindsley et al., 2011), suggesting alcohol may destroy the effect of neurotrophic factors on axon growth and guidance. Exposure 7-day-old rat pups to alcohol inhibited the formation of neurite and activation of Rac1 in cerebellar granule neurons, demonstrating that Rho GTPases played a regulatory role in the differentiation of cerebellar neurons, and alcohol-related impairment of Rac1 signaling may be one of the causes of brain defects observed in fetal alcohol syndrome (Joshi et al., 2006).

4.7. Rho GTPases in nicotine dependence

Nicotine dependence is one of the most expensive health problems worldwide. A microarray study on the time-course of acute response to nicotine in the VTA of mice showed that RhoA expression levels increased significantly with the duration of nicotine treatment, and one SNP of RhoA gene, rs2878298, showed a highly significant genotypic association with the initiation of smoking and nicotine dependence (Chen et al., 2007). Given the role of RhoA in cytoskeleton rearrangement and formation of dendritic spines, these results suggested RhoA's regulation of neuroplasticity may be involved in nicotine abuse. Tyrosine hydroxylase (TH) is a key rate-limiting enzyme in the biosynthesis of catecholamine such as DA. Nicotine could significantly activate RhoA and increase the expression and enzyme activity of TH in culture rat pheochromocytoma PC 12 cells, and treatment with Y27632 or C3 toxin significantly to block RhoA signaling remarkably inhibited the nicotine-induced increase of TH and catecholamine biosynthesis in PC12 cells (Fukuda et al., 2005), indicating RhoA may be involved in the increase of catecholamine neurotransmitters such as dopamine caused by nicotine and the activation of reward circuits.

5. Considerations for clinical use and outlook

The Rho/ROCK pathway is abnormally activated in various diseases of the central nervous system, and blocking of the Rho/ROCK pathway has been shown to be effective in animal models of Alzheimer's disease, neuropathic pain and stroke (Mueller et al., 2005). ROCK was also abnormally expressed in many brain regions of the addicted animals, therefore, inhibitors of ROCK may also have the potential to treat drug abuse. To date, only two inhibitors of ROCK, fasudil (Eril®) and its derivative ripasudil (Glanatec®), have been approved for clinical use. Fasudil is a small molecule ROCK inhibitor, which was first approved in 1995 in Japan for the prevention and treatment of cerebral vasospasm and subarachnoid hemorrhage (Abedi et al., 2020). Fasudil has been proved to stimulate neuroregeneration and prevent neurodegeneration in many neurological diseases (Tatenhorst et al., 2016). Fasudil could enhance action-outcome memory, leading to "goal-directed" behavior in mice, otherwise the mice would express "stimulus-response" habits, and fasudil can also prevent the habitual response to cocaine, and this effect would persist over a period of time based on the polymerized state of actin (Swanson et al., 2017). Fasudil administration could significantly ameliorate spatial learning and memory disorders and reduce the increase of inflammatory cytokines levels induced by smoking in the hippocampus, which may be related to the regulation of the Rho/ROCK/NF-κB pathway (Xueyang et al., 2016). In 2014, Pharmaceuticals and Medical DevicesAgency of Japan approved Ripasudil as an ophthalmic solution for the treatment of glaucoma with increased intraocular pressure (Koch et al., 2018). However, there have been no reports of ripasudil and drug addiction. RhoA activation may be involved in the up-regulating of the expression and activity of ileal P-gp protein, resulting in a decrease in the analgesic effect of oral morphine (Kobori et al., 2012), and inhibition of RhoA activation by rosuvastatin not only delayed, but also partially reversed the morphine tolerance (Li Y. et al., 2015).

Substance dependence is associated with mental disorders such as depression and anxiety, which are major factors leading to compulsive drug seeking and relapse. Opipramol, a sigma-1 receptor agonist, is approved in some European countries to treat anxiety disorders and depression. It has been reported that chronic opipramol administration could reduce cocain-seeking behavior in self- self-administrated rats. Further results suggested that Rac1 played a key role in the effect of opipramol on drug seeking, affecting the susceptibility of addicted rats to opipramol (Bareli et al., 2021b). As a drug used in clinical practice, opipramol reduced Rac1 and inhibited cocaine relapse, indicating its potential as a candidate for the treatment of substance dependence. Opipramol combined with baclofen significantly reduced cravings and depressive symptoms in substance abusers, according to a preliminary, double-blind, controlled clinical investigation. These findings suggest that opipramol and baclofen could be candidates for treatment in patients with substance abuse and comorbidities for mood/anxiety disorders, which may help improve their addiction status and promote rehabilitation (Bareli et al., 2021a).

Although there are preclinical studies that support the beneficial effects of Rac1, RhoA/ROCK inhibitors on drug abuse, human clinical studies and data confirming their beneficial effects are limited. More clinical trials are needed to determine whether fasudil or opipramol show beneficial effects in the treatment of drug dependence clinically and to research and develop more effective Rho GTPase-related compounds.

6. Conclusion

Accumulating studies have indicated that the Rho GTPases family and their regulatory factors regulators, in particular GEFs and GAPs, play crucial roles in substance dependence, which provide novel insights into the treatment. However, our work cannot tell the whole story because more and more findings are being discovered about the role of Rho GTPases and their regulators and effects in substance dependence, and even more have yet to be revealed. The cell specificity and brain region specificity of Rho GTPases indicate we remain far from a complete understanding of how they operate spatially and temporally in neuronal structure and function in substance dependence. A better understanding of regulatory mechanisms of these Rho GTPases will certainly highlight novel therapeutic targets and interventions for the treatment of substance dependence.

Author contributions

QR, LC, and YXW designed the study and wrote the manuscript. All authors contributed to the article and approved the final version.

Funding

This work was supported by the National Natural Science Foundation of China (Grant No. 81971775) to LC and (Grant No. 82071970) to YXW, the Young Talents Project of Hubei Provincial Health Commission (Grant No. WJ2021Q053) to QR, and the Science and Technology Project of Jianghan University (Grant No. 2022SXZX25).

Conflict of interest

The authors declare that the research was conducted in the absence of any commercial or financial relationships that could be construed as a potential conflict of interest.

Publisher's note

All claims expressed in this article are solely those of the authors and do not necessarily represent those of their affiliated organizations, or those of the publisher, the editors and the reviewers. Any product that may be evaluated in this article, or claim that may be made by its manufacturer, is not guaranteed or endorsed by the publisher.

References

Abdrabou, A., and Wang, Z. (2018). Post-translational modification and subcellular distribution of Rac1: An update. *Cells* 7:263. doi: 10.3390/cells7120263

Abedi, F., Hayes, A. W., Reiter, R., and Karimi, G. (2020). Acute lung injury: The therapeutic role of Rho kinase inhibitors. *Pharmacol. Res.* 155:104736. doi: 10.1016/j.phrs.2020.104736

Amin, E., Jaiswal, M., Derewenda, U., Reis, K., Nouri, K., Koessmeier, K. T., et al. (2016). Deciphering the molecular and functional basis of RhoGAP family proteins: A systematic approach toward selective inactivation of rho family proteins. *J. Biol. Chem.* 291, 20353–20371. doi: 10.1074/jbc.M116.736967

Bareli, T., Ahdoot, H. L., Ben Moshe, H., Barnea, R., Warhaftig, G., Gispan, I., et al. (2021a). Novel opipramol-baclofen combination alleviates depression and craving and facilitates recovery from substance use disorder-an animal model and a human study. *Front. Behav. Neurosci.* 15:788708. doi: 10.3389/fnbeh.2021.788708

Bareli, T., Ahdoot, H. L., Ben-Moshe, H., Barnea, R., Warhaftig, G., Maayan, R., et al. (2021b). Chronic opipramol treatment extinguishes cocaine craving through Rac1 in responders: A rat model study. *Addict. Biol.* 26:e13014. doi: 10.1111/adb.13014

Barrientos, C., Knowland, D., Wu, M. M. J., Lilascharoen, V., Huang, K. W., Malenka, R. C., et al. (2018). Cocaine-induced structural plasticity in input regions to distinct cell types in nucleus accumbens. *Biol. Psychiatry* 84, 893–904. doi: 10.1016/j.biopsych.2018.04.019

Baumeister, M. A., Martinu, L., Rossman, K. L., Sondek, J., Lemmon, M. A., and Chou, M. M. (2003). Loss of phosphatidylinositol 3-phosphate binding by the C-terminal Tiam-1 pleckstrin homology domain prevents *in vivo* Rac1 activation without affecting membrane targeting. *J. Biol. Chem.* 278, 11457–11464. doi: 10.1074/jbc.M211901200

Beltran-Campos, V., Silva-Vera, M., Garcia-Campos, M. L., and Diaz-Cintra, S. (2015). Effects of morphine on brain plasticity. *Neurologia* 30, 176–180. doi: 10.1016/j.nrl.2014.08.004

Benson, C. E., and Southgate, L. (2021). The DOCK protein family in vascular development and disease. *Angiogenesis* 24, 417–433. doi: 10.1007/s10456-021-09768-8

Bosco, E. E., Mulloy, J. C., and Zheng, Y. (2009). Rac1 GTPase: A "Rac" of all trades. *Cell Mol. Life Sci.* 66, 370–374. doi: 10.1007/s00018-008-8552-x

Butts, A. R., Ojelade, S. A., Pronovost, E. D., Seguin, A., Merrill, C. B., Rodan, A. R., et al. (2019). Altered actin filament dynamics in the drosophila mushroom bodies lead to fast acquisition of alcohol consumption preference. *J. Neurosci.* 39, 8877–8884. doi: 10.1523/JNEUROSCI.0973-19.2019

Cahill, M. E., Bagot, R. C., Gancarz, A. M., Walker, D. M., Sun, H., Wang, Z. J., et al. (2016). Bidirectional synaptic structural plasticity after chronic cocaine administration occurs through Rap 1 small GTPase signaling. *Neuron* 89, 566–582. doi: 10.1016/j.neuron.2016.01.031

Cahill, M. E., Browne, C. J., Wang, J., Hamilton, P. J., Dong, Y., and Nestler, E. J. (2018). Withdrawal from repeated morphine administration augments expression of the RhoA network in the nucleus accumbens to control synaptic structure. *J. Neurochem.* 147, 84–98. doi: 10.1111/jnc.14563

Cao, F., Zhou, Z., Pan, X., Leung, C., Xie, W., Collingridge, G., et al. (2017). Developmental regulation of hippocampal long-term depression by cofilin-mediated actin reorganization. *Neuropharmacology* 112, 66–75. doi: 10.1016/j.neuropharm.2016.08.017

Casalou, C., Ferreira, A., and Barral, D. C. (2020). The role of ARF family proteins and their regulators and effectors in cancer progression: A therapeutic perspective. *Front. Cell Dev. Biol.* 8:217. doi: 10.3389/fcell.2020.00217

Chang, J. Y., Nakahata, Y., Hayano, Y., and Yasuda, R. (2019). Mechanisms of $Ca^{(2+)}$/calmodulin-dependent kinase II activation in single dendritic spines. *Nat. Commun.* 10:2784. doi: 10.1038/s41467-019-10694-z

Chardin, P. (2003). GTPase regulation: Getting aRnd Rock and Rho inhibition. *Curr. Biol.* 13, R702–R704. doi: 10.1016/j.cub.2003.08.042

Chen, X., Che, Y., Zhang, L., Putman, A. H., Damaj, I., Martin, B. R., et al. (2007). RhoA, encoding a Rho GTPase, is associated with smoking initiation. *Genes Brain Behav.* 6, 689–697. doi: 10.1111/j.1601-183X.2006.00296.x

Chen, Z. G., Liu, X., Wang, W., Geng, F., Gao, J., Gan, C. L., et al. (2017). Dissociative role for dorsal hippocampus in mediating heroin self-administration and relapse through CDK5 and Rho B signaling revealed by proteomic analysis. *Addict. Biol.* 22, 1731–1742. doi: 10.1111/adb.12435

Chen, Z. G., Wang, Y. J., Chen, R. S., Geng, F., Gan, C. L., Wang, W. S., et al. (2021). Ube 2b-dependent degradation of DNMT3a relieves a transcriptional brake on opiate-induced synaptic and behavioral plasticity. *Mol. Psychiatry* 26, 1162–1177. doi: 10.1038/s41380-019-0533-y

Chou, F. S., and Wang, P. S. (2016). The Arp2/3 complex is essential at multiple stages of neural development. *Neurogenesis* 3:e1261653. doi: 10.1080/23262133.2016.1261653

Christoffel, D. J., Walsh, J. J., Hoerbelt, P., Heifets, B. D., Llorach, P., Lopez, R. C., et al. (2021). Selective filtering of excitatory inputs to nucleus accumbens by dopamine and serotonin. *Proc. Natl. Acad. Sci. U. S. A.* 118:e2106648118. doi: 10.1073/pnas.2106648118

Clamp, P. A., and Lindsley, T. A. (1998). Early events in the development of neuronal polarity *in vitro* are altered by ethanol. *Alcohol. Clin. Exp. Res.* 22, 1277–1284. doi: 10.1111/j.1530-0277.1998.tb03909.x

Corbit, L. H., and Balleine, B. W. (2003). The role of prelimbic cortex in instrumental conditioning. *Behav. Brain Res.* 146, 145–157. doi: 10.1016/j.bbr.2003.09.023

DePoy, L. M., Noble, B., Allen, A. G., and Gourley, S. L. (2013). Developmentally divergent effects of Rho-kinase inhibition on cocaine-and BDNF-induced behavioral plasticity. *Behav. Brain Res.* 243, 171–175. doi: 10.1016/j.bbr.2013.01.004

di Volo, M., Morozova, E. O., Lapish, C. C., Kuznetsov, A., and Gutkin, B. (2019). Dynamical ventral tegmental area circuit mechanisms of alcohol-dependent dopamine release. *Eur. J. Neurosci.* 50, 2282–2296. doi: 10.1111/ejn.14147

Ding, B., Yang, S., Schaks, M., Liu, Y., Brown, A. J., Rottner, K., et al. (2022). Structures reveal a key mechanism of WAVE regulatory complex activation by Rac1 GTPase. *Nat Commun* 13:5444. doi: 10.1038/s41467-022-33174-3

Duman, J. G., Blanco, F. A., Cronkite, C. A., Ru, Q., Erikson, K. C., Mulherkar, S., et al. (2022). Rac-maninoff and Rho-vel: The symphony of Rho-GTPase signaling at excitatory synapses. *Small GTPases* 13, 14–47. doi: 10.1080/21541248.2021.1885264

Everitt, B. J., and Robbins, T. W. (2016). Drug addiction: Updating actions to habits to compulsions ten years on. *Annu. Rev. Psychol.* 67, 23–50. doi: 10.1146/annurev-psych-122414-033457

Fakira, A. K., Massaly, N., Cohensedgh, O., Berman, A., and Moron, J. A. (2016). Morphine-associated contextual cues induce structural plasticity in hippocampal CA1 pyramidal neurons. *Neuropsychopharmacology* 41, 2668–2678. doi: 10.1038/npp.2016.69

Fort, P., and Blangy, A. (2017). The evolutionary landscape of Dbl-Like Rho GEF families: Adapting eukaryotic cells to environmental signals. *Genome Biol. Evol.* 9, 1471–1486. doi: 10.1093/gbe/evx100

Fukuda, T., Takekoshi, K., Nanmoku, T., Ishii, K., Isobe, K., and Kawakami, Y. (2005). Inhibition of the RhoA/Rho kinase system attenuates catecholamine biosynthesis in PC 12 rat pheochromocytoma cells. *Biochim. Biophys. Acta* 1726, 28–33. doi: 10.1016/j.bbagen.2005.08.008

Gao, Z., Xing, K., Zhang, C., Qi, J., Wang, L., Gao, S., et al. (2019). Crystal structure and function of Rbj: A constitutively GTP-bound small G protein with an extra DnaJ domain. *Protein Cell* 10, 760–763. doi: 10.1007/s13238-019-0622-3

Garcia-Mata, R., Boulter, E., and Burridge, K. (2011). The 'invisible hand': Regulation of RHO GTPases by RHOGDIs. *Nat. Rev. Mol. Cell Biol.* 12, 493–504. doi: 10.1038/nrm3153

Govek, E. E., Newey, S. E., and Van Aelst, L. (2005). The role of the Rho GTPases in neuronal development. *Genes Dev* 19, 1–49. doi: 10.1101/gad.1256405

Hart, G., Leung, B. K., and Balleine, B. W. (2014). Dorsal and ventral streams: The distinct role of striatal subregions in the acquisition and performance of goal-directed actions. *Neurobiol. Learn. Mem.* 108, 104–118. doi: 10.1016/j.nlm.2013.11.003

Hasegawa, K., Matsui, T. K., Kondo, J., and Kuwako, K. I. (2022). N-WASP-Arp2/3 signaling controls multiple steps of dendrite maturation in Purkinje cells *in vivo*. *Development* 149:dev201214. doi: 10.1242/dev.201214

Hitchcock, L. N., and Lattal, K. M. (2018). Involvement of the dorsal hippocampus in expression and extinction of cocaine-induced conditioned place preference. *Hippocampus* 28, 226–238. doi: 10.1002/hipo.22826

Jaiswal, M., Dvorsky, R., and Ahmadian, M. R. (2013). Deciphering the molecular and functional basis of Dbl family proteins: A novel systematic approach toward classification of selective activation of the Rho family proteins. *J. Biol. Chem.* 288, 4486–4500. doi: 10.1074/jbc.M112.429746

Jaiswal, M., Dvorsky, R., Amin, E., Risse, S. L., Fansa, E. K., Zhang, S. C., et al. (2014). Functional cross-talk between ras and rho pathways: A Ras-specific GTPase-activating protein (p120RasGAP) competitively inhibits the RhoGAP activity of deleted in liver cancer (DLC) tumor suppressor by masking the catalytic arginine finger. *J. Biol. Chem.* 289, 6839–6849. doi: 10.1074/jbc.M113.527655

Joshi, S., Guleria, R. S., Pan, J., Bayless, K. J., Davis, G. E., Dipette, D., et al. (2006). Ethanol impairs Rho GTPase signaling and differentiation of cerebellar granule neurons in a rodent model of fetal alcohol syndrome. *Cell Mol. Life Sci.* 63, 2859–2870. doi: 10.1007/s00018-006-6333-y

Jung, H., Yoon, S. R., Lim, J., Cho, H. J., and Lee, H. G. (2020). Dysregulation of Rho GTPases in human cancers. *Cancers* 12:1179. doi: 10.3390/cancers12051179

Kiraly, D. D., Lemtiri-Chlieh, F., Levine, E. S., Mains, R. E., and Eipper, B. A. (2011). Kalirin binds the NR2B subunit of the NMDA receptor, altering its synaptic localization and function. *J. Neurosci.* 31, 12554–12565. doi: 10.1523/JNEUROSCI.3143-11.2011

Kiraly, D. D., Ma, X. M., Mazzone, C. M., Xin, X., Mains, R. E., and Eipper, B. A. (2010). Behavioral and morphological responses to cocaine require Kalirin7. *Biol Psychiatry* 68, 249–255. doi: 10.1016/j.biopsych.2010.03.024

Kiraly, D. D., Nemirovsky, N. E., LaRese, T. P., Tomek, S. E., Yahn, S. L., Olive, M. F., et al. (2013). Constitutive knockout of Kalirin-7 leads to increased rates of cocaine self-administration. *Mol. Pharmacol.* 84, 582–590. doi: 10.1124/mol.113.087106

Kobori, T., Kobayashi, M., Harada, S., Nakamoto, K., Fujita-Hamabe, W., and Tokuyama, S. (2012). RhoA affects oral morphine analgesia depending on functional variation in intestinal P-glycoprotein induced by repeated etoposide treatment. *Eur. J. Pharm. Sci.* 47, 934–940. doi: 10.1016/j.ejps.2012.08.019

Koch, J. C., Tatenhorst, L., Roser, A. E., Saal, K. A., Tonges, L., and Lingor, P. (2018). ROCK inhibition in models of neurodegeneration and its potential for clinical translation. *Pharmacol. Ther.* 189, 1–21. doi: 10.1016/j.pharmthera.2018.03.008

Kurt, A. H., Macit, E., Uzbay, T., and Buyukafsar, K. (2015). Effects of ethanol withdrawal on the activity of rho-kinase in rat brain. *Bratisl. Lek. Listy.* 116, 490–493. doi: 10.4149/BLL_2015_093

Langdon, A. J., and Daw, N. D. (2020). Beyond the average view of dopamine. *Trends Cogn. Sci.* 24, 499–501. doi: 10.1016/j.tics.2020.04.006

LaRese, T. P., Yan, Y., Eipper, B. A., and Mains, R. E. (2017). Using Kalirin conditional knockout mice to distinguish its role in dopamine receptor mediated behaviors. *BMC Neurosci.* 18:45. doi: 10.1186/s12868-017-0363-2

Li, J., Gu, J., Wang, B., Xie, M., Huang, L., Liu, Y., et al. (2015). Activation of dopamine D1 receptors regulates dendritic morphogenesis through Rac1 and RhoA in prefrontal cortex neurons. *Mol. Neurobiol.* 51, 1024–1037. doi: 10.1007/s12035-014-8762-1

Li, J., Liu, N., Lu, K., Zhang, L., Gu, J., Guo, F., et al. (2012). Cocaine-induced dendritic remodeling occurs in both D1 and D2 dopamine receptor-expressing neurons in the nucleus accumbens. *Neurosci. Lett.* 517, 118–122. doi: 10.1016/j.neulet.2012.04.040

Li, Y., Shu, Y., Ji, Q., Liu, J., He, X., and Li, W. (2015). Attenuation of morphine analgesic tolerance by rosuvastatin in naive and morphine tolerance rats. *Inflammation* 38, 134–141. doi: 10.1007/s10753-014-0015-y

Lin, R., Liang, J., and Luo, M. (2021). The raphe dopamine system: Roles in salience encoding, memory expression, and addiction. *Trends Neurosci* 44, 366–377. doi: 10.1016/j.tins.2021.01.002

Lin, R., Liang, J., Wang, R., Yan, T., Zhou, Y., Liu, Y., et al. (2020). The raphe dopamine system controls the expression of incentive memory. *Neuron* 106, 498–514.e8. doi: 10.1016/j.neuron.2020.02.009

Lindsley, T. A., Shah, S. N., and Ruggiero, E. A. (2011). Ethanol alters BDNF-induced Rho GTPase activation in axonal growth cones. *Alcohol. Clin. Exp. Res.* 35, 1321–1330. doi: 10.1111/j.1530-0277.2011.01468.x

Liu, C., Tose, A. J., Verharen, J. P. H., Zhu, Y., Tang, L. W., de Jong, J. W., et al. (2022). An inhibitory brainstem input to dopamine neurons encodes nicotine aversion. *Neuron* 110, 3018–3035.e7. doi: 10.1016/j.neuron.2022.07.003

Ma, X. M. (2010). Kalirin-7 is a key player in the formation of excitatory synapses in hippocampal neurons. *ScientificWorldJournal* 10, 1655–1666. doi: 10.1100/tsw.2010.148

Ma, X. M., Huang, J. P., Xin, X., Yan, Y., Mains, R. E., and Eipper, B. A. (2012). A role for kalirin in the response of rat medium spiny neurons to cocaine. *Mol. Pharmacol.* 82, 738–745. doi: 10.1124/mol.112.080044

Magee, J. C., and Grienberger, C. (2020). Synaptic plasticity forms and functions. *Annu. Rev. Neurosci.* 43, 95–117. doi: 10.1146/annurev-neuro-090919-022842

Mah, S. J., Fleck, M. W., and Lindsley, T. A. (2011). Ethanol alters calcium signaling in axonal growth cones. *Neuroscience* 189, 384–396. doi: 10.1016/j.neuroscience.2011.05.042

Marchant, N. J., Kaganovsky, K., Shaham, Y., and Bossert, J. M. (2015). Role of corticostriatal circuits in context-induced reinstatement of drug seeking. *Brain Res.* 1628, 219–232. doi: 10.1016/j.brainres.2014.09.004

Marie-Claire, C., Salzmann, J., David, A., Courtin, C., Canestrelli, C., and Noble, F. (2007). Rnd family genes are differentially regulated by 3, 4-methylenedioxymethamphetamine and cocaine acute treatment in mice brain. *Brain Res.* 1134, 12–17. doi: 10.1016/j.brainres.2006.11.065

Mateos-Aparicio, P., and Rodriguez-Moreno, A. (2020). Calcium dynamics and synaptic plasticity. *Adv. Exp. Med. Biol.* 1131, 965–984. doi: 10.1007/978-3-030-12457-1_38

Matsuda, J., Asano-Matsuda, K., Kitzler, T. M., and Takano, T. (2021). Rho GTPase regulatory proteins in podocytes. *Kidney Int.* 99, 336–345. doi: 10.1016/j.kint.2020.08.035

Mazzone, C. M., Larese, T. P., Kiraly, D. D., Eipper, B. A., and Mains, R. E. (2012). Analysis of Kalirin-7 knockout mice reveals different effects in female mice. *Mol. Pharmacol.* 82, 1241–1249. doi: 10.1124/mol.112.080838

Mueller, B. K., Mack, H., and Teusch, N. (2005). Rho kinase, a promising drug target for neurological disorders. *Nat. Rev. Drug. Discov.* 4, 387–398. doi: 10.1038/nrd1719

Nara, A., Aki, T., Funakoshi, T., and Uemura, K. (2010). Methamphetamine induces macropinocytosis in differentiated SH-SY5Y human neuroblastoma cells. *Brain Res.* 1352, 1–10. doi: 10.1016/j.brainres.2010.07.043

Nara, A., Aki, T., Funakoshi, T., Unuma, K., and Uemura, K. (2012). Hyperstimulation of macropinocytosis leads to lysosomal dysfunction during exposure to methamphetamine in SH-SY5Y cells. *Brain Res.* 1466, 1–14. doi: 10.1016/j.brainres.2012.05.017

Narita, M., Takagi, M., Aoki, K., Kuzumaki, N., and Suzuki, T. (2003). Implication of Rho-associated kinase in the elevation of extracellular dopamine levels and its related behaviors induced by methamphetamine in rats. *J. Neurochem.* 86, 273–282. doi: 10.1046/j.1471-4159.2003.01784.x

Natividad, L. A., Buczynski, M. W., Parsons, L. H., Torres, O. V., and O'Dell, L. E. (2012). Adolescent rats are resistant to adaptations in excitatory and inhibitory mechanisms that modulate mesolimbic dopamine during nicotine withdrawal. *J. Neurochem.* 123, 578–588. doi: 10.1111/j.1471-4159.2012.07926.x

Ojelade, S. A., Acevedo, S. F., Kalahasti, G., Rodan, A. R., and Rothenfluh, A. (2015). RhoGAP18B isoforms act on distinct Rho-family GTPases and regulate behavioral responses to alcohol *via* cofilin. *PLoS One* 10:e0137465. doi: 10.1371/journal.pone.0137465

Paskus, J. D., Herring, B. E., and Roche, K. W. (2020). Kalirin and Trio: RhoGEFs in synaptic transmission, plasticity, and complex brain disorders. *Trends Neurosci.* 43, 505–518. doi: 10.1016/j.tins.2020.05.002

Pelloux, Y., Hoots, J. K., Cifani, C., Adhikary, S., Martin, J., Minier-Toribio, A., et al. (2018). Context-induced relapse to cocaine seeking after punishment-imposed abstinence is associated with activation of cortical and subcortical brain regions. *Addict. Biol.* 23, 699–712. doi: 10.1111/adb.12527

Peru, Y., Colón de Portugal, R. L., Acevedo, S. F., Rodan, A. R., Chang, L. Y., Eaton, B. A., et al. (2012). Adult neuronal Arf6 controls ethanol-induced behavior with Arfaptin downstream of Rac1 and RhoGAP18B. *J Neurosci* 32, 17706–17713. doi: 10.1523/JNEUROSCI.1944-12.2012

Qu, L., Wang, Y., Li, Y., Wang, X., Li, N., Ge, S., et al. (2020). Decreased neuronal excitability in medial prefrontal cortex during morphine withdrawal is associated with enhanced SK channel activity and upregulation of small GTPase Rac1. *Theranostics* 10, 7369–7383. doi: 10.7150/thno.44893

Rahman, M. M., Islam, M. R., Yamin, M., Islam, M. M., Sarker, M. T., Meem, A. F. K., et al. (2022). Emerging role of neuron-glia in neurological disorders: At a glance. *Oxid. Med. Cell Longev.* 2022:3201644. doi: 10.1155/2022/3201644

Raimondi, F., Portella, G., Orozco, M., and Fanelli, F. (2011). Nucleotide binding switches the information flow in ras GTPases. *PLoS Comput. Biol.* 7:e1001098. doi: 10.1371/journal.pcbi.1001098

Rojas, A. M., Fuentes, G., Rausell, A., and Valencia, A. (2012). The Ras protein superfamily: Evolutionary tree and role of conserved amino acids. *J. Cell Biol.* 196, 189–201. doi: 10.1083/jcb.201103008

Rothenfluh, A., Threlkeld, R. J., Bainton, R. J., Tsai, L. T., Lasek, A. W., and Heberlein, U. (2006). Distinct behavioral responses to ethanol are regulated by alternate RhoGAP18B isoforms. *Cell* 127, 199–211. doi: 10.1016/j.cell.2006.09.010

Saunders, C., and Galli, A. (2015). Insights in how amphetamine ROCKs (Rho-associated containing kinase) membrane protein trafficking. *Proc. Natl. Acad. Sci. U. S. A.* 112, 15538–15539. doi: 10.1073/pnas.1520960112

Serafini, R. A., Pryce, K. D., and Zachariou, V. (2020). The mesolimbic dopamine system in chronic pain and associated affective comorbidities. *Biol. Psychiatry* 87, 64–73. doi: 10.1016/j.biopsych.2019.10.018

Shan, L., Galaj, E., and Ma, Y. Y. (2019). Nucleus accumbens shell small conductance potassium channels underlie adolescent ethanol exposure-induced anxiety. *Neuropsychopharmacology* 44, 1886–1895. doi: 10.1038/s41386-019-0415-7

Shibata, A. C. E., Ueda, H. H., Eto, K., Onda, M., Sato, A., Ohba, T., et al. (2021). Photoactivatable CaMKII induces synaptic plasticity in single synapses. *Nat. Commun.* 12:751. doi: 10.1038/s41467-021-21025-6

Shin, H. J., Lee, S. Y., Na, H. S., Koo, B. W., Ryu, J. H., and Do, S. H. (2020). Effects of tranexamic acid on the activity of glutamate transporter EAAT3. *Anesth. Pain Med.* 15, 291–296. doi: 10.17085/apm.20004

Shutes, A., and Der, C. J. (2004). *Small GTPases*. Amsterdam: Elsevier.

Smith, A. C. W., and Kenny, P. J. (2018). Micro RNAs regulate synaptic plasticity underlying drug addiction. *Genes Brain Behav.* 17:e12424. doi: 10.1111/gbb.12424

Speranza, L., di Porzio, U., Viggiano, D., de Donato, A., and Volpicelli, F. (2021). Dopamine: The neuromodulator of long-term synaptic plasticity, reward and movement control. *Cells* 10:735. doi: 10.1242/dev.201214

Stradal, T. E., and Scita, G. (2006). Protein complexes regulating Arp2/3-mediated actin assembly. *Curr. Opin. Cell Biol.* 18, 4–10. doi: 10.1016/j.ceb.2005.12.003

Sun, Y., and Giocomo, L. M. (2022). Neural circuit dynamics of drug-context associative learning in the mouse hippocampus. *Nat. Commun.* 13:6721. doi: 10.1038/s41467-022-34114-x

Swanson, A. M., DePoy, L. M., and Gourley, S. L. (2017). Inhibiting Rho kinase promotes goal-directed decision making and blocks habitual responding for cocaine. *Nat. Commun.* 8:1861. doi: 10.1038/s41467-017-01915-4

Takayama, N., and Ueda, H. (2005). Morphine-induced chemotaxis and brain-derived neurotrophic factor expression in microglia. *J. Neurosci.* 25, 430–435. doi: 10.1523/JNEUROSCI.3170-04.2005

Tatenhorst, L., Eckermann, K., Dambeck, V., Fonseca-Ornelas, L., Walle, H., Lopes da Fonseca, T., et al. (2016). Fasudil attenuates aggregation of alpha-synuclein in models of Parkinson's disease. *Acta Neuropathol. Commun.* 4:39. doi: 10.1186/s40478-016-0310-y

Tcherkezian, J., and Lamarche-Vane, N. (2007). Current knowledge of the large RhoGAP family of proteins. *Biol. Cell* 99, 67–86. doi: 10.1042/BC20060086

Tolias, K. F., Duman, J. G., and Um, K. (2011). Control of synapse development and plasticity by Rho GTPase regulatory proteins. *Prog. Neurobiol.* 94, 133–148. doi: 10.1016/j.pneurobio.2011.04.011

Tu, G., Ying, L., Ye, L., Zhao, J., Liu, N., Li, J., et al. (2019). Dopamine D1 and D2 receptors differentially regulate Rac1 and Cdc42 signaling in the nucleus accumbens to modulate behavioral and structural plasticity after repeated methamphetamine treatment. *Biol Psychiatry* 86, 820–835. doi: 10.1016/j.biopsych.2019.03.966

Underhill, S. M., Wheeler, D. S., Li, M., Watts, S. D., Ingram, S. L., and Amara, S. G. (2014). Amphetamine modulates excitatory neurotransmission through endocytosis of the glutamate transporter EAAT3 in dopamine neurons. *Neuron* 83, 404–416. doi: 10.1016/j.neuron.2014.05.043

Valentinova, K., Tchenio, A., Trusel, M., Clerke, J. A., Lalive, A. L., Tzanoulinou, S., et al. (2019). Morphine withdrawal recruits lateral habenula cytokine signaling to reduce synaptic excitation and sociability. *Nat. Neurosci.* 22, 1053–1056. doi: 10.1038/s41593-019-0421-4

Vega, F. M., and Ridley, A. J. (2007). SnapShot: Rho family GTPases. *Cell* 129:1430. doi: 10.1016/j.cell.2007.06.021

Wang, X., Cahill, M. E., Werner, C. T., Christoffel, D. J., Golden, S. A., Xie, Z., et al. (2013). Kalirin-7 mediates cocaine-induced AMPA receptor and spine plasticity, enabling incentive sensitization. *J. Neurosci.* 33, 11012–11022. doi: 10.1523/JNEUROSCI.1097-13.2013

Wang, Q., Chen, M., Schafer, N. P., Bueno, C., Song, S. S., Hudmon, A., et al. (2019). Assemblies of calcium/calmodulin-dependent kinase II with actin and their dynamic regulation by calmodulin in dendritic spines. *Proc. Natl. Acad. Sci. U. S. A.* 116, 18937–18942. doi: 10.1073/pnas.1911452116

Wheeler, D. S., Underhill, S. M., Stolz, D. B., Murdoch, G. H., Thiels, E., Romero, G., et al. (2015). Amphetamine activates Rho GTPase signaling to mediate dopamine transporter internalization and acute behavioral effects of amphetamine. *Proc. Natl. Acad. Sci. U. S. A.* 112, E7138–E7147. doi: 10.1073/pnas.1511670112

Wright, W. J., Graziane, N. M., Neumann, P. A., Hamilton, P. J., Cates, H. M., Fuerst, L., et al. (2020). Silent synapses dictate cocaine memory destabilization and reconsolidation. *Nat. Neurosci.* 23, 32–46. doi: 10.1038/s41593-019-0537-6

Xue, Y., He, J. T., Zhang, K. K., Chen, L. J., Wang, Q., and Xie, X. L. (2019). Methamphetamine reduces expressions of tight junction proteins, rearranges F-actin cytoskeleton and increases the blood brain barrier permeability *via* the RhoA/ROCK-dependent pathway. *Biochem Biophys Res Commun* 509, 395–401. doi: 10.1016/j.bbrc.2018.12.144

Xueyang, D., Zhanqiang, M., Chunhua, M., and Kun, H. (2016). Fasudil, an inhibitor of Rho-associated coiled-coil kinase, improves cognitive impairments induced by smoke exposure. *Oncotarget* 7, 78764–78772. doi: 10.18632/oncotarget.12853

Yang, X., Cao, Z., Zhang, J., Shao, B., Song, M., Han, Y., et al. (2018). Dendritic spine loss caused by AlCl(3) is associated with inhibition of the Rac 1/cofilin signaling pathway. *Environ. Pollut.* 243, 1689–1695. doi: 10.1016/j.envpol.2018.09.145

Yang, X., Liu, Y., Liu, C., Xie, W., Huang, E., Huang, W., et al. (2013). Inhibition of ROCK2 expression protects against methamphetamine-induced neurotoxicity in PC12 cells. *Brain Res.* 1533, 16–25. doi: 10.1016/j.brainres.2013.08.009

Yanni, P. A., and Lindsley, T. A. (2000). Ethanol inhibits development of dendrites and synapses in rat hippocampal pyramidal neuron cultures. *Brain Res. Dev. Brain Res.* 120, 233–243. doi: 10.1016/S0165-3806(00)00015-8

Yasuda, R., Hayashi, Y., and Hell, J. W. (2022). CaMKII: A central molecular organizer of synaptic plasticity, learning and memory. *Nat. Rev. Neurosci.* 23, 666–682. doi: 10.1038/s41583-022-00624-2

Yin, L. T., Xie, X. Y., Xue, L. Y., Yang, X. R., Jia, J., Zhang, Y., et al. (2020). Matrix metalloproteinase-9 overexpression regulates hippocampal synaptic plasticity and decreases alcohol consumption and preference in mice. *Neurochem. Res.* 45, 1902–1912. doi: 10.1007/s11064-020-03053-8

Zhao, J., Ying, L., Liu, Y., Liu, N., Tu, G., Zhu, M., et al. (2019). Different roles of Rac1 in the acquisition and extinction of methamphetamine-associated contextual memory in the nucleus accumbens. *Theranostics* 9, 7051–7071. doi: 10.7150/thno.34655

Zheng, Y., Zangrilli, D., Cerione, R. A., and Eva, A. (1996). The pleckstrin homology domain mediates transformation by oncogenic dbl through specific intracellular targeting. *J. Biol. Chem.* 271, 19017–19020. doi: 10.1074/jbc.271.32.19017

Zhu, Y., Xing, B., Dang, W., Ji, Y., Yan, P., Li, Y., et al. (2016). AUTS2 in the nucleus accumbens is essential for heroin-induced behavioral sensitization. *Neuroscience* 333, 35–43. doi: 10.1016/j.neuroscience.2016.07.007

Zhu, S., Zhao, C., Wu, Y., Yang, Q., Shao, A., Wang, T., et al. (2015). Identification of a Vav 2-dependent mechanism for GDNF/Ret control of mesolimbic DAT trafficking. *Nat. Neurosci.* 18, 1084–1093. doi: 10.1038/nn.4060

frontiers | Frontiers in Molecular Neuroscience

TYPE Original Research
PUBLISHED 30 March 2023
DOI 10.3389/fnmol.2023.1112927

OPEN ACCESS

EDITED BY
Juan Marín-Lahoz,
Hospital Universitario Miguel Servet,
Spain

REVIEWED BY
Mohammad Farhan,
Hamad Bin Khalifa University,
Qatar
Fabio Marti,
Institut National de la Santé et de la Recherche Médicale (INSERM),
France

*CORRESPONDENCE
Henning Schneider
✉ hschneider@depauw.edu

SPECIALTY SECTION
This article was submitted to Neuroplasticity and Development, a section of the journal Frontiers in Molecular Neuroscience

RECEIVED 30 November 2022
ACCEPTED 21 February 2023
PUBLISHED 30 March 2023

CITATION
Schneider H, Pearson A, Harris D, Krause S, Tucker A, Gardner K and Chinyanya K (2023) Identification of nicotine-seeking and avoiding larval zebrafish using a new three-choice behavioral assay.
Front. Mol. Neurosci. 16:1112927.
doi: 10.3389/fnmol.2023.1112927

Identification of nicotine-seeking and avoiding larval zebrafish using a new three-choice behavioral assay

Henning Schneider*, Anna Pearson, Drew Harris, Sabrina Krause, Andrew Tucker, Kaitlyn Gardner and Kuzivakwashe Chinyanya

Department of Biology, DePauw University, Greencastle, IN, United States

Introduction: Nicotine dependence is one of the main causes of preventable diseases in the United States. Nicotine-seeking and avoidance behavioral assays in larval zebrafish could be used for identifying potential new pharmacotherapeutics in an early phase of drug discovery and could facilitate the identification of genes and genomic variations associated with nicotine-seeking and avoidance behavior.

Methods: A new three-choice behavioral assay has been developed for the identification of nicotine-seeking and avoiding larval zebrafish. The three choices are represented by three compartments of a gradient maze. Video-recording and subsequent quantitative analysis of the swimming track was carried out using EthovisionXT (Noldus).

Results: Three behavioral phenotypes could be identified. Nicotine-seeking larval zebrafish occupied nicotine compartments for longer periods and entered the nicotine-containing compartments most frequently. Nicotine-avoiders spent most of the cumulative time in the water compartment or entered the water compartment most frequently. Non-seekers remained in the center compartment for most of the time. In the gradient maze, about 20–30% of larval zebrafish had a preference for low nicotine concentrations whereas nicotine avoidance was stronger at higher nicotine concentrations. Lower concentrations of nicotine (0.63 μM, 6.3 μM) resulted in higher percentages of nicotine seekers whereas high nicotine concentrations (63 μM, 630 μM) resulted in higher percentages of nicotine avoiders. Pre-treatment of larval zebrafish with nicotine slightly increased the percentage of nicotine avoiders at lower nicotine concentrations. Treatment with varenicline strongly increased the percentage of nicotine avoiders at lower nicotine concentrations.

Conclusion: The results show that larval zebrafish have individual preferences for nicotine that could change with drug treatment. The three-choice gradient maze assay for larval zebrafish provides a new testing paradigm for studying the molecular and cellular mechanisms of nicotine action and the discovery of potential new pharmacotherapeutics for the treatment of smoking cessation.

KEYWORDS

addiction, self-administration, drug-use, varenicline, smoking cessation

1. Introduction

The use of nicotine products remains one of the leading causes of preventable diseases in the United States.[1] Cigarette smoking leads to diseases such as lung cancer, heart disease, and COPD. Although smoking tobacco products in the United States has declined from 20.9% in 2005 to 12.5% in 2020, about 30.8 million adults, in the United States still smoke or regularly use some form of nicotine product. Adults, 45–64 years old, represent the age group with the highest percentage of smokers (14.9%). The rate of smoking is the highest among non-Hispanic American Indian/Alaska native adults (27.1%) and the highest in adults with an annual household income of less than $35,000 (20.2%). Youth use of tobacco product in the US is at 4.5% for middle school students and 16.5% for high school students (Park-Lee et al., 2022). Vaping liquids used in Juul's, and e-cigarettes contain nicotine and are popular among teenagers. Because the success rate of quitting smoking is low as 75% of individuals who quit smoking relapse within 3 months and 90% within 12 months, additional treatments and therapies are needed to improve the rate of smoking cessation (Ebbert et al., 2010; Jordan and Zhen-Xiong, 2018; Hurt et al., 2022). The use of nicotine products varies between individuals. Most nicotine users experience nicotine in adolescence for the first time. Transitions to avoidance (no nicotine use), controlled nicotine use and nicotine dependence (uncontrolled use) depend on both genetic and environmental factors (Wang et al., 2021).

While rodents are the standard model for studying the actions of drugs of addiction such as nicotine and for discovering potential new chemicals for nicotine cessation treatments, zebrafish (*Danio rerio*) have emerged as an alternative model (Pan et al., 2012; Parker et al., 2013; Kaleuff et al., 2014). Nicotine induces robust acute behavioral changes in all post-embryonic stages of zebrafish as well as nicotine-induced long term behavioral changes in adult zebrafish (Petzold et al., 2009; Brennan et al., 2011). The high fecundity and the fast development of zebrafish to the larval stage allows the screening of nicotine-seeking behavior as early as 5 days after fertilization (5 dpf) (Schneider, 2017). The genetic toolbox for analyzing and modifying the zebrafish genome is enormous and includes a sequenced reference genome and methods for genome modifications such as CRISPR and TALENs (Blackburn et al., 2013; Ata et al., 2016). In addition, the small size of larval zebrafish facilitates behavioral testing and fast screening of large number of chemicals (high throughput) (Rihel et al., 2010; MacRae and Peterson, 2015; Brady et al., 2016; Lee et al., 2022). While the behavioral response of larval zebrafish to acute exposures to nicotine (acute nicotine response, ANR) is routinely used in drug-development projects, they do not allow larval zebrafish to titrate their exposure to nicotine as in self-administration tests in rodents. Behavioral choice tests for drugs of dependence are less developed in larval zebrafish compared to adult zebrafish (Schneider, 2017; Nathan et al., 2022).

The initial experience associated with nicotine use impacts the future user patterns of nicotine products such as avoidance, casual use and dependence of nicotine products (US Department of Health and Human Services, 2014). To better understand the underlying mechanisms of nicotine use, behavioral choice tests in which animals can self-administer drugs are more suitable (Perkins, 1999). The self-administration experiments for drugs of abuse in rodents have been essential for the discovery of neuronal mechanisms regulating nicotine use but are more difficult to conduct in zebrafish and especially in larval zebrafish (Krishnan et al., 2014; Bosse and Peterson, 2017; Bosse et al., 2021a,b; Gallois et al., 2022; Nathan et al., 2022). Based on mazes that have been successfully used for rodents and single-chamber behavioral choice tests for larval zebrafish, we developed a three-compartment gradient-maze for measuring nicotine-seeking and avoidance behavior of individual larval zebrafish. Because nicotine can be taken up into the body through the skin, freely swimming larvae can self-administer or titrate nicotine by choosing to stay in the nicotine, a center, and a water compartment. The gradient maze is designed to allow the selective delivery and exposure to drugs as larval zebrafish can move freely between compartments. In this study, nicotine seeking and avoidance behavior were tested in the gradient maze at different nicotine concentrations, after nicotine pre-treatment and treatment with the nicotinic acetylcholine receptor agonist varenicline, the active drug in the smoking cessation drug Chantix (Coe et al., 2005; Benowitz, 2009; Rigotti et al., 2022).

2. Methods

2.1. Zebrafish

Adult wildtype zebrafish (PWT) were obtained from a local supplier and maintained at 28–29 degrees Celsius on a 14-h light/ 10-h dark cycle at the zebrafish facility of DePauw University. Embryos were collected from breeding tanks and placed in 100 mm Petri dishes filled with 25 ml half-strength (0.5x) embryo water (15 mM NaCl, 0.5 mM KCl, 1.0 mM $MgSO_4$, 0.15 mM KH_2PO_4, 0.05 mM Na_2HPO_4, 1.0 mM $CaCl_2$ and 0.7 mM $NaHCO_3$; after Brand et al., 2002). Larval zebrafish were raised in Petri dishes in embryo water at 28–29 degrees Celsius on a 14-h light/10-h dark cycle on LED light boxes in an incubator or behavioral room. Experiments were carried out with larval zebrafish on days 6–8 post fertilization (6–8 dpf). All protocols involving zebrafish had been approved by IACUC at DePauw University.

2.2. Chemicals

Working concentrations of nicotine solutions were prepared by serial dilution of a 10 M L-nicotine stock solution (Acros, AC181420250) using embryo water. Varenicline tartrate (Tocris, #3754) was obtained in powder-form and dissolved in embryo water to obtain a 10^{-2} M stock solution. Subsequent serial dilutions were carried out as needed with embryo water to obtain the desired working concentrations.

2.3. Mazes

Gradient mazes were made with 1.5% agarose dissolved in boiling embryo water and reusable 3D-printed gradient maze molds. The molds

1 https://www.cdc.gov/ – Smoking and Tobacco Use – Fast Facts and Fact Sheet, accessed 11-27-22.

were designed using AutoCAD (Autodesk) (Supplementary Figure S1). The area of each compartment was 15 mm × 15 mm. The connectors between compartments were 10 mm long and 2 mm wide. These dimensions were selected after testing diffusion of chemicals and movement of larval zebrafish. The connectors were narrow enough to reduce the diffusion of directly added chemicals out of the compartment and wide enough for larval zebrafish to pass through and move between compartments. A center compartment was connected on two opposite sides to outer compartments (Figure 1). The height of molds was 30 mm to allow easy removal. Either five 3D-printed molds [polylactic acid (PLA) material] were positioned evenly spaced in a single one-well plate[2] (#229501) or three 3D-printed molds were placed into 100 mm polystyrene Petri dishes (VWR #25384-342). Agarose was added to embryo water and completely dissolved by boiling in a microwave oven. After cooling for 10 min at room temperature, 55 ml of agarose solution was poured into the dish containing the molds and allowed to solidify for at least 45 min at room temperature. Molds were removed and any thin layer of solidified agarose that had formed underneath the molds at the bottom of the mazes was carefully removed using a plastic pipette tip. Depth of mazes was 8–9 mm. Mazes were covered with the lid, sealed with parafilm and stored for up to 3 days. For experiments, each gradient maze was filled with 5.0 ml embryo water to a water level of 7–8 mm measured in the center of each compartment.

2.4. Behavioral experiments

A single behavioral setup consisted of a video-camera (Canon Vixia HF R80 and R82) mounted 24 inches above an LED – light box (Displays2go.com; #APFLP1117) on a black wooden frame (Supplementary Figure S2). One one-well plate with five gradients mazes or one Petri dish with three gradient mazes was placed onto the LED light box and centered in the viewfinder of the camera. White artboard shielding was placed to surround the plate or dish to block any visual stimulation that could interfere with the free movement of larval zebrafish in the gradient maze. The shielding was temporarily removed for pipetting nicotine into the gradient mazes and replaced after pipetting was completed. Experimenters left the behavioral lab during the video-recording periods. To scale up the number of larval zebrafish that could be tested in one experiment session, we constructed three behavioral setups and placed them next to each other onto the same bench in the behavioral lab. Three one-well plates with 15 larval zebrafish or three Petri-dishes with 9 larval zebrafish total were tested in each experiment session.

Because larval zebrafish are sensitive to the environmental and water temperature all experiments were performed with temperature equilibrated mazes, solutions, and plasticware in a dedicated behavioral lab in which the room temperature was maintained between 27 and 29 degrees Celsius. Mazes and embryo water brought in from outside the behavioral lab were temperature equilibrated for at least 24 h before use in the behavioral lab.

Zebrafish embryos that were obtained from breeding setups using standard procedures, were raised in 100 mm polystyrene Petri dishes filled with 25 ml embryo water to the larval developmental stage in a 28 degree Celsius incubator on a 14 h light/10 h dark cycle and tested on day 6–8 after fertilization (6–8 dpf). Petri dishes contained 25–30 embryos. On the day of the experiment, Petri dishes with larval zebrafish were transferred from the incubator onto the LED light box of the video recording setup in the behavioral lab, the lid of the dish was removed, and the larval zebrafish could temperature and light adapt for 60 min. Each temperature-equilibrated maze was filled with 5 ml temperature-equilibrated embryo water using temperature equilibrated serological pipettes. One larval zebrafish (6–8 dpf) was transferred into the center compartment of one gradient maze each in the dish or plate using temperature equilibrated plastic transfer pipettes. The dish or plate with gradient mazes was positioned in the viewfinder of a video camera and the focus was adjusted manually. Movement activity was recorded for 30 min before nicotine solution was added into one compartment (pre-nicotine phase). After the 30-min pre-nicotine phase, videorecording was stopped and 5 µl nicotine solution was pipetted into one outer compartment of each maze. White artboard shielding was always placed around the plate or dish before videorecording was started (Supplementary Figure S2). The calculated dilution factor of nicotine solution was 315 in the nicotine compartment. The 5 µl of a 200 mM nicotine solution pipetted into the nicotine compartment, would be diluted 315 times based on the surface area of each compartment (15 mm × 15 mm) and the height of the water level in the center of compartments (~7 mm) resulting in a concentration of approximately 635 µM. The 5 µl nicotine solution was directly pipetted into a lower corner of one outer compartment (Figure 1 and Supplementary Movie S3). Pipetting the nicotine solution into the lower corner of the compartment is critical for preventing diffusion of nicotine into the center compartment. To avoid adding nicotine directly onto larval zebrafish, any larval zebrafish in an outer compartment were transferred to the center compartment immediately before adding nicotine. The white artboard shielding was placed to surround the plates with the mazes and videorecording was turned on. After 2 h, videorecording was stopped and larval zebrafish were transferred into 6-well plates, one larval zebrafish per well, each filled with 5 ml embryo water. Larvae were transferred and raised in the zebrafish facility. After one-week, larval zebrafish were transferred to larger containers and ultimately into 1.4 l zebrafish tanks (Aquatic Ecosystem, Aquaneering) kept on a zebrafish tank system (AquaticEcosystems).

2.5. Nicotine pre-treatment and varenicline treatment of larval zebrafish

For nicotine pre-treatments, larval zebrafish were first placed on the day of the experiment into 100 mm Polystyrene Petri dishes filled with 25 ml nicotine solution (1 µM) and kept on the LED light panel of the behavioral setup for 1 h. Then, larval zebrafish were transferred to mazes for the 30-min pre-nicotine equilibration on the light panel (no nicotine exposure in equilibration period) and videorecorded after placing white artboard shielding around the plate or dishes. Then nicotine solution was added to the mazes as described above, and videorecording resumed for 2 h. For varenicline testing, gradient mazes were filled with 5 ml embryo water containing 20 µM varenicline tartrate, all temperature equilibrated and placed onto the light panel. Then larval zebrafish were transferred into the center compartment of the mazes containing varenicline and incubated and

2 Celltreat.com

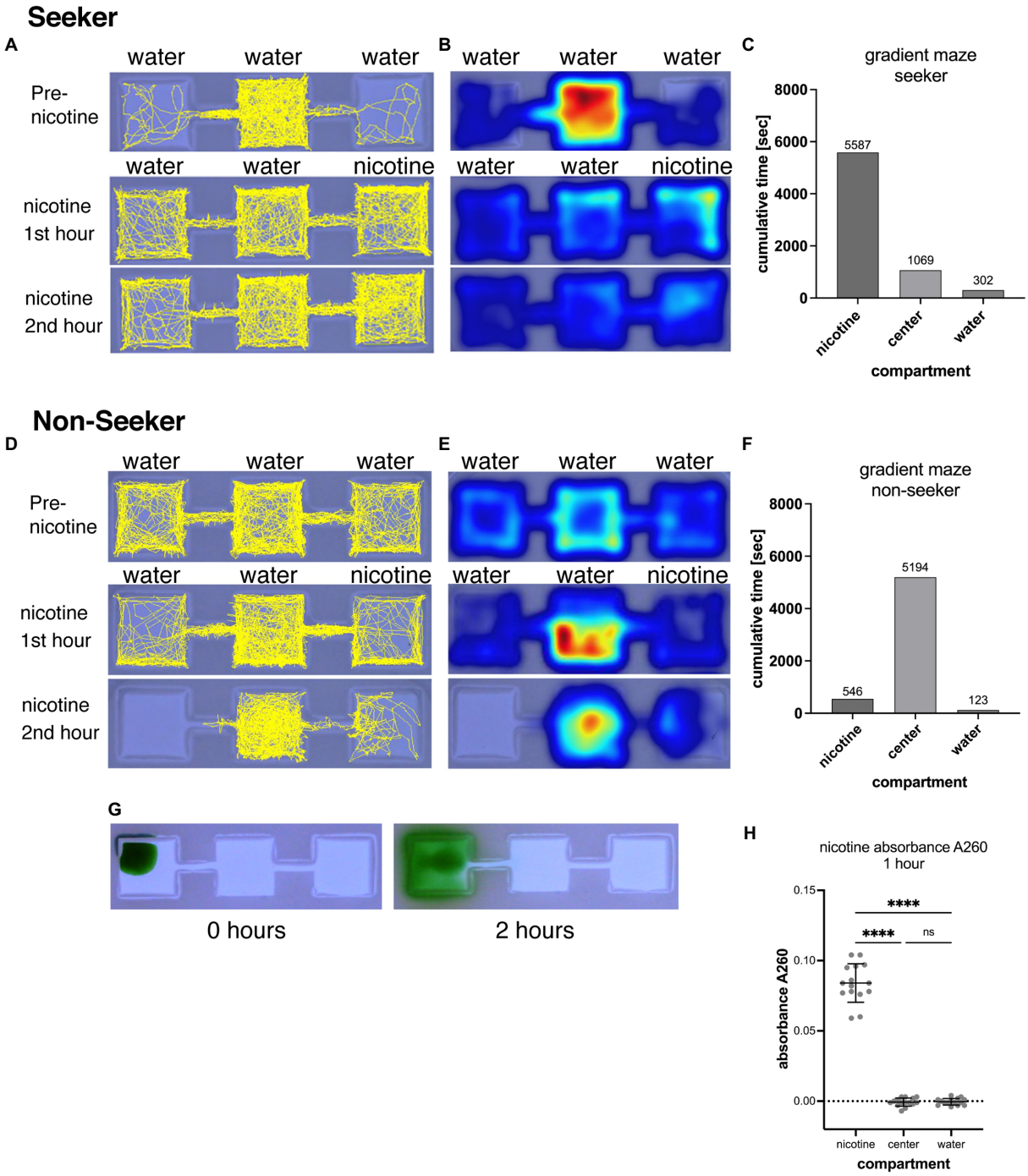

FIGURE 1
Shows the representation of swimming activities of a nicotine seeker **(A–C)** and a non-seeker **(D–F)**. Tracks of larval zebrafish (yellow) as generated by EthovisionXT are shown in **(A)** for a seeker and **(D)** for a non-seeker. Heatmaps of the corresponding experiments are shown in **(B)** for the seeker and **(E)** for the non-seeker. Warmer colors in heatmaps indicate more time spent in a location. Examples of the analysis for a single larval zebrafish are shown in **(C)** for the seeker and in **(F)** for the non-seeker. **(G)** Shows the diffusion of 5µl green food dye added to the left outer compartment of a gradient maze. After 2h the dye is mostly contained in the left compartment. **(H)** Absorbance measurements (at 260nm) of water samples (25µl) taken from the nicotine, center and water compartments of 15 gradient mazes 1h after pipetting 5µl of 200mM nicotine solution into the nicotine compartments. Each data point represents one measurement from one compartment. Absorbance could be detected in nicotine compartments but not in center and water compartment. Nicotine compartment: mean absorbance 0.084 (SD=0.0137; n=15); Center compartment: mean absorbance −0.0007 (SD=0.002895; n=15); Water compartments: mean absorbance −0.0004 (SD=0.002324; n=15). ****$p < 0.0001$; ns > 0.9999.

video-recorded for 1 h. After the 1-h equilibration period and varenicline treatment, nicotine was added to the mazes as described above. Videorecording was carried out during the 1 h of varenicline incubation period before addition of nicotine to compartment and the 2 h after pipetting of nicotine into the mazes. Both, varenicline and nicotine were present in the mazes over the 2-h video recording

period. For comparison, one experimental group of larval zebrafish was not treated with varenicline before addition of nicotine to nicotine compartments. Experiments without varenicline treatment and without the addition of water instead of nicotine served as additional control.

2.6. Dose dependency tests

When testing the nicotine seeking and avoidance behavior at different nicotine concentrations, experimental conditions were randomized. In one test session, three one-well plates with five gradient mazes each were setup and used simultaneously – one plate on each of three behavioral recording setups. Using this arrangement, three different nicotine concentrations were tested simultaneously on larval zebrafish from the same clutch. Each one of the three plates was set up with a different nicotine concentration or water (as control). In addition, the outer compartment into which the 5 µl nicotine solution (or water for controls) was pipetted varied between plates. Nicotine or water was pipetted into the left or right outer compartment. The randomization was carried out to account for potential clutch-specific behavioral variations.

2.7. Repeated testing

For repeated testing, individual larval zebrafish were tested on day 6, 7, and 8 post fertilization (dpf) using the same testing paradigm as described for behavioral testing above. After the first gradient maze test on 6 dpf, larval zebrafish were transferred to 6-well plates, one larval zebrafish per well, and kept in an incubator at 28 degrees Celsius and a 14 h light/10 h dark cycle until the testing on the second day. For the second test at 7 dpf, larval zebrafish were transferred from 6-well plates into new gradient mazes filled with embryo water. Behavioral experiments followed the same protocol on the first test day an as described above including the 30-min equilibration period (pre-nicotine) and a 2-h videorecording after nicotine had been added to one outer compartment. After this second day test, larval zebrafish were transferred back into the 6-well plates which were placed into the incubator under described temperature and light conditions. For the recording on the third day at 8 dpf, we followed again the same procedure as on the first 2 days of testing. Each larval zebrafish was tested on day 6, 7, and 8 post fertilization (pdf). For each experiment, 5 µl of 200 µM nicotine was added to the nicotine compartment as described above. For the statistical analysis, we used a two way ANOVA test to account for the different days of testing and the different compartments.

2.8. Data analysis and statistical test

Files of video recordings of experiments were imported into EthoVisionXT 15 (Noldus) for acquisition and subsequent analysis following the manufacturer's instructions. The acquisition parameters (arena and detection settings) were selected so that larval zebrafish were tracked continuously. To avoid that missing tracking coordinates introduced errors, especially for the analysis of entrances into compartments, we used the track editing tool in EthovisionXT. Swimming tracks were examined for accuracy of tracking quality (no tracks outside of a gradient maze). The swimming tracks of larval zebrafish were analyzed for the cumulative duration spent in compartments of mazes and the frequency of entering the nicotine compartment. Acquired data were exported to Excel (v16, Microsoft) for grouping results from all mazes in one plate or dish. The data were imported to Prism9 (Graphpad) that we used for graphing and statistical analyses including calculation of means and standard error means (±SEM). One-way ANOVA tests (Kruskal–Wallis with Dunn's posttest) were used for the analysis of cumulative duration and frequency of entering compartments in behavioral tests for the screening of nicotine seekers and avoiders, dose-dependency of nicotine seeking and avoidance behavior, nicotine pre-treatment experiments and varenicline experiments. A two-way ANOVA test was used for the analysis of repeated testing experiments.

3. Results

3.1. Nicotine-seeking in the gradient-maze for identification of nicotine-seekers and avoiders

A gradient-maze was developed for direct application of nicotine into the maze and identification of nicotine seekers and avoiders. A center compartment was linked by a narrow connector to outer compartments, one on each side (Figure 1). In experiments, nicotine was added to one outer compartment (nicotine compartment) while the other outer compartment opposite to the nicotine-compartment did not receive nicotine (water compartment). Following a 30-min acclimation period that started immediately after placing a single larval zebrafish into the central compartment, a nicotine solution (5 µl, 200-times concentrated) was added to one of the outer compartments. Nicotine-seeking larval zebrafish were defined by the cumulative time and number of entrances (frequency) into the nicotine compartment over the 2-h observation period. Larval zebrafish with the highest cumulative time in the nicotine compartment were identified as duration seekers (Figures 1A–C). Larval zebrafish with the longest cumulative duration spent in the water compartment were identified as duration avoiders. Larval zebrafish that entered the nicotine compartment most frequently compared to the center and water compartment were identified as frequency seekers. Larval zebrafish that entered the water compartment most frequently were identified as frequency avoiders. Larval zebrafish that spent most of the time in the center compartment or entered the center compartment most frequently were identified as non-seekers. (Figures 1D–F). The example of the track map in Figure 1A shows a nicotine seeker that spent most of the time in the center compartment before nicotine application but shifted toward the nicotine compartment after nicotine was added to the maze. Corresponding heat maps (Figure 1B) provided information about the activity pattern and were used only to determine if a larval zebrafish had stationary phases during which they a did not move. The example of a non-seeker (Figures 1D,E) showed the shifted away from the nicotine compartment once nicotine was added as well as shifting away from the water

compartment and became more stationary in the center compartment (Figure 1E). A significant shifting of larval zebrafish between compartments after application of nicotine was used to determine responses to nicotine and drug treatments.

The volume and concentration of nicotine solution that was pipetted into the nicotine compartment was selected to limit diffusion of nicotine out of the compartment and generating a concentration around 1 µM in the nicotine compartment. Larval zebrafish had a 100% 24 h-survival rate at 1 µM nicotine and seemed to be attracted by nicotine (Krishnan et al., 2014). Indeed, the narrow link between the center compartment suppressed the diffusion of added liquids from the outer (nicotine) to the center compartment over the 2-h video-recording phase as shown (Figure 1G). When 5 µl of concentrated food dye was pipetted into an outer compartment, only a small amount of liquid could diffuse into the center compartment, and none into other outer compartment which did not appear to contain any food dye after 2 h. To determine the concentration and potential diffusion of nicotine in the gradient maze we measured the absorbance of nicotine at 260 nm (Willits et al., 1950). Solutions were sampled from all three compartments after the first hour of adding 5 µl of nicotine (200 mM) to the nicotine compartment when the gradient maze was filled with 5.0 ml embryo water. After 1 h mean positive absorbance of 0.084 (SD = 0.0137; $n = 15$) could be detected in the nicotine but not in the center (mean = −0.0007; SD = 0.002895; $n = 15$) and water compartments (mean = −0.0004; SD = 0.002324; $n = 15$) indicating that nicotine did not diffuse from the nicotine compartment into the center compartment (Figure 1F). However, the calibration measurements for this spectrophotometric nicotine measurement showed that absorbances of concentrations below 10 µM could not be detected reliably because of negative absorbances. Based on the A260 values, adding a 5 µl volume of nicotine (200 mM) resulted in a mean concentration of 630 µM (using the obtained standard curve $y = 0.1633x - 0.019$; $n = 15$) in the nicotine compartments after 1 h of adding nicotine. Based on these results we concluded that adding 5 µl of 200 mM nicotine to the compartment would results in a concentration of 630 µM nicotine, 5 µl of 20 mM nicotine in a nicotine concentration of 63 µM, 5 µl of 2 mM nicotine in a nicotine concentration of 6.3 µM and 5 µl of 200 µM in a nicotine concentration of 0.63 µM. The design of the gradient maze allowed easy delivery and retention of nicotine in compartments in which larval zebrafish can swim freely following their preferences.

3.2. Identification of nicotine-seekers and avoiders

The first series of experiment established behavioral phenotype profiles. The preferences for nicotine were tested on 390 larval zebrafish and a nicotine concentration of 0.63 µM in the nicotine compartment (Figure 2). The cumulative time and the frequency of entering the compartment was analyzed. In gradient maze tests ($n = 390$), larval zebrafish spent most of the time (3,974 s; SEM ± 101.6) in the center compartment (Figure 2A). The nicotine compartment and the water compartment were occupied for similar average cumulative times (nicotine: 1204 s; SEM ± 81.75; water: 1162 s; SEM ± 73.44). The difference between the time spent in the nicotine and water compartment was not significantly different ($p > 0.9999$).

When analyzing the preference of all tested larval zebrafish (cohort), 22.8% or 89 out of 390 tested larval zebrafish were identified as nicotine-seekers at 0.63 µM nicotine. These 89 seekers included 36 super seekers (spent most time in the nicotine compartment and entered the nicotine compartment most frequently), 22 duration seekers (spent most time in the nicotine compartment) and 31 frequency seekers (entered the nicotine compartment most frequently) (Table 1).

Larval zebrafish with a nicotine duration seeker profile ($n = 58$, duration seekers and super seekers) spent a mean time of 4,513 s (SEM ± 196) in the nicotine compartment, 1,350 s in the center compartment (SEM ± 139) and 605 s (SEM ± 134) in the water compartment (Figure 2B). In comparison, larval zebrafish with a nicotine duration avoider profile ($n = 67$, duration avoiders and super avoiders) spent a mean time of 413 s in the nicotine compartment (SEM ± 65), 1809 s (SEM ± 137) in the center compartment and 3,953 s (SEM ± 170) in the water compartment (Figure 2C). Non-seekers including larval zebrafish that spent most of the time in the center compartment or entered the center compartment most frequently ($n = 208$) made up 53.3% of the tested larval zebrafish in the gradient maze, spent a mean time of 4,945 s (SEM ± 130) in the center compartment, 740 s (SEM ± 61.09) in the nicotine compartment and 651 s (SEM ± 57.81) in the water compartment.

The frequency analysis of larval zebrafish entering the three compartments for the entire cohort ($n = 390$) mirrored the duration results (Figure 2D). The center compartment was entered most frequently (mean 343.9; SEM ± 19.0), while entrances into the nicotine compartment (mean 167.5; SEM ± 13.37) and the water compartment (mean 164.8; SEM ± 15.09) were similar and not significantly different ($p = 0.1124$, $n = 390$). The differences between the number of entrances into the nicotine and center compartments were significantly different ($p < 0.001$); also, the number of entrances into the water compartment compared to the center compartment were significantly different ($p < 0.001$). Larval zebrafish with a frequency seekers profile ($n = 60$, including frequency seekers and super seekers) preferred the nicotine compartment (mean 433 entrances; SEM ± 56) over the center compartment (mean 164 entrances; SEM ± 26) and the water compartment (mean 84 entrances; SEM ± 21) (Figure 2E). The differences recorded for the three compartments varied significantly (nicotine vs. center – $p < 0.0001$; nicotine vs. water – $p < 0.0001$; center vs. water $p = 0.0018$). Larval zebrafish with a nicotine frequency avoider profile ($n = 62$, frequency avoiders and super avoiders) entered the water compartment most frequently (mean 521 entrances; SEM ± 66) compared to the center (mean 211 entrances; SEM ± 29) and nicotine compartments (mean 110 entrances; SEM ± 26) (Figure 2F). The number of entrances between the nicotine and the water compartment ($p < 0.0001$), between the nicotine and the center compartment ($p = 0.0021$) and between the center and the water compartment ($p < 0.0001$) were significantly different.

Out of 390 larval zebrafish that were tested in the gradient maze, 93 (23.8%) were identified as nicotine-avoiders including 36 super avoiders (spent most of the time in the water compartment and entered the water compartment most frequently), 31 duration avoiders (spent most of the time in the water compartment) and 26 frequency avoiders (entered the water compartment most frequently). (Table 1).

Overall, the analysis of cumulative time spent in compartments and the frequency of entering compartments identified behavioral

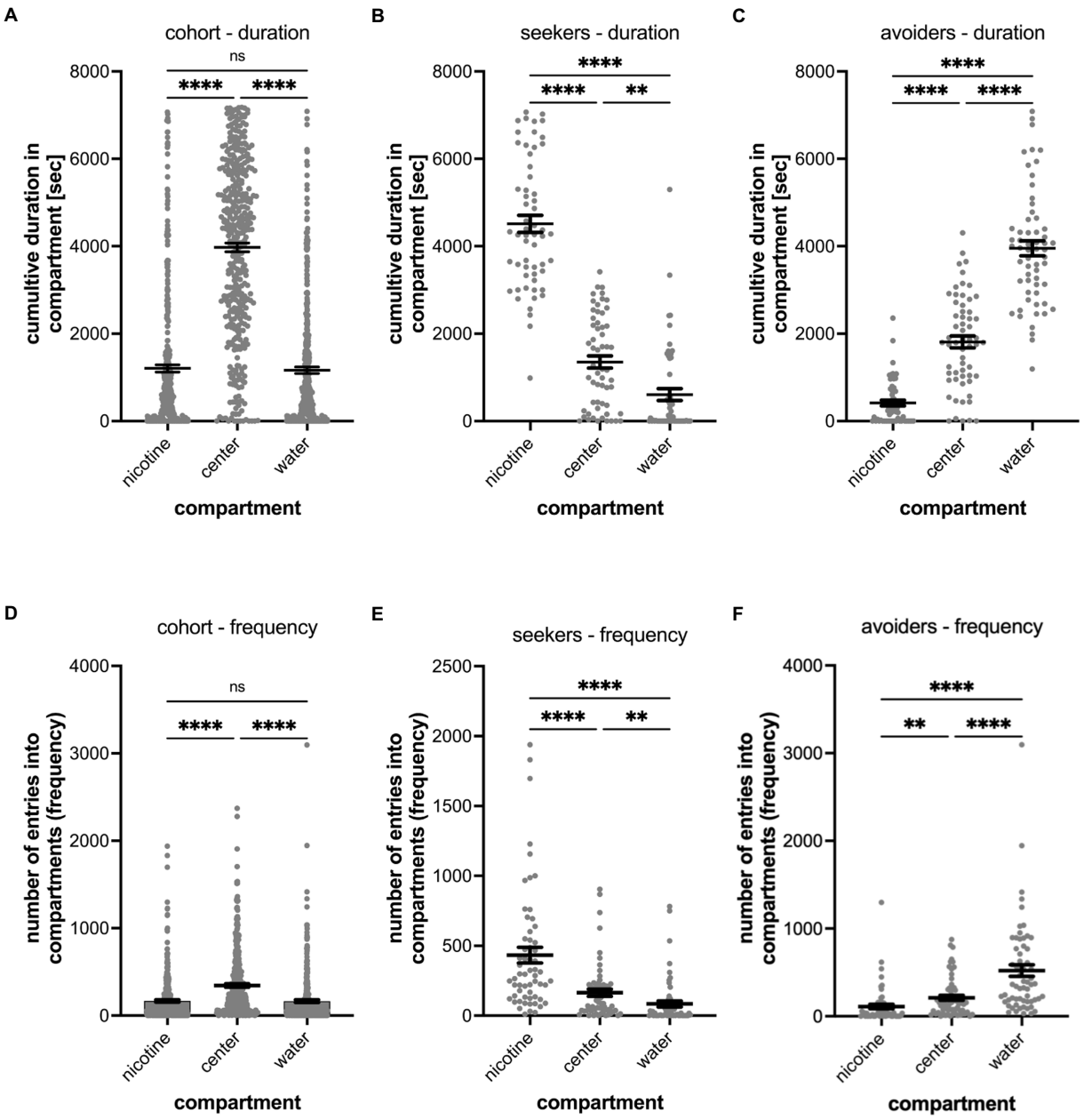

FIGURE 2
Shows the quantitative analysis of the cumulative duration spent in compartments of the gradient maze **(A–C)** and the number of entrances into compartments (frequency) **(D–F)**. The results for the entire cohort are shown in **(A,D)**, for nicotine seekers in **(B,E)** and for nicotine avoiders in **(C,F)**. Each graph shows the individual datapoints for the nicotine compartment (nicotine), center compartment (center), and the water compartment (water). Data are shown as mean with ±SEM. Statistical significance was tested using a one-way ANOVA Kruskal–Wallis test with Dunn's comparison test. The results for the cumulative duration of the cohort **(A)** and for the frequency of entering a compartment for the cohort (n =390) establish the behavioral profile baseline for the nicotine-seeker and avoidance test. Nicotine-seekers spent significantly more time in the center compartment compared to the nicotine and water compartment (nicotine vs. center p <0.0001; nicotine vs. water $p \geq 0.9999$, center vs. water p <0.0001). In **(B)** the behavioral profile of nicotine duration seekers (n =58) has shifted to the nicotine compartment (nicotine vs. center: p <0.0001; nicotine vs. water: p <0.0001, center vs. water: p =0.0046). For nicotine duration avoiders (n =60) in **(C)** the behavioral profile has shifted to the water compartment. **(D)** Nicotine vs. center: p <0.0001; nicotine vs. water: p <0.0001, center vs. water: p <0.0001). The results for entering the nicotine, center and water compartments of the cohort (n =390) are similar compared to the duration profile (nicotine vs. center: p <0.0001; nicotine vs. water: p =0.7969, center vs. water: p =0.0026). In **(E)** the behavioral profile of frequency seekers has shifted to the nicotine compartment (nicotine vs. center: p <0.0001; nicotine vs. water: p <0.0001, center vs. water: p =0.0018). In **(F)** the behavioral profile for frequency avoiders has shifted to the water compartment (nicotine vs. center: p =0.0021; nicotine vs. water: p <0.0001, center vs. water: $p < 0.0001$). Data are shown as mean with ±SEM. Statistical significance was tested using a one-way ANOVA Kruskal–Wallis test with Dunn's comparison test. ****$p < 0.0001$; **$p < 0.0056$; *$p < 0.046$; ns > 0.9999.

profiles for (1) nicotine-seekers, (2) nicotine-avoiders, and (3) non-seekers. The experimental setup allowed the testing of large numbers of larval zebrafish easily. Environmental and genetic factors associated with behavioral responses to nicotine could potentially be identified by significant shifting of behavioral profiles in test groups.

TABLE 1 Behavioral Phenotypes in a Cohort of 390 larval zebrafish (100%).

Behavioral Phenotype	Total	%
All Seekers	89	22.8
Duration Seeker	22	5.6
Frequency Seekers	31	7.9
Super Seekers	36	9.2
Duration + Super Seekers	58	14.9
All Avoiders	93	23.8
Duration Avoiders	31	7.9
Frequency Avoiders	26	6.7
Super Avoiders	36	9.2
Duration + Super Avoiders	67	17.2
All Non-seekers	208	53.3

3.3. Dose-dependency of nicotine seeking and avoidance

To explore whether nicotine concentrations impacted nicotine-seeking and avoidance in larval zebrafish, nicotine concentrations ranging from 0.63 to 630 µM were tested in the gradient maze assay (Figure 3 and Tables 2A,B). Control experiments were carried out in parallel on one of three behavioral setups while nicotine tests were performed on the two additional setups simultaneously with larval zebrafish from the same clutch. In controls, 5 µl embryo water were added to an outer compartment instead of a nicotine solution. For comparison, the movement activity over a 30-min period immediately before the addition of nicotine (pre-nic) to one compartment of the maze was video-recorded and analyzed.

Before adding nicotine to the nicotine compartment or water in case of the control, no statistically significant differences were detected for the cumulative duration (Figures 3A,C) in different test groups in the nicotine compartment (water, $n = 35$; 0.63 µM nicotine, $n = 30$; 6.3 µM nicotine, $n = 75$; 63 µM nicotine, $n = 20$; and 630 µM nicotine, $n = 20$). Cumulative durations in the nicotine compartment during the 30-min phase prior to adding nicotine were not significantly different between test groups (Figure 3A). Compared to the water control group (mean 355.6 s; SEM ± 96.94; $n = 35$), the mean cumulative durations at 0.63 µM nicotine (563.4 s; SEM ± 126.5 s; $n = 30$), at 6.3 µM nicotine (405.6 s; SEM ± 73.94; $n = 75$), at 63 µM nicotine (629.6 s; SEM ± 161.6; $n = 20$) and at 630 µM nicotine (mean 527.2 s; SEM ± 148.4; $n = 20$) were not significantly different ($p > 0.9999$ for water vs. 0.63 µM, water vs. 6.3 µM, and water vs. 63 µM; $p = 0.0909$ for water vs. 630 µM; one-way ANOVA; Kruskal–Wallis with Dunn's multiple comparison test).

Cumulative durations in the nicotine compartment significantly increased after addition of nicotine in the 0.63 and 6.3 µM nicotine groups (Figure 3B). Compared to the water control (mean 1,056 s, SEM ± 323.2, $n = 35$), 0.63 and 6.3 µM nicotine increased the cumulative time in the nicotine compartment significantly (0.63 µM: mean 1853 s; SEM ± 293.8; $n = 35$; 6.3 µM – mean 2,222 s, SEM ± 277.3; $n = 75$). At 63 µM nicotine the cumulative time (1752 s ± SEM 404.7; $n = 20$) was longer compared to the mean of the water control experiment but was not significantly different potentially because of the wide range (Figure 3B and Table 2A). At 630 µM nicotine the mean cumulative time in the nicotine compartment was reduced (901.1 s; SEM ± 481.6; $n = 20$) compared to the water controls, but not significantly different from the water control group (Figure 3B). Overall, nicotine concentrations ranging from 0.63 to 630 µM significantly increased the cumulative time spent in the nicotine compartment, while higher concentrations did not affect the time spent in the nicotine compartment. The differences between water controls and 0.63 µM nicotine ($p = 0.0158$) and between controls and 6.3 µM nicotine ($p = 0.0092$) were significant. Calculated means for 63 and 630 µM nicotine were not significantly different from the mean of the water control. Cumulative durations for the different test groups in the water compartments before (Figure 3C) and after nicotine addition (Figure 3D) were not significantly different from the water controls at all tested nicotine concentrations (0.63, 6.3, 63, and 630 µM).

The different nicotine concentrations resulted in fewer changes in the number of entrances into the nicotine compartment compared to the duration (Figures 3F,H and Table 2B). Before the addition of nicotine into the nicotine compartment and during 30 min pre-nicotine phase entrances into the water compartment (mean 2; SEM ± 1; $n = 35$), the nicotine compartment at 0.63 µM (mean 3; SEM ± 1; $n = 30$), the nicotine compartment at 6.3 µM (mean 2; SEM ± 0; $n = 75$), the nicotine compartment at 63 µM (mean 2; SEM ± 1; $n = 20$) and the nicotine compartment at 630 µM (mean 2; SEM ± 0; $n = 20$) were not significantly different (Figure 3E). After the addition of nicotine (Figure 3F) and over the 2-h nicotine phase, significantly more entrances occurred at 0.63 µM nicotine (mean 13; SEM ± 2; $n = 30$; $p = 0.0478$) and at 6.3 µM nicotine (mean 6; SEM ± 0.9; $n = 75$), but not at 63 µM nicotine (mean 7; SEM ± 2; $n = 20$) and 630 µM nicotine (mean 2; SEM ± 0.5; $n = 20$) compared to the number of entrances in water controls (mean 6; SEM ± 1; $n = 35$). The number of entrances into the water compartment in controls before addition of nicotine (mean 6; SEM ± 0.9; $n = 35$), at 0.63 µM nicotine (mean 10; SEM ± 2; $n = 30$), 6.3 µM nicotine (mean 7; SEM ± 1; $n = 75$), 63 µM nicotine (mean 10; SEM ± 4; $n = 20$) and 630 µM nicotine (mean 4; SEM ± 0.8; $n = 20$) did not differ significantly ($p > 0.9999$) (Figure 3G). Addition of nicotine did not result in significant differences ($p > 0.9999$) in the frequency of entering the water compartment between water (mean, SEM ± 0.9, $n = 35$), 0.63 µM nicotine (mean 10, SEM ± 2, $n = 30$), 6.3 µM nicotine (mean 7, SEM ± 1, $n = 75$), 63 µM nicotine (mean 10, SEM ± 4, $n = 20$) and 630 µM nicotine (mean 4, SEM ± 0.8, $n = 20$) (Figure 3H). Overall, the frequency of entering nicotine and water compartments did not change significantly with nicotine concentrations, except for the nicotine compartment at 0.63 and 6.3 µM nicotine.

The analysis of the percentages of behavioral phenotypes (Figure 3I) showed that nicotine caused the highest percentages of seekers for 0.63 µM nicotine (30%) and 6.3 µM nicotine (26.7%). Fewer nicotine-seekers were identified in water controls (20%) and at nicotine concentrations of 63 µM (20.0%) and 630 µM nicotine (20.0%). The percentage of nicotine avoiders was the lowest at 0.63 µM nicotine (16.7%) and highest at 63 µM nicotine (35.0%). In control experiments in which water was added to the test compartment, 22.9% of tested larval zebrafish were avoiders. Percentages of non-seekers were 57.1% for water controls, 53.3% for 0.63 µM nicotine, 45.3% for 6.3 µM nicotine, 45.0% for 63 µM nicotine and 50% for 630 µM nicotine. Thus, lower nicotine concentrations (0.63–6.3 µM) caused more nicotine-seeking while higher concentrations (63, 630 µM) were associated with more nicotine avoidance.

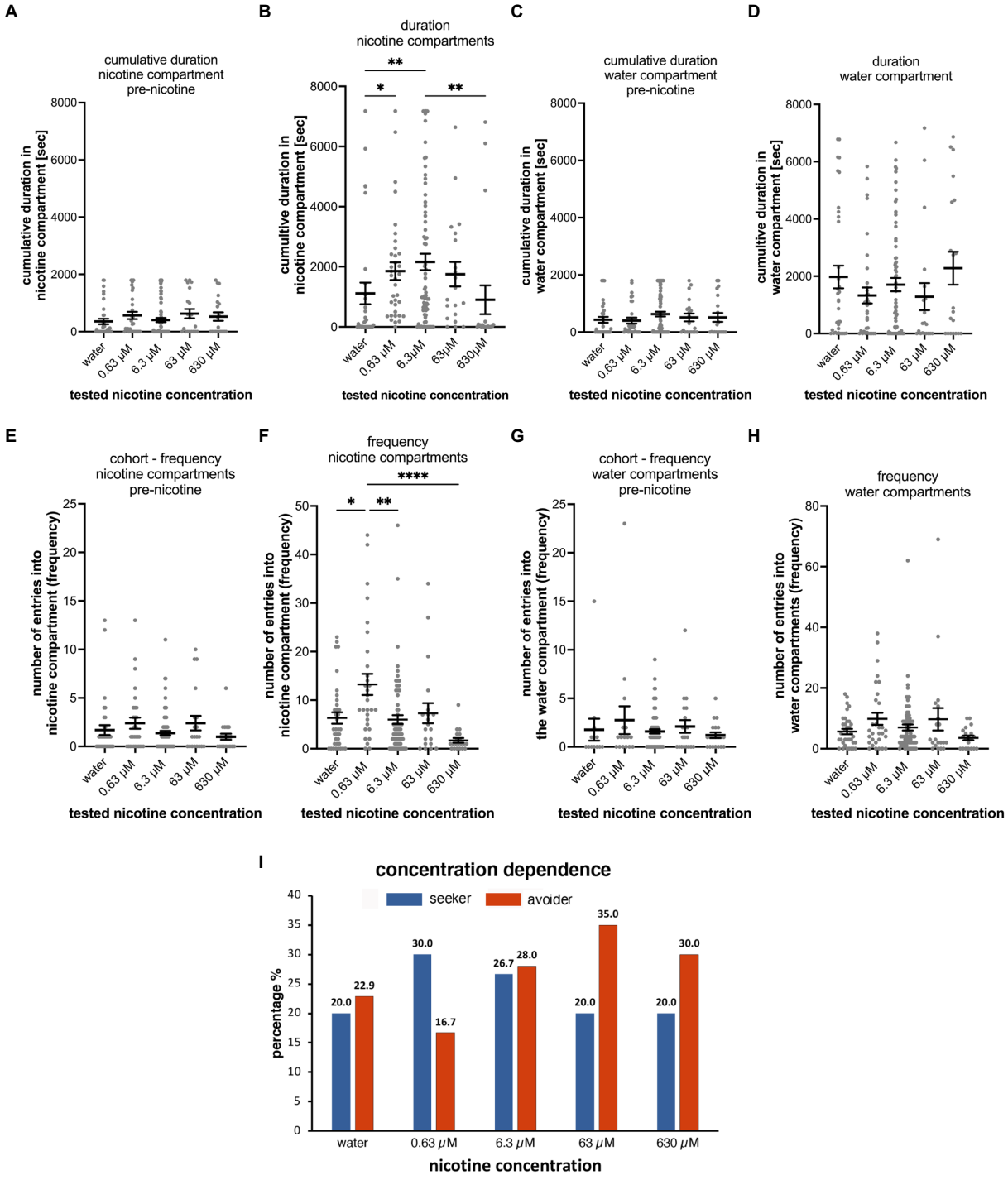

FIGURE 3
Concentration dependence of nicotine-seeking and avoidance in larval zebrafish. **(A)** Shows the duration spent in the "nicotine" compartment before the addition of nicotine (pre-nicotine). No significant differences (p>0.9999) were detected between water controls (water) and different nicotine concentrations (0.63, 6.3, 63µM nicotine, and 630µM nicotine) for the cumulative duration in the pre-nicotine phase of experiments. The duration of the pre-nicotine phase was 30min compared to the duration of the 2-h nicotine phase after adding nicotine. **(B)** The concentration of nicotine increased the cumulative duration in the nicotine compartment compared to water controls for 0.63µM nicotine (p=0.0158), and for 6.3µM nicotine (p=0.0092), but not for 63µM nicotine (p=0.2627) and 630µM nicotine (p>0.9999). The difference in cumulative duration in 630µM nicotine decreased significantly (p=0.0015) compared to the 6.3µM nicotine concentration. No significant differences in the cumulative duration in the water compartment were apparent in the 30-min pre-nicotine phase **(C)** and the 2-h nicotine phase **(D)** of the experiments. **(E)** The number of entrances into the "nicotine" compartment (frequency) before the addition of nicotine (pre-nicotine) were not significantly different. **(F)** After the addition of nicotine at a final concentration as indicated (0.63, 6.3, 63, and 630µM) compared to water controls (water) the number of entrances increased in 0.63µM nicotine (p<0.0001), but not in 6.3µM nicotine (p=0.7926), 63µM nicotine (p>0.9999) and 630µM nicotine (p>0.9999). The number of entrances into the water compartment (frequency) before the addition of nicotine (**G**, pre-nicotine) and after the addition of nicotine **(H)** at tested concentrations were not significantly different. Data are shown as mean ±SEM. Statistical significance was tested using a Kruskal–Wallis test with Dunn's comparison test. Levels

(Continued)

FIGURE 3 (Continued)
of significance are indicated. **(I)** The percentage of nicotine-seekers (combined duration seekers, frequency seekers, and super seekers) and avoiders (combined duration avoiders, frequency avoiders and super avoiders) for each tested nicotine concentration (0.63, 6.3, 63, and 630μM) as well as water controls (water) showed an increase in seekers at 0.63 and 6.3μM nicotine followed by a decrease in 63 and 630μM nicotine. Data labels above columns indicate percentages. Most avoiders were counted at 63 and 630μM nicotine. The lowest percentage of avoiders was found at 0.63μM nicotine and a slightly higher percentage at 6.3μM. Individual data points are shown with the mean ±SEM. Statistical significance was tested using a one-way ANOVA Kruskal–Wallis test with Dunn's comparison test. ****$p < 0.0001$; **$p < 0.0058$; *$p < 0.049$.

TABLE 2A Statistical analysis of nicotine dose-dependency - duration in nicotine compartment.

Duration	Water	0.63μM	6.3μM	63μM	630μM
n	35	30	75	20	20
Mean	1,114	1853	2,161	1752	901.1
SD	2004	1738	2,282	1810	2,154
SEM	360	293.8	272.7	404.7	481.6
Min	0	0	0	0	0
Max	7,177	7,178	7,177	6,641	6,813
Range	7,177	7,178	7,177	6,641	6,813

TABLE 2B Statistical analysis of nicotine dose-dependency - frequency in nicotine compartment.

Duration	Water	0.63μM	6.3μM	63μM	630μM
n	35	30	75	20	20
Mean	6	13	6	7	2
SD	7	12	8	9	2
SEM	1	2	0.9	2	0.5
Min	0	0	0	0	0
Max	23	44	46	34	9
Range	23	44	46	34	9

3.4. Repeated testing

To determine the consistency of nicotine seeking and avoidance behavior, 30 individual larval zebrafish were tested repeatedly over 3 days at 6, 7, and 8 dpf, one time on each day at the same time of the day and at a concentration of 0.63 μM nicotine. Results from one larval zebrafish on 1 day were not included because of a fly that entered the maze. The analysis of the cumulative durations of the entire cohort on each tested day did not show significant differences [two way ANOVA; $F(2,261) = 0.002750$; $p = 0.9973$; $n = 29$] (Figure 4A). Larval zebrafish spent similar times in the nicotine compartment on day 1 (Figure 4A1) (963.5 s; SEM ± 215.8; $n = 29$), day 2 (1,491 s; SEM ± 482.0; $n = 29$), and day 3 (1,021 s; SEM ± 373.0; $n = 29$). These durations were not significantly different between day 1 and day 2 ($p = 0.7706$, n = 29), day1 and day3 ($p = 0.935$, $n = 29$) and day2 and day 3 ($p = 0.9214$; n = 29). Cumulative durations for the center compartment (Figure 4A2) were higher compared to the nicotine compartment on day 1 (5,080 s; SEM ± 325.0; $n = 29$) day 2 (4,658 s; SEM ± 523.5; $n = 29$), and day 3 (4,894 s; SEM ± 491.1; $n = 29$). No differences were seen for the cumulative durations between day1 and day 2 ($p \geq 0.9999$, $n = 29$), day 1 and day 3 ($p > 0.9999$, $n = 29$) and day 2 and day 3 ($p > 0.9999$, $n = 29$). The cumulative durations for the water compartment also were not significantly different (Figure 4A3) on day1 (1,007 s; SEM ± 235.7; $n = 29$), day 2 (1,047 s; SEM ± 359.7; $n = 29$) and day 3 (1,265 s; SEM ± 441.7; $n = 29$). Comparisons of cumulative durations in the water compartment between day 1 and day 2 (0.3852, $n = 29$), day 1 and day 3 ($p = 0.2258$, $n = 29$) and day 2 and day 3 ($p > 0.9999$, $n = 29$) did not indicate significant differences. The analysis of the frequency of entering compartments for the entire cohort on each tested day showed a significant shift in activity [two way ANOVA; $F(2,252) = 16.44$; $p < 0.0001$; $n = 29$] (Figure 4B). Larval zebrafish entered compartments more frequently on the first day and less on the second and third day of testing (Figures 4B1–B3). The frequency of entering the nicotine compartment (Figure 4B1) was the highest on day1 (11.3, SEM ± 2.7; $n = 29$) compared to day2 (3.1; SEM ± 0.8, $n = 29$) and day 3 (2.5; SEM ± 0.8, $n = 29$). The frequency on day 1 was significantly higher compared to day 2 ($p = 0.0198$, $n = 29$) and day 3 ($p = 0.145$, $n = 29$). No significant change was found between day 2 and day 3 ($p = 0.8527$, $n = 29$). The difference between entrances into the center compartment (Figure 4B2) also were the highest on the first test day (19.2; SEM ± 3.6; $n = 29$) compared to the second (9.4; SEM ± 1.8, $n = 29$) and third day (9.1; SEM ± 1.7 n = 29). The differences between day 1 and day 3 were statistically significant ($p = 0.0005$) but not between day 1 and day 2 ($p = 0.1026$) and between day 2 and 3 day 3 ($p = 0.2975$). Frequency of entrances into the water compartment (Figure 4B3) were not significantly different on all days (Day1 vs. Day2 $p = 0.1762$; day1 vs. day 2 $p = 0.1773$; day 2 vs. day 3 $p > 0.9999$). The results of repeated experiments showed a high degree of consistency for the cumulative duration on all three test days. The frequency of entering compartments were similar on day 2 and day 3 of testing with less movement between compartments compared to test in day 1 when movement activity between compartments was about twice as high as on day 2 and 3. Otherwise, major shifts between days to or from the nicotine and water compartments were not detected for the cohort.

Variations of the behavioral phenotype – seeker vs. avoider – were found in individual zebrafish. Overall, the behavioral phenotype was consistent on two or more days in 79.3% of tested larval zebrafish. Of the 29 tested larval zebrafish, 11 (37.9%) showed the same seeking behavior on all 3 days (example #103B in Figures 4C,F), 12 (41.4%) showed the same behavior on 2 out of 3 days (example #102A in Figures 4D,G), and 6 (20.7%) showed different behavioral phenotypes on all 3 days (example #104D in Figures 4E,H). The larval zebrafish that had a similar behavioral phenotype based on duration on 2 out of 3 days included 5 that were non-seekers on 2 days and seekers on 1 day, 2 larval zebrafish that were seekers on 2 days and non-seekers on 1 day, 2 larval zebrafish that were avoiders on 1 day and non-seekers on 2 days and 2 larval zebrafish that were avoiders on 2 days and non-seekers on 1 day. The behavioral phenotypes for frequency were like those for duration in examples #103B and #104D. Example #102A was a frequency seeker on day1 of testing, a duration seeker on day 3 of testing, and a non-seeker on day2 of testing. Testing larval zebrafish throughout their larval life (up to 30 dpf) was challenging because of high mortality rates. Individual

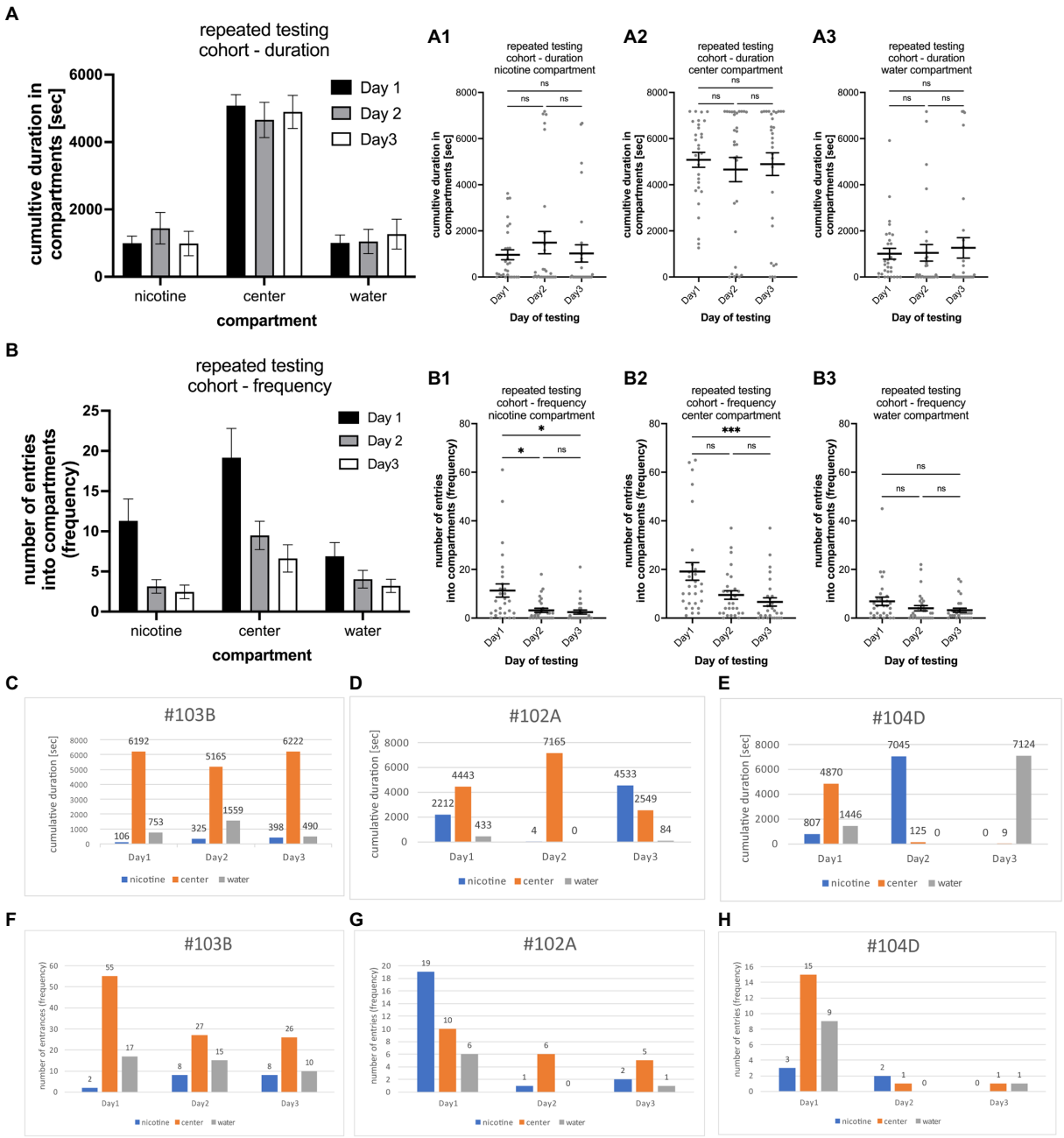

FIGURE 4
Shows the results of repeated testing of individual larval zebrafish for nicotine-seeking and avoidance in the gradient maze over the course of 3days. **(A)** Cumulative durations in the nicotine, center and water compartments of the entire cohort (n =29) show now similar behavioral activities on all 3days [two way ANOVA; $F(2,261)=0.002750$; p =0.9973; n =29] **(A1–A3)** show that the cumulative times for each compartment [**(A1)** nicotine compartment; **(A2)** center compartment; **(A3)** water compartment] were similar with no significant (ns) differences. **(B)** The number of entrances into the compartments was higher on the first day of testing for all three compartments (nicotine, center, and water). On day 2 and 3 of the testing lower number of entrances were recorded than on day 1 [two way ANOVA; $F(2,252)=16.44$; p <0.0001; n =29]. **(B1)** The number of entrances into the nicotine compartment was significantly higher on day 1 in comparison to day 2 and 3 (day1 vs. day2, p =0.0198; day1 vs. day 3, p =0.0145). **(B2)** Larval zebrafish also entered the center compartment more frequently on day 1 compared to day 3 of testing (p =0.0005). **(B3)** The number of entrances into the water compartment were not different on all three testing days. Individual data points are shown with the mean ±SEM. Statistical significance was tested using a one-way ANOVA Kruskal–Wallis test with Dunn's comparison test. Representative examples of larval zebrafish that showed similar behavioral profiles on all three testing days [#103B, **(C)** duration, **(F)** frequency], on two of the three testing days [#102A, **(D)** duration, **(G)** frequency]. In the third example (#104D, **E,H**) different behavioral profiles were recorded on each day of testing. Numbers on top of bars represent the cumulative duration spent in the compartment in **(C–E)** and the number of entrances into the compartment in **(F–H)**. ***p < 0.0005; *p < 0.0198.

larval zebrafish showed more consistency than variation in their behavioral phenotypes in repeated three-choice gradient maze tests which contributed to the overall consistency in the cohort results. However, individual differences and switching of nicotine preferences have been observed and could be based on individual genomic or developmental variations.

3.5. Treatment with nicotine and varenicline changes nicotine-seeking and avoidance behavior

3.5.1. Nicotine pre-treatment

Since exposure to nicotine in preferred place preference tests of adult zebrafish results in behavioral changes, we carried out nicotine-pretreatment experiments in the gradient maze to determine if nicotine-seeking and avoidance behavior could change with nicotine exposure. Overall, the pre-treatment seemed to affect the seeking and avoidance behavior only weakly. The mean time of the entire cohort spent in the water compartment (2,538 s; SEM ± 316, $n = 45$), compared to the nicotine compartment (mean 1,558 s; SEM ± 301; $n = 45$) was significantly longer ($p = 0.0364$) and similar to the cumulative time spent in the center compartment (Figure 5A). The cumulative times spent in the nicotine compartment (Figure 5B) between not-pretreated (–PT) and pretreated (+PT) larval zebrafish was similar (not pretreated – 1853 s, SEM ± 293.8; $n = 35$; pretreated- 1,558 s; SEM ± 300.6; n = 45) and not significantly different ($p = 0.1124$). Compared to the water control group (mean 1,056 s; SEM ± 323.3, $n = 35$), nicotine alone without pretreatment resulted in significantly more cumulative time spent in the nicotine compartment ($p = 0.0014$) but nicotine pretreatment did not ($p = 0.3143$). The cumulative time spent in the water compartment by the not pretreated nicotine group (nic -PT, mean 1,329 s, SEM ± 278.7, $n = 35$) was significantly lower compared to the nicotine pre-treatment group (2,538 s, SEM ± 316.0, $n = 45$) ($p = 0.0287$) (Figure 5C). However, the mean cumulative duration in the water compartment of pre-treated larval zebrafish (nicotine + PT) was not significantly different from water controls (water –PT; mean 1975 s, SEM ± 395.9, $n = 35$) ($p = 0.3816$). Thus, the nicotine pre-treatment did not change the time spent in nicotine or water compartments clearly.

Result of entrances into the gradient maze compartments showed similar patterns as results for the cumulative duration and provided no strong indication of a shift in nicotine-seeking or avoidance behavior. The entire cohort of larval zebrafish in the nicotine pre-treatment experiments entered the center compartment most frequently (mean number of entrances 15; SEM ± 3) and both the nicotine compartment (mean 8; SEM ± 2) and the water compartment (mean 8; SEM ± 1) at similar frequencies (Figure 5D). The center compartment was entered more frequently than the nicotine compartment ($p = 0.008$). But there was no significant difference between entrances into the center and water compartments. Nicotine pretreatment reduced the number of entrances into the nicotine compartment significantly (not pretreated vs. pretreated $p = 0.0175$, Figure 5E) as the mean number of entrances into the nicotine compartment by treated larval zebrafish (mean 7.5; SEM ± 2.1; $n = 45$) was lower compared to not pretreated larval zebrafish (mean 13.23; SEM ± 2.1; $n = 30$) and levels more similar to water controls without pretreatment (mean 6.314; SEM ± 1.2; $n = 35$). Number of entrances into the water compartment in water controls (mean 5.7, SEM ± 0.9, $n = 35$), nicotine not pretreated (mean 9.833, SEM ± 1.974, $n = 30$) and nicotine pretreated groups (mean 8.311, SEM ± 1.5, $n = 45$) did not differ significantly (Figure 5F).

The nicotine pretreatment did not shift the percentage of nicotine-seekers compared to other test groups (Figure 3I). Out of 45 tested larval zebrafish 9 (20%) were identified as nicotine seekers (4 super seekers, 4 duration seekers, 1 frequency seeker). In contrast, the percentage of nicotine avoiders was higher 35.6% (16 out of 45 tested larval zebrafish). The 16 nicotine-avoiding larval zebrafish included 9 duration avoiders, 3 frequency avoiders and 4 super avoiders.

Overall, the nicotine pre-treatment facilitated only slight changes more toward nicotine avoidance behavior and a larger percentage of nicotine avoiders but that shift was not significant when compared to not nicotine pretreated larval zebrafish.

3.5.2. Varenicline treatment

Varenicline is the active substance in the smoking cessation drug Chantix that reduces nicotine craving (Coe et al., 2005). To explore whether varenicline could change nicotine-seeking and avoidance behavior in the gradient maze test, larval zebrafish were treated with varenicline (20 μM) for 1 h in the gradient maze before the nicotine was added to the maze compartments. Moreover, varenicline has been used at concentrations up to 50 μM for larval zebrafish in overnight treatment (Cousin et al., 2014). We used 20 μM varenicline, because this concentration resulted in significant reduction of movement activity in acute nicotine response tests without indication of detrimental effects (Schneider, unpublished results). Over the first hour of the experiment, varenicline was added directly to the gradient maze and movement activity of larval zebrafish was recorded for 1 h. Nicotine was applied to the nicotine compartment to reach a final concentration around 3.15 μM (based on calculations of concentrations described above for 5 μl of 1 mM nicotine added) and in between the effective nicotine concentrations of 0.63 and 6.3 μM as shown in the dose-dependency experiments (Figure 3B). During the varenicline treatment phase, larval zebrafish spent most of the time in the center compartment (1804 s; SEM ± 368.7; $n = 15$) and significantly less time ($p = 0.0037$, $n = 15$) in the "nicotine compartment" (402.7 s; SEM ± 250.0; $n = 15$) (Figure 6A). The cumulative duration between times spent in the center and the water compartment (1,356 s; SEM ± 356.1; $n = 15$) were not significantly different ($p = 0.9581$, $n = 15$). After addition of nicotine to a final concentration of 3.15 μM and the 2-h recording in the presence of both nicotine and varenicline, the cumulative duration spent in the water compartment increased (3,397 s, SEM ± 680.6, $n = 15$) while the cumulative time spent in the center compartment (2,496 s, SEM ± 587.3, $n = 15$) decreased for the cohort (Figure 6B) making the difference in cumulative duration between the water compartment and the nicotine compartment (1,182 s SEM ± 436.3, $n = 15$) significant (Nicotine vs. center: $p = 0.2432$, $n = 15$; nicotine vs. water: $p = 0.0307$, $n = 15$; center vs. water $p > 0.9999$, $n = 15$). The cumulative duration after adding nicotine in the nicotine compartment (1,182 s; SEM ± 436 s), water controls (1983; SEM ± 624 s) and untreated larval zebrafish (1935; SEM ± 348 s) did not indicate significant differences (Figure 6C). In addition, the cumulative time in the water compartment of varenicline treated larval zebrafish (nic + varT: 3397 s; SEM ± 681) had significantly increased ($p = 0.0198$) compared to untreated larval zebrafish (nic -varT: 1729 s; SEM ± 414) (Figure 6D).

During the varenicline treatment and before addition of nicotine the number of entrances into the nicotine compartment were significantly lower (1.13; SEM ± 0.551; $n = 15$) compared to the center compartment (3.33; SEM ± 10.8; $n = 15$) ($p = 0.0242$, $n = 15$) (Figure 6E). The addition of nicotine to the nicotine compartment resulted in number of entrances (nicotine: 1.733 SEM ± 0.5812, $n = 15$, center: 6.333 SEM ± 3.238, $n = 15$; water: 2.933 SEM ± 0.6652, $n = 15$)

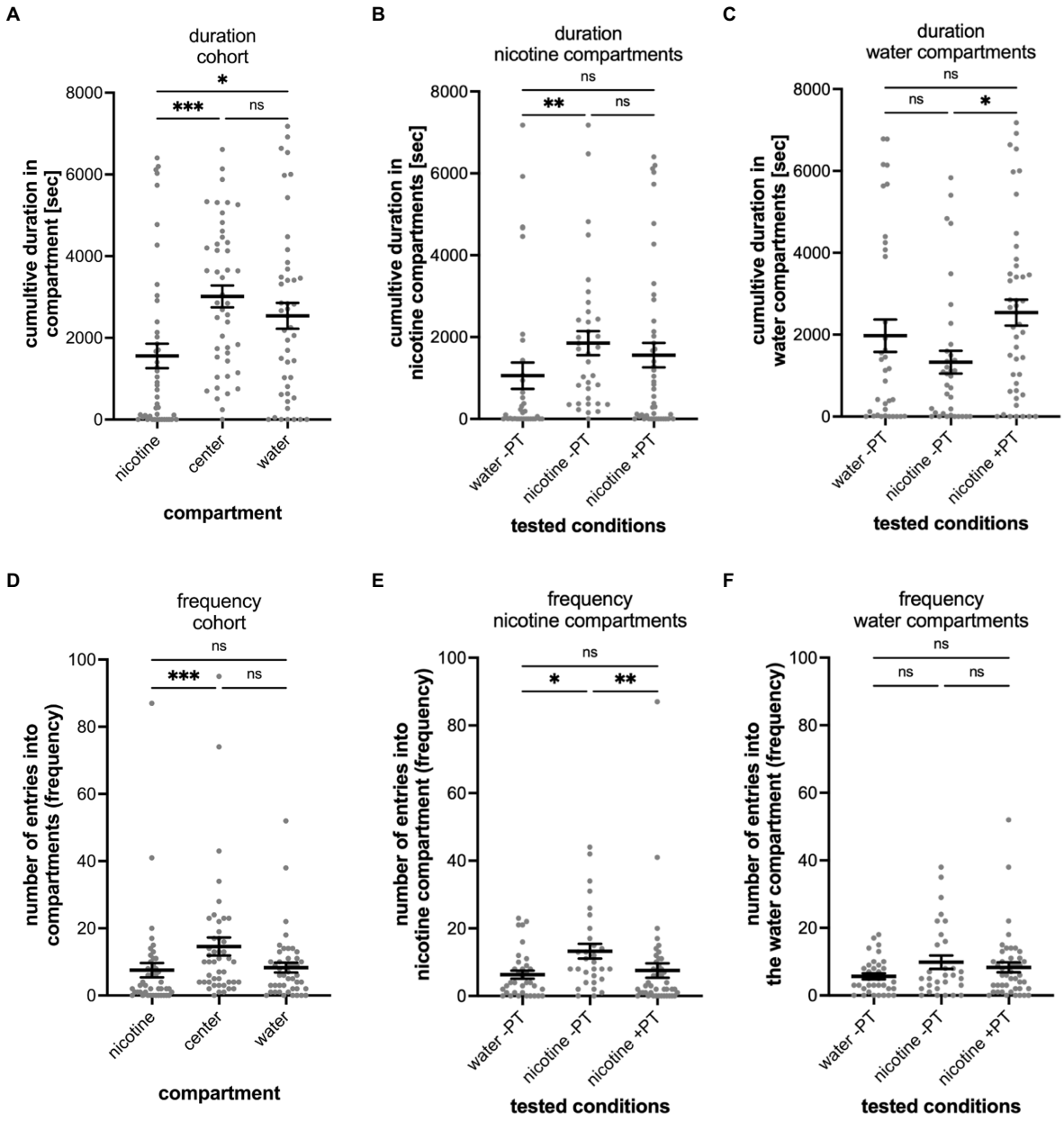

FIGURE 5
Shows the results of nicotine pre-treatment (PT) experiments. **(A)** The results of the entire tested cohort (n =45) are shown for the cumulative duration spent in compartments and the number of entrances into compartment (frequency; D). **(B)** Compares the durations spent in the nicotine compartment under different experimental conditions including water controls without nicotine pretreatment when water was added to the "nicotine compartment" (water -PT, n =35), at a 0.63 μM nicotine concentration in the nicotine compartment without nicotine pretreatment (nicotine -PT, n=30), and at 0.63 μM nicotine in the nicotine compartment with a 1 μM nicotine pretreatment (nicotine +PT, n=45). The cumulative duration increased in nicotine without pre-treatment compared to water (p =0.0014) but did not change with nicotine-pretreatment (p =0.1124). **(C)** Comparison of the cumulative time spent in the water compartment under the indicated experimental conditions as in **(B)** (water −PT, nicotine −PT, and nicotine +PT). Nicotine pre-treatment increased the duration spent in the water compartment (p =0.0287). **(D)** The results of the entire tested cohort (n =45) are shown for the number of entrances into the nicotine, center, and water compartments (frequency). The number of entrances into the nicotine compartment (nicotine) were lower compared to the entrances into the center compartment (p =0.0008). Entrances into the water compartment compared to the center compartment were not significantly different (p =0.0851). **(E)** Comparison of the number of entrances (frequency) into the nicotine compartment under the same indicated condition as in **(B)** (water −PT, nicotine −PT, and nicotine +PT). The number of entrances increased (p =0.0175) when nicotine was added into the nicotine compartment without nicotine pre-treatment (nicotine −PT) compared to water controls (water −PT) but not with a nicotine pretreatment (nicotine +PT) (p =0.3816). Nicotine pretreatment reduced the number of entrances into the nicotine compartment (nicotine +PT) when compared to the nicotine without nicotine pretreatment (nicotine -PT) (p =0.0036). **(F)** Entrances into the water compartment under the three different experimental conditions (water −PT, nicotine −PT, and nicotine +PT) were not significantly different. Individual data points are shown with means ±SEM. Statistical significance was tested using a Kruskal–Wallis test with Dunn's comparison test. ***p < 0.0008; **p < 0.0036, *p < 0.0364; ns > 0.0851.

that were not significantly different from each other (nicotine vs. center: p = 0.0771, n = 15; nicotine vs. water: p = 0.3352, n = 15; center vs. water: p > 0.9999, n = 15).

The number of entrances into the three compartments of the varenicline treated group (n = 15) were not significantly different and varied between 1.7 (SEM ± 0.5812) in the nicotine compartment, 6.3 in

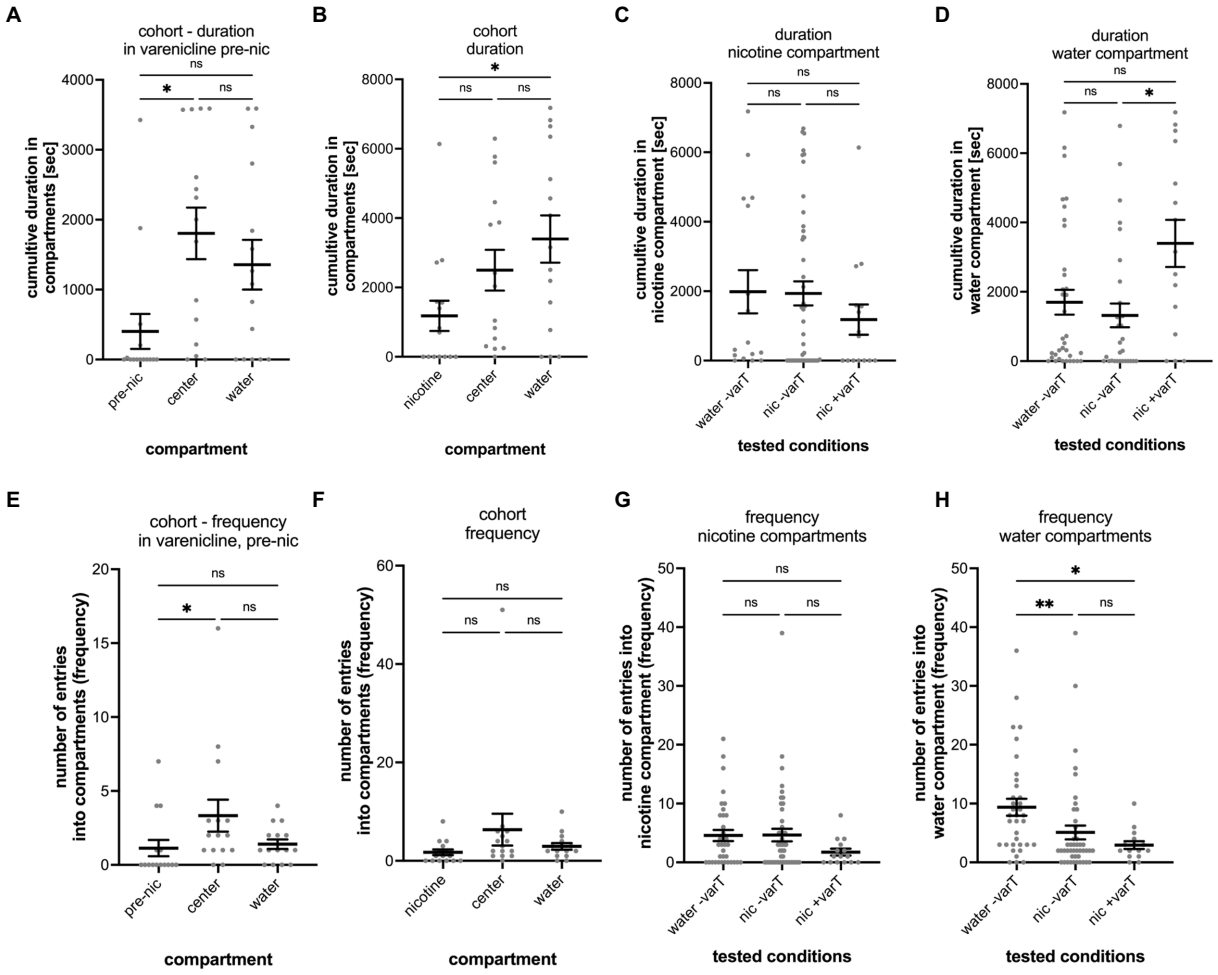

FIGURE 6
Analysis of varenicline treatment experiments. The results of the entire cohort (n =15) are shown in **(A)** for the cumulative duration in the nicotine (pre-nic), center and water compartments during the 1-h varenicline phase before addition of nicotine into the nicotine compartment (pre-nic). The difference between the cumulative duration in the nicotine and center compartment was significant (p =0.0037) but not between the center compartment and the water compartment (p =0.9581) and the pre-nicotine compartment and the water compartment (p =0.0766). **(B)** Shows the cumulative duration in the nicotine nicotine, center, and water compartments in varenicline after addition of nicotine into the nicotine compartment (nicotine). The cumulative duration in the water increased (nicotine vs. water, p =0.0307) whereas the duration in the center compartment decreased (nicotine vs. center, p =0.2432) and was not significantly different as before the addition of nicotine. **(C)** No difference was found between the three experimental conditions for the cumulative duration in the nicotine compartment. **(D)** The cumulative duration in the water compartment in varenicline and after nicotine addition (nic+varT) was significantly larger than the without varenicline (nic -varT) (p =0.0198). **(E)** Comparison of the number of entrances (frequency) into the nicotine, center and water compartment during varenicline treatment and before addition of nicotine shows a significant difference between the nicotine and center compartment (p =0.0242). **(F)** Addition of nicotine eliminated this difference. **(G)** No differences for the number of entrances into the nicotine compartment were found when comparing the different treatments. **(H)** Nicotine decreased the number of entrances into the water compartment without (water −varT vs. nic −varT, p=0.0021) and with varenicline treatment (nic −varT vs. nic+varT; p=0.0161). Varenicline did not change the number of entrances with nicotine in the nicotine compartment (p=0.6111). Individual data points are shown with the mean ±SEM. Statistical significance was tested using a Kruskal–Wallis test with Dunn's comparison test. **$p < 0.0037$; *$p < 0.0307$; ns > 0.0766.

the center compartment (SEM ± 3.238) and 2.9 (SEM ± 0.6652) in the water compartment (Figure 6F). The number of entrances into nicotine compartments between varenicline treated and un-treated groups were also not significantly different (Figure 6G). Compared to the number of entrances into the water compartment in controls (water added to the nicotine compartment, no varenicline treatment) the number of entrances into water compartments was significantly lower after nicotine had been added in both varenicline untreated (−varT, p=0.0021; n=15) and varenicline treated (+varT, p=0.0161, n=15) tests (Figure 6H). Varenicline treatment did not change the number of entrances into the water compartment after nicotine had been added ($p > 0.9999$, n=15).

The varenicline treatment before the addition of nicotine, generated 20% seekers, 40% avoiders and 40% non-seekers. The addition of nicotine to the nicotine compartment in the presence of varenicline resulted in an increase in the percentage of avoiders from 40 to 60%, a decrease of the percentage of nicotine seekers from 20 to 13.3% and a decrease of non-seekers from 40 to 26.7%.

4. Discussion

4.1. Testing individual larval zebrafish

The study presents a new three-choice behavioral assay for measuring responses of larval zebrafish to chemicals such as nicotine. The new approach of measuring the behavioral responses of individual

larval zebrafish in a three-choice assay generated robust and reproducible results and demonstrated that individuals within one cohort differ in their response to nicotine by seeking, avoiding and non-seeking. The mazes were kept small so that larval zebrafish could easily explore the entire maze during recording periods. By separating three compartments by narrow links, we could contain the diffusion of nicotine and generate one nicotine compartment on one side and a compartment without nicotine on the other. The gradient design has been applied successfully in a copper avoidance test for zebrafish (Araújo et al., 2019). Based on food dye diffusion experiments some nicotine it likely to diffuse into the center compartment but to a much lesser degree into the water compartment connected to the center compartment. The measurement of absorbance of nicotine at 260 nm also supports that nicotine is contained in the nicotine compartment over the 2-h nicotine phase of the experiments. Because of the low sensitivity of the spectrophotometric assay, some diffusion into the center compartment or the water compartment cannot be ruled out, but the highest concentration of nicotine would be in the nicotine compartment and the lowest in the water compartment. The link between compartments was wide enough for larval zebrafish to turn around in the link. Thus, freely moving larval zebrafish had the choice to enter the water and nicotine-free compartment. The observational period was kept at 2 h to allow neuronal cell signaling mechanisms and potential gene expression changes to contribute to the nicotine seeking behavior (Kily et al., 2008). Tracking the path of larval zebrafish in the maze and calculating the time spent in the nicotine compartment allowed the differentiation of behavioral phenotypes of nicotine seeker, avoider and non-seeker in addition to a quantitative analysis of the test groups. Previously, choice experiments were used to measure the preference for morphine (Bretaud et al., 2007) and nicotine (Krishnan et al., 2014) in larval zebrafish. In both studies larval zebrafish could swim freely within the test chamber. However, groups of larval zebrafish were used for the morphine study. Once introduced into a continuous rectangular choice chamber (25 cm × 16.5 cm × 6.5 cm; L × W × H), morphine was delivered on one end and water on the opposite end. A drain in the center of the chamber reduced the diffusion of morphine in the water compartment. Snapshots were taken in 10 s intervals and the number of larval zebrafish in each compartment was used for the analysis. Using this approach, it remains unclear if the same larval zebrafish spent more time in the morphine compartment or if different larval zebrafish explored the morphine compartment for a short period. Individual variations were not accounted for. In a different experiment (Krishnan et al., 2014) nicotine was delivered and contained *via* microfluidic pump system in a corner of a rectangular test chamber (76 mm × 32 mm × 30 mm (L × W × H). While no physical barriers interfered with the movement of the single larval zebrafish in the experiment, the test chamber was virtually divided into the areas for the analysis of experiments that used distance between the larval zebrafish and the source of fluid delivery as a criterion for attraction and avoidance of the chemical. The three-choice behavioral test chamber introduced in our study is suitable for measuring behavioral responses to nicotine of individual freely swimming larval zebrafish and has the advantages of scalability and simple delivery of nicotine in a restricted area of the maze without the need for special perfusion systems. Both nicotine-seeking and avoiding larval zebrafish could be identified and significant responses to changes in nicotine concentrations could be observed in individual larval zebrafish. By measuring the behavior of single larval zebrafish, in contrast to groups (Bretaud et al., 2007) individual variations in behavioral responses could be measured in future studies.

4.2. Nicotine-seeking and avoidance behavior

The results show that a subset of ~20–30% of larval zebrafish spent most of the time the nicotine-containing compartment, a behavior that we named nicotine-seeking. That 20–30% of larval zebrafish preferred the nicotine compartment under our experimental conditions appears to be dependent on the concentration of nicotine. Along the same lines, nicotine avoidance behavior is also apparent in a subset of larval zebrafish within a cohort. Such mixed variations in individual behavioral responses are common. Self-administration experiments of nicotine (and other drugs of dependence) using mice demonstrated differences among strains of mice. In zebrafish, differences of inhibitory avoidance behavior, cortisol levels and gene expression between the AB and TL strains of zebrafish have been described (Gorissen et al., 2015). Locomotor activity has been described to vary consistently between individual adult zebrafish (Tran and Gerlai, 2013). Swimming activity of adult zebrafish measured by distance traveled varied between low, medium and high activity fish. In addition, females travelled longer distances than males (Tran and Gerlai, 2013). Moreover, individual variations have been described in zebrafish for the exposure to alcohol (Araujo-Silva et al., 2018), attraction and avoidance of odorants (Krishnan et al., 2014), exploratory behavior (Rajput et al., 2022), and learning and memory (Gerlai, 2016). Moreover, repeated testing in the gradient maze showed a certain degree of consistency indicating that nicotine-seeking and avoidance behavior is not random but switching of preferences has been observed. Thus, the characterization of nicotine-seekers, avoiders and non-seekers or variation in nicotine seeking and avoidance behavior among individual larval zebrafish described here are in line with individual variations reported in several experimental approaches. Since nicotine preference and avoidance are known to be associated with different neuronal circuits (Fowler and Kenny, 2014), the three-choice assay might be used to study the neuronal dynamics between seeking and avoidance. The application of nicotine to the nicotine compartment could be improved in future experiments.

4.3. Larval zebrafish respond to different nicotine concentrations

The behavioral choice experiment allows larval zebrafish to choose or avoid nicotine and adjust their nicotine uptake in a self-administration-like mode. The nicotine concentration in the compartment plays a critical role for the separation of seeking and avoidance behavior. The shifting of seeking and avoidance behavior with concentrations in the nicotine compartment is an indication that the exposure to nicotine is controlled by an underlying mechanism and does not occur randomly. Similar to studies in rodents, the behavioral response of larval zebrafish in the three-choice test follows an inverted-U shape with stronger nicotine seeking occurring at lower nicotine concentrations (0.63, 6.3 μM) and nicotine avoidance at higher nicotine concentrations (63 μM, 630 μM). A similar relationship

has been described for larval zebrafish in acute nicotine response tests (Petzold et al., 2009). These results could indicate that larval zebrafish titrate their nicotine intake and actively adjust their exposure to nicotine by moving between compartments. The cumulative time spent in the nicotine compartment and the percentage of nicotine seekers correlates stronger with an inverted U-shaped dose–response curve, but not the cumulative time and the number of entrances into the water compartment. In rodents, the inverted U-shaped relationships between nicotine concentration and behavioral responses is robust (e.g., Fowler and Kenny, 2014) and has been also described for conditioned place preference tests, for example (Braida et al., 2020). Aversion behavior also follows an inverted-U shaped dose–response curve over higher nicotine concentrations. Nicotine avoidance has been described in mice (Fowler and Kenny, 2014) and has been suggested in larval zebrafish (Krishnan et al., 2014). While a clear correlation between the nicotine-concentration and the percentage of nicotine seekers has been found in form of an inverted-U shaped curve, the number of entrances into the nicotine compartment is only weakly correlated with the nicotine concentration. A correlation between the cumulative time spent in the water compartment is absent. The relationship and dynamic between time spent in a compartment vs. entering a compartment could indicate separate regulatory entities or neural circuits. Overall, the nicotine dose–response relationships measured in the nicotine-seeking and avoidance assay align with the typical nicotine dose-relationships reported for rodents and zebrafish.

4.4. Varenicline-induced changes in nicotine-seeking and avoidance

Varenicline represents the gold standard of nicotine cessation treatment as it is widely used in smoking cessation treatment and reduces craving for smoking cigarettes (Ebbert et al., 2010). That larval zebrafish showed stronger nicotine avoidance behavior when treated with varenicline supports the use of the three-choice gradient maze for screening of potential pharmacotherapeutics for improved nicotine cessation treatment. An increase in nicotine avoidance aligns with a reduced nicotine exposure and intake. Alternatively, increased avoidance could be associated with increased desensitization of acetylcholine receptors at high concentrations of varenicline (Ortiz et al., 2012). The zebrafish genome contains nicotinic alpha4 and beta2 nicotinic acetylcholine receptor genes that interact with varenicline (Klee et al., 2012). Both genes of the alpha4 and beta2 nicotinic acetylcholine receptor subunit are expressed in the brain of larval zebrafish (Ackerman et al., 2009; Garcia-Gonzalez et al., 2020). In conditioned place preference tests using adult zebrafish, varenicline reduced the time spent in the nicotine-paired side of the behavioral chamber (Ponzoni et al., 2014). Rodents have been used in pre-clinical experiments for the study of varenicline actions. Self-administration of nicotine was reduced by varenicline treatment in rats (Scuppa et al., 2015; Zheng-Ming et al., 2021). Varenicline has been shown in rodents to decrease nicotine-induced hyperlocomotion, reduce nicotine-induced sensitization and improve the performance times in the Morris water maze (Zaniewska et al., 2008; King et al., 2011). Thus, the increased nicotine avoidance behavior in varenicline treated larval zebrafish in the gradient maze aligns with results obtained in adult zebrafish and rodent models.

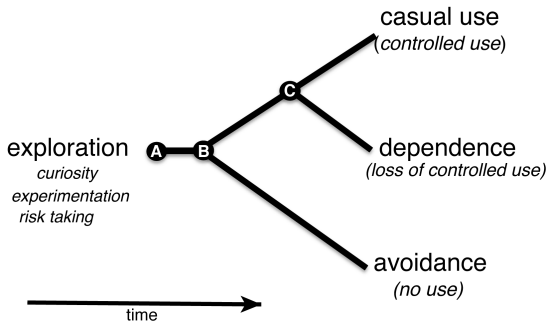

FIGURE 7
Shows a simplified behavioral cladogram of types of nicotine use behavior. The model is based on Jordan and Andersen (2017). **(A)** Use of nicotine is initiated early in development in an exploratory phase when curiosity, risk taking and experimentation drive behavior. The associated experience could lead to avoidance or continued nicotine use at the second transition point **(B)**. Continued use could put an organism on a path to a third transition point **(C)** at which loss of control over nicotine use could take place leading to nicotine dependence.

That the response to nicotine at an early developmental stage of zebrafish (6–8 dpf) could be dependent on previous nicotine-encounters is only weakly supported by results from nicotine-pretreatment experiments. Under our experimental conditions a slight shift to nicotine avoidance was measured that was weaker than the behavioral shift caused by varenicline treatment. The pretreatment did not result in a shift toward nicotine compartments. Similarly, learning in larval zebrafish appears to be limited as shown in certain learning paradigms (Valente et al., 2012; Roberts et al., 2013). Thus, mechanism needed for behavioral changes to occur in response to nicotine-pretreatment potentially could be lacking in the early larval stage of zebrafish.

5. Outlook

Studies of nicotine use in humans suggested that exploratory use of nicotine in early adolescence is an indicator of future nicotine-dependence (Jordan and Andersen, 2017). In the absence of an aversive response to nicotine in an exploratory phase, continued regular use of nicotine could result in a transition toward nicotine dependence (Figure 7; Smith et al., 2015). The model can be adopted for larval zebrafish with an exploratory phase in early development. The gradient maze test for the identification of nicotine-seekers and avoiders in the larval zebrafish model in combination with selected breeding or genome modifications could help to discover genetic risk factors that contribute directly to the transition from exploratory to regular (controlled) use of nicotine.

Data availability statement

The original contributions presented in the study are included in the article/Supplementary material, further inquiries can be directed to the corresponding author.

Ethics statement

The animal study was reviewed and approved by IACUC at DePauw University.

Author contributions

All authors listed have made a substantial, direct, and intellectual contribution to the work and approved it for publication.

Funding

This study was supported by grants from DePauw University (HS, AP, DH, AT, SK, KG, and KC), Arthur Vining Davis Foundations (HS), and the Buehler Family Foundation, A.C. Buehler and E. Buehler.

Acknowledgments

The authors like to thank S. C. Ekker and K. J. Clark and their teams at the Mayo Clinic for suggestions and general support.

Conflict of interest

The authors declare that the research was conducted in the absence of any commercial or financial relationships that could be construed as a potential conflict of interest.

Publisher's note

All claims expressed in this article are solely those of the authors and do not necessarily represent those of their affiliated organizations, or those of the publisher, the editors and the reviewers. Any product that may be evaluated in this article, or claim that may be made by its manufacturer, is not guaranteed or endorsed by the publisher.

Supplementary material

The Supplementary material for this article can be found online at: https://www.frontiersin.org/articles/10.3389/fnmol.2023.1112927/full#supplementary-material

References

Ackerman, K. M., Nakkula, R., Zirger, J. M., Beattie, C. E., and Boyd, R. T. (2009). Cloning and spatiotemporal expression of Zebrafish neuronal nicotinic acetylcholine receptor alpha 6 and alpha 4 subunit RNAs. *Dev. Dyn.* 238, 980–992. doi: 10.1002/dvdy.21912

Araújo, C. V. M., Pontes, J. R. S., and Blasco, J. (2019). Does the previous exposure to copper alter the pattern of avoidance by zebrafish in a copper gradient scenario? Hypothesis of time-delayed avoidance due to pre-acclimation. *Sci. Total Environ.* 694:133703. doi: 10.1016/j.scitotenv.2019.133703

Araujo-Silva, H., Pinheiro-da-Silva, J., Silva, P. F., and Luchiari, A. C. (2018). Individual differences in response to alcohol exposure in zebrafish (*Danio rerio*). *PLoS One* 13:e0198856. doi: 10.1371/journal.pone.0198856

Ata, H., Clark, K. J., and Ekker, S. C. (2016). The zebrafish genome editing toolkit. *Methods Cell Biol* 135, 149–170. doi: 10.1016/bs.mcb.2016.04.023

Benowitz, N. L. (2009). Pharmacology of nicotine: addiction, smoking-induced disease, and therapeutics. *Annu. Rev. Pharmacol. Toxicol.* 49, 57–71. doi: 10.1146/annurev.pharmtox.48.113006.094742

Blackburn, P. R., Campbell, J. M., Clark, K. J., and Ekker, S. C. (2013). The CRISPR system–keeping zebrafish gene targeting fresh. *Zebrafish* 10, 116–118. doi: 10.1089/zeb.2013.9999

Bosse, G. D., Cadeddu, R., Floris, G., Farero, R. D., Vigato, E., Lee, S. J., et al. (2021a). The 5alpha-reductase inhibitor finasteride reduces oioid self-administration in animal models of opioid use disorder. *J. Clin. Invest.* 131:e143990. doi: 10.1172/JCI143990

Bosse, G. D., and Peterson, R. T. (2017). Development of an opioid self-administration assay to study drug seeking in zebrafish. *Behav. Brain Res.* 335, 158–166. doi: 10.1016/j.bbr.2017.08.001

Bosse, G. D., Urcino, C., Watkins, M., Florez Salcedo, P., Kozel, S., Chase, K., et al. (2021b). Discovery of a potent conorfamide from Conus episcopatus using a novel zebrafish larvae assay. *J. Nat. Prod.* 84, 1232–1243. doi: 10.1021/acs.jnatprod.0c01297

Brady, C. A., Rennekamp, A. J., and Peterson, R. T. (2016). Chemical screening in zebrafish. *Methods Mol. Biol.* 1451, 3–16. doi: 10.1007/978-1-4939-3771-4_1

Braida, D., Ponzoni, L., Moretti, M., Viani, P., Pallavicini, M., Bolchi, C., et al. (2020). Behavioural and pharmacological profiles of zebrafish administrated pyrrolidinyl benzodioxanes and prolinol aryl ethers with high affinity for heteromeric nicotinic acetylcholine receptors. *Psychopharmacology* 237, 2317–2326. doi: 10.1007/s00213-020-05536-6

Brand, M., Granato, M., and Nüsslein-Volhard. (2002). "Keeping and raising zebrafish" in *Zebrafish – a practical approach*. eds. C. Nüsslein-Volhard and R. Dahm, vol. *2002* (Oxford: Oxford University Press), 7–37.

Bretaud, S., Li, Q., Lockwood, B. L., Kobayashi, K., Lin, E., and Guo, S. (2007). A choice behavior for morphine reveals experience-dependent drug preference and underlying neural substrates in developing larval zebrafish. *Neuroscience* 146, 1109–1116. doi: 10.1016/j.neuroscience.2006.12.073

Brennan, C. H., Parmar, A., Kily, L. K. M., Ananthathevan, A., Doshi, A., Paterl, S., et al. (2011). "Conditioned plave preference models of drug dependence and relapse to drug seeking: studies with nicotine and ethanol," in *Zebrafish Models in Neurobehavioral Research. Neuromethods, vol 52*. eds. A. Kalueff and J. Cacha (Totowa, NJ: Humana Press), 163–180.

Coe, J. W., Brooks, P. R., Vetelino, M. G., Wirtz, M. C., Arnold, E. P., Huang, J., et al. (2005). Varenicline: an alpha4beta2 nicotinic receptor partial agonist for smoking cessation. *J. Med. Chem.* 48, 3474–3477. doi: 10.1021/jm050069n

Cousin, M. A., Ebbert, J. O., Winamaki, A. R., Urban, M. D., Argue, D. P., and Ekker, S. C. (2014). Larval zebrafish model for FDA-approved drug repositioning for tobacco dependence treatment. *PLoS One* 9:e90467. doi: 10.1371/journal.pone.0090467

Ebbert, J. O., Wyatt, K. D., Hays, J. T., Klee, E. W., and Hurt, R. D. (2010). Varenicline for smoking cessation: efficacy, safety, and treatment recommendations. *Patient Prefer. Adherence* 4, 355–362. doi: 10.2147/ppa.s10620

Fowler, C. D., and Kenny, P. J. (2014). Nicotine aversion: neurobiological mechanisms and relevance to tobacco dependence. *Neuropharmacology* 76, 533–544. doi: 10.1016/j.neuropharm.2013.09.008

Gallois, B., Pontani, L. L., Debregeas, G., and Candelier, R. (2022). A scalable assay for chemical preference of small freshwater fish. *Front. Behav. Neurosci.* 16:990792. doi: 10.3389/fnbeh.2022.990792

Garcia-Gonzalez, J., Brock, A. J., Parker, M. O., Riley, R. J., Joliffe, D., Sudwarts, A., et al. (2020). Identification of slit3 as a locus affecting nicotine preference in zebrafish and human smoking behavior. *elife* 9:e51295. doi: 10.7554/eLife.51295

Gerlai, R. (2016). Learning and memory in zebrafish (*Danio rerio*). *Methods Cell Biol.* 134, 551–586. doi: 10.1016/bs.mcb.2016.02.005

Gorissen, M., Manuel, R., Pelgrim, T. N., Mes, W., de Wolf, M. J., Zethof, J., et al. (2015). Differences in inhibitory avoidance, cortisol and brain gene expression in TL and AB zebrafish. *Genes Brain Behav.* 14, 428–438. doi: 10.1111/gbb.12220

Hurt, R. T., Croghan, I. T., Schroeder, D. R., Choi, D. S., Fischer, K., Fokken, S., et al. (2022). Varenicline and lorcaserin for smoking cessation and weight gain prevention: a randomized clinical trial. *Mayo Clin Proc Innov Qual Outcomes* 6, 465–474. doi: 10.1016/j.mayocpiqo.2022.01.004

Jordan, C. J., and Andersen, S. L. (2017). Sensitive periods of substrate abuse: early risk for the transition to dependence. *Dev. Cognitive Neurosci.* 25, 29–44. doi: 10.1016/j.dcn.2016.10.004

Jordan, C. J., and Zhen-Xiong, X. (2018). Discovery and development of varenicline for smoking cessation. *Expert. Opin. Drug. Discov.* 13, 671–683. doi: 10.1080/17460441.2018.1458090

Kaleuff, A. V., Stewart, A. M., and Gerlai, R. (2014). Zebrafish as an emerging model for studying complex brain disorders. *Trends Pharmacol.* 35, 63–75. doi: 10.1016/j.tips.2013.12.002

Kily, L. J., Cowe, Y. C., Hussain, O., Patel, S., McElwaine, S., Cotter, F. E., et al. (2008). Gene expression changes in a zebrafish model of drug dependency suggest conservation of neuro-adaptation pathways. *J. Exp. Biol.* 211, 1623–1634. doi: 10.1242/jeb.014399

King, J., Huang, W., Chen, W., Heffernan, M., Shields, J., Rane, P., et al. (2011). A comparison of brain and behavioral effects of varenicline and nicotine in rats. *Behav. Brain Res.* 223, 42–47. doi: 10.1016/j.bbr.2011.04.012

Klee, E. W., Schneider, H., Clark, K. J., Cousin, M. A., Ebbert, J. O., Hooten, W. M., et al. (2012). Zebrafish: a model for the study of addiction genetics. *Hum. Genet.* 131, 977–1008.

Krishnan, S., Mathuru, A. S., Kibat, C., Rahman, M., Lupton, C. E., Stewart, J., et al. (2014). The right dorsal habenula limits attraction to an odor in zebrafish. *Curr. Biol.* 24, 1167–1175. doi: 10.1016/j.cub.2014.03.073

Lee, D. A., Oikonomou, G., and Prober, D. A. (2022). Large-scale analysis of sleep in Zebrafish. *Bio Protoc* 12:e4313. doi: 10.21769/BioProtoc.4313

MacRae, C. A., and Peterson, R. T. (2015). Zebrafish as tools for drug discovery. *Nat. Rev. Drug Discov.* 14, 721–731. doi: 10.1038/nrd4627

Nathan, F. M., Kibat, C., Goel, T., Stewart, J., Claridge-Chang, A., and Mathuru, A. S. (2022). Contingent stimulus delivery assay for zebrafish reveals a role for CCSER1 in alcohol preference. *Addict. Biol.* 27:e13126. doi: 10.1111/adb.13126

Ortiz, N. C., O'Neill, H. C., Marks, M. J., and Grady, S. R. (2012). Varenicline blocks beta2-nAchR mediated response and activates beta4-nAchr-mediated responses in mice in vivo. *Nicotine Tob. Res.* 14, 711–719. doi: 10.1093/ntr/ntr284

Pan, Y., Chatterjee, D., and Gerlai, R. (2012). Strain dependent gene expression and neuro- chemical levels in the brain of zebrafish: focus on a few alcohol related targets. *Physiol. Behav* 107, 773–780. doi: 10.1016/j.physbeh.2012.01.017

Parker, M. O., Bock, A. J., Walton, R. T., and Brennan, C. H. (2013). The role of zebrafish (Danio rerio) in dissecting the genetics and neural circuits of executive function. *Front. Neural Cricuits* 7:63. doi: 10.3389/fncir.2013.00063

Park-Lee, E., Ren, C., Cooper, M., Cornelius, M., Jamal, A., and Cullen, K. A. (2022). Tobacco product use among middle and high school students – National Youth Tobacco Survey, United States 2021. *Morb. Mortal. Wkly Rep.* 71, 1–29. doi: 10.15585/mmwr.mm7145a1

Perkins, K. A. (1999). Nicotine self-administration. *Nicotine Tob. Res.* 1, S133–S137.

Petzold, A. M., Balciunas, D., Sivasubbu, S., Clark, K. J., Bedell, V. M., Westcot, S. E., et al. (2009). Nicotine response genetics in the zebrafish. *Proc. Natl. Acad. Sci. U. S. A.* 106, 18662–18667. doi: 10.1073/pnas.0908247106

Ponzoni, L., Braida, D., Pucci, L., Andrea, D., Fasoli, F., Manfredi, I., et al. (2014). The cytisine derivatives, CC4 and CC26, reduce nicotine-induced conditioned place preference in zebrafish by acting on heteromeric neuronal nicotinic acetylcholine receptors. *Psychopharmacology* 231, 4681–4693. doi: 10.1007/s00213-014-3619-x

Rajput, N., Parikh, K., and Kenney, J. W. (2022). Beyond bold versus shy: zebrafish exploratory behavior fals into several behavioral clusters and is influenced by strain and sex. *Biol. Open.* 11:bio059443. doi: 10.1242/bio.059443

Rigotti, N. A., Kruse, G. R., Livingstone-Banks, J., and Hartmann-Boyce, J. (2022). Treatment of tobacco smoking: a review. *JAMA* 327, 566–577. doi: 10.1001/jama.2022.0395

Rihel, J., Prober, D. A., Arvanites, A., Lam, K., Zimmerman, S., Jang, S., et al. (2010). Zebrafish behavioral profiling links drugs to biological targets and rest/wake regulation. *Science* 327, 348–351. doi: 10.1126/science.1183090

Roberts, A. C., Bill, B. R., and Glanzman, D. L. (2013). Learning and memory in zebrafish larvae. *Front Neural. Circuits* 7:126. doi: 10.3389/fncir.2013.00126

Schneider, H. (2017). "Zebrafish neurobehavioral assays for addiction research" in *The rights and wrongs of Zebrafish: Principles of behavioral Phenotyping and CNS disease modeling*. ed. A. V. Kalueff (Cham: Springer International Publishing), 171–205.

Scuppa, G., Cippitelli, A., Toll, L., Ciccocioppo, R., and Ubaldi, M. (2015). Varenicline decreases nicotine but not alcohol self-administration in genetically selected marchigian sardianan alcohol-preferring (msP) rats. *Drug Alcohol Depend.* 156, 126–132. doi: 10.1016/j.drugalcdep.2015.09.002

Smith, R. F., McDonald, C. G., Bergstrom, H. C., Ehlinger, D. G., and Brielmaier, J. M. (2015). Adolescent nicotine induces persisting changes in development of neural connectivity. *Neurosci. Biobehav. Rev.* 55, 432–443. doi: 10.1016/j.neubiorev.2015.05.019

Tran, S., and Gerlai, R. (2013). Individual differences in activity levels in zebrafish (Danio rerio). *Behav. Brain Res.* 257, 224–229.

US Department of Health and Human Services (2014) *The health consequences of smoking – 50 years of progress: a report of the surgeon general*, Atlanta: US US Department of Health and Human Services, Centers for Disease Control and Prevention, National Center for Chronic Disease Prevention and Health Promotion, Office on Smoking and Health.

Valente, A., Huang, K. H., Portugues, R., and Engert, F. (2012). Ontogeny of classical and operant learning behaviors in zebrafish. *Learn. Mem.* 19, 170–177. doi: 10.1101/lm.025668.112

Wang, T. W., Gentzke, A. S., Neff, L. N., Glidden, E. V., Jamal, A., Park-Lee, E., et al. (2021). Characteristics of e-cigarettes use behaviors among US youth, 2022. *JAMA Netw. Open* 4:e2111336. doi: 10.1001/jamanetworkopen.2021.11336

Willits, C. O., Swain, M. L., Connelly, J. A., and Brice, B. A. (1950). Spectrophotometric determination of nicotine. *Anal. Chem.* 22, 430–433. doi: 10.1021/ac60039a013

Zaniewska, M., McCreary, A. C., Stefanski, R., Przegalinski, E., and Filip, M. (2008). Effect of varenicline on the acute and repeated locomotor responses to nicotine in rats. *Synapse* 62, 935–939. doi: 10.1002/syn.20564

Zheng-Ming, D., Gao, Y., Sentir, A. M., and Xiaoying, T. (2021). Self-administration of cotinine in wistar rats: comparisons to nicotine. *J. Pharmacol. Exp. Ther.* 376, 338–347. doi: 10.1124/jpet.120.000367

frontiers | Frontiers in Molecular Neuroscience

TYPE Original Research
PUBLISHED 11 May 2023
DOI 10.3389/fnmol.2023.1160157

OPEN ACCESS

EDITED BY
Juan Marín-Lahoz,
Hospital Universitario Miguel Servet, Spain

REVIEWED BY
Ron Keiflin,
University of California, Santa Barbara, United States
Ana Domi,
University of Gothenburg, Sweden

*CORRESPONDENCE
Kristen A. Keefe
✉ k.keefe@utah.edu

†These authors share first authorship

RECEIVED 06 February 2023
ACCEPTED 17 April 2023
PUBLISHED 11 May 2023

CITATION
Giangrasso DM, Veros KM, Timm MM, West PJ, Wilcox KS and Keefe KA (2023) Glutamate dynamics in the dorsolateral striatum of rats with goal-directed and habitual cocaine-seeking behavior.
Front. Mol. Neurosci. 16:1160157.
doi: 10.3389/fnmol.2023.1160157

Glutamate dynamics in the dorsolateral striatum of rats with goal-directed and habitual cocaine-seeking behavior

Danielle M. Giangrasso[1,2†], Kaliana M. Veros[1,2†], Maureen M. Timm[1], Peter J. West[1,2,3], Karen S. Wilcox[1,2,3] and Kristen A. Keefe[1,2*]

[1]Department of Pharmacology & Toxicology, University of Utah, Salt Lake City, UT, United States, [2]Interdepartmental Program in Neuroscience, University of Utah, Salt Lake City, UT, United States, [3]Anticonvulsant Drug Development Program, Department of Pharmacology & Toxicology, University of Utah, Salt Lake City, UT, United States

The shift from drug abuse to addiction is considered to arise from the transition between goal-directed and habitual control over drug behavior. Habitual responding for appetitive and skill-based behaviors is mediated by potentiated glutamate signaling in the dorsolateral striatum (DLS), but the state of the DLS glutamate system in the context of habitual drug-behavior remains undefined. Evidence from the nucleus accumbens of cocaine-experienced rats suggests that decreased transporter-mediated glutamate clearance and enhanced synaptic glutamate release contribute to the potentiated glutamate signaling that underlies the enduring vulnerability to relapse. Preliminary evidence from the dorsal striatum of cocaine-experienced rats suggests that this region exhibits similar alterations to glutamate clearance and release, but it is not known whether these glutamate dynamics are associated with goal-directed or habitual control over cocaine-seeking behavior. Therefore, we trained rats to self-administer cocaine in a chained cocaine-seeking and -taking paradigm, which yielded goal-directed, intermediate, and habitual cocaine-seeking rats. We then assessed glutamate clearance and release dynamics in the DLS of these rats using two different methods: synaptic transporter current (STC) recordings of patch-clamped astrocytes and the intensity-based glutamate sensing fluorescent reporter (iGluSnFr). While we observed a decreased rate of glutamate clearance in STCs evoked with single-pulse stimulation in cocaine-experienced rats, we did not observe any cocaine-induced differences in glutamate clearance rates from STCs evoked with high frequency stimulation (HFS) or iGluSnFr responses evoked with either double-pulse stimulation or HFS. Furthermore, GLT-1 protein expression in the DLS was unchanged in cocaine-experienced rats, regardless of their mode of control over cocaine-seeking behavior. Lastly, there were no differences in metrics of glutamate release between cocaine-experienced rats and yoked-saline controls in either assay. Together, these results suggest that glutamate clearance and release dynamics in the DLS are largely unaltered by a history of cocaine self-administration on this established cocaine seeking-taking paradigm, regardless of whether the control over the cocaine seeking behavior was habitual or goal directed.

KEYWORDS

dorsal striatum, cocaine, habitual and goal-directed processes, devaluation, astrocytes, glutamate transporter, synaptic transport currents, iGluSnFr

1. Introduction

Drug addiction is a chronic, relapsing disorder wherein individuals experience inflexible, uncontrollable drug use that persists despite adverse consequences (Vanderschuren and Everitt, 2004; Belin et al., 2009). Initially, drugs are intentionally consumed to obtain a reinforcing outcome, which reflects motivated, flexible behavior that is under goal-directed control (Vanderschuren and Everitt, 2004; Ersche et al., 2016). In contrast, as drug use continues, these drug-seeking and taking behaviors become automatically performed in response to drug-associated environmental stimuli, which is considered to reflect habitual control (Everitt and Robbins, 2005; Pierce and Vanderschuren, 2010). Over time, these habits have the ability to become compulsive, wherein drug-seeking and taking behaviors persist despite adverse consequences, which is a cardinal symptom of end-stage drug addiction (Belin et al., 2013). As such, elucidating the behavioral processes involved in the progression of drug use and their underlying neurobiological processes is a critical area of study.

Goal-directed and habitual behavior are mediated by distinct subregions within the striatum (Dolan and Dayan, 2013). Goal-directed behavior is mediated by the dorsomedial striatum (DMS) and is engaged during early behavioral learning (Yin et al., 2005a,b, 2009). In contrast, habitual behavior is mediated by the dorsolateral striatum (DLS) and is engaged after repeated behavioral practice (Packard and Knowlton, 2002; Yin et al., 2004; Yin and Knowlton, 2006; Yin et al., 2009; Dolan and Dayan, 2013). Classic studies have demonstrated that inactivation or lesion of the DMS results in early emergence of habitual actions (Yin et al., 2005a,b; Yin and Knowlton, 2006), whereas inactivation of the DLS results in maintenance of goal-directed behavior despite prolonged training (Yin et al., 2004; Yin and Knowlton, 2006). Similarly, in cocaine self-administration paradigms, transient inactivation of the DLS reverts habitual cocaine-seeking behavior back to goal-directed control (Zapata et al., 2010), attenuates cue-controlled drug-seeking (Jonkman et al., 2012), and increases sensitivity to punishment (Belin et al., 2013). To date, however, the neurobiological mechanisms within the DLS that mediate habitual drug behavior are undefined.

The development of habitual behavior is associated with enduring glutamatergic changes in the DLS (Lipton et al., 2019; Malvaez, 2020). For example, extended skill training significantly increases neuronal excitability and synaptic strength (Yin et al., 2009), suggesting that habitual behavior is mediated by potentiated glutamate signaling in the DLS. Further, disruption of postsynaptic glutamate NMDA or AMPA receptor activation during task acquisition (Palencia and Ragozzino, 2005), consolidation (Goodman et al., 2017), or performance (Corbit et al., 2014) prevents the formation or expression of habitual behavior. Thus, altered glutamate signaling mediates the development and maintenance of habitual behavior, but relatively little is known about the state of glutamate signaling in the DLS in the context of habitual drug behavior.

Astrocytes, through glutamate transporters, play a key role in regulating extracellular glutamate dynamics within the tripartite synapse (Mahmoud et al., 2019). In particular, the glutamate transporter-1 (GLT-1) is predominantly expressed on astrocytes and accounts for ~90% of glutamate clearance in the mature brain (Danbolt et al., 1992; Haugeto et al., 1996). Through the clearance of extracellular glutamate, astrocytic GLT-1 largely regulates both the time course and extracellular concentration of glutamate (Danbolt, 2001), which are critical to the modulation of neuronal excitatory signaling (Mahmoud et al., 2019). As such, the astrocytic GLT-1 system is well-poised to regulate various aspects of glutamate signaling and homeostasis that underlie addictive behavior.

To date, the majority of studies examining the effects of cocaine self-administration on glutamate signaling and clearance have focused on the nucleus accumbens (NAc), the ventral subregion of the striatum that mediates reward and motivation-based behavior (Kalivas, 2009; D'Souza, 2015). Most notably, extended cocaine self-administration and withdrawal are associated with decreased GLT-1 uptake capacity (Knackstedt et al., 2010; Trantham-Davidson et al., 2013) and decreased GLT-1 expression (Knackstedt et al., 2010; Reissner et al., 2012; Fischer-Smith et al., 2013; LaCrosse et al., 2017). Consequently, the synaptic dwell time of glutamate, synaptic spillover, and duration of glutamate signaling in the NAc are increased in response to drug cues (Niedzielska-Andres et al., 2021). In addition to altered clearance, the glutamate system is primed for enhanced synaptic release of glutamate in the NAc during cocaine reinstatement (McFarland et al., 2003; Madayag et al., 2007; Li et al., 2010). Together, these alterations in NAc glutamate clearance and release are associated with the enduring vulnerability to relapse that is central to drug addiction (Kalivas, 2009; Niedzielska-Andres et al., 2021). However, less is known about glutamate dynamics in the DLS and its role in the formation of habitual drug-seeking behavior. Interestingly, one study demonstrated increased extracellular glutamate levels in the DLS in response to acute cocaine challenge in rats withdrawn for 24 h from cocaine self-administration (Gabriele et al., 2012). In addition, GLT-1 protein expression is reportedly decreased in the DLS following extended, long-access to cocaine self-administration (Ducret et al., 2016). While these studies have begun to identify cocaine-induced alterations to the DLS glutamate system, the status of this system in the context of goal-directed verses habitual cocaine-seeking behavior remains an undefined and important area of study.

The objective of the present study, therefore, was to assess the state of the DLS glutamate system of rats characterized as being goal-directed verses habitual in their cocaine-seeking behavior, as well as in comparison to yoked-saline controls. Rats were trained in a chained cocaine self-administration paradigm that involved distinct cocaine-seeking and -taking behaviors, outcome devaluation, and an assessment of the mode of control over cocaine-seeking behavior. We then assessed glutamate clearance and release in the DLS of these rats with synaptic transporter current (STC) recordings of patch-clamped astrocytes and the intensity-based glutamate-sensing reporter (iGluSnFr). In both of these assays, we found that glutamate clearance and release were largely unchanged across goal-directed and habitual cocaine-seeking rats, as well as in comparison to yoked-saline controls. Consistent with these findings, GLT-1 protein expression in the DLS was unchanged. Overall, the present results suggest that the DLS glutamate system is largely unaltered by a history of cocaine self-administration, whether the drug-seeking behavior is under goal-directed or habitual control.

2. Materials and methods

2.1. Animals

Male Long Evans rats (300–350 g) that were surgically prepared with right jugular vein catheters were obtained from Charles River

Laboratories (Wilmington, MA, United States). Catheter patency was verified upon arrival to the University of Utah animal facility and maintained by daily infusions of heparin-dextrose catheter locking solution (500 IU/50% dextrose; SAI Infusion, IL, United States). Rats also received daily prophylactic Baytril (10 mg/kg, i.v.; Norbrook, Newry, United Kingdom). Rats were single-housed in standard housing conditions. Three days before the start of cocaine self-administration training, rats were food-restricted to 25 g of standard chow per day, with *ad libitum* access to water, and were maintained on this feeding schedule throughout the experiment. Rats were fed every day following behavioral training. Rats were randomly assigned to receive either cocaine training or to serve as yoked-saline controls. Animal care, surgeries, and experimental procedures followed the *Guide for the Care and Use of Laboratory Animals* (8th Edition) and were approved by the Institutional Animal Care and Use Committee at the University of Utah. Rats used in electrophysiology experiments began self-administration training 5–7 days after arrival. Rats used in fluorescent indicator studies underwent stereotaxic surgery for infusion of iGluSnFr into the DLS 6–8 days after arrival at the University of Utah and were allowed to recover for 5–7 days before the start of cocaine self-administration training.

2.2. Stereotaxic surgery

Only rats used in fluorescent indicator studies underwent stereotaxic surgery for viral induction of iGluSnFr in astrocytes. Rats were anesthetized with isoflurane (2.0–2.5% induction; 1.5–2.0% maintenance) and placed in a stereotaxic apparatus (Stoelting, IL, United States). A small hole was drilled in the skull and a 28-gage infusion cannula (P1 Technologies, VA, United States) was inserted into the DLS (in mm relative to bregma: AP +0.7, ML -3.6, DV -5.0; Yin et al., 2004). A total of 3 µL of pENN.AAV1.GFAP.iGluSnFr.WPRE.SV40 (RRID:Addgene_98,930; http://n2t.net/addgene:98930; RRID:Addgene_98,930) was infused into the DLS over the course of 30 min, after which the cannula was left in place for an additional 5 min before removal to ensure maximal diffusion. Rats were given 10 mg/kg Baytril i.v. and 0.1 mL of 500 IU/mL heparin-50% dextrose catheter-Lock Solution (SAI infusions, IL, United States) on the day of surgery, as well as once daily, along with 5 mg/kg carprofen s.c., for 3 days post-surgery. For the remainder of the recovery period and throughout the cocaine self-administration training and testing, rats were given daily infusions of i.v. Baytril and the heparin-dextrose catheter-lock solution following daily training. Rats were allowed to recover from stereotaxic surgery for 3–5 days before food restriction began, and 5–7 days before self-administration training.

2.3. Cocaine self-administration paradigm

The cocaine self-administration paradigm, adapted from Zapata et al. (2010), was conducted in eight standard operant chambers that were enclosed in sound and light-attenuating cabinets (Coulbourn Instruments, PA, United States). One wall of the chamber had two retractable levers on the right and left sides and the opposite wall was equipped with a 3-W, 24-V house light. Graphic State 4.0 software (Coulbourn Instruments, PA, United States) was used to control chamber equipment and experimental protocols, as well as to record the number of lever presses and session time. Male Long-Evans rats were trained to press one lever (designated as the drug "taking" lever) for intravenous cocaine•HCl infusion (0.33 mg/50 µL infusion; calculated as the salt; NIDA Drug Supply Program, NC, USA) under a fixed ratio 1 (FR1) schedule. In addition to cocaine infusion, each taking-lever press was accompanied by a retraction of the taking lever, illumination of a cue light, and extinction of the house light for a 30-s time-out (TO) period. Rats were trained daily on the taking lever for 2 h or 40 infusions per session, whichever came first. After reliable taking-lever self-administration was established (2 consecutive sessions with >10 infusions/session; average intake across all rats = 9.82 mg/kg/h), rats progressed to a chained seeking-taking schedule in which an additional, different lever (designated as the "seeking" lever) was introduced. The drug-taking and -seeking levers were counterbalanced across the left and right levers in the operant chambers. The first press of the seeking lever, under a 2-s random interval (RI) schedule, resulted in retraction of the seeking lever and presentation of the taking lever. Responding on the taking lever was kept on FR1 schedule of cocaine administration, followed by the 30-s TO period. Following the TO period, the seeking lever was reinserted, and the cycle began again. This seeking-taking chained schedule is denoted as: RI(2 s)/FR1:TO(30s) or "Chain #1." Rats underwent daily training on this schedule (3 h or 12 infusions, whichever came first) until they reached criterion of two consecutive sessions with 12 infusions/session. Rats then progressed through increasing chained schedules: Chain #2 RI(20s)/FR1:TO(120 s) and Chain #3 RI(60s)/FR1:TO(300 s) using the same training criteria. They then advanced to Chain #4 RI(120 s)/FR1:TO(600 s), which continued for six sessions (12 infusions/session), at which point all rats had achieved stable responding (<20% variability in drug infusions; average intake per Chain 4 session across all rats = 4.6 mg/kg/h). Yoked-saline controls received response-independent saline infusions identical to that of their paired experimental rat and lever-pressing had no scheduled consequences.

Once stable chained responding was established, rats progressed to 13 days of outcome devaluation; that is, the taking lever was available, but no cocaine was delivered upon lever-pressing, thereby devaluing the drug-taking lever via outcome omission. After the last day of outcome devaluation, seeking behavior was assessed under these "devalued" conditions in a 5-min test session. In this seeking test, only the seeking-lever was available and responding did not result in any scheduled consequences. Following the devalued seeking test, the taking-lever was then re-valued across two daily sessions identical to the initial FR1 taking lever training sessions (2 h or 40 infusions, whichever came first). The following day, another 5-min seeking test was conducted, but now under "valued" conditions. Comparing the number of cocaine-seeking lever presses made under the "devalued" vs. the "valued" test conditions gives insight into the sensitivity of drug-seeking to outcome devaluation, which enables the classification of cocaine-seeking behavior as either under goal-directed or habitual control (Zapata et al., 2010; Lerner, 2020). A "cocaine-seeking score" was determined for each rat as the number of seeking responses made under the *devalued* test condition expressed as a percentage of seeking responses made under the *valued* test condition. Rats with cocaine-seeking scores ≤70% were classified as having "goal-directed" cocaine-seeking behavior and scores ≥80% were classified as "habitual," similar to that previously reported by Zapata et al. (2010). As a small percentage of rats had cocaine-seeking scores that fell between 71–79%,

we termed these rats as "intermediate" and analyzed them as a separate group. All rats were sacrificed within 1–4 days following completion of the final seeking test, given the throughput of the electrophysiological recordings and iGluSnFr imaging. We limited this time course to 1–4 days after the testing as the seminal work on incubation of cocaine craving showed no significant changes in drug seeking over days 1–4 (Grimm et al., 2001) and subsequent studies of incubation variably use 1–4 days as "early" withdrawal time points. The 1–4 day period should therefore mitigate potential confounding effects of withdrawal and incubation of craving on the dependent measures.

2.4. Brain slice preparation

From the point of brain slice preparation onward through final data analysis, the experimenter was blinded to the treatment group (saline or cocaine) and behavioral classification (goal-directed, intermediate, habitual) of the rats. Within 4 days after the final seeking test, rats were anesthetized with 3% isoflurane or sodium pentobarbital (50 mg/kg) and immediately decapitated. The brain was then divided into two hemispheres longitudinally. For electrophysiology recordings, sagittal brain slices (400 μm) containing the DLS were collected in an oxygenated ice-cold NMDG-HEPES cutting solution (in mM: 92 NMDG, 2.5 KCl, 1.2 NaH_2PO_4, 30 $NaHCO_3$, 20 HEPES, 25 glucose, 2 thiourea, 5 Na-ascorbate, 3 Na-pyruvate, 10 $MgSO_4$, and 0.5 $CaCl_2$). Slices were then transferred to a pre-warmed (32–24°C) holding chamber containing NMDG-HEPES for 30 min as a protective recovery period. Stepwise, a Na^+ spike-in procedure was carried out according to an optimal age-dependent schedule (Ting et al., 2014). After 30 min, slices were transferred to a holding chamber containing room-temperature oxygenated HEPES-aCSF holding solution (in mM: 92 NaCl, 2.5 KCl, 1.2 NaH_2PO_4, 30 $NaHCO_3$, 20 HEPES, 25 glucose, 2 thiourea, 5 Na-ascorbate, 3Na-pyruvate, 2 $MgSO_4$, and 2 $CaCl_2$). Slices were then transferred to a pre-warmed (30°C) holding chamber for 20 min prior to recording for astrocyte labeling with 0.5 μM SR101 (Sigma-Aldrich, MO, United States) in recording aCSF (in mM: 119 NaCl, 2.5 KCl, 1.25 NaH_2PO_4, 24 $NaHCO_3$, 12.5 glucose, 2 $MgCl_2$, and 2 $CaCl_2$) (Takahashi et al., 2010). For iGluSnFr imaging, coronal brain slices (400 μm) containing the right hemisphere DLS were cut on a Vibratome 3,000 (Vibratome, MO, United States) in an ice-cold, sucrose solution (in mM: 185 sucrose, 2.5 KCl, 1.2 NaH_2PO_4, 25 $NaHCO_3$, 25 glucose, 10 $MgSO_4$, 0.5 $CaCl_2$). Brain slices were then transferred to a recovery chamber containing oxygenated aCSF at room temperature (in mM: 126 NaCl, 2.5 KCl, 1 NaH_2PO_4, 26 $NaHCO_3$, 10.5 glucose, 1.3 $MgSO_4$, 2 $CaCl_2$). All slices, regardless of slice method, were allowed to recover for a minimum of 1 h before recording or imaging. All solutions were bubbled with 95% O_2/5% CO_2 throughout the experiment, pH corrected to 7.30–7.35, and adjusted for an osmolarity between 295–300 mOsm. The non-injected hemisphere from iGluSnFr-transfected rats was flash-frozen in 2-methylbutane (MilliporeSigma, MA, United States) and stored at −80°C for later use in western blot analyses.

2.5. Electrophysiology

Whole-cell patch-clamp recordings of astrocytes were obtained by recording in the voltage-clamp configuration through a Multiclamp 700B amplifier, a Digidata 1440A data acquisition board, and pClamp10 software (Molecular Devices, CA, USA). Slices were visualized with a 40x water immersion objective (NA 0.8; Carl Zeiss, Thornwood, NY) using infrared differential interference contrast (IR-DIC) microscopy on an upright Axioskop2 microscope (Carl Zeiss, Thornwood, NY) prior to specific astrocyte identification. Only cells displaying SR101 fluorescence (excitation 586 nm, emission 605 nm) deep in the tissue were targeted for electrophysiology with pipettes containing a K^+ gluconate intracellular solution (in mM: 120 K gluconate, 20 HEPES, 10 EGTA, and 0.2 Na_2GTP), pH corrected to 7.28–7.33, and osmolarity between 290–295 mOsm. Astrocytes were voltage-clamped at -70 mV and further distinguished from neurons by their hyperpolarized resting membrane potential, low input resistance, and lack of voltage-dependent inward currents at depolarized potentials. Resting membrane potential was periodically determined in the $I = 0$ mode and monitored throughout recordings. Cells with variations in resting membrane potential greater than ±10 mV were excluded from analyses. Membrane and access resistance were monitored and only stable recordings were included in the study. Upon successfully obtaining the whole-cell patch configuration, a pharmacological cocktail containing $BaCl_2$ (200 μM), APV (50 μM), CNQX (10 μM), and picrotoxin (50 μM) was perfused for 15 min to isolate STCs.

A bipolar nichrome/formvar stimulating electrode placed 100–200 μm from the patch pipette in the DLS was used to deliver a single pulse or a high frequency stimulation train (10 pulses, 100 Hz). Stimulation strength was set as the intensity at which stimulation produced a half-maximal response amplitude following an input–output curve of increasing stimulation intensities, and this strength was used for all subsequent STC recordings. A maximum of two astrocytes were patched per slice. Signals were acquired at 10 kHz and filtered at 2 kHz. All response amplitude and time course analyses were performed on averaged, baseline corrected STCs in ClampFit (Molecular Devices, CA, United States). Rise times were calculated as the time it took for the current to rise from baseline to peak amplitude. Decay tau values were obtained by curve fitting the decay phase to a second order standard exponential equation, with only fast decay tau values included for analyses. Curves were fit from just after peak STC amplitude of the single pulse or the final (10th) pulse of HFS, to the end of the trace when currents have returned to baseline. Half-width was calculated as the time between the 50% values of the rise and decay times. Pulse ratios were determined by STC amplitude of the 10^{th} pulse to the 1st pulse of the HFS train. All analyses, with the exception of peak amplitude and pulse ratios, were also performed in traces normalized to peak current.

2.6. iGluSnFr imaging

iGluSnFr fluorescence was excited by a 470-nm LED light (Excelitas, Mississauga, Canada) and captured with an Axiocam 702 monochrome camera coupled with ZEN 3.1 (blue edition) software (Zeiss, MA, United States). All video recordings of evoked iGluSnFr signals were kept at constant imaging settings within the Zen software to allow for an image acquisition rate of 92 Hz (ROI size: 480 × 510; Exposure time: 10 ms; Intensity: 100%; Binning: 5 × 5; Gain: 2x). A bipolar, nichrome/formvar electrode was positioned within the DLS at a depth of ~100 μm below the tissue surface to deliver a 1-mA

double-pulse stimulation (two, 0.1 ms pulses, 10 ms apart). Three to five stimulation trials, conducted in the same location and spaced 1 min apart, were averaged together to produce one "evoked iGluSnFr response" that was used for analysis. After the final double-pulse stimulation trial was conducted in a given area, the electrode was kept in the same position and three stimulation trials were conducted with 1 mA high frequency stimulation (HFS; 0.1 ms pulses delivered at 10 Hz for 1 s) following the same trial protocol as above. Each stimulation trial was video recorded for 15 s, and included 4 s of baseline iGluSnFr fluorescence. Rats with low levels of iGluSnFr expression, no expression, or expression outside the DLS were not included in the final data analysis.

Evoked iGluSnFr responses were analyzed in ImageJ by placing a 158×158 pixel ROI (30×30 unit in ImageJ) at the location surrounding the highest peak iGluSnFr signal, typically adjacent to the stimulating electrode. Fluorescence intensity changes were baseline-corrected and used for analysis of decay kinetics in GraphPad Prism (GraphPad Software Inc., CA, United States). Decay tau was calculated by fitting the evoked iGluSnFr trace from the peak dF/*F* value to one-second post-peak with a one-phase, non-linear regression (Parsons et al., 2016; Pinky et al., 2018). For HFS trials, the response was fit from the final peak dF/F value in the HFS train to one-second post-peak (Parsons et al., 2016). Area under the curve (AUC) was calculated from the peak dF/F or final peak dF/F to one-second post-peak for both double-pulse stimulation and HFS, respectively.

A series of iGluSnFr control experiments were conducted in rats that were not enrolled in the chained cocaine self-administration paradigm, but were imaged within the same timeframe that experimental rats were imaged (approximately 6 weeks post-stereotaxic surgery). For temperature control experiments, evoked iGluSnFr responses were recorded in the same location within the DLS at 24°C and 32°C. Three stimulation trials (1 mA double-pulse stimulation) were first recorded at 24°C, and then three additional stimulation trials were recorded in the same location at 32°C. Bath temperature within the recording chamber was monitored and maintained with an in-line heater system (TC-324C, Warner Instruments, MA, United States). For all pharmacological control experiments, three baseline iGluSnFr responses (1 mA double-pulse) were first evoked in the DLS; next, three iGluSnFr responses (1 mA double-pulse) were evoked in the same location within the DLS in the presence of the pharmacological agent after the specified waiting period. For tetrodotoxin (TTX) experiments, 1 µM TTX citrate (Abcam, Cambridge, United Kingdom) in aCSF was perfused into the recording chamber for 15 min before imaging evoked iGluSnFr responses under TTX conditions. For TBOA experiments, the non-selective glutamate transporter inhibitor DL-threo-β-Benzyloxyaspartic acid (DL-TBOA, 100 µM) (Tocris, MN, United States) was perfused into the recording chamber for 10 min before imaging evoked iGluSnFr responses under TBOA conditions. For all experiments, three stimulation trials (1 mA double-pulse), spaced 1-min apart, were conducted for each experimental condition and were averaged together for later analysis.

2.7. Western blot

Non-injected hemispheres from iGluSnFr-transfected rats were used for western blot analysis of GLT-1 expression in the DLS. The frozen hemisphere was sectioned to bregma 1.44 mm at −16°C in a cryostat (Leica). Punches of the DLS (~1-mm^3) were taken and then sonicated in 2% SDS with protease inhibitor (cOmplete™ Mini, Sigma Roche; #11836153001), and centrifuged for 10 min (10,000 g at 4°C). The supernatant was collected and used for western blotting. Equal amounts of total protein, as determined by BCA assay, were prepared in 4x Laemmli sample buffer (Bio-Rad, #1610747). Samples were heated at 70°C for 10 min and 15 µL loaded onto 4–15% TGX gels (Bio-Rad Criterion #5671085). One well contained the ladder for determining molecular weights (Bio-Rad Precision Plus Protein Standard). Gels were run at 75 V for 15 min and then 125 V for 45–70 min. Gels were then transferred to nitrocellulose membranes at 100 V for 1.5 h at 4°C. Blots were stained with 1x Ponceau stain for 2 min and imaged on the FluorChem M (Protein Simple, Bio-Techne) to determine total protein in each lane. Gels were then blocked for 1 h in blocking solution (TBS-T) and incubated with anti-GLT1 primary antibody overnight at 4°C (1:2000, Millipore #AB1783, RRID: AB_90949). After washing in TBS-T, blots were incubated with Goat anti-guinea pig HRP secondary antibody (1:10,000; Jackson ImmunoResearch Laboratories #106–035–003, RRID: AB_2337402) for 1 h at room temperature. Blots were developed using the enhanced chemiluminescence reagent Western Lighting Plus Luminol Kit (Perkin Elmer NEL103001) and scanned using FluorChem M. The fluorescent intensity of each band was normalized to Ponceau as a loading control, and the resulting ratio was used to assess protein concentrations.

2.8. Statistical analysis

All statistical analyses were performed in GraphPad Prism (GraphPad Software Inc., CA, United States). For all analyses, alpha was set to 0.05. D-Agostino & Pearson normality tests were performed on all data sets to determine if the data was normally distributed. If the data were normally distributed ($p > 0.05$), parametric tests were used, including: one-way ANOVA, paired t-tests, unpaired t-tests, and Pearson correlation. If the data were not normally distributed ($p < 0.05$), nonparametric versions of the aforementioned tests were used, including: Kruskall Wallis test, Mann–Whitney *U* test, Wilcoxon matched-pairs signed rank test, and Spearman correlation, respectively. As noted above, all electrophysiology recordings, iGluSnFr imaging, and data analyses were conducted with the experimenter blinded to the treatment and behavioral classification of the subject.

3. Results

3.1. Cocaine-seeking and -taking behavior

Rats in the electrophysiology ($n = 21$) and iGluSnFr imaging ($n = 15$) cohorts were enrolled in cocaine self-administration training and DLS glutamate dynamics were assessed within 1–4 days after the final cocaine-seeking test (Figure 1). We used a chained cocaine self-administration paradigm, adapted from Zapata et al. (2010), to train distinct cocaine-seeking and -taking behaviors. Importantly, the number of seeking-lever responses made under devalued and valued conditions were used to calculate the cocaine-seeking score, which

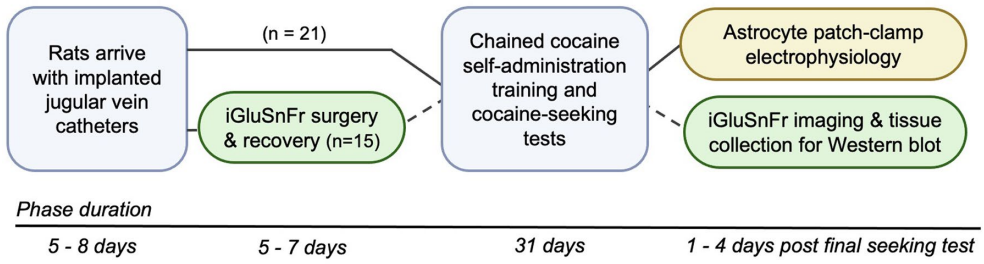

FIGURE 1
Schematic of experimental timeline. All rats arrived with implanted jugular vein catheters and were given 5–8 days to acclimate to animal facility housing. Rats in the electrophysiology cohort (n =21, black lines) were directly advanced into the chained cocaine self-administration paradigm, whereas rats in the imaging cohort (n =15, dashed lines) first underwent stereotaxic surgery to transfect DLS astrocytes with iGluSnFr and then were advanced to the self-administration paradigm 5–7 days later. Upon completion of the cocaine self-administration paradigm and testing for cocaine seeking under devalued and valued conditions, electrophysiological recordings, iGluSnFr imaging, and tissue collection were conducted within 1–4 days of the final cocaine-seeking test.

classified rats as either goal-directed (≤ 70%) or habitual (≥ 80%) in their cocaine-seeking behavior (Figure 2). We observed a subset of iGluSnFr-transfected rats (n =4) whose cocaine-seeking scores fell between 71–79%, which we termed "intermediate." As the non-transfected group only had one intermediate cocaine-seeking rat, it was excluded from subsequent STC analyses.

Both non-transfected and iGluSnFr-transfected rats readily met criteria for all cocaine-seeking and taking responses throughout training, extinguished cocaine-taking upon devaluation, and reinstated their cocaine-taking behavior upon revaluation (Supplementary Figures S1 and S2). Moreover, there was no significant difference in the average cocaine-seeking score between iGluSnFr-transfected and non-transfected rats (*Mann–Whitney U = 117.5, p = 0.21*; Supplementary Figure S1A). Next, there was no main effect of transfection on the number of taking-lever presses made across devaluation sessions (*two-way RM ANOVA,* $F_{(1,34)} = 0.0003$, $p = 0.99$; Supplementary Figure S1B). There was, however, a significant transfection x day interaction for the number of seeking-lever presses made during chained training (*two-way RM ANOVA,* $F_{(11,418)} = 3.49$, $p = 0.0001$; Supplementary Figure S1C), with iGluSnFr-transfected rats making significantly more seeking-responses than non-transfected rats during the first 5 sessions, but not the final session, of chain 4 training (*Sidak's multiple comparisons test, sessions 1–5: p < 0.01, session 6: p = 0.07*). However, there was no significant correlation between the average number of chain 4 seeking-responses and cocaine-seeking score for both non-transfected rats (*Spearman r = −0.30, p = 0.19*; Supplementary Figure S1D) and iGluSnFr-transfected rats (*Spearman r = 0.13, p = 0.65*; Supplementary Figure S1E). Similarly, iGluSnFr-transfected rats had a significantly higher average number of taking-lever presses than non-transfected rats during both the initial FR1 (*Mann–Whitney U = 47, p < 0.001*; Supplementary Figure S2A) and revaluation FR1 (*Mann–Whitney U = 39.5, p < 0.0001*; Supplementary Figure S2B) training sessions. However, the average number of taking-lever presses made in either stage did not correlate with cocaine-seeking score for both non-transfected rats (Initial: *Spearman r = −0.42, p = 0.052*; Revaluation: *Spearman r = −0.26, p = 0.25*; Supplementary Figure S2C) and iGluSnFr-transfected rats (Initial: *Spearman r = 0.06, p = 0.84*; Revaluation: *Spearman r = −0.12, p = 0.66*; Supplementary Figure S2D). In addition, both non-transfected and iGluSnFr-transfected rats reinstated taking-lever presses to at or above the level of their initial FR1 training (Supplementary Figure S2E). Taken together, while we observed some

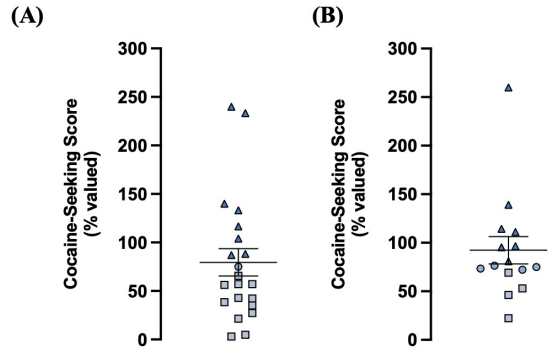

FIGURE 2
A chained cocaine seeking-taking self-administration paradigm reliably establishes rats with goal-directed and habitual control over cocaine-seeking behavior. **(A)** Distribution of cocaine-seeking scores from non-transfected animals (n =21; goal-directed: n =12, intermediate n =1, habitual: n =8). **(B)** Distribution of cocaine-seeking scores from iGluSnFr-transfected animals (n =15; goal-directed: n =4, intermediate: n =4, habitual: n =7). Cocaine-seeking scores (devalued seeking responses expressed as a percentage of valued seeking responses) are classified as goal- directed (≤70%, squares), intermediate (71–79%, circles), and habitual (≥80%, triangles). Data expressed as the mean±SEM.

training differences between transfected and non-transfected rats during cocaine self-administration sessions, these differences did not impact the generation or classification of goal-directed, intermediate, and habitual cocaine-seeking behavior in either group. Moreover, as we reliably generated goal-directed and habitual cocaine-seeking rats in both groups, we proceeded to assess the state of the DLS glutamate system of these rats with their respective assays of glutamate clearance and release.

3.2. Analyses of synaptic transporter currents in astrocytes reveal minimal changes in glutamate clearance in cocaine-experienced rats

We recorded evoked STCs of voltage-clamped astrocytes in the DLS of acute brain slices obtained from yoked-saline controls and rats classified as goal-directed or habitual in their cocaine-seeking to assess

astrocyte-mediated glutamate clearance. Each aspect of evoked STCs reflects various components of glutamate signaling as assessed through glutamate transporters on the astrocytes (Figure 3). The rise phase of the STC reflects the concerted uptake activity of glutamate transporters expressed on the astrocyte membrane in response to glutamate, whereas STC amplitude reflects the amount of glutamate released at the synapse and sensed by the astrocyte in question (Diamond and Jahr, 2000; Diamond, 2005; Tzingounis and Wadiche, 2007). STC rise times were not significantly different between slices obtained from yoked control (6.8 ± 0.2 ms; $n = 19$ cells, 15 slices, 10 rats) or cocaine-experienced (6.6 ± 0.2 ms; $n = 27$ cells, 23 slices, 16 rats) rats (*unpaired t-test, $t = 0.85$, $p = 0.40$;* Figure 3A). STC peak amplitudes were also not significantly different between slices from yoked-saline (−92.2 ± 10.2pA) and cocaine-experienced (−94.8 ± 8.0pA) rats when stimulated at an intensity that produced a half-maximal response amplitude (*unpaired t-test, $t = 0.20$, $p = 0.84$;* Figure 3A). Similarly, there were no significant differences in STC rise times recorded in slices from goal-directed (6.6 ± 0.3 ms; $n = 16$ cells, 14 slices, 10 rats) vs. habitual (6.6 ± 0.3 ms; $n = 11$ cells, 9 slices, 6 rats) classifications and in comparison to yoked-saline controls (*Kruskall-Wallis statistic = 0.30, $p = 0.86$;* Figure 3B). Peak amplitudes were also similar between slices from goal-directed (−93.2 ± 10.2pA) vs. habitual (−97.4 ± 13.8pA) cocaine-seeking rats, as well as yoked-saline controls (*one-way ANOVA: $F_{(2, 41)} = 0.05$, $p = 0.95$;* Figure 3B). Therefore, STC rise times and amplitudes from astrocytes in the DLS of acute brain slices suggest that there are no disruptions in transporter-mediated glutamate uptake into astrocytes or the amount of glutamate released at the synapse in cocaine-experienced rats regardless of their behavioral classification.

The time course of STCs reflects the rate of glutamate clearance from the synaptic cleft, with the decay phase being proportional to the decrease in the amount of extracellular glutamate available for transport (Diamond and Jahr, 2000; Diamond, 2005; Tzingounis and Wadiche, 2007). Analysis of the decay tau and half-width values of STCs in acute brain slices taken from cocaine-experienced and yoked-saline control rats revealed significantly slower decay kinetics in DLS astrocytes of rats with a history of cocaine self-administration. Specifically, decay tau values from cocaine-experienced rats (12.9 ± 0.3 ms) were significantly slower than those in yoked-saline controls (11.9 ± 0.3 ms; *unpaired t-test, $t = 2.03$, $p < 0.05$;* Figure 4A). Half-width values were also significantly longer in cocaine-experienced rats (17.8 ± 0.3 ms) in comparison to yoked-saline controls (16.7 ± 0.3 ms; *unpaired t-test, $t = 2.15$, $p < 0.05$;* Figure 4A). Together, STC decay kinetics indicate a significantly slower rate of glutamate clearance in astrocytes of cocaine-experienced rats. However, when STC decay kinetics were assessed in accordance with behavioral classifications of cocaine-seeking rats, there were no overall differences between the yoked-saline, goal-directed, and habitual cocaine-seeking groups (Figure 4B). Specifically, STC decay tau values from goal-directed (12.7 ± 0.5 ms) or habitual (13.1 ± 0.5 ms) classification groups did not significantly differ from each other or from yoked-saline controls (11.9 ± 0.3 ms; *one-way ANOVA: $F_{(2, 43)} = 2.26$, $p = 0.12$;* Figure 4B). STC half-width values were also not significantly different between slices from rats classified as

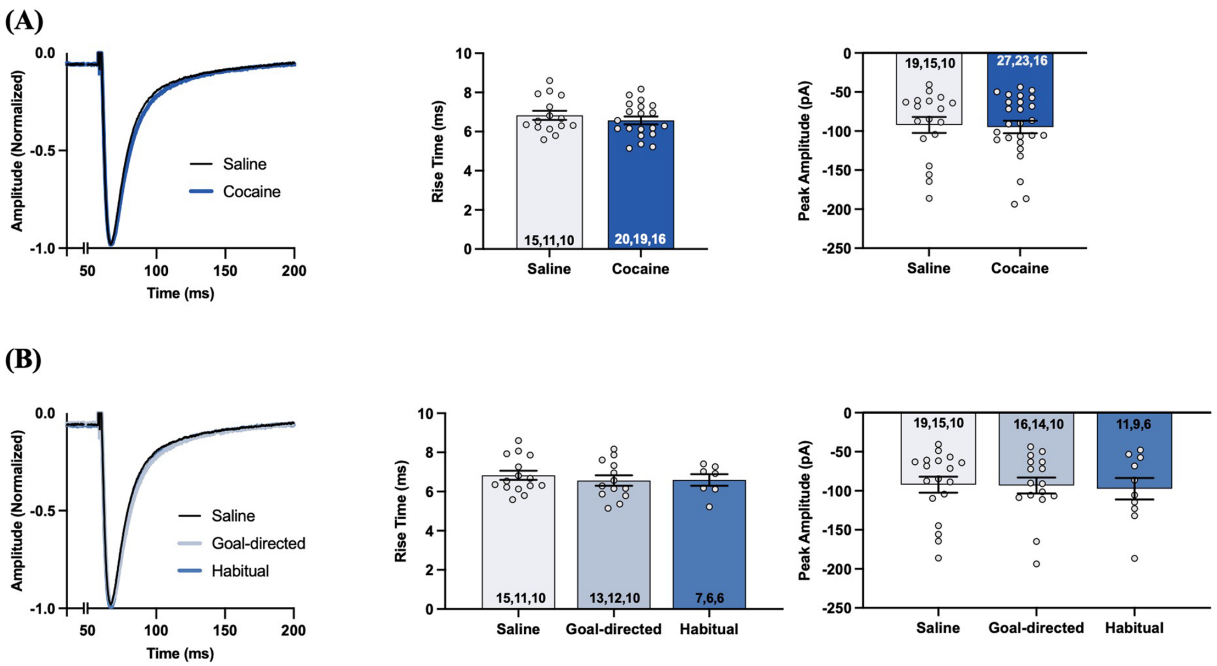

FIGURE 3
Synaptic transporter currents (STCs) in the DLS of acute brain slices from cocaine-experienced animals display no differences in the rise time or the peak amplitude of the STCs in astrocytes. **(A)** Representative peak-normalized STCs from slices of cocaine-experienced rats and yoked-saline controls following single-pulse stimulation at an intensity that produced a half maximal response amplitude. The STC rise time (0–100%) is quantified in the associated bar graph, along with peak STC amplitude (unpaired *t*- test, $p > 0.05$). **(B)** Representative peak-normalized STCs from slices of saline, goal-directed, and habitual rats following single-pulse stimulation, with the corresponding quantified STC rise time and peak amplitude (one-way ANOVA with Dunnet's *post hoc* test, Kruskal-Wallis test, $p > 0.05$, respectively). Data are expressed as the mean±SEM. Sample sizes for each group are denoted in each corresponding bar as: number of cells, number of slices, number of animals.

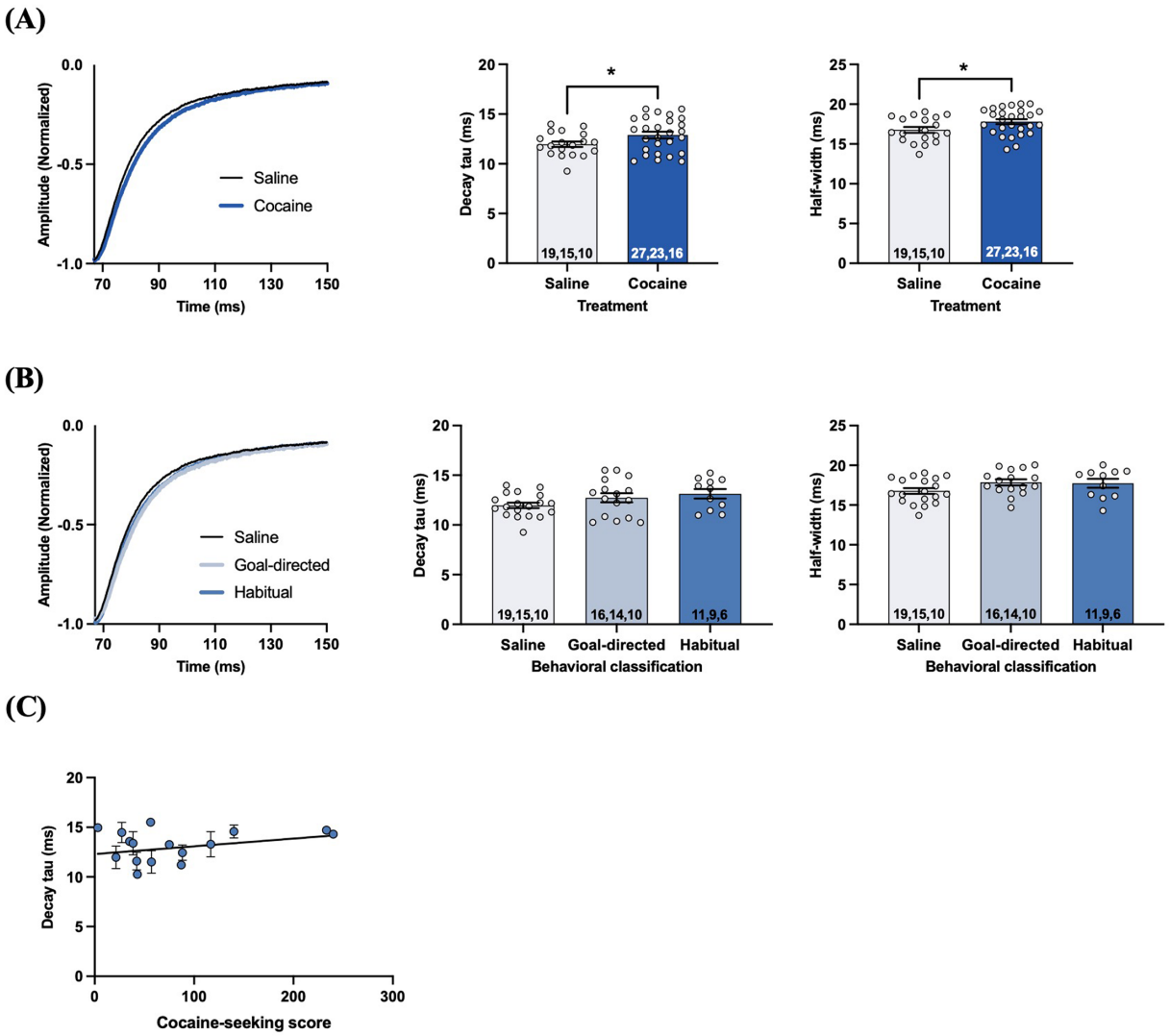

FIGURE 4
STCs in the DLS of slices obtained from cocaine-experienced animals display slower glutamate clearance kinetics. **(A)** Representative peak-normalized STC response decay phase, decay tau rate constant, and STC half-width following single pulse stimulation in the DLS of acute brain slices from yoked-saline and cocaine-experienced animals (unpaired t-test, $p < 0.05$). **(B)** Representative peak-normalized STC response decay phase, decay tau, and STC half-width in slices from yoked-saline rats or rats classified as goal-directed and habitual in their cocaine seeking (one-way ANOVA, with Dunnet's *post hoc* test, $p > 0.05$). **(C)** Relationship between decay tau and cocaine-seeking score (Spearman correlation, $p > 0.05$). Data fit with a linear regression line of best fit. Bar graphs expressed as the mean±SEM. *$p < 0.05$. Sample sizes for each group **(A,B)** are denoted in each corresponding bar as: number of cells, number of slices, number of animals.

goal-directed (17.8 ± 0.4 ms) or habitual (17.7 ± 0.5 ms) or from yoked-saline controls (16.7 ± 0.3 ms; *one-way ANOVA:* $F_{(2, 43)} = 2.28$, $p = 0.11$; Figure 4B). Moreover, there was no significant correlation between decay tau values and cocaine-seeking score (*Spearman* $r = 0.035$, $p = 0.90$; Figure 4C). Together, these data suggest that rats with a history of cocaine self-administration, regardless of whether their cocaine-seeking behavior is under goal-directed or habitual control, have a statistically slower rate of glutamate clearance in the DLS.

The difference in decay tau values of astrocyte STCs evoked by single-pulse stimulation in slices from cocaine-experienced and yoked-saline rats may not fully reflect the extent of possible biologically meaningful changes. Indeed, STCs resulting from different physiologically relevant synaptic events may be differentially affected. For example, a high frequency stimulation (HFS) protocol (10 pulses, 100 Hz) which elicits large amounts of synaptically-released glutamate has previously been shown to reveal impairments in glutamate clearance that were not apparent, or well-defined, under low frequency conditions (*c.f.,* Diamond and Jahr, 2000; Tanaka et al., 2013; Umpierre et al., 2019). Therefore, we also evoked STCs using the HFS stimulation protocol. Unexpectedly, decay tau values from STCs evoked with the HFS protocol did not significantly differ between slices obtained from yoked-saline (49.2 ± 3.8 ms) and cocaine-experienced rats (46.1 ± 2.9 ms; *unpaired t-test,* $t = 0.69$, $p = 0.49$; Figure 5A). Likewise, decay tau values of STCs from rats classified as goal-directed (46.2 ± 4.2 ms) or habitual (45.9 ± 3.6 ms) in their cocaine-seeking behavior were not significantly different relative to each other or to yoked-saline controls (49.2 ± 3.8 ms; *one-way ANOVA:* $F_{(2, 41)} = 0.23$, $p = 0.79$; Figure 5B). Also, there was no significant

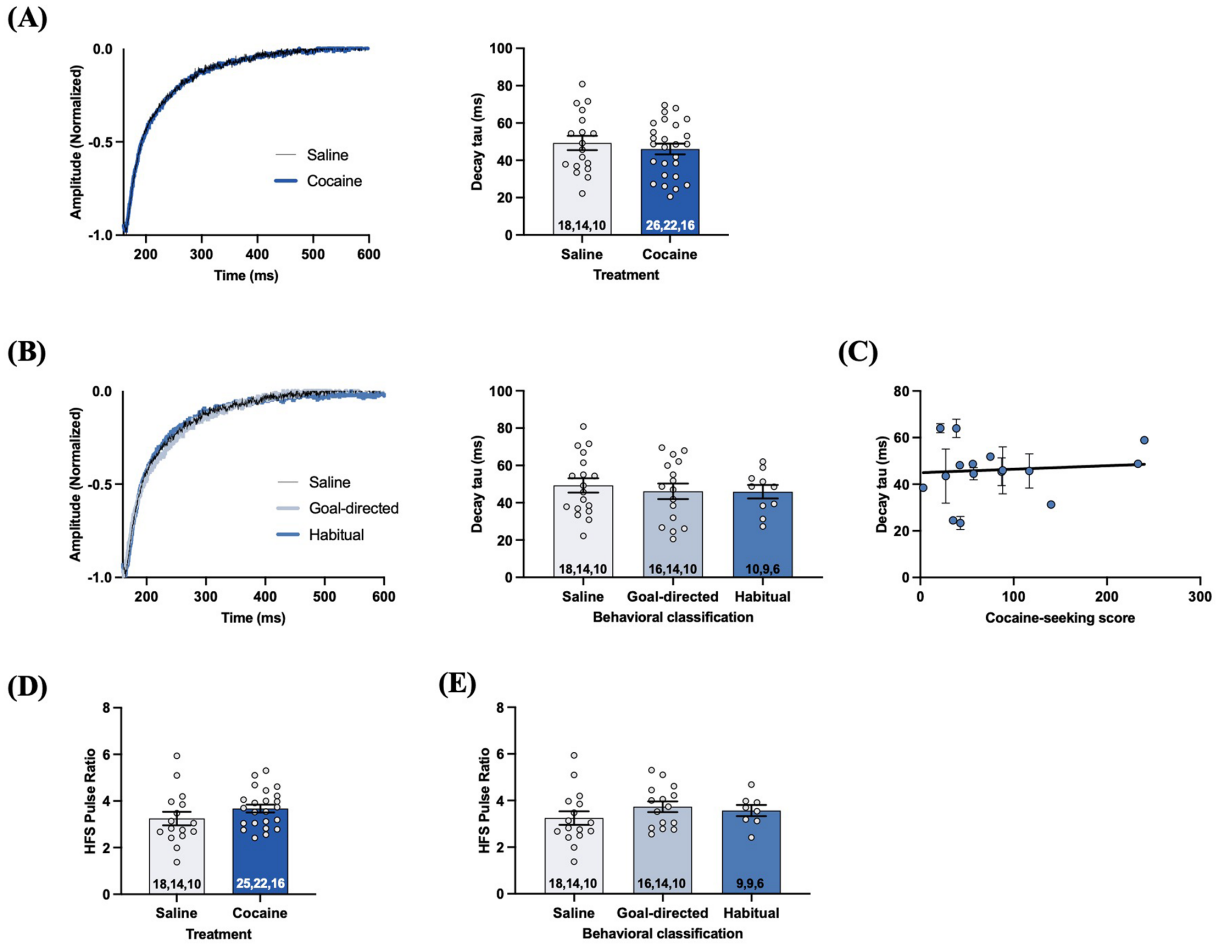

FIGURE 5
STCs following HFS in slices obtained from cocaine-experienced animals display no differences in glutamate clearance or presynaptic release in the DLS. **(A)** Representative STC decay phase, peak-normalized to the 10th stimulus, following HFS (10 pulses, 100 Hz) in slices from yoked-saline control and cocaine-experience animals. HFS STC decay tau from slices of saline and cocaine- treated animals (unpaired *t*-test, $p > 0.05$). **(B)** Representative STC decay phase following HFS in slices from yoked-saline controls and rats classified as goal-directed or habitual in their cocaine-seeking behavior and corresponding decay tau (one-way ANOVA with Dunnet's *post hoc* test, $p > 0.05$). **(C)** Relationship between HFS decay tau and cocaine-seeking score (Spearman correlation, $p > 0.05$). Data fit with a linear regression line of best fit. **(D)** HFS pulse ratio (10th: 1st pulse amplitude) between slices from yoked-saline and cocaine self- administering animals (unpaired *t*-test, $p > 0.05$). **(E)** HFS pulse ratio between slices from yoked-saline controls and rats classified as goal-directed and habitual in their cocaine-seeking behavior (one-way ANOVA with Dunnet's *post hoc* test, $p > 0.05$). Bar graphs expressed as the mean±SEM. Sample sizes for each group **(A,B,D,E)** are denoted in each corresponding bar as: number of cells, number of slices, number of animals.

correlation between HFS decay tau values and cocaine-seeking scores (*Spearman* $r = 0.15$, $p = 0.57$; Figure 5C). Together, these data suggest that DLS glutamate clearance following HFS is unaffected by cocaine self-administration, as well as the nature of control over the cocaine-seeking behavior. Finally, we also assessed short term plasticity mechanisms of presynaptic facilitation by analyzing the STC pulse amplitude ratio for the 10th: 1st pulse of the HFS train (Umpierre et al., 2019). HFS pulse ratios were not significantly different between yoked-saline (3.3 ± 0.3) and cocaine-experienced rats (3.6 ± 0.2; *unpaired t-test*, $t = 1.37$, $p > 0.05$; Figure 5D). Likewise, further sub-group analysis of HFS pulse ratios from rats classified as goal-directed (3.7 ± 0.2) or habitual (3.6 ± 0.2) in their cocaine-seeking behavior did not reveal any significant differences relative to each other or to the yoked-saline controls (3.3 ± 0.3; *one-way ANOVA:* $F_{(2, 36)} = 0.99$, $p = 0.38$; Figure 5E). These findings suggest that glutamate release and presynaptic facilitation in the DLS is also unaltered in cocaine-experienced rats, regardless of apparent goal-directed or habitual control over their cocaine-seeking behavior.

3.3. Evoked iGluSnFr response kinetics in the DLS are unaltered in cocaine-experienced rats

Next, we investigated extracellular glutamate dynamics using the intensity-based glutamate-sensing fluorescent reporter (iGluSnFr) (Marvin et al., 2013). Unlike STCs, iGluSnFr enables the measurement of rapid glutamate release and clearance dynamics at the regional level and can be expressed in a cell-type specific manner (Marvin et al., 2013). As the fine processes of astrocytes are in close contact with the pre- and post-synaptic components of excitatory synapses (Mahmoud et al., 2019), we selectively expressed

iGluSnFr under the GFAP promotor in the DLS and confirmed selective expression by astrocytes based on the morphology of the cells expressing the iGluSnFr (Supplementary Figure S3A). The kinetics of evoked iGluSnFr responses reflect different properties of extracellular glutamate dynamics (Supplementary Figures S3B,C), including the rate of glutamate clearance (decay tau) and the magnitude of evoked synaptic glutamate release (peak signal), and the total amount of extracellular glutamate sensed by iGluSnFr-expressing cells (area under the curve; AUC) (Marvin et al., 2013, Parsons et al., 2016, Koch et al., 2018; Pinky et al., 2018; Parker et al., 2021). Control experiments using bath-applied tetrodotoxin (TTX) abolished evoked iGluSnFr responses, confirming that evoked iGluSnFr signals occur in response to local stimulation-induced, synaptic glutamate release (Supplementary Figure S3D). Next, bath-application of the non-specific glutamate transporter antagonist DL-TBOA decreased the rate of decay of the evoked-iGluSnFr response (Supplementary Figure S3E), demonstrating that iGluSnFr imaging is capable of detecting changes in glutamate clearance resulting from altered glutamate transporter function. Finally, the decay rate of evoked iGluSnFr responses was faster when the bath temperature was increased to 32°C, as compared to evoked responses measured at 24°C (Supplementary Figure S3F). Importantly, each of these iGluSnFr control experiments have been previously performed to verify iGluSnFr functioning (Parsons et al., 2016). Together, these control experiments demonstrate that iGluSnFr is properly functioning in our experimental preparation and is capable of detecting both increases and decreases in glutamate clearance as well as changes in clearance arising from altered glutamate transporter function.

We examined iGluSnFr response decay kinetics to determine the rate of regional glutamate clearance following 1 mA double-pulse stimulation. The decay tau of evoked iGluSnFr responses was not significantly different between yoked-saline (143.8 ± 3.3 ms) and cocaine-experienced rats (140 ± 3.4 ms; *unpaired t-test, t = 0.69, p = 0.49*; Figure 6A). Analysis of the decay tau across the cocaine-experienced rats classified as goal-directed (138.7 ± 6.5 ms),

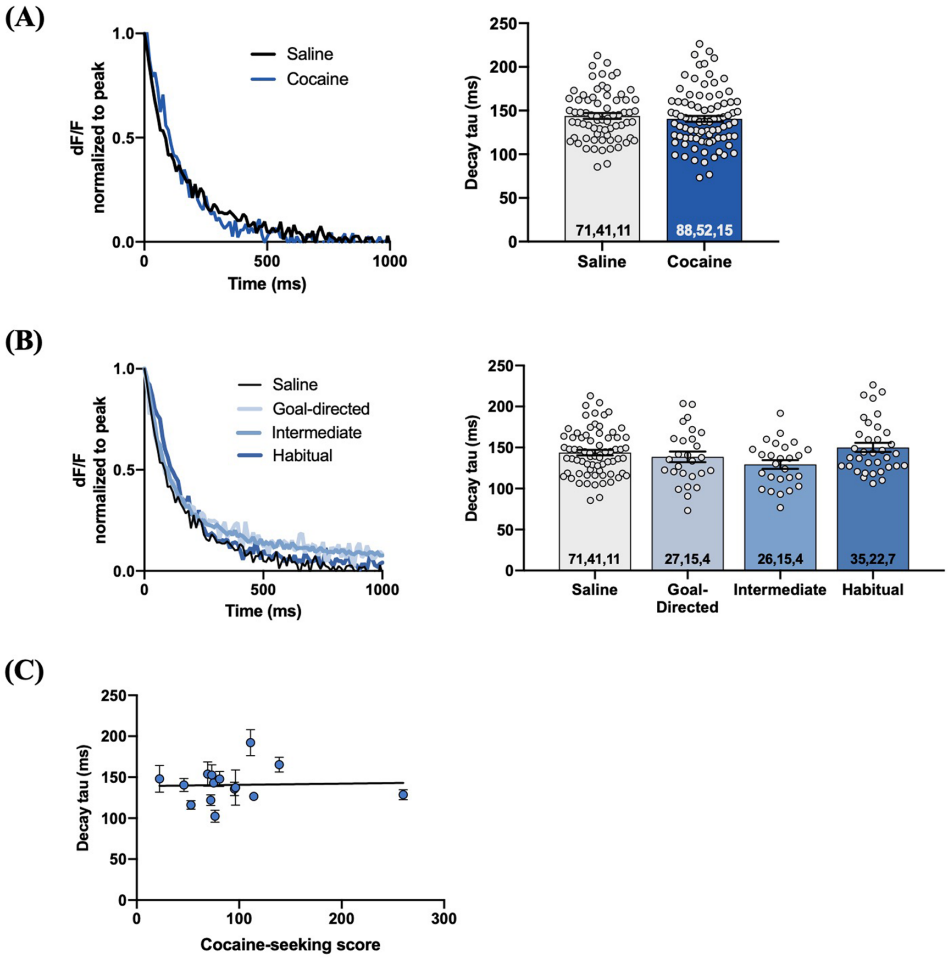

FIGURE 6
Evoked iGluSnFr responses in the DLS of slices from cocaine-experienced animals display no differences in glutamate clearance rate.
(A) Representative peak-normalized iGluSnFr response decay following 1 mA double pulse stimulation from slices of yoked-saline and cocaine-experienced animals. Decay tau quantified in the associated bar graph (unpaired t-test, $p>0.05$). **(B)** Representative iGluSnFr response decay and decay tau values of yoked-salibe controls and goal-directed, intermediate, and habitual classifications (one-way ANOVA, $p=0.05$). **(C)** Relationship between cocaine-seeking score and decay tau of evoked iGluSnFr responses (Spearman correlation, $p>0.05$); data fit with a linear regression line of best fit. iGluSnFr responses were evoked with 1mA double-pulse stimulation. Bar graphs expressed as mean ± SEM. Sample sizes for each group **(A,B)** are denoted in each corresponding bar as: number of averaged responses, number of slices, number of animals.

intermediate (129.4 ± 5.3 ms), and habitual (150.2 ± 5.5 ms) and yoked-saline controls (143.8 ± 3.3 ms) did reveal an overall significant effect (*one-way ANOVA:* $F_{(3, 155)} = 2.6$, $p = 0.05$; Figure 6B). *Post hoc* analyses, however, failed to identify significant differences in decay tau between yoked-saline controls and each behavioral classification of cocaine-experienced rats (*Dunnett's multiple comparisons adjusted p values*; *goal-directed:* $p = 0.82$, *intermediate:* $p = 0.10$, *habitual:* $p = 0.65$). Moreover, there was no significant correlation between cocaine-seeking score and decay tau of evoked iGluSnFr responses (*Spearman* $r = 0.05$, $p = 0.87$; Figure 6C). We observed similar results when iGluSnFr responses were evoked with 1 mA-HFS (0.1 ms pulses, 10 Hz for 1 s). The decay tau of HFS-evoked iGluSnFr responses did not significantly differ between yoked-saline (186.0 ± 6.6 ms) and cocaine-experienced rats (199.8 ± 8.6 ms; *unpaired t-test,* $t = 1.23$, $p = 0.22$; Figure 7A). Furthermore, there were no significant differences in decay tau across rats classified as goal-directed (199.4 ± 13.1 ms), intermediate (180.7 ± 19.0 ms), or habitual (214.2 ± 10.9 ms) in their cocaine seeking, both relative to each other and compared to yoked-saline controls (*Kruskall-Wallis statistic* $= 5.13$, $p = 0.16$; Figure 7B). Lastly, there was no significant correlation between decay tau and cocaine-seeking score (*Spearman* $r = 0.23$, $p = 0.40$; Figure 7C). Taken together, these results suggest that glutamate clearance in the DLS is unaffected by a history of cocaine self-administration as well as the development of habitual control over cocaine-seeking behavior.

As iGluSnFr provides the means to assess aspects of synaptic glutamate release (Marvin et al., 2013; Parsons et al., 2016; Koch et al., 2018), we also investigated these metrics in the DLS of cocaine-experienced rats. We first assessed these measures in iGluSnFr responses evoked with local 1 mA double pulse stimulation. There was no significant difference in the peak signal of evoked responses between cocaine-experienced and yoked saline rats (saline: 0.052 ± 0.003dF/F; cocaine: 0.053 ± 0.003dF/F; *Mann–Whitney* $U = 3{,}101$, $p = 0.94$; Figure 8A). Similarly, the peak signal was unchanged across goal-directed (0.046 ± 0.005 dF/F), intermediate (0.06 ± 0.005 dF/F), and habitual (0.05 ± 0.005 dF/F) cocaine-seeking rats and yoked-saline controls (*Kruskall-Wallis statistic* $= 3.46$, $p = 0.33$;

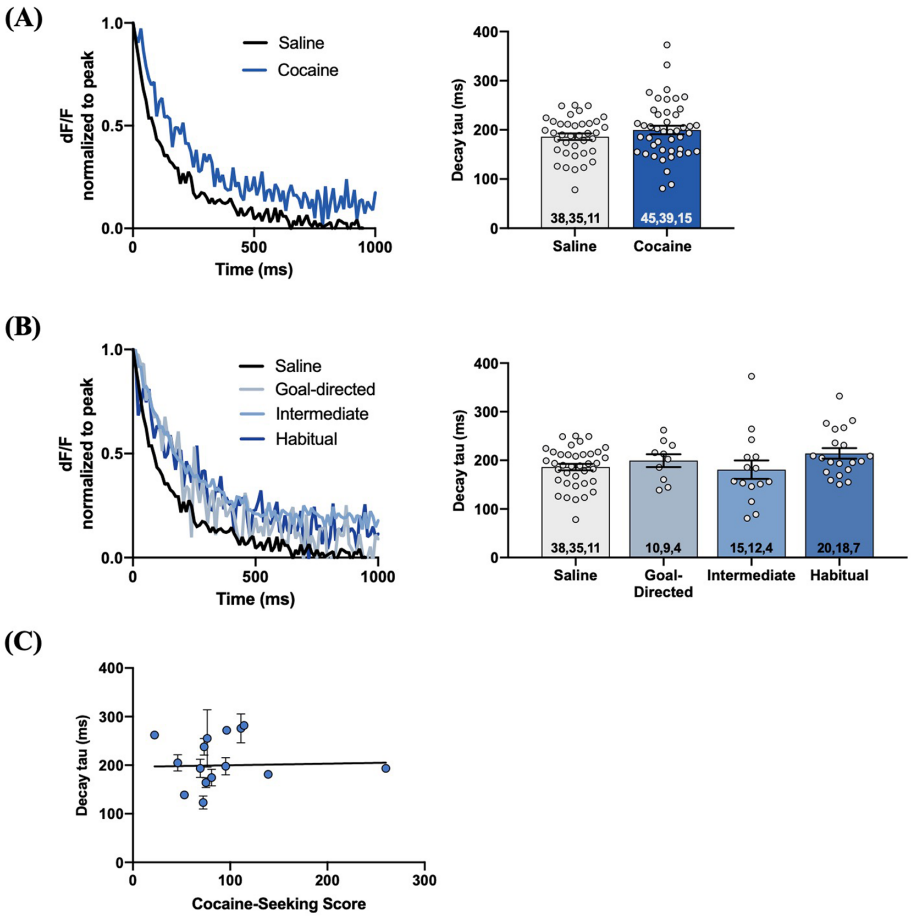

FIGURE 7
HFS-evoked iGluSnFr responses display no differences in glutamate dynamics in the DLS of cocaine-experienced animals and saline controls. **(A)** Representative peak-normalized iGluSnFr response decay evoked by 1 mA HFS (10 Hz, 1 s) in slices from drug-naïve control and cocaine-experienced animals. Decay tau quantified in the corresponding bar graph (unpaired *t*-test, $p > 0.05$). **(B)** Representative peak-normalised, HFS-evoked iGluSnFr response decay of goal-directed, intermediate, and habitual classifications. Decay tau quantified in the corresponding bar graphs (one-way ANOVA with Dunnet's *post hoc* test, $p > 0.05$). **(C)** Relationship between cocaine-seeking score and decay tau of evoked iGluSnFr responses (Spearman correlation, $p > 0.05$), data fit with a linear regression line of best fit). iGluSnFr responses were evoked with 10 Hz HFS stimulation in the DLS of acute brain slices. Bar graphs are expressed as mean ± SEM. Sample sizes for each group **(A,B)** are denoted in each corresponding bar as: number of responses, number of slices, number of animals.

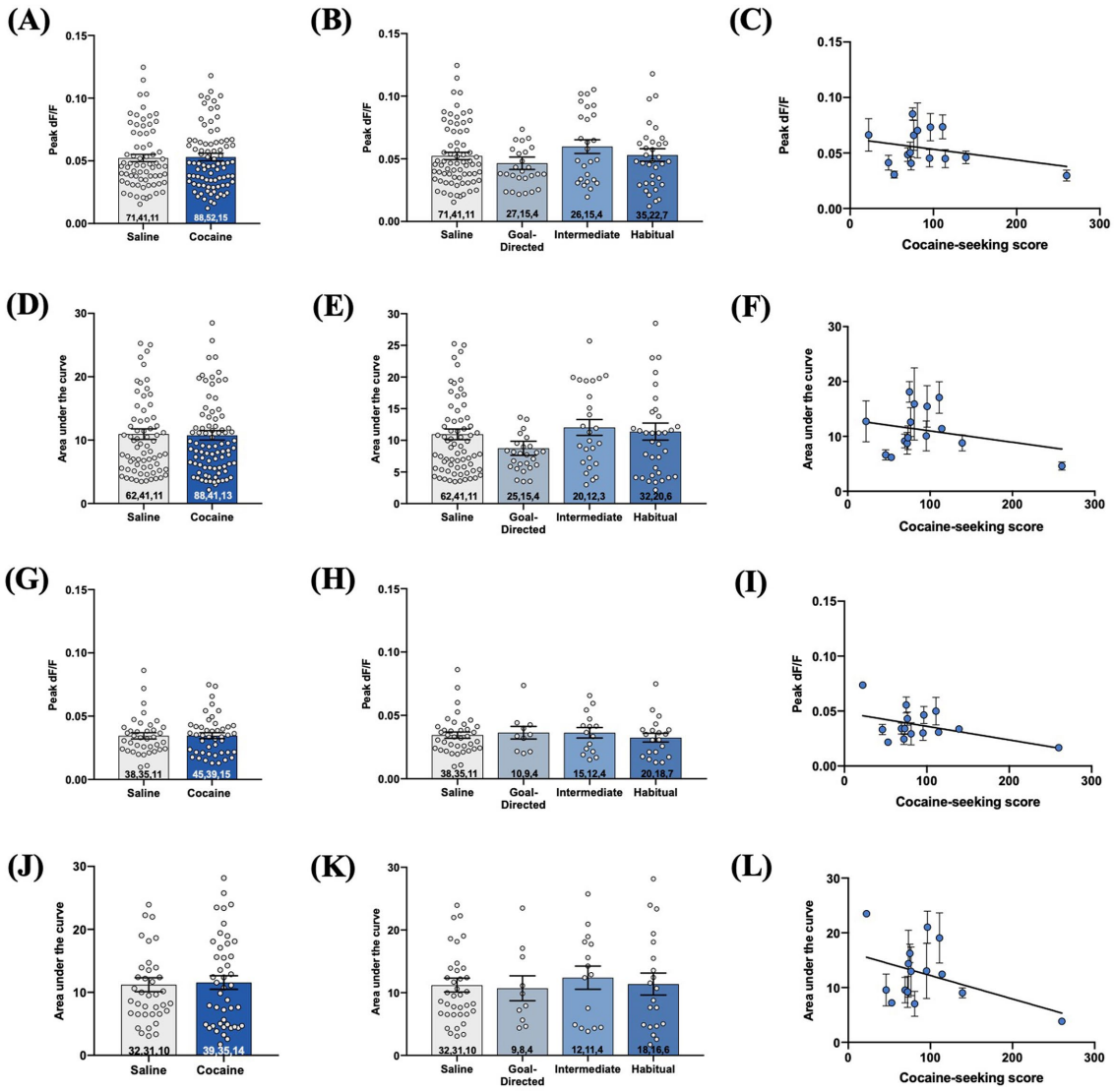

FIGURE 8
Evoked iGluSnFr responses in acute brain slices obtained from cocaine-experienced animals display no differences in synaptically-released glutamate in the DLS. iGluSnFr responses were evoked with either 1 mA double-pulse stimulation **(A-F)** or high-frequency stimulation **(G-L)**. **(A,G)** Peak signal (dF/F) of iGluSnFr responses in the DLS of yoked saline and cocaine- experienced animals (Mann-Whitney test, $p > 0.05$) and **(B,H)** across behavioral classification groups (Kruskall-Wallis test, $p > 0.05$). **(C,I)** Relationship between cocaine-seeking score and peak dF/F (Spearman correlation, $p > 0.05$). AUC of evoked iGluSnFr responses in the DLS of **(D,J)** yoked saline and cocaine-experienced animals (Mann-Whitney test, $p > 0.05$) and **(E,K)** across cocaine-seeking behavioral classification groups (Kruskall-Wallis test, $p > 0.05$). **(F,L)** Relationship between cocaine-seeking score and AUC (Spearman correlation, $p > 0.05$). iGluSnFr responses were evoked with either 1 mA double-pulse stimulation or 1 mA HFS (10 Hz, 1 s). Bar graphs expressed as mean ± SEM. Sample sizes for each group are denoted in each corresponding bar as: number of averaged responses, number of slices, number of animals.

Figure 8B). Furthermore, peak signal and cocaine-seeking score were not significantly correlated (*Spearman* $r = 0.01$, $p = 0.98$, Figure 8C). Next, there was no significant difference in the AUC of double-pulse-evoked responses between cocaine-experienced (10.76 ± 0.74) and yoked-saline (10.95 ± 0.84) rats (*Mann–Whitney* $U = 3{,}100$, $p = 0.93$; Figure 8D), as well as across behavioral classification groups (goal-directed: 8.7 ± 1.12; intermediate: 12.03 ± 1.25; habitual: 11.38 ± 1.35) and controls (*Kruskall-Wallis statistic* $= 4.25$, $p = 0.24$; Figure 8E). Finally, there was no significant correlation between AUC and cocaine-seeking score (*Spearman* $r = 0.12$, $p = 0.68$, Figure 8F). Similar results were observed when iGluSnFr responses were evoked with 1 mA-HFS. There were no significant differences in peak signal between cocaine-experienced (0.03 ± 0.002 dF/F) and yoked-saline (0.03 ± 0.002 dF/F) rats (*Mann Whitney* $U = 854.5$, $p = 0.99$, Figure 8G), as well as across behavioral classification groups (goal-directed: 0.04 ± 0.005 dF/F; intermediate: 0.04 ± 0.004 dF/F; habitual: 0.03 ± 0.003 dF/F) and yoked-saline controls (*Kruskall-Wallis statistic* $= 0.89$, $p = 0.83$, Figure 8H). In addition, there was no significant correlation between HFS-evoked peak signal and cocaine-seeking score (*Spearman* $r = -0.175$, $p = 0.53$, Figure 8I). Finally, there were no significant differences in the AUC between cocaine-experienced (11.57 ± 1.07) and yoked-saline (11.21 ± 1.1) rats (*Mann Whitney* $U = 840$, $p = 0.89$, Figure 8J), as well as across behavioral classification groups (goal-directed: 10.70 ± 1.98; intermediate:

12.40 ± 1.85; habitual: 11.37 ± 1.75) and yoked-saline controls (*Kruskall-Wallis statistic = 0.34, p = 0.95,* Figure 8K). Lastly, there was no significant correlation between the AUC of HFS-evoked iGluSnFr responses and cocaine-seeking score (*Spearman r = −0.17, p = 0.54,* Figure 8L). Taken together, these data suggest that iGluSnFr metrics of glutamate release in the DLS are unaltered in cocaine-experienced rats, regardless of the mode of control over their cocaine-seeking behavior.

3.4. GLT-1 protein expression in the DLS is unaltered following chained cocaine self-administration

Given the extensive literature reporting decreased GLT-1 expression in the accumbens of rats with a history of cocaine self-administration and withdrawal (Kalivas, 2009; Niedzielska-Andres et al., 2021) and one report of decreased expression in the DLS (Ducret et al., 2016), we investigated GLT-1 protein expression via western blotting of the DLS of cocaine-experienced rats and across cocaine-seeking behavioral classifications (Figure 9A). There was no significant difference in ponceau-corrected GLT-1 band intensity in cocaine-experienced (1.30 ± 0.04) rats in comparison to yoked-saline controls (1.40 ± 0.08; *unpaired t-test, t = 1.14, p = 0.26*; Figure 9B). Similarly, sub-group analysis of the cocaine-experienced rats showed that there was no difference in GLT-1 expression in the DLS of rats classified as goal-directed (1.15 ± 0.06), intermediate (1.47 ± 0.04), or habitual (1.32 ± 0.06) in their cocaine-seeking relative to each other and the yoked-saline controls (*one-way ANOVA:* $F_{(3, 27)} = 2.39$, *p = 0.09*; Figure 9C). Finally, there was no significant correlation between cocaine-seeking score and GLT-1 expression in the DLS (*Spearman r = 0.21, p = 0.37*; Figure 9D). These results suggest that extended cocaine self-administration, regardless of apparent goal-directed, intermediate, or habitual control over cocaine-seeking behavior, is not associated with altered GLT-1 protein expression in the DLS.

4. Discussion

The transition between recreational drug use and addiction is considered to arise from the shift between goal-directed and habitual control over drug behaviors. While the development of habitual appetitive and motor skill behaviors has been shown to be mediated by potentiated glutamatergic signaling in the DLS (Yin et al., 2009; Goodman et al., 2017), the state of the DLS glutamate system in the context of habitual drug behaviors has remained undefined. Therefore, this study profiled the state of the DLS glutamate system across rats whose cocaine-seeking behavior was classified as goal-directed, intermediate, and habitual based on sensitivity to outcome omission. Overall, we found that glutamate clearance and release dynamics and GLT-1 protein expression in the DLS are largely unchanged across cocaine-experienced rats, both relative to the apparent nature of the behavioral control over the cocaine-seeking behavior and relative to yoked-saline controls.

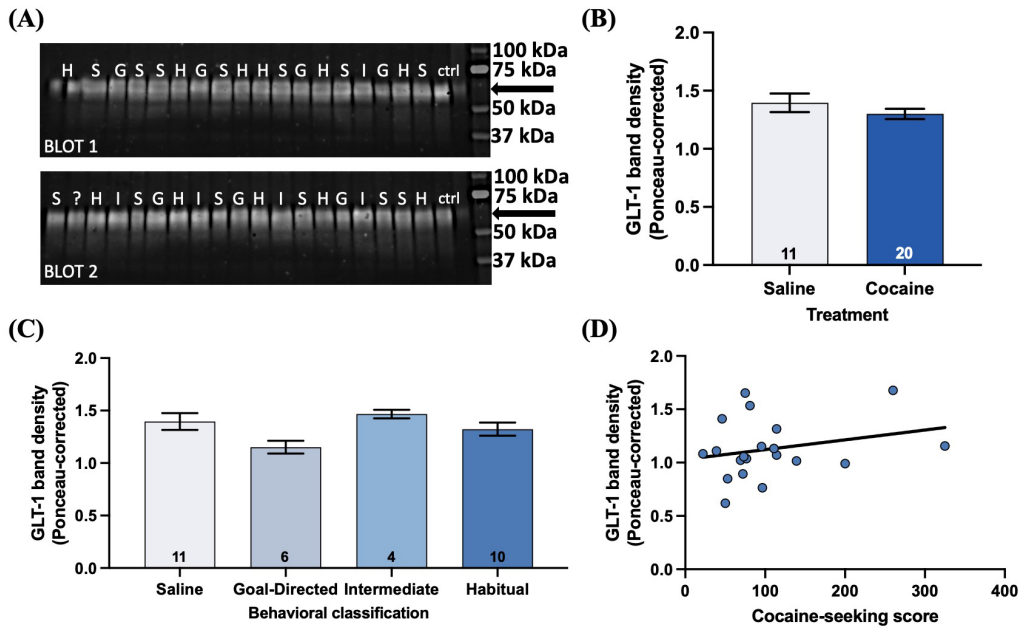

FIGURE 9
GLT-1 expression in the DLS is unaltered by cocaine-experience or the mode of behavioral control over cocaine-seeking. **(A)** Illustrative western blots from saline (S), goal-directed (G), intermediate (I), and habitual (H) groups for GLT-1 protein obtained from micro-punches of the DLS. The GLT-1 band resolved at ~62kDa (arrow). "?" indicates sample from an animal who failed to respond on either seeking test and therefore could not be behaviorally classified. "ctrl" indicates control lanes. **(B)** GLT-1 band density in saline and cocaine-treated animals (unpaired *t*-test, $p > 0.05$). **(C)** Ponceau-corrected GLT-1 band density across goal-directed, intermediate, and habitual classification groups (one-way ANOVA with Dunnet's *post hoc* test, $p > 0.05$). **(D)** Relationship between cocaine-seeking score and GLT-1 band density (Spearman correlation, $p > 0.05$). Data fit with a linear regression line of best fit. Bar graphs expressed as mean±SEM. Sample sizes for each group **(B,C)** are denoted in each corresponding bar as number of animals.

The present study capitalized on a previously published behavioral paradigm that enabled the classification of cocaine-seeking as either goal-directed or habitual (Zapata et al., 2010). Similar to Zapata et al. (2010), training on this paradigm reliably produced goal-directed and habitual cocaine-seeking rats. However, we also observed a subset of a rats whose cocaine-seeking scores fell between the goal-directed and habitual categories, which we termed "intermediate." An intermediate cocaine-seeking score likely represents a rat whose cocaine-seeking behavior was transitioning between goal-directed and habitual control at the time of testing or were, perhaps, more flexible in their behavioral control. Indeed, Zapata et al. (2010) demonstrated that rats with goal-directed cocaine-seeking behavior transitioned to habitual cocaine-seeking with extended training. Next, rats in the present study, as well as in Zapata et al. (2010), demonstrated a wide range of sensitivity of their cocaine-seeking behavior to outcome devaluation, despite being given the same daily access to cocaine self-administration sessions. Whether this wide range in cocaine-seeking scores is due to individual differences in learning strategy or vulnerability to addiction (Belin et al., 2009) remains an interesting avenue of future study. Finally, we observed some minor differences in lever press behavior between iGluSnFr-transfected rats and non-transfected rats during self-administration training. Namely, iGluSnFr-transfected rats made more taking-lever presses than non-transfected rats during the initial FR1 and revaluation FR1 training sessions and also made more seeking-lever presses during chain 4 training. These training differences may have stemmed from the stereotaxic surgery and/or DLS infusion itself that the iGluSnFr group received, as stress, for example, has been shown to influence instrumental responding (Schwabe and Wolf, 2009; Smeets et al., 2019). In addition, iGluSnFr itself introduces an artificial, competitive binding site for extracellular glutamate (Marvin et al., 2018; Armbruster et al., 2020), which needs to be acknowledged when combined with behavioral studies. Indeed, computational analyses suggest that iGluSnFr expression on astrocytes decreases the rate of glutamate uptake into astrocytes, which can result in an increased time course and concentration of extracellular glutamate (Armbruster et al., 2020). It is, therefore, plausible that the iGluSnFr expression in the DLS of rats in the present study may have altered glutamate dynamics within the DLS and affected their instrumental training, but further study is needed. Nevertheless, we found that none of these training differences were related to the final cocaine-seeking score of rats in either group and, importantly, iGluSnFr transfection did not significantly affect the average cocaine-seeking score of rats. Moreover, as training on this behavioral paradigm reliably produced goal-directed and habitual cocaine-seeking rats, and it has previously been used to demonstrate that habitual cocaine-seeking is dependent on DLS activity (Zapata et al., 2010), we considered it to be an ample platform to assess the state of the DLS glutamate system in goal-directed and habitual cocaine-seeking rats.

We used whole-cell patch-clamp electrophysiology of DLS astrocytes in acute brain slices to assess glutamate dynamics in rats with a history of cocaine self-administration exhibiting goal-directed or habitual cocaine-seeking behavior. STCs evoked by single pulse stimulation displayed significantly slower rates of glutamate clearance in slices obtained from cocaine-experienced rats, as observed by an increase in the decay tau and half-width values. Interestingly, when decay tau and half-width values were compared between saline and either the goal-directed or habitual groups, there were no significant differences, nor was there any relationship between cocaine-seeking scores and decay tau values. Single-pulse evoked STCs, therefore, suggest that cocaine-experience, independent of goal-directed or habitual control over cocaine-seeking behavior, is associated with a slower rate of glutamate clearance in the DLS. In contrast, analysis of STC recordings evoked by HFS indicate no significant differences in decay tau values between yoked-saline controls and rats with a history of cocaine self-administration. Similarly, there were no differences observed in accordance with any of the behavioral classification groups, nor a significant relationship between cocaine-seeking score and HFS decay tau. As HFS does not overwhelm astrocyte transporters (Diamond and Jahr, 2000) and has been shown to reveal impairments in glutamate clearance that are not apparent or well-defined under low frequency conditions (Tanaka et al., 2013; Umpierre et al., 2019), the lack of a significant difference in HFS decay tau values seemingly contradicts our findings from single-pulse STCs. However, given the small, albeit statistically significant, difference in single-pulse decay tau values between saline (11.9 ± 0.3 ms) and cocaine-experienced (12.9 ± 0.3 ms) rats, the lack of a significant difference in HFS decay tau likely reflects that there are no biologically relevant changes. Therefore, taken together, our results from evoked STCs suggest that there are seemingly negligible changes to the rate of glutamate clearance in the DLS of cocaine-experienced rats, regardless of whether such cocaine-seeking behavior is classified as goal-directed or habitual. It is important to acknowledge that STC recordings may reflect the intrinsic properties of the glutamate transporter, not necessarily the rate of glutamate clearance (Wadiche et al., 2006), and do not provide insight to other cellular events occurring at the synapse. Alternative glutamate homeostatic mechanisms of the tripartite synapse including GLAST expression, cysteine-glutamate exchanger, astrocytic ensheathment of neurons, and neuronal function may act in a compensatory manner (Mahmoud et al., 2019), resulting in no detectable changes in STC recordings. Future studies of these aspects of glutamate dynamics are needed to fully characterize synapse properties in the DLS of cocaine-experienced rats classified as goal-directed or habitual in their cocaine-seeking behavior.

We also expressed iGluSnFr on astrocytes and astrocyte processes in the DLS to visualize real-time extracellular glutamate dynamics at a regional level. The rate of glutamate clearance, as reflected by the decay tau of evoked iGluSnFr signals, did not differ across goal-directed, intermediate, and habitual cocaine-seeking rats and yoked-saline controls. In addition, no group differences were observed in the magnitude of evoked glutamate release and the total amount of glutamate sensed by iGluSnFr-expressing astrocytes, as reflected by the peak signal and area under the curve of evoked iGluSnFr signals, respectively. Notably, these results were observed in response to both double-pulse stimulation as well as HFS, suggesting that the glutamate clearance system is intact under low-stimulation conditions and in glutamate spillover conditions (Umpierre et al., 2019). Importantly, we verified that iGluSnFr imaging in our laboratory was functioning properly, as we demonstrated that evoked iGluSnFr responses were sensitive to a wide range of experimental manipulations (Parsons et al., 2016), including TTX-induced blockade of action-potential dependent glutamate release, blockade of glutamate transporters with TBOA, and an increased bath temperature. As such, the data suggest that there is little difference in extracellular glutamate dynamics in the DLS of cocaine-experienced rats, regardless of whether their cocaine-seeking behavior is characterized as habitual, intermediate, or goal-directed.

In line with the negligible differences in glutamate clearance observed by STCs and iGluSnFr assays, the level of GLT-1 protein expression in the DLS was also unchanged between cocaine-experienced rats, regardless of behavioral classification, and yoked-saline controls. This finding further builds the profile of an intact glutamate clearance system in the DLS of habitual cocaine-seeking rats, as GLT-1 is the predominant glutamate transporter and accounts for ~90% of glutamate clearance in the brain (Danbolt, 2001; Magi et al., 2019).

The present results are surprising, as enduring changes in the glutamate system have been observed in the NAc of cocaine-experienced rats (Kalivas, 2009; Niedzielska-Andres et al., 2021). Specifically, rats with a history of cocaine self-administration exhibit decreased GLT-1 expression and decreased uptake capacity of glutamate transporters in the NAc (Knackstedt et al., 2010; Sari et al., 2010; Reissner et al., 2012, 2014; Sondheimer and Knackstedt, 2012; Fischer-Smith et al., 2013; Trantham-Davidson et al., 2013; LaCrosse et al., 2017). In addition, the magnitude of synaptically-released glutamate in the NAc is also increased upon cue or cocaine-primed reinstatement (McFarland et al., 2003; Madayag et al., 2007; Li et al., 2010). Together, these alterations to presynaptic glutamate release and glutamate clearance largely contribute to the enduring vulnerability to relapse (Kalivas, 2009; Niedzielska-Andres et al., 2021). In comparing the present results to this literature, it is important to consider the methodologies used and how they provide different perspectives into the glutamate system. First, the assessments of glutamate clearance in the NAc were conducted with the tritiated glutamate uptake assay, which measures the total uptake capacity of glutamate transporters on the timescale of minutes (Knackstedt et al., 2010; Trantham-Davidson et al., 2013). This differs from the rapid clearance of glutamate that occurs on the millisecond time scale (Clements et al., 1992) that is detected through STC recordings (Diamond and Jahr, 2000; Diamond, 2005) and iGluSnFr imaging (Marvin et al., 2013; Parsons et al., 2016; Pinky et al., 2018). Similarly, seemingly contradictory results across these different assays of glutamate clearance have been observed in the dorsal striatum of mice with Huntington's disease (HD). Here, HD mice exhibited decreased GLT-1 expression and decreased uptake capacity of glutamate transporters, but the rate of glutamate clearance was unaffected, and even increased, when measured with iGluSnFr imaging and STCs (Parsons et al., 2016; Raymond, 2017). Therefore, as these assays measure different dimensions of glutamate clearance, the present results should be viewed as providing a more comprehensive, rather than contradictory, view of glutamate dynamics in the cocaine-experienced striatum.

While less profiled than the NAc, changes in the DLS glutamate system have also been reported in the context of cocaine self-administration. That is, decreased GLT-1 protein expression was observed in rats given long (6 h), but not short (2 h), access to repeated cocaine self-administration (Ducret et al., 2016). Given that the short-access condition is similar to the 1–3 h timeframe of cocaine access used in the present study, differences in the glutamate system may emerge if rats are given longer daily access to cocaine self-administration. Indeed, GLT-1 expression in the NAc has been shown to be differentially affected by the length of daily cocaine access sessions as well as the length of cocaine withdrawal (Fischer-Smith et al., 2013; Ducret et al., 2016). Further, rats in Ducret et al. (2016) were sacrificed after numerous tests, including punishment-induced abstinence, which may have contributed to changes in GLT-1 expression in the DLS. It has also been reported that rats withdrawn from cocaine self-administration for 24 h exhibit increased extracellular glutamate levels in the DLS in response to an acute cocaine challenge (Gabriele et al., 2012). Notably, our rats were not challenged prior to sacrifice, which occurred 1–4 days after the final drug-seeking test (and 2–5 days after the last day of cocaine self-administration). Thus, although these two prior studies have reported changes in aspects of glutamate signaling in the DLS in rats with a history of cocaine self-administration, the present data suggest that those changes may be unique to the behavioral history of the animals and/or acute drug challenge. However, the present results suggest that a history of cocaine-seeking and taking, regardless of whether the learned cocaine-seeking behavior is apparently goal-directed or habitual, is not associated with changes in glutamate clearance or release nor changes in GLT-1 expression in the DLS.

The present results may have implications for the use of treatments aimed at restoring glutamate homeostasis in individuals with cocaine use disorder. To date, there are no FDA-approved medications for the treatment of cocaine use disorder (National Institute on Drug Abuse, 2021). However, given the large body of work detailing the decreased expression of GLT-1 and xCT (the catalytic subunit of the cysteine-glutamate exchanger xC-) in the NAc (Niedzielska-Andres et al., 2021), agents that restore expression and function of these proteins, such as N-acetylcysteine and Ceftriaxone, have received increasing therapeutic attention (Nocito Echevarria et al., 2017; Spencer and Kalivas, 2017). In light of the present results, however, the effect of these systemically-administered glutamate-targeted interventions on the DLS glutamate system and habitual responding need to be considered. Given that the present results suggest that glutamate release, clearance, and GLT-1 expression are not altered in the DLS of cocaine-experienced rats, administering agents that increase glutamate clearance and basal levels of extracellular glutamate may adversely impact instrumental responding. As such, further study is needed to explore the effect of NAC and Ceftriaxone on habitual responding for cocaine, as well as the underlying glutamate dynamics in the DLS, in order to further elucidate their efficacy in treating the striatally-based behavioral aspects of cocaine use disorder. Importantly, as the present study was conducted only in male rats, assessing these measures in female rats is needed in order to obtain a comprehensive understanding of cocaine abuse disorder and to adequately inform the development of treatment strategies.

Overall, we found that the dynamics of glutamate release and clearance as well as GLT-1 protein expression in the DLS are largely unchanged across rats with goal-directed, intermediate, and habitual cocaine-seeking behavior, as well as in comparison to yoked saline controls. These results provide a more comprehensive, rather than contrasting, profile of glutamate dynamics in the cocaine-experienced striatum and spark a deeper conversation into the state of the striatal glutamate system in the context of cocaine use. Namely, it is imperative to consider both the specific glutamate assay and cocaine paradigm employed when conducting and comparing studies on rats with a history of cocaine self-administration and different addiction-related phenotypes. Moreover, this study urges that more comprehensive profiles of the DLS glutamate system and habitual cocaine-related behavior are not only developed, but considered, as glutamate-targeted therapies for cocaine use disorder advance to clinical application.

Data availability statement

The raw data supporting the conclusions of this article will be made available by the authors, without undue reservation.

Author contributions

KK and KW conceived the project. KK, KW, DG, and KV designed the experiments. DG and KV carried out the iGluSnFr and STC experiments, respectively, and collected the data. DG and MT established the cocaine self-administration paradigm and stereotaxic surgical methods. MT, DG, KV, and KK carried out the cocaine self-administration training. MT conducted the stereotaxic surgeries. PW assisted with electrophysiology experiments and data analysis. DG and KV analyzed the data and wrote the final manuscript. All authors contributed to the article and approved the submitted version.

Funding

This work was supported by the National Institutes of Health (R21DA0466000), University of Utah Skaggs Graduate Research Fellowship, Roy Kuramoto Award, and University of Utah Neuroimmunology Training Grant (T32NS115664).

Acknowledgments

Special thanks to Augstin Zapata for his thoughtful counsel in establishing the chained cocaine self-administration paradigm in our laboratory. The authors also thank Lynn Raymond and Ellen Koch for hosting iGluSnFr imaging training sessions, Patrick Parker and Matt Parsons for their iGluSnFr technical support, and John Wagner for his assistance in developing iGluSnFr data processing systems. iGluSnFr data included in the present study was originally conducted in the dissertation work of Danielle Giangrasso at the University of Utah.

Conflict of interest

The authors declare that the research was conducted in the absence of any commercial or financial relationships that could be construed as a potential conflict of interest.

Publisher's note

All claims expressed in this article are solely those of the authors and do not necessarily represent those of their affiliated organizations, or those of the publisher, the editors and the reviewers. Any product that may be evaluated in this article, or claim that may be made by its manufacturer, is not guaranteed or endorsed by the publisher.

Supplementary material

The Supplementary material for this article can be found online at: https://www.frontiersin.org/articles/10.3389/fnmol.2023.1160157/full#supplementary-material

References

Armbruster, M., Dulla, C. G., and Diamond, J. S. (2020). Effects of fluorescent glutamate indicators on neurotransmitter diffusion and uptake. *elife* 9:e54441. doi: 10.7554/eLife.54441

Belin, D., Balado, E., Piazza, P. V., and Deroche-Gamonet, V. (2009). Pattern of intake and drug craving predict the development of cocaine addiction-like behavior in rats. *Biol. Psychiatry* 65, 863–868. doi: 10.1016/j.biopsych.2008.05.031

Belin, D., Belin-Rauscent, A., Murray, J. E., and Everitt, B. J. (2013). Addiction: failure of control over maladaptive incentive habits. *Curr. Opin. Neurobiol.* 23, 564–572. doi: 10.1016/j.conb.2013.01.025

Clements, J. D., Lester, R. A. J., Tong, G., Jahr, C. E., and Westbrook, G. L. (1992). The time course of glutamate in the synaptic cleft. *Science* 258, 1498–1501. doi: 10.1126/science.1359647

Corbit, L. H., Chieng, B. C., and Balleine, B. W. (2014). Effects of repeated cocaine exposure on habit learning and reversal by N-acetylcysteine. *Neuropsychopharmacology* 39, 1893–1901. doi: 10.1038/npp.2014.37

Danbolt, N. C. (2001). Glutamate uptake. *Prog. Neurobiol.* 65, 1–105. doi: 10.1016/S0301-0082(00)00067-8

Danbolt, N. C., Storm-Mathisen, J., and Kanner, B. I. (1992). An [Na+ + K+]coupled L-glutamate transporter purified from rat brain is located in glial cell processes. *J. Neurosci.* 51, 295–310. doi: 10.1016/0306-4522(92)90316-T

Diamond, J. S. (2005). Deriving the glutamate clearance time course from transporter currents in CA1 hippocampal astrocytes: transmitter uptake gets faster during development. *J. Neurosci.* 25, 2906–2916. doi: 10.1523/JNEUROSCI.5125-04.2005

Diamond, J. S., and Jahr, C. E. (2000). Synaptically released glutamate does not overwhelm transporters on hippocampal astrocytes during high-frequency stimulation. *J. Neurophysiol.* 83, 2835–2843. doi: 10.1152/jn.2000.83.5.2835

Dolan, R. J., and Dayan, P. (2013). Goals and habits in the brain. *Neuron* 80, 312–325. doi: 10.1016/j.neuron.2013.09.007

D'Souza, M. S. (2015). Glutamatergic transmission in drug reward: implications for drug addiction. *Front. Neurosci.* 9:404. doi: 10.3389/fnins.2015.00404

Ducret, E., Puaud, M., Lacoste, J., Belin-Rauscent, A., Fouyssac, M., Dugast, E., et al. (2016). N-acetylcysteine facilitates self-imposed abstinence after escalation of cocaine intake. *Biol. Psychiatry* 80, 226–234. doi: 10.1016/j.biopsych.2015.09.019

Ersche, K. D., Gillan, C. M., Simon Jones, P., Williams, G. B., Ward, L. H. E., Luijten, M., et al. (2016). Carrots and sticks fail to change behavior in cocaine addiction. *Science* 352, 1468–1471. doi: 10.1126/science.aaf3700

Everitt, B. J., and Robbins, T. W. (2005). Neural systems of reinforcement for drug addiction: from actions to habits to compulsion. *Nat. Neurosci.* 8, 1481–1489. doi: 10.1038/nn1579

Fischer-Smith, K. D., Houston, A. C. W., and Rebec, G. V. (2013). Differential effects of cocaine access and withdrawal on GLT1 expression in rat nucleus accumbens core and shell. *J. Neurosci.* 210, 333–339. doi: 10.1016/j.neuroscience.2012.02.049

Gabriele, A., Pacchioni, A. M., and See, R. E. (2012). Dopamine and glutamate release in the dorsolateral caudate putamen following withdrawal from cocaine self-administration in rats. *Pharmacol. Biochem. Behav.* 103, 373–379. doi: 10.1016/j.pbb.2012.09.015

Goodman, J., Ressler, R. L., and Packard, M. G. (2017). Enhancing and impairing extinction of habit memory through modulayion of NMDA receptors in the dorsolateral striatum. *J. Neurosci.* 352, 216–225. doi: 10.1016/j.neuroscience.2017.03.042

Grimm, J. W., Hope, B. T., Wise, R. A., and Shaham, Y. (2001). Neuroadaptation. Incubation of cocaine craving after withdrawal. *Nature* 412, 141–142. doi: 10.1038/35084134

Haugeto, O., Ullensvang, K., Levy, L. M., Chaudhry, F. A., Honore, T., Nielsen, M., et al. (1996). Brain glutamate transporter proteins form homomultimers. *J. Biol. Chem.* 271, 27715–27722. doi: 10.1074/jbc.271.44.27715

Jonkman, S., Pelloux, Y., and Everitt, B. J. (2012). Differential roles of the dorsolateral and midlateral striatum in punished cocaine seeking. *J. Neurosci.* 32, 4645–4650. doi: 10.1523/JNEUROSCI.0348-12.2012

Kalivas, P. W. (2009). The glutamate homeostasis hypothesis of addiction. *Nat. Rev. Neurosci.* 10, 561–572. doi: 10.1038/nrn2515

Knackstedt, L. A., Melendez, R. I., and Kalivas, P. W. (2010). Ceftriaxone restores glutamate homeostasis and prevents relapse to cocaine seeking. *Biol. Psychiatry* 67, 81–84. doi: 10.1016/j.biopsych.2009.07.018

Koch, E. T., Woodard, C. L., and Raymond, L. A. (2018). Direct assessment of presynaptic modulation of cortico-striatal glutamate release in a Huntington's disease mouse model. *J. Neurophysiol.* 120, 3077–3084. doi: 10.1152/jn.00638.2018

LaCrosse, A. L., O'Donovan, S. M., Sepulveda-Orengo, M. T., McCullumsmith, R. E., Reissner, K. J., Schwendt, M., et al. (2017). Contrasting the role of xCT and GLT-1 upregulation in the ability of ceftriaxone to attenuate the cue-induced reinstatement of cocaine seeking and normalize AMPA receptor subunit expression. *J. Neurosci.* 37, 5809–5821. doi: 10.1523/JNEUROSCI.3717-16.2017

Lerner, T. N. (2020). Interfacing behavioral and neural circuit models for habit formation. *J. Neurosci. Res.* 98, 1031–1045. doi: 10.1002/jnr.24581

Li, X., Li, J., Gardner, E. L., and Xi, Z. X. (2010). Activation of mGluR7s inhibits cocaine-induced reinstatement of drug-seeking behavior by a nucleus accumbens glutamate mGluR2/3 mechanism in rats. *J. Neurochem.* 114, 1368–1380. doi: 10.1111/j.1471-4159.2010.06851.x

Lipton, D. M., Gonzales, B. J., and Citri, A. (2019). Dorsal striatal circuits for habits, compulsions and addictions. *Front. Syst. Neurosci.* 13:28. doi: 10.3389/fnsys.2019.00028

Madayag, A., Lobner, D., Kau, K. S., Mantsch, J. R., Abdulhameed, O., Hearing, M., et al. (2007). Repeated N-acetylcysteine administration alters plasticity- dependent effects of cocaine. *J. Neurosci.* 27, 13968–13976. doi: 10.1523/JNEUROSCI.2808-07.2007

Magi, S., Piccirillo, S., Amoroso, S., and Lariccia, V. (2019). Excitatory amino acid transporters (EAATS): glutamate transport and beyond. *Int. J. Mol. Sci.* 20:5674. doi: 10.3390/ijms20225674

Mahmoud, S., Gharagozloo, M., Simard, C., and Gris, D. (2019). Astrocytes maintain glutamate homeostasis in the CNS by controlling the balance between glutamate uptake and release. *Cells* 8:184. doi: 10.3390/cells8020184

Malvaez, M. (2020). Neural substrates of habit. *J. Neurosci. Res.* 98, 986–997. doi: 10.1002/jnr.24552

Marvin, J. S., Borghuis, B. G., Tian, L., Cichon, J., Harnett, M. T., Akerboom, J., et al. (2013). An optimized fluorescent probe for visualizing glutamate neurotransmission. *Nat. Methods* 10, 162–170. doi: 10.1038/nmeth.2333

Marvin, J. S., Scholl, B., Wilson, D. E., Podgorski, K., Kazemipour, A., Mueller, J. A., et al. (2018). Stability, affinity and chromatic variants of the glutamate sensor iGluSnFR. *Nat. Methods* 15, 936–939. doi: 10.1101/235176

McFarland, K., Lapish, C. C., and Kalivas, P. W. (2003). Prefrontal glutamate release into the core of the nucleus accumbens mediates cocaine-induced reinstatement of drug-seeking behavior. *J. Neurosci.* 23, 3531–3537. doi: 10.1523/jneurosci.23-08-03531.2003

National Institute on Drug Abuse. (2021). Cocaine DrugFacts. Available at: https://www.drugabuse.gov/publications/drugfacts/cocaine

Niedzielska-Andres, E., Pomierny-Chamioło, L., Andres, M., Walczak, M., Knackstedt, L. A., Filip, M., et al. (2021). Cocaine use disorder: a look at metabotropic glutamate receptors and glutamate transporters. *Pharmacol. Ther.* 221:107797. doi: 10.1016/j.pharmthera.2020.107797

Nocito Echevarria, M. A., Andrade Reis, T., Ruffo Capatti, G., Siciliano Soares, V., da Silveira, D. X., and Marques Fidalgo, T. (2017). N-acetylcysteine for treating cocaine addiction: a systematic review. *Psychiatry Res.* 251, 197–203. doi: 10.1016/j.psychres.2017.02.024

Packard, M. G., and Knowlton, B. J. (2002). Learning and memory functions of the basal ganglia. *Annu. Rev. Neurosci.* 25, 563–593. doi: 10.1146/annurev.neuro.25.112701.142937

Palencia, C. A., and Ragozzino, M. E. (2005). The contribution of NMDA receptors in the dorsolateral striatum to egocentric response learning. *Behav. Neurosci.* 119, 953–960. doi: 10.1037/0735-7044.119.4.953

Parker, P. D., Suryavanshi, P., Melone, M., Sawant-Pokam, P. A., Reinhart, K. M., Kaufmann, D., et al. (2021). Non-canonical glutamate signaling in a genetic model of migraine with aura. *Neuron* 109, 611–628.e8. doi: 10.1016/j.neuron.2020.11.018

Parsons, M. P., Vanni, M. P., Woodard, C. L., Kang, R., Murphy, T. H., and Raymond, L. A. (2016). Real-time imaging of glutamate clearance reveals normal striatal uptake in Huntington disease mouse models. *Nat. Commun.* 7:11251. doi: 10.1038/ncomms11251

Pierce, R. C., and Vanderschuren, L. J. M. J. (2010). Kicking the habit: the neural basis of ingrained behaviors in cocaine addiction. *Neurosci. Biobehav. Rev.* 35, 212–219. doi: 10.1016/j.neubiorev.2010.01.007

Pinky, N. F., Wilkie, C. M., Barnes, J. R., and Parsons, M. P. (2018). Region- and activity- dependent regulation of extracellular glutamate. *J. Neurosci.* 38, 5351–5366. doi: 10.1523/JNEUROSCI.3213-17.2018

Raymond, L. A. (2017). Striatal synaptic dysfunction and altered calcium regulation in Huntington disease. *Biochem. Biophys. Res. Commun.* 483, 1051–1062. doi: 10.1016/j.bbrc.2016.07.058

Reissner, K. J., Brown, R. M., Spencer, S., Tran, P. K., Thomas, C. A., and Kalivas, P. W. (2014). Chronic administration of the methylxanthine propentofylline impairs reinstatement to cocaine by a GLT-1-dependent mechanism. *Neuropsychopharmacology* 39, 499–506. doi: 10.1038/npp.2013.223

Reissner, K. J., Gipson, C. D., Tran, P. K., Knackstedt, L. A., Scofield, M. D., and Kalivas, P. W. (2012). Glutamate transporter GLT-1 mediates N-acetylcysteine inhibition of cocaine reinstatement. *Addict. Biol.* 20, 316–323. doi: 10.1111/adb.12127

Sari, Y., Smith, K. D., Ali, P. K., and Rebec, G. V. (2010). Up-regulation of GLT1 attenuates cue- induced reinstatement of cocaine-seeking behavior in rats. *J. Neurosci.* 29, 9239–9243. doi: 10.1523/JNEUROSCI.1746-09.2009

Schwabe, L., and Wolf, O. T. (2009). Stress prompts habit behavior in humans. *J. Neurosci.* 29, 7191–7198. doi: 10.1523/JNEUROSCI.0979-09.2009

Smeets, T., van Ruitenbeek, P., Hartogsveld, B., and Quaedflieg, C. W. E. M. (2019). Stress- induced reliance on habitual behavior is moderated by cortisol reactivity. *Brain Cogn.* 133, 60–71. doi: 10.1016/j.bandc.2018.05.005

Sondheimer, I., and Knackstedt, L. A. (2012). Ceftriaxone prevents the induction of cocaine sensitization and produces enduring attenuation of cue- and cocaine-primed reinstatement of cocaine-seeking. *Behav. Brain Res* 225, 252–258. doi: 10.1016/j.bbr.2011.07.041

Spencer, S., and Kalivas, P. W. (2017). Glutamate transport: a new bench to bedside mechanism for treating drug abuse. *Int. J. Neuropsychopharmacol.* 20, 797–812. doi: 10.1093/ijnp/pyx050

Takahashi, D. K., Vargas, J. R., and Wilcox, K. S. (2010). Increased coupling and altered glutamate transport currents in astrocytes following kainic-acid-induced status epilepticus. *Neurobiol. Dis.* 40, 573–585. doi: 10.1016/j.nbd.2010.07.018

Tanaka, M., Shih, P. Y., Gomi, H., Yoshida, T., Nakai, J., Ando, R., et al. (2013). Astrocytic Ca2+ signals are required for the functional integrity of tripartite synapses. *Mol. Brain* 6, 1–13. doi: 10.1186/1756-6606-6-6

Ting, J. T., Daigle, T. L., Chen, Q., and Feng, G. (2014). Acute brain slice methods for adult and aging animals: application of targeted patch clamp analysis and optogenetics. *Methods Mol. Biol.* 1183, 221–242. doi: 10.1007/978-1-4939-1096-0_14

Trantham-Davidson, H. H., LaLumiere, R. T., Reissner, K. J., Kalivas, P. W., and Knackstedt, L. A. (2013). Ceftriaxone normalizes nucleus accumbens synaptic transmission, glutamate transport and export following cocaine self-administration and extinction training. *J. Neurosci.* 32, 12406–12410. doi: 10.1523/JNEUROSCI.1976-12.2012

Tzingounis, A. V., and Wadiche, J. I. (2007). Glutamate transporters: confining runaway excitation by shaping synaptic transmission. *Nat. Rev. Neurosci.* 8, 935–947. doi: 10.1038/nrn2274

Umpierre, A. D., West, P. J., White, J. A., and Wilcox, K. S. (2019). Conditional knock-out of mGluR5 from astrocytes during epilepsy development impairs high-frequency glutamate uptake. *J. Neurosci.* 39, 727–742. doi: 10.1523/JNEUROSCI.1148-18.2018

Vanderschuren, L. J. M. J., and Everitt, B. J. (2004). Drug seeking becomes compulsive after prolonged cocaine self-administration. *Science* 305, 1017–1019. doi: 10.1126/science.1098975

Wadiche, J. I., Tzingounis, A. V., and Jahr, C. E. (2006). Intrinsic kinetics determine the time course of neuronal synaptic transporter currents. *Proc. Natl. Acad. Sci. U. S. A.* 103, 1083–1087. doi: 10.1073/pnas.0510476103

Yin, H. H., and Knowlton, B. J. (2006). The role of the basal ganglia in habit formation. *Nat. Rev. Neurosci.* 7, 464–476. doi: 10.1038/nrn1919

Yin, H. H., Knowlton, B. J., and Balleine, B. W. (2004). Lesions of dorsolateral striatum preserve outcome expectancy but disrupt habit formation in instrumental learning. *Eur. J. Neurosci.* 19, 181–189. doi: 10.1111/j.1460-9568.2004.03095.x

Yin, H. H., Knowlton, B. J., and Balleine, B. W. (2005a). Blockade of NMDA receptors in the dorsomedial striatum prevents action-outcome learning in instrumental conditioning. *Eur. J. Neurosci.* 22, 505–512. doi: 10.1111/j.1460-9568.2005.04219.x

Yin, H. H., Mulcare, S. P., Hilário, M. R. F., Clouse, E., Holloway, T., Davis, M. I., et al. (2009). Dynamic reorganization of striatal circuits during the acquisition and consolidation of a skill. *Nat. Neurosci.* 12, 333–341. doi: 10.1038/nn.2261

Yin, H. H., Ostlund, S. B., Knowlton, B. J., and Balleine, B. W. (2005b). The role of the dorsomedial striatum in instrumental conditioning. *Eur. J. Neurosci.* 22, 513–523. doi: 10.1111/j.1460-9568.2005.04218.x

Zapata, A., Minney, V. L., and Shippenberg, T. S. (2010). Shift from goal-directed to habitual cocaine seeking after prolonged experience in rats. *J. Neurosci.* 30, 15457–15463. doi: 10.1523/JNEUROSCI.4072-10.2010

frontiers | Frontiers in Molecular Neuroscience

TYPE Original Research
PUBLISHED 24 May 2023
DOI 10.3389/fnmol.2023.1106765

OPEN ACCESS

EDITED BY
Vidhya Kumaresan,
Boston University, United States

REVIEWED BY
Peter Vanhoutte,
Centre National de la Recherche Scientifique (CNRS), France
Giordano de Guglielmo,
University of California, San Diego, United States

*CORRESPONDENCE
Dasiel O. Borroto-Escuela
✉ dasiel.borroto.escuela@ki.se;
✉ dasiel@uma.es

RECEIVED 24 November 2022
ACCEPTED 12 April 2023
PUBLISHED 24 May 2023

CITATION
Borroto-Escuela DO, Lopez-Salas A, Wydra K, Bartolini M, Zhou Z, Frankowska M, Suder A, Benitez-Porres J, Romero-Fernandez W, Filip M and Fuxe K (2023) Combined treatment with Sigma1R and A2AR agonists fails to inhibit cocaine self-administration despite causing strong antagonistic accumbal A2AR-D2R complex interactions: the potential role of astrocytes. *Front. Mol. Neurosci.* 16:1106765. doi: 10.3389/fnmol.2023.1106765

Combined treatment with Sigma1R and A2AR agonists fails to inhibit cocaine self-administration despite causing strong antagonistic accumbal A2AR-D2R complex interactions: the potential role of astrocytes

Dasiel O. Borroto-Escuela[1,2,3]*, Alexander Lopez-Salas[2], Karolina Wydra[4], Marco Bartolini[1,5], Zilong Zhou[1,6], Malgorzata Frankowska[4], Agata Suder[4], Javier Benitez-Porres[2], Wilber Romero-Fernandez[1,7], Malgorzata Filip[4] and Kjell Fuxe[1]

[1]Department of Neuroscience, Karolinska Institutet, Stockholm, Sweden, [2]Department of Human Physiology, Physical Education and Sport, Universidad de Málaga, Málaga, Spain, [3]Department of Biomolecular Science, Section of Physiology, University of Urbino, Urbino, Italy, [4]Maj Institute of Pharmacology Polish Academy of Sciences, Department of Drug Addiction Pharmacology, Kraków, Poland, [5]Department of Medical Biotechnology and Translational Medicine, University of Milan, Milan, Italy, [6]National Engineering Laboratory for Druggable Gene and Protein Screening, Northeast Normal University, Changchun, China, [7]Department of Neurology, Vanderbilt University Medical Center, Nashville, TN, United States

Previous studies have indicated that acute treatment with the monoamine stabilizer OSU-6162 (5 mg/kg), which has a high affinity for Sigma1R, significantly increased the density of accumbal shell D2R-Sigma1R and A2AR-D2R heteroreceptor complexes following cocaine self-administration. *Ex vivo* studies using the A2AR agonist CGS21680 also suggested the existence of enhanced antagonistic accumbal A2AR-D2R allosteric interactions after treatment with OSU-6162 during cocaine self-administration. However, a 3-day treatment with OSU-6162 (5 mg/kg) failed to alter the behavioral effects of cocaine self-administration. To test these results and the relevance of OSU-6162 (2.5 mg/kg) and/or A2AR (0.05 mg/kg) agonist interactions, we administered low doses of receptor agonists during cocaine self-administration and assessed their neurochemical and behavioral effects. No effects were observed on cocaine self-administration; however, marked and highly significant increases using the proximity ligation assay (PLA) were induced by the co-treatment on the density of the A2AR-D2R heterocomplexes in the nucleus accumbens shell. Significant decreases in the affinity of the D2R high- and low-affinity agonist binding sites were also observed. Thus, in low doses, the highly significant neurochemical effects observed upon cotreatment with an A2AR agonist and a Sigma1R ligand on the A2AR-D2R heterocomplexes and their enhancement of allosteric inhibition of D2R high-affinity binding are not linked to the modulation of cocaine self-administration. The explanation may be related to an increased release of ATP and adenosine from astrocytes in the nucleus accumbens shell in cocaine self-administration. This can lead to increased activation of the A1R protomer in a putative A1R-A2AR-D2R

complex that modulates glutamate release in the presynaptic glutamate synapse. We hypothesized that the integration of changes in presynaptic glutamate release and postjunctional heteroreceptor complex signaling, where D2R plays a key role, result in no changes in the firing of the GABA anti-reward neurons, resulting in no reduction in cocaine self-administration in the present experiments.

KEYWORDS

A2AR-D2R heteroreceptor complexes, allosteric receptor-receptor interactions, cocaine use disorder, monoamine stabilizer, G protein coupled receptor (GPCR), oligomerization, Sigma 1 receptor

1. Introduction

GPCR homoreceptor and heteroreceptor complexes in the central nervous system (CNS) are integrated through allosteric receptor–receptor interactions. These interactions modulate the recognition, signaling, and trafficking of these receptor complexes, making them important targets for drug use disorders (Fuxe et al., 2014; Navarro et al., 2015; Borroto-Escuela et al., 2017a; Lazim et al., 2021; Nguyen et al., 2021). In addition, adenosine A2AR-dopamine D2R heteroreceptor complexes have been found to play a role in cocaine reward and addiction (Borroto-Escuela et al., 2018a). Upon cocaine self-administration, modulation of antagonistic allosteric A2AR-D2RR interactions was observed in A2AR-D2R heterocomplexes located in the nucleus accumbens. Furthermore, A2AR agonists blocked cocaine-induced reinstatement of seeking cocaine (Romero-Fernandez et al., 2022).

Cocaine can also produce pathological A2AR-D2R-Sigma1R heterocomplexes that lead to a strong brake on D2R protomer signaling, causing cocaine addiction through the presence of the Sigma1R protomer (Borroto-Escuela et al., 2018a). The Sigma1R is an intracellular chaperone that can be translocated into the plasma membrane by cocaine, where it can interact with the D2R (Kourrich et al., 2012). It has been shown in previous studies that cocaine can target the Sigma1R, which can counteract its effects (Kourrich et al., 2012). However, the Sigma1R ligand OSU-6162, which in low doses (5 mg/kg) selectively binds to the Sigma1R (Sahlholm et al., 2013), failed to alter the behavior found during cocaine self-administration in rats (Borroto-Escuela et al., 2020). Nevertheless, the low dose (5 mg/kg) of OSU-6162 could still produce significant increases in the density of the A2AR-D2R and D2R-Sigma1R heterocomplexes in the nucleus accumbens shell in rats self-administering cocaine (Borroto-Escuela et al., 2020). Furthermore, the effects of the A2AR agonist CGS 21680 on its inhibition of D2R affinity, given *ex vivo*, were significantly enhanced by the OSU-6162 treatment vs. vehicle treatment. Thus, neurochemical effects on the heteroreceptor complexes were observed in the absence of changes in cocaine infusion and active lever pressing.

Based on the studies of Arvid Carlsson and Pia Steensland et al. (Lahti et al., 2007; Steensland et al., 2012; Fredriksson et al., 2019), OSU-6162 dopamine stabilizer has a direct effect on the D2R as a partial agonist in the range of 15–25 mg/kg. They hypothesized that the partial D2R agonist OSU-6162 taken in the abovementioned doses has a stabilizing function. OUS-6162 acts both on D2R located at the post-junctional level, increasing D2R signaling, and at the pre-junctional level, activating D2 auto-receptors and reducing the release of dopamine. As a result, D2R is stabilized.

In this study, we aimed to test the effect of combined threshold doses of A2AR agonist (CGS21680, 0.05 mg/kg) and Sigma1R ligand (OSU-6162, 2.5 mg/kg, to fully exclude dopamine receptor stabilizer actions) on cocaine self-administration while still producing significant changes in the A2AR-D2R heteroreceptor complexes and their allosteric receptor–receptor interactions. We anticipated that combined threshold doses of A2AR agonist and Sigma1R ligand through allosteric inhibition could counteract D2R protomer signaling. This finding would improve our understanding of heterogeneities in the ventral striatal-pallidal GABA anti-reward neurons' responses to cocaine self-administration. Additionally, this study examined the effect of cocaine self-administration with and without OSU-6162 treatment on the number of astrocytes and their process branching in the nucleus accumbens shell, considering their ability to release adenosine and ATP, which undergoes hydrolysis to adenosine extracellularly (Acton and Miles, 2017). Astrocytes can have an impact on neuronal function in the nucleus accumbens shell involving changes in their ability to alter, e.g., the allosteric interactions in A1R-A2AR heterocomplexes (Ciruela et al., 2006; Cristovao-Ferreira et al., 2013; Navarro et al., 2018) and putative A1R-A2AR-D2R heterocomplexes in the presynaptic glutamate synapses on the GABA antireward neurons modulating glutamate release and the firing of these GABA neurons.

2. Material and methods

2.1. Animals

We used male Sprague–Dawley rats (obtained from the licensed animal breeder Charles River, Sulzfeld, Germany) weighing between 250 and 270 g at the beginning of the experiment. All animals used in the study were experimentally tested. The animals were housed individually in standard plastic rodent cages in a colony room maintained at 22 ± 2°C and 55 ± 10% humidity under a 12-h light-dark cycle (lights on at 6:00 am). Rodent food (VRF1 pellets, UK) and water were available *ad libitum* except for the period of the initial lever pressing training, during which the rats were maintained on limited food. All protocols were conducted during the light phase of the light-dark cycle, between 9:00 and 15:00 h. The experiments were carried out in accordance with the European Directive 2010/63/EU and were approved by the Ethical

Committee (76/2019, 2020/2019) at the Institute of Pharmacology, Polish Academy of Sciences, Krakow. The total number of subjects used for behavioral procedures was 38 (six animals did not meet the self-administration procedure criteria). For statistical analysis, a total of 32 rats were used (eight rats per group).

2.2. Drugs

Cocaine HCl ((1R, 2R, 3S, 5S)-3-(benzoyloxy-8-methyl-8-azabicyclo [3.2.1] octane-2-carboxylic acid methyl ester hydrochloride); Toronto Research Chemicals, Canada) was dissolved in sterile 0.9% NaCl. It was administered *i.v.* at a volume of 0.1 ml per infusion. OSU-6162 hydrochloride ((3S)-3-[3-(methyl sulfonyl)phenyl]-1-propylpiperidine hydrochloride; Tocris, UK, 2.5 mg/kg, *s.c.*) and CGS 21680 hydrochloride (4-[2-[[6-Amino-9-(N-ethyl-β-D-ribofuranuronamidosyl)-9H-purin-2-yl]amino]ethyl]benzenepropanoic acid hydrochloride; Tocris, UK, 0.05 mg/kg, *i.p.*) were dissolved in 0.9% NaCl and administered for 60 and 10 min, respectively, before the start of the 2 h self-administration session at a volume of 0.1 ml/kg.

2.3. Surgery

All the animals were anesthetized with ketamine HCl (Biowet, Pluawy, Poland, 75 mg/kg, *i.m.*) and xylazine (Biowet, Poland; 5 mg/kg, *i.m.*) given as a cocktail and chronically implanted with a silastic catheter in the external jugular vein, as described in a previous study (Filip et al., 2006). During the 3 days after surgery, meloxicam (*Metacam*, Boehringer Ingelheim; 5 mg/kg, *s.c.*) was used to reduce postoperative pain.

Rats were allowed 7–9 days to recover from surgery before the start of the experiments. Catheters were flushed daily with 0.2 ml of saline solution containing heparin (Biochemie, Austria; 100 U/ml) and 0.1 ml of a cephazolin solution (Biochemie GmbH, Austria; 100 mg/ml) to prevent catheter non-patency. No problems with catheter patency were reported in the tested rats.

2.4. Initial training (lever pressing)

During lever pressing training (2–3 days), each rat had food (VRF1 pellets, UK) limited to 25 g/day in a home cage. The animals were trained in standard operant chambers (Med-Associates, St. Albans, USA) in 2-h daily sessions. Presses on an "active" lever in the chamber resulted in the delivery of 0.1 ml of sweetened milk (SM Gostyń, Poland). After ensuring the criteria for initial training (100 rewards) under the fixed ratio (FR) as a schedule of reinforcement were met, the FR was subsequently increased to 5.

2.5. Cocaine self-administration

After the recovery period, all animals began lever pressing for cocaine reinforcement during daily 2-h sessions performed 6 days per week (Monday–Saturday). The house light was illuminated throughout each session. Each press on the "active" lever (FR-5 schedule of reinforcement) resulted in a 5-s infusion of cocaine (0.5 mg/kg per 0.1 ml) and a 5-s presentation of a stimulus complex (activation of the white stimulus light directly above the "active" lever and the tone generator). After each injection, there was a 20-s time-out period during which the responses were recorded but had no programmed consequences. Presses on the "inactive" lever were recorded but not reinforced. Seven days after acquisition, rats were used to complete a cocaine (0.25–0.5 mg/kg/infusion) dose-response procedure. Cocaine self-administration was conducted daily for 17 sessions. The animals exhibited a stable number of lever presses during the last three sessions, with <10% differences in their daily intake of cocaine. Following the stabilization of response rates with cocaine (0.25 mg/kg/infusion) self-administration, the animals were divided into separate groups ($n = 8$) to undergo test procedures. Vehicle, or OSU-6162, was administered daily for the three last cocaine SA sessions, while CGS 21680 was administered only before the last cocaine self-administration session. Immediately after the last cocaine self-administration sessions, animals were either euthanized (for biochemical analysis) or injected with pentobarbital and perfused intracardially (for IHC and *in situ* PLA analysis).

2.6. Yoked "procedure"

In yoked "procedure", each rat that was actively self administering cocaine was assigned to the rats that passively received intravenous saline in the same amount and manner as the active animal. Lever pressing by the "yoked" rats was recorded, but it had no programmed consequences. The yoked saline group was euthanized at the same time as the corresponding group of rats that were self-administering cocaine after a 2-h experimental session of cocaine self-administration. The plan of the experiment is presented in Figure 1.

2.7. Biochemical binding experiments

2.7.1. Membrane preparation

Frozen tissue was homogenized in an ice-cold preparation buffer using a sonicator (Soniprep 150). The buffer contained 50 mM Tris-HCl, pH 7.4, 7 mM $MgCl_2$, 1 mM EDTA, a cocktail of protease inhibitors (Roche Diagnostics, Mannheim, Germany), and 0.3 IU/ml adenosine deaminase (EC 3.5.4.4, Sigma-Aldrich). The membranes were precipitated using centrifugation at 4°C for 40 min at 40,000 × *g* (Thermo Scientific, Sorvall Lynx 6000, Stockholm, Sweden) and washed through re-homogenization in the same buffer one more time. The protein concentration of the membrane homogenates was determined using the BCA Protein Assay (Pierce, Sweden), using standard bovine serum albumin. Pelleted membranes were resuspended at a concentration of 0.15 mg/ml, immediately used, or stored at −80°C until required.

2.7.2. [^{3}H]-raclopride competition binding experiments

[^{3}H]-raclopride binding was displaced by quinpirole to determine the proportion of receptors in the high-affinity state

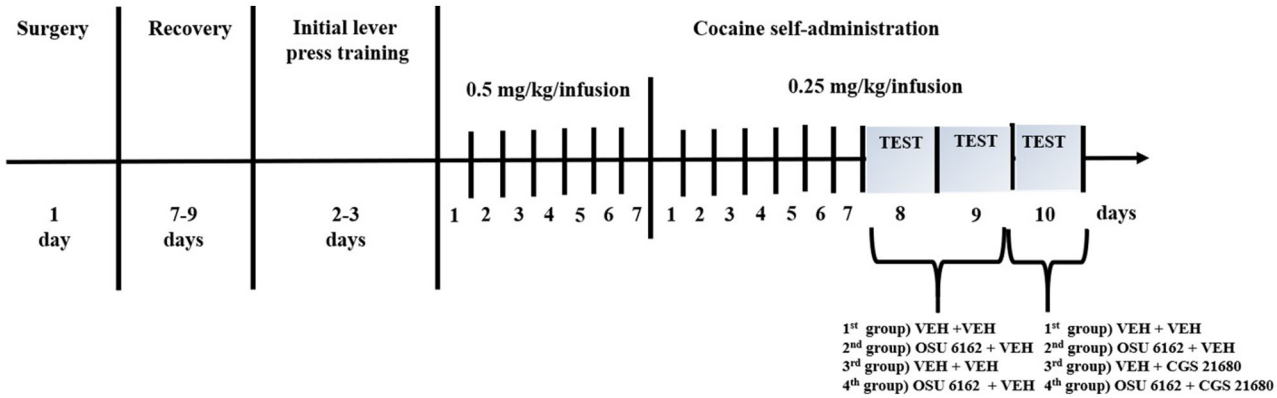

FIGURE 1
Experimental design of the study. Schematic diagram illustrating the experimental procedure. VEH, vehicle.

(RH), the high-affinity value (Ki, High), and the low-affinity (Ki, Low) value. Ventral striatum membrane preparations (60 μg protein/ml) were incubated with increasing concentrations of quinpirole (0.01 nM to 1 mM) and 2 nM [^{3}H]-raclopride (75 Ci/mmol, Novandi Chemistry AB, Sweden) in 250 μl of incubation buffer (50 mM Tris-HCl, 100 mM NaCl, 7 mM $MgCl_2$, 1 mM EDTA, 0.05% BSA, 1 mM DTT) and 0.3 IU/ml adenosine deaminase (EC 3.5.4.4, Sigma-Aldrich). The incubation took place for 90 min at 30°C in the presence or absence of 100 nM of the A2AR agonist CGS-21680. Non-specific binding was defined by radioligand binding in the presence of 100 μM (+)-butaclamol (Sigma-Aldrich, Sweden). The incubation was terminated by rapid filtration using Whatman GF/B filters (Millipore Corp, Sweden) and a MultiScreenTM Vacuum Manifold 96-well, followed by five washes (250 μl per wash) with ice-cold washing buffer (50 mM Tris-HCl pH 7.4). The filters were dried, 5 ml of scintillation cocktail was added, and the amount of bound ligand was determined after 12 h by liquid scintillation spectrometry.

2.8. *In situ* proximity ligation assay (*in situ* PLA)

To study the effects of OSU-6162, a Sigma1R ligand, in low doses on the D2R-A2AR and D2R-Sigma1R heteroreceptor complexes and the density changes after cocaine self-administration, *in situ* PLA was performed as described previously (Borroto-Escuela et al., 2017b). Formalin-fixed, free-floating brain sections (30 μm-thick, cut using a cryostat) at the Bregma level (1.0 mm) from rats after cocaine self-administration were employed using the following primary antibodies: rabbit monoclonal anti-A2AR (AB1559F, 1:250; Millipore, Sweden), mouse monoclonal anti-D2R (MABN53, 1:600, Millipore, Sweden), and rabbit monoclonal antisigma1R (ab53852, 1:500, Abcam, Sweden). The primary antibodies had been validated previously by means of immunohistochemistry in both rat brain tissue and the HEK293 cell line (Borroto-Escuela et al., 2017b, 2018b; Feltmann et al., 2018). To localize the heteroreceptor complexes in relation to neurons and astrocytes in the brains, traditional immunohistochemistry (IHC) was employed in parallel to *in situ* PLA. For this purpose, a glial marker (GFAP) and a nucleic marker (DAPI) were used. Control experiments for *in situ* PLA procedures were performed in free-floating, formalin-fixed rat brain sections employing only one primary antibody (mouse monoclonal anti-D2R (MABN53), 1:600, Millipore, Sweden). The *in situ* PLA analysis of this negative control showed 15.6% false-positive clusters compared to the positive control group value (100%). This false-positive signal was reduced even further (<4%) when the brain sections were kept in a citric acid buffer for 45–60 min at 65°C prior to the primary antibody incubation. Control experiments with similar results were also performed in cells transfected with cDNAs encoding only one type of receptor. The PLA signal was visualized and quantified using a Leica TCS-SL SP5 confocal microscope (Leica, USA) and the Duo Link Image Tool software. Briefly, fixed free-floating rat brain sections (stored at −20°C in Hoffman solution) were washed four times with PBS and quenched with 10 mM glycine buffer for 20 min at room temperature. Then, after three PBS washes, incubation took place with a permeabilization buffer [10% fetal bovine serum (FBS) and 0.5% Triton X-100 or Tween 20 in Tris buffer saline (TBS), pH 7.4] for 30 min at room temperature. The sections were washed twice for 5 min each with PBS at room temperature and incubated with the blocking buffer (0.2% BSA in PBS) for 30 min at room temperature. The brain sections were then incubated with the primary antibodies diluted to a suitable concentration in the blocking solution for 1–2 h at 37°C or at 4°C overnight. The sections were washed two times the day after, and the proximity probe mixture (minus and plus probes; for details, please refer to the Duolink instructions) was applied to the sample and incubated for 1 h at 37°C in a humidity chamber.

The unbound proximity probes were removed by washing the slides twice for 5 min each time with the blocking solution kept at room temperature under gentle agitation. The sections were incubated with the hybridization-ligation solution [BSA (250 g/ml), T4 DNA ligase (final concentration of 0.05 U/μl), Tween-20 (0.05%), NaCl 250 mM, ATP 1 mM, and the circularization or connector oligonucleotides (125–250 nM)] and incubated in a humidity chamber at 37°C for 30 min. The excess of connector oligonucleotides was removed by washing twice for 5 min each

with the washing buffer A [Sigma-Aldrich, Duolink Buffer A (8.8 g NaCl, 1.2 g Tris Base, 0.5 ml Tween 20)] dissolving in 800 ml of high-purity water (pH 7.4) at room temperature under gentle agitation, and the rolling circle amplification buffer was added to the sections and incubated in a humidity chamber for 100 min at 37°C. Then, the sections were incubated with the detection solution through hybridization (fluorescent oligonucleotide probes) in a humidity chamber at 37°C for 30 min. In the last step, the sections were washed twice in the dark for 10 min each with the washing buffer B (Sigma-Aldrich, Duolink Buffer B (5.84 g NaCl, 4.24 g Tris Base, 26.0 g Tris-HCl), dissolved in 500 ml of high-purity water, pH 7.5) at room temperature under gentle. The free-floating sections were put on a microscope slide, and a drop of appropriate mounting medium containing DAPI, giving blue staining of the nuclei (e.g., VectaShield or Dako), was applied. The coverslip was placed on the section and sealed with nail polish. The sections were protected against light and stored for several days at −20°C before confocal microscope analysis.

2.9. GFAP IHC and *in situ* PLA image acquisition and analysis

Images of the samples were taken with a confocal microscope, i.e., the LEICA TCS-SL SP5 confocal microscope. Three different areas of the nucleus accumbens shell (AcbSh) were selected, from which two randomly chosen magnified sample fields (150 x 150μm) were used for image acquisition, yielding a total of six pictures per animal. Images were inspected before being analyzed to exclude unrepresentable pictures, e.g., pictures containing blood vessels (which naturally attract astrocytes). As described previously, nuclei and PLA signal quantification were performed with DuoLink Image Tool software (Borroto-Escuela et al., 2013, 2016). Astrocyte quantification, including branch analysis, was performed with the open-source Fiji ImageJ software using the Ridge detection plugin. Using Sholl morphological analysis, we evaluated the development of astrocytes and quantified their morphological and structural changes in cocaine-self-administering rats vs. yoked saline groups. Sholl analysis was performed by overlaying circles of increasing diameter (in 1.5 mm steps) out from the center of the astrocyte soma and by counting the number of intersections the astrocytes make with each circle. A total of 10 astrocytes per group were investigated.

2.10. Statistical analysis

Data were analyzed using GraphPad Prism 5.0 (GraphPad Software Inc., San Diego, CA). All the data were shown as means ± SEM. In behavioral experiments, the number of responses on the "active" and "inactive" levers or the number of cocaine infusions were analyzed using the factorial analysis of variance (ANOVA) for factors (groups and levers). Data from competition experiments were analyzed by nonlinear regression analysis. The absolute values and the percent changes induced by A2AR agonist CGS 21680 in the dopamine D2R high-affinity, low-affinity, and proportion of receptors in the high-affinity state were evaluated using a paired Student's *t*-test and a non-parametric Mann–Whitney *U*-test, respectively. Data from *in situ* PLA experiments showing cluster density (clusters per nucleus per sampled field) were analyzed using a one-way ANOVA followed by a *post-hoc* Tukey's test. The number of rats (n) in each experimental condition is indicated in the figure legends. Data from GFAP experiments were analyzed using the Mann–Whitney *U*-test and a two-way ANOVA (see Supplementary Figure 1). A p-value of 0.05 and lower was considered statistically significant.

3. Results

3.1. Behavioral, pharmacological analysis of cocaine self-administration

After 17 sessions, the rats completed cocaine self-administration (i.e., they received ≥23 infusions at 2-h sessions under 0.25 mg/kg/infusion of cocaine) and displayed <10% variation in the number of cocaine infusions (Figure 1). The mean group number of cocaine infusions per day during the last three self-administration days varied from 23 to 28. The total cocaine intake during the 17 days (means ± SEM of 8 rats) was 103 ± 10 mg/rat for the vehicle group, 148 ± 33 mg/rat for the OSU-6162 group, 123 ± 18 mg/rat for the CGS 21680 group (see Figure 2 for more details), and 134 ± 15 mg/rat for the OSU-6162 + CGS 21680 groups (Figure 2).

No difference was observed between the groups assigned as vehicles or the OSU-6162 or CGS 21680 groups in the context of "active" and "inactive" lever presses and cocaine infusions (Figure 2). OSU-6162 in a dose of 2.5 mg/kg given in combination with CGS 21680, 0.05 mg/kg, did not change the number of "active" and "inactive" lever presses [group × lever $F_{(3,56)} = 0.174$, $p = 0.91$; group $F_{(3,56)} = 0.045$, $p = 0.71$; lever $F_{(1,56)} = 28.58$; $p = 0.0001$] and cocaine infusions [$F_{(3,28)} = 0.14$; $p = 0.09$; Figure 3].

3.2. Studies with *in situ* PLA on the effects of very low doses of OSU-6162 and CGS 21680 in cocaine self-administration on A2AR-D2R heteroreceptor complexes of the nucleus accumbens shell

OSU-6162 treatment in cocaine-self-administrating rats at the very low dose of 2.5 mg/kg, given once daily over 3 days, produced a significant increase in the density of red fluorescent PLA puncta (A2AR-D2R heteroreceptor complexes) per nucleus in the sampled field in the nucleus accumbens shell vs. vehicle-treated cocaine-self-administrating rats (Figure 4). A combination with a low dose (0.05 mg/kg) of the A2AR agonist CGS 21680, which by itself did not change the density of the PLA complexes, significantly enhanced the density of the red PLA complexes in the nucleus accumbens shell compared to treatment with OSU-6162 or CGS 21680 alone and especially with the vehicle-alone treatment (Figure 4). Representative images of the A2AR-D2R density increases in red positive puncta in the nucleus accumbens shell are shown upon combined treatment with OSU-6162 and CGS 21680 compared to vehicle treatment (Figure 4). For comparison, the D2R-Sigma1R heteroreceptor complexes were studied in

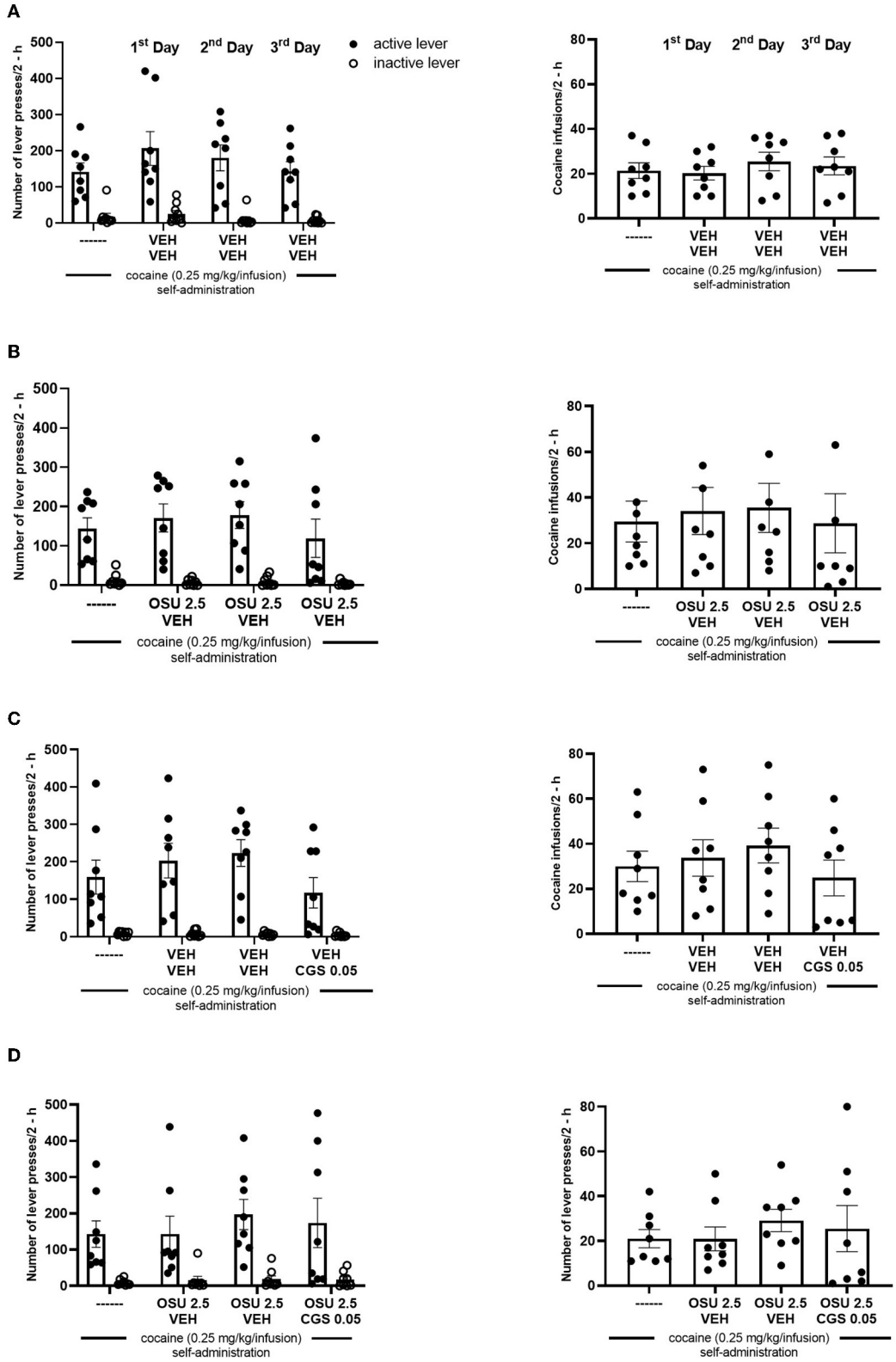

FIGURE 2
(A) Effects of repeated administration of vehicle (VEH; 0.9% NaCl, *s.c. or i.p.*), **(B)** OSU-6162 (OSU; 2.5 mg/kg, *s.c.*), **(C)** CGS 21680 (CGS; 0.05 mg/kg, *i.p.*), and **(D)** OSU-6162 (OSU; 2.5 mg/kg, *s.c.*) plus CGS 21680 (CGS; 0.05 mg/kg, *i.p.*) treatments on cocaine (0.25 mg/kg/infusion) self-administration under the FR-5 schedule of reinforcement in rats. The numbers of "active" and "inactive" lever presses (left panels) as well as cocaine infusions (right panels) after 2-h sessions are expressed as the means ± SEM of the data from eight rats/group.

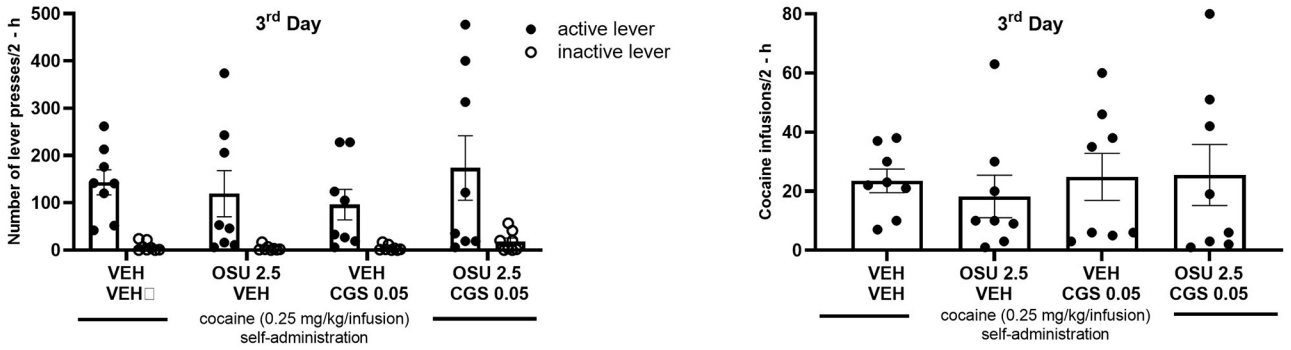

FIGURE 3
Effects of repeated administration of OSU-6162 (OSU; 2.5 mg/kg, *s.c.*) with or without combination with CGS 21680 (CGS; 0.05 mg/kg, *i.p.*) on cocaine (0.25 mg/kg/infusion) self-administration under the FR-5 schedule of reinforcement in rats. The numbers of "active" and "inactive" lever presses (left panels) as well as cocaine infusions (right panels) after 2-h sessions are expressed as the means ± SEM of the data from eight rats/group.

cocaine self-administration after single or combined treatment with a low dose (0.05 mg/kg) of the A2AR agonist CGS 21680 and a very low dose of 2.5 mg/kg of Sigma1R ligand OSU-6162. Daily treatment for 3 days did not produce a significant increase in the density of these heteroreceptor complexes in the nucleus accumbens shell vs. the vehicle-treated group in cocaine self-administration (Figure 4). An overall high density of A2AR-D2R and D2R-Sigma1R PLA positive clusters was found in the nucleus accumbens of the ventral striatum (Figure 4, bottom panels) based on the average number of clusters per nucleus (in blue) per sample field. They were both significantly different from the number of PLA positive clusters in the myelinated bundles of the crus cerebri (CC) and the anterior limb of the anterior commissure (aca), and negative controls were regarded as background values (please refer to Supplementary Figure 2).

3.3. Effects of single and combined systemic OSU-6162 and CGS 21680 treatment on the antagonistic allosteric A2AR-D2R receptor-receptor interactions in the ventral striatum in cocaine self-administering rats

Co-treatment was performed as mentioned above in the PLA experiments with OSU-6162 (2.5 mg/kg) and CGS 21680 (0.05 mg/kg). A2AR agonist (CGS 21680) was given on the last day 50 min after OSU-6162 with its 60-min pretreatment before the 120-min long cocaine self-administration session prior to euthanasia. The combined treatment resulted in a marked and significant increase in D2R $K_{i,High,}$ and D2R.

Figure 5 shows the effects of pharmacological treatments on cocaine self-administration (SA) on D2R high-and low-affinity K_i values in the ventral striatum produced by A2AR agonist CGS 21680 (CGS 0.05 mg/kg) and/or the Sigma 1R ligand OSU-6162 (OSU 2.5 mg/kg) and compared with vehicle (control group; VEH: 0.09% NaCl). It shows a strong reduction of D2R affinity in the nucleus accumbens after combined treatment with OSU-6162 and CGS 21680, involving both high-and low-affinity K_i values.

Treatment with either OSU-6162 or CGS 21680 alone did not lead to any changes in these D2R K_i values.

3.4. Effects of cocaine self-administration vs. yoked procedure on astrocytes in the nucleus accumbens shell

3.4.1. Density of astrocytes

Cocaine self-administration vs. yoked saline controls produced a significant increase in the density of astrocytes per nucleus per sample field ($^{**}p < 0.01$, Mann–Whitney *U*-test, mean, and SEM) in the nucleus accumbens shell, visualized in green with GFAP immunoreactivity (Figures 6A, B). In addition, a significant change in the area was observed (Figure 6C).

3.4.2. Astrocytic process branching

Cocaine self-administration caused a highly significant and substantial increase in the number of GFA-positive branches per astrocyte ($^{***}p < 0.001$, Mann–Whitney *U*-test, mean, and SEM) in the nucleus accumbens shell vs. yoked saline controls (Figure 6D). Representative GFAP images of the GFAP-positive astrocytes with their process branching are presented after cocaine self-administration or yoked procedures (Figure 6A). However, a non-significant change in the average branch length between the cocaine self-administration and the yoked saline groups was observed (Figure 6E).

3.4.3. Sholl morphological analysis of astrocytes

Using Sholl morphological analysis, we evaluated the development of astrocytes and quantified their morphological and structural changes after cocaine self-administration vs. yoked delivery of saline. Figure 6F (Top right) illustrates the Sholl method for an astrocyte labeled for GFAP in a cocaine self-administration accumbens shell sample. A total of 10 astrocytes per group were investigated, and the results indicated an increase in the number of intersections across the entire range of distance in the cocaine-self-administration group vs. the yoked saline group (Figure 6F).

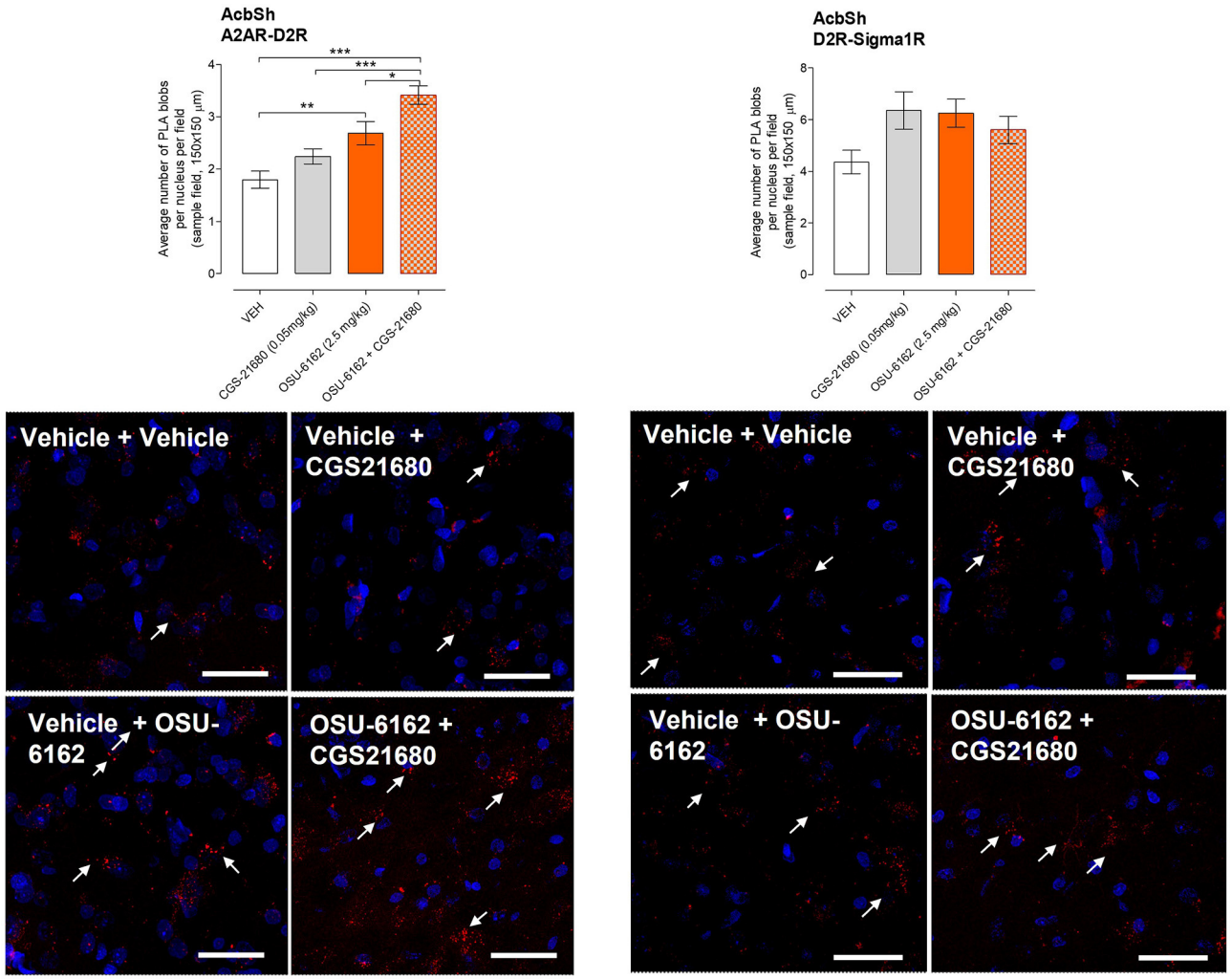

FIGURE 4
Effects of pharmacological treatment on cocaine self-administration (SA) on A2AR-D2R and D2R-Sigma1R heteroreceptor complexes using proximity ligation assay (PLA). (Bottom panels) The heteroreceptor complexes are shown as red puncta, and their average number has been determined per nucleus per sample field using confocal laser microscopy in the nucleus accumbens shell (AcbSh). (Top panels) The effects of CGS 21680 (CGS; 0.05 mg/kg, *i.p.*) and/or OSU-6162 (OSU; 2.5 mg/kg, *s.c.*) in cocaine-self-administrating rats using the same doses as reported in Figure 5 are shown in terms of density changes in their heterodimers compared to the density found in vehicle (VEH; 0.9% NaCl) treated cocaine-self-administrating rats. Significant changes were observed in the A2AR-D2R heterocomplexes as studied in the nucleus accumbens shell. The OSU-6162 treatment cocaine SA group was significantly increased compared to the vehicle SA group (**$p < 0.01$). The combined treatment group showed the strongest increase in its density with highly significant increases against the vehicle and CGS 21680 SA groups (***$p < 0.001$) and with a significant increase against the OSU-6162 group (*$p < 0.05$). Statistical analysis was performed by a one-way ANOVA followed by the Tukey *post hoc* analysis to obtain the means ± SEM of the data from four rats/group.

3.5. Effects of OSU-6162 (2.5 mg/kg) on astrocyte morphology in cocaine self-administration model and yoke saline rats

No significant difference was found in the density of astrocytes per nucleus per sample field ($p > 0.05$, Mann–Whitney test, mean, and SEM), visualized in green with GFAP immunoreactivity, in rats treated with OSU-6162 before cocaine self-administration compared to the yoked saline control group in the nucleus accumbens shell (Figure 7A). However, OSU-6162 2.5 mg/kg alone caused a highly significant increase in the number of GFAP-positive branches per astrocyte (***$p < 0.001$, Mann–Whitney *U*-test, mean, and SEM) in the nucleus accumbens shell vs. yoked saline controls (Figure 7B). In addition, a significant change in the average branch length after OSU-6162 treatment was observed in the cocaine self-administration group vs. the yoked saline group (Figure 7C). Representative GFAP images of the GFAP-positive astrocytes with their process branching are presented after OSU-6162 treatment in cocaine self-administration or yoked procedures (Figure 7D).

We also performed a two-way ANOVA analysis to test the effects of treatment (vehicle vs. OSU-6162) and drug use (cocaine vs. yoked saline) on the average number of astrocytes, average number of branches per astrocyte, and branch length (see Supplementary Figure 1). The analysis showed significant

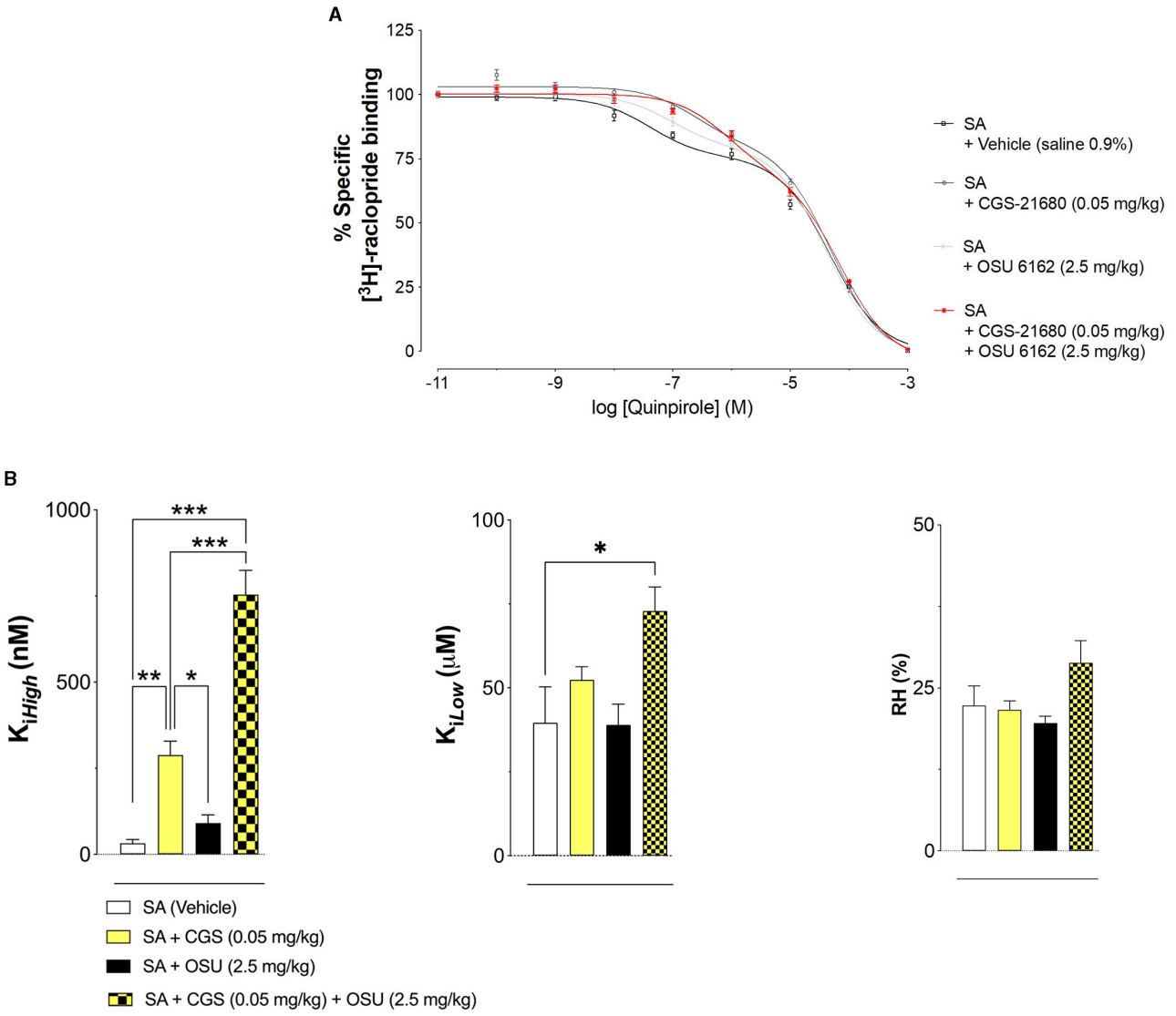

FIGURE 5
(A) Effects of pharmacological treatments on cocaine self-administration (SA) on D2R affinity. [^{3}H]-raclopride/quinpirole competition binding experiments were performed to study changes in D2R affinities produced by A2AR agonist CGS 21680 (CGS 0.05 mg/kg) and/or the Sigma 1R ligand OSU-6162 (OSU 2.5 mg/kg) and compared with vehicle (control group; VEH: 0.09% NaCl). Competition experiments involved the D2-likeR antagonist [^{3}H]-raclopride binding vs. increasing concentrations of quinpirole in ventral striatal membrane preparations from the control group (60 μg/ml). Non-specific binding was defined as the binding in the presence of 100 μM (+) −butaclamol. [^{3}H]-raclopride/quinpirole competition curves were obtained based on the values of four rats with each experiment performed in duplicate. The binding values were given in percentage of specific binding at the lowest concentration of quinpirole employed **(B)**. Modulation of D2R affinity was found with CGS 21680 and OSU-6162 and their combined treatment which induced changes in the high affinity value (D2R $K_{i\ high}$). In the low-affinity component (K_{ilow}), a significant change (*$p < 0.05$) was only found in the combined treatment group with no significant changes in the values of the proportion of the D2R-like receptors in the high-affinity state (RH; upper right and lower left). Means ± SEM are given from four independent experiments performed in duplicate. Statistical analysis was performed by a one-way ANOVA followed by the *post hoc* analysis, **$p < 0.01$. The group of rats exposed to combined treatment was significantly different compared to the group receiving only vehicle treatment.

interactions between the two factors for all three measures ($p < 0.01$ for an average number of astrocytes and branch length and $p < 0.05$ for the average number of branches per astrocyte). Furthermore, we found that the effect of OSU-6162 was distinctly different in the yoked saline group and the cocaine self-administration group. Specifically, in the yoked saline group, treatment with OSU-6162 produced a significant increase in the mean number of astrocytes and in the number of branches per astrocyte while resulting in no changes in the average branch length. In contrast, in the cocaine self-administration group, the mean number of astrocytes and the number of branches per astrocyte were not altered by the low-dose treatment with OSU-6162, while a significant increase in the average branch length was observed. These findings suggest that the effects of OSU-6162 on astrocytes are dependent on both drug use and treatment type.

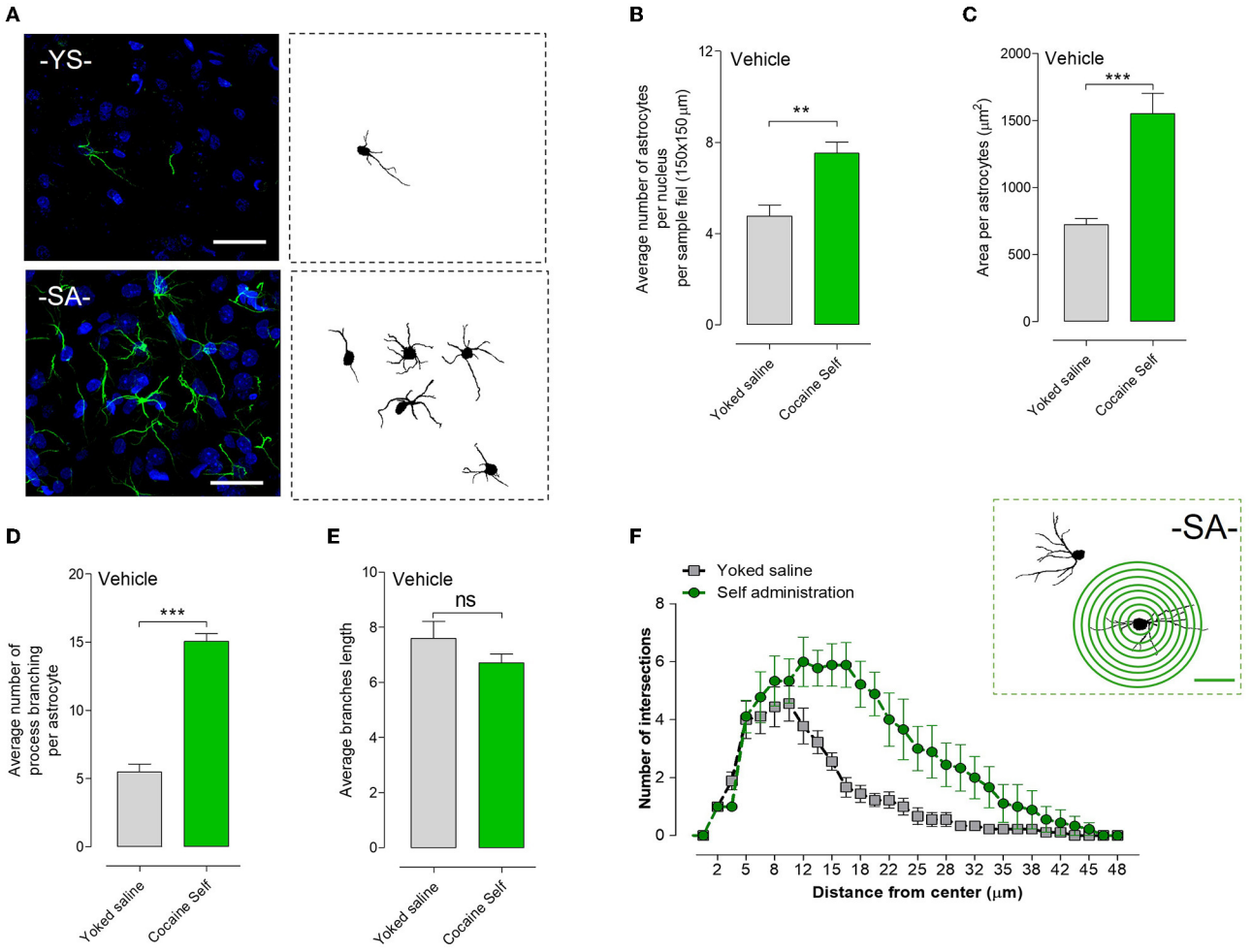

FIGURE 6
Structural changes in astrocytes after cocaine self-administration compared to the yoked saline controls procedure in rats in terms of the number of astrocytes and their process branching in the nucleus accumbens shell. **(A)** Representative GFAP images of the GFAP-positive astrocytes with their process branching are presented after cocaine self-administration or after the yoked saline procedure are also given. **(B)** Cocaine self-administration vs. yoked saline controls produced a significant increase in the density of astrocytes per nucleus per sample field (**$p < 0.01$, Mann–Whitney *U*-test, means ± SEM, $n = 8$ rats) in the nucleus accumbens shell, visualized in green with GFAP immunoreactivity. **(C)** In addition, a significant change in the area was observed. **(D)** Cocaine self-administration caused a highly significant and substantial increase in the number of GFAP-positive branches per astrocyte (***$p < 0.001$, Mann–Whitney test, means ± SEM, $n = 8$ rats) in the nucleus accumbens shell vs. yoked saline controls. **(E)** However, a non-significant (ns) change in the average branch length was observed. **(F)** illustrates the Sholl method for an astrocyte, labeled GFAP, in cocaine self-administration of an accumbens shell sample. A total of 10 astrocytes per group were investigated, and the results clearly indicated an increase in the number of intersections (hence cell processes) with the entire range of astrocytes being compared between the cocaine-self administration group and the yoked saline group in **(B, C)**.

4. Discussion

Previous studies have failed to demonstrate that the monoamine stabilizer OSU-6162 (Steensland et al., 2012) in a low dose (5 mg/kg), which mainly activates the Sigma1R (Sahlholm et al., 2013), altered cocaine self-administration in terms of active lever pressing and total cocaine intake (Borroto-Escuela et al., 2020). However, experiments involving 3-day treatments with OSU-6162 have revealed significant increases in the density of the A2AR-D2R and D2R-Sigma1R heterocomplexes in the nucleus accumbens shell during cocaine self-administration. This may also involve an increased formation of putative trimeric A2AR-D2R-Sigma1R heterocomplexes (Pinton et al., 2015a,b; Borroto-Escuela et al., 2018a). When an A2AR agonist was added *ex vivo* to membrane preparations from OSU-6162-treated rats undergoing cocaine self-administration, a substantial and significant enhancement of the A2AR-mediated allosteric inhibition of the D2R protomer affinity was observed (Borroto-Escuela et al., 2020). The mechanism may involve a cocaine-induced increase in the expression of Sigma1R in the ventral striatum (Romieu et al., 2002; Pinton et al., 2015a,b; Borroto-Escuela et al., 2020).

The present experiments further explored the previous study on the pharmacology of cocaine self-administration by administering an even lower dose of OSU-6162 (2.5 mg/kg) given daily for 3 days, along with systemic treatment with a threshold dose of the A2AR agonist CGS 21680 (0.05 mg/kg), with or without combined systemic treatment with OSU-6162. No significant effects of

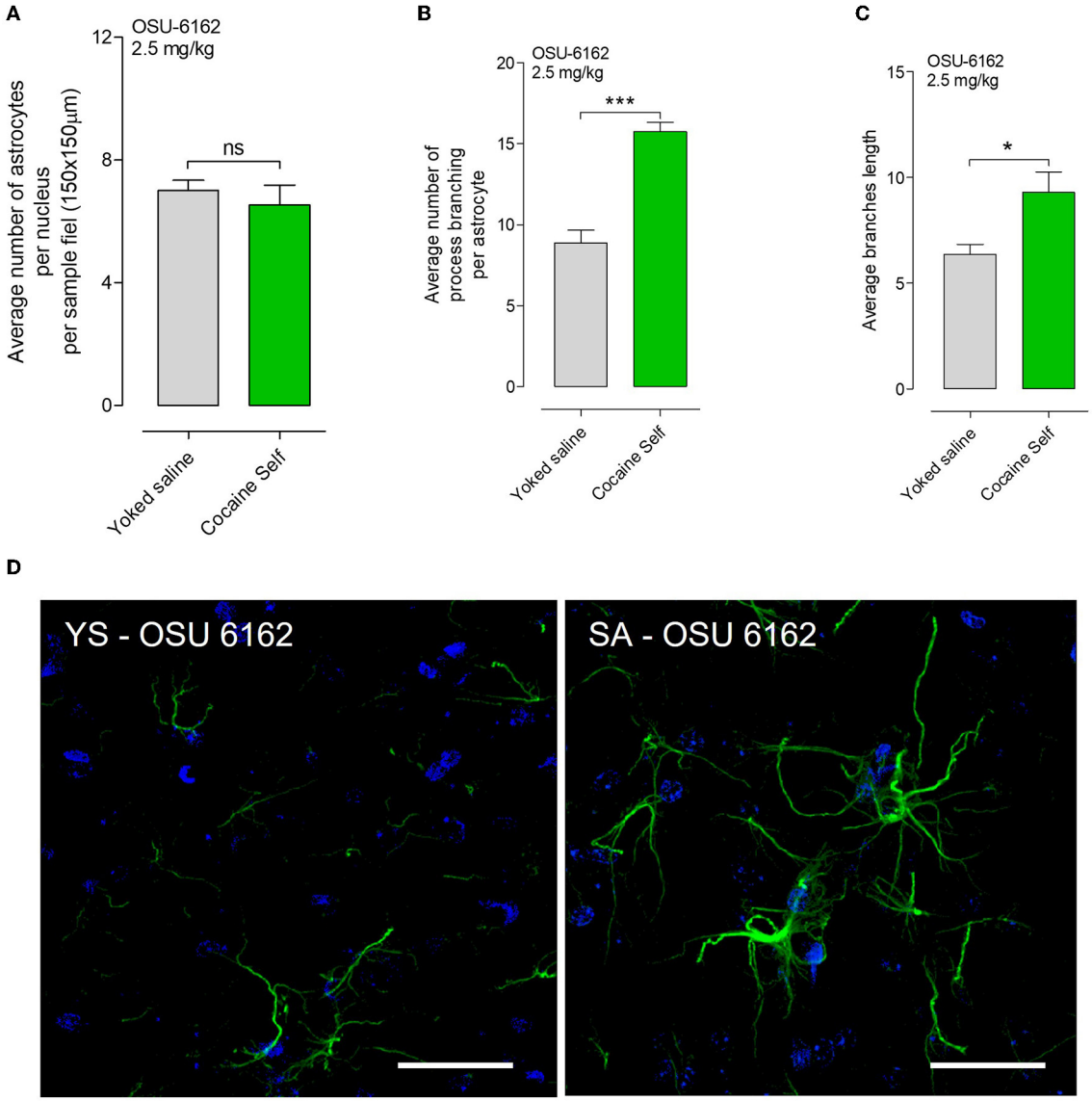

FIGURE 7
(A) OSU-6162 with low dose (OSU 2.5 mg/kg) treatment produced a non-significant (ns) change in the density of astrocytes per nucleus per sample field ($p > 0.05$, Mann–Whitney *U*-test, means ± SEM, $n = 8$ rats) in the nucleus accumbens shell, visualized in green with GFAP immunoreactivity after cocaine self-administration vs. yoked saline controls. **(B)** However, OSU-6162 treatment caused a highly significant and substantial increase in the number of GFAP-positive branches per astrocyte (***$p < 0.001$, Mann–Whitney *U*-test, means ± SEM, $n = 8$ rats) in the nucleus accumbens shell of cocaine-self administration rats vs. yoked saline controls. **(C)** Moreover, significant changes in the average branch length were observed (*$p < 0.01$, Mann–Whitney *U*-test, means ± SEM, $n = 8$ rats). **(D)** Representative GFAP images of the GFAP-positive astrocytes with their process branching are presented in cocaine self-administration or yoked procedure after OUS-6162 low-dose treatment (OSU 2.5 mg/kg). There is a clear-cut increase visualized in the GFAP branching of the astrocytes after OSU6162 treatment in cocaine self-administration compared to its treatment in yoked saline rats.

these treatments on cocaine self-administration were observed, including active lever pressing and total cocaine intake. However, it was possible to demonstrate that combined treatment with a threshold dose of OSU-6162 and CGS 21680 caused significant increases in the A2AR-D2R heterocomplexes in the nucleus accumbens shell compared to vehicle-treated animals, while there was no significant change in the densities of the D2R-Sigma1R heteroreceptor complexes. Treatment with a low dose of OSU-6162 alone but not with CGS 21680 alone produced significant but reduced increases in the density of A2AR-D2R heteroreceptor complexes compared to vehicle-treated animals in the nucleus accumbens shell.

These results enhanced the impact of previous studies. Thus, it is important to understand why there were no reductions in cocaine self-administration despite evidence that the A2AR agonist and Sigma1R ligand, when combined, significantly increased the densities of the A2AR-D2R heterocomplexes in the nucleus accumbens shell. Moreover, enhanced antagonistic A2A-D2R interactions developed upon combined treatment with the Sigma1R ligand in these heterocomplexes, reducing D2R function,

which should bring down cocaine self-administration. Based on the neurochemical results, it seems likely that a significant molecular target can be the putative A2AR-D2R-Sigma1R heterocomplex, which was located extrasynaptically in the postsynaptic part of the glutamate synapses on the ventral striatal-pallidal GABA antireward neurons (Borroto-Escuela et al., 2018a; Wydra et al., 2020). However, another mechanism involved in reducing the effects of the inhibition of the D2R protomer signaling in the A2AR-D2R-Sigma1R heterocomplex on cocaine self-administration can be a substantial increase in the number of astrocytes per sampled field and of branches per astrocyte in the nucleus accumbens shell compared to the yoked saline animals.

The cocaine self-administration-induced changes in the mean number of astrocytes and the number of branches per astrocyte were not altered by the low-dose treatment with OSU-6162. However, OSU-6162 treatment in the yoked saline group significantly increased the mean number of astrocytes and the number of branches per astrocyte. The latter results indicate that Sigma 1R can be involved in mediating certain structural changes in astrocytes in the absence of cocaine.

The increased structural plasticity developed in astrocytes upon cocaine self-administration supported the possibility that astrocytes may modulate cocaine actions on neuronal function in the nucleus accumbens shell. It may develop via the alteration of astrocytic-neuronal crosstalk through changes in the release of astrocytic signals, especially adenosine and ATP, with hydrolysis to adenosine (Acton and Miles, 2017). They operate via astrocytic volume transmission (Borroto-Escuela et al., 2015; Fuxe et al., 2015; Fuxe and Borroto-Escuela, 2016) to reach and activate, especially, neuronal A1R protomers with a higher affinity for adenosine than A2AR (Canals et al., 2005; Ciruela et al., 2006; Cristovao-Ferreira et al., 2013). They may form presynaptic A1R-A2AR heterocomplexes (Ciruela et al., 2006; Cristovao-Ferreira et al., 2013) that can inhibit the A2AR protomer signaling in the cortical-striatal glutamate terminals, forming synapses on the ventral striatal-pallidal GABA anti-reward neurons. It has also been proposed that A1R-A2AR-D2R higher-order complexes may exist on the presynaptic part of the glutamate synapses on the GABA anti-reward neurons in the nucleus accumbens.

Consequently, the reduced inhibition of presynaptic D2R protomer signaling by the A2AR protomer through its inhibition by the A1R protomer may lead to increased inhibition of glutamate release by the presynaptic D2R protomer onto the ventral striatal-pallidal GABA antireward neurons. Further, the astrocytic release of adenosine may contribute to the reduction of activity in the GABA anti-reward neurons due to the reduction of their glutamate drive through preferential A1R protomer activation, inhibiting the A2AR protomer, leading to reduced inhibition of the D2R protomer signaling, which causes enhanced D2R mediated inhibition of glutamate release from the presynaptic region of the glutamate synapse. Such events should aim to reduce the activity of the GABA anti-reward neurons through the reduction of their glutamate drive, which favors the enhancement of cocaine self-administration.

As stated above, a possible explanation for the lack of inhibition of cocaine self-administration in the current experiments may be the cocaine-induced increase in the number of astrocytes and their branching process in the nucleus accumbens shell. This increase can lead to increased extracellular levels of adenosine that are released from astrocytes (Acton and Miles, 2017). Adenosine has an enhanced affinity for the A1R vs. the A2AR and may, therefore, preferentially activate the A1R protomer upon cocaine self-administration, which inhibits the A2AR protomer signaling in A1R-A2AR heterodimers (Ciruela et al., 2006). In the glutamate synapses on the GABA anti-reward neurons, presynaptic A1R-A2AR-D2R heterocomplexes are proposed to exist, with allosteric inhibition of the A2AR protomer being set free from the presynaptic D2R protomer signaling to inhibit glutamate release from the glutamate synapse onto the GABA anti-reward neurons, reducing their firing of the GABA anti-reward neurons. The combined balance of reduced glutamate release onto the GABA antireward neurons and reduced D2R protomer inhibitory signaling in the A2AR-D2R-Sigma1R heterocomplexes located close to the glutamate synapses on these GABA anti-reward neurons may be the mechanism for the lack of change in cocaine self-administration in the current experiments. The post-junctional D2R protomer-mediated inhibition of the GABA anti-reward neurons is lost through presynaptic D2R protomer-mediated inhibition of glutamate release, resulting in a lack of changes in cocaine self-administration.

Taken together, the present findings help to understand the mechanism that led to the failure of combined A2AR agonist and Sigma 1R ligand treatment with their subthreshold dose on cocaine self-administration despite significant and substantial increases in the density of the A2AR-D2R heterocomplexes in the nucleus accumbens. The explanation may be an increased release by cocaine of ATP and adenosine from astrocytes in the nucleus accumbens shell and a putative integration of presynaptic glutamate release and post-junctional heteroreceptor complex signaling where D2R plays a key role. The potential existence of such integrative mechanisms between presynaptic and postjunctional mechanisms in glutamate synapses on GABA antireward neurons is highly interesting and should be further investigated.

Data availability statement

The raw data supporting the conclusions of this article will be made available by the authors, without undue reservation.

Ethics statement

The animal study was reviewed and approved by Ethical Committee (76/2019, 2020/2019) at the Institute of Pharmacology, Polish Academy of Sciences, Krakow.

Author contributions

All authors listed have made a substantial, direct, and intellectual contribution to the work and approved it for publication.

Funding

This study was supported by the Swedish Medical Research Council 2019 (62X-00715-50-3), Stiftelsen Olle Engkvist Byggmästare 2018 and 2021 to KF and DB-E. Moreover, from Hjärnfonden (F02018-0286), Hjärnfonden (F02019-0296), Karolinska Institutet Forskningsstiftelser, and from EMERGIA 2020-39318 (Plan Andaluz de Investigación, Desarrollo e Innovación 2020) to DB-E. DB-E, which belongs to the Academia de Biólogos Cubanos.

Conflict of interest

The authors declare that the research was conducted in the absence of any commercial or financial relationships that could be construed as a potential conflict of interest.

Publisher's note

Supplementary material

The Supplementary Material for this article can be found online at: https://www.frontiersin.org/articles/10.3389/fnmol.2023.1106765/full#supplementary-material

References

Acton, D., and Miles, G. B. (2017). Gliotransmission and adenosinergic modulation: insights from mammalian spinal motor networks. *J. Neurophysiol.* 118, 3311–3327. doi: 10.1152/jn.00230.2017

Borroto-Escuela, D. O., Agnati, L. F., Bechter, K., Jansson, A., Tarakanov, A. O., and Fuxe, K. (2015). The role of transmitter diffusion and flow versus extracellular vesicles in volume transmission in the brain neural-glial networks. *Philos. Trans. R. Soc. Lond,. B. Biol. Sci.* 370, 20140183. doi: 10.1098/rstb.2014.0183

Borroto-Escuela, D. O., Carlsson, J., Ambrogini, P., Narvaez, M., Wydra, K., Tarakanov, A. O., et al. (2017a). Understanding the role of GPCR heteroreceptor complexes in modulating the brain networks in health and disease. *Front. Cell. Neurosci.* 11, 37. doi: 10.3389/fncel.2017.00037

Borroto-Escuela, D. O., Hagman, B., Woolfenden, M., Pinton, L., Jiménez-Beristain, A., Oflijan, J., et al. (2016). "*In situ* proximity ligation assay to study and understand the distribution and balance of GPCR homo- and heteroreceptor complexes in the brain," in *Receptor and Ion Channel Detection in the Brain,* eds R. Lujan and F. Ciruela (Berlin: Springer), 109–126. doi: 10.1007/978-1-4939-3064-7_9

Borroto-Escuela, D. O., Narvaez, M., Wydra, K., Pintsuk, J., Pinton, L., Jimenez-Beristain, A., et al. (2017b). Cocaine self-administration specifically increases A2AR-D2R and D2R-sigma1R heteroreceptor complexes in the rat nucleus accumbens shell. Relevance for cocaine use disorder. *Pharmacol. Biochem. Behav.* 155, 24–31. doi: 10.1016/j.pbb.2017.03.003

Borroto-Escuela, D. O., Romero-Fernandez, W., Garriga, P., Ciruela, F., Narvaez, M., Tarakanov, A. O., et al. (2013). G protein-coupled receptor heterodimerization in the brain. *Meth. Enzymol.* 521, 281–294. doi: 10.1016/B978-0-12-391862-8.00015-6

Borroto-Escuela, D. O., Romero-Fernandez, W., Wydra, K., Zhou, Z., Suder, A., Filip, M., et al. (2020). OSU-6162, a Sigma1R ligand in low doses, can further increase the effects of cocaine self-administration on accumbal D2R heteroreceptor complexes. *Neurotox. Res.* 37, 433–444. doi: 10.1007/s12640-019-00134-7

Borroto-Escuela, D. O., Wydra, K., Filip, M., and Fuxe, K. (2018a). A2AR-D2R heteroreceptor complexes in cocaine reward and addiction. *Trends Pharmacol. Sci.* 39, 1008–1020. doi: 10.1016/j.tips.2018.10.007

Borroto-Escuela, D. O., Wydra, K., Li, X., Rodriguez, D., Carlsson, J., Jastrzebska, J., et al. (2018b). Disruption of A2AR-D2R heteroreceptor complexes After A2AR transmembrane 5 peptide administration enhances cocaine self-administration in rats. *Mol. Neurobiol.* 55, 7038–7048. doi: 10.1007/s12035-018-0887-1

Canals, M., Angulo, E., Casado, V., Canela, E. I., Mallol, J., Vinals, F., et al. (2005). Molecular mechanisms involved in the adenosine A and A receptor-induced neuronal differentiation in neuroblastoma cells and striatal primary cultures. *J. Neurochem.* 92, 337–348. doi: 10.1111/j.1471-4159.2004.02856.x

Ciruela, F., Casado, V., Rodrigues, R. J., Lujan, R., Burgueno, J., Canals, M., et al. (2006). Presynaptic control of striatal glutamatergic neurotransmission by adenosine A1-A2A receptor heteromers. *J. Neurosci.* 26, 2080–2087. doi: 10.1523/JNEUROSCI.3574-05.2006

Cristovao-Ferreira, S., Navarro, G., Brugarolas, M., Perez-Capote, K., Vaz, S. H., Fattorini, G., et al. (2013). A1R-A2AR heteromers coupled to Gs and G i/0 proteins modulate GABA transport into astrocytes. *Purinergic Signal.* 9, 433–449. doi: 10.1007/s11302-013-9364-5

Feltmann, K., Borroto-Escuela, D. O., Ruegg, J., Pinton, L., de Oliveira Sergio, T., Narvaez, M., et al. (2018). Effects of long-term alcohol drinking on the dopamine D2 receptor: gene expression and heteroreceptor complexes in the striatum in rats. *Alcohol. Clin. Exp. Res.* 42, 338–351. doi: 10.1111/acer.13568

Filip, M., Bubar, M. J., and Cunningham, K. A. (2006). Contribution of serotonin (5-HT) 5-HT2 receptor subtypes to the discriminative stimulus effects of cocaine in rats. *Psychopharmacology* 183, 482–489. doi: 10.1007/s00213-005-0197-y

Fredriksson, I., Wirf, M., and Steensland, P. (2019). The monoamine stabilizer (-)-OSU6162 prevents the alcohol deprivation effect and improves motor impulsive behavior in rats. *Addict. Biol.* 24, 471–484. doi: 10.1111/adb.12613

Fuxe, K., Agnati, L. F., Marcoli, M., and Borroto-Escuela, D. O. (2015). Volume transmission in central dopamine and noradrenaline neurons and its astroglial targets. *Neurochem. Res.* 40, 2600–2614. doi: 10.1007/s11064-015-1574-5

Fuxe, K., and Borroto-Escuela, D. O. (2016). Volume transmission and receptor-receptor interactions in heteroreceptor complexes: understanding the role of new concepts for brain communication. *Neural Regen Res* 11, 1220–1223. doi: 10.4103/1673-5374.189168

Fuxe, K., Borroto-Escuela, D. O., Romero-Fernandez, W., Palkovits, M., Tarakanov, A. O., Ciruela, F., et al. (2014). Moonlighting proteins and protein-protein interactions as neurotherapeutic targets in the G protein-coupled receptor field. *Neuropsychopharmacology* 39, 131–155. doi: 10.1038/npp.2013.242

Kourrich, S., Su, T. P., Fujimoto, M., and Bonci, A. (2012). The sigma-1 receptor: roles in neuronal plasticity and disease. *Trends Neurosci.* 35, 762–771. doi: 10.1016/j.tins.2012.09.007

Lahti, R. A., Tamminga, C. A., and Carlsson, A. (2007). Stimulating and inhibitory effects of the dopamine "stabilizer" (-)-OSU6162 on dopamine D2 receptor function *in vitro*. *J. Neural. Transm.* 114, 1143–1146. doi: 10.1007/s00702-007-0784-7

Lazim, R., Suh, D., Lee, J. W., Vu, T. N. L., Yoon, S., and Choi, S. (2021). Structural characterization of receptor-receptor interactions in the allosteric modulation of G protein-coupled receptor (GPCR) dimers. *Int. J. Mol. Sci.* 22, 3241. doi: 10.3390/ijms22063241

Navarro, G., Cordomi, A., Brugarolas, M., Moreno, E., Aguinaga, D., Perez-Benito, L., et al. (2018). Cross-communication between G(i) and G(s) in a G-protein-coupled receptor heterotetramer guided by a receptor C-terminal domain. *BMC Biol.* 16, 24. doi: 10.1186/s12915-018-0491-x

Navarro, G., Quiroz, C., Moreno-Delgado, D., Sierakowiak, A., McDowell, K., Moreno, E., et al. (2015). Orexin-corticotropin-releasing factor receptor heteromers in the ventral tegmental area as targets for cocaine. *J. Neurosci.* 35, 6639–6653. doi: 10.1523/JNEUROSCI.4364-14.2015

Nguyen, K. D. Q., Vigers, M., Sefah, E., Seppala, S., Hoover, J. P., Schonenbach, N. S., et al. (2021). Homo-oligomerization of the human adenosine A(2A) receptor is driven by the intrinsically disordered C-terminus. *Elife* 10, e66662. doi: 10.7554/eLife.66662.sa2

Pinton, L., Borroto-Escuela, D. O., Narváez, M., Jiménez-Beristain, A., Oflijan, J., Ferraro, L., et al. (2015a). Dopamine D2 receptor dynamic and modulation in the D2R-Sigma1R heteroreceptor complexes: role in cocaine actions. *Eur. Neuropsychopharmacol.* 25, S609–S610. doi: 10.1016/S0924-977X(15)30860-9

Pinton, L., Borroto-Escuela, D. O., Narváez, M., Oflijan, J., Agnati, L. F., and Fuxe, K. (2015b). Evidence for the existence of dopamine D2R and Sigma 1 allosteric receptor-receptor interaction in the rat brain: role in brain plasticity and cocaine action. *SpringerPlus* 4, (Suppl 1), P37. doi: 10.1186/2193-1801-4-S1-P37

Romero-Fernandez, W., Wydra, K., Borroto-Escuela, D. O., Jastrzebska, J., Zhou, Z., Frankowska, M., et al. (2022). Increased density and antagonistic allosteric interactions in A2AR-D2R heterocomplexes in extinction from cocaine use, lost in cue induced reinstatement of cocaine seeking. *Pharmacol. Biochem. Behav.* 215, 173375. doi: 10.1016/j.pbb.2022.173375

Romieu, P., Phan, V. L., Martin-Fardon, R., and Maurice, T. (2002). Involvement of the sigma(1) receptor in cocaine-induced conditioned place preference: possible dependence on dopamine uptake blockade. *Neuropsychopharmacology* 26, 444–455. doi: 10.1016/S0893-133X(01)00391-8

Sahlholm, K., Arhem, P., Fuxe, K., and Marcellino, D. (2013). The dopamine stabilizers ACR16 and (-)-OSU6162 display nanomolar affinities at the sigma-1 receptor. *Mol. Psychiatry* 18, 12–14. doi: 10.1038/mp.2012.3

Steensland, P., Fredriksson, I., Holst, S., Feltmann, K., Franck, J., Schilstrom, B., et al. (2012). The monoamine stabilizer (-)-OSU6162 attenuates voluntary ethanol intake and ethanol-induced dopamine output in nucleus accumbens. *Biol. Psychiatry* 72, 823–831. doi: 10.1016/j.biopsych.2012.06.018

Wydra, K., Gawlinski, D., Gawlinska, K., Frankowska, M., Borroto-Escuela, D. O., Fuxe, K., et al. (2020). Adenosine A2A receptors in substance use disorders: a focus on cocaine. *Cells* 9, 1372. doi: 10.3390/cells9061372

Frontiers in
Molecular Neuroscience

Leading research into the brain's molecular structure, design and function

Part of the most cited neuroscience series, this journal explores and identifies key molecules underlying the structure, design and function of the brain across all levels.

Discover the latest Research Topics

See more →

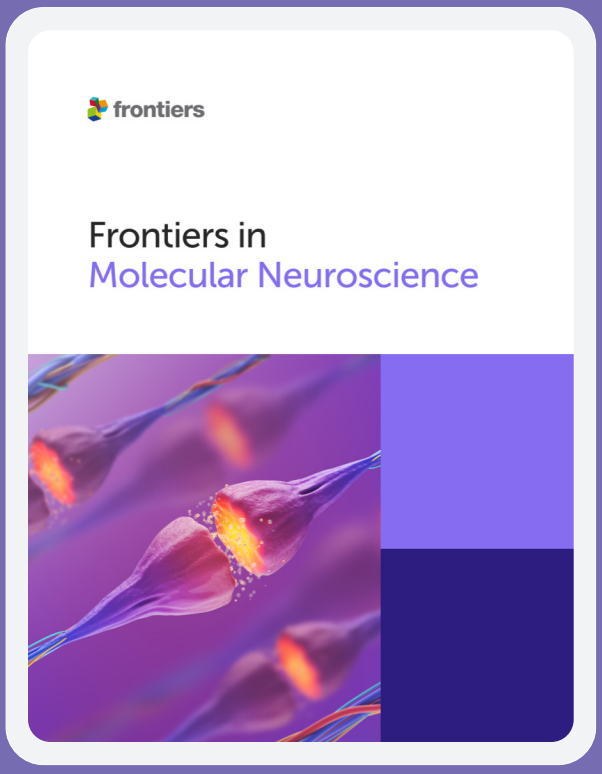

Frontiers

Avenue du Tribunal-Fédéral 34
1005 Lausanne, Switzerland
frontiersin.org

Contact us

+41 (0)21 510 17 00
frontiersin.org/about/contact